Development of Simple Performance Tests Using Laboratory Test Procedures to Illustrate the Effects of Moisture Damage on Hot Mix Asphalt

Jason Bausano[1]
Andrea Kvasnak[1]
R. Christopher Williams[1]**, Ph.D.**

Final Report

DISCLAIMER

This document is disseminated under the sponsorship of the Federal Highway Administration (FHWA) in the interest of information exchange. FHWA assumes no liability for its content or use thereof.

The contents of this report reflect the views of the contracting organization, which is responsible for the accuracy of the information presented herein. The contents may not necessarily reflect the views of FHWA and do not constitute standards, specifications, or regulations.

1. Report No. RC-1521	2. Government Accession No.	3. Recipient's Catalog No.	
4. Title and Subtitle Development of Simple Performance Tests Using Laboratory Test Procedures to Illustrate the Effects of Moisture Damage on Hot Mix Asphalt		5. Report Date April 5, 2006	
7. Author(s) Jason Bausano, Andrea Kvasnak, & R. Christopher Williams, Ph.D.		6. Performing Organization Code	
9. Performing Organization Name and Address Michigan Technological University Department of Civil and Environmental Engineering 1400 Townsend Drive Houghton, MI 49931		8. Performing Org Report No.	
12. Sponsoring Agency Name and Address Federal Highway Administration		10. Work Unit No. (TRAIS)	
		11. Contract/Grant No. DTFH61-02-C-00074	
		11a. 00-MTU-5	
15. Supplementary Notes		13. Type of Report and Period Covered Final Report	
		14. Sponsoring Agency Code	

16. Abstract

It has been extensively documented since the late 1970's that moisture damage occurs in hot mix asphalt (HMA) pavements. A variety of test methods are available that test an HMAs' ability to resist moisture sensitivity. There are also some test methods that look at an asphalt binder's moisture susceptibility. The current test method for detecting moisture sensitivity in HMA is American Association of State Highway and Transportation Officials (AASHTO) T283: Resistance of Compacted Bituminous Mixture to Moisture-Induced Damage. Inclusion of this test method in Superpave did not consider the change in specimen size from 100mm to 150mm nor difference in compaction method. The procedures in AASHTO T283 consider the loss of strength due to freeze/thaw cycling and the effects of moisture existing in specimens compared to unconditioned specimens. However, mixtures do not experience such a pure phenomenon. Pavements undergo cycling of environmental conditions, but when moisture is present, there is repeated hydraulic loading with the development of pore pressure in mixtures. Thus, AASHTO T283 does not consider the effect of pore pressure, but rather considers a single load effect on environmentally conditioned specimens.

This report develops moisture susceptibility procedures which would utilize repeated loading test devices (dynamic modulus or asphalt pavement analyzer) of specimens in saturated conditions and be compared to unconditioned specimens in a dry test environment. In addition to HMA mixture testing, a modified dynamic shear rheometer will be used to determine if an asphalt binder or mastic is moisture susceptible. Moisture susceptible criteria was developed using the dynamic complex modulus, asphalt pavement analyzer, and dynamic shear rheometer. Evaluation of AASHTO T283 for 150mm Superpave Gyrtaory compacted specimens is also detailed in this report along with a new criterion.

17. Key Words: Hot Mix Asphalt, Moisture Damage, Dynamic Modulus, and Flow Number	18. Distribution Statement No restrictions. This document is available to the public through the Federal Highway Administration.		
19. Security Classification (report) Unclassified	20. Security Classification (Page) Unclassified	21. No of Pages 366	22. Price

Form DOT F 1700.7 (8-72)

TABLE OF CONTENTS

LIST OF TABLES

LIST OF FIGURES

LIST OF ACRONYMS

A	Witczak Predictive Equation Regression Intercept
APA	Asphalt Pavement Analzyer
AAPT	Association of Asphalt Paving Technologists
AASHTO	American Association of State and Highway Transportation Officials
ASTM	American Society for Testing and Materials
BSG (G_{mb})	Bulk Specific Gravity
COV	Coefficient of Variation
CTAA	Canadian Technical Asphalt Association
D60	Grain size that corresponds to 60 percent passing
DSR	Dynamic Shear Rheometer
E* and $\lvert E^* \rvert$	Complex Modulus and Dynamic Modulus, respectively
E' and E"	Elastic and Viscous Modulus, respectively
ESAL	Equivalent Single Axle Load
FHWA	Federal Highway Administration
F_N	Flow Number
G_b	Asphalt Specific Gravity
G_{sb}	Aggregate Bulk Specific Gravity
G_{se}	Aggregate Effective Specific Gravity
HRB	Highway Research Board
HMA	Hot Mix Asphalt
IDT	Indirect Tension Test
JMF	Job Mix Formula
LVDT	Linear Variable Differential Transducer
M-E	Mechanistic-Empirical
MTSG (G_{mm})	Maximum Theoretical Specific Gravity
MTU	Michigan Technological University
NCAT	National Center for Asphalt Technology
NCHRP	National Cooperative Highway Research Program
NMAS	Nominal Maximum Aggregate Size
P_b	Asphalt Binder Content
P_{eff}	Effective Asphalt Binder Content
R^2	Coefficient of Determination
RAP	Recycled Asphalt Pavement
RTFO	Rolling Thin Film Oven
SGC	Superpave Gyratory Compactor
SHRP	Strategic Highway Research Program
SSD	Saturate Surface Dry
SPT	Simple Performance Test
SST	Superpave Shear Tester
TAI	The Asphalt Institute
UTM	Universal Testing Machine
V	Witczak Predictive Equation Regression Slope

VFA	Voids Filled with Asphalt
VMA	Voids in the Mineral Aggregate
ε_o	Strain
ϕ	Phase Angle
σ_o	Stress

Executive Summary

Introduction

The accelerated damage of hot mix asphalt (HMA) due to moisture is of significant concern to transportation agencies and researchers. It is of primary interest in the northern states due to freeze/thaw action during the spring months, but it can be a problem wherever there is the availability of moisture. Currently, there are many tests available to test HMA or binder to determine if it is a mix, a binder, or both are moisture susceptible. Many of these tests have produced varied results and a more mechanistic test is being sought that considers the micro-mechanical behavior and/or chemical behavior of moisture damage. A significant amount of time and money has been spent on trying to validate these tests and to determine how well the results relate to the field performance of HMA.

Moisture susceptibility is the loss of strength in HMA mixtures due to the effects of moisture. In HMA, there are three components: aggregates, asphalt binder, and air voids. Moisture damage can occur in two ways; loss of adhesion between asphalt binder and aggregate, or the weakening of asphalt mastic in the presence of moisture. Thus, selection of appropriate aggregates (aggregate chemistry) and asphalt binder (binder chemistry) play an important role in deterring moisture damage. Moisture damage can occur from a loss of adhesion between aggregates and binder. This is due to the chemistry of the aggregates. Siliceous aggregate sources are prone to stripping due to a high silica dioxide component. The asphalt binder cannot bond to siliceous aggregate thus when moisture is present and HMA is loaded repeatedly, asphalt binder strips from the aggregate resulting in a loss of adhesion (the binder holds the aggregates together). Moisture damage is a significant concern because it diminishes the performance and service life of HMA pavements resulting in increased maintenance and rehabilitation costs to

highway agencies. Moisture susceptibility is best identified by developing tests that illustrate the effects of moisture damage whether it is on the HMA mixture or asphalt binder. Identification of moisture susceptibility allows the issue to appropriately addressed if necessary.

Literature Review

According to Little and Jones (2003), moisture damage can be defined as the loss of strength and durability in asphalt mixtures due to the effects of moisture. Moisture can damage the HMA in two ways: 1) loss of bond between asphalt cement or mastic and fine and coarse aggregates or 2) weakening of mastic due to the presence of moisture. There are six contributing factors that have been attributed to causing moisture damage in HMA: detachment, displacement, spontaneous emulsification, pore-pressure induced damage, hydraulic scour, and environmental effects (Roberts et al. 1996, Little and Jones 2003). Not one of the above factors necessarily works alone in damaging an HMA pavement, as several of these factors can have a combined affect on damaging a pavement. Therefore there is a need to look at the adhesive interface between aggregate and asphalt and the cohesive strength and durability of the mastic (Graff 1986, Roberts et al. 1996, Little and Jones 2003, Cheng et al. 2003). A loss of the adhesive bond between aggregate and asphalt can lead to stripping and raveling while a loss of cohesion can lead to a weakened pavement that is susceptible to premature cracking and pore pressure damage (Majidzadeh and Brovold 1966, Kandhal 1994, Birgission et al. 2003).

Several tests are available that are conducted on loose HMA mixtures, asphalt binders, or compacted HMA mixtures. The most notable loose mixture test is the boiling water test. Some notable asphalt binder tests are the pull-off tensile strength test and the Wilhelmy plate test. Some widely used compacted mixture tests are AASHTO T283 (Lottman 1998, Lottman 1992, Tunnicliff and Root 1982, Kennedy et al. 1983, Tunnicliff and Root 1984, Coplantz and

Newcomb 1988, Kennedy and Ping 1991, Stroup-Gardiner and Epps 1992, Epps et al. 2000), Hamburg Wheel Track test device (Aschenbrener et al. 1995), Asphalt Pavement Analyzer (APA) (Cross et al 2000, APA Manual 2002, Mallick et al. 2003, West et al. 2004, Johnston et al 2005), and the Environmental Conditioning System (ECS (Terrel et al. 1994). The current method for evaluating the moisture susceptibility of compacted bituminous mixtures is AASHTO T283. AASHTO T283 is based on the Marshall mix design method, but current research and highway agencies are evaluating the moisture susceptibility of Superpave mixtures based on AASHTO T283. The Superpave volumetric mix design procedure does not include a simple, mechanical test that is analogous to the Marshall stability and flow test criteria. The Superpave mix design system relies on material specifications and volumetric criteria in order to ensure a quality performing mix design. Inclusion of AASHTO T283 in Superpave did not consider the change in specimen size from 100mm to 150mm and resulted in the initiation of NCHRP 9-13 in 1996 (Epps et al. 2000). The researchers concluded that either AASHTO T283 does not evaluate moisture susceptibility or the criterion, the tensile strength ratio (TSR), is incorrectly specified. NCHRP 9-13 examined mixtures that have historically been moisture susceptible and ones that have not. The researchers also examined the current criteria using Marshall and Hveem compaction, which was considered in the previously mentioned conclusions.

The procedures in AASHTO T283 and NCHRP 9-13 consider the loss of strength due to freeze/thaw cycling and the effects of moisture existing in specimens compared to unconditioned specimens. However, mixtures do not experience such a pure phenomenon. Pavements undergo cycling of environmental conditions, but when moisture is present, there is repeated hydraulic loading with development of pore pressure in mixtures. Thus, AASHTO T283 and the NCHRP

9-13 study do not consider the effect of pore pressure, but rather consider a single load effect on environmentally conditioned specimens. This project has developed moisture susceptibility procedures which utilizes the dynamic loading of specimens in saturated conditions and compared to the results to unconditioned specimens in a dry test environment. The developed test procedure considered the simple performance test, AASHTO T283, and the APA to determine the moisture susceptibility of the mixtures.

Material Collection

During the summer of 2004, when the majority of sampling occurred, it was realized that not all of the mixes could be sampled during the 2004 construction season. Thus, it was decided that previous HMA mixtures that were sampled during the 2000 construction season could be used coupled with additional sampling during the 2005 construction season. The 2000 construction projects that were sampled were stored in a heated, metal building where the material was protected from rain, heat, and snow.

This research was been divided into two phases. Phase I testing was used to determine the number of freeze/thaw cycles that will cause the equivalent damage to AASHTO T283 specimens for different methods of compaction and specimen sizes. Phase II testing of mixes for moisture damage used the results of Phase I for AASHTO T283 testing on 150mm specimens and the results of Phase I and Phase II for dynamic modulus testing. APA testing was based on results from Phase I. In the ensuing sections, the mixture experimental plan and laboratory testing experimental plan are outlined.

The experimental plan considers different mix types, aggregate sources, laboratory test systems, conditioning approaches, and test specimen size. The experimental plan includes two integrated plans: one for the mixes and one for the planned laboratory tests. A sensitivity study

on the effects of specimen size and compaction method was conducted on a limited number of mixes to determine the amount of conditioning that should be needed on larger Superpave compacted specimens to obtain analogous conditioning as AASHTO T283 Marshall mix specimens. Table 1 below outlines the sensitivity study experimental plan.

Table 1 Sensitivity Study Experimental Plan for Mix and Aggregate Types

PHASE 1 MOISTURE		
NMAS (mm)	Traffic Level (ESAL)	
	≤ 3,000,000	>3,000,000
25.0 or 19.0	Limestone - M50 Dundee	Limestone - M59 Brighton
	Gravel - M21 St. Johns	
12.5 or 9.5	Limestone - BL96 Howell	Limestone - I-196 Grand Rapids
	Gravel - M21 Owosso	Slag/Trap Rock - I-75 Clarkston

The Phase II experimental plan considers different mix types, aggregate sources, and laboratory test systems. Table 2 below outlines the expanded experimental plan.

Table 2 Expanded Experimental Plan for Phase II Projects

PHASE 2 MOISTURE		
NMAS (mm)	Traffic Level (ESAL's)	
	≤ 3,000,000	>3,000,000
25.0 or 19.0	Limestone - M50 Dundee	Limestone - M59 Brighton
	Limestone - M36 Pinckney	Limestone - Michigan Ave. Detroit
	Gravel - M45 Grand Rapids	Limestone - Vandyke Detroit
	Gravel - M21 St. Johns	Limestone - US23 Hartland
	Limestone - M84 Saginaw	Gravel - I-75 Levering Road
12.5 or 9.5	Limestone - BL96 Howell	Limestone - I-196 Grand Rapids
	Gravel - M21 Owosso	Slag/Gabbro - I-75 Clarkston
	Gravel - M66 Battle Creek	Gravel - M53 Detroit
	Limestone - M50 Dundee	Limestone - Michigan Ave. Detroit
	Limestone - US12 MIS	Gabbro I-75 Toledo (in MI)
SMA	N/A	Gabbro - I-94 SMA Ann Arbor

Phase I HMA Results

The Phase I sensitivity study considered the factors affecting the wet strength of a specimen and a new TSR criteria for AASHTO T283 when Superpave compaction method is

employed in lieu of the Marshall compaction method. AASHTO T283 was developed based on 100mm Marshall compacted specimens. With the transition from Marshall compacted specimens to Superpave compacted specimens it was felt that the requirements outlined in AASHTO T283 should be re-evaluated. It was discovered that three freeze/thaw cycles for conditioning is satisfactory when using specimens created via the Superpave method. However, to maintain the same probability level as attained with a TSR value of 80% for 100mm Marshall compacted specimens, a TSR value of 87% and 85% should be used with 150mm and 100mm Superpave compacted specimens, respectively. Alternatively, an 80% TSR for 150mm Superpave specimens corresponds to a TSR to 70% for 100mm Marshall specimens.

Phase I Binder Results

A new moisture susceptibility test was developed using modified DSR parts. Testing was conducted to determine if material interface affects complex shear modulus results. It was determined that material interface does affect complex shear modulus results. Hence, for the new test protocol, ceramic discs would be used to allow for water to access the top of a binder sample in addition to the circumference of a sample. Further testing was conducted to establish an appropriate gap size for a new testing procedure. The gap size selected was 1000μm. Subsequent testing indicated that the new test procedure is sensitive to binder type and addition of filler. The test also appears to be able to distinguish between two filler types, hydrated lime and silica based fillers. Additional testing indicated that statistically different complex shear modulus results were obtained from unsaturated asphalt binder samples versus saturated specimens. However, no additional differences were observed when the samples were moisture saturated and had endured one freeze/thaw cycle. There were also no statistical differences in

complex shear modulus readings when leaving a specimen in a heated water bath anywhere from zero to 20 minutes prior to testing.

Based on laboratory testing and statistical analysis a new test procedure was established in this report. Specimens would be tested first unsaturated with ceramic discs at a gap of 1000µm. Second, the specimens would soak in a water bath for a period of 24 hours at 25˚C. After 24 hours of soaking, specimens would be tested again in a DSR using ceramic discs.

Phase II Results

Phase II testing of HMA mixtures outlines moisture susceptibility procedures and preliminary criteria utilizing the dynamic loading on saturated and unconditioned specimens. The two devices used were a loaded wheel tester, an APA, and an unconfined compressive tester, for dynamic modulus testing. Specimens tested in the APA were tested unconditioned in air, saturated and freeze/thaw conditioned tested in air, and saturated and freeze/thaw conditioned tested in water. The proposed criterion is a ratio of conditioned specimen rut depths obtained in a moisture saturated environment divided by unconditioned specimen rut depths obtained in an air chamber accounting for a maximum allowable rut depth. The dynamic modulus test procedure uses a retained dynamic modulus of 60% of conditioned specimens to unconditioned specimens. This initial criterion was derived as it is the same percentage of mixtures that fail the AASHTO T283 criteria of the 21 field mixes. Comparison of mixtures performance ranked via AASHTO T283 and the proposed retained dynamic modulus criteria are considerably different.

The dynamic modulus and APA tests were selected to simulate hydraulic effects occurring in a pavement with the application of a load. In the field, pavements undergo cycling of environmental conditions, but when moisture is present, there is repeated hydraulic loading with the development of pore pressure in mixtures. AASHTO T283 does not consider the effect

of pore pressure, but rather considers a single load effect on environmentally conditioned specimens.

The binders from the mixes tested using AASHTO T283, APA, and dynamic modulus were evaluated using the modified DSR parts and test procedure developed in Phase I. The binders were tested as unconditioned and moisture saturated conditioned. Two fillers, a hydrated lime and silica, were added at three percentage levels to determine if the new test procedure could detect changes to binder and yield differing results for a moisture prone and a moisture resistant materials. The testing results indicated that the test procedure could distinguish between original binders and filler modified binders.

A moisture criterion was developed for the new binder moisture susceptibility test. Initially the Superpave criterion for unaged binders was considered. However, none of the binders examined in this report failed the Superpave minimum criteria of $G^*/\sin(\delta)$ being at least 1.0kPa, however several of the binders did exhibit degradation during testing. During the saturation process many of the binders maintained the original shape prior to saturation, however there were a few binders that tended to spread and even lose small sections of the binder. The binders which did tend to creep during saturation also emitted a visible oil sheen. Specimens displaying creep and oil sheens tended to yield $G^*/\sin(\delta)$ close to the Superpave minimum of 1.0kPa indicating that another criterion should be used for moisture susceptibility testing. The criterion suggested in this report is based on the ability to evaluate the viscous and elastic components.

A number of factors exist that cause or accelerate moisture damage. Test results from the AASHTO T283, dynamic modulus, and APA tests were used to determine the significant statistical factors affecting moisture damage. The factors considered were gradation, nominal

maximum aggregate size (NMAS), traffic level, polymer modification, aggregate type, permeability, asphalt content, fine aggregate angularity (FAA), and recycled asphalt pavement (RAP). In the case of the dynamic modulus testing, frequency was also considered. It appears that the factors affecting AASHTO T283 are polymer modification, aggregate type, permeability, and RAP. The factors affecting dynamic modulus are traffic, polymer modification, aggregate type, permeability, RAP, and frequency. Factors affecting APA rut depth results are temperature and traffic level for conditioned specimens tested in a water bath. For conditioned specimens tested in an air chamber, the factors affecting rut depth are test temperature, polymer modification, binder content, fines to binder ratio, NMAS, and traffic level. It is known that aggregate type, polymer modification, and permeability affect moisture damage. RAP may have been deemed a statistically significant factor since it is highly variable. No two RAP samples will have the same material properties since RAP often is obtained from several pavements.

CHAPTER 1 INTRODUCTION

1.1 Moisture Susceptibility

A number of factors exist that are detrimental to hot mix asphalt (HMA). Moisture damage is a major factor that impacts HMA; which includes the binder and the mixture component. Thus, there is a need for highway agencies to combat moisture susceptibility. In order to first solve this problem, several questions need to be answered:

- What is moisture susceptibility?
- Where does it occur?
- Why does it happen?
- Why is it important? and
- How can we fix it?

Moisture susceptibility is the loss of strength in HMA mixtures due to the effects of moisture. In HMA, there are three main components: aggregates, asphalt binder, and air voids. Moisture damage can occur in two ways; loss of adhesion between asphalt binder and aggregate, or the weakening of asphalt mastic in the presence of moisture. Thus, selection of appropriate aggregates (aggregate chemistry) and asphalt binder (binder chemistry) play an important role in moisture damage. Moisture damage can occur from a loss of adhesion between aggregates and binder. This is due to the chemistry of the aggregates. Siliceous aggregate sources are prone to stripping due to a high silica dioxide component. The asphalt binder cannot bond to these siliceous aggregates; thus when moisture is present and the HMA is loaded repeatedly, the asphalt binder strips from the aggregate resulting in a loss of adhesion (the binder holds the aggregates together). Moisture damage is a significant concern since it can diminish the performance and service life of HMA pavements, resulting in increased maintenance and

rehabilitation costs to highway agencies. Moisture susceptibility is best identified by developing tests that illustrate the effects of moisture damage whether it is on HMA mixture or asphalt binder. Identification of moisture susceptible prone materials enables remediation of a mix prior to usage in the field.

1.2 Project Objectives

The objectives of this study were to develop moisture susceptibility test criteria using 150mm Superpave gyratory compacted specimens and binders from these mixes used for procuring 150mm Superpave gyratory compacted specimens. Laboratory testing of HMA included testing specimens according to current American Association of State Highway and Transportation Officials (AASHTO) and American Society of Testing and Materials (ASTM) specifications, the simple performance test using the modified Lottman conditioning procedure, and an asphalt pavement analyzer (APA). Varying durations of freeze/thaw cycling and number of cycles will be detailed in the experimental plan. The test temperature also was used as an experimental factor. Laboratory testing of asphalt binders required the development of a new test procedure. A modified dynamic shear rheometer (DSR) was utilized to determine if an asphalt binder or mastic is moisture susceptible.

1.3 Current State of the Practice for Moisture Testing

The current method for evaluating the moisture susceptibility of compacted bituminous mixtures is based on AASHTO T283. AASHTO T283 was developed using Marshall mix design, yet current research and highway agencies are evaluating the moisture susceptibility of Superpave mixtures with the AASHTO T283 procedure. The Marshall and Superpave mix design methods differ from one another in several respects. The Superpave volumetric mix design procedure does not include a simple mechanical test that is analogous to the Marshall

stability and flow test criteria. The Superpave mix design system relies on material specifications and volumetric criteria in order to ensure a quality performing mix design. Inclusion of AASHTO T283 in Superpave did not consider the change in specimen size from 100mm to 150mm nor the difference in compaction effort, which resulted in the initiation of NCHRP 9-13 in 1996 (Epps et al. 2000). The researchers concluded that either AASHTO T283 does not evaluate moisture susceptibility or the criterion, the tensile strength ratio (TSR), is incorrectly specified. NCHRP 9-13 examined mixtures that have historically been moisture susceptible and ones that have not.

The procedures in AASHTO T283 and NCHRP 9-13 consider the loss of strength due to freeze/thaw cycling and effects of moisture existing in specimens compared to unconditioned specimens. However, mixture field conditions are not as controlled as laboratory testing. Pavements undergo cycling of environmental conditions. Pore pressures in the air void system develop in the presence of moisture and dynamic loading. Unfortunately, AASHTO T283 and NCHRP Report 444 do not account for the effects of pore pressure, but rather consider a single load effect on environmentally conditioned specimens. This project developed moisture susceptibility procedures evaluating both mix and binder. The mix test procedures utilized the dynamic loading of specimens to evaluate specimens in saturated conditions and compared those results to unconditioned specimens tested in a dry environment. The test procedures use the simple performance test, AASHTO T283, and an APA to determine the moisture susceptibility of the mixtures. The binder test procedure used a modified dynamic shear rheometer (DSR) to evaluate the moisture susceptibility of binders and mastic.

1.4 Overall Project Experimental Plan

The experimental considered different mix types, aggregate sources, laboratory test systems, and conditioning approaches. The experimental plan included two integrated plans: one for the mixes and one for the planned laboratory tests (both mix and binder). A sensitivity study on the effects of specimen size and compaction method was conducted on a limited number of mixes to determine the amount of conditioning that should occur on larger Superpave compacted specimens.

1.5 Hypotheses for Testing Results

Hypotheses were formulated regarding the factors considered in the experimental plan based upon past research and testing from the literature review. The statistical analyses are outlined in Chapter 4 for the sensitivity study. The following hypotheses were analyzed:

- Which test procedure better simulates moisture damage: AASHTO T283, APA, or the simple performance test?
- Do these HMA mixture tests rank the HMA mixtures the same?
- Can a DSR be utilized to determine if an asphalt binder or mastic is moisture sensitive?
- What kind of criteria should be used to determine if a HMA mixture or asphalt binder is moisture susceptible?

1.6 Contents of this Document

Chapter 2 of this final report discusses past research and studies that have been related to moisture damage or moisture susceptibility. Included is a brief description of the research conducted along with major findings of the study that directly apply to this research. Chapters 3 and 4 outline the experimental plan used and procedures used to sample, prepare, and test specimens for the project. Chapter 5 reviews the mixtures that were used and specimen

preparation in terms of volumetric properties in relation to the job mix formula (JMF). Chapter 6 outlines the testing setup for AASHTO T283, dynamic complex modulus (DCM), APA testing, and DSR testing. Chapter 7 presents the preliminary results of the sensitivity study using AASHTO T283. Chapter 8 relates the results of a preliminary asphalt binder and mastic study using a modified DSR. Chapter 9 presents the evaluation of all the mixes and asphalt binders used in the experimental plan and analyzes the results that were tested using AASHTO T283, the simple performance test, APA, and a modified DSR. Included in this chapter is the evaluation of the hypotheses that were formulated in Chapter 1. Chapter 10 presents the summary, conclusions, and recommendations for further research.

CHAPTER 2 LITERATURE REVIEW

2.1 Introduction

The accelerated damage of HMA due to moisture is of significant concern to transportation agencies and researchers. It is of primary interest in northern states due to freeze/thaw action during the spring months, but it can be a problem wherever there is the availability of moisture. Currently, there are many tests available to evaluate either HMA or binder to determine if it is a mix problem, a binder problem, or both are moisture susceptible. Many of these tests have produced ambiguous results and a more mechanistic test is being sought that considers the micro-mechanical behavior and/or chemical behavior of moisture damage. A significant amount of time and money has been spent on trying to validate these tests and to determine how well the results relate to the field performance of HMA.

2.2 Causes of Moisture Damage

According to Little and Jones (2003), moisture damage can be defined as the loss of strength and durability in asphalt mixtures due to the effects of moisture. Moisture can damage HMA in two ways: 1) Loss of bond between asphalt cement or mastic and fine and coarse aggregate or 2) Weakening of mastic due to the presence of moisture. There are six contributing factors that have been attributed to causing moisture damage in HMA: detachment, displacement, spontaneous emulsification, pore-pressure induced damage, hydraulic scour, and environmental effects (Roberts et al. 1996, Little and Jones, 2003). Not one of the above factors necessarily works alone in damaging an HMA pavement, as they can work in a combination of processes. Therefore there is a need to look at the adhesive interface between aggregates and asphalt and the cohesive strength and durability of mastics (Graff 1986, Roberts et al. 1996, Little and Jones 2003, Cheng et al. 2003). A loss of the adhesive bond between aggregate and

asphalt can lead to stripping and raveling while a loss of cohesion can lead to a weakened pavement that is susceptible to premature cracking and pore pressure damage (Majidzadeh and Brovold 1966, Kandhal 1994, Birgission et al. 2003).

2.2.1 Detachment

Majidzah and Brovold (1968) describe detachment as the separation of an asphalt film from an aggregate surface by a thin film of water without an obvious break in the film. Adhesive bond energy theory explains the rationale behind detachment. In order for detachment not to happen, a good bond must develop between asphalt and aggregate; this is known as wettability (Scott 1978). As free surface energy of adhesion or surface tension decreases the bond between the aggregate and asphalt increases. Consider a three phase system of aggregate, asphalt, and water. Water reduces the surface energy of a system since aggregate surfaces have a stronger preference for water than asphalt because the asphalt is hydrophilic (Majidzadeh and Brovold 1968). Cheng et al. (2002) calculated adhesive bond strengths by measuring the surface energies of components, the asphalt-aggregate interface, in the presence of water and when under dry conditions.

2.2.2 Displacement

Displacement can occur at a break in the asphalt film at the aggregate surface where water can intrude and displace asphalt from aggregate (Fromm 1974, Tarrer and Wagh 1991). The break in an asphalt film can come from an incomplete coating of aggregate particles, inadequate coating at sharp edges of aggregates, or pinholes in asphalt film. Chemical reaction theory can be used to explain stripping as a detachment mechanism according to Scott (1978). The pH of water at the point of film rupture can increase the process of displacement thereby

increasing the separation of asphalt from aggregate (Scott 1978, Tarrer and Wagh 1991, Little and Jones 2003).

2.2.3 Spontaneous Emulsification

Spontaneous emulsification occurs due to inverted emulsion of water droplets in asphalt cement (Little and Jones 2003). The water diffuses into asphalt cement thereby attaching itself to an aggregate causing a separation between asphalt and aggregate. A loss of adhesive bond occurs between asphalt and aggregate. Clays and asphalt additives can further aggravate the emulsification process (Scott 1978, Fromm 1974, Asphalt Institute 1981).

2.2.4 Pore Pressure

Pore pressure can develop in an HMA pavement due to entrapped water or water that traveled into air void systems in vapor form (Little and Jones, 2003, Kandhal 1994). The pore pressure in an HMA pavement can increase due to repeated traffic loading and/or increases in temperature as well. If an HMA pavement is permeable, then water can escape and flow out. However, if it is not permeable, the resulting increased pore pressure may surpass the tensile strength of an HMA and strips asphalt film from an aggregate, causing microcracking (Majidzadeh and Brovold 1968, Little and Jones, 2003). Microcracking can also be seen in a mastic under repeated loading thus resulting in an adhesive and/or cohesive failure (Little and Jones 2003). The rate of microcracking is accelerated by an increase in pore pressure and the presence of water in HMA. The air void system or permeability of a pavement is an important property in order to control pore pressure in an HMA pavement.

2.2.5 Hydraulic Scour

Hydraulic scour (stripping) occurs at a pavement surface and is a result of repeated traffic tires on a saturated pavement surface. Water is sucked into a pavement by tire rolling action

(Little and Jones 2003). Hydraulic scour may occur due to osmosis or pullback (Fromm 1974). Osmosis is the movement of water molecules from an area of high concentration to an area of low concentration. In the case of HMA, osmosis occurs in the presence of salts or salt solutions in aggregate pores. The movement of these molecules creates a pressure gradient that sucks water through the asphalt film (Mack 1964, Little and Jones 2003). The salt solution moves from an area of high concentration to an area of low concentration. Cheng et al. (2002) show that there is a considerable amount of water that diffuses through the asphalt cement and asphalt mastics can hold a significant amount of water.

2.2.6 Environmental Effects

Factors such as temperature, air, and water have deleterious effects on the durability of HMA (Terrel and Shute 1989, Tandon et al. 1998). Other mechanisms such as high water tables, freeze/thaw cycles, and aging of binder or HMA can affect the durability of HMA (Scherocman et al. 1986, Terrel and Al-Swailmi 1992, Choubane et al. 2000). Other considerations such as construction (segregation and raveling) and traffic are also important.

2.3 Adhesion Theories

Chemical reaction, surface energy, molecular orientation, and mechanical adhesion are four theories used to describe the adhesion characteristics between asphalt and aggregate (Terrel and Al-Swailmi 1992). The above four theories are affected by the following aggregate and asphalt properties: surface tension of asphalt cement and aggregate, chemical composition of asphalt and aggregate, asphalt viscosity, surface texture of aggregates, aggregate porosity, aggregate clay/silt content, aggregate moisture content, and temperature at the time of mixing with asphalt cement and aggregate (Terrel and Al-Swailmi 1992).

2.3.1 Chemical Reaction

The reaction of acidic and basic components of asphalt and aggregate form water insoluble compounds that resist stripping (Terrel and Al-Swailmi 1992). A chemical bond forms that allows an asphalt-aggregate mix to resist stripping. Using aggregates that are basic instead of acidic can lead to better adhesion of asphalt to aggregates (Terrel and Al-Swailmi 1992).

2.3.2 Surface Energy and Molecular Orientation

Surface energy can be described by how well asphalt or water coats aggregate particles (Terrel and Al-Swailmi 1992). Water is a better wetting agent because of it's lower viscosity and lower surface tension than asphalt (Little and Jones 2003). Using surface energy theory to calculate adhesive bond energies between asphalt and aggregate and cohesive strength of a mastic is rather complex and will be discussed further under the *Tests on Loose Mixtures* in Section 2.5.1.

The structuring of asphalt molecules at an asphalt-aggregate interface is molecular orientation. The adhesion between asphalt and aggregate is facilitated by a surface energy reduction at the aggregate surface where asphalt is adsorbed onto a surface (Terrel and Al-Swailmi 1992, Little and Jones 2003).

2.3.3 Mechanical Adhesion

Mechanical adhesion is a function of various aggregate physical properties such as surface texture, porosity, absorption, surface coatings, surface area, and particle size (Terrel and Al-Swailmi 1992, Little and Jones 2003). In short, an aggregate with desirable properties that will not show a propensity to moisture damage within an HMA is wanted.

2.4 Cohesion Theories

According to Little and Jones (2003), cohesion is developed in a mastic and it is influenced by the rheology of the filled binder. The cohesive strength of a mastic is a function of the interaction between the asphalt cement and mineral filler, not just of the individual components alone. The cohesive strength of a mastic is weakened due to the presence of water through increased saturation and void swelling or expansion (Terrel and Al-Swailmi 1992, Little and Jones 2003). Cheng et al. (2002) showed that the cohesive strength can be damaged in various mixtures by the diffusion of water into asphalt mastics.

2.5 Tests for Determining Moisture Susceptibility

Moisture damage has been a concern to highway agencies and asphalt researchers for many years as it can lead to a shortened pavement life. Therefore, there is a need to develop a test method that predicts and/or identifies the moisture susceptibility of HMA. Table 2.1 lists tests on loose mixtures while Table 2.2 lists tests on compacted mixtures. All of these tests predict laboratory moisture susceptibility, but lack the reliability of predicting moisture damage in the field. The preceding sections will give a brief description of each test method and how well it predicts field moisture damage.

2.5.1 Tests on Loose Mixture and Asphalt Binders

The tests on loose mixtures are conducted on only asphalt coated particles in the presence of water. Examples of these tests are listed in Table 2.1. The two biggest advantages of these tests are conducting simplicity and inexpensive nature in comparison compacted specimen test expenses. Another significant advantage is the use of simple equipment and procedures to conduct experiments (Solaimanian et al. 2003).

Table 2.1 Moisture Sensitivity Tests on Loose Samples (Solaimanian et al. 2003)

Test Method	ASTM	AASHTO	Other
Methylene Blue			Technical Bulletin 145, International Slurry Seal Association
Film Stripping			California Test 302
Static Immersion	D1664*	T182	
Dynamic Immersion			No standard exists
Chemical Immersion			Standard Method TMH1 (Road Research Laboratory 1986, England)
Quick Bottle			Virginia Highway and Transportation Research Council (Maupin 1980)
Boiling	D3625		Tex 530-C Kennedy et al. 1984
Rolling Bottle			Isacsson and Jorgensen, Sweden, 1987
Net Adsorption			SHRP-A-341 (Curtis et al. 1993)
Surface Energy			Thelen 1958, HRB Bulletin 192 Cheng et al., AAPT 2002
Pneumatic Pull-Off			Youtcheff and Aurilio (1997)

*No longer available as ASTM standard.

2.5.1.1 Methylene Blue Test

The methylene blue test is used to identify "dirty" aggregates which contain harmful clays and dust (Solaimanian et al. 2003). If dust or harmful clays are on aggregate particles, an asphalt binder will not be able to fully coat aggregate particles, and thus a potential for stripping may occur in the HMA. This test is used to identify aggregates that contain clays or dust. Since no asphalt is used, this test cannot measure a potential for HMA stripping.

2.5.1.2 Static Immersion Test (AASHTO T182)

A sample of HMA mix is cured for 2 hours at 60ºC before being placed in a jar and covered with water. The jar is left undisturbed for 16 to 18 hours in a water bath at 25ºC. Again the amount of stripping is visually estimated by looking at the HMA sample in the jar. The results of this test are given as either less than or greater than 95% of an aggregate surface is stripped (Solaimanian et al. 2003).

2.5.1.3 Film Stripping Test (California Test 302)

The film stripping test is a modified version of the static immersion test (AASHTO T182). Basically, a loose mixture of asphalt coated aggregates are placed in a jar filled with water. The mix is aged in an oven at 60ºC for 15 to 18 hours before being placed in a jar to cool. The jar with loose mix is rotated at 35 revolutions per minute (rpm) for 15 minutes to stir up the mix. Baffels in a jar stir up the mix to accelerate the stripping process. After 15 minutes the sample is removed, the loose mixture is viewed under a fluorescent light, and the %age of stripping is estimated. The results of this test are given in %age of total aggregate surface stripped (Solaimanian et al. 2003).

2.5.1.4 Dynamic Immersion Test

The dynamic immersion test (DIM) is similar to the static immersion test, but the DIM test is used to accelerate the stripping effect. Loose mixture is agitated in a jar filled with water in order to produce a dynamic effect (Solaimanian et al. 2003). Again, the results show that as the period of agitation increases, the amount of stripping increases, however the tests fail to simulate pore pressure and traffic which is the case with all loose mixture tests.

2.5.1.5 Chemical Immersion Test

A loose sample of asphalt coated aggregate is placed in boiling water while increasing the amount of sodium carbonate. The concentration of sodium carbonate is slowly increased until stripping occurs and the concentration of sodium carbonate is recorded. The recorded number is referred to as the Riedel and Weber (R&W) number. Zero refers to distilled water, 1 refers to 0.41 g of sodium carbonate and 9 refers to the highest concentration of sodium carbonate or 106 g. The sample is removed from the water and sodium carbonate solution and examined for stripping (Solaimanian et al. 2003).

2.5.1.6 Surface Reaction Test

A major problem with the tests reviewed in the previous section is the dependence on visual observation for identifying stripping. The surface reaction test allows a researcher to quantify the level of stripping on loose asphalt mixtures. This procedure was developed by Ford et al. (1974). The surface reaction test evaluates the reactivity of calcareous or siliceous aggregates and reaction response to the presence of highly toxic and corrosive acids. As part of the chemical reaction, gas is emitted, which generates a pressure and this pressure is proportional to the aggregate surface area (Solaimanian et al. 2003). This test is based on the premise that different levels (severity) of stripping result in exposed surface areas of aggregates.

2.5.1.7 Boiling Water Test

Several versions of a boiling water test have been developed by various state agencies including one from the Texas State Department of Highways and Public Transportation (Kennedy et al. 1983 and 1984). A visual inspection of stripping is made after the sample has been subjected to the action of water at an elevated temperature for a specified time (Kennedy et al. 1983 and 1984, Solaimanian et al. 2003). This test identifies mixes that are susceptible to moisture damage, but it does not account for mechanical properties nor include the effects of traffic (Kennedy et al. 1983 and 1984; Solaimanian et al. 2003).

2.5.1.8 Rolling Bottle Test

Isacsson and Jorgenson developed the Rolling Bottle Test in Sweden in 1987. The test is similar to the DIM in that aggregate chips are coated in asphalt and placed in a glass jar filled with water. The glass jar is rotated to agitate loose HMA. A visual inspection is completed to note how much asphalt has been stripped from aggregates (Solaimanian et al. 2003).

2.5.1.9 Net Adsorption Test

The Strategic Highway Research Program (SHRP) developed a test called the net adsorption test (NAT) in the early 1990's and is documented under SHRP-A-341 (Curtis et al. 1993). This test examines the asphalt-aggregate system and its affinity and compatibility (Solaimanian et al. 2003). In addition, this test also evaluates the sensitivity of the asphalt-aggregate pair. In terms of other tests, the NAT yields mixed results when compared to the indirect tensile test with moisture conditioned specimens (Solaimanian et al. 2003). The NAT was modified by researchers at the University of Nevada - Reno and the results were correlated with the environmental conditioning chamber (ECS) (Scholz et al. 1994). The water sensitivity of a binder as estimated by NAT showed little or no correlation to wheel-tracking tests on the mixes according to SHRP-A-402 (Scholz et al. 1994).

2.5.1.10 Wilhelmy Plate Test and Universal Sorption Device

Researchers at Texas A&M University lead in investigating cohesive and adhesive failure models based on surface energy theory and a moisture diffusion model based on results from the Universal Sorption Device (USD) (Cheng et al. 2003). The principle behind surface energy theory is that the surface energy of an asphalt and aggregate is a function of the adhesive bond between asphalt and aggregate and the cohesive bonding within an asphalt (Solaimanian et al. 2003). The Wilhelmy plate is used to determine the surface free energy of an asphalt binder where the dynamic contact angle is measured between asphalt and a liquid solvent (Cheng et al. 2003, Solaimanian et al. 2003). The USD test is used to determine the surface free energy of an aggregate (Cheng et al. 2003, Solaimanian et al. 2003). The surface free energy is then used to compute the adhesive bond between an asphalt binder and aggregate. Cheng et al. (2002) showed that the adhesive bond per unit area of aggregate is highly dependent on the aggregate

and asphalt surface energies. Also, this test shows that stripping occurs because the affinity of an aggregate for water is much greater than that for asphalt thus weakening the bond at the asphalt-aggregate interface (Cheng et al. 2002).

Current research at Texas A & M University (Bhasin et al. 2006, Masad et al. 2006) has shown that the moisture resistance of asphalt-aggregate combinations depends on surface energies of asphalt binders and aggregates. The factors considered are film thickness, aggregate shape characteristics, surface energy, air void distribution and permeability. The ratio of adhesive bond energy under dry conditions to adhesive bond energy under wet conditions can be used to identify moisture susceptible asphalt-aggregate combinations and a ratio of 0.80 should be used as a criterion to separate good and poor combinations of materials. Dynamic mechanical analysis tests were conducted to evaluate a mixtures ability to accumulate damage under dry and moisture conditions. A mechanistic approach using a form of the Paris law was used for the evaluation of moisture damage. The mechanical properties are influenced by aggregate gradation, aggregate shape characteristics, and film thickness. This approach captures the influence of moisture on crack growth and is able to distinguish good and poor performing HMA mixtures.

2.5.1.11 Pneumatic Pull-Off Test

Another method for evaluating the moisture susceptibility of asphalt binders is the pneumatic pull-off test. The properties being measured by this test are the tensile and bonding strength of a bitumen applied to a glass plate as a function of time while being exposed to water (Solaimanian et al. 2003). Test results by Youtcheff et al. (1998) showed that soak time appears to be an important factor. Additional results using the pneumatic pull-off test indicate that

asphaltenes provide the viscosity structure and is disrupted by the presence of water while the maltenes provide the resistance to moisture damage (Youtcheff et al. 1997).

2.5.1.12 Dynamic Shear Rheometer

Modified DSR parts were incorporated into a DSR by Rottermond (2004) to establish a moisture susceptibility test for asphalt binders. Rottermond extended the work conducted by Scholz and Brown (1996). Kanitpong and Bahia (2003) evaluated the effects of antistrip agents using ceramic interfaces and a DSR. The modified DSR parts were a base plate and spindle. A ceramic disc was inset in a base plate and spindle. A test specification was not developed, but several gap sizes were evaluated.

2.5.2 Tests on Compacted Mixtures

Tests conducted on compacted mixtures include laboratory compacted specimens, field cores, and/or slabs compacted in a laboratory or taken from the field. Table 2.2 provides moisture sensitivity tests which have been performed on compacted specimens. From these tests, physical, fundamental/mechanical properties can be measured while accounting for traffic/water action and pore pressure effects (Solaimanian et al. 2003). Some disadvantages of conducting tests on compacted mixtures are the expensive laboratory testing equipment, longer testing times, and potentially labor intensive test procedures.

Table 2.2 Moisture Sensitivity Tests on Compacted Samples (Solaimanian et al. 2003)

Test Method	ASTM	AASHTO	Other
Moisture Vapor Susceptbility			California Test 307 Developed in late 1940's
Immersion-Compression	D1075	T165	ASTM STP 252 (Goode 1959)
Marshal Immersion			Stuart 1986
Freeze/thaw Pedestal Test			Kennedy et al. 1982
Original Lottman Indirect Tension			NCHRP Report 246 (Lottman 1982); Transportation Research Record 515 (1974)
Modified Lottman Indirect Tension		T283	NCHRP Report 274 (Tunnicliff and Root 1984), Tex 531-C
Tunnicliff-Root	D4867		NCHRP Report 274 (Tunnicliff and Root 1984)
ECS with Resilient Modulus			SHRP-A-403 (Al-Swailmi and Terrel 1994)
Hamburg Wheel Tracking			1993 Tex-242-F
Asphalt Pavement Analyzer			Pavement Technology Inc., Operating Manual
ECS/SPT			NCHRP 9-34 (2002-03)
Multiple Freeze/thaw			No standard exists

2.5.2.1 Immersion-Compression Test

The immersion-compression test (ASTM D1075 and AASHTO T165-155) is among the first moisture sensitivity tests developed based on testing 100mm diameter compacted specimens. A more detailed explanation of this test can be reviewed in ASTM Special Technical Publication 252 (Goode 1959). This test consists of compacting two groups of specimens: a control group and a moisture conditioned group at an elevated temperature (48.8°C water bath) for four days (Roberts et al. 1996). The compressive strength of the conditioned and control group are then measured (Roberts, et al. 1996). The average strength of the conditioned specimens over that of the control specimens is a measure of strength lost due to moisture

damage (Solaimanian et al. 2003). Most agencies specify a minimum retained compressive strength of 70%.

2.5.2.2 Marshall Immersion Test

The procedure for producing and conditioning two groups of specimens is identical to the immersion-compression test. The only difference is, the Marshall stability test is used as the strength parameter as opposed to the compression test (Solaimanian et al. 2003). A minimum retained Mashall stability number could not be found in the literature.

2.5.2.3 Moisture Vapor Susceptibility

The moisture vapor susceptibility test was developed by the California Department of Transportation (California Test Method 307). A California kneading compactor is used to compact two specimens. The compacted surface of each specimen is sealed with an aluminum cap and a silicone sealant is applied to prevent the loss of moisture (Solaimanian, et al. 2003). After the specimens have been conditioned at an elevated temperature and suspended over water, testing of the specimens commences. The Hveem stabilometer is used to test both dry and moisture conditioned specimens. A minimum Hveem stabilometer value is required for moisture conditioned specimens, which is less than that required for dry specimens used in the mix design (Solaimanian et al. 2003).

2.5.2.4 Repeated Pore Water Pressure Stressing and Double-Punch Method

The repeated pore water pressure stressing and double punch method was developed by Jimenez at the University of Arizona (1974). This test accounts for the effects of dynamic traffic loading and mechanical properties. In order to capture the effects of pore water pressure, the specimens are conditioned by a cyclic stress under water. After the specimen has undergone the pore pressure stressing the tensile strength is measured using the double punch equipment.

Compacted specimens are tested through steel rods placed at either end of the specimen in a punching configuration.

2.5.2.5 Original Lottman Method

The original Lottman test was developed at the University of Idaho by Robert Lottman (1978). The laboratory procedure consists of compacting three sets of 100mm diameter by 63.5mm Marshall specimens to be tested dry or under accelerated moisture conditioning (Lottman et al. 1974). Below are the following laboratory conditions for each of the groups:

- Group 1: Control group, dry;
- Group 2: Vacuum saturated with water for 30-minutes; and
- Group 3: Vacuum saturation followed by freeze cycle at -18°C for 15- hours and then subjected to a thaw at 60°C for 24-hours (Lottman et al. 1974).

After the conditioning phase the indirect tensile equipment is used to conduct tensile resilient modulus and tensile strength of conditioned and dry specimens. All specimens are tested at 13°C or 23°C at a loading rate of 1.65mm/min. The severity of moisture damage is based on a ratio of conditioned to dry specimens (TSR) (Lottman et al. 1974, Lottman 1982). A minimum TSR value of 0.70 is recommended (NCHRP 246). Laboratory compacted specimens were compared to field cores and plotted against each other on a graph. The laboratory and field core specimens line up fairly close to the line of equality.

2.5.2.6 Modified Lottman Test (AASHTO T283)

"Resistance of Compacted Bituminous Mixture to Moisture Induced Damage" AASHTO T283, is the most commonly used test method for determining moisture susceptibility of HMA. This test is similar to the original Lottman test with only a few exceptions which are:

- Two groups, control versus moisture conditioned,

- Vacuum saturation until a saturation level of 70% to 80% is achieved, and
- Test temperature and loading rate change to 50mm/min at 25ºC.

A minimum TSR value of 0.70 is recommended (Roberts et al., 1996). AASHTO T283 was adopted by the Superpave system as the moisture test method of choice even though AASHTO T283 was developed for Marshall mixture design. State highway agencies have reported mixed results when using AASHTO T283 and comparing the results to field performance (Stroup-Gardiner et al. 1992, Solaimanian et al. 2003). NCHRP Project 9-13 looked at different factors affecting test results such as types of compaction, diameter of specimen, degree of saturation, and freeze/thaw cycles. Conclusions from looking at the previously mentioned factors can be seen in the NCHRP 9-13 report (Epps et al. 2000). The researchers concluded that either AASHTO T283 does not evaluate moisture susceptibility or the criterion, TSR, is incorrectly specified. NCHRP 9-13 examined mixtures that have historically been moisture susceptible and ones that have not. The researchers also examined the current criteria using Marshall and Hveem compaction. A recent study at the University of Wisconsin found no relationship exists between TSR and field performance in terms of pavement distress index and moisture damage (surface raveling and rutting) (Kanitpong et al. 2006). Additional factors such as production and construction, asphalt binder and gradation play important roles. Mineralogy does not appear to be an important factor in relation to pavement performance.

2.5.2.7 ASTM D4867 (Tunnicliff-Root Test Procedure)

"Standard Test Method for Effect of Moisture on Asphalt Concrete Paving Mixtures," ASTM D4867 is comparable to AASHTO T283. The only difference between AASHTO T283 and ASTM D4867 is that the curing of loose mixture at 60°C in an oven for 16 hours is

eliminated in ASTM D4867. A minimum TSR of 0.70 to 0.80 are specified by highway agencies (Roberts et al. 1996).

2.5.2.8 Texas Freeze/Thaw Pedestal Test

The water susceptibility test was developed by Plancher et al. (1980) at Western Research Institute but was later modified into the Texas freeze/thaw pedestal by Kennedy et al. (1983). Even though this test is rather empirical in nature, it is fundamentally designed to maximize the effects of bond and to minimize the effects of mechanical properties such as gradation, density, and aggregate interlock by using a uniform gradation (Kennedy et al. 1983). An HMA briquette is made according to the procedure outlined by Kennedy et al. (1982). The specimen is then placed on a pedestal in a jar of distilled water and covered. The specimen is subjected to thermal cycling and inspected each day for cracks. The number of cycles to induce cracking is a measure of the water susceptibility (Kennedy et al. 1983). The benefits of running this test are some key failures can be seen:

- Bond failure at the asphalt-aggregate interface (stripping) and
- Fracture of the thin asphalt films bonding aggregate particles (cohesive failure) by formation of ice crystals (Solaimanian et al. 2003).

2.5.2.9 Hamburg Wheel-Tracking Device (HWTD)

The Hamburg wheel tracking device was developed by Esso A.G. and is manufactured by Helmut-Wind, Inc. of Hamburg, Germany (Aschenbrener et al. 1995, Romero and Stuart 1998). Two samples of hot mix asphalt beams with each beam having a geometry of 26mm wide, 320mm long, and 40mm thick. This device measures the effects of rutting and moisture damage by running a steel wheel over the compacted beams immersed in hot water (typically 50ºC) (Aschenbrener et al. 1995). The steel wheel is 47mm wide and applies a load of 705N while

traveling at a maximum velocity of 340mm/sec in the center of the sample. A sample of HMA is loaded for 20,000 passes or 20mm of permanent deformation occurs (Aschenbrener et al. 1995). Some important results the HWTD gives are:

- Postcompaction consolidation: Deformation measured after 1,000 wheel passes;
- Creep Slope: Number of wheel passes to create a 1 mm rut depth due to viscous flow;
- Stripping Slope: Inverse of the rate of deformation in the linear region of the deformation curve; and
- Stripping Inflection Point: Number of wheel passes at the intersection of the creep slope and stripping slope (Aschenbrener et al. 1995).

2.5.2.10 Asphalt Pavement Analyzer

The APA is a type of loaded wheel test. Rutting, moisture susceptibility, and fatigue cracking can all be examined with an APA. The predecessor to the APA is the Georgia Loaded Wheel Tester (GLWT). Similar to the GLWT, an APA can test either cylindrical or rectangular specimens. Using either specimen geometry, the conditioned and unconditioned samples are subjected to a steel wheel that transverses a pneumatic tube, which lies on top of an asphalt sample. As the wheel passes back and forth over the tube, a rut is created in a sample. Numerous passes lead to a more defined rut and eventually, stress fractures can begin to manifest as cracks. Modeling these ruts and cracks helps to predict how different combinations of aggregate and binder for given criteria such as temperature and loading, will react under varying circumstances. The conditioning of a sample is based upon the characteristic an APA is testing. One of the main differences between an APA and a GLWT is an APA's ability to test samples

under water as well as in air. Testing submerged samples allows researchers to examine moisture susceptibility of mixes (Cooley et al. 2000).

An APA results are comparable to field data. A study that compared WesTrack, a full-scale test track, data with APA results found a strong relationship between field data and laboratory data (Williams and Prowell 1999). An additional study at the University of Tennessee revealed that an APA sufficiently predicted the potential for rutting of 30 HMAs commonly used in Tennessee (Jackson and Baldwin 1999).

To test moisture susceptible HMA samples, specimens are created in the same manner as the specimens for testing rutting potential without moisture. The samples are placed in an APA, which has an inner box that can be filled with water. The samples are completely submerged at all times during testing; therefore effects of evaporation do not need to be taken into account. The water bath is heated to a desired test temperature and the air in the chamber is also heated to the same desired test temperature.

2.5.2.11 Environmental Conditioning System (ECS)

The ECS was developed by Oregon State University as part of the SHRP-A-403 and later modified at Texas Technological University (Alam et al. 1998). The ECS subjects a membrane encapsulated HMA specimen that is 102mm in diameter by 102mm in height to cycles of temperature, repeated loading, and moisture conditioning (SHRP-A-403 1992, Al-Swailmi et al. 1992, Al-Swailmi et al. 1992, Terrel et al. 1993). Some important fundamental material properties are obtained from using an ECS. These properties are resilient modulus (M_R) before and after conditioning, air permeability, and a visual estimation of stripping after a specimen has been split open (SHRP-A-403, 1992). One of the significant advantages of using an ECS is the ability to influence the HMA specimens to traffic loading and the resulting effect of pore water

pressure (Solaimanian et al. 2003) which is close to field conditions. The downfall of the test is, it does not provide a better relationship to field observation than what was observed using AASHTO T283. Also, AASHTO T283 is much less expensive to run and less complex than the ECS.

2.5.2.12 Flexural Fatigue Beam Test with Moisture Conditioning

Moisture damage has been known to accelerate fatigue damage in pavements. Therefore, conditioning of flexural fatigue beams was completed by Shatnawi et al. (1995). Laboratory compacted beams were prepared from HMA sampled at jobs and corresponding field fatigue beams were cut from the pavement. The conditioning of the beams is as follows:

- Partial vacuum saturation of 60% to 80%;
- Followed by 3 repeated 5-hour cycles at 60ºC followed by 4-hours at 25ºC while remaining submerged; and
- One 5-hour cycle at -18ºC (Shatnawi et al. 1995).

The specimens are then removed from a conditioning chamber and tested according to AASHTO TP8. Initial stiffness and fatigue performance were affected significantly by conditioning the specimens (Shatnawi et al. 1995).

2.5.2.13 ECS/Simple Performance Test Procedures

As a result of NCHRP Projects 9-19, 9-29, and 1-37; new test procedures such as simple performance tests (SPTs) are being evaluated. According to Witczak et al. (2002), an SPT is defined as "A test method(s) that accurately and reliably measures a mixture response or characteristic or parameter that is highly correlated to the occurrence of pavement distress (e.g. cracking and rutting) over a diverse range of traffic and climatic conditions." The mechanical tests being looked at are the dynamic modulus |E*|, repeated axial load (F_N), and static axial

creep tests (F_T). These tests are conducted at elevated temperatures to determine a mixtures resistance to permanent deformation. The dynamic modulus test is conducted at an intermediate and lower test temperature to determine a mixtures susceptibility to fatigue cracking. Witczak et al. (2002) have shown that dynamic modulus, flow time, and flow number yield promising correlations to field performance. The advantages and disadvantages can be seen in Table 2.3 from the work of Brown et al. (2001) and Witczak et al. (2002).

Table 2.3 SPT Advantages and Disadvantages (Witczak et al. 2002 and Brown et al. 2001)

Test	Parameter	Test Condition	Model	R^2	Se/Sy	Advantages	Disadvantages
Dynamic Modulus	$E^*/\sin\phi$	Sinusoidal Linear 130°F 5 Hz	Power	0.91	0.310	Direct input for 2002 Pavement Design Guide Not forced to use master curves Easily linked to established regression equations Non destructive tests	Coring and sawing Arrangement of LVDTs Confined testing gave poor results Need further study of reliability of confined open graded specimens Equipment is more complex Difficult to obtain 1.5:1height-to-diameter ratio specimens in lab
Repeated Loading (Flow Number)	F_N	Unconfined 130°F Various Frequencies	Power	0.88	0.401	Better simulates traffic conditions	Equipment is more complex Restricted test temperature and load levels does not simulate field conditions Difficult to obtain 1.5:1height-to-diameter ratio specimens in lab

NCHRP 9-34 is currently looking at the aforementioned tests along with the ECS to develop new test procedures to evaluate moisture damage (Solaimanian et al. 2003). Solaimanian et al. (2006) reported that the results of the Phase I and Phase II testing of NCHRP 9-34 show that the dynamic complex modulus (DCM) test should be coupled with the ECS for moisture sensitivity testing. Some preliminary findings out of NCHRP 9-34 show that the ECS/DM test appear to separate good performing mixes from poor performing mixes in the field compared with TSR testing from ASTM D4867. The dynamic complex modulus is determined by applying a uniaxial sinusoidal vertical compressive load to an unconfined or confined HMA cylindrical sample as shown in Figure 2.1.

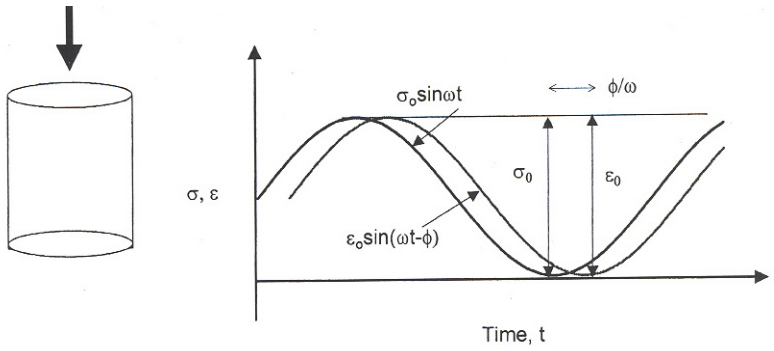

Figure 2.1 Haversine Loading Pattern or Stress Pulse for the Dynamic Modulus Test (Witczak et al. 2002)

The stress-to-strain relationship under a continuous sinusoidal load pattern for a liner viscoelastic material is defined by the complex modulus (dynamic modulus), E*. Mathematically, E* is equal to the maximum peak dynamic stress (σ_o) divided by the peak recoverable strain (ε_o):

$$\left|E^*\right| = \frac{\sigma_o}{\varepsilon_o} \qquad \text{(equation 2.1)}$$

The real and imaginary parts of the dynamic modulus can be written as

$$E^* = E' + iE'' \qquad \text{(equation 2.2)}$$

The previous equation shows that E* has two components; a real and an imaginary component. E' is referred to as the storage or elastic modulus component, while E" is referred to as the loss or viscous modulus. The angle by which the peak recoverable strain lags behind the peak dynamic stress is referred to as the phase angle, ϕ. The phase angle is an indicator of the viscous properties of the material being evaluated.

Mathematically, this is expressed as

$$E^* = |E^*|\cos\phi + i\,|E^*|\sin\phi \qquad \text{(equation 2.3)}$$

$$\phi = \frac{t_i}{t_p} \times 360 \qquad \text{(equation 2.4)}$$

where

t_i = time lag between a cycle of stress and strain(s),

t_p = time for a stress cycle(s), and

i = imaginary number.

For a purely viscous material, the phase angle is 90°, while for a purely elastic material the phase angle is 0° (NCHRP 465 2002). The dynamic modulus, a measurable, "fundamental" property of an HMA mixture is the relative stiffness of a mix. Mixes that have a high stiffness at elevated temperatures are less likely to deform. But, stiffer mixes at an intermediate test temperature are more likely to crack for thicker pavements (Shenoy and Romero 2002). Therefore, the dynamic modulus test is conducted at intermediate and elevated temperatures to evaluate the fatigue properties and the rutting propensity of HMA.

The dynamic creep test (i.e. repeated load test, flow number test) is based on the repeated loading and unloading of an HMA specimen where the permanent deformation of a specimen is recorded as a function of the number of load cycles. The loading is for 0.1sec. followed by a 0.9sec. unloading of a specimen. There are three types of phases that occur during a repeated load test: primary, secondary, and tertiary flow. In the primary flow region, there is a decrease in strain rate with time followed by a constant strain rate in the secondary flow region, and finally an increase in strain rate in the tertiary flow region. Tertiary flow signifies that a specimen is beginning to deform significantly and individual aggregates that make up the matrix start to "flow". The flow number is based upon the onset of tertiary flow (or the minimum strain rate recorded during the course of the test). The following description is shown graphically in Figure 2.2.

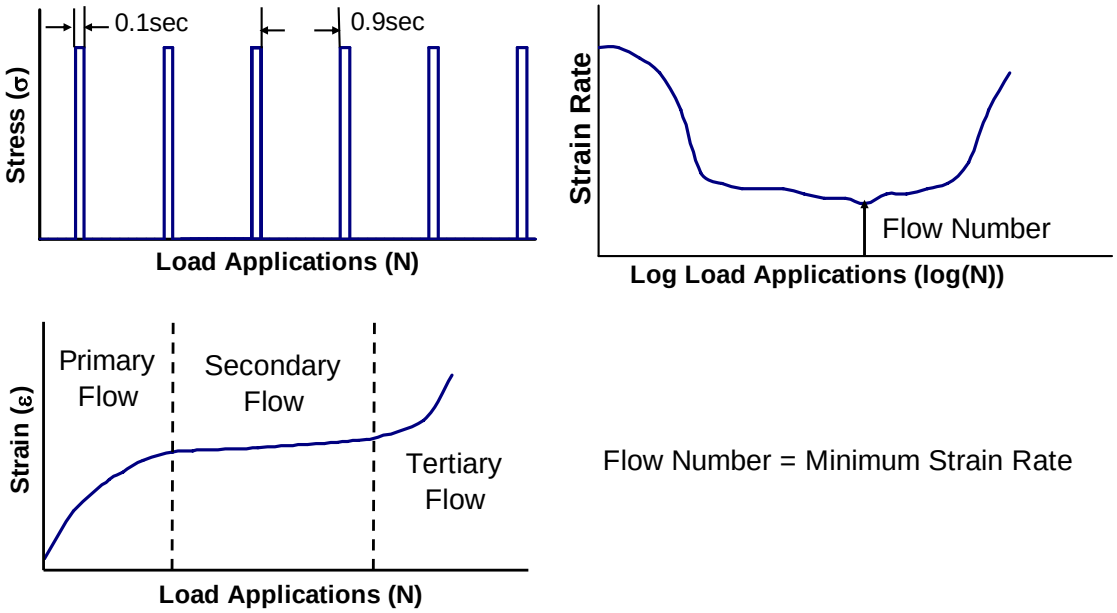

Figure 2.2 Flow Number Loading (Robinette 2005)

Flow number testing is similar to pavement loading because pavement loading is not continuous; there is a dwell period between loadings. This allows a pavement a certain amount of time to recover some strain induced by the loading. Additional reports on dynamic modulus and repeated loading can be seen elsewhere (Robinette 2005, NCHRP Report 465, and NCHRP Report 547).

CHAPTER 3 EXPERIMENTAL PLAN

3.1 Experimental Plan

This research has been divided into two phases. Phase I testing was used to determine the number of freeze/thaw cycles that will cause the equivalent damage to AASHTO T283 specimens. Phase II testing of mixes for moisture damage used the results of Phase I for the AASHTO T283 testing on 150mm specimens and the results of Phase I and Phase II for dynamic modulus testing. In the following sections below, the mixture experimental plan and laboratory testing experimental plan is outlined.

3.1.1 Phase I Testing – Sensitivity Study

The experimental plan considers different mix types, aggregate sources, laboratory test systems, and conditioning approaches. The experimental plan includes two integrated plans: one for mixes and one for laboratory tests. A sensitivity study on the effects of specimen size and compaction method was conducted on a limited number of mixes to determine the amount of conditioning that should occur for larger Superpave compacted specimens. Table 3.1 below outlines the sensitivity study experimental plan.

Table 3.1 Sensitivity Study Experimental Plan for Mix and Aggregate Types

PHASE 1 MOISTURE		
NMAS (mm)	Traffic Level (ESAL)	
	≤ 3,000,000	>3,000,000
25.0 or 19.0	Limestone - M50 Dundee	Limestone - M59 Brighton
	Gravel - M21 St. Johns	
12.5 or 9.5	Limestone - BL96 Howell	Limestone - I-196 Grand Rapids
	Gravel - M21 Owosso	Slag/Gabbro - I-75 Clarkston

Table 3.2 outlines the laboratory test plan for the sensitivity study. As previously mentioned, this plan partially duplicates the work conducted and reported in NCHRP Report 444. Twenty specimens per project per compaction method/diameter size were procured. This resulted in a

total of 420 specimens tested for the sensitivity study. Superpave designed mixes were used in the study, but the method of compaction (Marshall or Superpave) to achieve 7.0% air voids will vary. It was also be necessary to determine the conditioning time necessary to produce the same tensile strength ratios in larger specimens undergoing Superpave compaction compared with 100mm Marshall compacted specimens. The standard conditioning of specimens was the same as outlined by AASHTO T283 for 150mm specimens. The 150mm specimens for Phase I testing will be used for the results for the AASHTO T283 testing for Phase II.

Table 3.2 Sensitivity Study Experimental Plan for Effect of Compaction Method and Conditioning Period on Performance

Conditioning Period	Unconditioned			Conditioned		
	100mm Marshall	100mm Superpave	150mm Superpave	100mm Marshall	100mm Superpave	150mm Superpave
AASHTO T283, Standard Conditioning Time	XXXXX[1]	XXXXX	XXXXX	XXXXX	XXXXX	XXXXX
AASHTO T283, 2 Times Standard Conditioning Time	N/A[2]	N/A	N/A	XXXXX	XXXXX	XXXXX
AASHTO T283, 3 Times Standard Conditioning Time	N/A	N/A	N/A	XXXXX	XXXXX	XXXXX

[1]One X represents a specimen tested per job.
[2]Not applicable.

3.1.2 Phase I – Preliminary Binder Study

Two experimental plans for asphalt binder and mastic were executed. The first set of experiments determined which testing conditions should be employed in the final testing procedure. Verification of the hypothesis that an "aggregate type" material would yield significantly different results than a steel interface occurred during the initial test set.

Two binders were selected with known characteristics, AAA-1 and AAM-1. These binders were selected because one is moisture prone and the other is not. Two types of discs were employed to determine if the hypothesis of the material interface would yield a significant difference. The control disc was stainless steel. The selection of the aggregate-type of material

was a bit more complex than the selection for a control disc. The material desired was an aggregate-type, but a neutral material to reduce inconsistencies from source was coveted. Manufactured ceramic discs were selected as a neutral aggregate-type disc for the testing. The properties of the ceramic material, Cordierite, are detailed in Table 3.3. The chemical composition of Cordierite is $Mg_2Al_4Si_5O_{18}$, and it is referred to as Magnesium Aluminum Silicate.

Table 3.3 Properties of Ceramic Discs (Rottermond, 2004)

Property		Units
Name	Cordierite	
Color	Tan	
Hardness	6	Mohs
Water Absorption	10	%
Specific Gravity	2.0	
Tensile Strength	3,700	PSI
Compressive Strength	40,000	PSI
Flexural Strength	9,500	PSI
Max. Operating Temp. Non-Loading Conditions	1,300	Celsius

3.1.2.1 Gap Size and Interface Selection

Since it was hypothesized that ceramic discs would be a better interface for moisture susceptibility testing of asphalt binders, the hypothesis needed to be tested. Both ceramic and stainless steel interfaces were tested using the AAA-1 and AAM-1 asphalt binders at different gap sizes. The gap sizes evaluated were 200µm, 300µm, 500µm, and 1000µm for both binders and interface types. Table 3.4 displays the experimental plan followed for determining the appropriate gap size and interface material. Each replication of original binder tested is represented by an "X".

Table 3.4 Gap Size and Interface Selection Experimental Plan

Binder	Condition	Testing Environment	Gap Size (μm)	Stainless Steel	Ceramic
AAA-1	*Unaged Unconditioned*	*Water Bath*	*200*	XXX	XXX
	Aged Unconditioned			XXX	XXX
	Unaged Unconditioned		*300*	XXX	XXX
	Aged Unconditioned			XXX	XXX
	Unaged Unconditioned		*500*	XXX	XXX
	Aged Unconditioned			XXX	XXX
	Unaged Unconditioned		*1000*	XXX	XXX
	Aged Unconditioned			XXX	XXX
	Unaged Unconditioned	*Air Chamber*	*200*	XXX	XXX
	Aged Unconditioned			XXX	XXX
	Unaged Unconditioned		*300*	XXX	XXX
	Aged Unconditioned			XXX	XXX
	Unaged Unconditioned		*500*	XXX	XXX
	Aged Unconditioned			XXX	XXX
	Unaged Unconditioned		*1000*	XXX	XXX
	Aged Unconditioned			XXX	XXX
AAM-1	*Unaged Unconditioned*	*Water Bath*	*200*	XXX	XXX
	Aged Unconditioned			XXX	XXX
	Unaged Unconditioned		*300*	XXX	XXX
	Aged Unconditioned			XXX	XXX
	Unaged Unconditioned		*500*	XXX	XXX
	Aged Unconditioned			XXX	XXX
	Unaged Unconditioned		*1000*	XXX	XXX
	Aged Unconditioned			XXX	XXX
	Unaged Unconditioned	*Air Chamber*	*200*	XXX	XXX
	Aged Unconditioned			XXX	XXX
	Unaged Unconditioned		*300*	XXX	XXX
	Aged Unconditioned			XXX	XXX
	Unaged Unconditioned		*500*	XXX	XXX
	Aged Unconditioned			XXX	XXX
	Unaged Unconditioned		*1000*	XXX	XXX
	Aged Unconditioned			XXX	XXX

It was anticipated that the new test procedure would be used for both unmodified and modified binders. To ensure that the selected gap size for the new test procedure was adequate for modified binders, fillers were added to AAA-1 and AAM-1. Only two gap sizes were used to test the filler modified binders since the other two gap sizes had been eliminated. Further discussion of gap size selection is in Chapter 7. Table 3.5 displays the experimental plan conducted for the 500μm and 1000μm. This second experimental plan not only evaluated gap size, interface material, but also different levels of conditioning. Three conditioning types were

considered, unconditioned (control), moisture saturated, and moisture saturated with one freeze/thaw cycle.

Table 3.5 Experimental Plan for AAA-1 and AAM-1 Asphalt Binders

Test Condition							
Environment	Disk	Saturation	Freeze/Thaw	Mastic	Percent	AAA-1	AAM-1
Water	Ceramic	Unconditioned	No	Hydrated Lime	5	XXX	XXX
					10	XXX	XXX
					20	XXX	XXX
				Silica	5	XXX	XXX
					10	XXX	XXX
					20	XXX	XXX
				None	0	XXX	XXX
		Conditioned	No	Hydrated Lime	5	XXX	XXX
					10	XXX	XXX
					20	XXX	XXX
				Silica	5	XXX	XXX
					10	XXX	XXX
					20	XXX	XXX
				None	0	XXX	XXX
			Yes	Hydrated Lime	5	XXX	XXX
					10	XXX	XXX
					20	XXX	XXX
				Silica	5	XXX	XXX
					10	XXX	XXX
					20	XXX	XXX
				None	0	XXX	XXX
	Steel	Unconditioned	No	Hydrated Lime	5	XXX	XXX
					10	XXX	XXX
					20	XXX	XXX
				Silica	5	XXX	XXX
					10	XXX	XXX
					20	XXX	XXX
				None	0	XXX	XXX

3.1.3 Phase II Testing

Phase II testing was focused on evaluating the adequacy of various test procedures for evaluating the moisture susceptibility of HMA materials. The test temperature and moisture conditioning of specimens was determined in the sensitivity studies for mix and binders for the Phase II experimental plan. Table 3.6 summarizes the overall experimental plan for Phase II.

Table 3.6 Laboratory Experimental Plan for Phase II

		Unconditioned	Conditioned
Test System	AASHTO T283	XXXXX	XXXXX
	Dynamic Complex Modulus	XXX	XXX
	Asphalt Pavement Analyzer	XXX	XXX

	Dynamic Shear Rheometer – Asphalt Binder	XXX	XXX
	Dynamic Shear Rheometer – Mastic	XXX	XXX

3.2 Sampled Projects

The majority of projects were sampled during the 2004 construction season. Two projects were used from the 2000 construction season sampling and three projects were sampled in the 2005 construction season. The 2000 construction projects that were sampled were stored in a heated, metal building where the material was protected from rain, heat, and snow. By sampling materials from across the state, a better cross section of materials will be represented by the different contractors and available materials that are in the state. The majority of high volume mixes were found around the Detroit metro area whereas lower volume mixes were found around the state. Figure 3.1 illustrates the locations of the mixes sampled for this research project, a dot represents the approximate project location, whereas Appendix A: Project JMFs contains all the material properties related to each project.

Figure 3.1 Project Locations

3.3 Sampling

For this research project all HMA was sampled from mini-stockpiles. The locations for sampling were selected from the base to the top of a pile and around its perimeter, while keeping in mind the different strata of the stockpile, in that, the bottom of the piles comprises the greatest percentage of the material and hence the greatest percentage of the material was sampled from

this location. Figure 3.2 illustrates the composition of a cone stockpile in terms of its percentages with height. The type of sampling used for this project was mini-stock pile sampling due to the amount of material being sampled. Sampling from the mini-stock pile was done in accordance with ASTM D140. Typically, sampling occurs behind the paver or out of the truck but because one to two tons of material was sampled, the mini-stock pile was the easiest and simplest way to sample. In addition to the material being sampled, the job mix formula (JMF) was collected in order to verify the HMA volumetrics.

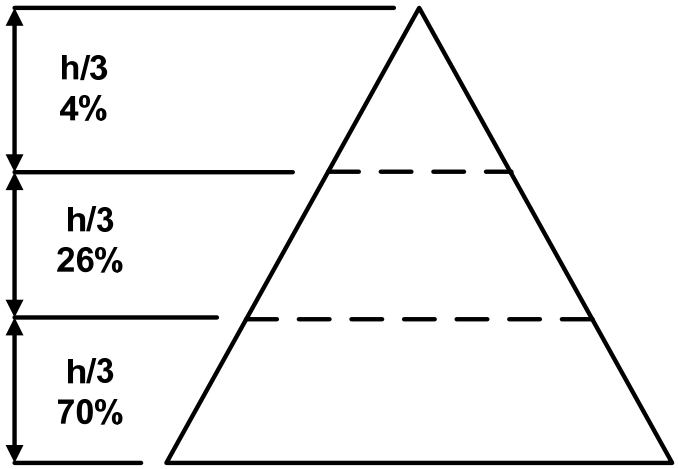

Figure 3.2 Stockpile Cone Proportions (Robinette 2005)

The sampled materials were brought back from the various plant sites and stored either in the Water Resources Building or in the basement of Dillman Hall at Michigan Technological University prior to sample preparation.

CHAPTER 4 PROCEDURES AND SAMPLE PREPARATION

4.1 Materials Collection

According to AASHTO T283 and NCHRP 465, three replicate specimens are required for testing the moisture sensitivity of HMA mixtures; three for the control group and three for the moisture conditioned group. Testing three specimens reduces the amount of testing variability inherent in each test procedure versus testing one or two specimens. For Phase I testing, twenty specimens per project (seven total projects) are required for AASHTO T283 testing. For Phase II testing, ten specimens per project (twenty-one total projects) are required. Therefore, thirty-four five gallon buckets of loose mix and two five gallon buckets of asphalt binder were sampled for Phase I projects and twenty five gallon buckets of loose mix and two five gallon buckets of asphalt binder were sampled for Phase II projects. Any additional material may then be used for supplemental testing. Specimen Preparation and Testing

Specimen preparation used to procure Superpave gyratory and Marshall specimens are outlined below. This also includes splitting samples, maximum theoretical specific gravity, specimen compaction, bulk specific gravity, and specimen cutting and coring.

4.1.1 Splitting

The loose mix that was sampled from the twenty-one jobs was heated up to 145 to 160°C for approximately two hours depending on the asphalt binder that was used. Each five gallon bucket of HMA contained roughly 30 to 40kg of mix. Splitting was conducted in accordance with ASTM C702. Sample sizes included two 2,000g samples for maximum theoretical specific gravity tests. For Phase I testing, 20 samples per project were batched for 100mm Superpave specimens, 20 samples per project were batched for 150mm Superpave specimens, and 20 samples per project were batched for 100mm Marshall specimens. Phase II testing required 10

specimens per project for AASHTO T283 testing, dynamic complex modulus, and APA testing each, for a total of 30 specimens for Phase II mix testing.

4.1.2 Maximum Theoretical Specific Gravity (G_{mm})

Maximum theoretical specific gravity testing (G_{mm}) was conducted in accordance with ASTM 2041 for two 2,000g samples. The G_{mm} was used to determine the volumetric properties of gyratory specimens and Marshall specimens, as well as the sawed and cored specimens. In addition, the G_{mm} was used to verify the G_{mm} on the JMF.

The maximum theoretical specific gravity (G_{mm}), also known as the Rice specific gravity, was measured according to AASHTO T209. The precision outlined in the specification states that the acceptable range of two test results for a single operator is ±0.011 standard deviations from the mean which is the difference of two properly conducted tests. For this research project field mix was used in which there is not as much control as with laboratory mixtures. In order to achieve a representative sample, quartering of the mixture occurred to mitigate differences between samples. In reviewing the standard deviations of the two G_{mm} samples for each project, it was found that all of the sampled mixtures fell within the single operator precision. Table 4.1shows the mean and standard deviations for each of the mixes. Of the twenty-one mixes presented in Table 4.1, six of the HMA mixtures do not contain recycled asphalt pavement (RAP). RAP is a variable aggregate product since one stockpile can constitute several sources of RAP and each source has a unique gradation, binder content, age, and depth of milling. The addition of RAP to a mix can contribute to the variability in the characteristics of field samples.

Table 4.1 G_{mm} Mean and Standard Deviation for Each Project

Project	Mix Type/Traffic	Mean ISU G_{mm}	Std. Dev.	Contractor JMF G_{mm}	RAP (%)
M-50 Dundee	3E1	2.519	0.0011	2.511	10.0
M-36 Pinckney	3E3	2.511	0.0028	2.488	15.0
M-45 Grand Rapids	3E3	2.513	0.0000	2.509	-
M-84 Saginaw	3E3	2.543	0.0151	2.550	20.0
M-21 St. Johns	3E3	2.489	0.0003	2.488	13.0
BL I-96 Howell	4E3	2.501	0.0089	2.480	15.0
M-21 Owosso	5E3	2.470	0.0031	2.470	10.0
M-66 Battle Creek	4E3	2.470	0.0043	2.480	15.0
M-50 Dundee	4E3	2.538	0.0025	2.520	-
US-12 MIS	4E3	2.491	0.0054	2.490	17.0
M-59 Brighton	3E10	2.502	0.0034	2.485	15.0
Michigan Ave. Dearborn	3E10	2.493	0.0025	2.496	15.0
VanDyke, Detroit	3E30	2.604	0.0103	2.577	-
US-23 Hartland	3E30	2.492	0.0019	2.494	15.0
I-75 Levering Road	3E10	2.443	0.0042	2.430	18.0
I-196 Grand Rapids	5E10	2.499	0.0018	2.499	-
I-75 Clarkston	4E30	2.487	0.0007	2.467	12.0
M-53 Detroit	4E10	2.563	0.0023	2.553	8.0
Michigan Ave. Dearborn	4E10	2.485	0.0012	2.464	10.0
I-75 Toledo	5E30	2.507	0.0074	2.510	-
I-94 Ann Arbor	4E30	2.515	0.0000	2.514	-

A comparison was made between ISU's and the contractor's G_{mm} supplied in the JMF. Figure 4.1 illustrates the comparison of laboratory G_{mm} and contractor G_{mm}. Some differences do exist between the ISU and contractor JMF G_{mm} as shown in Figures 4.1 and 4.2. As the asphalt content increases, the G_{mm} decreases due to the fact that asphalt cement has a lower specific gravity (approximately 1.020 to 1.030) than the aggregate. The increase of asphalt binder to a mixture results in a decrease in aggregate weight of a mix on a unit volume basis. Some of the mixtures do not fall within the multilaboratory precision of 0.019. There are several explanations for this in addition to the RAP component. One reason for the difference is that these samples are from the field and there are numerous sources where variability and segregation can occur. Every attempt was made to obtain representative field samples by sampling from mini stock piles, but prior construction processes could be not be controlled. A second possible reason for the difference is that the changes could have been made to a mix

design in production that deviates from the JMF. A third reason is that the binder content in a JMF could be higher or lower than what was stated. This will be commented on in the next section.

A two-way analysis of variance (ANOVA) with no interaction was used to compare the two methods of obtaining a G_{mm} (JMF versus laboratory obtained) by project. Table 4.2 shows that there is statistical difference between the contractor JMF and the laboratory obtained G_{mm} value. This could be due to changes in aggregate percentages, gradation, binder content, sampling, and RAP.

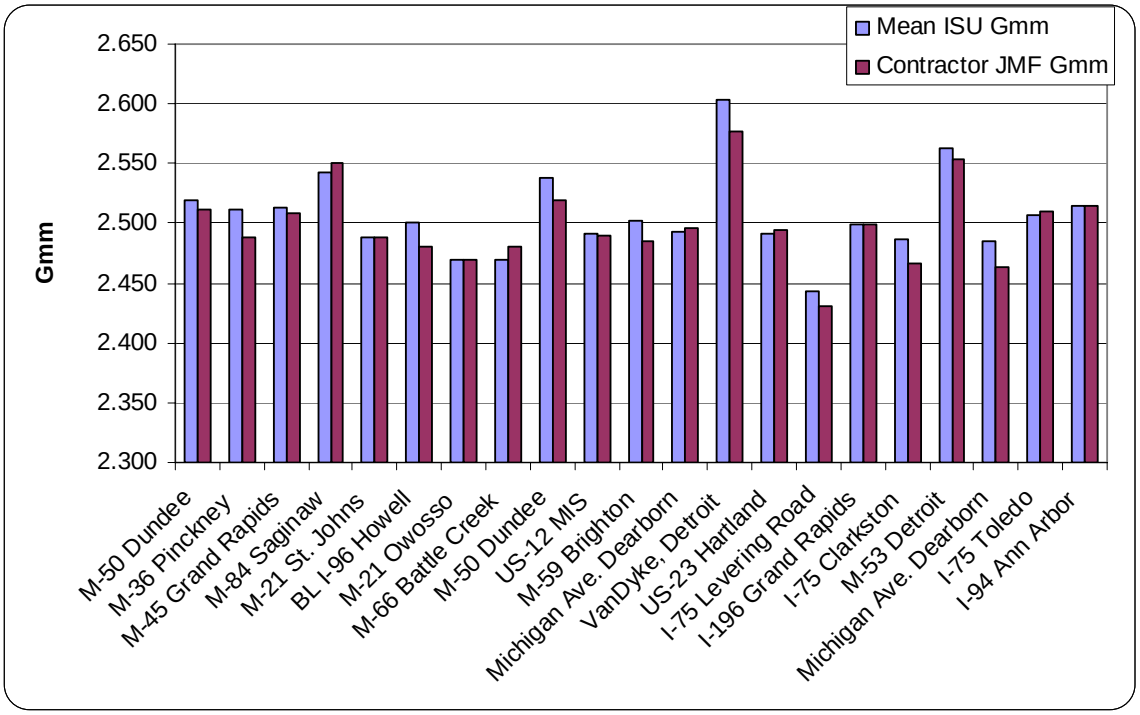

Figure 4.1 ISU and Contractor JMF G_{mm}

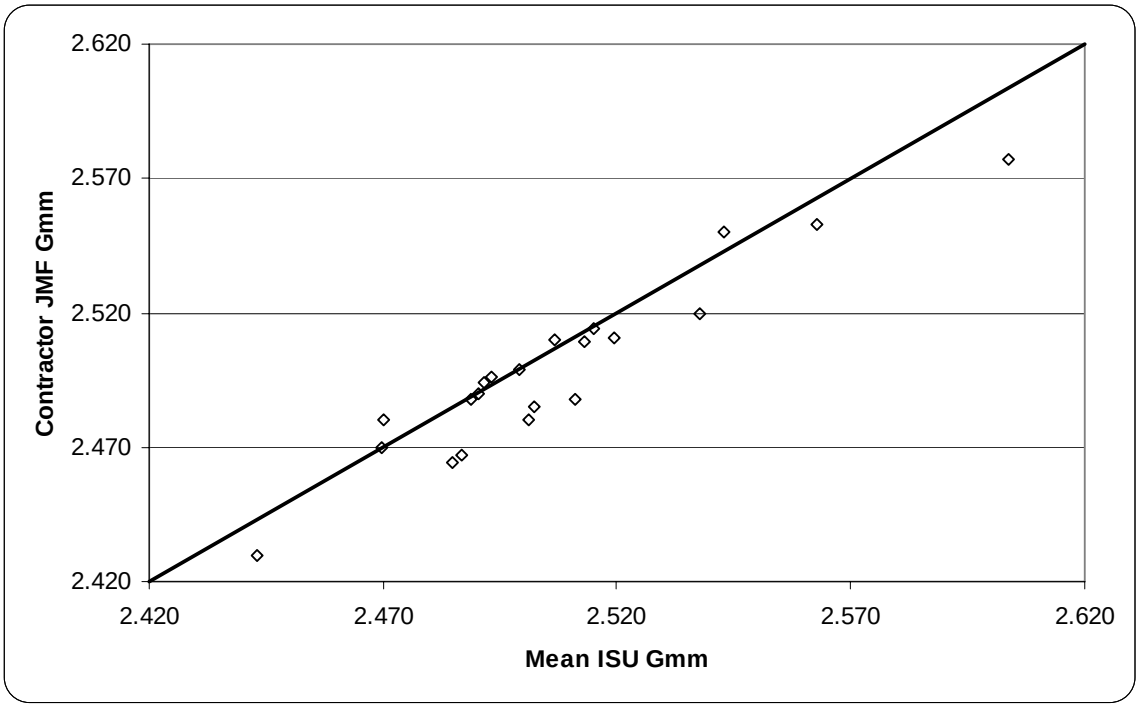

Figure 4.2 ISU and Contractor JMF G_{mm}

Table 4.2 2-Way ANOVA Comparing Laboratory G_{mm} to Contractor JMF

Source of Variation	*SS*	*df*	*MS*	*F*	*P-value*	*F crit*
Project	0.0444	20	0.00222	35.8551	1.6E-11	2.12416
Gmm Method	0.0006	1	0.0006	9.63832	0.00559	4.35124
Error	0.0012	20	6.2E-05			
Total	0.0462	41				

Asphalt binder constitutes the most expensive part of the HMA mixture. The differences in G_{mm} values between the contractor and ISU may be a result of differences in binder contents. Most contractors want to decrease the amount of asphalt in the mix to make the mix more economical in a low bid situation. In the state of Michigan, the production and placement of HMA is a single bid item and not separated between asphalt binder and aggregates nor their placement. Thus, a decrease in the binder content, yet still within specification tolerance could save a contractor a substantial amount of money on a paving project.

4.2 Extraction Test

An important property of an HMA mixture is asphalt content. Satisfactory performance of an HMA mixture is a function of asphalt content since mixtures with low asphalt contents are not durable while one with a high asphalt content is not stable. The asphalt content directly affects the volumetric properties such as air voids, voids in the mineral aggregate (VMA), voids filled with asphalt (VFA), and film thickness. Asphalt content can also have an effect on HMA performance in terms of |E*|, flow number, and rutting.

The asphalt content of mixtures were measured by an extraction test using the Abson method (ASTM D2172). The extraction test uses solvents to dissolve asphalt cement in a mix. The recovered asphalt cement and solvent are passed through filter report not allowing the aggregate to pass through it. The advantage of this test is that it allows for the determination of the aggregate gradation and comparison then to the JMF.

Table 4.3 gives the results of running extractions on each HMA mixture and comparing them to the JMF binder content. This table shows that fourteen of the twenty-one projects have lower binder contents than what the JMFs report. Another benefit of running an extraction is that a sieve analysis can be conducted on the extracted aggregate and compared with a JMF. The JMF and the resulting extracted gradation can be seen in Appendix A. Figure 4.3 and Figure 4.4 show graphically the extracted binder content versus the JMF binder content. The figures clearly illustrate that the asphalt binder for a majority of the projects is less than the reported value on the JMF. This can result in G_{mm} values lower than what is reported in a JMF.

Table 4.3 Extracted Binder Content versus JMF Binder Content

Project	Mix Type/Traffic	Extracted Binder Content (%)	JMF Binder Content (%)
M-50 Dundee	3E1	5.0	5.4
M-36 Pinckney	3E3	5.2	5.8
M-45 Grand Rapids	3E3	4.9	5.1
M-84 Saginaw	3E3	4.7	4.6
M-21 St. Johns	3E3	4.5	5.4
BL I-96 Howell	4E3	5.0	5.5
M-21 Owosso	5E3	5.7	5.9
M-66 Battle Creek	4E3	5.4	5.5
M-50 Dundee	4E3	5.6	5.6
US-12 MIS	4E3	5.9	5.8
M-59 Brighton	3E10	5.2	5.7
Michigan Ave. Dearborn	3E10	5.9	5.6
VanDyke, Detroit	3E30	4.7	5.2
US-23 Hartland	3E30	5.7	5.5
I-75 Levering Road	3E10	4.7	5.5
I-196 Grand Rapids	5E10	5.7	5.6
I-75 Clarkston	4E30	5.3	5.8
M-53 Detroit	4E10	5.2	5.6
Michigan Ave. Dearborn	4E10	5.6	5.8
I-75 Toledo	5E30	5.4	5.4
I-94 Ann Arbor	4E30	6.0	6.6

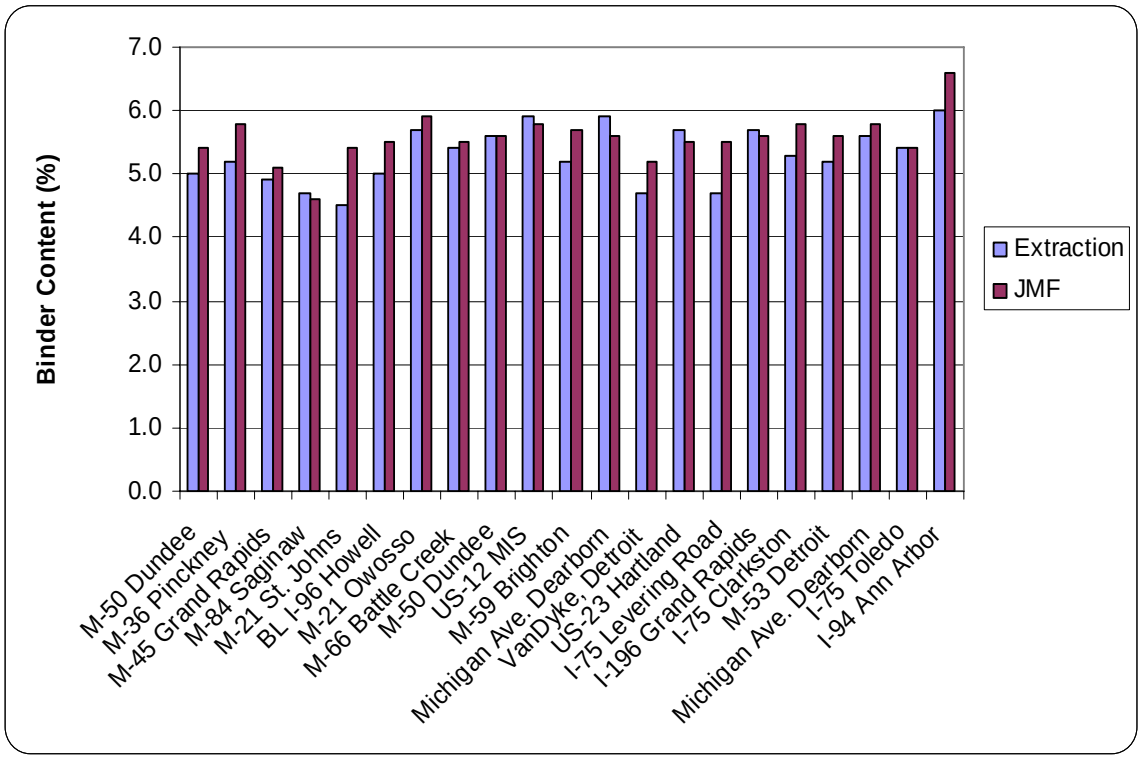

Figure 4.3 ISU and Contractor Binder Contents

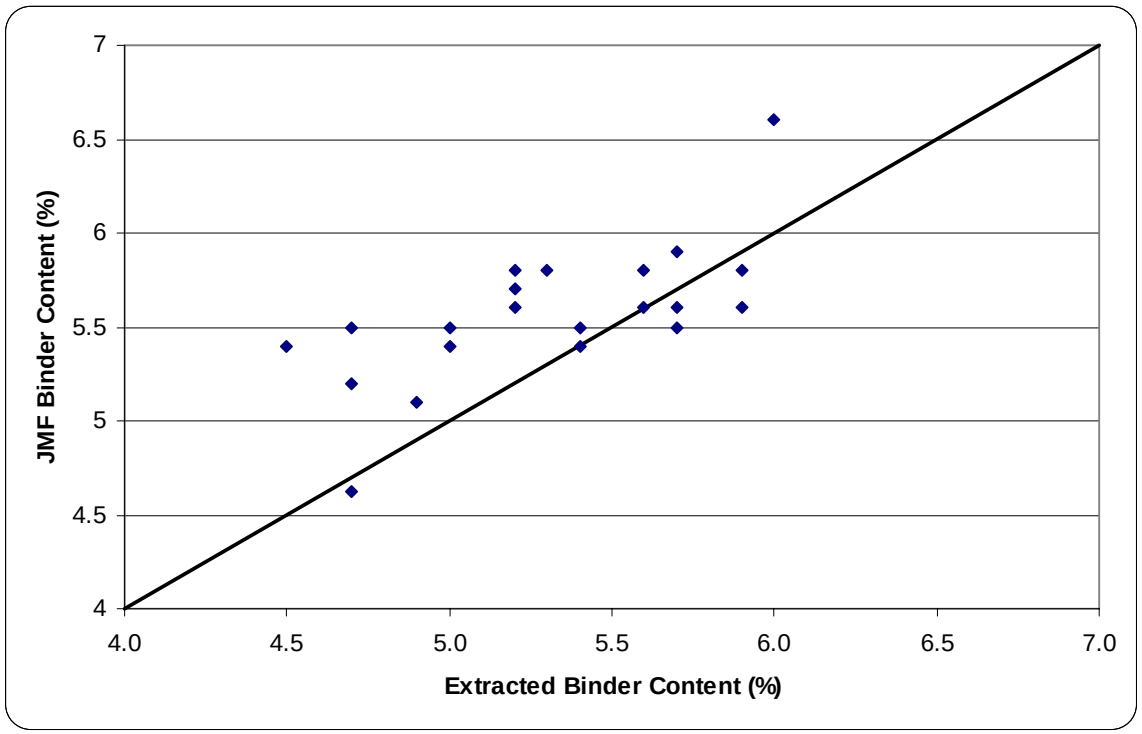

Figure 4.4 ISU versus Contractor Binder Contents

A two-way ANOVA with no interaction was the statistical tool used to analyze the binder contents obtained from the laboratory and the JMF. Table 4.4 shows that there is a statistical difference between the contractor JMF and the laboratory obtained binder content. This can be due to changes in gradation, RAP content, or a decrease in the binder content at the plant.

Table 4.4 2-Way ANOVA Comparing Laboratory Extracted Binder Content to Contractor JMF

Source of Variation	*SS*	*df*	*MS*	*F*	*P-value*	*F crit*
Project	5.61219	20	0.28061	4.93948	0.00038	2.12416
Method	0.75201	1	0.75201	13.2374	0.00164	4.35124
Error	1.13619	20	0.05681			
Total	7.50039	41				

After solvents are used to dissolve the asphalt cement off of the aggregate, then the asphalt cement and solvent are passed through filter report not allowing the aggregate to pass through. The advantage of this test is that it allows for the determination of the aggregate gradation and comparison then to the JMF. Two-way ANOVAs with no interaction were used at each sieve size to determine if the percentage of the aggregate weight has changed on the sieves. Table 4.5 shows that the gradation at each sieve size is statistically the same except at the #200 sieve where statistical differences result. For the most part the contractor's JMF compares well with the gradation from the extraction procedure. Figure 4.5 shows a comparison of the sieve analysis results from the #200 sieve. The figure shows that there is a difference in #200 material between the contractor JMF and the results from the extraction and sieve analysis.

Table 4.5 2-Way ANOVA Comparing Laboratory Extracted Gradation to JMF Gradation

Sieve Size (mm)	2-Way ANOVA Results JMF vs. Extraction
1 (25)	Statistically the Same
3/4 (19)	Statistically the Same
1/2 (12.5)	Statistically the Same
3/8 (9.5)	Statistically the Same
#4 (4.75)	Statistically the Same
#8 (2.36)	Statistically the Same
#16 (1.18)	Statistically the Same
#30 (0.60)	Statistically the Same
#50 (0.30)	Statistically the Same
#100 (0.15)	Statistically the Same
#200 (0.075)	Statistically Different

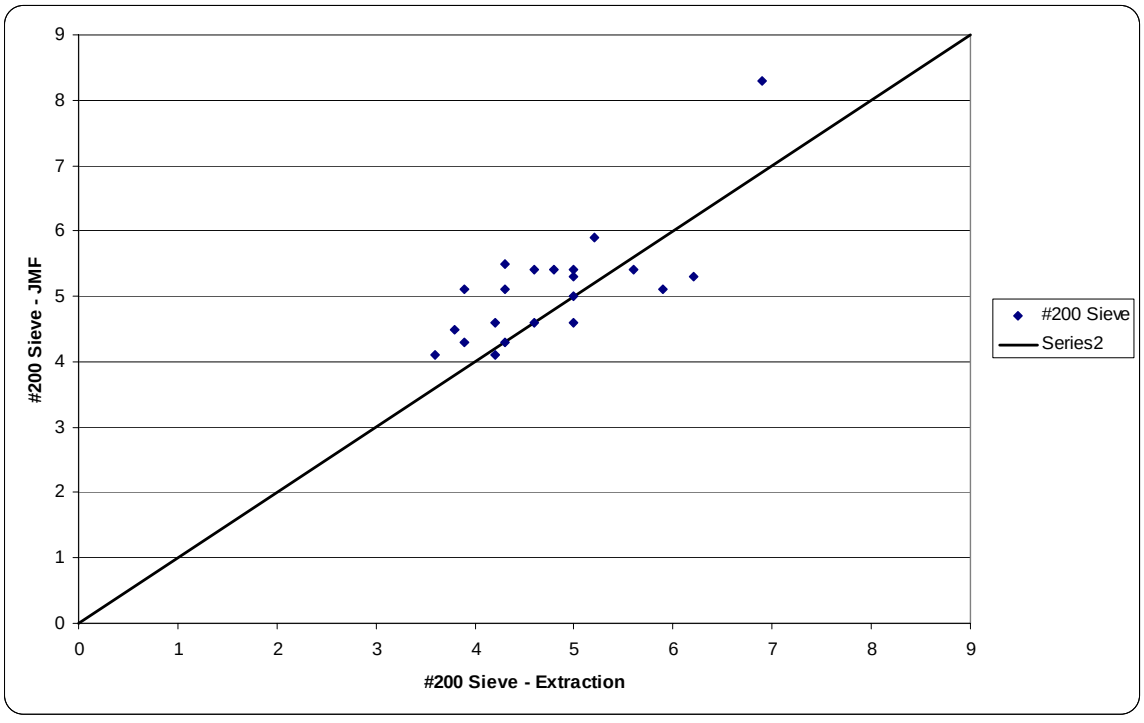

Figure 4.5 Comparison of #200 Sieve

4.2.1 Superpave Gyratory Compaction

Superpave gyratory specimens were compacted with a Pine AFGC125X SGC. The 100mm diameter specimens were compacted to approximately 63.5mm in height and the 150mm diameter specimens were compacted to approximately 95mm in height for Phase I. For Phase II,

150mm diameter specimens were compacted to 95mm in height for AASHTO T283 testing and APA testing. Dynamic complex modulus specimens were compacted to 170mm in height. All specimens were compacted to 7±1% air voids. An assumed appropriate correction factor was used based on gradation and NMAS. A new correction factor was calculated if the air voids were out of range and additional specimens were procured.

4.2.2 Marshall Compaction

The Marshall compaction method was only used for Phase I of this research project. A double-sided, automated Marshall hammer was used to compact specimens that were 100mm by 63.5mm in height. A double-sided mechanical compactor was selected instead of using the hand compactor for three reasons; first, the variability of the compaction procedure would be minimized, secondly, if this study was extended further, the compaction procedure would be uniform, and thirdly, 140 specimens had to be procured so this method was better suited for mass production of the samples. Before performance specimens could be procured, the determination of the number of blows to achieve 7±1% air voids was needed for each mix. Four specimens per job were compacted to 10, 25, 75 and 125 blows per side. A graph of air voids versus number of blows per side was used to determine the number of blows required to achieve 7±1% air voids.

4.3 Compaction of Gyratory and Marshall Specimens

In Michigan, mix designs are based on compacting specimens to N_{des}, which allows for the air voids of the specimen to be measured according to AASHTO T166. In order to compact gyratory specimens, a correction factor is needed to compact the specimens to height. The ratio of the estimated G_{mb} via volumetric measurements of weight, height, and diameter to that of the measured G_{mb} via saturated surface dried constitutes the correction factor. Typically, HMA mixtures have a correction factor of 1.0 to 1.03. For Phase I and Phase II Superpave gyratory

specimens, a correction factor of 1.02 was used for fine mixes and a correction factor of 1.04 was used for coarse mixtures. The correction factor was refined when the measured air voids were not between 7±1% and additional specimens were procured with a new correction factor and the air voids measured again. For the Marshall specimens, the sample mass was kept constant and graphs of air voids versus number of blows were constructed for each project. The number of blows to achieve 7% air voids was estimated from the graphical relationship for each mix. The air voids were measured for the specimens and if they were not within 7±1% then additional specimens were made by adjusting the number of blows.

All Superpave gyratory specimens for Phase I and Phase II were compacted with a Pine Superpave Gyratory (SGC) model AFGC125X. This machine was selected because of its familiarity and higher production capability. The SGC was fully calibrated to ensure that the specimens were compacted to the correct height at an angle of 1.25° with a pressure of 600kPa in accordance with Superpave compaction criterion.

Samples were split according to the weights required to achieve 63.5, 95, and 170mm for the SGC specimens. The Marshall specimens used a batch weight of 1200g and then compacted to the required number of blows per side to achieve 7±1% since the Marshall specimen height is to be about 63.5mm in height. These SGC specimen weights were determined using the G_{mm} test results and the guidance outlined in SP-2 (1996).

Specimens were left to cool until room temperature was achieved. At that time they were labeled and prepared for bulk specific gravity testing (G_{mb}). A total of 420 samples were compacted for Phase I and 420 samples were compacted for Phase II.

4.3.1 Bulk Specific Gravity (G_{mb})

The bulk specific gravity was determined for all laboratory compacted specimens and those specimens that were cut and cored. The testing was conducted in accordance with ASTM D2726. During the sawing and coring procedure, the specimens were exposed to water due to the fact that the saw blades and core barrel are water cooled. The dry weight of the specimen after cutting and coring is needed in order to determine the bulk specific gravity. According to ASTM D2726, the bulk specific gravity of a wet specimen must undergo a test temperature of 52°C for 24 hours in order to ensure a dry weight. Unfortunately, at this temperature, the HMA specimen could undergo creep, thus changing the dimensions and volumetrics of the sample. Robinette (2005) found that specimens after two days of drying on a wire rack in front of fan was adequate since the rate of weight change became asymptotical towards its true dry weight. This can be seen in Figure 4.6. Therefore, the submerged and saturated surface dry weight were taken immediately after sawing and coring, and the dry weight was taken two or more days after the submerged and saturated surface dry weight.

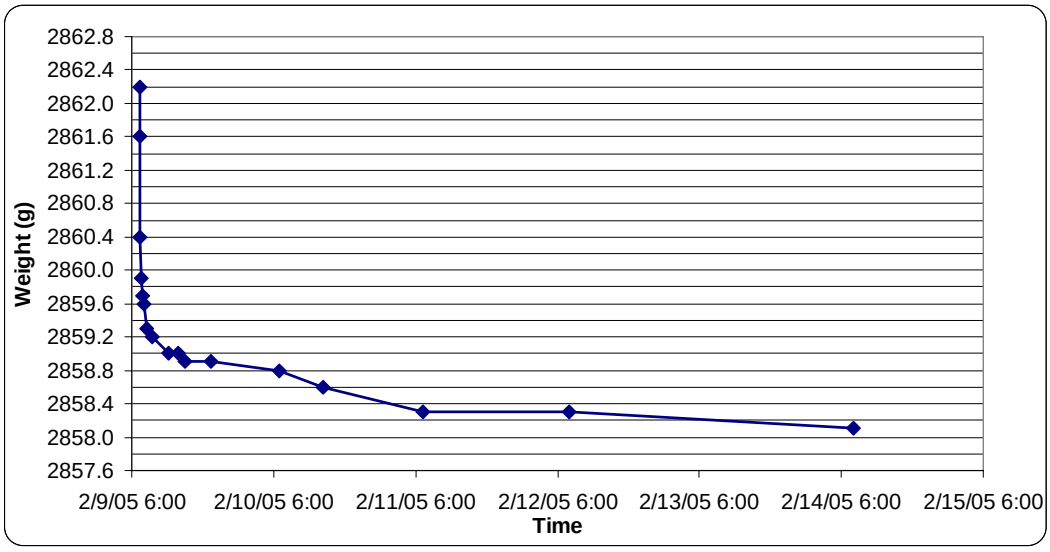

Figure 4.6 Changes in Weight of Specimen After G_{mb} Determination (Robinette 2005)

4.4 Bulk Specific Gravity of Gyratory and Marshall Specimens

The bulk specific gravity (G_{mb}) was measured on all the specimens using AASHTO T166. There was noticeable variability in the measured G_{mb} and air voids for specimens from the same job. This variability is likely due to HMA mixing at the plant, sampling of the mixture, or splitting processes. In according with AASHTO T283, all specimens (Superpave and Marshall) must have measured air voids of 7±1%. The air voids were measured using AASHTO T269. For those specimens that are cut and cored it was anticipated that the air voids would not change significantly, hence the 7±1% air void specification applies to gyratory compacted specimens. All volumetric data for the specimens of this project can be found in Appendix B.

4.4.1 Specimen Cutting and Coring

Specimen cutting and coring was only used for Phase II specimen preparation for subsequent dynamic complex modulus testing of the samples. The draft test protocol from NCHRP 9-19 calls for 100mm by 150mm specimens after coring. A sawing and coring device was developed by Shedworks, Inc. that does the sawing and coring in one piece of equipment. First, the diametrical ends of the specimen are sawed off with a water cooled, double-bladed, diamond tip saw in order to give the specimens a height of 150mm and to ensure parallelism between the top and bottom of a specimen. A coring machine was used to obtain the 100mm diameter specimen from the 150mm gyratory specimen.

Specimens created in a Superpave gyratory compactor were wet sawed to 75mm in height for APA testing. After sawing, the specimens were dried and volumetric measurements recalculated.

4.5 Specimen Measurement

The AASHTO T283 and APA samples were measured in accordance with AASHTO T283. Two diameter and four height measurements were recorded with a digital caliper and averaged. The dynamic complex modulus required a total of six diameter measurements (top, middle, and bottom of specimen) and four height measurements at 0°, 90°, 180°, and 270° and averaged. According to NCHRP 9-29 Interim Report, the diameter standard deviation was required to be less than 2.5mm, otherwise the specimen should be discarded. The only requirement on specimen height was that it should be within the range of 148 and 152mm.

4.6 Volumetrics of Sawed/Cored Test Specimens

The volumetrics of the sawed/cored specimens was measured on all the specimens using AASHTO T269. The volumetric properties of the sawed/cored specimens can be seen in Appendix B. It was noticed that on average, the air voids of sawed/cored specimens were lower than that of the gyratory specimens, this relationship can be seen in Figure 4.7. This relationship makes sense because high air voids exist around the perimeter and at the ends of gyratory compacted specimens. When the ends of the specimens are removed and the sample cored from the center of the Superpave gyratory compacted sample, some of the air voids are removed. The change in air voids ranged from -2.1 to +1.1%.

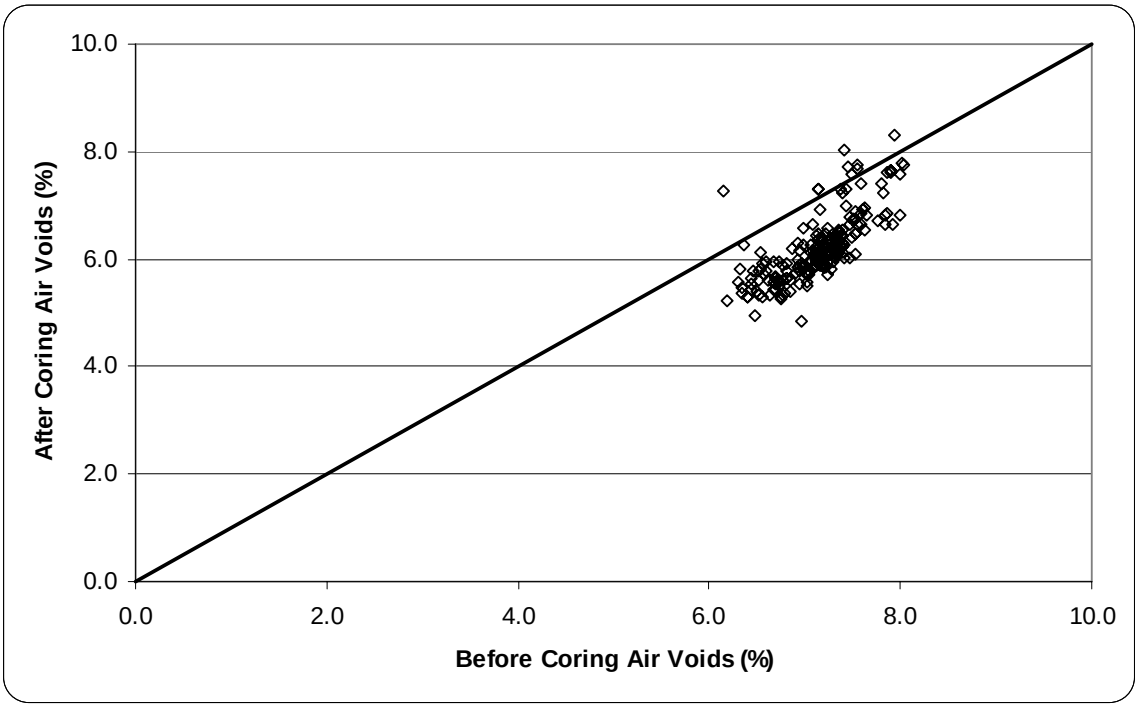

Figure 4.7 Air Voids Before and After Sawing/Coring

4.7 Testing and Calculations

Outlined below are the testing procedures and calculations associated with this research project. The types of tests are indirect tensile strength, dynamic complex modulus, and APA tests.

4.7.1 Indirect Tensile Strength Testing

The testing procedure described herein is derived from the AASHTO T283 Resistance of Compacted Bituminous Mixture to Moisture Induced Damage. Specimens were compacted according to section 4.2.3 and divided into two subsets so that each subset had the same average air voids. The dry subset (control group) were wrapped with plastic or placed in a heavy-duty, leak-proof plastic bag and stored in a water bath at 25±0.5°C for 2 hours ± 10 minutes prior to testing. The conditioned subset specimens were placed in a pycnometer with a spacer. Approximately 25mm of water was placed above the specimen. The specimen was vacuum

saturated for 5 to 10 minutes at 13-67 kPa. The specimen is left submerged in water bath for 5 to 10 minutes after vacuum saturating. The mass of the saturated, surface dry specimen was determined after partial vacuum saturation. Next, the volume of absorbed water was calculated. Finally, the degree of saturation was calculated. If the degree of saturation was between 70% and 80% testing proceeded. If the degree of saturation was less than 70%, the vacuum saturation procedure was repeated. If saturation was greater than 80%, the specimen was considered damaged and discarded. Each vacuum saturated specimen is tightly covered with plastic wrap and placed in a plastic bag with approximately 10±0.5 ml of water, and sealed. The plastic bags are placed in a freezer at -18±3°C for a minimum of 16 hours. The specimens are removed from the freezer and placed in a water bath at 60±1°C for 24±1 hour with 25mm of water above the specimens. Repeat the above steps for conducting multiple freeze thaw cycles. After 24 hours in the 60±1°C water bath, remove specimens and place in a water bath at 25±0.5°C for 2 hours ± 10 minutes. Approximately 25mm of water should be above the specimens. It may be necessary to add ice to the water bath to prevent the temperature from rising above 25±0.5°C. Not more than 15 minutes should be required for the water bath to reach 25±0.5°C. Remove specimens from water bath and test.

The indirect tensile strength of the dry and conditioned specimens can be determined at 25°C. Place the specimen between two bearing plates in the testing machine such that the load is applied along the diameter of the specimen. A Universal Testing Machine (UTM) 100 by Industrial Process Controls Ltd. (IPC) was used to conduct the testing. The load is applied at a constant rate of movement of the testing machine head of 50mm per minute. The maximum load is recorded and placed in the following equation in order to calculate tensile strength.

$$S_t = \frac{2000 \times P}{\pi \times t \times D} \qquad \text{(equation 4.1)}$$

where:

S_t = tensile strength (kPa),

P = maximum load (N),

t = specimen thickness (mm), and

D = specimen diameter (mm).

A numerical index or resistance of an HMA mixture to the effects of water is the ratio of the original strength that is retained to that of the moisture conditioned strength.

$$TSR = \frac{S_2}{S_1} \quad \text{(equation 4.2)}$$

where:

TSR = tensile strength ratio,

S_2 = average tensile strength of conditioned subset, and

S_1 = average tensile strength of dry subset.

4.7.2 Dynamic Modulus Testing

The testing procedure for dynamic modulus testing was derived from NCHRP 9-29 Simple Performance Tester for Superpave Mix Deign. The conditioning the specimens followed the procedure outline in AASHTO T283.

A 100mm diameter by 150mm high cylindrical specimen was tested under a repeated uniaxial, compressive, haversine unconfined load at the appropriate test temperatures. A Universal Testing Machine (UTM) 100 was used to conduct the testing with a temperature controlled testing chamber. The testing configurations for the dynamic modulus test are shown in Table 4.6.

Table 4.6 Dynamic Modulus Testing Configurations

	Fatigue	Rutting
Temperature	$T_{eff\ fatigue}$	$T_{eff\ rutting}$
Dynamic Load	Induce 75-150μstrain	Induce 75-150μstrain
Loading Rates	0.02 to 25Hz	0.02 to 25Hz

The effective test temperatures for fatigue and rutting are presented further in this final report. The dynamic stress was determined based on the 25 Hz conditioning cycle that caused corresponding strain in the HMA specimen that exceeded 75 – 150 microstrain.

There was a total of six test frequencies that were run at each test temperature. These test frequencies along with the number of loading cycles are given in Table 4.7. The testing sequence was conducted from high to low frequencies to mitigate the amount of deformation induced upon the specimens during testing.

Table 4.7 Cycles for Test Sequence

Frequency, Hz	Number of Cycles
25	200
10	100
5	50
1	20
0.1	6
0.02	6

Three axial linear variable differential transducers (LVDTs) were fixed at 120° around the perimeter of the specimen in order to record the strain at the middle of the specimen over the length of the test. Witczak et al. (2002), found that as you increase the number of LVDTs and the number of replicate specimens, the standard error of the mean decreases. Three LVDTs were used as part of this study because of the availability of the device developed by Shedworks, Inc. The LVDTs were adjusted to the end of their linear range so the entire range of the LVDT is available during the course of testing.

Specimens were placed in the testing chamber until the effective test temperature was attained in the test specimen. This was found with the aid of a dummy specimen with a temperature sensor embedded in the center of the specimen placed in the test chamber. There was another temperature probe that was placed in the temperature chamber that measured the air (skin) temperature. After the effective test temperature was reached, the specimen was then centered under the loading platens so as to not place an eccentric load on the specimen, and tested.

There are four main calculations that are performed by the associated software. The first is the loading stress, σ_o, that is applied to the specimen during the test.

$$\sigma_o = \frac{\bar{P}}{A} \qquad \text{(equation 4.3)}$$

where:

σ_o = stress (kPa),

$\bar{P}$ = average load amplitude (kN), and

A = area of specimen (m^2).

The recoverable axial strain from the individual strain gauges, ε_o, is determined as follows:

$$\varepsilon_o = \frac{\bar{\Delta}}{GL} \qquad \text{(equation 4.4)}$$

where:

ε_o = strain (mm/mm),

$\bar{\Delta}$ = average deformation amplitude (mm), and

GL = gauge length (mm).

Dynamic modulus, $|E^*|$ for each LVDT:

$$|E^*| = \frac{\sigma_o}{\varepsilon_o} \quad \text{(equation 4.5)}$$

The final equation is to determine the phase angle, for each LVDT:

$$\phi = \frac{t_i}{t_p}(360) \quad \text{(equation 4.6)}$$

where:

ϕ = phase angle,

t_i = average time lag between a cycle of stress and strain (sec), and

t_p = average time for a stress cycle (sec).

The software that was available for this project performed the above calculations was developed by IPC Global. It reported the |E*| and the phase angle for all three LVDTs as well as the permanent and resilient micro-strain and the applied stress for each load cycle.

4.7.3 Asphalt Pavement Analyzer

APA testing followed the APA's User Manual. HMA was compacted using a Superpave Gyratory Compactor. Once the specimens were made, volumetric testing and properties were obtained. A preliminary study on two mixes was conducted to determine which testing conditions should be employed for all 21 mixes. The selection of the two mixes was based on moisture susceptibility testing which evaluated the tensile strength ratio of several mixes. Testing conditions evaluated with the two mixes were unconditioned submerged in water, unconditioned in air, one freeze/thaw condition submerged in water, and one freeze/thaw condition in air. Three cylindrical specimens were subjected to APA testing for each condition. The unconditioned specimens were tested in accordance with guidelines established by the APA's User Manual (Pavement Technology, 2002). The freeze/thaw conditioned specimens

were prepped in accordance with the conditioning process outlined in AASHTO T283. HMAs with a high temperature grade of 58 or 64 were tested at their respective high temperature. The polymer modified mixes with a high temperature grade of 70 were also tested at 64, since this was the prescribed field temperature; the higher grade of 70 provides improved rutting resistance. The samples were heated to the high temperature (either 58 or 64˚C) since permanent deformation typically occurs during the warmer months when the binder is more fluid or less viscous.

All specimens were cut to the appropriate height (75mm) for circular specimens using a circular saw. New geometries of the specimens were recorded after sawing along with new bulk specific gravity measurements using the saturated surface dry method (ASTM D2726). Specimens were grouped in sets of three based on bulk specific gravity measurements.

Control specimens were preheated at the high performance grade a minimum time of 6 hours in accordance with the APA testing guidelines. After preheating, a pneumatic tube and steel wheel were lowered over the central axis of each specimen and an APA was set to run 8,000 cycles. As mentioned previously, a cycle is equivalent to a wheel passing one time forward and back to its starting position. Once the inner chamber of the APA reheated to the appropriate testing temperature, a test was initiated. The reheating usually took less than 2 minutes, since the chamber was heated to the appropriate test temperature prior to the placement of specimens. The reheating was necessary since there was some heat loss upon the opening of the APA doors to install the specimens locked inside the molds. After a completion of 8,000 cycles, test data was automatically transferred to an Excel file and saved for future analysis.

Specimens in either the freeze/thaw tested in air condition state or freeze/thaw tested submerged condition state were prepared in the same manner, except these specimens were

moisture saturated and endured one freeze/thaw cycle prior to testing. These specimens were vacuum saturated to a maximum of 80% air voids filled with water. Specimens were wrapped in Glad Press n' Seal® with ends of the wrap taped down with packing tape. Wrapped specimens and 10ml of water were placed inside a plastic freezer bag labeled with mix information, specimen number, and condition state group. Specimens inside the freezer bags were then placed in a freezer (-18 ± 3˚C) for a period of 24 hours. To minimize the amount of heat entering the freezer, all specimens in a particular group were prepared first and then entered into the freezer at the same time instead of individually. After 24 hours, specimens were placed in a 60˚C water bath to thaw. Once thawing was complete, specimens were preheated to the appropriate APA testing temperature for the 6 hour minimum conditioning time. Specimens to be tested in air were placed in an air chamber for preheating, while those to be tested in water were placed in a water bath for preheating. After the allotted 6 hours of preheating, specimens were placed in an APA for testing. Specimens tested in air were placed in an APA and a steel wheel lowered on top of a pneumatic tube and the APA chamber was allowed to re-establish the test temperature prior to the initiation of 8,000 cycles. Specimens tested in water were placed in an APA chamber and the doors sealed shut. Once the APA doors were shut, a metal box elevated to surround the APA molds. Once the metal box had reached its highest point, water heated to the appropriate temperature flowed into the chamber to fill the metal box. The heated water at all times kept specimens completely immersed. Once the metal box was filled and the water and test chamber re-established the appropriate test temperature, 8,000 cycles commenced. Data of the specimens freeze/thaw tested in air condition state or freeze/thaw tested submerged condition state were automatically transferred to an Excel file to be saved and analyzed later.

4.7.4 Dynamic Shear Rheometer (DSR)

Asphalt binder testing was conducted using a modified DSR. The initial modifications to a DSR for moisture susceptibility testing were developed by Rottermond (2004). Additional modifications were developed for this study since the initial modifications did not adequately allow for moisture saturation of a specimen during testing.

The new moisture susceptibility testing procedure is similar to the traditional DSR test procedures outlined in AASHTO T315. The main difference between AASHTO T315 and the new test procedure is in regards to modifications to a base plate and spindle. Instead of asphalt interacting with a stainless steel interface, a new base plate and spindle were devised that allowed for a ceramic interface with the asphalt binder. The stainless steel interface was deemed an unrealistic material for simulating in-situ conditions. Previous studies also identified the disadvantage of using stainless steel (Rottermond 2004, Scholz and Brown 1996). The ceramic material used was the same utilized by Youtcheff in developing a moisture sensitivity test of asphalt binder via a pneumatic pull-off test (Youtcheff and Aurilio 1997). A modification was deemed necessary to simulate moisture accessibility to asphalt binder. The stainless steel interface not only was an unrealistic representation of field conditions, but also did not allow for water to interact as the top and bottom of a specimen. Figure 4.8 through Figure 4.10 depict the alterations to the DSR parts incorporated into the new test procedure for determining moisture susceptibility. The modification to the DSR allows for any material to be used as an interface with asphalt as long as it meets the geometric dimensions of the space allowed for the disc. A manufactured ceramic disc was selected as the interface to reduce the variability contributed by an aggregate with possible material variations. An additional modification was incorporated into

the spindle to allow for moisture to penetrate the asphalt via the ceramic disc. Three holes 120˚ apart were created in the spindle head.

Figure 4.8 Modified DSR Base plate

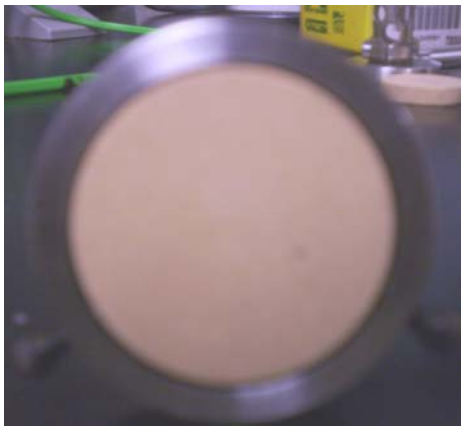

Figure 4.9 Modified DSR Spindle

Figure 4.10 Modified DSR Spindle with Three Holes

The final modification allowed for a disc of any material type to be place within the base plate and spindle. Set screws are used to hold the disc in place for both the base plate and the spindle. The set screws are at 120˚ intervals as are the holes through the top of the spindle. Figure 4.10 illustrates the placement of the holes that allow for water flow from the top down. Figure 4.11 through Figure 4.15 illustrate the dimensions and modifications of the modified spindle.

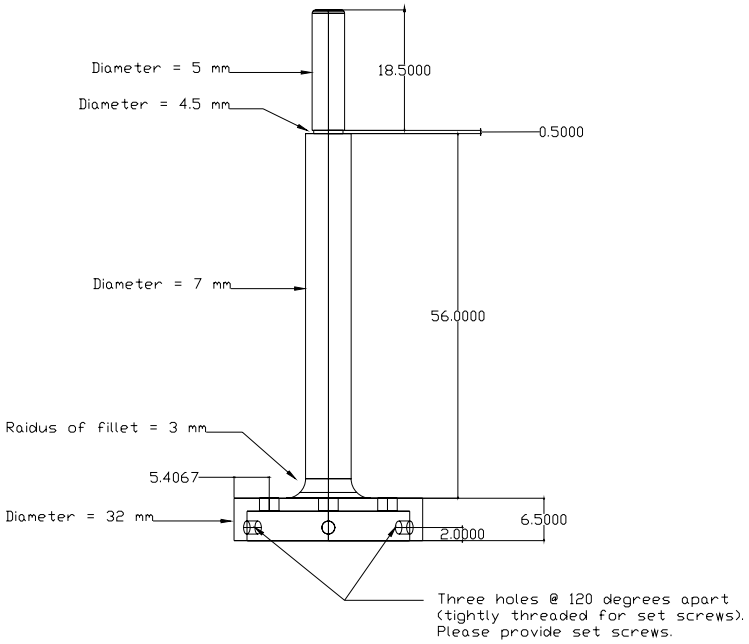

Figure 4.11 Dimensions Of Modified Spindle(Bausano, 2005)

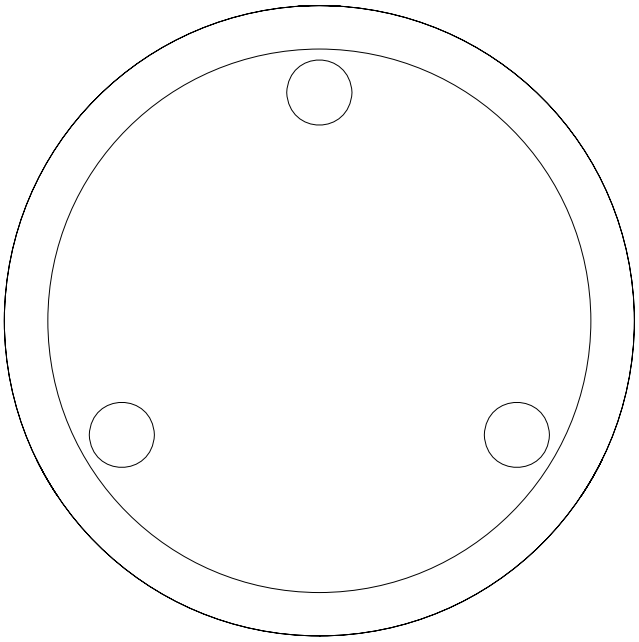

Figure 4.12 View of Spindle Through The Base (Bausano 2005)

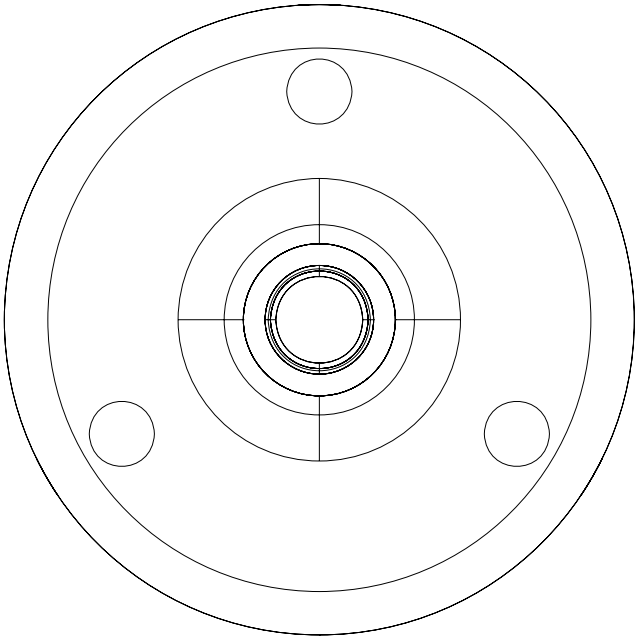

Figure 4.13 View of Modified Spindle From Top Down (Bausano 2005)

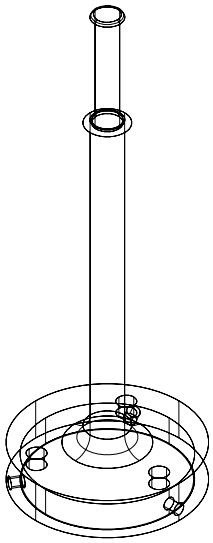

Figure 4.14 Side View of Modified Spindle (Bausano 2005)

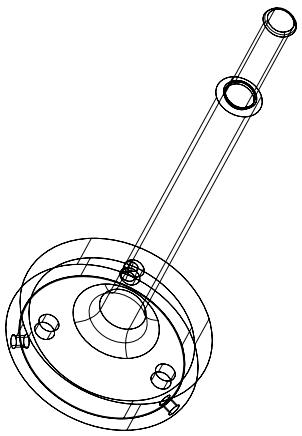

Figure 4.15 Angled View of Modified Spindle (Bausano 2005)

Hydrated lime and silica were used as the mastic material added to the asphalt binders to examine the binder interaction with aggregates. Both the hydrated lime and silica fillers passed the #200 sieve. Prior to mixing the filler into the binder, both the binder and filler were heated. Each filler was added by weight and stirred into the binder until it appeared homogenous.

All samples were poured into a standard 25mm mold in conjunction with the DSR. Each specimen rested for a minimum of 10 minutes prior to testing. In all cases, the disks were screwed into the base plate and spindle prior to initiation of testing. Once the DSR was zeroed, the spindle was raised to enable to application of the asphalt binder sample. The spindle was then lowered to a gap of 1050µm. If the sample required trimming it occurred at this point and then the spindle was lowered to 1000µm. Testing did not initiate until the water bath once again reached the desired testing temperature. After testing, the set screws in the modified spindle were unscrewed and then the spindle raised. The base plate with the specimen was then removed from the DSR. The specimen was then removed from the base plate by unscrewing the set screws holding the bottom of the specimen.

The binders tested with the ceramic disks were tested with the DSR for three different conditioning states. The first examination occurred with unconditioned samples. After the first test, the disk and binder cylinder were placed in a water bath with distilled 25˚C water for a period of 24 hours. After 24 hours of saturation, the specimens were retested as conditioned specimens. After the second round of testing, the specimen was wrapped in cellophane and placed in a freezer for 24 hours. After 24 hours in the freezer, the specimen was returned to the water bath to thaw and be conditioned for another 24 hours prior to being retested.

CHAPTER 5 TESTING SETUP

5.1 Testing Parameters – Phase I

The testing parameters of conditioning period, compaction method, and diameter of specimen were examined before Phase II testing commenced. To address the conditioning period, the objective was to determine what number of freeze/thaw cycles will cause the same damage to the Superpave gyratory compactor specimen compared to Marshall specimens for testing the resistance of compacted bituminous mixtures to moisture-induced damage using AASHTO T283. Section 3.2.1 provides a summary for conducting AASHTO T283.

5.2 Testing Parameters – Phase II

In order to address to issues related to testing parameters, past literature was consulted, engineering judgment was exercised, and contacts were utilized and specimens were tested to verify the parameters if needed. The testing parameters are discussed in section 6.2.1 for AASHTO T283 and 6.2.2 for dynamic modulus testing.

5.2.1 AASHTO T283

The only testing parameter for AASHTO T283 testing for Phase II is the number of freeze/thaw cycles determined from Phase I. Additional parameters that are stated in the test procedure are air voids, saturation level, test temperature for freezing and thawing along with time requirements at each temperature, test temperature prior to testing, and loading rate. Refer to section 3.4.1 to the testing parameters that are outlined for AASHTO T283.

5.2.2 Dynamic Modulus

The testing parameters of test temperature, confinement, and stress level were determined prior to testing. The number of freeze/thaw cycles was determined from Phase I. Each parameter is discussed in more detail in the subsequent sections.

5.2.2.1 Test Temperatures

The testing temperatures for intermediate and high temperature dynamic modulus and flow number testing are stipulated by an effective temperature (T_{eff}) reported in NCHRP Report 465 (Witczak et al. 2002). Effective temperature is defined as "a single test temperature at which an amount of permanent deformation would occur equivalent to that measured by considering each season separately throughout the year" (Robinette, 2005). The equation for effective temperature for rutting (dynamic modulus and flow number) is (Robinette 2005):

$$T_{eff\ rutting} = 30.8 - 0.12\ z_{cr} + 0.92\ MAAT_{design} \quad \text{(equation 6.1)}$$

where:

z_{cr} = critical depth down from pavement surface (mm), and

$MAAT_{design}$ = mean annual air temperature (ºC).

$$MAAT_{design} = MAAT_{average} + K_{\alpha}\sigma_{MAAT} \quad \text{(equation 6.2)}$$

where:

$MAAT_{average}$ = mean annual air temperature (ºC),

K_{α} = appropriate reliability level of 95% (1.645), and

σ_{MAAT} = standard deviation of distribution of MAAT for site location.

The critical depth is to be considered was 20mm from the surface. The $MAAT_{average}$ was collected from the Michigan State Climatology Office from stations that were located in close proximity to where each job was paved. The σ_{MAAT} was found in LTPPBind v2.1 as the high air temperature standard deviation. LTPPBind is a software program that provides guidance on asphalt binder grade selection based on climatic information. The rutting effective test temperatures based on equation 6.1 are summarized in Table 5.1.

Table 5.1 Rutting Effective Test Temperatures

Site	$MAAT_{design}$ (°C)	σ_{MAAT} (°C)	$T_{eff\ rutting}$ (°C)
M-45 Grand Rapids	10.4	1.1	37.9
Michigan Ave, Detroit 3E10	11.8	1.1	39.2
Michigan Ave, Detroit 4E10	11.8	1.1	39.2
M-66 Battle Creek	10.8	1.1	38.3
I-75 Levering	7.0	1.1	34.8
US-12 MIS	11.6	1.4	39.1
Vandyke	11.8	1.1	39.2
M-21 St. Johns	10.5	1.0	38.0
M-36 Pinckney	11.6	1.2	39.1
I-94 Ann Arbor SMA	11.6	1.2	39.1
Dundee M-50 3E1	11.2	1.3	38.7
M-53 Detroit 8 Mile	11.8	1.1	39.2
US-23 Hartland	10.0	1.1	37.6
Saginaw M-84	10.1	1.2	37.7
Toledo I-75	12.1	1.3	39.5
I-196 Grand Rapids	10.4	1.1	37.9
I-75 Clarkston	10.7	1.0	38.2
M-59 Brighton	10.1	1.0	37.7
M-21 Owosso	10.1	1.0	37.7
BL I-96 Howell	10.1	1.0	37.7
Dundee M-50 4E3	11.2	1.3	38.7

The effective pavement temperature for fatigue was determined by using the Strategic Highway Research Program (SHRP) equation and is shown in the following equations.

$$T_{eff\ fatigue} = 0.8\ MAPT - 2.7 \qquad \text{(equation 6.3)}$$

where:

MAPT = mean annual pavement temperature (ºC).

$$MAPT = T_{air} - 0.00618\ lat^2 + 0.2289\ lat + 42.2\ (0.9545) - 17.78 \qquad \text{(equation 6.4)}$$

where:

MAPT = T_{20mm} = temperature at 20mm depth from pavement surface (ºC),

T_{air} = mean annual air temperature (ºC), and

lat = latitude of location (degrees).

The $MAAT_{average}$ from equation 6.2 was used for T_{air} in equation 6.4. The latitude was determined by location of where the project was paved.

Based on the above methods the following effective test temperatures were used for each individual project listed in Table 5.2 for fatigue testing.

Table 5.2 Fatigue Effective Test Temperatures

Site	T_{air} (°C)	Latitude (degrees)	MAPT (°C)	$T_{eff\ fatigue}$ (°C)
M-45 Grand Rapids	10.4	42.88	29.5	20.9
Michigan Ave, Detroit 3E10	11.8	42.42	31.0	22.1
Michigan Ave, Detroit 4E10	11.8	42.42	31.0	22.1
M-66 Battle Creek	10.8	42.37	30.0	21.3
I-75 Levering	7.0	45.57	25.3	17.5
US-12 MIS	11.6	42.23	30.4	21.6
Vandyke	11.8	42.42	31.0	22.1
M-21 St. Johns	10.5	43.02	29.7	21.1
M-36 Pinckney	11.6	42.30	30.8	21.9
I-94 Ann Arbor SMA	11.6	42.30	30.8	21.9
Dundee M-50 3E1	11.2	41.92	30.3	21.5
M-53 Detroit 8 Mile	11.8	42.42	31.0	22.1
US-23 Hartland	10.0	42.58	29.3	20.7
Saginaw M-84	10.1	43.53	28.9	20.4
Toledo I-75	12.1	41.83	31.2	22.3
I-196 Grand Rapids	10.4	42.88	29.5	20.9
I-75 Clarkston	10.7	42.65	30.1	21.4
M-59 Brighton	10.1	42.97	29.4	20.8
M-21 Owosso	10.1	42.97	29.4	20.8
BL I-96 Howell	10.1	42.97	29.4	20.8
Dundee M-50 4E3	11.2	41.92	30.3	21.5

5.2.2.2 Unconfined or Confined Testing

Due to the large volume of specimens that were tested for this project, all specimens were tested unconfined. Past research was consulted and it was found that Witczak et al. (2002) determined that both unconfined and confined testing for the two test configurations yielded high correlations with field recorded pavement deformation and there was no significant statistical difference.

5.2.2.3 Stress Level

Finally the magnitude of the stress level had to be determined for each test setup. A review of the testing conducted as part of NCHRP Report 465 yielded no definitive stress level

for each test setup (Witczak et al. 2002). The stress levels used were a function of test temperature and location. According to Robinette (2005), it was found that the stress level for dynamic modulus was dependent on the materials response to the loading. FHWA recommended that the permanent strain at the different frequencies should be between 75 to 150 micro-strain and the load should be adjusted accordingly. Thus through the conditioning cycles the stress levels were determined for the dynamic modulus test at the intermediate and high temperatures on an iterative basis.

5.2.3 Testing Parameters – Asphalt Pavement Analyzer

Four testing conditions were considered. The first condition was the control set where a set of specimens were tested in air without any moisture conditioning. The second set were tested in water without any moisture conditioning. The third set of specimens were tested in air after moisture saturation and one freeze/thaw cycle. The fourth set of specimens were tested in water after moisture saturation and one freeze/thaw cycle. All specimens endured 8,000 cycles. The hose pressure was set to 700 ± 35kPa (100 ± 5 PSI), which is the suggested pressure according to the APA manual (APA, 2001). The load applied to each specimen was 445 ± 22N (l00 ± 5lbs.). Table 5.3 summarizes the test temperatures used for each mix.

Table 5.3 APA Test Temperatures

Site	Test Temperature
M-45 Grand Rapids	58
Michigan Ave, Detroit 3E10	58
Michigan Ave, Detroit 4E10	64
M-66 Battle Creek	64
I-75 Levering	58
US-12 MIS	64
Vandyke	64
M-21 St. Johns	58
M-36 Pinckney	64
I-94 Ann Arbor SMA	64
Dundee M-50 3E1	64
M-53 Detroit 8 Mile	64
US-23 Hartland	64
Saginaw M-84	58
Toledo I-75	64
I-196 Grand Rapids	64
I-75 Clarkston	64
M-59 Brighton	58
M-21 Owosso	64
BL I-96 Howell	64
Dundee M-50 4E3	64

5.2.4 Testing Parameters – Dynamic Shear Rheometer

Each binder was split seven ways. One split was original binder, the following 6 splits were mixed with fillers, silica and hydrated lime, at 5%, 10%, and 20% by weight. Each binder or binder/filler was tested in air unconditioned, water unconditioned, air after saturation, water after saturation, air after saturation and one freeze/thaw cycle, and water after moisture saturation and one freeze/thaw cycle. The moisture saturation occurred in a 25˚C bath of distilled water. The water bath and air chamber were preheated prior to specimens being placed in the DSR. Once the specimens were placed in the DSR, the water bath and air chamber were reheated prior to initiating testing.

CHAPTER 6 SENSITIVITY STUDY – EVALUATION OF AASHTO T283

6.1 Introduction

The objectives of Phase I was to examine a number of field mixes to find an equivalent number of freeze/thaw cycles that would produce moisture damage effects of the original AASHTO T283 specification, which are based upon Marshall compaction, using the newer Superpave gyratory compaction method. The effects of size and compaction method on results obtained following AASHTO T283 procedure were analyzed. Finally, a new minimum TSR was determined by the analysis instead of using the original TSR ratio of 80% which is based on the original AASHTO T283 specification.

6.2 AASHTO T283 Test Results

Figures 6.1 through 6.7 show the results of AASHTO T283 testing by displaying the average of five test specimens per freeze/thaw cycle along with the 95% confidence interval about the mean. Most of these projects illustrate that 100mm Marshall specimens produce lower tensile strength ratios (TSRs) than 100mm and 150mm Superpave specimens. For the most part, there is a decrease in TSR with an increasing number of freeze/thaw cycles. These trends are consistent for the two trafficking levels considered. However, some mixes did show an increase in TSR as the number of freeze/thaw cycles increased similar to the previous research conducted by Lottman (1978), Root and Tunicliff (1982), and Epps et al. (2000).

Table 6.1 ranks the mixtures for each project based on the number of freeze/thaw cycles, compaction, and size of specimens. The ranking is on a scale from one to seven where one is most moisture susceptible and seven is least moisture susceptible. In general, the projects had the same ranking based on number of freeze/thaw cycles. Based on compaction method and

diameter size, some projects were more variable and their rankings fluctuated based on compaction method, diameter size, and freeze/thaw cycles. Overall, I-196 Grand Rapids was the most moisture susceptible followed by M-50 Dundee and M-59 Brighton. M-21 Owosso ranked in the middle. The least moisture susceptible mix was BL I-96 Howell and M-21 St. Johns followed by I-75 Clarkston.

Figures 6.8 and 6.9 show that the average lowest TSR were obtained by 100mm Marshall compacted specimens. In general, the 100mm Superpave specimens exhibited the highest TSR. The method and specimens with the lowest standard deviation were the 150mm Superpave specimens. Interestingly, according to Figures 6.1 through 6.7, the 100mm Superpave specimens had the highest level of variability. These results indicate that the 150mm Superpave specimens are more precise, the data is less spread out, than both the TSR values for the Marshall and 100mm Superpave specimens. The coefficient of variation supports the concept of the TSR results being less dispersed for the 150mm Superpave specimens as well.

As suspected, the TSR is lowest on average once the specimens endured three freeze/thaw cycles and the highest TSRs occurred after only one freeze/thaw cycle. The coefficients of variation indicate that for all three compaction and size categories, three freeze/thaw cycles led to less precise TSR values, while the most precise readings are obtained after one freeze/thaw for Marshall and 150mm Superpave and two freeze/thaw cycles for 100mm Superpave specimens, respectively.

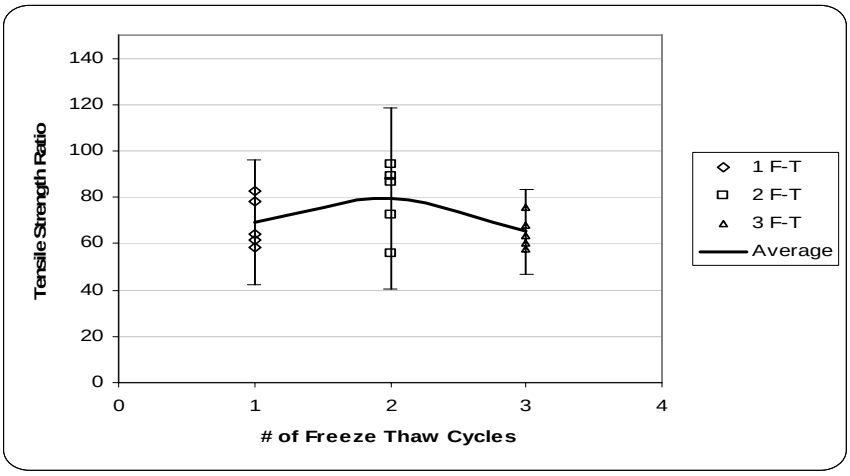

(a) 100mm Superpave

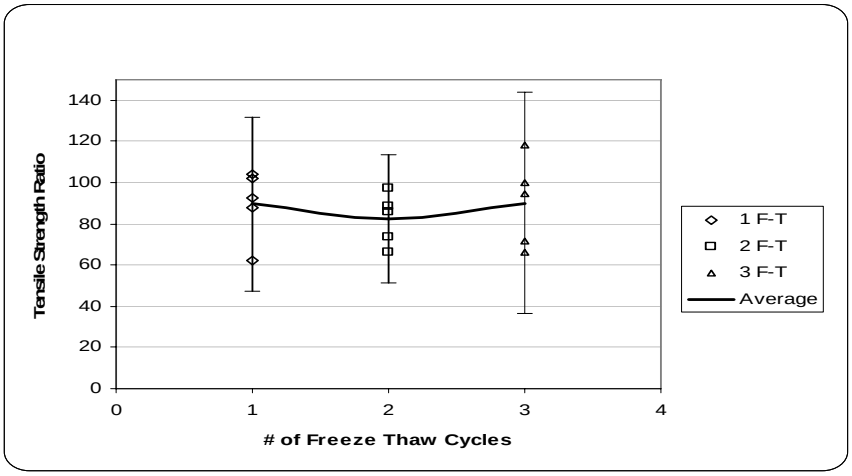

(b) 150mm Superpave

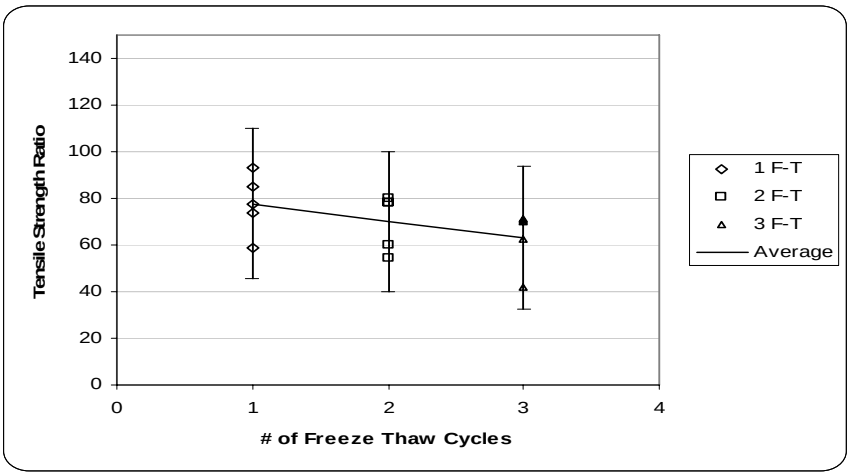

(c) 100mm Marshall

Figure 6.1 M-50 Dundee Average TSR versus Number of Freeze/thaw Cycles with 95% Confidence Intervals

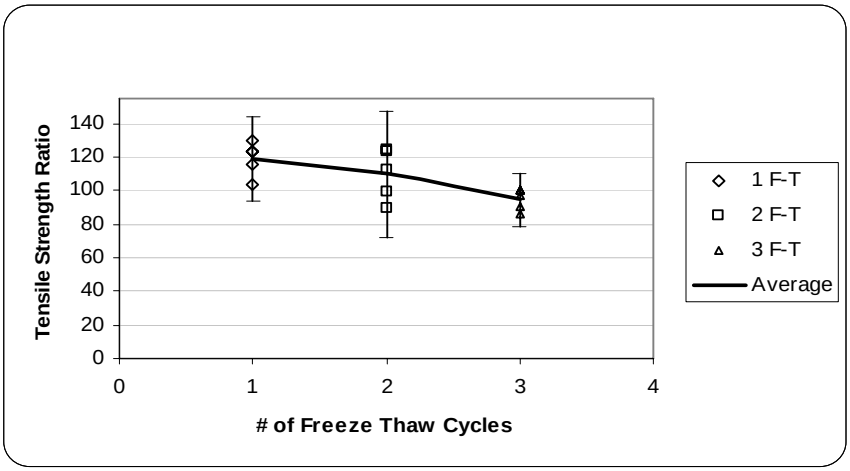

(a) 100mm Superpave

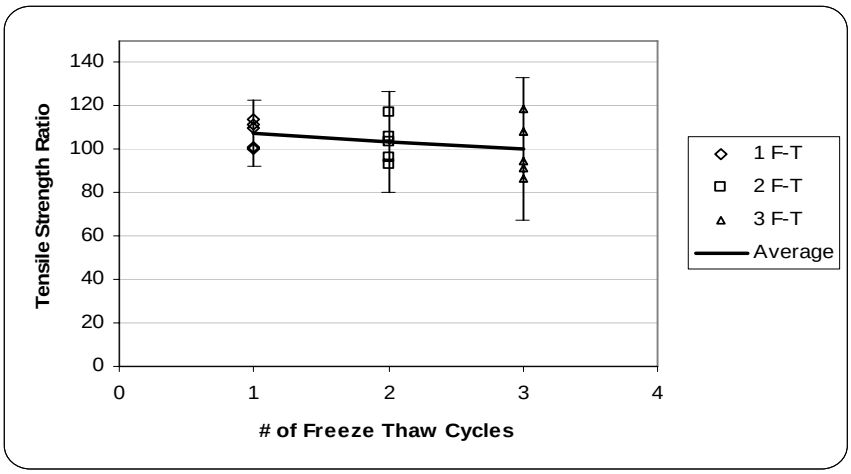

(b) 150mm Superpave

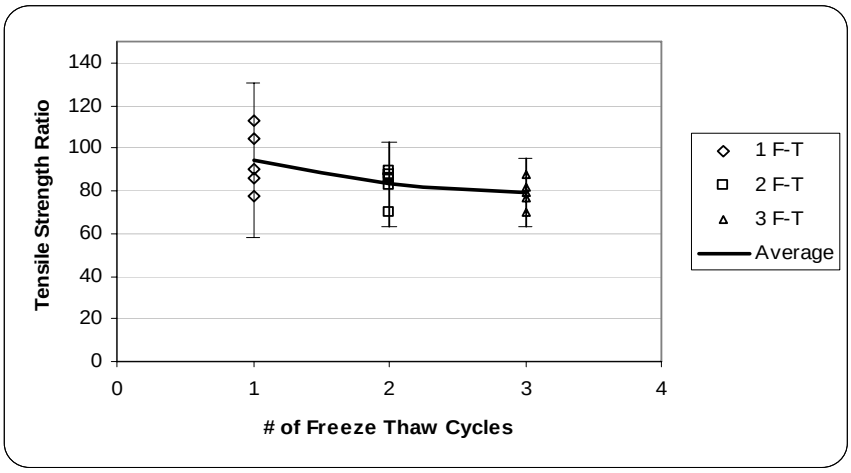

(c) 100mm Marshall

Figure 6.2 M-21 St. Johns Average TSR versus Number of Freeze/thaw Cycles with 95% Confidence Intervals

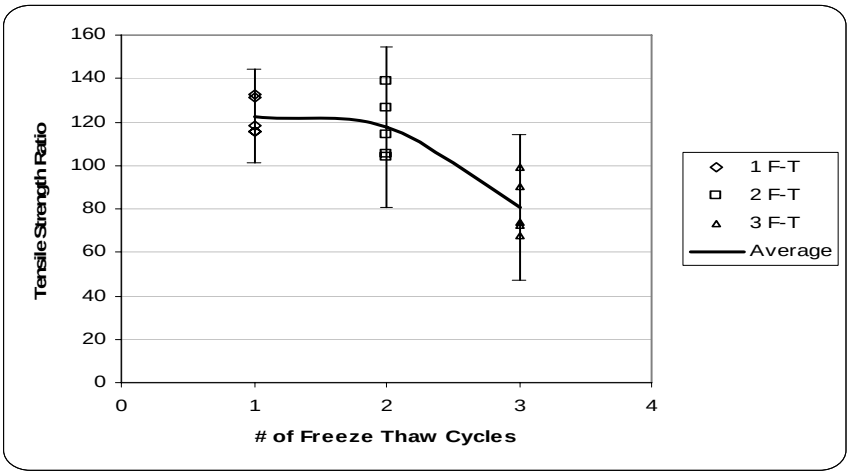

(a) 100mm Superpave

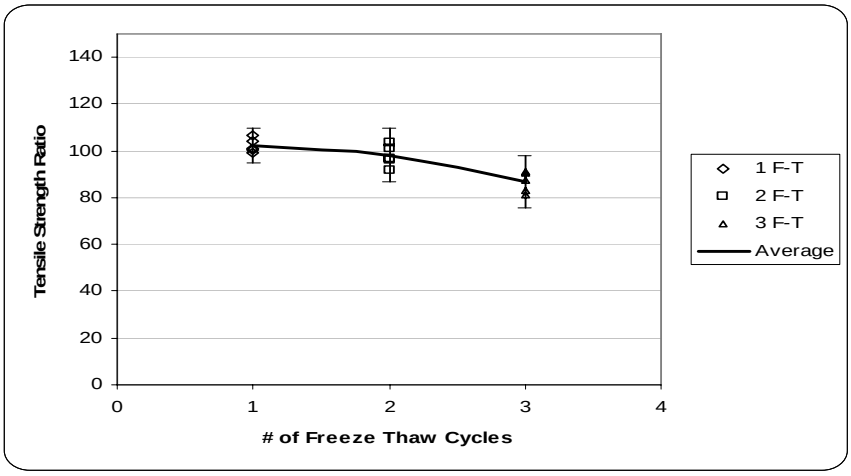

(b) 150mm Superpave

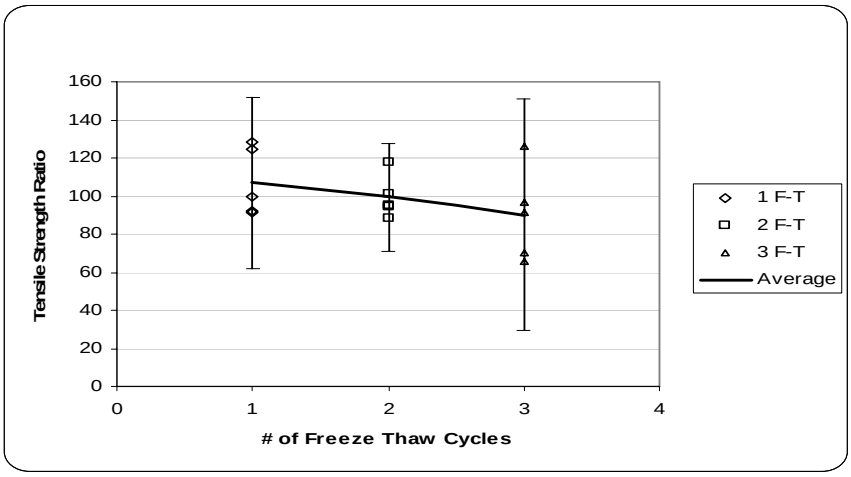

(c) 100mm Marshall

Figure 6.3 BL I-96 Howell Average TSR versus Number of Freeze/thaw Cycles with 95% Confidence Intervals

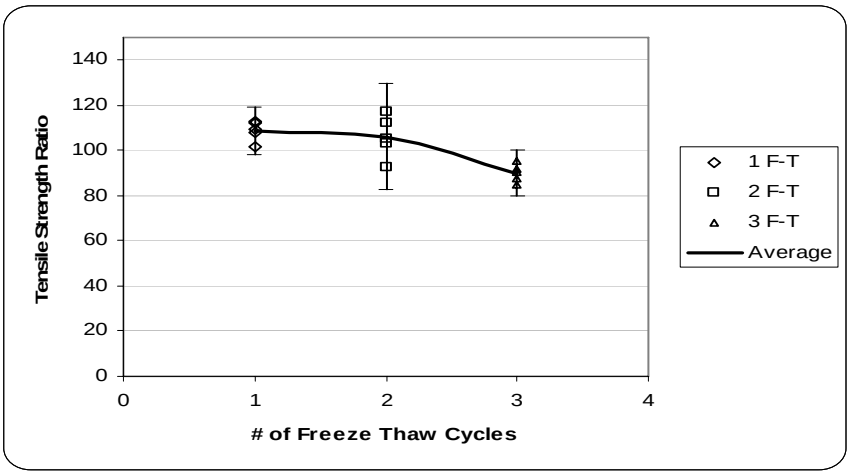

(a) 100mm Superpave

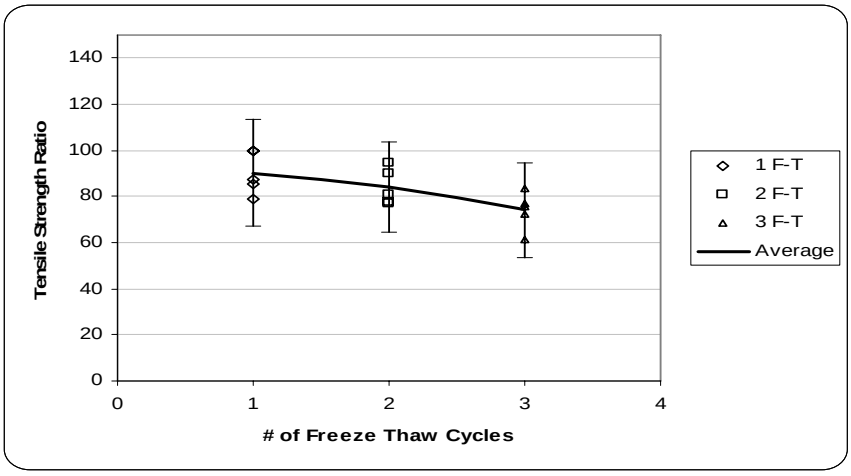

(b) 150mm Superpave

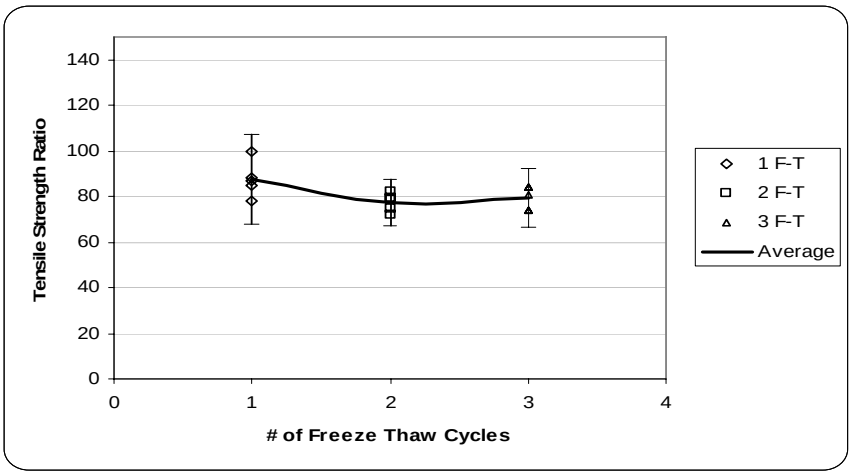

(c) 100mm Marshall

Figure 6.4 M-21 Owosso Average TSR versus Number of Freeze/thaw Cycles with 95% Confidence Intervals

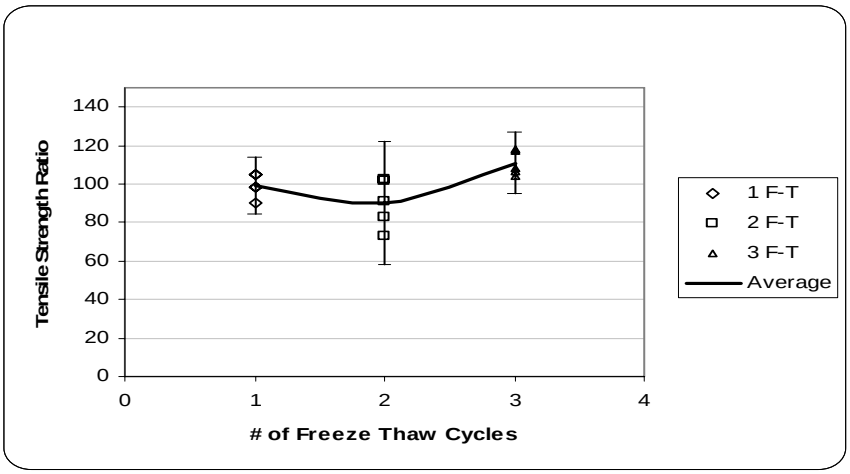

(a) 100mm Superpave

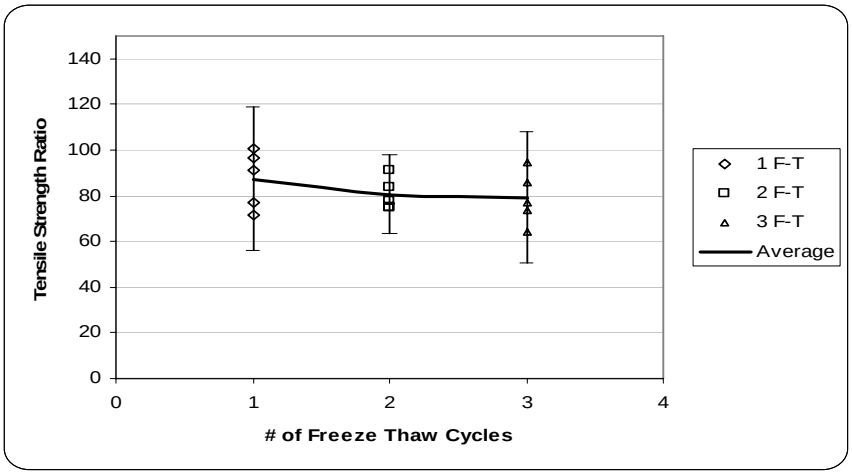

(b) 150mm Superpave

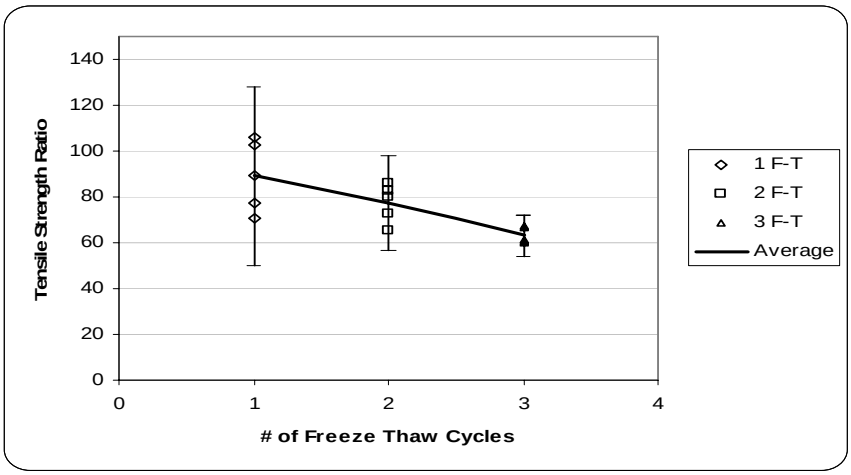

(c) 100mm Marshall

Figure 6.5 M-59 Brighton Average TSR versus Number of Freeze/thaw Cycles with 95% Confidence Intervals

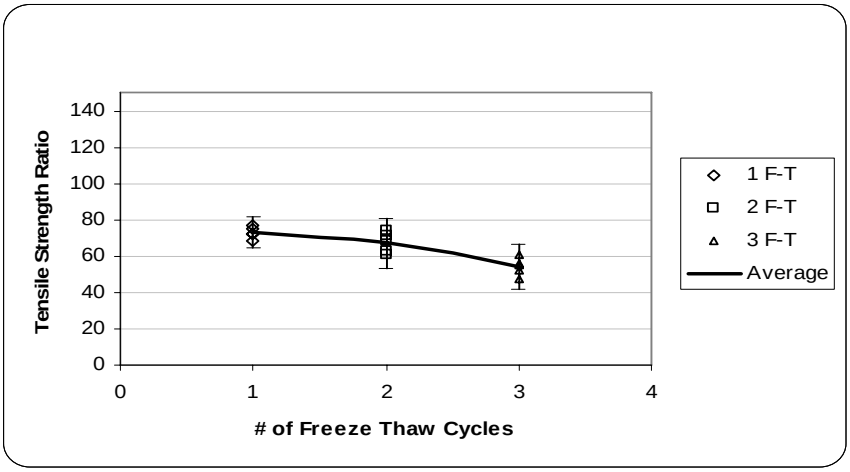

(a) 100mm Superpave

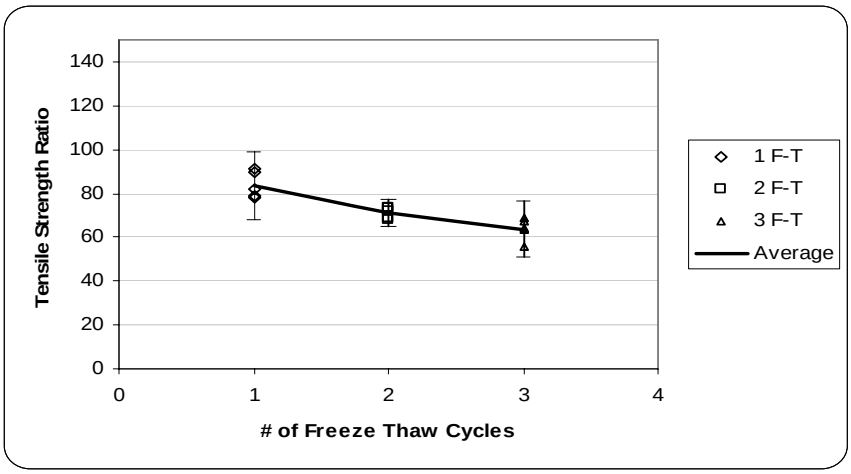

(b) 150mm Superpave

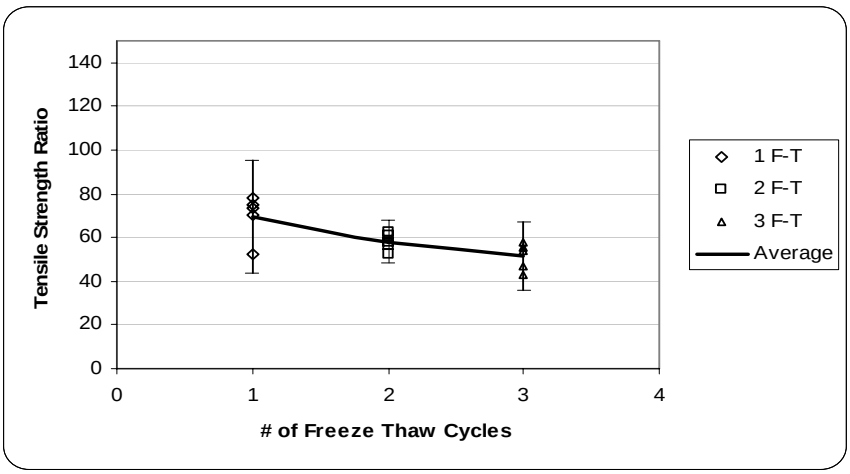

(c) 100mm Marshall

Figure 6.6 I-196 Grand Rapids Average TSR versus Number of Freeze/thaw Cycles with 95% Confidence Intervals

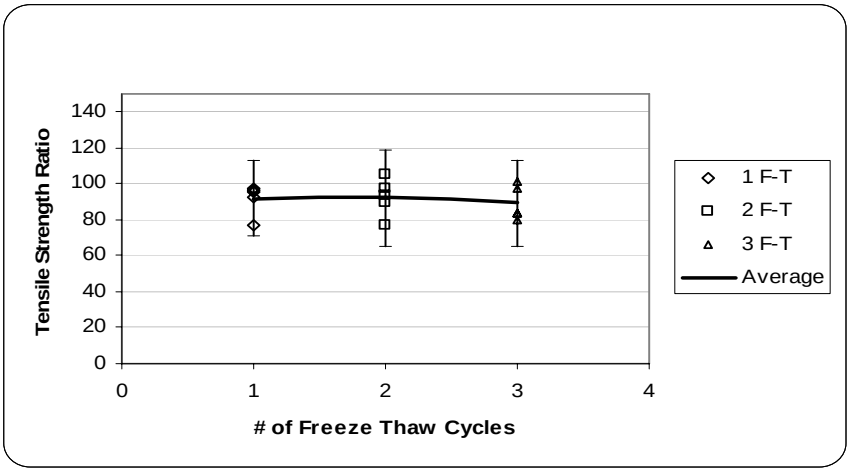

(a) 100mm Superpave

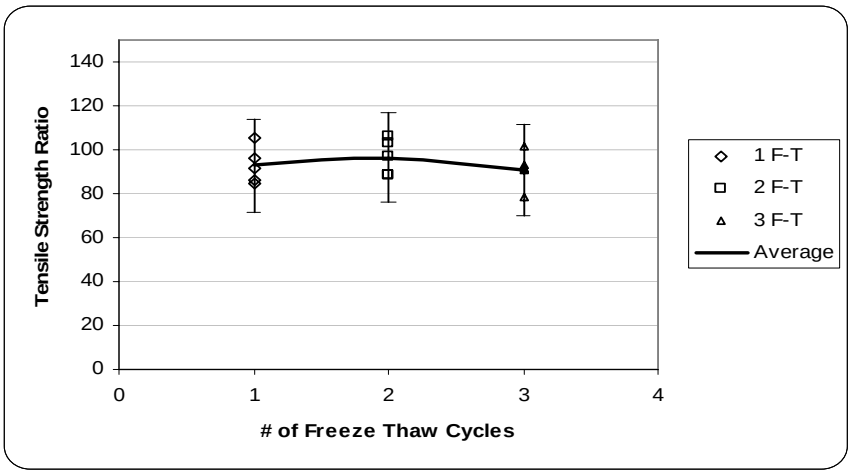

(b) 150mm Superpave

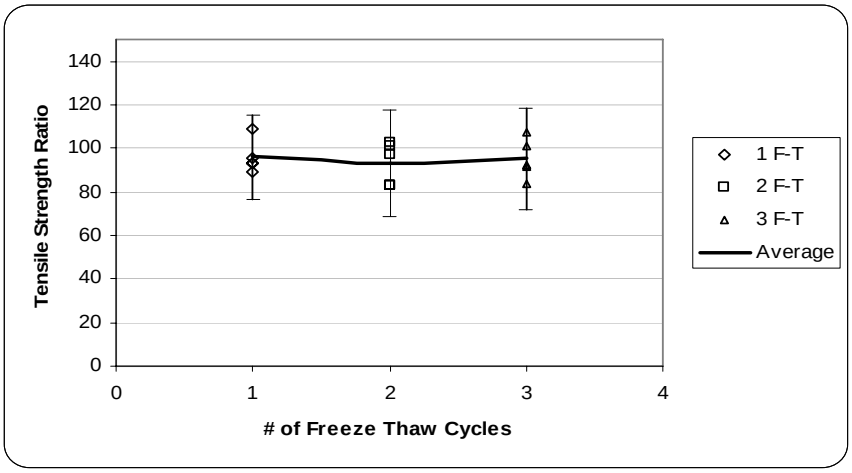

(c) 100mm Marshall

Figure 6.7 I-75 Clarkston Average TSR versus Number of Freeze/thaw Cycles wit 95% Confidence Intervals

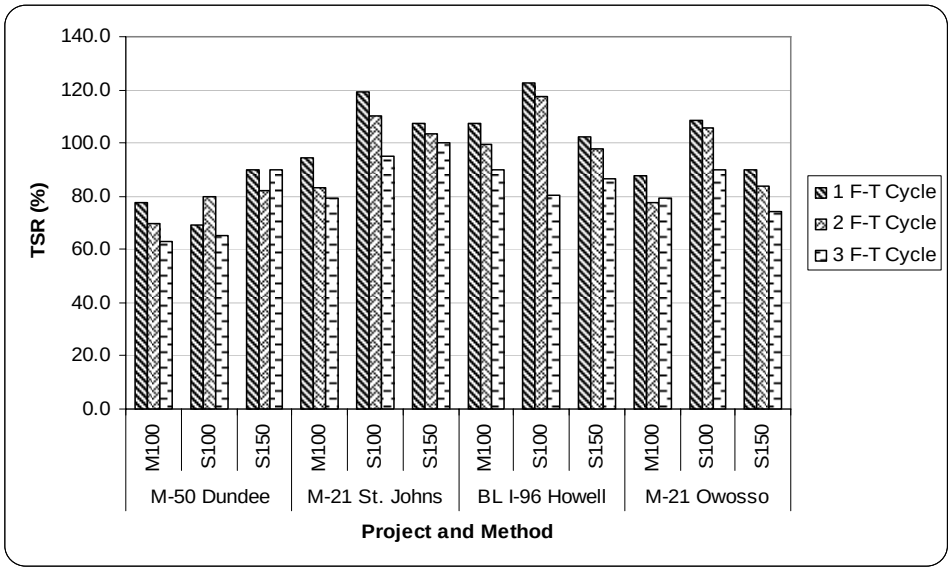

Figure 6.8 Average TSR Results for Traffic Level ≤3,000,000 ESAL's

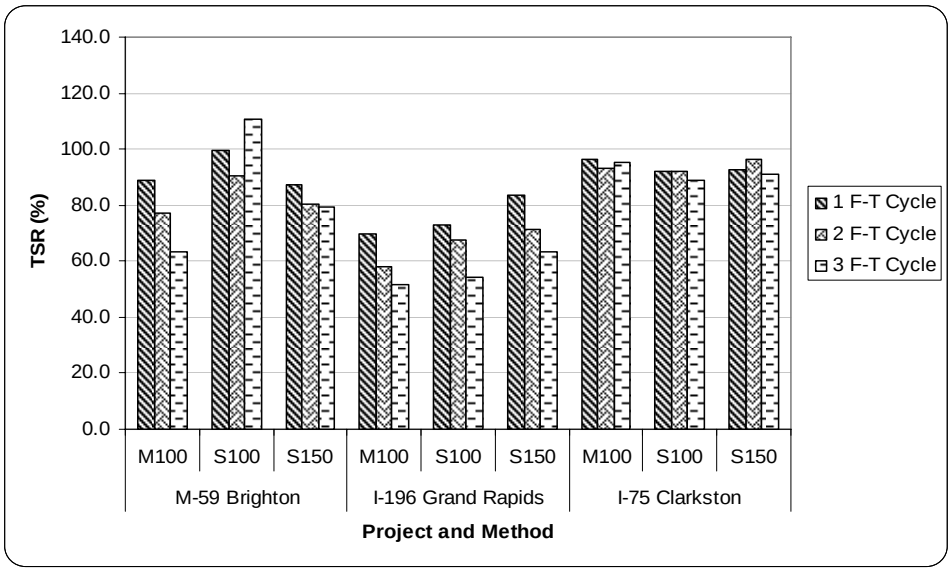

Figure 6.9 Average TSR Results for Traffic Level >3,000,000 ESAL's

Table 6.1 Ranking of Projects Based on TSR

Project	Average TSR for S100			Average TSR for M100			Average TSR for S150		
	TSR 1F-T	TSR 2F-T	TSR 3F-T	TSR 1F-T	TSR 2F-T	TSR 3F-T	TSR 1F-T	TSR 2F-T	TSR 3F-T
M-50 Dundee	1	2	2	2	2	3	3	3	5
BL I-96 Howell	7	7	3	7	7	6	6	6	4
M-21 Owosso	5	5	5	3	4	5	4	4	2
M-59 Brighton	4	3	7	4	3	2	2	2	3
I-196 Grand Rapids	2	1	1	1	1	1	1	1	1
I-75 Clarkston	3	4	4	6	6	7	5	5	6
M-21 St. Johns	6	6	6	5	5	4	7	7	7

6.3 Analysis of Results

Two approaches were used to analyze the above data. The first approach is a statistical approach that analyzes the effects of project, compaction method, and number of freeze/thaw cycles. The second approach used probabilistic analyses to determine a new minimum TSR ratio. The current minimum TSR ratio used is 80% for 100mm Marshall compacted specimens.

The first type of statistical test used is the two-way ANOVA with no interaction to compare the dependent variable, TSR, and two independent factors are project and method of compaction (100mm Superpave, 150mm Superpave, and 100mm Marshall). The goal of this analysis is to determine the number of freeze/thaw cycles required to attain an equivalent amount of damage of one freeze/thaw cycle for the 100mm Marshall specimens for 150mm Superpave gyratory compacted specimens. The compaction method, number of freeze/thaw cycles, and the change in size of the specimens are considered.

Five two-way ANOVAs with no interaction were constructed based on the amount of available data.

- 100mm Marshall versus 100mm Superpave versus 150mm Superpave at one freeze/thaw cycle shows that the TSRs are statistically the same based on method of compaction.

- 100mm Marshall versus 100mm Superpave versus 150mm Superpave at two freeze/thaw cycles show that the TSRs are statistically the same based on method of compaction.
- 100mm Marshall versus 100mm Superpave versus 150mm Superpave at three freeze/thaw cycles show that the TSRs are statistically the same based on method of compaction.
- 100mm Marshall at one freeze/thaw cycle versus 100mm Superpave at two freeze/thaw cycles versus 150mm Superpave at two freeze/thaw cycles show that the TSRs are statistically the same based on method of compaction.
- 100mm Marshall at one freeze/thaw cycle versus 100mm Superpave at three freeze/thaw cycles versus 150mm Superpave at three freeze/thaw cycles show that the TSRs are statistically different based on method of compaction.

Based on the results of the two-way ANOVA, in order to achieve the same moisture damage in the 100mm Marshall specimens, three-freeze/thaw cycles are needed for the 150mm and 100mm Superpave specimens. Generally, a highway agency does not have sufficient time to conduct three freeze/thaw cycles for each paving project during a construction season, therefore the criteria for the TSR ratio needs to be adjusted so one freeze/thaw cycle can still be used.

A second statistical analysis was undertaken to look at the effects of wet strength versus dry strength for each project. A two-sample t-test was used to compare the mean dry strength to the mean wet strength. The following hypothesis was used:

H_o : Dry Strength = Wet Strength
H_A : Dry Strength ≠ Wet Strength
$\alpha = 0.05$

Table 6.2 gives the results of the two-sample t-tests along with the mean TSR for each group. The results show that when dry and wet strengths are statistically different, the average TSR is quite low or close to the threshold value of 80% except in some limited cases. The shaded in cells show those projects that have statistically different strengths for each combination of compaction, diameter, and number of freeze/thaw cycles endured.

Table 6.2 Results of Two-Sample Paired t-Tests

Project	100 mm Marshall					
	1 Freeze-Thaw Cycle		2 Freeze-Thaw Cycle		3 Freeze-Thaw Cycle	
	Paired t-Test Results	Average TSR (%)	Paired t-Test Results	Average TSR (%)	Paired t-Test Results	Average TSR (%)
M-50 Dundee	*Statistically Different*	*78*	*Statistically Different*	*70*	*Statistically Different*	*63*
M-21 St. Johns	Statistically the Same	94	*Statistically Different*	*83*	*Statistically Different*	*79*
BL I-96 Howell	Statistically the Same	107	Statistically the Same	99	Statistically the Same	90
M-21 Owosso	*Statistically Different*	*88*	*Statistically Different*	*77*	*Statistically Different*	*79*
M-59 Brighton	Statistically the Same	89	*Statistically Different*	*77*	*Statistically Different*	*63*
I-196 Grand Rapids	*Statistically Different*	*70*	*Statistically Different*	*58*	*Statistically Different*	*51*
I-75 Clarkston	Statistically the Same	96	Statistically the Same	93	Statistically the Same	95
Project	**100 mm Superpave**					
	1 Freeze-Thaw Cycle		**2 Freeze-Thaw Cycle**		**3 Freeze-Thaw Cycle**	
	Paired t-Test Results	**Average TSR (%)**	**Paired t-Test Results**	**Average TSR (%)**	**Paired t-Test Results**	**Average TSR (%)**
M-50 Dundee	*Statistically Different*	*69*	Statistically the Same	80	*Statistically Different*	*65*
M-21 St. Johns	*Statistically Different*	*119*	Statistically the Same	110	Statistically the Same	95
BL I-96 Howell	*Statistically Different*	*123*	*Statistically Different*	*118*	*Statistically Different*	*81*
M-21 Owosso	*Statistically Different*	*109*	Statistically the Same	106	*Statistically Different*	*90*
M-59 Brighton	Statistically the Same	99	Statistically the Same	90	*Statistically Different*	*111*
I-196 Grand Rapids	*Statistically Different*	*73*	*Statistically Different*	*67*	*Statistically Different*	*54*
I-75 Clarkston	Statistically the Same	92	Statistically the Same	92	Statistically the Same	89
Project	**150 mm Superpave**					
	1 Freeze-Thaw Cycle		**2 Freeze-Thaw Cycle**		**3 Freeze-Thaw Cycle**	
	Paired t-Test Results	**Average TSR (%)**	**Paired t-Test Results**	**Average TSR (%)**	**Paired t-Test Results**	**Average TSR (%)**
M-50 Dundee	Statistically the Same	90	Statistically the Same	82	Statistically the Same	90
M-21 St. Johns	Statistically the Same	107	Statistically the Same	103	Statistically the Same	100
BL I-96 Howell	Statistically the Same	102	Statistically the Same	98	*Statistically Different*	*87*
M-21 Owosso	Statistically the Same	90	*Statistically Different*	*84*	*Statistically Different*	*74*
M-59 Brighton	Statistically the Same	87	*Statistically Different*	*81*	*Statistically Different*	*79*
I-196 Grand Rapids	*Statistically Different*	*84*	*Statistically Different*	*71*	*Statistically Different*	*64*
I-75 Clarkston	Statistically the Same	93	Statistically the Same	96	Statistically the Same	91

A probabilistic analysis was used to determine a new minimum TSR for HMA using 100 and 150mm Superpave gyratory compacted specimens. The lognormal distribution based on the Kolmogorov-Smirnov One-Sample Test using a p-value of 0.05 was selected for the TSR for the different compaction methods and number of freeze/thaw cycles since a lognormal distribution was applicable to all datasets investigated. In addition, a lognormal distribution is an appropriate selection since the TSR cannot be less than zero. The outputs containing the lognormal distribution and the appropriate test statistics can be seen in Appendix C and summarized below in Table 6.3.

Table 6.3 Goodness of Fit Statistics for Phase I Distributions

Compaction Method	Diameter Size (mm)	# of Freeze-Thaw Cycles	Kolmogorov-Smirnov Statistic Lognormal Distribution	p-value
Superpave	150	1	0.15094143	0.045
Superpave	150	2	0.10983981	>0.150
Superpave	150	3	0.10919085	>0.150
Superpave	100	1	0.10134991	>0.150
Superpave	100	2	0.14599732	0.058
Superpave	100	3	0.07556771	>0.150
Marshall	100	1	0.13930827	0.084
Marshall	100	2	0.11497959	>0.150
Marshall	100	3	0.13629187	0.096

Historically, the Michigan Department of Transportation uses a TSR value of 80% after one freeze/thaw cycle for 100mm Marshall specimens as the specification criteria for determining moisture susceptibility (Barak 2005). To determine an equivalent point with 150mm Superpave specimens, several lognormal cumulative probability plots were created. Each cumulative probability plot consisted of pooled strength data for each combination of compaction and diameter. The point on the 100mm Marshall cumulative probability plot that coincided with a TSR value of 80% was determined. A horizontal line was then extended from that point to intersect with the cumulative probability plot for the 150mm Superpave specimens tested after one freeze/thaw cycle. The point of intersection corresponded to a TSR value of 87%, as demonstrated in Figure 6.10. Thus, indicating that a threshold of 87% for TSR should be employed to maintain equivalent standards with the Marshall specimen usage. Following the same procedure, a threshold of 85% is recommended for 100mm Superpave compacted specimens, as can be seen in Figure 6.11. Figure 6.12 shows the current 80% TSR specification for 150mm Superpave gyratory compacted specimens is 70% TSR for 100mm Marshall compacted specimens. These three figures illustrate that the current TSR specification of 80%

needs to be changed if the same acceptance rate of mixtures is to be maintained (Bausano et al. 2006, Kvasnak 2006)

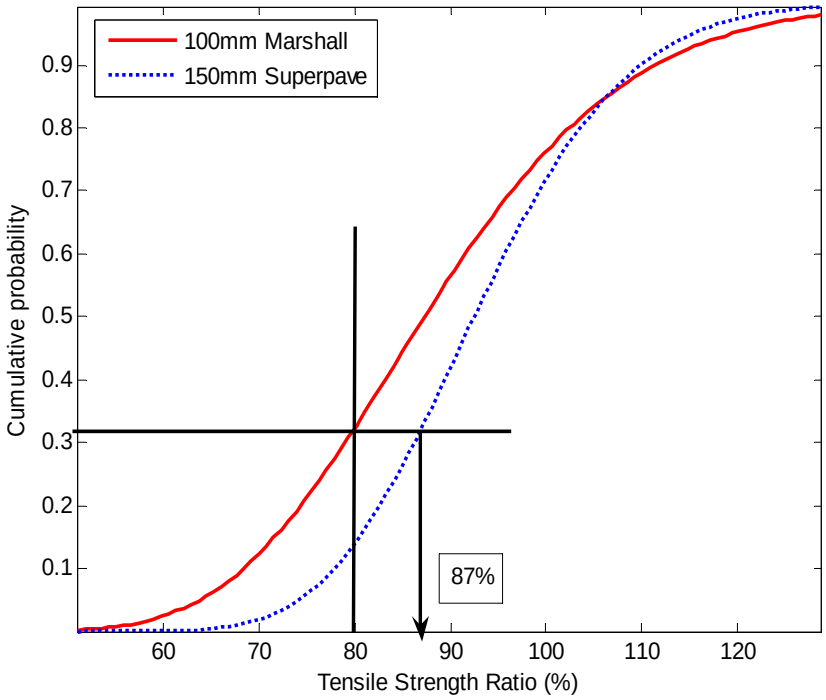

Figure 6.10 100mm Marshall versus 150mm Superpave at one freeze/thaw cycle

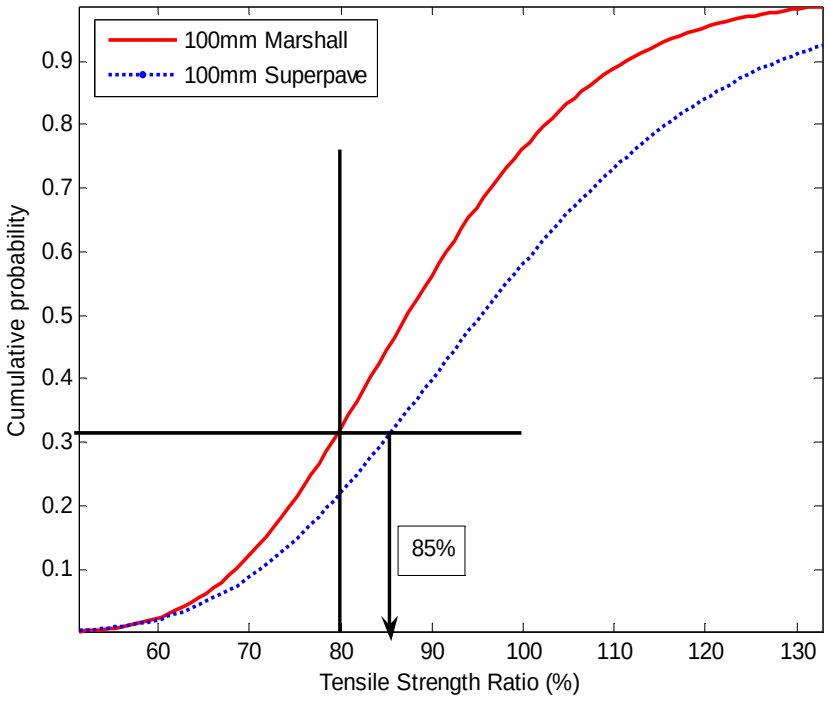

Figure 6.11 100mm Marshall versus 100mm Superpave at one freeze/thaw cycle

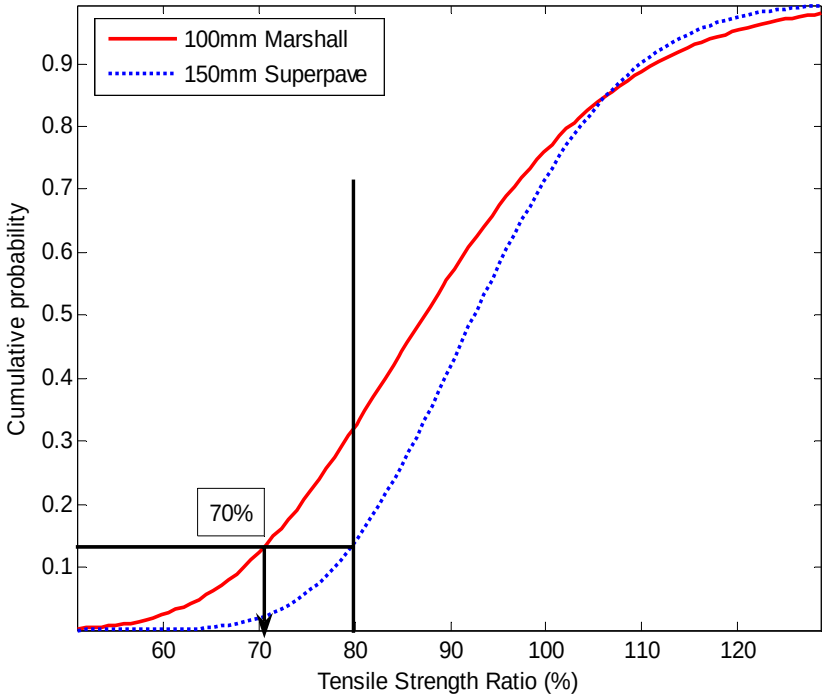

Figure 6.12 100mm Marshall versus 150mm Superpave at one freeze/thaw cycle

6.4 Conclusions

In this sensitivity study, the factors affecting wet strength of a specimen and new thresholds for AASHTO T283 when Superpave compaction method is employed in lieu of the Marshall compaction method are identified. Testing included 100mm Marshall, 100mm Superpave, and 150mm Superpave specimens. Four conditions of each mix type for every compaction and diameter combination were considered. The control condition was the dry state of a specimen and the other conditions were strength of conditioned specimens after one, two, or three freeze/thaw cycles.

AASHTO T283 was developed based on 100mm Marshall compacted specimens. With the transition from 100mm Marshall compacted specimens to 150mm Superpave compacted specimens, it was felt that the requirements outlined in AASHTO T283 should be re-evaluated. It was discovered that three freeze/thaw cycles for conditioning is needed when using specimens

created using 150mm Superpave specimens. However, to continue using one freeze/thaw cycle and maintain the same probability level as attained with a TSR value for 80% for 100mm Marshall compacted specimens, a TSR value of 87% and 85% should be used for 150mm and 100mm Superpave compacted specimens, respectively. If an 80% TSR for 150mm Superpave specimens is used, this would correspond to a TSR ratio of 70% for 100mm Marshall specimens (Bausano et al 2006, Kvasnak 2006).

CHAPTER 7 PRELIMINARY BINDER STUDY TEST RESULTS

7.1 Introduction

Statistical analyses were conducted to determine which factors significantly affected complex shear modulus results when using modified DSR parts. Both original binders and mastics were evaluated. The main type of analysis used was ANOVA with level of significance of 0.05. P-values from ANOVA tables will be presented. It should be remembered that a low (in this case below 0.05) indicates a significant factor, while a high p-value is associated with an insignificant factor.

7.2 Gap Size and Interface Selection

It was hypothesized that ceramic discs would be a better interface for moisture susceptibility testing of asphalt binders, and thus the hypothesis needed to be tested. Both ceramic and stainless steel interfaces were tested using AAA-1 and AAM-1 asphalt binders at different gap sizes. As mentioned earlier, original binders were used for all gap size tests while binders with fillers were only used for testing with a 500-µm and 1000µm gap. The gap sizes evaluated were 200µm, 300µm, 500µm, and 1000µm for both binders and interface types.

It has been hypothesized that a smaller gap size would yield more reliable results since a small gap size would be closer to actual film thicknesses found in pavements. However, the issue that emerged with the smaller gap size was unrepeatable results. It is speculated that one of the issues contributing to the lack of repeatability is non-parallel plates. DSRs were designed based on parallel plate theory, which assumes the surface of a spindle is parallel to the surface of a base plate. If a plate is slightly askew, thus violating the parallel plate requirement, readings may not be accurate. Lack of parallelism has a less significant effect when a larger versus a smaller gap size when the degree of skewness is the same gap size is used. The effects of an

angle created by an askew plate are magnified when a small gap size is used (Dongre 2006). Table 7.1 summarizes the repeatability analysis performed on the 200µm and 300µm gap size. Cells labeled "Yes" are results that were repeatable, whereas ones labeled "No" were not repeatable, based on a 5% level of significance. It can be seen that over half of the tests conducted were unrepeatable. The lack of repeatability indicates that a different gap sizes should be considered.

Table 7.1 Repeatability of 200µm and 300µm Gap Size

Complex Modulus									
Binder	Bath	Original Binder				RTFO Aged Binder			
		200 micrometer		300 micrometer		200 micrometer		300 micrometer	
		Stainless Steel	Ceramic	Stainless Steel	Ceramic	Stainless Steel	Ceramic	Stainless Steel	Ceramic
AAA-1	Water	No	Yes	No	No	No	No	Yes	No
AAA-1	Air	Yes	No	No	No	Yes	No	No	Yes
AAM-1	Water	Yes	Yes	Yes	No	Yes	No	Yes	Yes
AAM-1	Air	No	Yes	No	No	No	Yes	Yes	No

After examining the 200µm and 300µm gap sizes, 500µm and 1000µm gap sizes, evaluation of an appropriate gap size occurred. It should be noted that 1000µm is the current standard gap size for binders tested using the Superpave grading system. Both the 500µm and 1000µm gap sizes were statistically viable gap sizes for the unaged original binders.

Comparisons between a stainless steel interface and a ceramic one yielded varying results based on gap size. No statistical difference was observed for the complex shear modulus and phase angle results between a stainless steel and ceramic interface for 200µm and 300µm gap sizes. The inability of the test to distinguish between the two interfaces could be associated with a high level of variability of measurements acquired at these smaller gap sizes. Statistical differences between rheological properties of specimens tested with ceramic versus those tested with steel existed when gap sizes of 500µm and 1000µm were used for original binders.

Additional testing was conducted with the 500µm and 1000µm gap sizes using filler modified asphalt binders. Two fillers were selected; hydrated lime and a silica based ones.

500μm and 1000μm gap sizes were used to test AAA-1 and AAM-1 with 3 percentage levels of the two fillers. During testing with fillers, it was discovered that some of the binders with silica could not be measured for complex shear modulus and phase angle at the 500μm gap size. Further difficulties were faced with the 500μm gap size with some silica modified binders that yielded unrepeatable results. These issues were not observed with the 1000μm, hence the selection of a 1000μm gap size for testing with modified DSR parts.

Multiway ANOVAs were employed to determine which factors significantly contribute to different complex shear modulus values. The main effects considered were binder type (AAA-1 or AAM-1), filler type (hydrated lime or silica), percent of filler (5%, 10%, or 20%), disc material (stainless steel or ceramic), gap size (500μm or 1000μm), and testing environment (water bath or air chamber). Table 7.2 summarizes the calculated p-values obtained from an ANOVA. All of the main effects considered were deemed statistically significant. This implies that each of these factors contributed to changes in complex shear modulus readings. Interaction effects were also considered within this ANOVA. Interestingly, the interaction between binder type and filler type was not considered a significant contributor to the complex shear modulus variability. It has been speculated that chemical compatibility between binders and fillers would results in significantly different complex shear modulus values. It is hypothesized that certain levels of filler accounts for significant levels of complex shear modulus variability. It should be noted that the interaction between binder and percent level does not distinguish between hydrated lime and silica. Additional analysis will be presented that examines this more complex relationship. The interaction between binder type and disc type was also regarded as significant with respect to complex shear modulus variability. The precise reasoning for this interaction is not clear, but it is speculated that either absorption of binder into a disc or friction created

between a disc and binder results in different complex shear modulus readings. Since filler and disc interactions do not have an effect on complex shear modulus variability friction may not be the cause of low p-values for binder and disc interactions. Based on filler and disc not being a cause, it is likely possible that the absorption of the binder into a disc resulted in a low p-value. Another surprising relationship that did not significantly affect complex shear modulus measurements was the interaction between binder type and environmental testing condition (Kvasnak 2006).

Table 7.2 P-Values of Main and Interaction Effects on Complex Shear Modulus Results

Effect	P-Values
binder	<.0001
filler	<.0001
percent	<.0001
disc	0.0003
gap	<.0001
bath	<.0001
binder*filler	0.3524
binder*percent	0.0229
binder*disc	0.0033
filler*percent	0.0041
filler*disc	0.6379
filler*bath	0.3286
filler*gap	<.0001
binder*bath	0.4009

7.3 Saturation Effects on Asphalt Binders

Saturation effects were analyzed by testing unsaturated, saturated, saturated plus one freeze/thaw cycle specimens. For this testing only ceramic insets were used in the modified DSR parts. Analyses were conducted to determine if saturation or saturation plus one freeze/thaw cycle has an effect on complex shear modulus values. According to the analysis, there is a significant difference between unsaturated and saturated specimens. However, there is no statistical difference between saturation plus one freeze/thaw versus either unsaturated or saturated specimens. This would indicate that it is sufficient to test just unsaturated and saturated

specimens. More freeze/thaw cycles could be examined, but to remain consistent with current freeze/thaw testing procedures for HMA mix, only one freeze/thaw cycle was considered.

The viscous and elastic moduli results were examined next. For the AAA-1 binder, it was found that the viscous modulus changed much more than the elastic modulus when comparing between unsaturated, saturated, and saturated plus one freeze/thaw cycle. The significant difference between viscous moduli for AAM-1 asphalt binders was less than that of AAA-1. Both AAA-1 and AAM-1 yielded statistically different elastic moduli values for saturated and unsaturated specimens. Testing of binders also found that the elastic moduli values for saturated and saturated plus one freeze/thaw were statistically equivalent. The analysis shows that the viscous component of asphalt binders changes the most with saturation in comparison to the elastic component. In general, saturation caused the complex shear modulus to decrease for the original binders. Table 7.3 lists the p-values obtained by conducting mean comparisons between the listed groups (Kvasnak 2006).

Table 7.3 P-Values of Condition Comparisons of Original Binders

Binder	Condition Comparison	Elastic Modulus	Viscous modulus
AAA-1	*Saturated vs Unsaturated*	0.0006	0.0002
	Saturated vs Saturated Plus Freeze-Thaw	0.1526	0.0018
	Unsaturated vs Saturated Plus Freeze-Thaw	0.1530	0.0020
AAM-1	*Saturated vs Unsaturated*	0.0007	0.0006
	Saturated vs Saturated Plus Freeze-Thaw	0.6172	0.0304
	Unsaturated vs Saturated Plus Freeze-Thaw	0.0262	0.0031

7.4 Delay Effects on Asphalt Binders

Some of the modified binders were used to see if there was any effect on the specimens if left in a DSR. The time intervals considered were 0, 5, 10, and 20 minutes. Binders were tested at their high PG temperature. Both stainless steel and ceramic discs were employed in determining delay effects on complex shear modulus values. Comparisons were made between complex shear modulus values at different delay times. Table 7.4 summarizes the results of these comparisons. According to the results, there is no significant statistical difference in testing a specimen that has been in a water bath anywhere from zero to 20 minutes (Kvasnak 2006).

Table 7.4 P-Values Comparing Delay Times

Time Comparison (minutes)	P-value
0 vs 5	0.8697
0 vs 10	0.9158
0 vs 20	0.5386
5 vs 10	0.9740
5 vs 20	0.4639
10 vs 20	0.5330

7.5 AAA-1 and AAM-1 DSR Testing Conclusions

A new moisture susceptibility test was developed using modified DSR parts. Testing was conducted to determine if material interface affects complex shear modulus results. It was determined that material interface does affect complex shear modulus results. Hence for the new test protocol, ceramic discs would be used to allow for water to access the top of a binder sample in addition to the circumference of a sample. Further testing was conducted to establish an appropriate gap size for a new testing procedure. The gap size selected was 1000μm. Subsequent testing indicated that the new test procedure is sensitive to binder type and addition of filler. The test also appears to be able to distinguish between filler type. Additional testing

indicated that statistically different complex shear modulus results were obtained from unsaturated asphalt binder samples versus saturated specimens. However, no additional differences were observed with the samples were moisture saturated and had endured one freeze/thaw cycle. There were also no statistical differences in complex shear modulus readings when leaving a specimen in a heated water bath anywhere from zero to 20 minutes prior to testing.

Based on laboratory testing and statistical analysis a new test procedure was established in this report. Specimens would be tested first unsaturated with ceramic discs at a gap of 1000µm. Second the specimens would soak in a water bath for a period of 24 hours at 25˚C. After 24 hours of soaking, specimens would be tested again in a DSR using ceramic discs. Table 7.2 summarized results from an ANOVA indicating that binder type, filler type, percent of filler, disc material, gap size, testing environment, interaction between binder type and percent of filler, interaction between binder type and disc material, and interaction between filler type and gap size were all deemed significant factors contributing to differences in complex shear modulus (Kvasnak 2006).

CHAPTER 8 TESTING OF MICHIGAN MIXES FOR MOISTURE DAMAGE – PHASE II

8.1 Introduction

This chapter discusses the results of the expanded experimental plan which includes twenty-one HMA mixtures that were sampled throughout the state of Michigan. The test results for conducting AASHTO T283 and the proposed test procedure using dynamic modulus will be provided. The chapter will also provide the analysis of the testing results using statistical procedures to analyze the data and to look at properties that may affect moisture damage including gradation, nominal maximum aggregate size NMAS, traffic, polymer modification, aggregate type, permeability, asphalt content, FAA, RAP, and frequency (for dynamic modulus only).

8.2 Experimental Plan

The Phase II expanded experimental plan considers different mix types, aggregate sources, and laboratory test systems. The experimental plan includes two integrated plans: one for the mixes and one for the planned laboratory tests. A sensitivity study on the effects of specimen size and compaction method was accomplished in the Phase I testing to determine the amount of conditioning that should be done on larger Superpave compacted specimens. Table 8.1 below outlines the expanded experimental plan.

Table 8.1 Expanded Experimental Plan for Phase II Projects

PHASE 2 MOISTURE		
NMAS (mm)	Traffic Level (ESAL's)	
	≤ 3,000,000	>3,000,000
25.0 or 19.0	Limestone - M50 Dundee	Limestone - M59 Brighton
	Limestone - M36 Pinckney	Limestone - Michigan Ave. Detroit
	Gravel - M45 Grand Rapids	Limestone - Vandyke Detroit
	Gravel - M21 St. Johns	Limestone - US23 Hartland
	Limestone - M84 Saginaw	Gravel - I-75 Levering Road
12.5 or 9.5	Limestone - BL96 Howell	Limestone - I-196 Grand Rapids
	Gravel - M21 Owosso	Slag/Gabbro - I-75 Clarkston
	Gravel - M66 Battle Creek	Gravel - M53 Detroit
	Limestone - M50 Dundee	Limestone - Michigan Ave. Detroit
	Limestone - US12 MIS	Gabbro I-75 Toledo (in MI)
SMA	N/A	Gabbro - I-94 SMA Ann Arbor

Table 8.2 below outlines the laboratory testing experimental plan. The test temperature and moisture conditioning of the specimens is determined in the Phase I sensitivity study. The proposed methods of determining moisture susceptibility will be compared to the current method of determining moisture susceptibility from which any conclusions and recommendations will be drawn upon.

Table 8.2 Laboratory Experimental Plan for Phase II

		Unconditioned	Conditioned
Test System	AASHTO T283	XXXXX	XXXXX
	Dynamic Complex Modulus	XXX	XXX
	Asphalt Pavement Analyzer	XXX	XXX
	Dynamic Shear Rheometer – Asphalt Binder	XXX	XXX
	Dynamic Shear Rheometer – Mastic	XXX	XXX

8.3 AASHTO T283 Test Results

Figures 9.1 and 9.2 illustrate the variability of TSRs among each project. Ninety-five percent confidence intervals around the mean were fit to the data. Figure 8.1 shows the TSRs for low volume roads (≤3,000,000 ESALs) and Figure 8.2 shows the TSRs for high volume roads (>3,000,000 ESALs). The data shows that generally higher volume roads exhibited higher TSRs than lower volume roads. Figure 8.3 shows good agreement (correlation) between dry strength and wet strength. It appears that at low strengths the regression line is close to the line of equality but as the strength increases, the regression line diverges away from the line of equality.

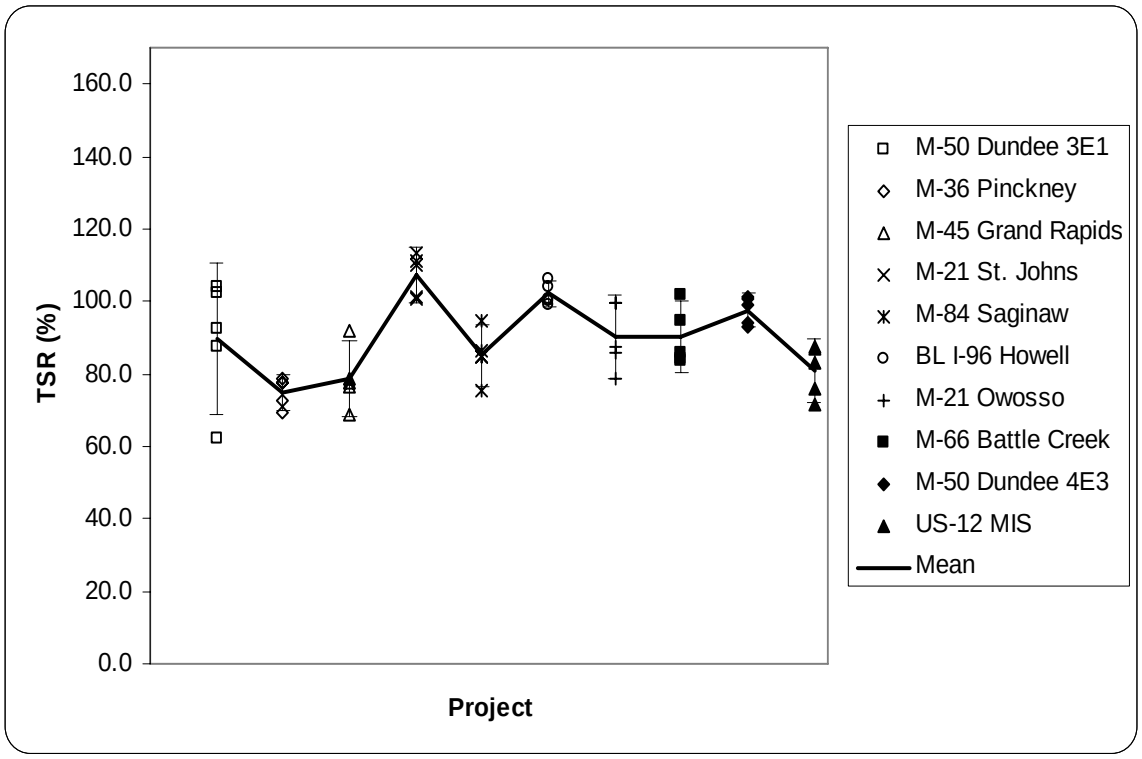

Figure 8.1 AASHTO T283 Test Results for Traffic Level ≤3,000,000 ESALs with 95% Confidence Intervals

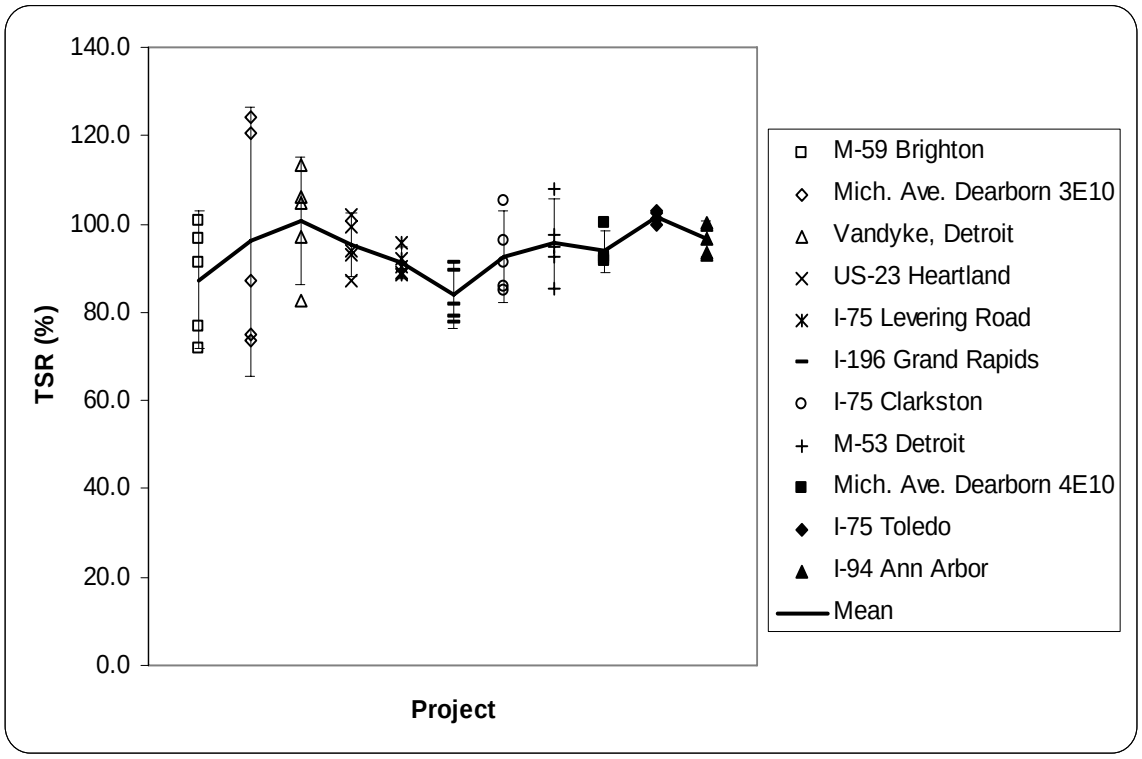

Figure 8.2 AASHTO T283 Test Results for Traffic Level >3,000,000 ESALs with 95% Confidence Intervals

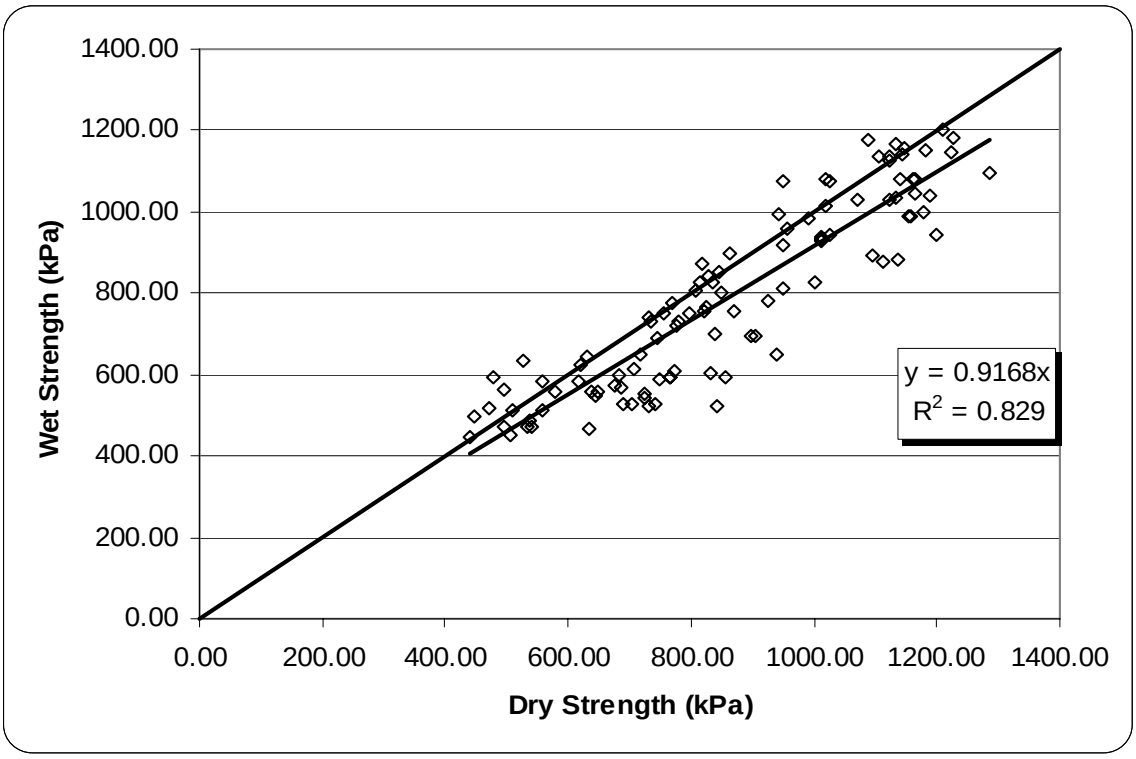

Figure 8.3 Dry Strength versus Wet Strength (Pooled Data)

8.4 Dynamic Modulus Test Results

Figures 8.4 to 8.15 illustrate the variability of E* ratios at each frequency among each project. Ninety-five percent confidence intervals around the mean were fit to the data. Figures 8.4 to 8.9 show the E* ratios for low volume roads (≤3,000,000 ESALs) and Figures 8.10, to 8.15 show the E* ratios for high volume roads (>3,000,000 ESALs). The test temperature that each project was conducted at was the effective test temperature for rutting. The data shows that higher volume roads have higher E* ratios than the lower volume roads. It should also be noted that E* ratio cannot be negative and the confidence interval cannot be negative. Figure 8.16 shows a good agreement between unconditioned E* values and moisture conditioned E* values. It appears that at low E* values the regression line is close to the line of equality but as the E* increases, the regression line diverges from the line of equality similar to that of AASHTO T283

strength values. It was noticed that the 95% confidence intervals were rather broad, and this is due to the fact that only three samples were tested. Additional testing of the samples is needed in order to reduce the variability. NCHRP Report 465 concludes that a coefficient of variation (COV) less than 30% is good, and the data shown in the figures below exhibit COV values below this level but evaluation of the 95% confidence intervals, much variability still exists. The variability is due to the fact that only three specimens were tested for the control group and three specimens for the conditioned group. Since the specimens that have been conditioned are prone to additional variabilitydue to the conditioning, additional specimens should be tested in the future to reduce the variability.

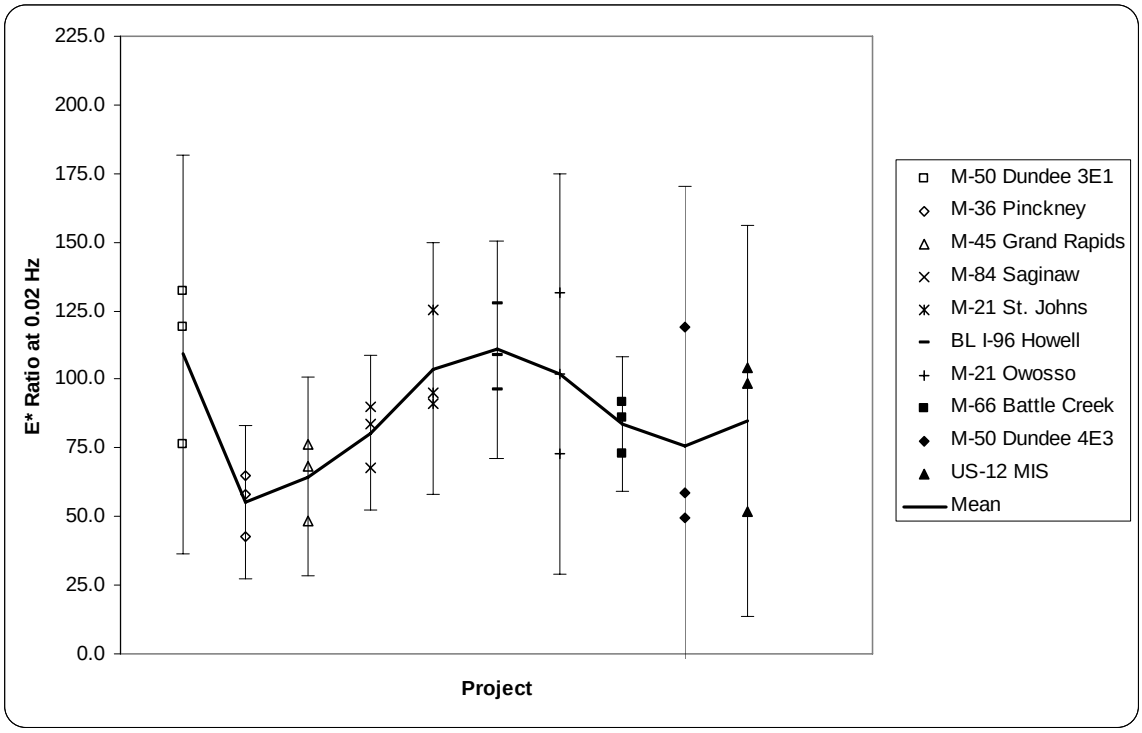

Figure 8.4 Dynamic Modulus With Freeze/Thaw Conditioning Test Results for Traffic Level ≤3,000,000 ESALs with 95% Confidence Intervals

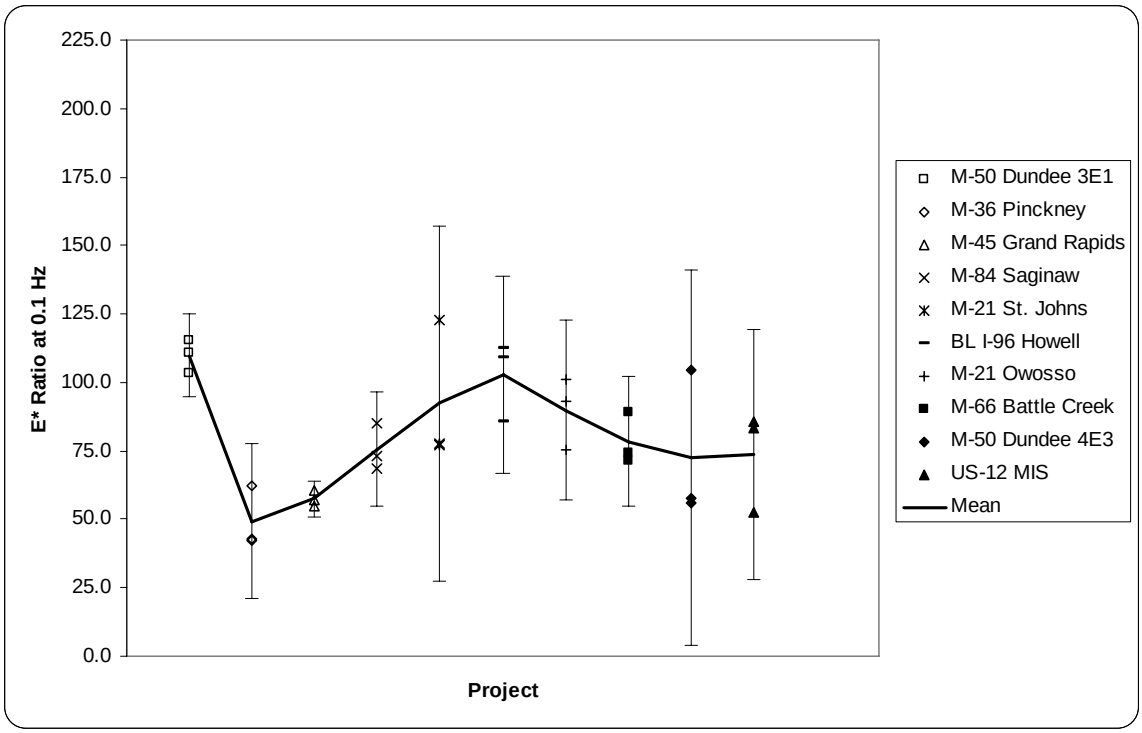

Figure 8.5 Dynamic Modulus with Freeze/Thaw Conditioning Test Results for Traffic Level ≤3,000,000 ESALs with 95% Confidence Intervals

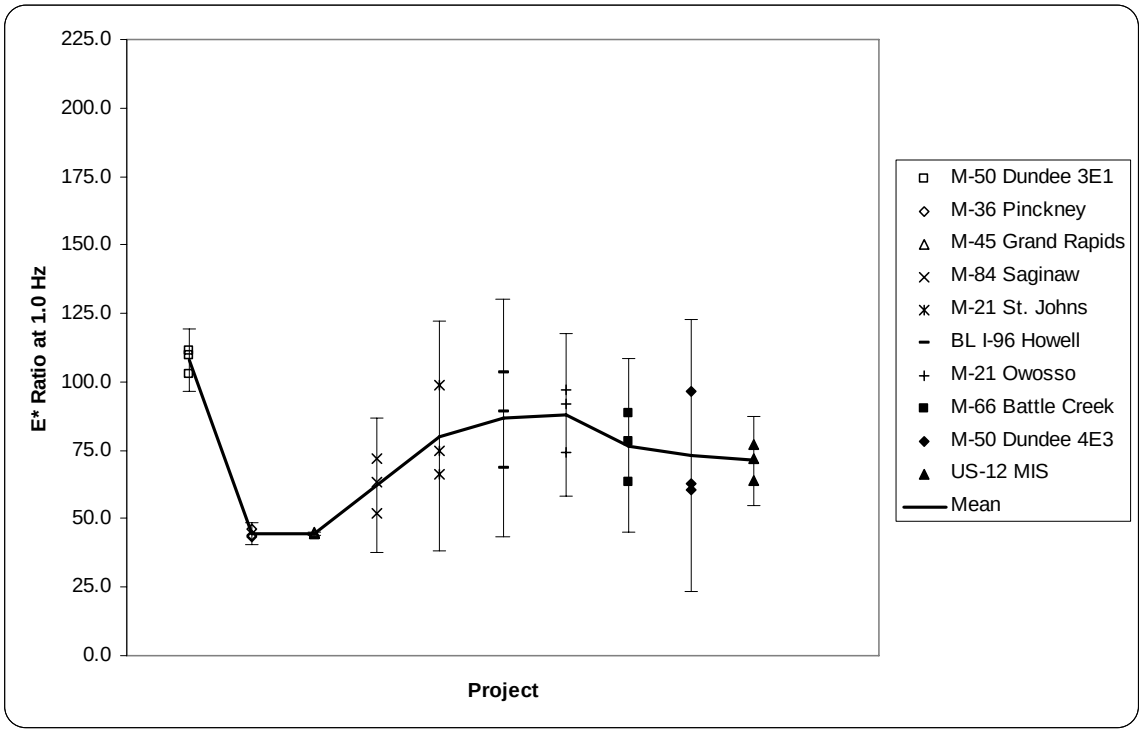

Figure 8.6 Dynamic Modulus with Freeze/Thaw Conditioning Test Results for Traffic Level ≤3,000,000 ESALs with 95% Confidence Intervals

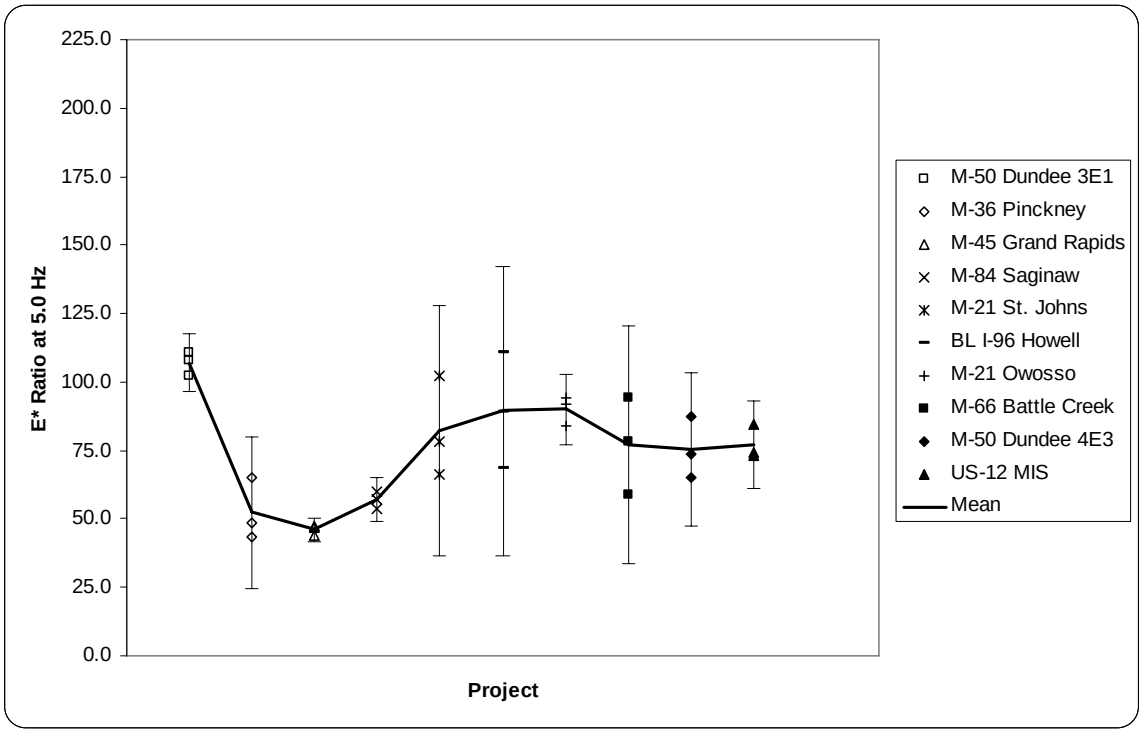

Figure 8.7 Dynamic Modulus with Freeze/Thaw Conditioning Test Results for Traffic Level ≤3,000,000 ESALs with 95% Confidence Intervals

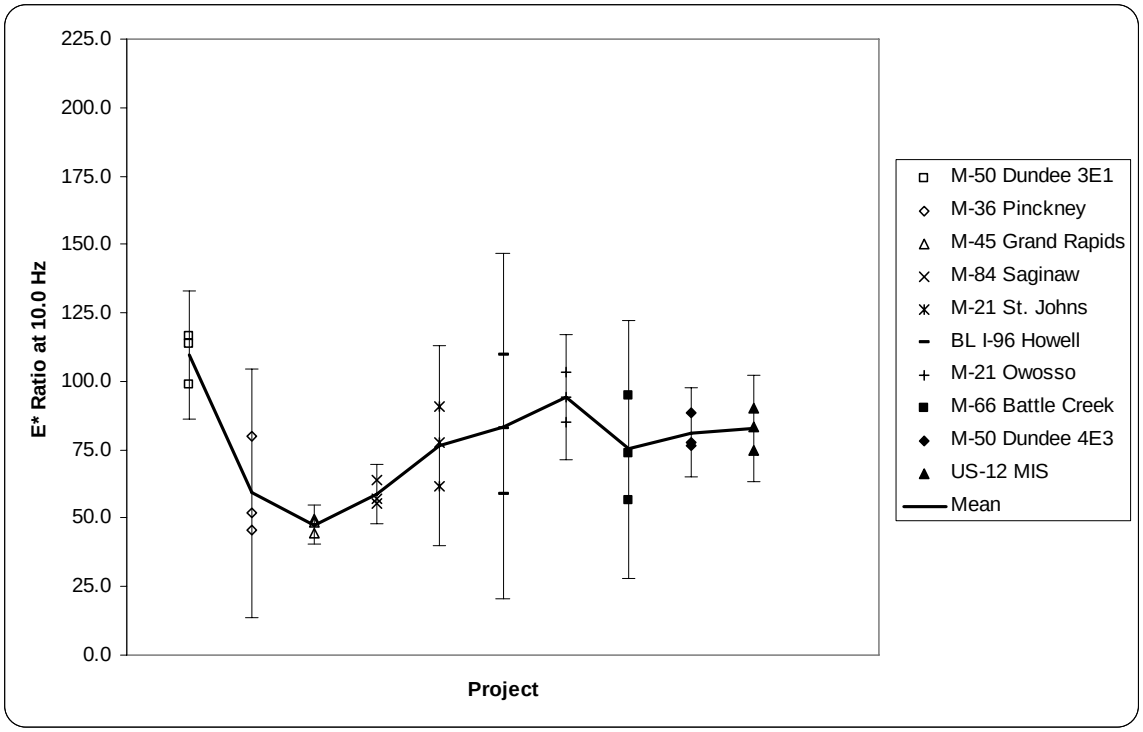

Figure 8.8 Dynamic Modulus with Freeze/Thaw Conditioning Test Results for Traffic Level ≤3,000,000 ESALs with 95% Confidence Intervals

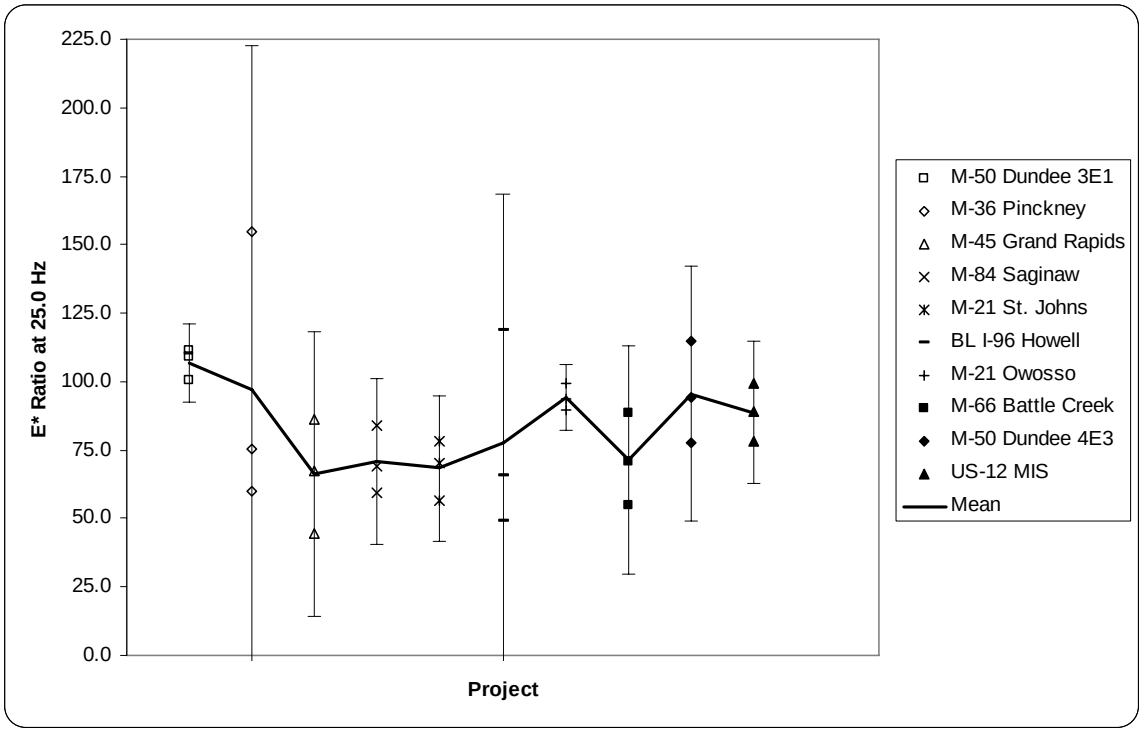

Figure 8.9 Dynamic Modulus with Freeze/Thaw Conditioning Test Results for Traffic Level ≤3,000,000 ESALs with 95% Confidence Intervals

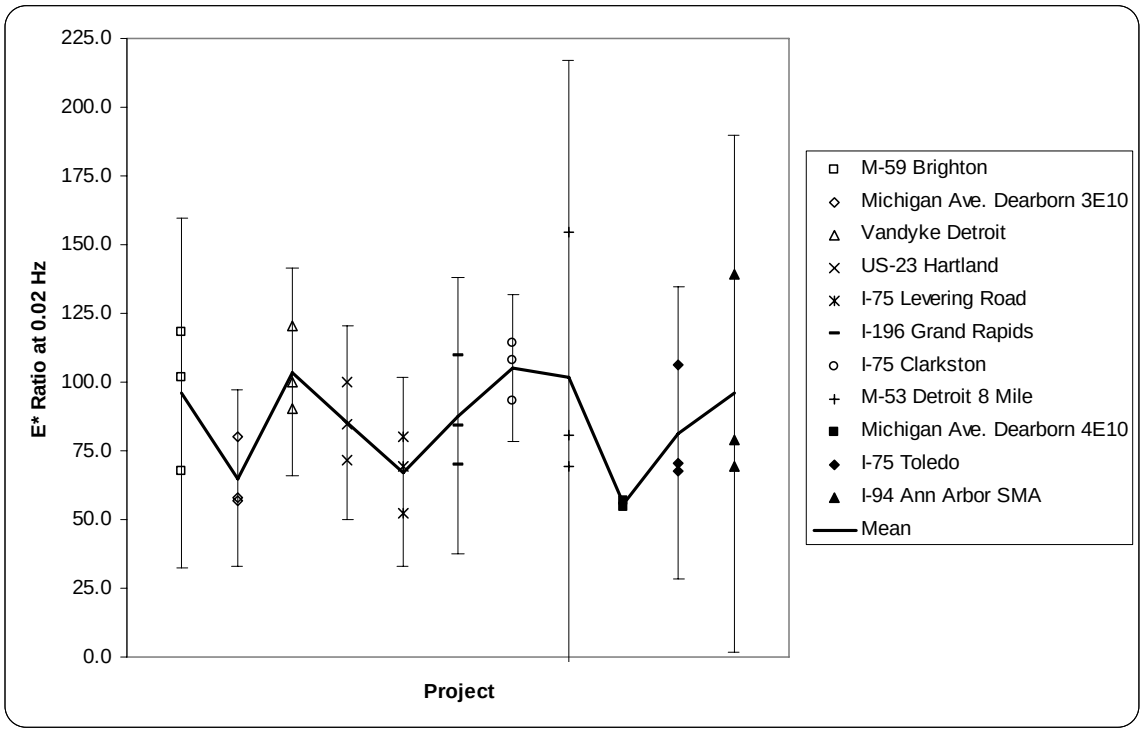

Figure 8.10 Dynamic Modulus With Freeze/Thaw Conditioning Test Results for Traffic Level >3,000,000 ESALs with 95% Confidence Intervals

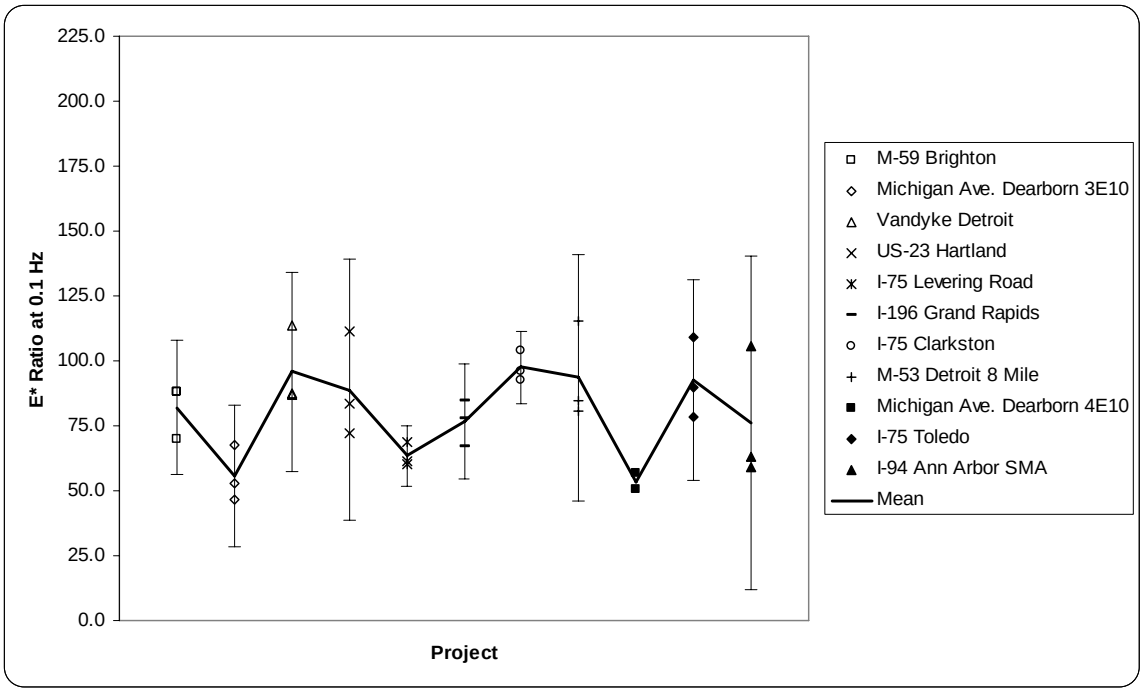

Figure 8.11 Dynamic Modulus with Freeze/thaw Conditioning Test Results for Traffic Level >3,000,000 ESALs with 95% Confidence Intervals

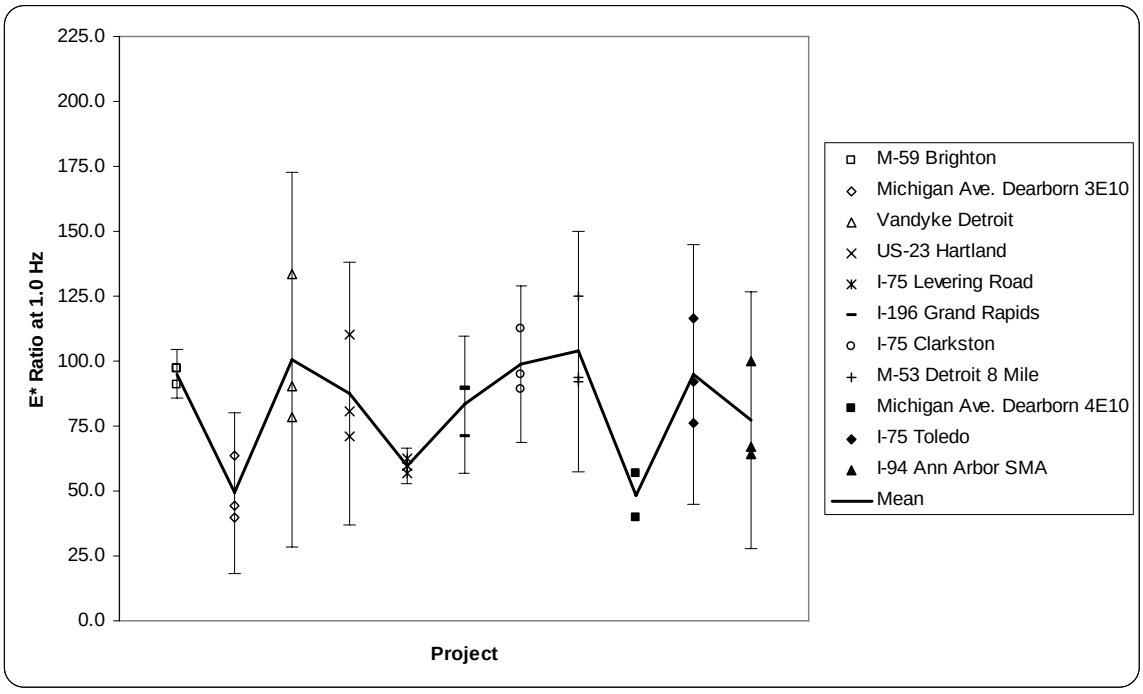

Figure 8.12 Dynamic Modulus with Freeze/Thaw Conditioning Test Results for Traffic Level >3,000,000 ESALs with 95% Confidence Intervals

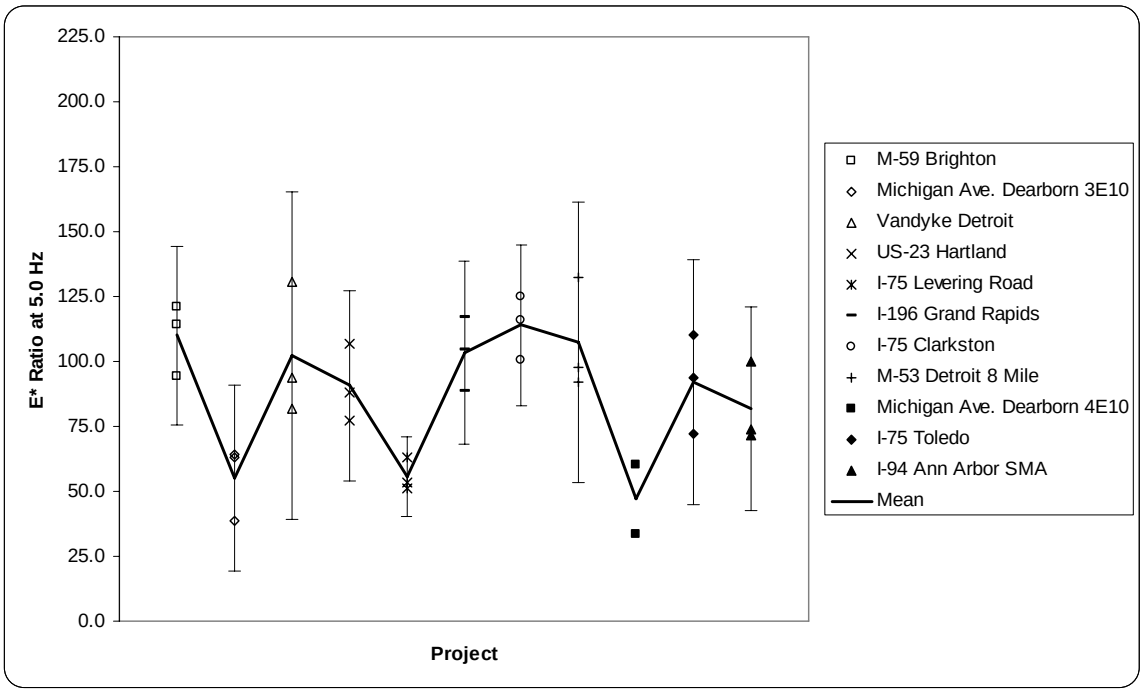

Figure 8.13 Dynamic Modulus with Freeze/Thaw Conditioning Test Results for Traffic Level >3,000,000 ESALs with 95% Confidence Intervals

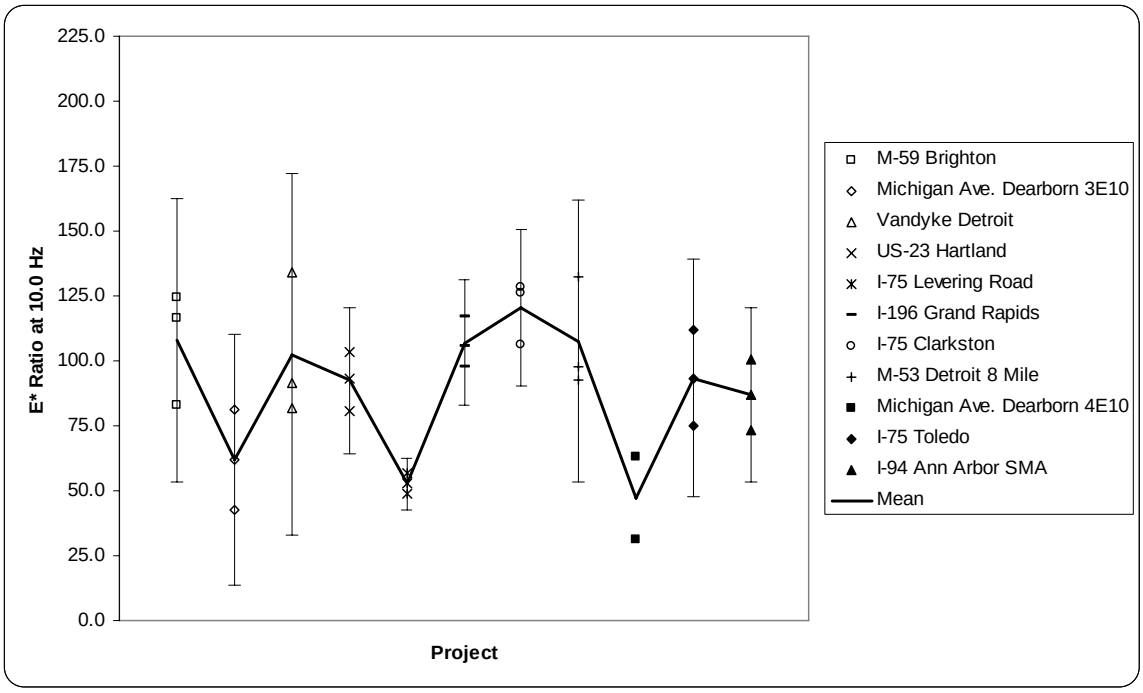

Figure 8.14 Dynamic Modulus with Freeze/Thaw Conditioning Test Results for Traffic Level >3,000,000 ESALs with 95% Confidence Intervals

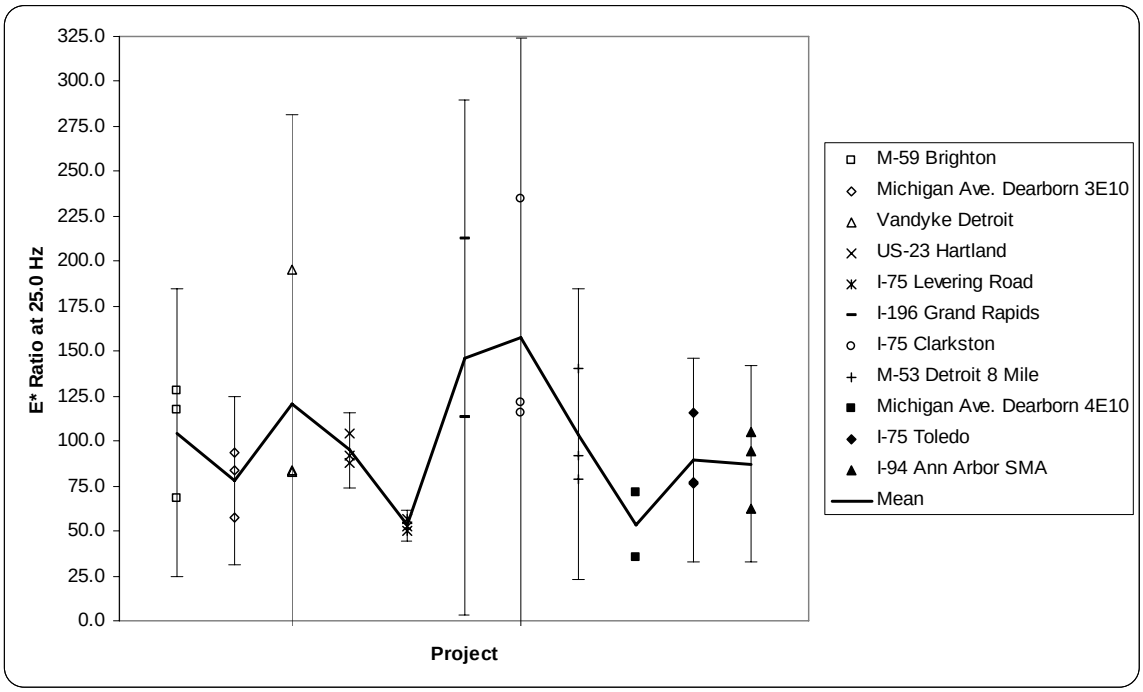

Figure 8.15 Dynamic Modulus with Freeze/Thaw Conditioning Test Results for Traffic Level >3,000,000 ESALs with 95% Confidence Intervals

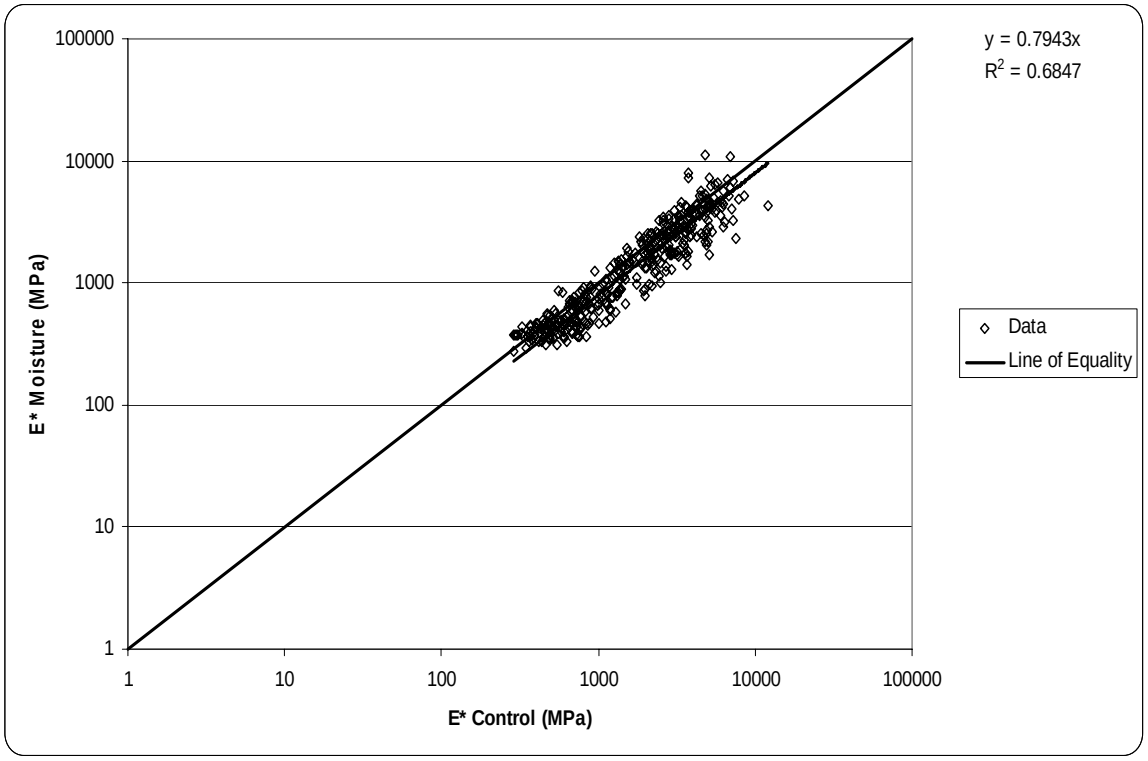

Figure 8.16 Dry E* versus Wet E* (Pooled Data)

8.5 DSR Test Results

As with the SHRP materials reference library (MRL) binders, binders collected from around Michigan were mixed with hydrated lime and silica filler. The hydrated lime and silica used for creating mastics was the same for both the SHRP MRL binders and Michigan binders. Mixing of the fillers with binders was conducted in the same manner as outlined previously for the SHRP MRL mastics. Once mastics had been procured 25mm specimens were made with standard 25mm molds and allowed to rest for the required 10 minutes prior to testing. Specimen attachment and DSR zeroing was conducted in the same manner as was detailed earlier for AAA-1 and AAM-1 binder testing.

The samples tested with the ceramic disks were examined with the DSR twice. The first examination occurred with unconditioned samples. After the first test, the disk and binder

cylinder were placed in a water bath with 25˚C distilled water for a period of 24 hours. After 24 hours of soaking, the specimens were retested as conditioned specimens. Both testing procedures were tested with the water bath and air chamber separately. Table 8.3 summarized the different testing conditions employed for each binder. As the table indicates, 28 different scenarios were conducted for each binder, yielding 588 scenarios for all 21 binders.

8.5.1 Materials for Field Binder Testing

The binders selected for analysis were collected from the field and encompassed a range of Performance Grades (PG). Three categories of PG high temperature were available for analysis: PG 58, 64, and 70. Binders were tested at the high temperature (e.g. 58˚C or 64˚C) with exception of the binders with a high temperature of 70, these were tested at 64˚C. The discrepancy in test temperature for the PG 70-X binders was based on the knowledge that the PG 70-X was only used to allow for better rutting performance in the field where high traffic volumes were expected. Some of the binders contained polymers while others were neat.

Table 8.3 summarizes the number of tests conducted for each condition state and filler-binder combination.

Table 8.3 Samples Tested

		Water Bath			Air Chamber		
		Performance High Grade			Performance High Grade		
		58	*64*	*70*	*58*	*64*	*70*
Original Binder	Unconditioned	18	27	18	18	27	18
	Saturated	18	27	18	18	27	18
5% Hydrated Lime	Unconditioned	18	27	18	18	27	18
	Saturated	18	27	18	18	27	18
10% Hydrated Lime	Unconditioned	18	27	18	18	27	18
	Saturated	18	27	18	18	27	18
20% Hydrated Lime	Unconditioned	18	27	18	18	27	18
	Saturated	18	27	18	18	27	18
5% Silica	Unconditioned	18	27	18	18	27	18
	Saturated	18	27	18	18	27	18
10% Silica	Unconditioned	18	27	18	18	27	18
	Saturated	18	27	18	18	27	18
20% Silica	Unconditioned	18	27	18	18	27	18
	Saturated	18	27	18	18	27	18

8.4 Testing Plan for Each Michigan Binder

Binder	Environment	Mastic	Percentage of Mastic	Unconditioned	Conditioned
1	Water	Lime	5	XXX	XXX
			10	XXX	XXX
			20	XXX	XXX
		Silica	5	XXX	XXX
			10	XXX	XXX
			20	XXX	XXX
		None	0	XXX	XXX
	Air	Lime	5	XXX	XXX
			10	XXX	XXX
			20	XXX	XXX
		Silica	5	XXX	XXX
			10	XXX	XXX
			20	XXX	XXX
		None	0	XXX	XXX

8.5.2 Statistical and Graphical Results of Michigan Binder Tests

Upon the conclusion of testing all 588 combinations, statistical analyses were conducted to determine statistically significant factors and moisture susceptible binders. All of the statistical analyses assumed a level of significance of 0.05.

8.5.3 Statistical and Graphical Comparisons of All Michigan Binders

The initial set of statistical analysis examined all of the data prior to categorizing the DSR test results by possible significant factors. Figure 8.17 displays the data collected from the modified DSR spindle and base plate configuration. It is difficult to distinguish a graphical trend using all of this data; thus indicating that there are no obvious trends that should be evaluated first. It is however apparent that the majority of complex modulus values are less than 10000 pascals. Several t-tests were employed to help ascertain important information. Figure 8.7 summarizes the t-tests calculated to obtain significant information.

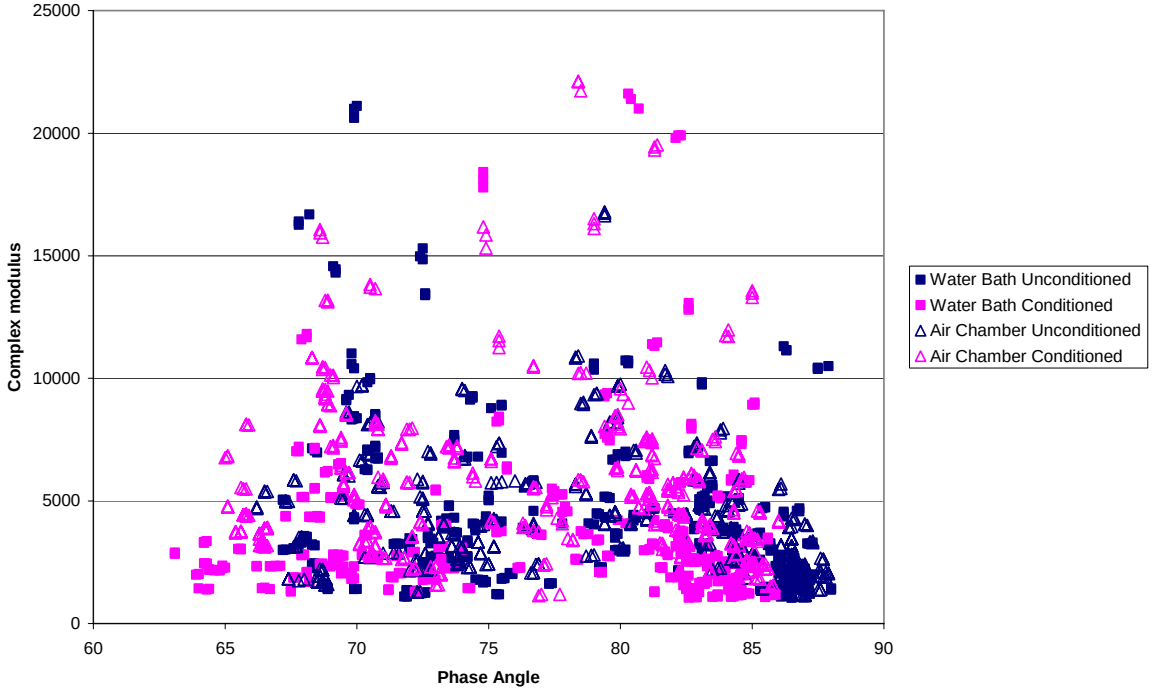

Figure 8.17 Graphical Comparison of Environmental Testing Conditions for All Data

8.6 Development of a Moisture Susceptibility Criteria

Twenty-one binders were collected from paving construction sites around the state of Michigan. The binders collected varied in performance grade. Table 8.5 summarizes the binders tested. The testing procedure developed in the previous chapter was used to evaluate the moisture susceptibility of the field binders.

Table 8.5 Summary of Binders Tested

Site	PG High Temperature	PG Low Temperature	Polymer	Polymer Percent	Asphalt Source
Ann Arbor	70	-22	Cellulose Fibers	0.3	T & M Oil
Battle Creek	64	-28	None	-	Michigan Paving and Materials
Brighton	58	-22	None	-	Marathon Detroit
Clarkston	70	-22	Modifier	Unknown	Marathon Detroit
Detroit	70	-22	Modifier	Unknown	Marathon Detroit
Dundee 12.5mm NMAS	64	-28	None	-	MTM Oil
Dundee 19mm NMAS	64	-28	None	-	Marathon Detroit
Grand Rapids I-196	64	-22	None	-	Michigan Paving and Materials
Grand Rapids M-45	58	-28	Antistrip	0.3	T & M Oil
Hartland	64	-22	None	-	Marathon Detroit
Howell	70	-28	Modifier	Unknown	Michigan Paving and Materials
Levering	58	-28	None	-	British Petroleum
Michigan Ave 12.5mm NMAS	70	-22	Modifier	Unknown	Marathon Detroit
Michigan Ave 19mm NMAS	58	-28	None	-	Marathon Detroit
Michigan International Speedway	64	-28	None	-	Marathon Detroit
Owosso	64	-28	None	-	Michigan Paving and Materials
Pinckney	64	-22	None	-	Marathon Detroit
Saginaw	58	-28	None	-	Marathon Detroit
St. Johns	58	-22	None	-	Michigan Paving and Materials
Toledo	70	-22	Modifier	Unknown	6505 MPM Oil
Van Dyke	64	-22	None	-	Marathon Detroit

As previously mentioned, several moisture susceptibility tests exist for HMA pavements. For example, the modified Lottman test is often used to determine the moisture susceptibility of a mix. Unfortunately, attempts at establishing a moisture susceptible test for asphalt binders have been fairly ineffective. Previously a new test method to determine the moisture susceptibility of asphalt binders was presented using a DSR (Rottermand 2004, Kvasnak 2006). The proceeding sections outline a preliminary moisture susceptibility criterion for the newly developed moisture susceptibility test for asphalt binders.

8.6.1 Hypotheses

It was initially hypothesized that specimens tested in a water bath would yield differing asphalt binder measurements than those tested in the temperature controlled air chamber. Conditioned specimens were predicted to generate different asphalt binder measurements than unconditioned specimens. Since differences in asphalt binder measurements were anticipated, it was decided that specimens would not be identified as moisture susceptible simply because of divergences in asphalt binder properties for water bath tested, temperature controlled air chamber

tested, unconditioned, or conditioned specimens. It was realized that a guideline for categorizing asphalt binders as either moisture susceptible or moisture resistant was needed that considered more than a difference between asphalt binder measurements. The following sections outline the development of a moisture susceptibility criterion for asphalt binders tested using a modified base plate and spindle in a DSR (Kvasnak 2006).

8.6.2 Asphalt Binder Criteria

When researchers established criteria for asphalt binder tests incorporated in the Superpave system a consensus of asphalt binder minimums was reached by an Expert Task Group. The minimum proposed by the Expert Task Group was verified by subsequent testing (Dongre, 2006). There was an initial inclination to only examine the change in the viscous component, but it was realized that the elastic component should be incorporated in the criteria system. The inclusion of both elastic and viscous components prompted the use of $G^*/\sin(\delta)$ in the Superpave criteria (Dongre 2006). The minimum criterion established for unaged binders is that $G^*/\sin(\delta)$ exceeds 1.0kPa.

The performance grade specification associated with the Superpave system was adapted for establishing a specification for surface treatments. Numerous Texas Department of Transportation (TxDOT) agencies completed surveys on distresses identified for surface treatments and rated the successfulness of certain surface treatments in the field. The information collected from the cooperating TxDOT was used in conjunction with laboratory tests to altar the performance grade system established in Superpave (Barcena et al. 2002). Unfortunately, there is no available field data for the materials researched for this study. However, the goal was to base a criterion on mechanistic properties.

8.6.3 Application of Superpave Asphalt Binder Criterion

The initial inclination was to determine if moisture was detrimental enough to change the performance grade of an asphalt binder. Since all of the binders tested with the modified DSR parts were unaged, the criterion that the G*/sin(δ) exceed 1.0kPa was applied to all binders tested. Original binders, hydrated lime treated binders, and silica treated binders all passed the minimum criterion that the G*/sin(δ) surpass 1.0kPa. It was noted however, that several of the filler treated binders were close to not meeting the minimum criterion.

Since the Superpave criterion for unaged binders did not identify moisture susceptible binders, another criterion was sought. It was concluded that a criterion similar to the Superpave system should be utilized. Thus, subsequent methods were employed to establish a new minimum criterion for binders established with the modified DSR parts. Visual observations had indicated which asphalt binders were severely affected by moisture, but this only indicated that the Superpave criterion was not a satisfactory measure and a new guideline needed to be established (Kvasnak 2006).

8.6.4 Viscous and Elastic Component Analysis

The final method used in conjunction with the previously mentioned methods in establishing a criterion for asphalt binders tested with modified DSR parts was an analysis of the change in viscous and elastic components of asphalt binders based on the different testing conditions.

The initial analysis only considered original binders. For each binder the viscous and elastic components were computed for unconditioned air chamber, unconditioned water bath, conditioned air chamber, and conditioned air chamber specimens. Viscous and elastic components were computed by using G* and δ data. The relationship between the viscous

component, elastic component and G* can be illustrated as a right triangle. Figure 8.18 illustrates the relationships with reference to the complex shear modulus. Knowing this relationship allowed for basic geometry and trigonometry to be used to calculate the viscous and elastic components.

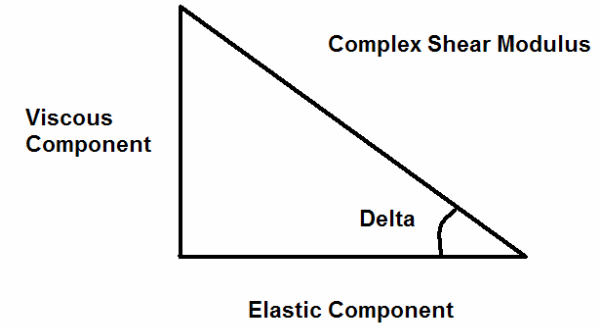

Figure 8.18 Complex Shear Modulus

The main difference considered was a contrast between conditioned water bath and unconditioned air chamber specimens. Differences were divided by an unconditioned air chamber sample to yield a percent change. Figure 8.19 illustrates the dispersion of the percent change of the viscous to elastic components for the comparison of unconditioned air chamber specimens to conditioned water bath specimens. Based on the dispersion, a four category ranking system was developed. Each section of a graph was labeled quandrant I, II, III, or IV. Quadrant I is the upper right hand corner where both the elastic and viscous components are positive. Quadrant II is the upper left corner. Quadrant III is the lower left corner. Quadrant IV is the lower right corner.

Binders in quadrant I were given a rank of 1, implying the most favorable asphalt binders since both the elastic and viscous properties increased with conditioning. Binders in quadrant II were ranked 2, these binder demonstrated a loss in the viscous component, but an improvement

in elasticity. Quadrant III binders were given the rank of 3, these binders exhibited a loss in both viscous and elastic properties. The level 3 binders were deemed the least favorable, fortunately only two original binders fell into this category. There were no data points in quadrant IV, loss in elastic component and gain in viscous component. The grey dashed lines represent one standard deviation above and below the normalized mean. The grey dotted line is the standard deviation limits for normalized viscous differences. The grey dashed and dotted line represents the standard deviation limits for normalized elastic differences. The standard deviations for normalized viscous and elastic components were calculated by pooling all of the data together.

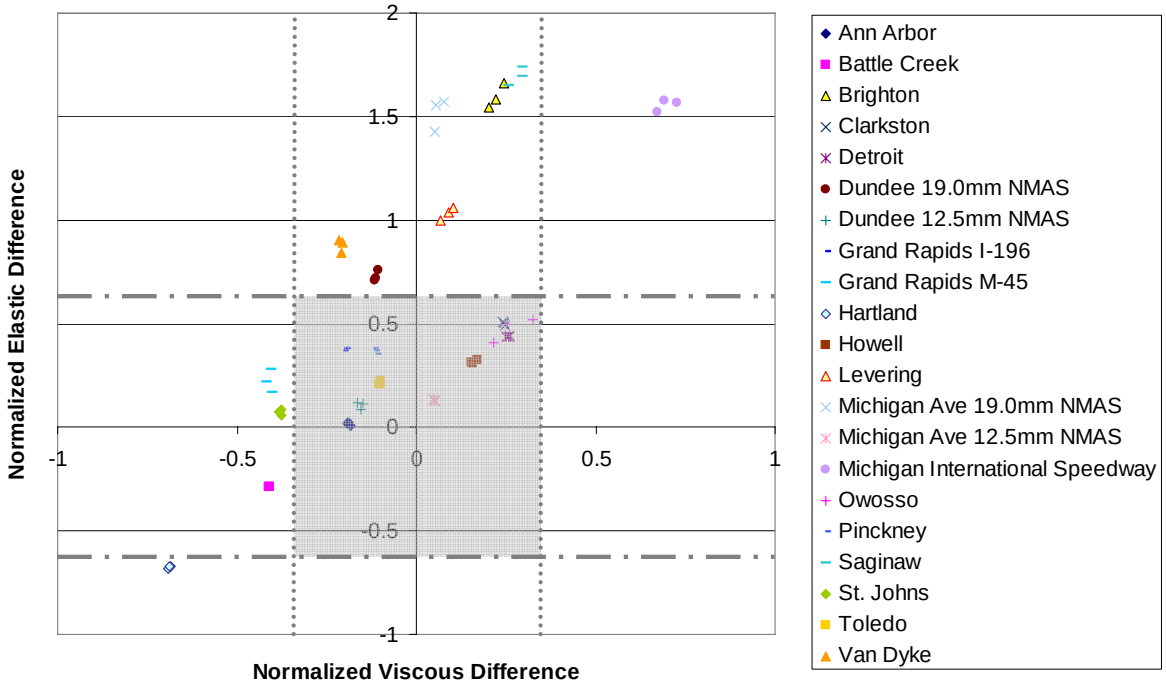

Figure 8.19 Comparison of Elastic and Viscous Percent Changes for Original Binders

Table 8.6 summarizes the binders which exist within one standard deviation, outside one standard deviation, and marginally within one standard deviation. Examining binders within one standard deviation allowed for the identification of binders which yielded drastic changes in elastic and viscous components. The marginal binders are binders that were either located on top

of a standard deviation line or relatively close to one. From Table 8.6, it can be seen that about half of the binders responded quite differently than the other half. After examining the wide range in normalized elastic and viscous component differences it was concluded that additional analysis was required to understand these differences.

Table 8.6 Normalized Viscous and Component of Original Binders Standard Deviation Analysis Summary

Within 1 Standard Deviation	Marginal Binders	Outside 1 Standard Deviation
Ann Arbor	Clarkston	Brighton
Battle Creek	Dundee 19.0mm NMAS	Detroit
Dundee 12.5mm NMAS	Howell	Michigan Ave 19.0mm NMAS
Grand Rapids I-196	Levering	Michigan Ave 12.5mm NMA
Grand Rapids M-45	Owosso	Saginaw
Hartland		VanDyke
Michigan International Speedway		
Pinckney		
Saginaw		
St. Johns		
Toledo		

An additional method of evaluating the normalized difference was employed to account for statistical noise associated with the data collected. Confidence ellipsoids were defined at a level of 95% for the normalized elastic and viscous component differences of each original binder. If the confidence ellipsoid existed completely in quadrant I and II, that binder would be considered not significantly affected by moisture. If the ellipsoid was in quadrant III, viscous and elastic components both decreased in value, then the binder was considered prone to moisture affects (Kvasnak 2006).

8.6.5 I-94 Ann Arbor

Figure 8.20 illustrates the relationship between the normalized differences for the elastic and viscous components. The confidence ellipsoid for I-94 Ann Arbor spans quadrants II and III. Since the ellipsoid overlaps into quadrant III, the binder collected from Ann Arbor is

considered possibly prone to moisture susceptibility. The correlation between the elastic and viscous components is negative but strong, with a value of -0.8889. Figure 8.21 displays the dispersion of the elastic and viscous components by filler. The normalized component values increase drastically with increasing hydrated lime levels.

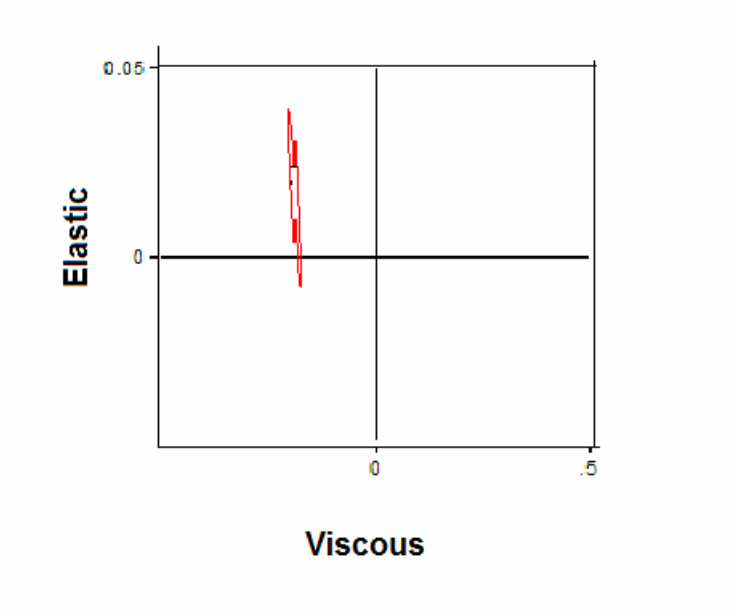

Figure 8.20 Ann Arbor Confidence Ellipsoid

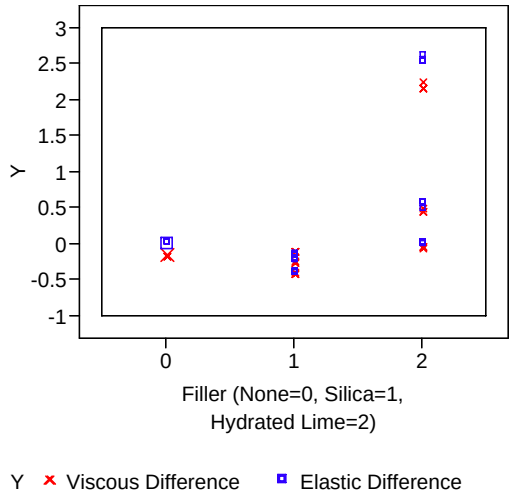

Figure 8.21 Plot of Normalized Elastic and Viscous Differences

8.6.6 M-66 Battle Creek

The confidence ellipsoid for the viscous and elastic components of the Battle Creek binder were extremely small since the changes in elastic and viscous components with conditioning were small. Figure 8.22 illustrates the confidence ellipsoid obtained for the normalized differences of elastic and viscous components for Battle Creek. The correlation between the differences in elastic and viscous components was -0.9779. Figure 8.23 illustrates the range in normalized difference measurements. The original binder normalized differences are close fitting with little dispersion. Binder specimens with hydrated lime display the greatest dispersion, however hydrated lime modified binders are the only specimens which should show improvement with conditioning.

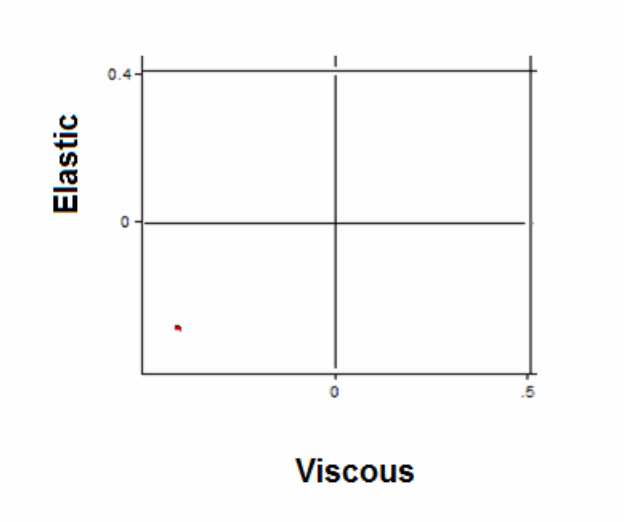

Figure 8.22 Confidence Ellipsoid for Battle Creek Original Binder

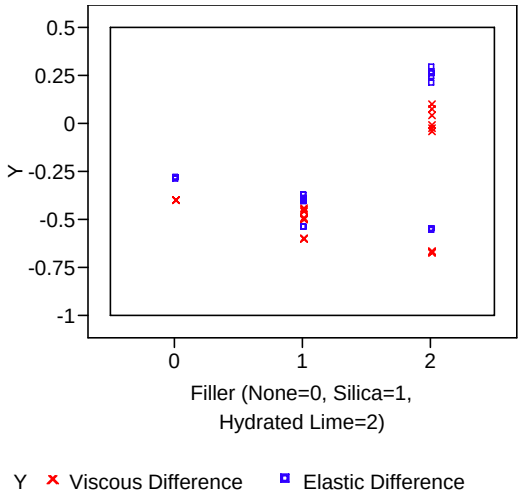

Figure 8.23 Plot of Normalized Viscous and Elastic Differences for Battle Creek

8.6.7 M-59 Brighton

The normalized elastic and viscous component differences are graphed along with a confidence ellipsoid in Figure 8.24. The figure showed that there is no overlap into an adjacent quadrant at a confidence level of 95%. The correlation between the normalized viscous and elastic differences is 0.9892. The range of values for the calculated normalized viscous and elastic component differences are displayed in Figure 8.25. The elastic component for original binders improves significantly, as can be seen in Figure 5.7.

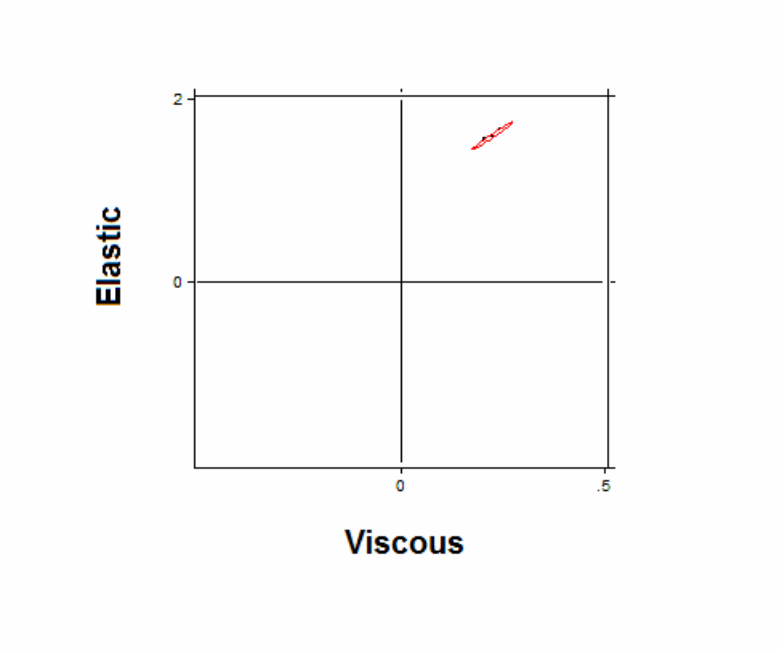

Figure 8.24 Confidence Ellipsoid of Normalized Elastic and Viscous Differences of Brighton Original Binder

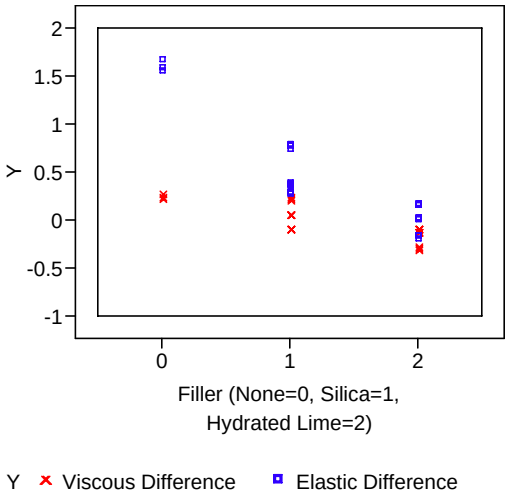

Figure 8.25 Plot of Viscous and Elastic Component Normalized Differences for Brighton

8.6.8 I-75 Clarkston

The differences in the elastic and viscous components were rather precise, thus resulting in rather small confidence ellipsoids. The confidence ellipsoids for viscous and elastic

differences of original binder obtained from Clarkston can be seen in Figure 8.26. From the figure, it can be seen that the region of 95% confidence limit is rather small, but all contained within quadrant I. Despite the small confidence ellipsoid, the data clearly falls within quadrant I therefore it is not deemed a binder prone to moisture damage. The correlation between the two normalized component differences is -0.9826. Figure 8.27 displays the diverse values for the normalized components.

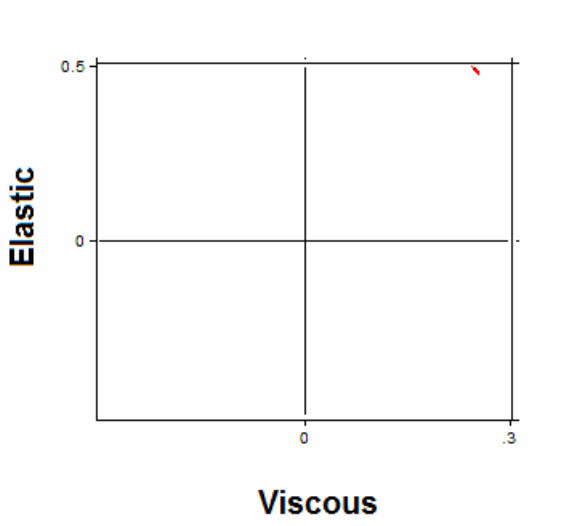

Figure 8.26 Confidence Ellipsoid for Elastic and Viscous Component Differences of Clarkston Original Binder

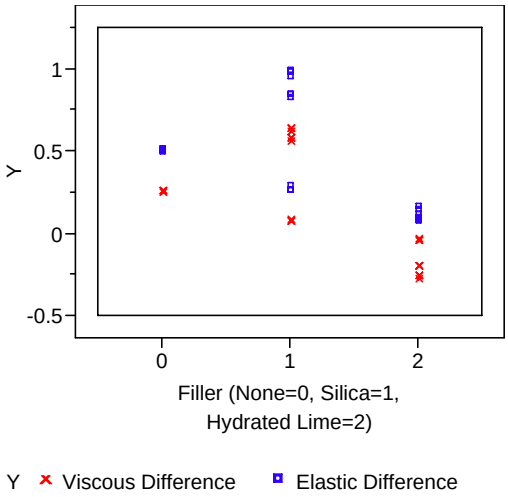

Figure 8.27 Plot of Normalized Elastic and Viscous Component Differences for Clarkston

8.6.9 M-53 Detroit

The confidence ellipsoids based on the normalized elastic and viscous component differences are illustrated in Figure 8.28. The confidence ellipsoid is clearly in quadrant I, thus implying that it is not a binder prone to moisture damage. The correlation between the normalized elastic and viscous component differences is 0.1286. The range of differences for original binder, binder with silica, and binder with hydrated lime is shown in Figure 8.29. It would appear that the addition of filler actually has a negative effect on this binder's ability to resist moisture absorption. This would indicate that the addition of hydrated lime does not always aid in improving a binder's resistance to moisture damage. In other words, the practice of adding hydrated lime to any binder to improve the moisture resistance should be reevaluated.

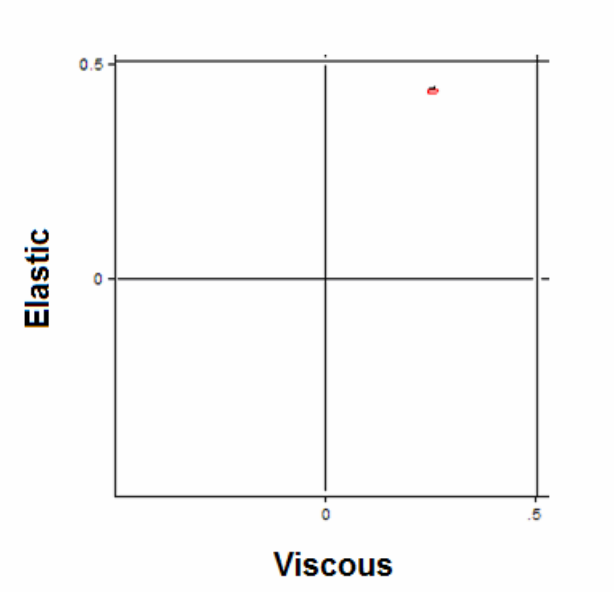

Figure 8.28 Confidence Ellipsoid of Normalized Elastic and Viscous Differences of Original Binder from Detroit

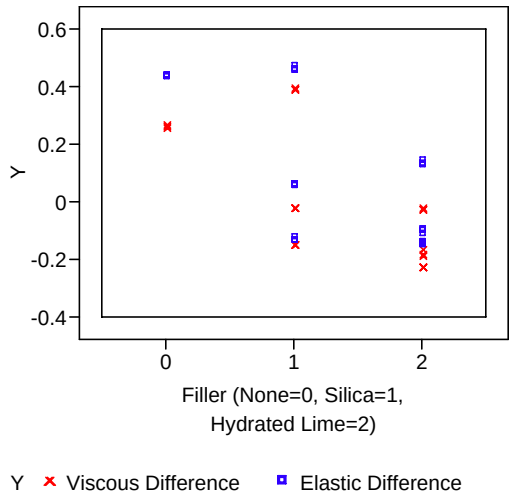

Figure 8.29 Plot of Normalized Elastic and Viscous Component Differences for Detroit Binder

8.6.10 M-50Dundee 19.0mm NMAS

The confidence ellipsoid for Dundee 19.0mm NMAS original binder is completely in quadrant II as can be seen in Figure 8.30. The correlation between the normalized elastic and

viscous component differences is 0.9739. The dispersion in the normalized differences for original binder, binder with silica, and binder with hydrated lime specimens can be seen in Figure 8.31. The improvement in the elastic and viscous components occurred with the higher percentages of filler in the binder.

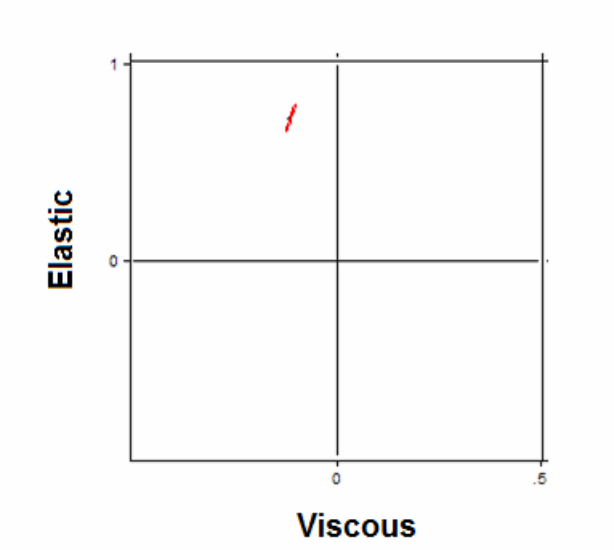

Figure 8.30 Confidence Ellipsoid for Original Binder Dundee 19.0mm NMAS

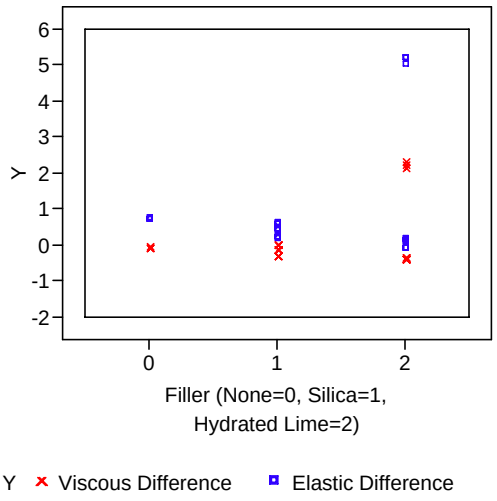

Figure 8.31 Plot of Normalized Elastic and Viscous Component Differences for Dundee 19.0mm NMAS Binder

8.6.11 M-50Dundee 125mm NMAS

The confidence ellipsoid of normalized elastic and viscous component differences of Dundee 12.5mm NMAS original binder exist completely in quadrant II, which can be seen in Figure 8.32. Existence in quadrant II implies that the elastic component is increasing while the viscous component is decreasing with moisture conditioning. The correlation between the two normalized component differences is -0.2617. The range of values for normalized difference is displayed in Figure 8.33. Silica has the most negative effect on the normalized elastic and viscous components, which can be seen in Figure 5.16.

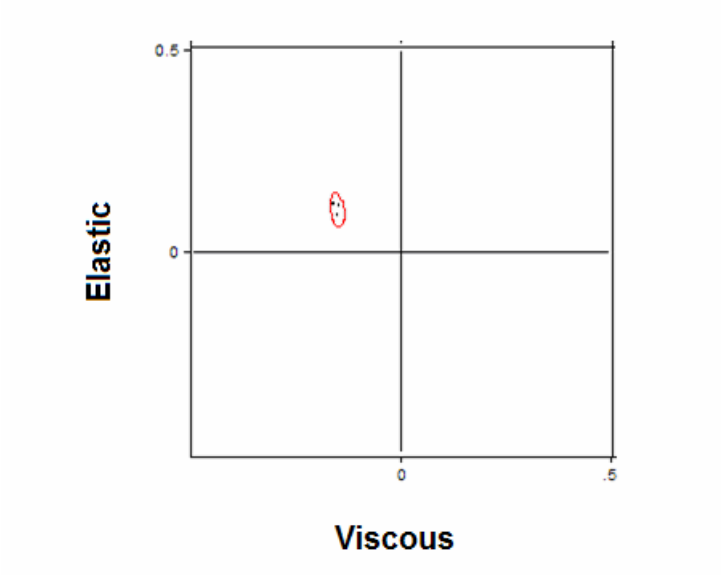

Figure 8.32 Confidence Ellipsoid of Dundee 12.5mm NMAS Original Binder

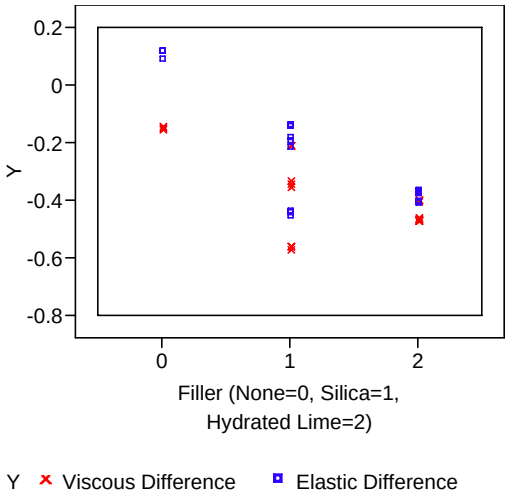

Figure 8.33 Plot of Normalized Elastic and Viscous Component Differences for Dundee 12.5mm NMAS Binder

8.6.12 Grand Rapids I-196

Grand Rapids I-196 original binder exists completely in quadrant II, as can be seen in Figure 8.34. The correlation between the normalized elastic and viscous component differences is 1, thus implying that the component differences are strongly related. Figure 8.35 illustrates the dispersion associated with normalized differences for binder from Grand Rapids I-196. As can be seen, the binder improves the most with the increased levels of hydrated lime.

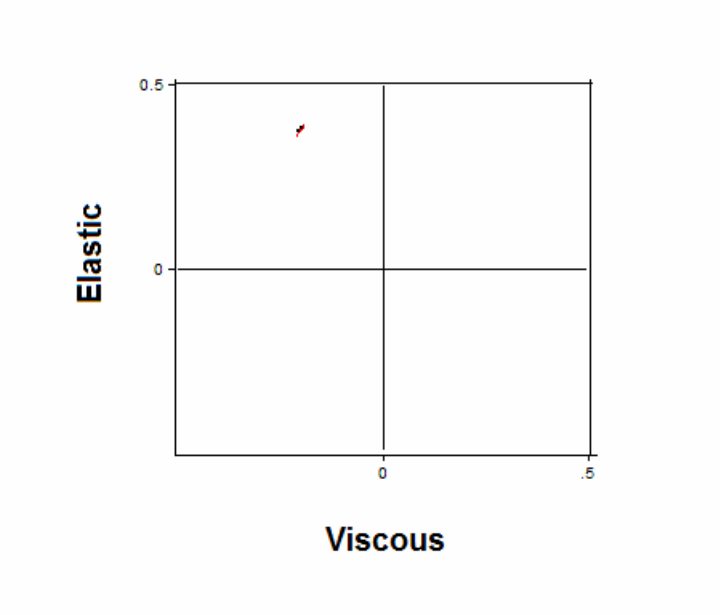

Figure 8.34 Confidence Ellipsoid of Grand Rapids I-196 Original Binder

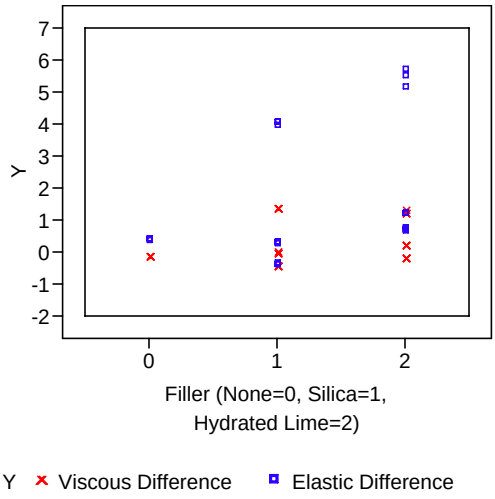

Figure 8.35 Plot of Normalized Elastic and Viscous Component Differences for Grand Rapids I-196 Binder

8.6.13 Grand Rapids M-45

Quadrant II surrounds the confidence ellipsoid for the Grand Rapids M-45 original binder normalized elastic and viscous component differences. The confidence ellipsoid is displayed in

Figure 8.36. The correlation between the normalized elastic and viscous component differences is -0.0938. Figure 8.37 illustrates the range of values of the normalized differences. The greatest improvements come with the addition of silica, followed closely by hydrated lime.

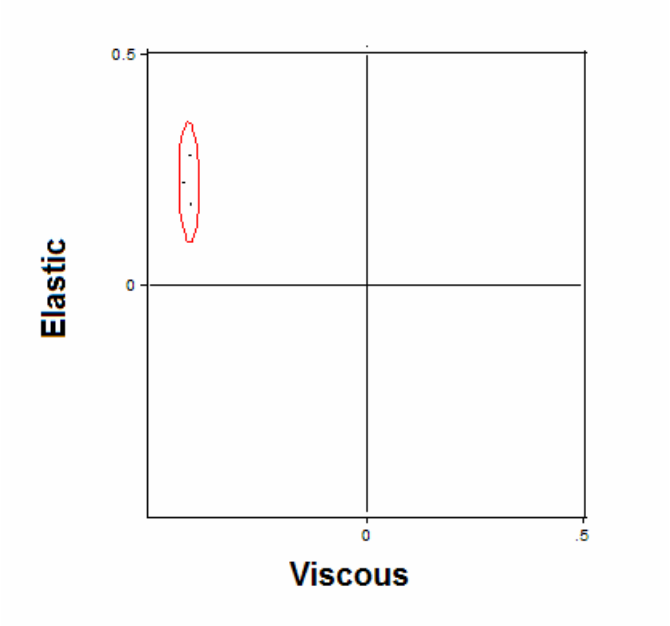

Figure 8.36 Confidence Ellipsoid for Grand Rapids M-45 Original Binder

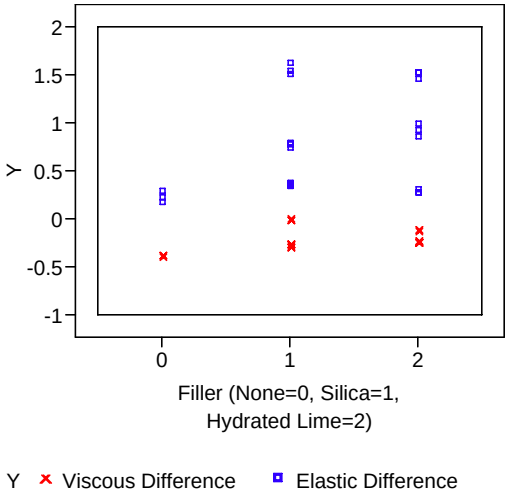

Figure 8.37 Plot of Normalized Elastic and Viscous Component Differences for Grand Rapids M-45 Original Binder

8.6.14 US-23 Hartland

The Hartland confidence ellipsoid based on normalized elastic and viscous component differences exists only in quadrant III. Figure 8.38 illustrates the confidence ellipsoids location in quadrant III. The correlation between the normalized elastic and viscous component differences is 0.7904. Normalized elastic and viscous component differences for the Hartland binder are displayed in Figure 8.39.

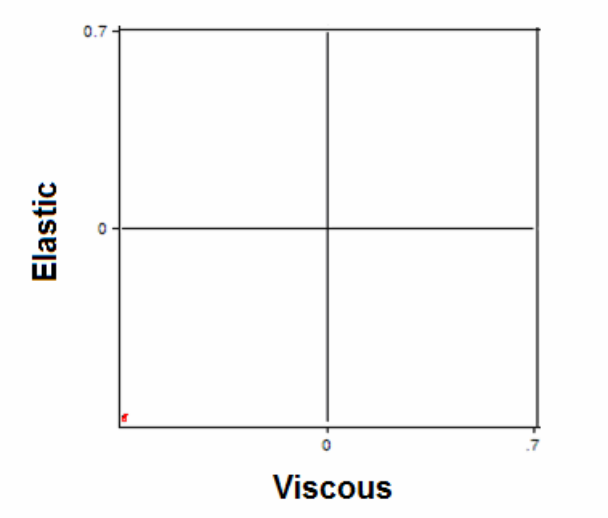

Figure 8.38 Confidence Ellipsoid for Hartland Original Binder

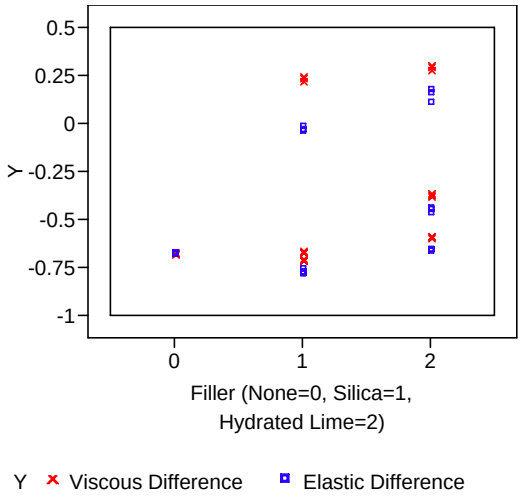

Figure 8.39 Plot of Normalized Elastic and Viscous Component Differences for Hartland Binder

8.6.15 BL I-96 Howell

Figure 8.40 illustrates the placement of the confidence ellipsoid for Howell original binder in quadrant I. The correlation between the normalized elastic and viscous component differences is 0.6988. Figure 8.41 illustrates the range of differences for the normalized elastic and viscous components of Howell binder specimens. The binder performs well without filler. The addition of silica and hydrated lime actually deteriorate the binders resistance to moisture.

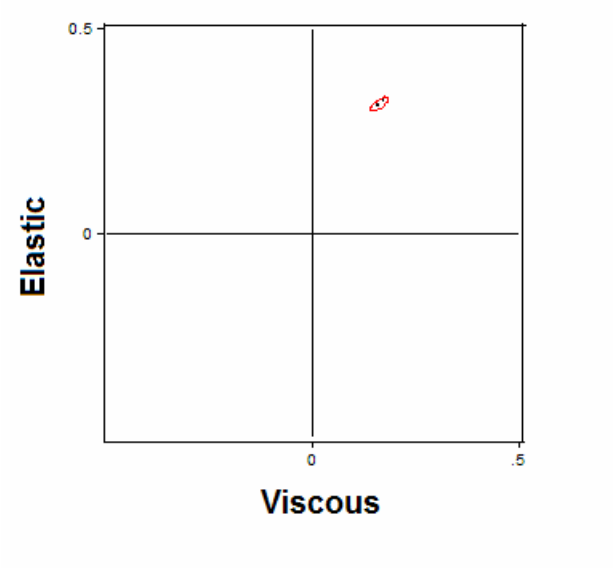

Figure 8.40 Confidence Ellipsoid for Howell Original Binder

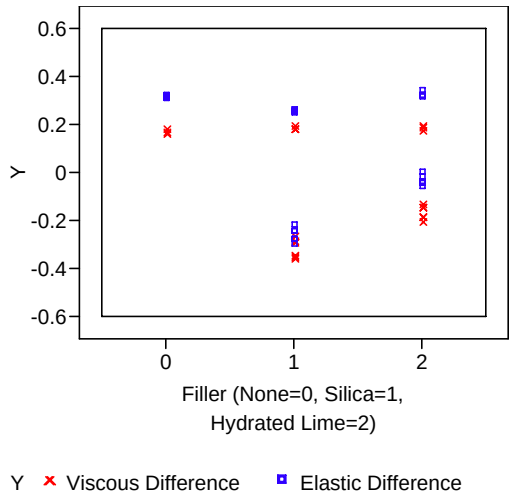

Figure 8.41 Plot of Normalized Elastic and Viscous Component Differences for Howell Binder

8.6.16 I-75 Levering Road

The confidence ellipsoid for the Levering original binder is located in quadrant I, as can be seen in Figure 8.42. The correlation between the normalized elastic and viscous component differences is 1, implying that there is an extremely strong relationship between the normalized

differences. Figure 8.43 displays the range of values obtained for the normalized elastic and viscous component differences.

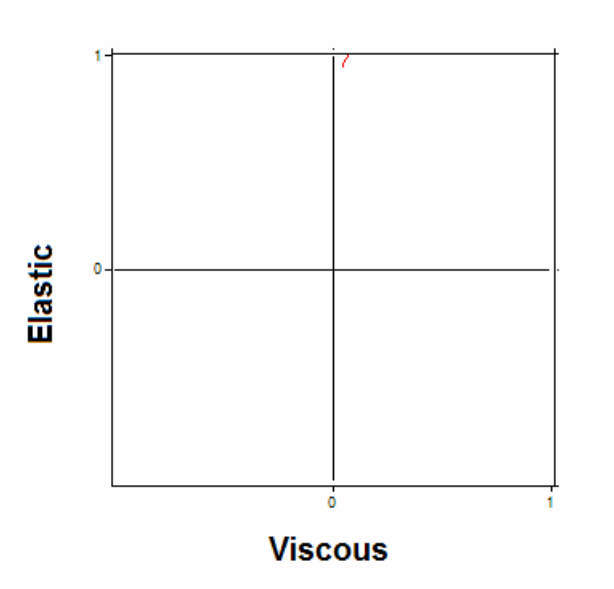

Figure 8.42 Confidence Ellipsoid for Levering Original Binder

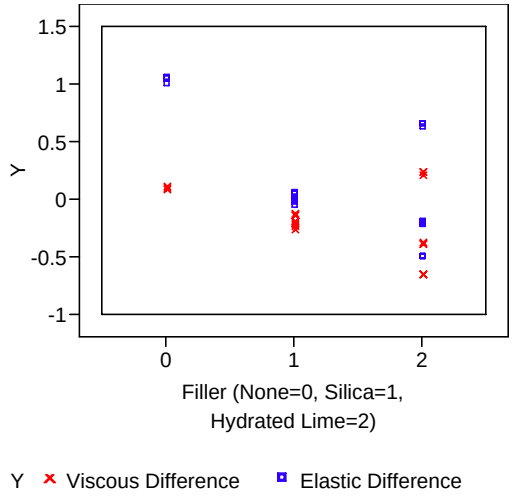

Figure 8.43 Plot of Normalized Elastic and Viscous Component Differences for Levering Binder

8.6.17 Michigan Ave 19.0mm NMAS

Figure 8.44 illustrates the placement of the confidence ellipsoid of the normalized elastic and viscous component differences for Michigan Ave. 19.0mm NMAS original binder. The correlation between the two component differences is 0.6684. The range of normalized component differences can be seen in Figure 8.45.

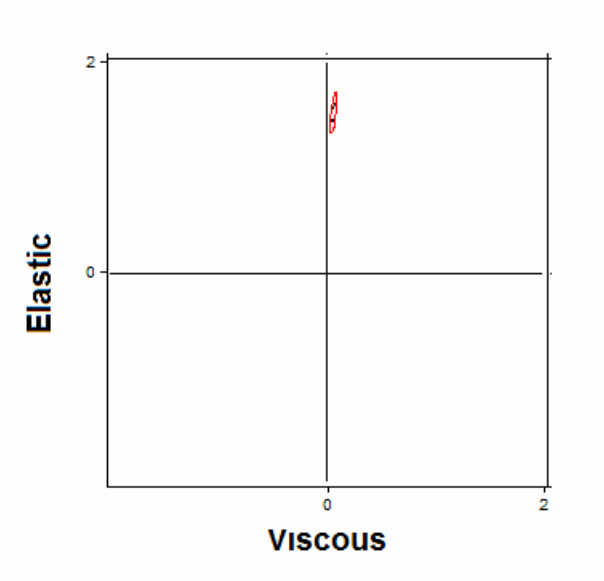

Figure 8.44 Confidence Ellipsoid for Michigan Ave 19.0mm NMAS Original Binder

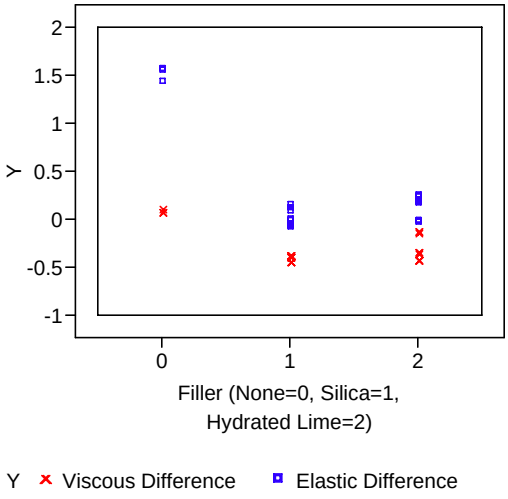

Figure 8.45 Plot of Normalized Elastic and Viscous Component Differences for Michigan Ave 19.0mm NMAS Binder

8.6.18 Michigan Ave 12.5mm NMAS

The confidence ellipsoid for the normalized elastic and viscous component differences lies completely in quadrant I, as shown in Figure 8.46. This indicates that this binder is not prone to moisture damage. The correlation between the two normalized components is -0.8426. From Figure 8.47, it can be seen that the improvement of the binder with either filler for resisting moisture effects is minimal if at all.

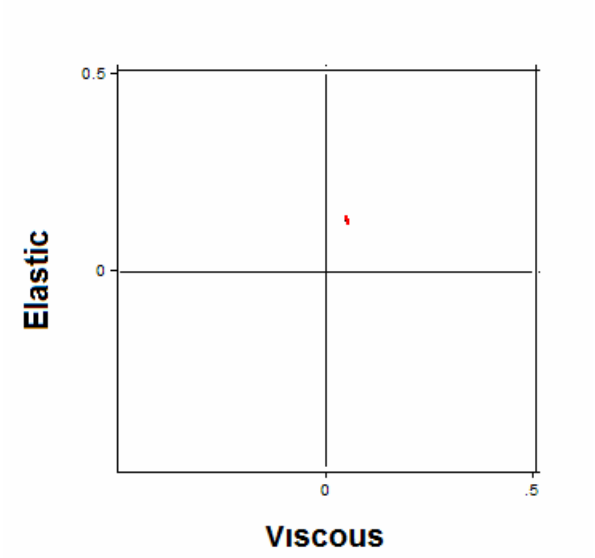

Figure 8.46 Confidence Ellipsoid for Michigan Avenue 12.5mm NMAS Original Binder

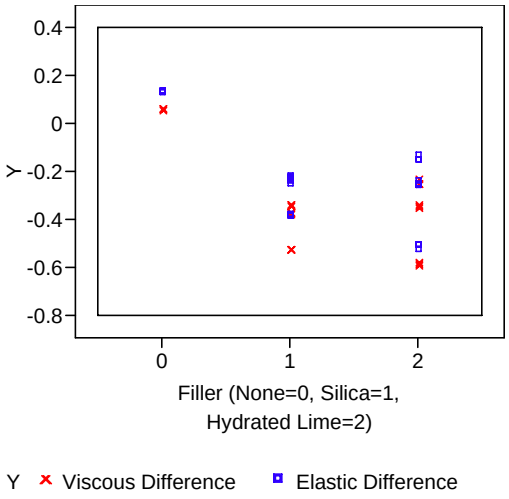

Figure 8.47 Overlay Plot of Normalized Elastic and Viscous Component Differences for Michigan Avenue 12.5mm NMAS Binder

8.6.19 Michigan International Speedway US-12

Quadrant I completely encompasses the confidence ellipsoid of the normalized elastic and viscous component differences for the original binder from Michigan International Speedway. An ellipse completely encompassed by quadrant I imples that the binder is not prone to moisture damage. The correlation between the two normalized component differences is 0.6614. The range of values obtained for the differences can be seen in Figure 8.49. The addition of filler hinders the binder's ability to resist moisture damage.

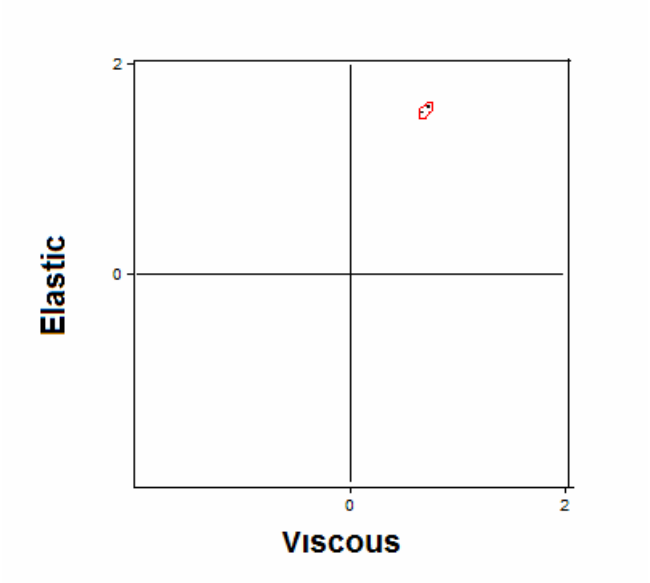

Figure 8.48 Confidence Ellipsoid for Michigan International Speedway US-12 Original Binder

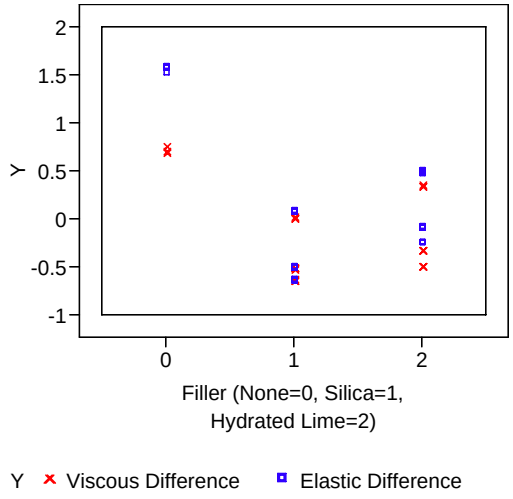

Figure 8.49 Overlay Plot of Normalized Elastic and Viscous Component Differences for Michigan International Speedway US-12 Binder

8.6.20 M-21 Owosso

binder from Owosso exists completely in quadrant I, seen in Figure 8.50. The correlation between the two normalized components is 0.8680. The range of values obtained when finding

the difference between normalized components can be seen in Figure 8.51. As the amount of filler was added to the binder, the moisture resistance increased.

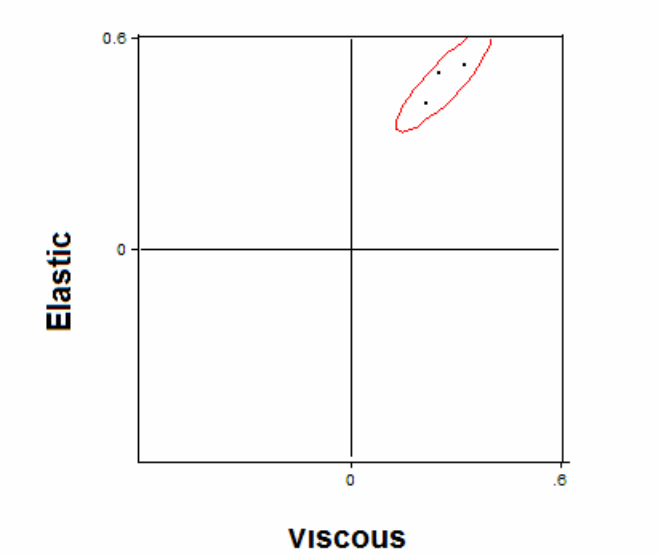

Figure 8.50 Confidence Ellipsoid for Owosso Original Binder

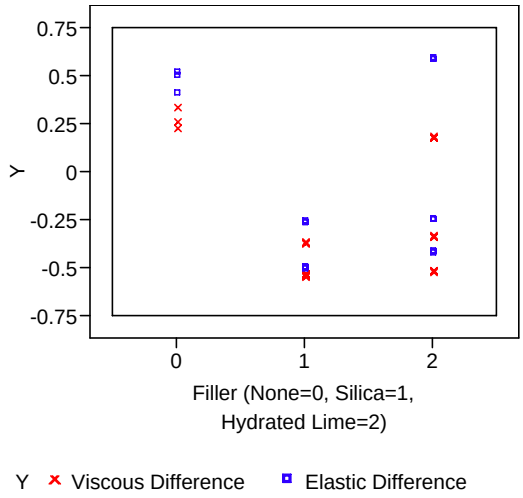

Figure 8.51 Overlay Plot of Normalized Elastic and Viscous Component Differences for Owosso Binder

8.6.21 M-36 Pinckney

The confidence ellipsoid for the normalized elastic and viscous component differences lies completely in quadrant II, see Figure 8.52, indicating that the elastic component increased and the viscous component decreased. The correlation between the two normalized differences is -0.8513. The range in difference values obtained can be seen in Figure 8.53. The addition of silica improves the moisture resistance and performance of the binder.

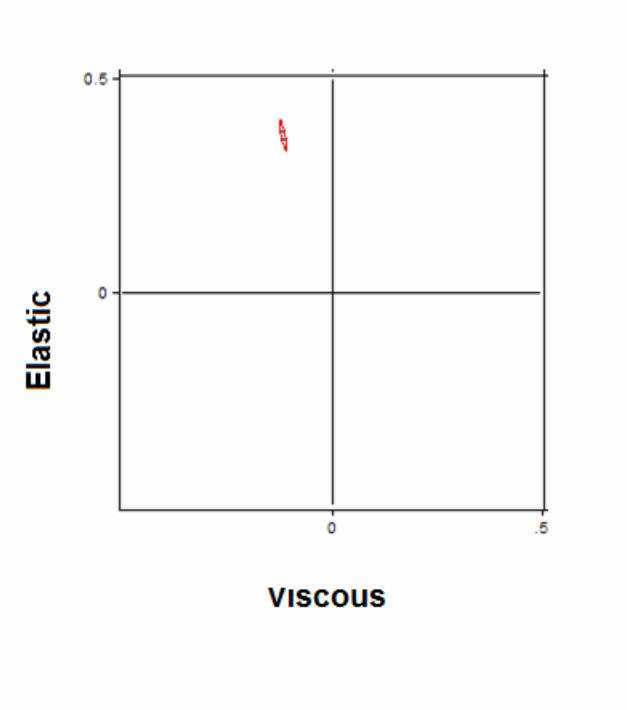

Figure 8.52 Confidence Ellipsoid for Pinckney Original Binder

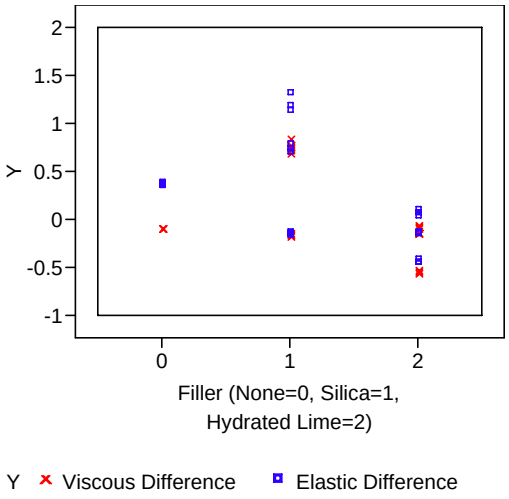

Figure 8.53 Overlay Plot of Normalized Elastic and Viscous Component Differences for Pinckney Binder

8.6.22 M-84 Saginaw

The confidence ellipsoid for the Saginaw original binder exists completely in quadrant I, as seen in Figure 8.54. Since the data falls in quadrant I, the binder is deemed moisture damage resistant. The correlation between the normalized elastic and viscous component differences is 0.8530. The range of normalized difference values can bee observed in Figure 8.55. The binder performs best without fillers.

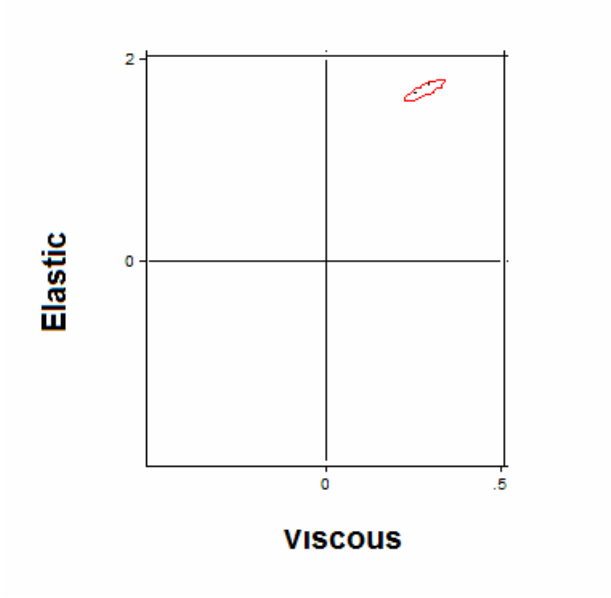

Figure 8.54 Confidence Ellipsoid for Saginaw Original Binder

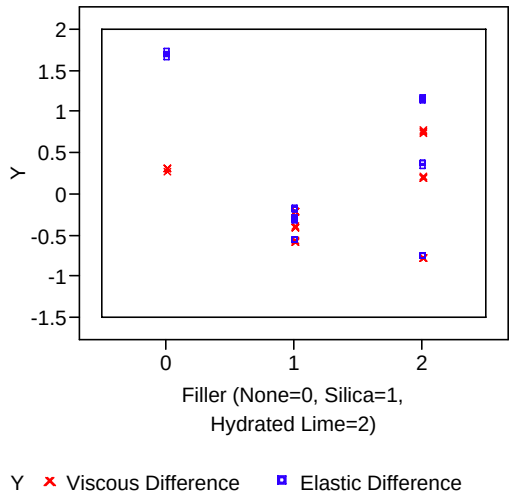

Figure 8.55 Overlay Plot of Normalized Elastic and Viscous Component Differences for Saginaw Binder

8.6.23 M-21 St. Johns

Figure 8.56 illustrates that the confidence ellipsoid for St. Johns of the normalized elastic and viscous component differences lies completely in quadrant II. The correlation between the two normalized component differences is -0.4764. The range of difference values can be seen in Figure 8.57. The binder performs best with hydrate lime followed by silica.

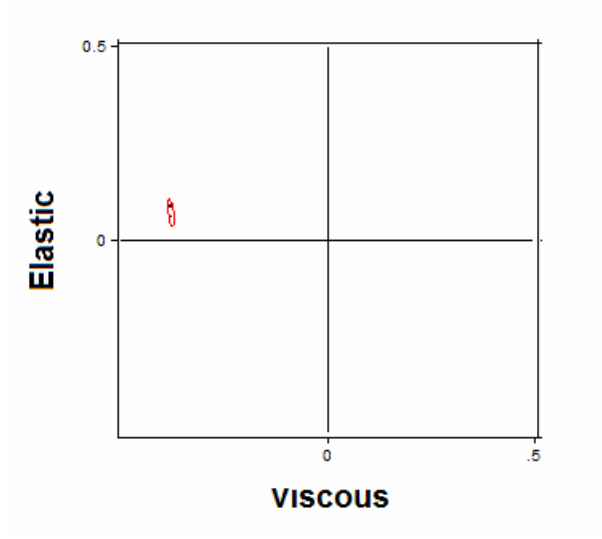

Figure 8.56 Confidence Ellipsoid of St. Johns Original Binder

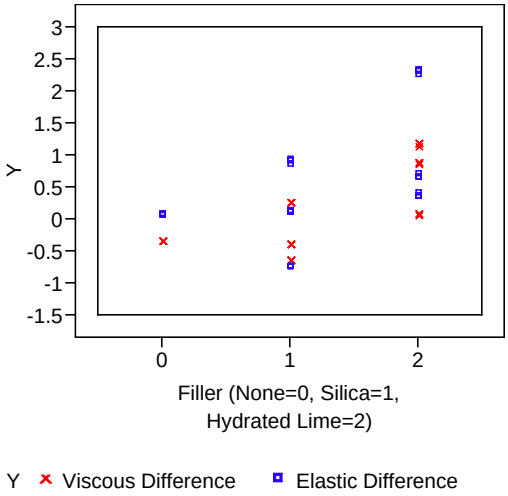

Figure 8.57 Overlay Plot of Normalized Elastic and Viscous Component Differences for St. Johns Binder

8.6.24 I-75 Toledo

Figure 8.58 displays the confidence ellipsoid of the normalized elastic and viscous component differences in quadrant II. The correlation between the two component differences is

0.3777. The range of difference values can be seen in Figure 8.59. The binder performs best with the addition of hydrated lime followed closely by the original binder.

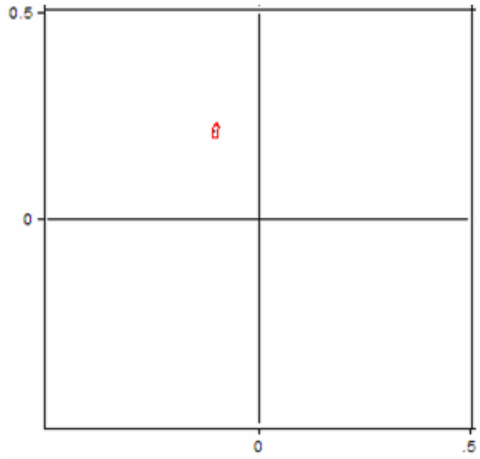

Figure 8.58 Confidence Ellipsoid for Toledo Original Binder

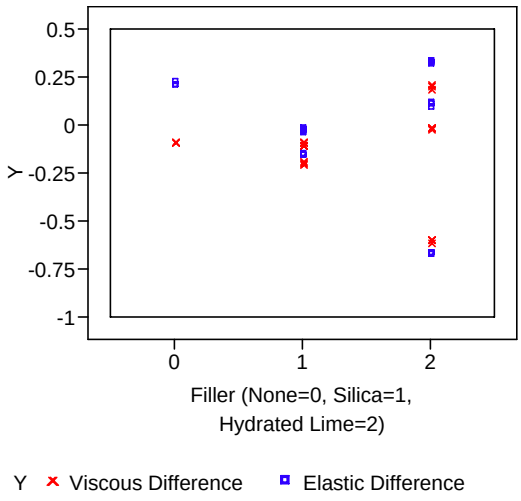

Figure 8.59 Overlay Plot of Normalized Elastic and Viscous Component Differences for Toledo Binder

8.6.25 Van Dyke, Detroit

Figure 8.60 illustrates the placement of the confidence ellipsoid in quadrant II. The correlation between the normalized elastic and viscous component differences is -0.1733. The

range of difference values for original binder and binder with filler can be seen in Figure 8.61. The binder performs best with higher levels of hydrated lime.

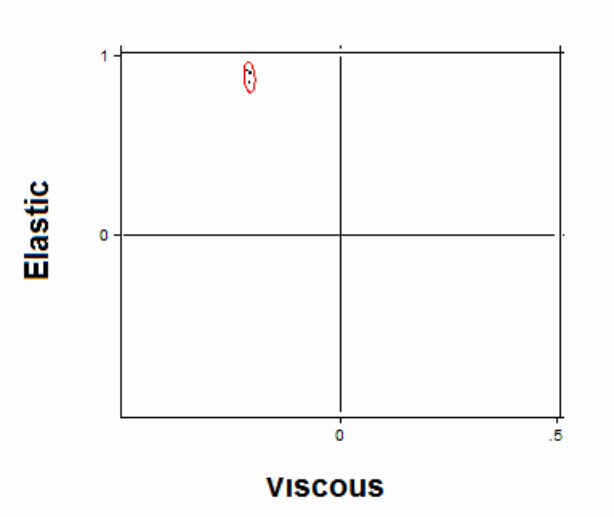

Figure 8.60 Confidence Ellipsoid of Van Dyke Original Binder

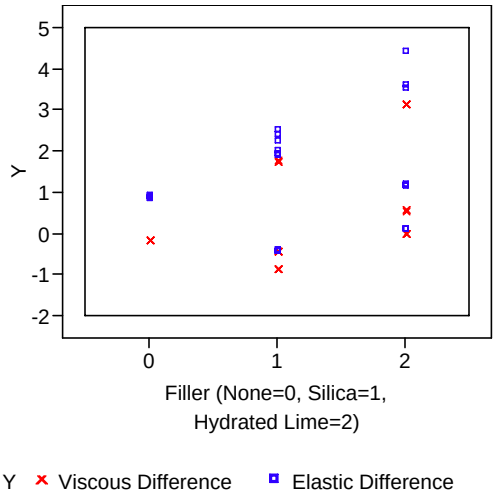

Figure 8.61 Overlay Plot of Normalized Elastic and Viscous Component Differences for Van Dyke Binder

8.6.26 Summary of Statistical Noise

Confidence ellipsoids were employed to evaluate the noise associated with the data obtained from the DSR testing. Evaluating whether or not all of the recorded data and confidence region lies completely encompassed in one quadrant aided in defining the moisture

susceptibility of a binder. Confidence ellipsoids account for the confidence regions of both the elastic and viscous normalized component differences. The confidence ellipsoids are based on a confidence level of 95%. Table 8.7 summarizes the locations of the various confidence ellipsoids. The only binder that spanned multiple quadrants was Ann Arbor. The binders completely contained in quadrant I improved in both elastic and viscous properties, thus indicating that moisture does not have a damaging effect on these binders. Binders completely in quadrant II exhibited increasing values for the elastic component, but decreasing values for the viscous component. These binders are slightly effected by moisture, but since the elastic component increased the affect is not considered significant. An increased elastic component indicated that a binder recovers better after a load application than prior to an elastic component increase. Binders in quadrant III were considered prone to moisture damage since both the elastic and viscous components decreased. Confidence ellipsoids of binders with filler can be found in Appendix B (Kvasnak 2006).

Table 8.7 Location of Confidence Ellipsoids

Quadrant I	Quadrant II	Quadrant III
Brighton, Clarkston, Detroit, Howell, Levering, Michigan Avenue 19.0mm NMAS, Michigan Avenue 12.5mm NMAS, Michigan International Speedway, Owosso, Saginaw	Ann Arbor, Dundee 19.0mm NMAS, Dundee 12.5mm NMAS, Grand Rapids I-196, Grand Rapids M-45, Pinckney, St. Johns, Toledo, VanDyke	Ann Arbor, Battle Creek, Hartland

8.6.27 Summary of Correlation of Normalized Component Differences

Normalized elastic and viscous components were computed to evaluate the affect of moisture on these components. The correlation of the difference between normalized components was computed to determine if the changes caused by moisture on each component was related. For negative and positive correlations, absolute values between 0 and 0.5 were

considered low, while values between 0.5 and 0.75 were deemed moderate, and all above 0.75 labeled as high. Table 8.8 summarizes the results of categorizing the correlations. Most of the binders have a strong (labeled as high) relationship, the difference is whether or not it is positive or negative. Strong relationships between the normalized components were considered auspicious. If the two components change with respect to one another as a result of moisture exposure, defining a relationship of how moisture affects binders will be much easier than if there was no relationship between the two normalized components (Kvasnak 2006).

Table 8.8 Correlation Ratings of Normalized Viscous and Elastic Component Differences

	Low	Moderate	High
Positive	Detroit, Dundee 12.5mm NMAS, Toledo	Howell, Michigan Ave 19.0mm NMAS	Brighton, Dundee 19.0mm NMAS, Grand Rapids I-196, Hartland, Levering, Michigan International Speedway, Owosso, Saginaw
Negative	Grand Rapids M-45, St. Johns, VanDyke		Ann Arbor, Battle Creek, Clarkston, Michigan Ave 12.5mm NMAS, Pinckney

8.7 Recommended Moisture Susceptibility Criterion

This test criterion is based on data obtainable from DSR testing software and water absorption. As previously mentioned, this criterion is based on theory and has been applied to laboratory results, but still needs to be verified with field results. It is recommended that binders are tested with a DSR using a modified spindle and base plate. The binder that should be tested is original binder and binder with a filler. A binder with filler should be tested to allow for breaks in an asphalt binder specimen membrane surface, which enables water to permeate a

specimen faster than a specimen without surface breaks. Surface breaks occur in pavements; therefore inducing breaks by adding a filler simulates, to an extent, reality.

Both of the original binder and binder with filler should be tested as unsaturated and saturated. The saturation should occur for a minimum of 24 hours in a 25˚C water bath. An evaluation of the change in viscous and elastic components should be conducted, as outlined in this chapter. Confidence ellipsoids should be developed to account for noise associated with data readings. The rating used in this chapter should be followed.

In conjunction with DSR testing results, specimens should be evaluated to determine water absorbing tendencies, following steps outlined in this chapter. If a binder exhibits an confidence ellipsoid that is close to crossing over into another quadrant, the water absorption test results should be consulted. This method should be validated with field data once the pavements where the material was collected from have aged properly.

8.8 Analysis of Results – AASHTO T283

Two statistical procedures were used to analyze the data. First, two sample t-tests were used to compare dry strength to wet strength and dry dynamic modulus to wet dynamic modulus at each frequency using the following hypotheses:

H_o : Dry Strength = Wet Strength
H_A : Dry Strength ≠ Wet Strength
$\alpha = 0.05$

H_o : Dry E^* = Wet E^*
H_A : Dry E^* ≠ Wet E^*
$\alpha = 0.05$

A probabilistic analysis was used to determine the criterion for moisture susceptibility for HMA based on the dynamic modulus test using moisture conditioning outlined in AASHTO T283. The lognormal distribution based on the Kolmogorov-Smirnov One-Sample Test using a

p-value of 0.05 was selected for the TSR and E* ratios since a lognormal distribution was applicable to most of the datasets investigated. A lognormal distribution is an appropriate selection since the TSR cannot be less than zero. Therefore a lognormal distribution was used to fit the TSR and E* ratio data at each frequency. The outputs containing the lognormal distribution and the appropriate test statistics can be seen in Appendix C and summarized below in Table 8.9.

Table 8.9 Goodness of Fit Statistics for Phase II

Test Parameter	Frequency (Hz)	Kolmogorov-Smirnov Statistic Lognormal Distribution	p-value
TSR	N/A	0.08659458	0.051
E* Ratio	0.02	0.06143057	>0.150
E* Ratio	0.1	0.08809599	>0.150
E* Ratio	1.0	0.14446214	<0.010
E* Ratio	5.0	0.10132484	0.113
E* Ratio	10.0	0.11101509	0.057
E* Ratio	25.0	0.07586343	>0.150

Table 8.10 shows the results of the two-sample t-tests comparing dry strength to wet strength. The t-tests show that for certain projects, there are significant statistical differences in strength. The bolded projects in Table 8.10 are those that are statistically different and have a TSR value less than the threshold value of 80%. Thus, the average TSR for each project is shown in Table 8.10, to understand if the t-test results are positive in that the TSR is greater than the criterion or negative if it is less than the criterion. The t-test shows mixed results, in some cases the strengths are statistically different and the TSRs are less than the criterion or close to it, while there are a few cases where the strengths are statistically different and the TSRs are greater than the criterion.

Table 8.10 Two-Sample t-test Results Comparing Dry Strength to Wet Strength

	AASHTO T283	
Project	**t-Test Results**	**Average TSR (%)**
M-50 Dundee 3E1	Not Statistically Different	89.7
M-36 Pinckney	***Statistically Different***	***75.1***
M-45 Grand Rapids	***Statistically Different***	***78.7***
M-21 St. Johns	Not Statistically Different	107.3
M-84 Saginaw	*Statistically Different*	*85.1*
BL I-96 Howell	Not Statistically Different	102.1
M-21 Owosso	Not Statistically Different	90.2
M-66 Battle Creek	*Statistically Different*	*90.1*
M-50 Dundee 4E3	Not Statistically Different	97.6
US-12 MIS	*Statistically Different*	*80.9*
M-59 Brighton	Not Statistically Different	87.3
Michigan Ave. Dearborn 3E10	Not Statistically Different	96.0
Vandyke Detroit	Not Statistically Different	100.7
US-23 Hartland	Not Statistically Different	95.1
I-75 Levering Road	*Statistically Different*	*91.1*
I-196 Grand Rapids	*Statistically Different*	*83.8*
I-75 Clarkston	Not Statistically Different	92.7
M-53 Detroit 8 Mile	Not Statistically Different	95.6
Michigan Ave. Dearborn 4E10	*Statistically Different*	*93.7*
I-75 Toledo	Not Statistically Different	101.5
I-94 Ann Arbor SMA	Not Statistically Different	96.6

Figure 8.62 shows the TSR data pooled together and a lognormal distribution fitted to the data. A vertical line is drawn at 80%, which is the TSR criterion and a horizontal line across to show how many specimens did not meet the criterion. Approximately 15% of the specimens failed to meet the TSR criterion of 80%.

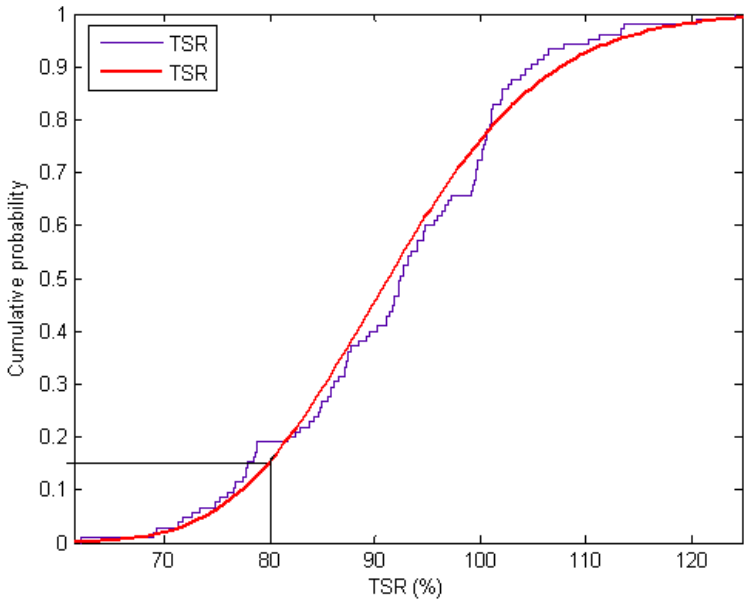

Figure 8.62 Lognormal Distribution of TSRs

8.9 Analysis of Results – E* Ratio

Table 8.11 shows the results of the two-sample t-tests comparing dry dynamic modulus to moisture conditioned dynamic modulus. The t-tests show that for certain projects, there are significant statistical differences in dynamic modulus. Thus, the average E* ratio for each project is shown in Table 8.11, to understand if the t-test results are propitious, E* ratio is greater than the criterion, or negative, E* less than the criterion. The t-test shows mixed results, in some cases dynamic modulus values are statistically different and the E* ratios are less than the criterion while there are cases where the results are statistically the same and the E* ratio is less than the criterion. The criterion used is 80% which is the same as TSR but this value will be examined later in this chapter.

Table 8.11 Two-Sample t-test Results Comparing Control E* to Moisture Conditioned E*

	0.02 Hz		0.1 Hz		1 Hz	
Project	**t-test Results**	**E* Ratio**	**t-test Results**	**E* Ratio**	**t-test Results**	**E* Ratio**
M-50 Dundee 3E1	Not Statistically Different	109.1	Not Statistically Different	109.8	Not Statistically Different	108.0
M-36 Pinckney	*Statistically Different*	*55.2*	*Statistically Different*	*49.2*	*Statistically Different*	*44.6*
M-45 Grand Rapids	Not Statistically Different	64.4	*Statistically Different*	*57.5*	*Statistically Different*	*44.5*
M-21 St. Johns	Not Statistically Different	103.8	Not Statistically Different	92.5	Not Statistically Different	80.0
M-84 Saginaw	Not Statistically Different	80.6	Not Statistically Different	75.6	*Statistically Different*	*62.3*
BL I-96 Howell	Not Statistically Different	110.9	Not Statistically Different	102.6	Not Statistically Different	86.9
M-21 Owosso	Not Statistically Different	102.0	Not Statistically Different	89.8	Not Statistically Different	87.8
M-66 Battle Creek	Not Statistically Different	83.7	Not Statistically Different	78.2	Not Statistically Different	76.7
M-50 Dundee 4E3	Not Statistically Different	75.7	Not Statistically Different	72.5	Not Statistically Different	73.2
US-12 MIS	Not Statistically Different	84.9	Not Statistically Different	73.8	*Statistically Different*	*71.1*
M-59 Brighton	Not Statistically Different	95.9	Not Statistically Different	82.0	Not Statistically Different	95.1
Michigan Ave. Dearborn 3E10	Not Statistically Different	65.0	Not Statistically Different	55.7	*Statistically Different*	*49.2*
Vandyke Detroit	Not Statistically Different	103.6	Not Statistically Different	95.9	Not Statistically Different	100.7
US-23 Hartland	Not Statistically Different	85.4	Not Statistically Different	88.9	Not Statistically Different	87.5
I-75 Levering Road	Not Statistically Different	67.3	*Statistically Different*	*63.4*	*Statistically Different*	*59.7*
I-196 Grand Rapids	Not Statistically Different	87.7	*Statistically Different*	*76.8*	Not Statistically Different	83.4
I-75 Clarkston	Not Statistically Different	105.3	Not Statistically Different	97.6	Not Statistically Different	99.0
M-53 Detroit 8 Mile	Not Statistically Different	101.5	Not Statistically Different	93.6	Not Statistically Different	103.8
Michigan Ave. Dearborn 4E10	*Statistically Different*	*55.5*	Not Statistically Different	53.7	Not Statistically Different	48.3
I-75 Toledo	Not Statistically Different	81.4	Not Statistically Different	92.5	Not Statistically Different	94.8
I-94 Ann Arbor SMA	Not Statistically Different	95.9	Not Statistically Different	76.0	Not Statistically Different	77.1

	5 Hz		10 Hz		25 Hz	
Project	**t-test Results**	**E* Ratio**	**t-test Results**	**E* Ratio**	**t-test Results**	**E* Ratio**
M-50 Dundee 3E1	Not Statistically Different	107.1	Not Statistically Different	109.7	Not Statistically Different	106.8
M-36 Pinckney	*Statistically Different*	*52.3*	Not Statistically Different	59.1	Not Statistically Different	96.8
M-45 Grand Rapids	*Statistically Different*	*46.2*	*Statistically Different*	*47.5*	Not Statistically Different	66.2
M-21 St. Johns	Not Statistically Different	82.3	Not Statistically Different	76.7	Not Statistically Different	68.4
M-84 Saginaw	*Statistically Different*	*57.0*	*Statistically Different*	*58.8*	Not Statistically Different	70.8
BL I-96 Howell	Not Statistically Different	89.4	Not Statistically Different	83.6	Not Statistically Different	77.8
M-21 Owosso	Not Statistically Different	90.0	Not Statistically Different	94.4	Not Statistically Different	94.3
M-66 Battle Creek	Not Statistically Different	77.1	Not Statistically Different	75.1	Not Statistically Different	71.4
M-50 Dundee 4E3	*Statistically Different*	*75.4*	*Statistically Different*	*81.1*	Not Statistically Different	95.5
US-12 MIS	*Statistically Different*	*77.2*	Not Statistically Different	82.7	Not Statistically Different	88.8
M-59 Brighton	Not Statistically Different	110.0	Not Statistically Different	108.1	Not Statistically Different	104.5
Michigan Ave. Dearborn 3E10	Not Statistically Different	55.3	Not Statistically Different	61.9	Not Statistically Different	78.3
Vandyke Detroit	Not Statistically Different	102.2	Not Statistically Different	102.5	Not Statistically Different	120.8
US-23 Hartland	Not Statistically Different	90.7	Not Statistically Different	92.4	Not Statistically Different	94.8
I-75 Levering Road	*Statistically Different*	*55.8*	*Statistically Different*	*52.7*	*Statistically Different*	*52.9*
I-196 Grand Rapids	Not Statistically Different	103.4	Not Statistically Different	106.9	Not Statistically Different	146.4
I-75 Clarkston	Not Statistically Different	114.0	Not Statistically Different	120.3	Not Statistically Different	157.3
M-53 Detroit 8 Mile	Not Statistically Different	107.5	Not Statistically Different	107.5	Not Statistically Different	103.8
Michigan Ave. Dearborn 4E10	Not Statistically Different	47.0	Not Statistically Different	47.0	Not Statistically Different	53.3
I-75 Toledo	Not Statistically Different	92.0	Not Statistically Different	93.2	Not Statistically Different	89.8
I-94 Ann Arbor SMA	Not Statistically Different	81.9	Not Statistically Different	87.0	Not Statistically Different	87.3

Figures 9.18 through 9.23 shows the E* ratio data pooled for each frequency and a lognormal distribution fitted to the data. A horizontal line is drawn at a cumulative probability of 0.15 and a vertical line drawn where the horizontal line intersects the fitted distribution. This cumulative probability value was selected because 15% of the TSR specimens failed the 80% criteria. By drawing the lines at a cumulative probability of 0.15 and drawing vertical lines where the horizontal line intersects the distribution function the E* ratio at 0.02, 0.1, 1.0, 5.0,

10.0 and 25.0 Hz are approximately 60%, 60%, 57%, 58%, 58%, and 58%, respectively. This results in a E* ratio criterion of 60% for each frequency.

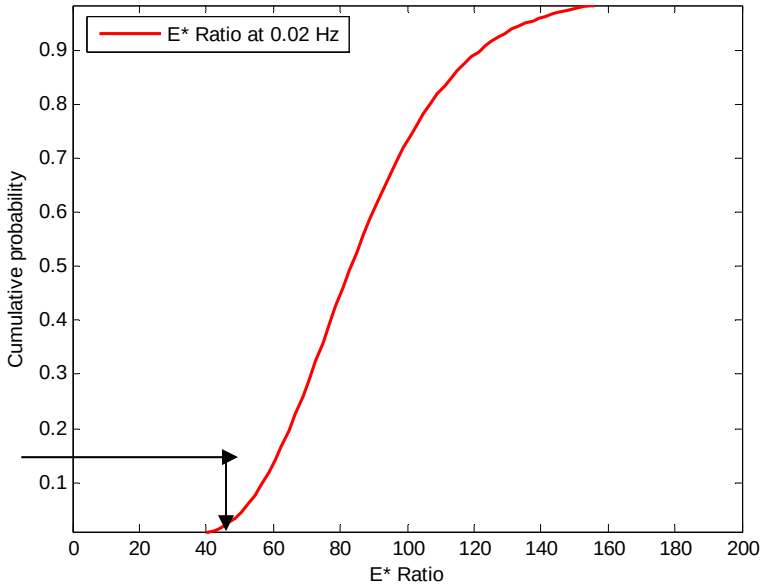

Figure 8.63 Lognormal Distribution of E* Ratios at 0.02 Hz

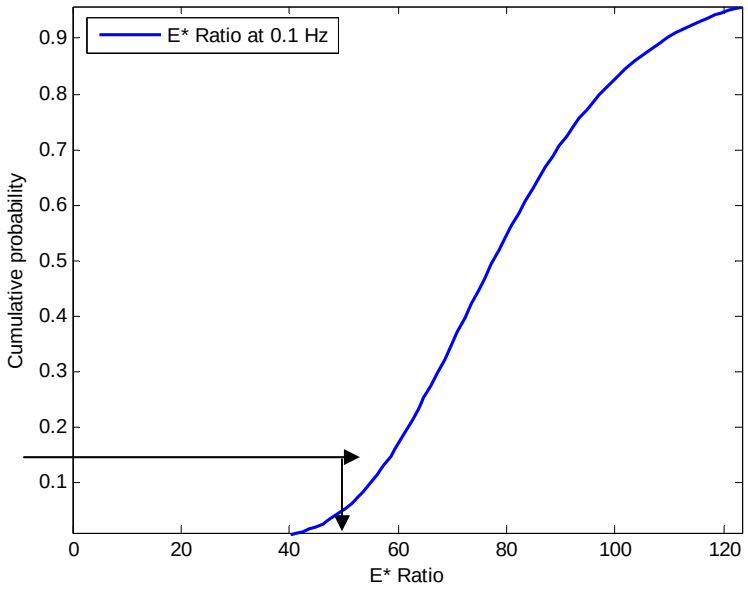

Figure 8.64 Lognormal Distribution of E* Ratios at 0.1 Hz

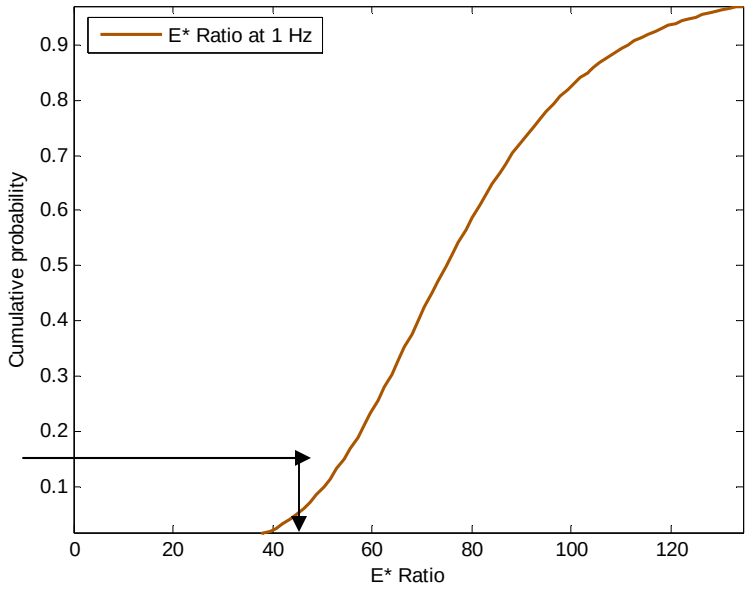

Figure 8.65 Lognormal Distribution of E* Ratios at 1.0 Hz

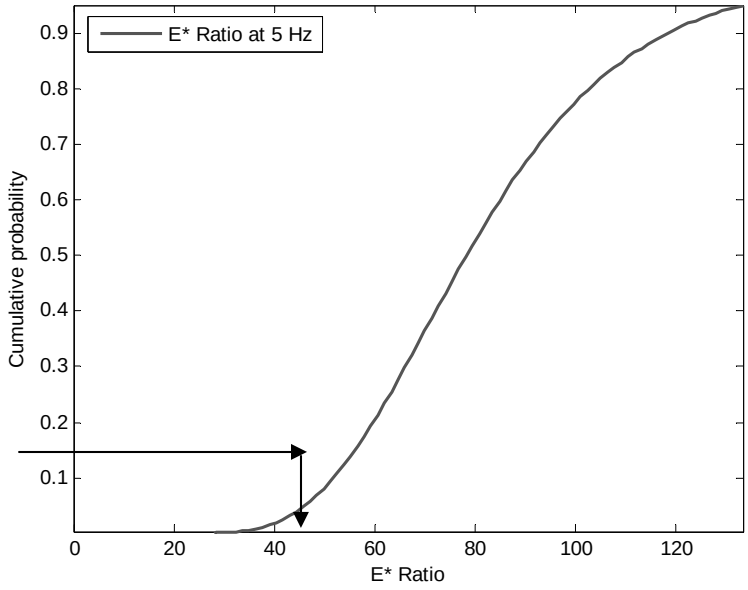

Figure 8.66 Lognormal Distribution of E* Ratios at 5.0 Hz

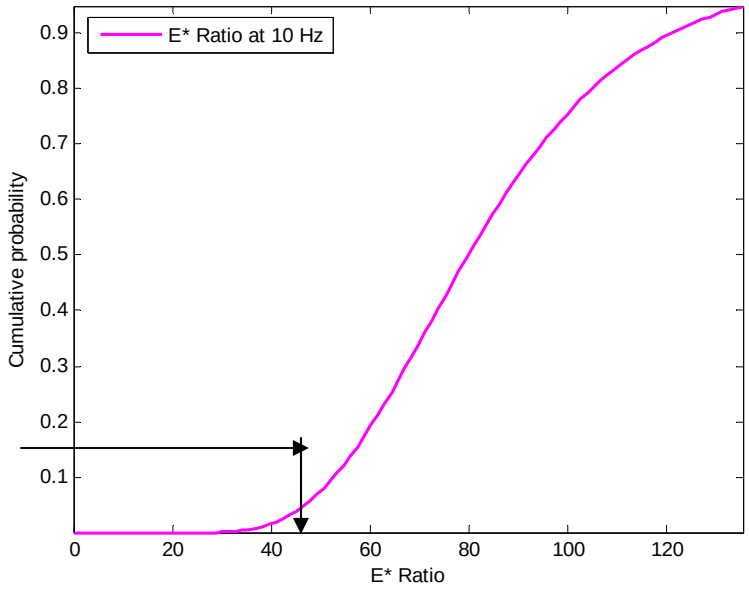

Figure 8.67 Lognormal Distribution of E* Ratios at 10.0 Hz

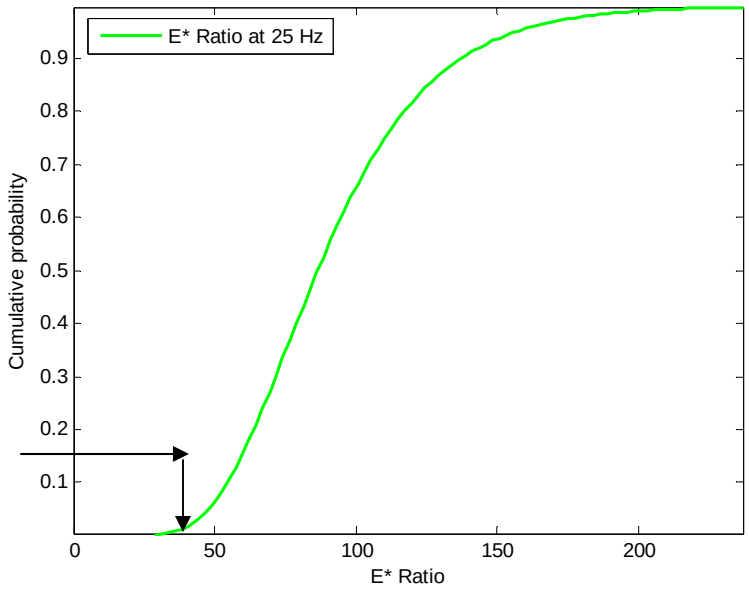

Figure 8.68 Lognormal Distribution of E* Ratios at 25.0 Hz

Table 8.12 provides a summary of both test procedure by ranking the mixtures for each project based AASHTO T283 TSR and the proposed moisture susceptibility test using E* ratio. The ranking is based on a scale from one to twenty-one where one is most moisture susceptible and twenty-one is least moisture susceptible. Both test procedures rank the first two mixtures

about the same otherwise the two methods diverge considerably in their ranking of the mixtures. The proposed method does produce lower retained strength ratios and this is due to the dynamic loading of a specimen which produces hydraulic loading in a specimen thus reducing the strength of the HMA mixture. There is a tendency for the proposed test procedure to identify additional mixes that are moisture susceptible than AASHTO T283.

Table 8.12 Ranking of Projects Based on TSR and E* Ratio

Project	T283	0.02 Hz	0.1 Hz	1.0 Hz	5.0 Hz	10.0 Hz	25.0 Hz
M-36 Pinckney	1	1	1	2	3	4	14
M-45 Grand Rapids	2	2	3	1	1	1	3
US-12 MIS	3	7	6	7	9	11	11
I-196 Grand Rapids	4	12	10	12	17	18	20
M-84 Saginaw	5	8	9	6	6	5	7
M-59 Brighton	6	13	12	17	20	17	16
M-50 Dundee 3E1	7	19	21	21	19	20	18
M-66 Battle Creek	8	11	11	9	7	7	6
M-21 Owosso	9	16	14	15	14	15	13
I-75 Levering Road	10	5	5	5	5	3	1
I-75 Clarkston	11	20	19	19	21	21	21
Michigan Ave. Dearborn 4E10	12	4	4	4	2	2	2
US-23 Hartland	13	10	13	14	13	13	12
M-53 Detroit 8 Mile	14	15	17	20	18	19	17
Michigan Ave. Dearborn 3E10	15	3	2	3	4	6	8
I-94 Ann Arbor SMA	16	14	8	10	11	12	9
M-50 Dundee 4E3	17	6	7	8	8	10	15
Vandyke Detroit	18	17	18	18	16	16	19
I-75 Toledo	19	9	16	16	15	14	10
BL I-96 Howell	20	21	20	13	12	9	5
M-21 St. Johns	21	18	15	11	10	8	4

8.10 Moisture Susceptibility Testing with the Asphalt Pavement Analyzer

The APA has been used for years to rank the rutting potential of HMA mixes. Several studies have concluded that the APA adequately ranks the rutting susceptibility of an HMA mix. One objective of this report was to determine if the APA could be used to rank not only the rutting potential of a mix, but also the moisture susceptibility of a mix. The Hamburg wheel

tracker has been used to rank the moisture susceptibility of mixes in various studies. One study concluded that the APA and Hamburg do an adequate job of ranking (West et al. 2004), while another concluded that the two were too severe (Cooley et al. 2000).

8.10.1 APA Sensitivity Study

Two mixes were used to establish testing conditions for moisture susceptibility evaluation using the APA. The two mixes selected were based on TSR results from the Phase I testing. One of the mixes was deemed moisture resistant while the other was considered to be moisture susceptible based on a TSR criterion of 80% retained tensile strength.

Four condition states were considered for moisture susceptibility evaluation. The first condition state consisted of unconditioned specimens tested in air. The second condition state encompassed unconditioned specimens tested in water. A third condition state consisted of moisture saturated specimens that had endured one freeze/thaw cycle prior to testing in air. The final condition considered moisture saturated specimens that had undergone one freeze/thaw cycle prior to testing in water.

An ANOVA (α=0.05) was conducted to determine if the different condition states yielded statistically different mean rut depths. The ANOVA indicated that no statistical differences existed between the four condition states when comparing mean rut depths. Since a statistical difference in mean rut depths was not detected, it was concluded that not all four condition states would be required for testing the remaining 19 field mixes. The condition state selected for the study were a control state (unconditioned specimens tested in air), and two condition states of moisture saturated specimens that had endured one freeze/thaw cycle with one set tested in air and another in water (Kvasnak 2006).

8.10.2 APA Testing of Field Sampled HMA

As mentioned, 21 HMA mixes were collected from the field. Two of the 21 mixes were evaluated during the sensitivity study to determine the testing conditions to be considered when examining the moisture damage of HMA with the APA. The 19 HMA mixes not evaluated during the sensitivity study were tested under three condition states. Previously mentioned in the last subsection, the three condition states considered were:

1. Unconditioned tested in air (control set/condition state 1),
2. Moisture saturated and one freeze/thaw cycle tested in air (condition state 2), and
3. Moisture saturated and one freeze/thaw cycle tested in water (condition state 3).

8.10.3 Conditioning of the HMA Specimens for APA Testing

All specimens were cut to the appropriate height (75mm) for circular specimens using a circular saw. New geometries of the specimens were recorded after sawing along with new bulk specific gravity measurements using the saturated surface dry method. Specimens were grouped in sets of three based on bulk specific gravity measurements.

Control specimens were preheated at the high performance grade for a minimum time of 6 hours in accordance with the APA testing guidelines. After preheating, a pneumatic tube and steel wheel were lowered over the central axis of each specimen and an APA was set to run 8,000 cycles. As mentioned previously, a cycle is equivalent to a wheel passing one time forward and back to its starting position over the test specimen. Once the inner chamber of the APA reheated to the appropriate testing temperature a test was initiated. The reheating usually took less than 2 minutes, since the chamber was heated to the appropriate test temperature prior to the placement of specimens. The reheating was necessary since there was some heat loss upon the opening of the APA doors to install the specimens locked inside the molds. After a

completion of 8,000 cycles, test data was automatically transferred to a spreadsheet file and saved for future analysis. Saturation occurred via vacuum saturation.

Specimens in either the condition state 2 or 3 were prepared in the same manner, except the specimens which were moisture saturated and endured one freeze/thaw cycle prior to testing. These specimens were moisture saturated to a maximum of 80% air voids filled with water. Specimens were wrapped in Glad Press n' Seal® with ends of the wrap taped down with packing tape. Wrapped specimens and 10mL of water were placed inside a plastic freezer bag labeled with mix information, specimen number, and condition state group. Specimens inside the freezer bags were then placed in a freezer for a period of 24 hours. To minimize the amount of heat entering the freezer, all specimens in a particular group were prepared first and then placed into the freezer at the same time instead of individually. After 24 hours, specimens were placed in a 60˚C water bath to thaw. Once thawing was complete, specimens were preheated to the appropriate APA testing temperature for the 6 hour minimum time. Specimens tested in air were placed in an air chamber for preheating, while those to be tested in water were placed in a water bath for preheating. After the allotted 6 hours of preheating, specimens were placed in an APA for testing. Specimens tested in air were placed in an APA and a steel wheel lowered on top of a pneumatic tube and the APA chamber was allowed to re-establish the test temperature prior to the initiation of 8,000 cycles. Specimens tested in water were placed in an APA chamber and the doors sealed shut. Once the APA doors were shut, a metal box elevated to surround the APA molds. Once the metal box had reached its highest point, water heated to the appropriate temperature flowed into the chamber to fill the metal box. The heated water at all times kept specimens completely immersed. Once the metal box was filled and the water and test chamber re-established the appropriate test temperature, 8,000 cycles commenced. Data from both

condition states 2 and 3 were automatically transferred to a spreadsheet file to be saved and analyzed later.

8.10.4 APA Test Results for Field Sampled HMA

ANOVA tables were employed to evaluate data collected from APA testing. A significance level of 0.05 was used for evaluating the ANOVA tables. Data from each mix was analyzed along with all of the data combined using an ANOVA.

8.10.5 Analysis of All APA Data

Analysis of data combined indicated that the significant factors affecting rut depths were condition state, PG high temperature, NMAS, and aggregate passing the #4, #8, #50, #100 sieves. Mean comparisons of the main effects were conducted using the Tukey method to determine whether or not means of different groups are statistically equivalent (α=0.05). Tables 7.1 through 7.6 outline the results of the mean comparisons. Effect levels considered statistically equivalent share the same group letter. Two group letters appear if an effect level is statistically similar to more than one group.

Table 8.13summarizes comparisons of mean rut depths grouped by condition state. Condition states 1 (unconditioned) and 3 are considered statistically equivalent. Condition state 2 differed from the rut depth means of the two other groups. The average rut depth for condition state 2 specimens was about 6mm while condition states 1 and 3 were 8.5mm and 9.5mm, respectively. It would appear that condition state 2 specimens performed better than condition state 1 and 3. It is hypothesized that the specimens stiffened during the combined freeze/thaw cycle and preheating for APA testing which resulted in the condition state 2 specimens

performing better. Condition state 1 was only preheated and condition state 3 was preheated in a water bath not an air chamber (Kvasnak 2006).

Table 8.13 Mean Comparison by Condition State

Condition	Group
Unconditioned Tested in Air	A
Conditioned, One Freeze-Thaw Tested in Air	B
Conditioned, One Freeze-Thaw Tested in Water	A

Table 8.14 compared average rut depths of specimens grouped by PG high temperature. Mixes with PG 58 and PG 64 binders were found statistically equivalent and PG 70 mixes differed. The rut depth for PG 70 mixes was 1.3mm and 3.4mm less than PG 64 and PG 58 mixes, respectively. It is hypothesized that the PG 70 mixes performed better since these mixes were tested at 64˚C instead of at 70˚C. It should be remembered that mixes with PG 70 binders were used in lieu of PG 64 binders to realize better performance for certain mixes; therefore, these mixes were tested at 64˚C to observe the improved performance if any (Kvasnak 2006).

Table 8.14 Mean Comparison by PG High Temperature

PG High Temperature	Group
PG 58	A
PG 64	A
PG 70	B

Table 8.15 summarizes the results of a rut depth mean comparison between specimens tested at 64˚C and 58˚C. The specimens tested at 64˚C performed better than the ones tested at 58˚C. It is hypothesized that the 64˚C specimens performed better since the PG 70 binders were included in this group (Kvasnak 2006).

Table 8.15 Mean Comparisons by Test Temperature

Test Temperature	Group
58˚C	A
64˚C	B

Table 8.16 summarizes a rut depth mean comparison grouping the specimens by NMAS. 19.0mm NMAS and 12.5mm NMAS were deemed statistically equivalent. 12.5mm NMAS and 9.5 mm NMAS were found to be statistically equivalent. 19.0mm NMAS and 9.5 mm NMAS differed statistically. Specimens having a 9.5 mm NMAS yielded the lowest rut depth while 19.0MM NMAS specimens yielded the deepest ruts (Kvasnak 2006).

Table 8.16 Mean Comparisons by NMAS

NMAS	Group
19.0mm	A
12.5mm	A B
9.5mm	B

Table 8.17 summarizes rut depth mean comparisons grouped by equivalent single axle load (ESAL) level. ESAL levels 3 (3 million ESALs) and 10 (10 million ESALs) were deemed statistically equivalent and 10 million ESALs and 30 million ESALs were also found to be statistically equivalent. Mixes made for 30 million ESALs performed the best and 1 million ESAL specimens performed the worst (Kvasnak 2006).

Table 8.17 Mean Comparisons by ESAL Level

ESAL	Group
1	A
3	B
10	B C
30	C

Table 8.18 summarizes a rut depth mean comparison by gradation. The mean rut depths for the two gradations were considered statistically similar.

Table 8.18 Mean Comparisons by Gradation

Gradation	Group
Fine	B
Coarse	B

Table 8.19 summarizes the results of the rut depth mean comparisons conducted on the APA Data. It can be seen that many of the mixes yielded statistically equivalent rut depths for the different combinations of testing environment and specimen conditioning (Kvasnak 2006).

Table 8.19 Summary of Rut Depth Mean Comparison

	Condition State		
Mix	1	2	3
Ann Arbor	A	A	A
Battle Creek	A	B	A
Brighton	A	A	A
Clarkston	A	A	A
Detroit	A	B	A
Dundee 19.0mm NMAS	A	B	B C
Dundee 12.5mm NMAS	A	A	A
Grand Rapids I-196	A	A	A
Grand Rapids M-45	A	A	A
Hartland	A	A	A
Howell	A	B	B C
Levering	A	A	A
Michigan Ave 19.0mm NMAS	A	A	A
Michigan Ave 12.5mm NMAS	A	B	B
Michigan International Speedway US-12	A	A	A
Owosso	A	A	B
Pinckney	A	A	A
Saginaw	A	A	A
St. Johns	A	A	A
Toledo	A	A	B
Van Dyke	A	A	B

8.10.6 General Linear Model Analysis of APA Data

General linear models (GLMs), ANOVA and stepwise regression, were used to evaluate the significance of several factors affecting the rut depth of a specimen. The first set of analyses evaluated all of the data without grouping by a factor. Table 8.20 summarizes the conclusions gleaned from the ANOVA. Dots in a cell indicate that a factor is deemed significant based on a level of significance of 0.05. The sum of squares associated with each factor was evaluated. Sum of squares relate how the variability of a factor affects a model. Type I sum of squares calculates a factor's effect with regards to the preceding factors have already been entered into a model. Factor order is not an issue for Type III sum of squares, which account for a factor's variation assuming that all factors have been entered into a model. According to the Type I sum of squares, the factors with a significant affect on rut depth are site, condition, high PG temperature, test temperature, material obtained on a 9.5mm sieve, and binder content. Type III sum of squares only identifies one factor as significantly affecting rut depth, test temperature and material retained on a 9.5mm sieve. From this analysis, it can be seen that conservatively speaking, test temperature and material retained on a 9.5mm sieve are significant factors. Closer examination indicates that overall, specimens tested at 64˚C exhibited lower rut depths, especially those with a high PG temperature of 70˚C (Kvasnak 2006).

Table 8.20 Summary of ANOVA for All of the APA data

Factor	Type I Sum of Squares Significance	Type III Sum of Squares Significance
Site	•	
Condition	•	•
High PG Temp	•	
Test Temperature		
25mm		
19mm		
12.5mm		
9.5mm	•	
4.75mm	•	
2.36mm	•	
1.18mm		
0.60mm		
0.30mm	•	
0.15mm		
0.075mm		
Binder Modification		
RAP		
Binder Content		
Fines/Binder	•	
NMAS	•	
ESAL		
Gradation		
Angularity		

Regression analysis was employed to evaluate the nature of the relationship of a factor and a model. Stepwise selection was used to develop a model. Table 8.21 summarizes the results of the regression analysis based on stepwise selection. The model selected consisted of six factors. The R^2, which quantitatively describes how well rut depth is predicted by a model, was 0.9982. Another statistical tool used to evaluate the regression model selected via stepwise selection was Mallow's Cp. Mallow's Cp is a statistical tool used to select an appropriate model. A propitious model will have a Cp value close to the number of variables in the model plus 1. Mallow's Cp is calculated as follows:

$$Cp = \frac{SSE}{MSE} - N + 2 \bullet p$$ Equation 8.1

where:

SSE= Residual sum of squares,

MSE= Mean sum of squares,

N= Number of observations, and

p=Number of factors +1.

Mallow's Cp for the selected regression model was 10.0917. The best value for this model would have been 7 since there are six factors; however a value of 10 is not a sign of a poorly fit model. The parameter estimates are the coefficients associated with each factor. A large parameter estimate indicates that a relationship is strong. The measure of significance is related in the column labeled Pr > F.

Table 8.21 Regression Parameter Estimated for All APA Data

Factor	Parameter Estimate	Pr > F
Intercept	775.15666	<0.0001
Site	0.32019	0.0001
Condition	0.52751	0.0287
High PG Temp	1.5151	0.0462
Test Temperature	-2.17985	0.0093
25mm		
19mm	-7.33037	<0.0001
12.5mm	1.67161	<0.0001
9.5mm	-1.31011	<0.0001
4.75mm		
2.36mm		
1.18mm		
0.60mm	0.38679	<0.0001
0.30mm		
0.15mm	-1.27069	0.0006
0.075mm		
Binder Modification	-5.42499	0.0134
RAP		
Binder Content		
Fines/Binder		
NMAS	4.70714	0.0005
ESAL		
Gradation		
Angularity	-1.36009	<0.0001

The next set of ANOVA and regression analyses grouped the data by condition state. The first condition state explored was the condition state 1 (the control set). The first GLM analysis evaluated was the ANOVA table for condition state 1. Table 8.22 summarizes the results of the ANOVA for condition state rut depth data. As with the previous ANOVA table analysis, information about Type I and Type III sum of squares is provided. The level of significance was α=0.05. The dots in the table indicate that a factor is significant. Nine factors were considered significant for Type I sum of squares, however no factors were considered significant for Type III sum of squares. The factors deemed significant by Type I sum of squares

included site, high PG temperature, several sieve sizes, and the fines to binder ratio (Kvasnak 2006).

Table 8.22 Summary of ANOVA for Condition State 1 APA Data

Factor	Type I Sum of Squares Significance	Type III Sum of Squares Significance
Site	•	
Condition		
High PG Temp	•	
Test Temperature		
25mm		
19mm	•	
12.5mm		
9.5mm	•	
4.75mm	•	
2.36mm	•	
1.18mm		
0.60mm		
0.30mm	•	
0.15mm	•	
0.075mm		
Binder Modification		
RAP		
Binder Content		
Fines/Binder	•	
NMAS		
ESAL		
Gradation		
Angularity		

The second set of analysis conducted for condition state 1 was regression analysis to evaluate the nature of the factor relationships. Table 8.23 summarizes the results of the regression analysis for condition state 1 APA rut depth data. The R^2 for the condition state 1 regression model was 0.7797 and Mallow's Cp was 22.5524. The model would be considered good based on the R^2 and Mallow's Cp. An excellent model would have yielded a higher R^2 and lower Mallow's Cp. Outside of the intercept, the fines to binder ratio has the largest parameter

estimate indicating that the rut depth of the control specimens is strongly related to the fines to binder ratio (Kvasnak 2006).

Table 8.23 Regression Parameter Estimates for Condition State 1 APA Rut Depth Data

Factor	Parameter Estimate	Pr > F
Intercept	369.62144	0.009
Site	-0.15442	0.0005
Condition		
High PG Temp		
Test Temperature	-0.2361	0.0226
25mm		
19mm	-3.29513	0.0031
12.5mm		
9.5mm		
4.75mm	-0.4561	<0.0001
2.36mm		
1.18mm		
0.60mm		
0.30mm	0.32202	0.0600
0.15mm	1.7956	0.0036
0.075mm		
Binder Modification		
RAP	0.12625	0.0756
Binder Content		
Fines/Binder	-15.43404	<0.0001
NMAS	4.04996	<0.0001
ESAL		
Gradation	-8.39689	<0.0001
Angularity		

After evaluating the data from condition state 1, condition state 2 was evaluated (moisture saturation plus one freeze/thaw cycle tested in air). Table 8.24 summarizes the ANOVA results of condition state 2 rut depth data obtained from APA testing. Nine factors were deemed significant based on Type I sum of squares. The factors deemed statistically significant for condition state 2 are not the same as the factors deemed statistically significant for condition state 1 ruts. Both condition state ruts were affected by site, high PG temperature, and the fines to binder ratio. However, condition state 2 ruts were also affected by binder

modification. There were also several differences in which sieve sizes affected the ruts (Kvasnak 2006).

Table 8.24 Summary of ANOVA for Condition State 2 APA Rut Depth Data

Factor	Type I Sum of Squares Significance	Type III Sum of Squares Significance
Site	•	
Condition		
High PG Temp	•	
Test Temperature		
25mm		
19mm	•	
12.5mm	•	
9.5mm		
4.75mm		
2.36mm	•	
1.18mm		
0.60mm	•	
0.30mm		
0.15mm	•	
0.075mm		
Binder Modification	•	
RAP		
Binder Content		
Fines/Binder	•	
NMAS		
ESAL		
Gradation		
Angularity		

Regression analysis was conducted after evaluating the ANOVA table for condition state 2. Table 8.25 summarizes the parameter estimates for condition state 2 rut depth data. Disregarding the intercept, gradation exhibits the largest parameter estimate, indicating that gradation (fine or coarse) is strongly related to rut depths of condition state 2 specimens (Kvasnak 2006).

Table 8.25 Regression Parameter Estimates for Condition State 2 APA Rut Depth Data

Factor	Parameter Estimate	Pr > F
Intercept	354.05987	<0.0001
Site	0.11773	0.0314
Condition		
High PG Temp	-0.14946	0.0127
Test Temperature		
25mm		
19mm	-3.00001	<0.0001
12.5mm		
9.5mm		
4.75mm	-0.38694	<0.0001
2.36mm	0.59923	0.0003
1.18mm		
0.60mm		
0.30mm		
0.15mm		
0.075mm	-0.78474	0.0220
Binder Modification		
RAP		
Binder Content		
Fines/Binder		
NMAS		
ESAL		
Gradation	6.65655	0.0017
Angularity	-0.92217	<0.0001

The final condition state to be evaluated was condition state 3 (moisture saturation plus one freeze/thaw cycle tested in water). Table 8.26 summarizes the ANOVA conclusions for condition state 3 rut depth data. Evaluation of condition state 3 ANOVA indicates that six factors were deemed statistically significant for Type I sum of squares. Like condition states 1 and 2, condition state 3 Type I sum of squares indicated that high PG temperature and fines to binder ratio are significant factors. No factors were deemed statistically equivalent for Type III sum of squares (Kvasnak 2006).

Table 8.26 Summary of ANOVA for Condition State 3 APA Rut Depth Data

Factor	Type I Sum of Squares Significance	Type III Sum of Squares Significance
Site		
Condition		
High PG Temp	•	
Test Temperature		
25mm		
19mm	•	
12.5mm		
9.5mm	•	
4.75mm	•	
2.36mm		
1.18mm		
0.60mm		
0.30mm		
0.15mm	•	
0.075mm		
Binder Modification		
RAP		
Binder Content		
Fines/Binder	•	
NMAS		
ESAL		
Gradation		
Angularity		

Once the ANOVA evaluation was completed, regression analysis was used to evaluate the nature of the relationships of the factors affecting condition state 3 rut depths. Table 8.27 displays the parameter estimates for the regression model selected based on condition state 3 rut depth data. Disregarding the intercept, the 19mm sieve yields the largest parameter estimate. Interestingly, in the stepwise regression model selected, the fines to binder ratio is marginally significant (Kvasnak 2006).

Table 8.27 Regresion Parameter Estimates for Condition State 3 APA Rut Depth Data

Factor	Parameter Estimate	Pr > F
Intercept	680.98121	<0.0001
Site		
Condition		
High PG Temp		
Test Temperature	-0.29178	0.0679
25mm		
19mm	-6.26604	<0.0001
12.5mm		
9.5mm		
4.75mm	-0.75907	<0.0001
2.36mm	0.58732	0.0042
1.18mm		
0.60mm	0.28329	0.1102
0.30mm		
0.15mm		
0.075mm		
Binder Modification		
RAP		
Binder Content	-4.32343	0.0034
Fines/Binder	-5.57584	0.0538
NMAS	4.98947	<0.0001
ESAL		
Gradation		
Angularity		

Evaluation of the data grouped by condition state offered some useful insight. According to the ANOVAs, there are several factors that consistently affect the rut depth of APA tested specimens. Those factors are high PG temperature, fines to binder ratio, and the sieve sizes 19mm and 0.15mm. The regression analysis differed between the three condition states. The factor exhibiting the largest parameter estimate was not consistent for all three condition states. This indicates that not only does testing environment, but also condition may be affecting the final rut depth created by an APA. Further inspection of the high PG temperature groupings revealed that the PG 70-X binders performed the best, smallest rut depths. The mixes with a PG 70-X binders were tested at 64˚C and performed better than the other mixes. Most likely these

mixes performed better since the binders were less fluid during testing. Binders that tend to be fluid easily move with the application of a load. Aggregates can also move when the binders are moving during this fluid state. Shifting of material in a specimen in the presence of water can allow for breaks in a binder membrane thus enabling the penetration of moisture. Once moisture penetrates a binder it tends to soften a binder making it less resistant to moisture damage (Kvasnak 2006).

8.10.7 APA Analysis Summary

The analysis conducted on rut depth obtained from APA testing was outlined in the above sections summarizing ANOVA table results and mean comparison results. Interestingly for the majority of comparisons where there were differences between the condition effect levels, the unconditioned and condition state 3 specimens were usually deemed statistically equivalent while condition state 2 was deemed statistically different from both. However, only 8 mixes were affected statistically different by the condition state. The majority of mixes yielded statistically equivalent rut depths for all three condition states. A second observation that is intriguing is that there is no statistical difference between the rut depths of coarse-graded and fine-graded mixes (Kvasnak 2006).

8.10.8 APA Moisture Criteria

A moisture criterion for APA testing was developed based on ratio of the rut depths. The ratio consisted of condition state 3 divided by condition state 1. Any value less than 1± 0.05 was considered not prone to moisture damage. Values greater than 1± 0.05 were deemed moisture damage prone. The assumption for this criterion is that as mix ages it becomes stiffer therefore the specimens that endured longer heating times are aged more than the unconditioned

specimens. Condition state 2 and 3 specimens therefore should be stiffer than condition state 1 specimens. Stiffer binders are less prone to rutting. The ratio of condition state 2 to condition state 1 should also be determined to see if the freeze/thaw cycle has an affect on rut depth results. Table 8.28 summarizes the results of applying the two criteria. It appears that the majority of mixes fail both the freeze/thaw and moisture criteria. This is possible, however, these results should be compared to field cores to better refine both criteria. It is suspected that the criterion is on the conservative side (Kvasnak 2006).

Table 8.28 Summarized Results of Field Mixes Based on Freeze/thaw and Moisture Criteria

	Moisture Damage Prone	**Moisture Damage Resistant**
Freeze-Thaw Damage Prone	Grand Rapids M-45, Hartland	MIS US12, Pinckney
Freeze-Thaw Damage Resistant	Battle Creek, Detroit, Dundee 19.0mm NMAS, Dundee 12.5mm NMAS, Howell, Levering, Michigan Ave 19.0mm NMAS, Owosso, Saginaw, St. Johns, Toledo, Vandyke	Ann Arbor, Michigan Ave 4, Brighton

Rutting results at WesTrack were compared to APA results (Epps Martin and Park, 2003). In the study, a rut of 12.5mm was considered dangerous and used as a failure marker. Tests with the APA of the same mixes yielded ruts of 9.1mm on average. The rut depth of 9.1mm created by the APA was then deemed the failure point for the mixes. Until field data can be acquired to relate APA results to Michigan mixes, a value of 9.1mm should be used as the failure criteria. The 9.1mm criteria was used to improve the criterion based on the ratio of the conditioned water tested specimens divided by the control specimens. Several specimen groups yielded high ratios which would be deemed moisture prone, however the rut depths were very small. Setting a failure rut depth and then calculating the ratio alleviates the issue of specimens

with small rut depths being labeled as moisture prone. Table 8.29 summarizes which conditions groups within a mix failed the rut depth criterion of 9.1mm. It can be seen that most of the specimens from condition state 2 (moisture saturation plus one freeze/thaw tested in air) specimens did not fail the rut depth criterion. Seven of the control groups failed and nine of the condition state 3 groups failed.

A further analysis was conducted to determine if these failure groups failed due to moisture damage or if the mix is merely susceptible to rutting. For this analysis, the ratio method of dividing water tested conditioned specimen rut depth values by control specimen rut depth values was implemented. If the ratio is greater than 1 the mix is considered moisture prone; whereas if the ratio is less than one it is not considered moisture prone. Table 8.30 summarizes the rut depth ratios of the mixes that failed the maximum rut depth criterion of 9.1mm. All of the mixes actually yielded lower rut depths for conditioned specimens tested in water except for the two mixes from Grand Rapids.

Table 8.29 Summary of Rut Depth Failure for all Three Condition States

Site	Control	Saturated and Freeze/Thaw Tested in Air	Saturated and Freeze/Thaw Tested in Water
Ann Arbor	Pass	Pass	Pass
Battle Creek	**Fail**	Pass	**Fail**
Brighton	Pass	Pass	Pass
Clarkston	Pass	Pass	Pass
Detroit	Pass	Pass	Pass
Dundee 19.0mm NMAS	**Fail**	Pass	**Fail**
Dundee 12.5mm NMAS	Pass	Pass	Pass
Grand Rapids I-196	**Fail**	**Fail**	**Fail**
Grand Rapids M-45	**Fail**	**Fail**	**Fail**
Hartland	Pass	Pass	Pass
Howell	**Fail**	Pass	**Fail**
Levering	**Fail**	**Fail**	**Fail**
Michigan Ave 19.0mm NMAS	Pass	Pass	**Fail**
Michigan Ave 12.5mm NMAS	Pass	Pass	Pass
Michigan International Speedway	Pass	Pass	Pass
Owosso	**Fail**	Pass	Pass
Pinckney	Pass	Pass	Pass
Saginaw	Pass	Pass	Pass
St. Johns	Pass	Pass	**Fail**
Toledo	Pass	Pass	Pass
Van Dyke	Pass	Pass	**Fail**

Table 8.30 Rut Depth Ratios of Mixes that Failed the Rut Depth Maximum Criterion

Site	Ratio of Conditioned Specimens Tested in Water by Control Specimens
Battle Creek	0.42
Dundee 19.0mm NMAS	0.62
Grand Rapids I-196	**1.05**
Grand Rapids M-45	**1.07**
Howell	0.66
Levering	0.84
Michigan Ave 19.0mm NMAS	0.90
St. Johns	0.76
Van Dyke	0.53

8.10.9 Summary of Phase I TSR and APA Comparison

Comparing factors that affect moisture damage test results and mixes deemed moisture prone for TSR and APA testing resulted in finding no relationship between the two test methods. Very few of the mixes were considered moisture damage susceptible by both test procedures. The same factors were considered for regression analysis with the exception of compaction and diameter, which were only accounted for in the TSR analysis. There were no similar factors affecting the results of these two tests. When the TSR values were grouped by compaction method and diameter it could be seen that binder PG was the one shared factor that may be affecting the moisture susceptibility (Kvasnak 2006).

8.10.10 Comparison of Moisture Susceptibility Testing of HMA Mixes and Asphalt Binders

One part of this research was developing and applying a moisture susceptibility test for asphalt binders. A second portion was examining the use of an APA for moisture susceptibility testing of HMA mixes. In this section data obtained during this research is evaluated to determine if there is a relationship between results obtained for mixes and asphalt binders. Regression analysis was employed to evaluate the relationship between mixes and binders in term of moisture susceptibility. The regression analysis indicated that there is a relationship between the APA, DSR, and water absorbed data. According to the analysis the weight of a binder specimen after 3 minutes and 48 hours has a significant effect on the rut depth of a moisture conditioned specimen tested in water. This indicates that changes in weight due to moisture saturation have an effect on rut depth. Other variables deemed significant were polymer modification, binder content %, gradation, and aggregate angularity (Kvasnak 2006).

Table 8.31 summarizes the materials deemed moisture susceptible by the three different procedures. The solid dots indicate that material collected from that location was deemed moisture susceptible. The strongest agreement occurs between the water absorbed procedure and APA test results. However, material from two sites, Battle Creek and Hartland, were deemed moisture susceptible by three procedures; thus indicating that there is a very strong possibility that these two mixes will be prone rutting caused by moisture damage (Kvasnak 2006).

Table 8.31 Moisture Susceptible Comparison

Site	Water Absorbed	Dynamic Shear Rheometer	Asphalt Pavement Analyzer Based on Ratio	Asphalt Pavement Analyzer Based on Ratio and Maximum Allowable Rut Depth
Ann Arbor				
Battle Creek	•	•	•	
Brighton	•			
Clarkston				
Detroit	•		•	
Dundee 19.0mm NMAS	•		•	
Dundee 12.5mm NMAS			•	
Grand Rapids I-196			•	•
Grand Rapids M-45			•	•
Hartland	•	•	•	
Howell	•		•	
Levering	•		•	
Michigan Ave 19.0mm NMAS			•	
Michigan Ave 12.5mm NMAS				
Michigan International Speedway	•			
Owosso			•	
Pinckney	•			
Saginaw			•	
St. Johns			•	
Toledo			•	
Van Dyke			•	

8.10.11APA Conclusions

In this chapter the use of an APA to evaluate the moisture susceptibility of HMA was explored. The criterion developed to determine whether or not a mix is moisture susceptible

indicated that 2 of the 21 mixes were moisture susceptible. Further analysis revealed that there is a strong relationship between water absorbed data and APA test data. There, however is not a strong relationship between DSR and APA test results, nor is there a strong relationship between TSR results and APA test results. It is recommended that if a loaded wheel tester is to be used for moisture susceptibility testing that more than three specimens be tested. The variability of the rut depth data was rather high and it is believed that additional specimens tested would yield data less affected by outliers (Kvasnak 2006).

8.11 Analysis of Results – DSR

The focus of the analysis was the affects of moisture on the rutting potential of an asphalt binder. The statistical evaluation of the data was grouped by individual filler-asphalt combinations and then comparisons between the groups. In all cases where hypothesis testing was conducted, a level of significance of 0.05 was used.

Part of the analysis conducted was determining if any of the binders failed the Superpave criterion that $G^*/\sin(\delta)$ be greater than 1.0 kPa for unaged binders. It should be noted that this criteria was established for stainless steel and not for a ceramic interfaces. Comparisons between the stainless steel interface and ceramic interface have revealed that the specimens tested with ceramic tend to give a slightly lower $G^*/\sin(\delta)$ value than those tested with a stainless steel interface for unsaturated specimens. The saturated specimens tend to yield greater differences between the two interfaces for $G^*/\sin(\delta)$ values.

The initial analysis examined the effects of moisture on the original binders. The null hypothesis for the following comparisons states that there is no statistical difference between the two original binder data sets examined. Table 8.32 summarizes the results of comparisons conducted to determine if there are significant differences between the testing conditions for

original binders. It can be seen that most of the comparisons indicated that there are statistical differences between the testing conditions; this however does not mean that all of the original binders with statistical differences will be moisture susceptible. It is expected that the varying testing conditions may yield different G* values. However, drastic changes in G* could be indicative of a moisture prone binder. In most cases, the phase angles were statistically equivalent, indicating that a closer examination of the results is needed to determine which binders are moisture susceptible (Kvasnak 2006).

The following analysis summarized in Table 8.32 examined whether the varying G* and G*/sin(δ) values would result in a revised binder high temperature grade. If different testing conditions result in a new grade, then the binder will be marked as moisture susceptible. The Superpave specification requirement is that G*/sin(δ) is at least 1.0 kPa at the given test temperature. All of the original binders tested within the varying environmental conditions pass the Superpave requirements, however there were several binders after moisture saturation that barely met the 1.0 kPa requirement. The original binders that were close to the 1.0 kPa requirement will be monitored closely for changes with the fillers (Kvasnak 2006).

Table 8.32 Comparison of Testing Conditions for All Data

		ALL	
		Hydrated Lime	Silica
Unconditioned Water Bath Vs. Conditioned Water Bath	Complex Modulus	***Reject***	***Reject***
	Phase Angle	***Reject***	***Reject***
	G*/ sin(δ)	***Reject***	***Reject***
Unconditioned Water Bath Vs. Unconditioned Air Chamber	Complex Modulus	***Reject***	Not Rejected
	Phase Angle	***Reject***	Not Rejected
	G*/ sin(δ)	***Reject***	Not Rejected
Conditioned Water bat Vs. Conditioned Air Chamber	Complex Modulus	***Reject***	***Reject***
	Phase Angle	Not Rejected	Not Rejected
	G*/ sin(δ)	***Reject***	***Reject***
Unconditioned Air Chamber Vs. Conditioned Air Chamber	Complex Modulus	***Reject***	***Reject***
	Phase Angle	***Reject***	***Reject***
	G*/ sin(δ)	***Reject***	***Reject***

Table 8.33 Comparison of Environmental Testing Conditions and Specimen Condition

Site	Water Bath Unconditioned vs Water Bath Conditioned				Water Bath Unconditioned vs Air Chamber Unconditioned				Water Bath Conditioned vs Air Chamber Conditioned				Air Chamber Unconditioned vs Air Chamber Conditioned			
	Complex Modulus	Phase Angle	Strain Amplitude	G*/ sin(delta)	Complex Modulus	Phase Angle	Strain Amplitude	G*/ sin(delta)	Complex Modulus	Phase Angle	Strain Amplitude	G*/ sin(delta)	Complex Modulus	Phase Angle	Strain Amplitude	G*/ sin(delta)
Pinckney	Accept	Reject	Accept	Accept	Accept	Reject	Reject	Accept	Reject	Reject	Accept	Reject	Accept	Reject	Accept	Accept
VanDyke	Accept	Accept	Accept	Accept	Reject	Reject	Accept	Reject	Reject	Accept	Reject	Accept	Reject	Reject	Accept	Reject
St. Johns	Reject	Reject	Accept	Reject	Reject	Reject	Reject	Reject	Reject	Reject	Reject	Reject	Reject	Reject	Accept	Reject
Grand Rapids M-45	Accept	Reject	Accept	Accept	Accept	Reject	Reject	Accept	Reject	Accept	Accept	Reject	Reject	Reject	Accept	Reject
Saginaw	Accept	Accept	Accept	Accept	Reject	Reject	Accept	Accept	Reject	Reject	Reject	Reject	Reject	Reject	Accept	Reject
Michigan Ave 3	Reject	Reject	Accept	Reject	Accept	Reject	Accept	Accept	Reject	Reject	Accept	Reject	Reject	Reject	Accept	Reject
Levering	Reject	Accept	Accept	Reject	Reject	Accept	Accept	Reject	Reject	Reject	Reject	Reject	Reject	Reject	Accept	Reject
Ann Arbor	Accept	Reject	Accept	Accept	Accept	Reject	Accept	Accept	Reject	Accept	Reject	Reject	Accept	Reject	Accept	Accept
Detroit	Reject	Reject	Accept	Reject	Reject	Accept	Reject	Reject	Reject	Reject	Reject	Reject	Reject	Reject	Accept	Reject
Toledo	Reject	Reject	Accept	Reject	Reject	Reject	Reject	Reject	Reject	Accept	Reject	Reject	Reject	Reject	Accept	Reject
Heartland	Reject	Reject	Accept	Reject	Reject	Reject	Reject	Reject	Accept	Accept	Reject	Accept	Reject	Reject	Accept	Reject
MIS	Accept	Reject	Accept	Accept	Accept	Accept	Reject	Accept	Reject	Accept	Accept	Reject	Accept	Reject	Accept	Accept
Battle Creek	Reject	Reject	Accept	Reject	Accept	Accept	Accept	Accept	Reject	Reject	Reject	Reject	Accept	Reject	Accept	Accept
Howell	Reject	Reject	Accept	Reject	Reject	Reject	Reject	Reject	Reject	Accept	Reject	Reject	Reject	Reject	Accept	Reject
Clarkston	Accept	Reject	Accept	Accept	Accept	Reject	Reject	Accept	Reject	Reject	Reject	Reject	Reject	Reject	Accept	Reject
Owosso	Reject	Reject	Accept	Reject	Accept	Accept	Accept	Reject	Reject	Reject	Reject	Reject	Accept	Reject	Reject	Accept
Dundee 3	Reject	Reject	Accept	Reject	Reject	Reject	Accept	Reject	Accept	Reject	Reject	Accept	Reject	Reject	Reject	Reject
Brighton	Reject	Reject	Accept	Reject	Accept	Accept	Accept	Accept	Reject	Accept	Reject	Reject	Reject	Reject	Reject	Reject
Michigan Ave 4	Reject	Reject	Accept	Reject	Accept	Accept	Reject	Accept	Reject	Reject	Reject	Reject	Reject	Reject	Accept	Reject
Grand Rapids I-196	Reject	Reject	Accept	Reject	Accept	Reject	Accept	Accept	Reject	Reject	Accept	Reject	Accept	Reject	Accept	Accept
Dundee 4	Accept	Reject	Accept	Accept	Reject	Accept	Reject	Reject	Reject	Accept	Reject	Reject	Accept	Reject	Accept	Accept

8.11.1 Statistical and Graphical Results of Michigan Binders Categorized by Filler Type

Moisture damage issues can arise in HMA pavements even if the asphalt binder has not been found to be moisture susceptible. The moisture susceptibility could be caused by either the aggregate or the interaction between the aggregate and asphalt binder. Two fillers and their interactions with asphalt binders were examined as part of this dissertation. Three percentages by weight were examined to see if different levels of each filler had dissimilar results. The mastics considered were hydrated lime and silica, both passing the #200 sieve. The following analysis explored the affects of each mastic associated with the 21 asphalt binders sampled.

In Table 8.34, comparisons are grouped by filler type and percentage levels. Not pooling the data allows certain trends to be observed. $G^*/\sin(\delta)$ values tend to be deemed statistically similar for comparison of specimens tested in a water bath or unconditioned. Differences begin to arise with an increase level of filler. $G^*/\sin(\delta)$ comparisons are also dissimilar when comparing conditioned specimens or ones tested in an air chamber (Kvasnak 2006).

Table 8.34 Results of Comparing Environmental Testing Conditions by Mastic Percentage Level

		5% Hydrated Lime	5% Silica	10% Hydrated Lime	10% Silica	20% Hydrated Lime	20% Silica
Unconditioned Water Bath Vs. Conditioned Water Bath	Complex Modulus	Not Rejected	Not Rejected	Not Rejected	***Reject***	***Reject***	***Reject***
	Phase Angle	***Reject***	***Reject***	***Reject***	***Reject***	***Reject***	***Reject***
	G*/ sin(δ)	Not Rejected	Not Rejected	Not Rejected	***Reject***	***Reject***	Not Rejected
Unconditioned Water Bath Vs. Unconditioned Air Chamber	Complex Modulus	Not Rejected	Not Rejected	Not Rejected	Not Rejected	Not Rejected	Not Rejected
	Phase Angle	Not Rejected	Not Rejected	Not Rejected	Not Rejected	***Reject***	***Reject***
	G*/ sin(δ)	Not Rejected	Not Rejected	Not Rejected	Not Rejected	***Reject***	Not Rejected
Conditioned Water Bath Vs. Conditioned Air Chamber	Complex Modulus	***Reject***	***Reject***	Not Rejected	***Reject***	***Reject***	***Reject***
	Phase Angle	Not Rejected	Not Rejected	***Reject***	Not Rejected	***Reject***	Not Rejected
	G*/ sin(delta)	***Reject***	***Reject***	Not Rejected	***Reject***	***Reject***	***Reject***
Unconditioned Air Chamber Vs. Conditioned Air Chamber	Complex Modulus	***Reject***	***Reject***	***Reject***	***Reject***	Not Rejected	***Reject***
	Phase Angle	***Reject***	***Reject***	***Reject***	***Reject***	***Reject***	***Reject***
	G*/ sin(δ)	***Reject***	***Reject***	***Reject***	***Reject***	***Reject***	***Reject***
Conditioned Water Bath Vs. Unconditioned Air Chamber	Complex Modulus	***Reject***	***Reject***	***Reject***	***Reject***	***Reject***	***Reject***
	Phase Angle	***Reject***	***Reject***	***Reject***	***Reject***	***Reject***	***Reject***
	G*/ sin(δ)	***Reject***	***Reject***	***Reject***	***Reject***	***Reject***	***Reject***

8.11.1.1 Effects of Hydrated Lime

Extensive research has been conducted analyzing the advantages of using hydrated lime in binders to resist moisture damage. Since past research has shown that hydrated lime is moisture resistant and aids in preventing moisture damage within HMA, the current research used hydrated lime as a mineral filler to prevent moisture damage. Table 8.35 outlines the results of comparisons conducted to determine if there is a statistical difference between testing conditions results within a certain percentage of filler. The comparisons with the unconditioned samples tested in the water bath for both 5% and 10% of hydrated lime yield statistically

equivalent results with conditioned specimens tested in water bath and unconditioned specimens tested in the air chamber. However, comparisons between conditioned specimens tested in the water bath and unconditioned specimens tested in the air chamber were statistically different for both G* and G*/sin(δ) implying that there is a shift in the distributions' location, with respect to the unconditioned air chamber specimens, for G* and G*/sin(δ) after water saturation. In general, binders with 20% hydrated lime are statistically different when comparing environmental test conditions (Kvasnak 2006).

Table 8.35 Results of Hydrated Lime Comparisons Grouped by Percentage of Filler

		5% Lime	10% Lime	20% Lime
Unconditioned Water Bath Vs. Conditioned	Complex Modulus	Not Rejected	Not Rejected	***Reject***
	G*/ sin(δ)	Not Rejected	Not Rejected	***Reject***
Unconditioned Water Bath Vs. Unconditioned	Complex Modulus	Not Rejected	Not Rejected	Not Rejected
	G*/ sin(δ)	Not Rejected	Not Rejected	***Reject***
Conditioned Water Bath Vs. Conditioned	Complex Modulus	***Reject***	Not Rejected	***Reject***
	G*/ sin(δ)	***Reject***	Not Rejected	***Reject***
Unconditioned Air Chamber Vs. Conditioned	Complex Modulus	***Reject***	***Reject***	Not Rejected
	G*/ sin(δ)	***Reject***	***Reject***	***Reject***
Conditioned Water Bath Vs. Unconditioned	Complex Modulus	***Reject***	***Reject***	***Reject***
	G*/ sin(δ)	***Reject***	***Reject***	***Reject***

Table 8.36 summarizes the results of comparisons by site, filler, and percentage of filler. As with the comparisons for the original binders by site, most of the results indicate that the environmental testing conditions yield different G* and G*/sin(δ) measurements (Kvasnak 2006).

Since the comparisons indicate that there are significant statistical differences between test condition measurements of G* and G*/sin(δ), the raw data was examined to determine if the addition of hydrated lime was beneficial, detrimental, or had little affect on the G* and G*/sin(δ) measurements. This was a twofold process where the minimum Superpave requirements were applied and then a comparison between the original binder results and hydrated lime results commenced (Kvasnak 2006).

All of the binders with hydrated lime met the Superpave minimum requirement for G*/sin(δ). However, G*/sin(δ) values did tend to increase for the binders with hydrated lime. The increase in G*/sin(δ) could mean the filler changes to a higher temperature grade, thus enabling the binder to perform better in summer months. Also, a higher G*/sin(δ) for the materials tested in the water bath and/or saturated indicates that the hydrated lime is preventing moisture damage (Kvasnak 2006).

Table 8.37 displays the results of calculating the G*/sin(δ) ratio of hydrated lime to original binders. The values close to 1 indicate that little change occurred and is neither beneficial nor detrimental. Values less than 1, displayed in bold in the table, indicate binders that performed poorly with the hydrated lime when compared with the performance of the binder without hydrated lime. In most cases, the values were greater than 1, which indicates that the hydrated lime improved the performance and resistance to moisture damage. The ratio increases with an increasing percentage of hydrated lime for all but four binders. This increase in the ratio indicates that the hydrated lime is improving the rut resistance of a binder (Kvasnak 2006).

Table 8.36 Results of Hydrated Lime Comparing Testing Conditions

			Unconditioned Water Bath vs Saturated Water Bath		Unconditioned Water Bath vs Unconditioned Air Chamber		Saturated Water Bath vs Saturated Air Chamber		Unconditioned Air Chamber vs Saturated Air Chamber		Saturated Water Bath vs Unconditioned Air Chamber	
Site	Mastic	Percentage	Complex Modulus	G*/ sin(delta)	Complex Modulus	G*/ sin(delta)	Complex Modulus	G*/ sin(delta)	Complex Modulus	G*/ sin(delta)	Complex Modulus	G*/ sin(delta)
Ann Arbor	Lime	5	Reject	Reject	Reject	Reject	Reject	Reject	Reject	Reject	Reject	Reject
Battle Creek	Lime	5	Reject	Reject	Reject	Reject	Reject	Reject	Reject	Reject	Not Rejected	Not Rejected
Brighton	Lime	5	Reject	Reject	Reject	Reject	Reject	Reject	Reject	Reject	Reject	Reject
Clarkston	Lime	5	Reject	Reject	Reject	Reject	Reject	Reject	Reject	Reject	Reject	Reject
Detroit	Lime	5	Reject	Reject	Reject	Reject	Reject	Reject	Reject	Reject	Reject	Not Rejected
Dundee 19.0mm NMAS	Lime	5	Reject	Reject	Reject	Reject	Reject	Reject	Reject	Reject	Reject	Reject
Dundee 12.5mm NMAS	Lime	5	Reject	Reject	Reject	Reject	Reject	Reject	Reject	Reject	Reject	Reject
Grand Rapids M-45	Lime	5	Reject	Reject	Reject	Reject	Reject	Reject	Reject	Reject	Reject	Reject
Grand Rapids I-196	Lime	5	Reject	Reject	Reject	Reject	Reject	Reject	Reject	Reject	Reject	Reject
Hartland	Lime	5	Reject	Reject	Reject	Reject	Reject	Reject	Reject	Reject	Reject	Reject
Howell	Lime	5	Reject	Reject	Reject	Reject	Reject	Reject	Reject	Reject	Reject	Reject
Levering	Lime	5	Reject	Reject	Reject	Reject	Reject	Reject	Reject	Reject	Reject	Reject
Michigan Ave 19.0mm NMAS	Lime	5	Reject	Reject	Reject	Reject	Reject	Reject	Reject	Reject	Reject	Reject
Michigan Ave 12.5mm NMAS	Lime	5	Reject	Reject	Reject	Reject	Reject	Reject	Reject	Reject	Reject	Reject
Michigan International Speedway	Lime	5	Reject	Reject	Reject	Reject	Reject	Reject	Reject	Reject	Reject	Reject
Owosso	Lime	5	Reject	Reject	Reject	Reject	Reject	Reject	Reject	Reject	Reject	Reject
Pinckney	Lime	5	Reject	Reject	Not Rejected	Not Rejected	Reject	Reject	Reject	Reject	Reject	Reject
Saginaw	Lime	5	Reject	Reject	Reject	Reject	Reject	Reject	Reject	Reject	Reject	Reject
St. Johns	Lime	5	Reject	Reject	Reject	Reject	Reject	Reject	Reject	Reject	Reject	Reject
Toledo	Lime	5	Reject	Reject	Reject	Reject	Reject	Reject	Reject	Reject	Reject	Not Rejected
Van Dyke	Lime	5	Reject	Reject	Reject	Reject	Reject	Reject	Reject	Reject	Reject	Reject
Ann Arbor	Lime	10	Reject	Reject	Reject	Reject	Reject	Reject	Reject	Reject	Reject	Reject
Battle Creek	Lime	10	Reject	Reject	Reject	Reject	Reject	Reject	Reject	Reject	Reject	Reject
Brighton	Lime	10	Reject	Reject	Reject	Reject	Reject	Reject	Reject	Reject	Reject	Reject
Clarkston	Lime	10	Reject	Reject	Reject	Reject	Reject	Reject	Reject	Reject	Reject	Not Rejected
Detroit	Lime	10	Reject	Reject	Reject	Reject	Reject	Reject	Reject	Reject	Reject	Reject
Dundee 19.0mm NMAS	Lime	10	Not Rejected	Not Rejected	Reject	Reject	Reject	Reject	Reject	Reject	Reject	Reject
Dundee 12.5mm NMAS	Lime	10	Reject	Reject	Reject	Reject	Reject	Reject	Reject	Reject	Reject	Reject
Grand Rapids M-45	Lime	10	Reject	Reject	Reject	Reject	Not Rejected	Not Rejected	Reject	Reject	Reject	Reject
Grand Rapids I-196	Lime	10	Reject	Reject	Reject	Reject	Reject	Reject	Reject	Reject	Reject	Reject
Hartland	Lime	10	Reject	Reject	Reject	Reject	Reject	Reject	Reject	Reject	Reject	Reject
Howell	Lime	10	Reject	Reject	Reject	Reject	Reject	Reject	Reject	Reject	Reject	Reject
Levering	Lime	10	Reject	Reject	Reject	Reject	Reject	Reject	Reject	Reject	Reject	Reject
Michigan Ave 19.0mm NMAS	Lime	10	Reject	Reject	Reject	Reject	Reject	Reject	Reject	Reject	Reject	Reject
Michigan Ave 12.5mm NMAS	Lime	10	Reject	Reject	Reject	Reject	Reject	Reject	Reject	Reject	Reject	Reject
Michigan International Speedway	Lime	10	Reject	Reject	Reject	Reject	Reject	Reject	Reject	Reject	Reject	Reject
Owosso	Lime	10	Reject	Reject	Reject	Reject	Reject	Reject	Reject	Reject	Reject	Reject
Pinckney	Lime	10	Reject	Reject	Reject	Reject	Reject	Reject	Reject	Reject	Reject	Reject
Saginaw	Lime	10	Reject	Reject	Not Rejected	Not Rejected	Reject	Reject	Reject	Reject	Reject	Reject
St. Johns	Lime	10	Reject	Reject	Reject	Reject	Reject	Reject	Reject	Reject	Reject	Reject
Toledo	Lime	10	Reject	Reject	Reject	Reject	Reject	Reject	Reject	Reject	Reject	Reject
Van Dyke	Lime	10	Reject	Reject	Reject	Reject	Reject	Reject	Reject	Reject	Reject	Reject
Ann Arbor	Lime	20	Reject	Reject	Reject	Reject	Reject	Reject	Reject	Reject	Reject	Reject
Battle Creek	Lime	20	Reject	Reject	Reject	Reject	Reject	Reject	Reject	Reject	Reject	Reject
Brighton	Lime	20	Not Rejected	Not Rejected	Reject	Reject	Reject	Reject	Reject	Reject	Reject	Reject
Clarkston	Lime	20	Reject	Reject	Reject	Reject	Reject	Reject	Reject	Reject	Reject	Reject
Detroit	Lime	20	Reject	Reject	Reject	Reject	Reject	Reject	Reject	Reject	Reject	Reject
Dundee 19.0mm NMAS	Lime	20	Reject	Reject	Reject	Reject	Reject	Reject	Reject	Reject	Reject	Reject
Dundee 12.5mm NMAS	Lime	20	Reject	Reject	Reject	Reject	Reject	Reject	Reject	Reject	Reject	Reject
Grand Rapids M-45	Lime	20	Reject	Reject	Reject	Reject	Reject	Reject	Reject	Reject	Reject	Reject
Grand Rapids I-196	Lime	20	Reject	Reject	Reject	Reject	Reject	Reject	Reject	Reject	Reject	Reject
Hartland	Lime	20	Reject	Reject	Reject	Reject	Reject	Reject	Reject	Reject	Reject	Reject
Howell	Lime	20	Reject	Reject	Reject	Reject	Reject	Reject	Reject	Reject	Reject	Reject
Levering	Lime	20	Reject	Reject	Reject	Reject	Reject	Reject	Reject	Reject	Reject	Reject
Michigan Ave 19.0mm NMAS	Lime	20	Reject	Reject	Reject	Reject	Reject	Reject	Reject	Reject	Reject	Reject
Michigan Ave 12.5mm NMAS	Lime	20	Reject	Reject	Reject	Reject	Reject	Reject	Reject	Reject	Reject	Reject
Michigan International Speedway	Lime	20	Reject	Reject	Not Rejected	Not Rejected	Reject	Reject	Reject	Reject	Reject	Reject
Owosso	Lime	20	Reject	Reject	Reject	Reject	Reject	Reject	Reject	Reject	Reject	Reject
Pinckney	Lime	20	Reject	Reject	Reject	Reject	Reject	Reject	Reject	Reject	Reject	Reject
Saginaw	Lime	20	Reject	Reject	Reject	Reject	Reject	Reject	Reject	Reject	Reject	Reject
St. Johns	Lime	20	Reject	Reject	Reject	Reject	Reject	Reject	Reject	Reject	Reject	Reject
Toledo	Lime	20	Reject	Reject	Reject	Reject	Reject	Reject	Reject	Reject	Reject	Reject
Van Dyke	Lime	20	Reject	Reject	Reject	Reject	Not Rejected	Not Rejected	Reject	Reject	Reject	Reject

Table 8.37 Ratio G*/sin(δ) of Hydrated Lime to Original Binder

			Averages Ratio of Hydrated Lime:Original Binder			
Site	**Mastic**	**Percentage**	**WC**	**AC**	**WO**	**AO**
Ann Arbor	***Lime***	***5***	1.65	1.74	2.57	1.46
Ann Arbor	***Lime***	***10***	7.99	2.51	3.39	2.06
Ann Arbor	***Lime***	***20***	3.66	2.79	3.95	2.09
Battle Creek	***Lime***	***5***	1.74	2.51	2.05	**1.03**
Battle Creek	***Lime***	***10***	1.67	3.22	2.16	**0.92**
Battle Creek	***Lime***	***20***	1.69	3.64	9.41	2.93
Brighton	***Lime***	***5***	**0.60**	**0.89**	**0.69**	**0.87**
Brighton	***Lime***	***10***	**0.60**	**0.64**	**0.95**	1.09
Brighton	***Lime***	***20***	1.31	1.03	1.32	1.83
Clarkston	***Lime***	***5***	**0.86**	5.00	2.42	1.31
Clarkston	***Lime***	***10***	1.02	2.42	2.41	1.33
Clarkston	***Lime***	***20***	1.58	3.39	5.02	2.61
Detroit	***Lime***	***5***	1.55	2.29	2.57	1.97
Detroit	***Lime***	***10***	1.82	2.71	3.27	2.96
Detroit	***Lime***	***20***	2.50	3.97	4.44	3.85
Dundee 19.0mm NMAS	***Lime***	***5***	3.97	**0.86**	1.88	1.11
Dundee 19.0mm NMAS	***Lime***	***10***	**0.97**	1.22	1.30	1.44
Dundee 19.0mm NMAS	***Lime***	***20***	1.61	1.61	1.93	2.56
Dundee 12.5mm NMAS	***Lime***	***5***	**0.73**	1.16	1.27	1.18
Dundee 12.5mm NMAS	***Lime***	***10***	1.19	2.42	**0.97**	1.95
Dundee 12.5mm NMAS	***Lime***	***20***	2.25	3.97	2.11	3.30
Grand Rapids M-45	***Lime***	***5***	**0.79**	**0.74**	1.10	**0.82**
Grand Rapids M-45	***Lime***	***10***	**0.99**	**0.34**	1.59	**0.68**
Grand Rapids M-45	***Lime***	***20***	3.02	**0.86**	8.11	1.08
Grand Rapids I-196	***Lime***	***5***	1.16	1.19	1.20	**0.92**
Grand Rapids I-196	***Lime***	***10***	1.60	1.39	1.52	1.28
Grand Rapids I-196	***Lime***	***20***	2.84	2.69	3.29	1.96
Hartland	***Lime***	***5***	2.80	1.65	1.63	2.20
Hartland	***Lime***	***10***	5.13	1.52	2.30	2.62
Hartland	***Lime***	***20***	18.39	2.33	3.41	4.52
Howell	***Lime***	***5***	**0.66**	1.18	1.68	**0.93**
Howell	***Lime***	***10***	1.07	1.19	0.88	1.06
Howell	***Lime***	***20***	1.39	2.17	4.37	1.91
Levering	***Lime***	***5***	2.04	**0.73**	1.67	1.83
Levering	***Lime***	***10***	**0.71**	1.93	2.42	2.31
Levering	***Lime***	***20***	1.66	2.28	3.41	2.97
Michigan Ave 19.0mm NMAS	***Lime***	***5***	**0.70**	**0.74**	1.17	1.19
Michigan Ave 19.0mm NMAS	***Lime***	***10***	1.05	1.47	1.37	2.04
Michigan Ave 19.0mm NMAS	***Lime***	***20***	2.02	0.94	1.66	2.54
Michigan Ave 12.5mm NMAS	***Lime***	***5***	**0.42**	**0.66**	**0.20**	**0.67**
Michigan Ave 12.5mm NMAS	***Lime***	***10***	**0.57**	1.10	**0.29**	**0.79**
Michigan Ave 12.5mm NMAS	***Lime***	***20***	**0.50**	1.35	**0.36**	1.26
Michigan International Speedway	***Lime***	***5***	**0.73**	**0.91**	2.04	2.48
Michigan International Speedway	***Lime***	***10***	**0.88**	1.40	3.19	2.31
Michigan International Speedway	***Lime***	***20***	2.96	1.55	4.71	3.82
Owosso	***Lime***	***5***	1.45	1.15	**0.75**	1.50
Owosso	***Lime***	***10***	1.45	1.19	1.17	2.82
Owosso	***Lime***	***20***	1.27	1.74	1.67	3.30
Pinckney	***Lime***	***5***	2.71	5.61	3.37	2.88
Pinckney	***Lime***	***10***	2.93	2.30	4.24	2.88
Pinckney	***Lime***	***20***	2.92	**0.57**	5.55	5.92
Saginaw	***Lime***	***5***	1.06	**0.56**	2.20	1.16
Saginaw	***Lime***	***10***	3.21	**0.77**	2.63	2.37
Saginaw	***Lime***	***20***	**0.62**	**0.42**	4.08	4.05
St. Johns	***Lime***	***5***	5.04	1.06	**0.59**	1.71
St. Johns	***Lime***	***10***	4.18	2.09	1.30	1.22
St. Johns	***Lime***	***20***	3.26	2.40	2.18	1.96
Toledo	***Lime***	***5***	2.27	1.76	2.69	2.16
Toledo	***Lime***	***10***	1.25	2.74	3.23	3.19
Toledo	***Lime***	***20***	4.82	3.00	6.36	3.77
VanDyke	***Lime***	***5***	3.67	1.37	2.41	1.92
VanDyke	***Lime***	***10***	18.18	1.73	3.50	3.52
VanDyke	***Lime***	***20***	5.25	2.34	6.14	4.46

WC= Conditioned Water Bath Specimens, AC= Conditioned Air Chamber Specimens

WO= Unconditioned Water Bath Specimens,, AO=Unconditioned Air Chamber Specimens

8.11.1.2 Effects of Silica

The second filler selected for determining the sensitivity of the new moisture susceptibility test was silica since siliceous materials are known to be moisture prone. The analysis conducted for the binders with hydrated lime were repeated for the binders with silica, as previously described in section 8.11.1.1.

Table 8.38 summarizes the results of comparisons conducted to determine if G* and G*/sin(δ) are statistically different when measured in dissimilar testing environments. As the table relates, almost all of the comparisons indicate that G* and G*/sin(δ) are not the same with the exception of the comparison between the unconditioned water bath and unconditioned air chamber. The results indicate that water saturation has a significant impact on G* and G*/sin(δ) (Kvasnak 2006).

Table 8.38 Results of Comparing Testing Conditions for Binders with Silica

		5% Silica	10% Silica	20% Silica
Unconditioned Water Bath Vs. Conditioned	Complex Modulus	Not Rejected	***Reject***	***Reject***
	G*/ sin(δ)	Not Rejected	***Reject***	Not Rejected
Unconditioned Water Bath Vs. Unconditioned	Complex Modulus	Not Rejected	Not Rejected	Not Rejected
	G*/ sin(δ)	Not Rejected	Not Rejected	Not Rejected
Conditioned Water Bath Vs. Conditioned	Complex Modulus	***Reject***	***Reject***	***Reject***
	G*/ sin(δ)	***Reject***	***Reject***	***Reject***
Unconditioned Air Chamber Vs. Conditioned	Complex Modulus	***Reject***	***Reject***	***Reject***
	G*/ sin(δ)	***Reject***	***Reject***	***Reject***
Conditioned Water Bath Vs. Unconditioned	Complex Modulus	***Reject***	***Reject***	***Reject***
	G*/ sin(δ)	***Reject***	***Reject***	***Reject***

The comparison results comparing environmental testing condition measurements for G* and G*/ sin(δ) are displayed in Table 8.39. It can be seen that very few of the comparisons yield statistically equivalent results.

G*/ sin(δ) ratios of binders with silica to original binders were computed to determine any trends. The computed ratios are displayed in Table 8.40. Unlike the ratios computed with the hydrated lime filler, many of the binders with silica make only a small advantageous contribution if any at all. There are quite a few more silica results with a lower G*/ sin(δ) in comparison to the original binder G*/ sin(δ). Unlike the hydrated lime, less than half of the binders exhibit an increasing ratio with increasing silica amounts (Kvasnak 2006).

Table 8.39 Results of Comparing Testing Conditions of Binders with Silica by Site

			Unconditioned Water Bath vs. Conditioned Water Bath		Unconditioned Water Bath vs. Unconditioned Air Chamber		Conditioned Water Bath vs. Conditioned Air Chamber		Unconditioned Air Chamber vs. Conditioned Air Chamber		Conditioned Water Bath vs. Unconditioned Air Chamber	
Site	Mastic	Percentage	Complex Modulus	G*/ sin(δ)	Complex Modulus	G*/ sin(delta)	Complex Modulus	G*/ sin(delta)	Complex Modulus	G*/ sin(delta)	Complex Modulus	G*/ sin(delta)
Ann Arbor	Silica	5	Reject	Reject	Reject	Reject	Reject	Reject	Reject	Reject	Reject	Reject
Battle Creek	Silica	5	Reject	Reject	Reject	Reject	Reject	Reject	Reject	Reject	Reject	Reject
Brighton	Silica	5	Reject	Reject	Reject	Reject	Reject	Reject	Reject	Reject	Reject	Reject
Clarkston	Silica	5	Reject	Reject	Reject	Reject	Reject	Reject	Reject	Reject	Reject	Reject
Detroit	Silica	5	Reject	Reject	Reject	Reject	Reject	Reject	Reject	Reject	Reject	Not Rejected
Dundee 19.0mm NMAS	Silica	5	Reject	Reject	Reject	Reject	Reject	Reject	Reject	Reject	Reject	Reject
Dundee 12.5mm NMAS	Silica	5	Reject	Reject	Reject	Reject	Reject	Reject	Reject	Reject	Reject	Reject
Grand Rapids M-45	Silica	5	Reject	Reject	Reject	Reject	Not Rejected	Not Rejected	Reject	Reject	Reject	Reject
Grand Rapids I-196	Silica	5	Reject	Reject	Not Rejected	Not Rejected	Reject	Reject	Reject	Reject	Reject	Reject
Hartland	Silica	5	Reject	Reject	Reject	Reject	Reject	Reject	Reject	Reject	Reject	Reject
Howell	Silica	5	Reject	Reject	Reject	Reject	Reject	Reject	Reject	Reject	Reject	Reject
Levering	Silica	5	Reject	Reject	Reject	Reject	Reject	Reject	Reject	Reject	Reject	Reject
Michigan Ave 19.0mm NMAS	Silica	5	Reject	Reject	Reject	Reject	Reject	Reject	Reject	Reject	Reject	Reject
Michigan Ave 12.5mm NMAS	Silica	5	Reject	Reject	Reject	Reject	Reject	Reject	Reject	Reject	Reject	Reject
Michigan International Speedway	Silica	5	Reject	Reject	Reject	Reject	Reject	Reject	Reject	Reject	Reject	Reject
Owosso	Silica	5	Reject	Reject	Not Rejected	Not Rejected	Reject	Reject	Not Rejected	Not Rejected	Reject	Reject
Pinckney	Silica	5	Reject	Reject	Reject	Reject	Reject	Reject	Reject	Reject	Reject	Reject
Saginaw	Silica	5	Reject	Reject	Reject	Reject	Reject	Reject	Reject	Reject	Reject	Reject
St. Johns	Silica	5	Reject	Reject	Reject	Reject	Reject	Reject	Reject	Reject	Reject	Reject
Toledo	Silica	5	Reject	Reject	Reject	Reject	Not Rejected	Not Rejected	Reject	Reject	Reject	Reject
Van Dyke	Silica	5	Reject	Reject	Reject	Reject	Reject	Reject	Reject	Reject	Reject	Reject
Ann Arbor	Silica	10	Reject	Reject	Reject	Reject	Reject	Reject	Reject	Reject	Reject	Reject
Battle Creek	Silica	10	Reject	Reject	Reject	Reject	Reject	Reject	Reject	Reject	Reject	Reject
Brighton	Silica	10	Reject	Not Rejected	Reject	Reject	Reject	Reject	Reject	Reject	Reject	Reject
Clarkston	Silica	10	Reject	Reject	Reject	Reject	Reject	Reject	Reject	Reject	Reject	Reject
Detroit	Silica	10	Reject	Not Rejected	Reject	Not Rejected	Reject	Reject	Reject	Reject	Reject	Reject
Dundee 19.0mm NMAS	Silica	10	Reject	Reject	Reject	Reject	Reject	Reject	Reject	Reject	Reject	Reject
Dundee 12.5mm NMAS	Silica	10	Reject	Reject	Reject	Reject	Reject	Reject	Reject	Reject	Reject	Reject
Grand Rapids M-45	Silica	10	Reject	Reject	Reject	Reject	Reject	Reject	Reject	Reject	Reject	Reject
Grand Rapids I-196	Silica	10	Reject	Reject	Reject	Reject	Reject	Reject	Reject	Reject	Reject	Reject
Hartland	Silica	10	Reject	Reject	Reject	Reject	Reject	Reject	Reject	Reject	Reject	Reject
Howell	Silica	10	Reject	Reject	Reject	Reject	Reject	Reject	Reject	Reject	Reject	Reject
Levering	Silica	10	Reject	Reject	Reject	Reject	Reject	Reject	Reject	Reject	Reject	Reject
Michigan Ave 19.0mm NMAS	Silica	10	Reject	Reject	Reject	Reject	Reject	Reject	Reject	Reject	Reject	Reject
Michigan Ave 12.5mm NMAS	Silica	10	Reject	Reject	Reject	Reject	Reject	Reject	Reject	Reject	Reject	Reject
Michigan International Speedway	Silica	10	Reject	Reject	Reject	Reject	Reject	Reject	Reject	Reject	Not Rejected	Not Rejected
Owosso	Silica	10	Reject	Reject	Reject	Reject	Reject	Reject	Not Rejected	Reject	Reject	Reject
Pinckney	Silica	10	Reject	Reject	Reject	Reject	Reject	Reject	Reject	Reject	Reject	Reject
Saginaw	Silica	10	Reject	Reject	Reject	Reject	Reject	Reject	Reject	Reject	Reject	Reject
St. Johns	Silica	10	Reject	Reject	Reject	Reject	Reject	Reject	Reject	Reject	Reject	Reject
Toledo	Silica	10	Reject	Not Rejected	Reject	Reject	Reject	Reject	Reject	Reject	Reject	Reject
Van Dyke	Silica	10	Reject	Reject	Not Rejected	Not Rejected	Reject	Reject	Reject	Reject	Reject	Reject
Ann Arbor	Silica	20	Reject	Reject	Reject	Reject	Reject	Reject	Not Rejected	Not Rejected	Reject	Reject
Battle Creek	Silica	20	Reject	Reject	Reject	Reject	Reject	Reject	Reject	Reject	Reject	Reject
Brighton	Silica	20	Reject	Reject	Reject	Reject	Reject	Reject	Reject	Reject	Reject	Reject
Clarkston	Silica	20	Reject	Reject	Reject	Reject	Reject	Reject	Reject	Reject	Reject	Reject
Detroit	Silica	20	Reject	Reject	Reject	Reject	Reject	Reject	Reject	Reject	Reject	Reject
Dundee 19.0mm NMAS	Silica	20	Reject	Reject	Reject	Reject	Reject	Reject	Reject	Reject	Reject	Reject
Dundee 12.5mm NMAS	Silica	20	Reject	Reject	Reject	Reject	Reject	Reject	Reject	Reject	Reject	Reject
Grand Rapids M-45	Silica	20	Reject	Reject	Reject	Reject	Reject	Reject	Reject	Reject	Reject	Reject
Grand Rapids I-196	Silica	20	Reject	Reject	Not Rejected	Not Rejected	Reject	Reject	Reject	Reject	Reject	Reject
Hartland	Silica	20	Reject	Reject	Reject	Reject	Reject	Reject	Reject	Reject	Reject	Reject
Howell	Silica	20	Not Rejected	Not Rejected	Reject	Reject	Reject	Reject	Reject	Reject	Reject	Reject
Levering	Silica	20	Reject	Reject	Reject	Reject	Reject	Reject	Reject	Reject	Reject	Reject
Michigan Ave 19.0mm NMAS	Silica	20	Reject	Reject	Reject	Reject	Reject	Reject	Reject	Reject	Reject	Reject
Michigan Ave 12.5mm NMAS	Silica	20	Reject	Reject	Reject	Reject	Reject	Reject	Reject	Reject	Reject	Reject
Michigan International Speedway	Silica	20	Reject	Reject	Reject	Reject	Reject	Reject	Reject	Reject	Reject	Reject
Owosso	Silica	20	Reject	Reject	Reject	Reject	Reject	Reject	Reject	Reject	Reject	Reject
Pinckney	Silica	20	Reject	Reject	Not Rejected	Not Rejected	Reject	Reject	Reject	Reject	Reject	Reject
Saginaw	Silica	20	Reject	Reject	Reject	Reject	Reject	Reject	Reject	Reject	Reject	Reject
St. Johns	Silica	20	Reject	Reject	Reject	Reject	Reject	Reject	Reject	Reject	Reject	Reject
Toledo	Silica	20	Reject	Reject	Reject	Reject	Reject	Reject	Reject	Reject	Reject	Reject
Van Dyke	Silica	20	Reject	Reject	Reject	Reject	Reject	Reject	Reject	Reject	Reject	Reject

Table 8.40 G*/sin(δ) Ratio of Silica to Original Binder

			Averages Ratio of Silica:Original Binder			
Site	**Mastic**	**Percentage**	**WC**	**AC**	**WO**	**AO**
Ann Arbor	***Silica***	***5***	1.36	2.80	2.27	1.54
Ann Arbor	***Silica***	***10***	2.42	3.04	4.12	3.50
Ann Arbor	***Silica***	***20***	2.79	3.02	1.85	2.67
Battle Creek	***Silica***	***5***	1.29	2.08	1.90	1.93
Battle Creek	***Silica***	***10***	1.47	1.77	2.19	1.72
Battle Creek	***Silica***	***20***	1.99	2.15	2.63	2.16
Brighton	***Silica***	***5***	**0.91**	**0.40**	**0.90**	**0.93**
Brighton	***Silica***	***10***	**0.64**	**0.65**	**0.67**	**0.89**
Brighton	***Silica***	***20***	**0.70**	**0.80**	**0.77**	**0.84**
Clarkston	***Silica***	***5***	**0.76**	1.19	**0.82**	**0.60**
Clarkston	***Silica***	***10***	1.02	1.08	**0.98**	1.19
Clarkston	***Silica***	***20***	1.29	1.40	**0.93**	1.01
Detroit	***Silica***	***5***	1.53	1.79	6.40	1.97
Detroit	***Silica***	***10***	2.51	2.02	10.24	2.29
Detroit	***Silica***	***20***	1.80	2.36	2.82	2.71
Dundee 19.0mm NMAS	***Silica***	***5***	**0.96**	**0.87**	**0.93**	1.33
Dundee 19.0mm NMAS	***Silica***	***10***	1.14	**0.92**	**0.98**	1.08
Dundee 19.0mm NMAS	***Silica***	***20***	1.32	1.12	1.18	1.42
Dundee 12.5mm NMAS	***Silica***	***5***	**0.78**	3.68	**0.65**	1.53
Dundee 12.5mm NMAS	***Silica***	***10***	1.07	1.34	**0.93**	1.40
Dundee 12.5mm NMAS	***Silica***	***20***	1.47	1.12	1.11	1.62
Grand Rapids M-45	***Silica***	***5***	1.90	**0.67**	**0.99**	**0.66**
Grand Rapids M-45	***Silica***	***10***	**0.78**	1.05	1.01	**0.68**
Grand Rapids M-45	***Silica***	***20***	**0.84**	**0.54**	**0.98**	1.38
Grand Rapids I-196	***Silica***	***5***	1.14	3.82	1.39	**0.94**
Grand Rapids I-196	***Silica***	***10***	1.69	1.45	7.43	1.02
Grand Rapids I-196	***Silica***	***20***	1.89	1.57	2.33	1.62
Hartland	***Silica***	***5***	9.80	2.30	2.00	2.53
Hartland	***Silica***	***10***	2.44	2.49	1.05	2.43
Hartland	***Silica***	***20***	2.60	1.61	1.89	2.95
Howell	***Silica***	***5***	**0.85**	1.04	2.63	**0.85**
Howell	***Silica***	***10***	**0.60**	**0.91**	1.51	1.01
Howell	***Silica***	***20***	**0.65**	1.03	**0.86**	1.20
Levering	***Silica***	***5***	1.05	**0.75**	1.87	1.53
Levering	***Silica***	***10***	1.41	**0.80**	1.98	1.96
Levering	***Silica***	***20***	1.34	**0.56**	2.00	1.72
Michigan Ave 19.0mm NMAS	***Silica***	***5***	**0.75**	**0.68**	**0.92**	1.35
Michigan Ave 19.0mm NMAS	***Silica***	***10***	**0.65**	**0.41**	**0.80**	1.27
Michigan Ave 19.0mm NMAS	***Silica***	***20***	**0.87**	1.29	1.21	1.56
Michigan Ave 12.5mm NMAS	***Silica***	***5***	**0.41**	**0.58**	**0.18**	**0.68**
Michigan Ave 12.5mm NMAS	***Silica***	***10***	**0.36**	**0.80**	**0.21**	**0.76**
Michigan Ave 12.5mm NMAS	***Silica***	***20***	**0.55**	**0.78**	**0.28**	**0.88**
Michigan International Speedway	***Silica***	***5***	**0.67**	1.01	2.04	2.46
Michigan International Speedway	***Silica***	***10***	1.68	1.49	7.17	2.89
Michigan International Speedway	***Silica***	***20***	**0.83**	2.81	2.47	4.16
Owosso	***Silica***	***5***	**0.88**	1.00	1.06	1.78
Owosso	***Silica***	***10***	**0.96**	1.51	1.10	2.70
Owosso	***Silica***	***20***	1.07	2.16	1.02	3.07
Pinckney	***Silica***	***5***	4.30	2.02	8.77	2.16
Pinckney	***Silica***	***10***	3.70	1.95	3.65	4.02
Pinckney	***Silica***	***20***	6.03	7.71	3.57	3.12
Saginaw	***Silica***	***5***	1.01	1.66	2.18	2.25
Saginaw	***Silica***	***10***	1.79	**0.47**	2.87	3.04
Saginaw	***Silica***	***20***	1.16	**0.70**	2.99	3.76
St. Johns	***Silica***	***5***	**0.92**	1.91	1.02	0.99
St. Johns	***Silica***	***10***	1.73	1.95	1.11	0.88
St. Johns	***Silica***	***20***	1.82	3.09	1.36	3.61
Toledo	***Silica***	***5***	2.13	1.50	2.74	2.23
Toledo	***Silica***	***10***	2.53	2.15	2.39	2.68
Toledo	***Silica***	***20***	2.66	2.44	3.78	3.16
VanDyke	***Silica***	***5***	5.49	2.26	1.87	2.38
VanDyke	***Silica***	***10***	2.09	2.00	2.83	3.25
VanDyke	***Silica***	***20***	11.79	2.20	3.17	3.45

All of the binders with silica met the minimum Superpave requirement of 1.0 kPa, but there were several that barely passed. A few of the binders that barely passed were originally well above the minimum requirement, thus indicating that attention should be paid to the interaction between aggregates and binders to prevent moisture damage.

A further analysis of the affects of silica on the moisture susceptibility of asphalt binders was conducted by comparing $G^*/\sin(\delta)$ of specific groupings. The first set of groupings compared conditioned specimens to unconditioned specimens within silica percentage, testing environment, and temperature. The ratio of $G^*/\sin(\delta)$ was used to determine the loss, if any, of $G^*/\sin(\delta)$ of moisture saturated specimens (Kvasnak 2006).

Table 8.41 summarizes the results of this first set of analyses. It can be seen that several groups exhibit a loss of $G^*/\sin(\delta)$ after moisture saturation, to ascertain whether or not the change is due to a viscous or elastic loss, G^* and δ of the respective groups were examined. In all of the cases where there is a loss of $G^*/\sin(\delta)$ with moisture saturation, the viscous component decreases the most in comparison to the elastic component. The decrease in viscosity was the most extreme for the groups containing 10% silica. The loss of elasticity was only apparent in about half of the groups and was slight. Binders with 20% and 5% silica exhibited the greatest decrease in elasticity (Kvasnak 2006).

The second set of analyses examining the ratio of $G^*/\sin(\delta)$ compared environmental testing conditions. $G^*/\sin(\delta)$ computed from specimens tested in a water bath were divided by $G^*/\sin(\delta)$ values determined from specimens tested in the air chamber. The results of these comparisons are displayed in Table 8.41. The comparisons indicate that in most cases $G^*/\sin(\delta)$ measured from specimens tested in a water bath are less than those measured in an air chamber. The groupings exhibiting a loss in $G^*/\sin(\delta)$ were further investigated to determine if the

decrease is due to a loss in the viscous or elastic component. In almost all cases where G*/sin(δ) decreases, the loss of elasticity is greater than the loss of viscosity. The viscosity decrease was greater than the elasticity loss for binders with 10% and 20% silica conditioned tested at 64˚C and 5% and 20% silica unconditioned tested at 58˚C (Kvasnak 2006).

Table 8.41 Ratio of G*/sin(δ) Conditioned to Unconditioned Specimens

Percentage of Silica	Test Environment	Temperature	G*/sin(δ) Conditoned: Unconditioned
5	Air Chamber	58	1.36
		64	1.25
		All	1.28
	Water Bath	58	***0.76***
		64	1.06
		All	***0.99***
	All	All	1.15
10	Air Chamber	58	2.71
		64	1.36
		All	1.65
	Water Bath	58	***0.84***
		64	***0.71***
		All	***0.73***
	All	All	1.14
20	Air Chamber	58	1.63
		64	1.08
		All	1.19
	Water Bath	58	***0.90***
		64	***0.51***
		All	***0.57***
	All	All	***0.84***

The most extreme comparison case for relating moisture damage was between the unconditioned air chamber samples and conditioned water bath samples. The G*/sin(δ) ratio computed for the extreme case are outlined in Table 8.42. The ratio analysis indicates that there is a loss of G*/sin(δ) after moisture saturation and water bath testing for all classifications. In all cases the decrease in viscosity was greater than the reduction of elasticity. Proportionally, binders with 10% silica exhibited the greatest decline in viscosity compared to elasticity, followed by binders with 20% silica. The loss in viscosity indicates that the binder is more prone to causing rutting issues in HMA pavements. Determining which binders will exhibit a drastic

change in viscosity in advance of its use allows for owner/agencies to replace the binder with a more moisture resistant binder, which is likely less expensive than adjusting the aggregate (Kvasnak 2006).

Table 8.42 Ratio of G*/sin(δ) of Specimens Tested in a Water Bath to Those Tested in an Air Chamber

Percentage of Silica	Condition State	Temperature	G*/sin(δ) Water Bath: Air Chamber
5	Conditioned	58	***0.37***
		64	***0.66***
		All	***0.58***
	Unconditioned	58	***0.66***
		64	***0.78***
		All	***0.75***
10	Conditioned	58	***0.31***
		64	***0.68***
		All	***0.55***
	Unconditioned	58	1.01
		64	1.31
		All	1.24
20	Conditioned	58	***0.52***
		64	***0.66***
		All	***0.62***
	Unconditioned	58	***0.94***
		64	1.40
		All	1.31

Table 8.43 Ratio of G*/sin(δ) for Conditioned Water Bath Specimens Versus Unconditioned Air Chamber Specimens with Silica

Percentage of Silica	Temperature	G*/sin(δ) Conditioned Water Bath: Unconditioned Air Chamber
5	58	*0.85*
	64	*0.93*
	All	*0.91*
10	58	*0.84*
	64	*0.72*
	All	*0.74*
20	58	*0.50*
	64	*0.83*
	All	*0.74*

8.11.1.3 Comparison of Hydrated Lime to Silica

The previous sections outlined the advantages and disadvantageous of the fillers detected by the new test method. This section summarizes a comparison of the sensitivity of the new test methods to the selected fillers. Figure 8.69 displays the variability of G*/sin(δ) with the data grouped by environmental testing condition (water bath or air chamber), condition status (unconditioned or saturated), filler percentage, and filler. The variability of the original binders is rather slight in comparison to many of the mastics (Kvasnak 2006).

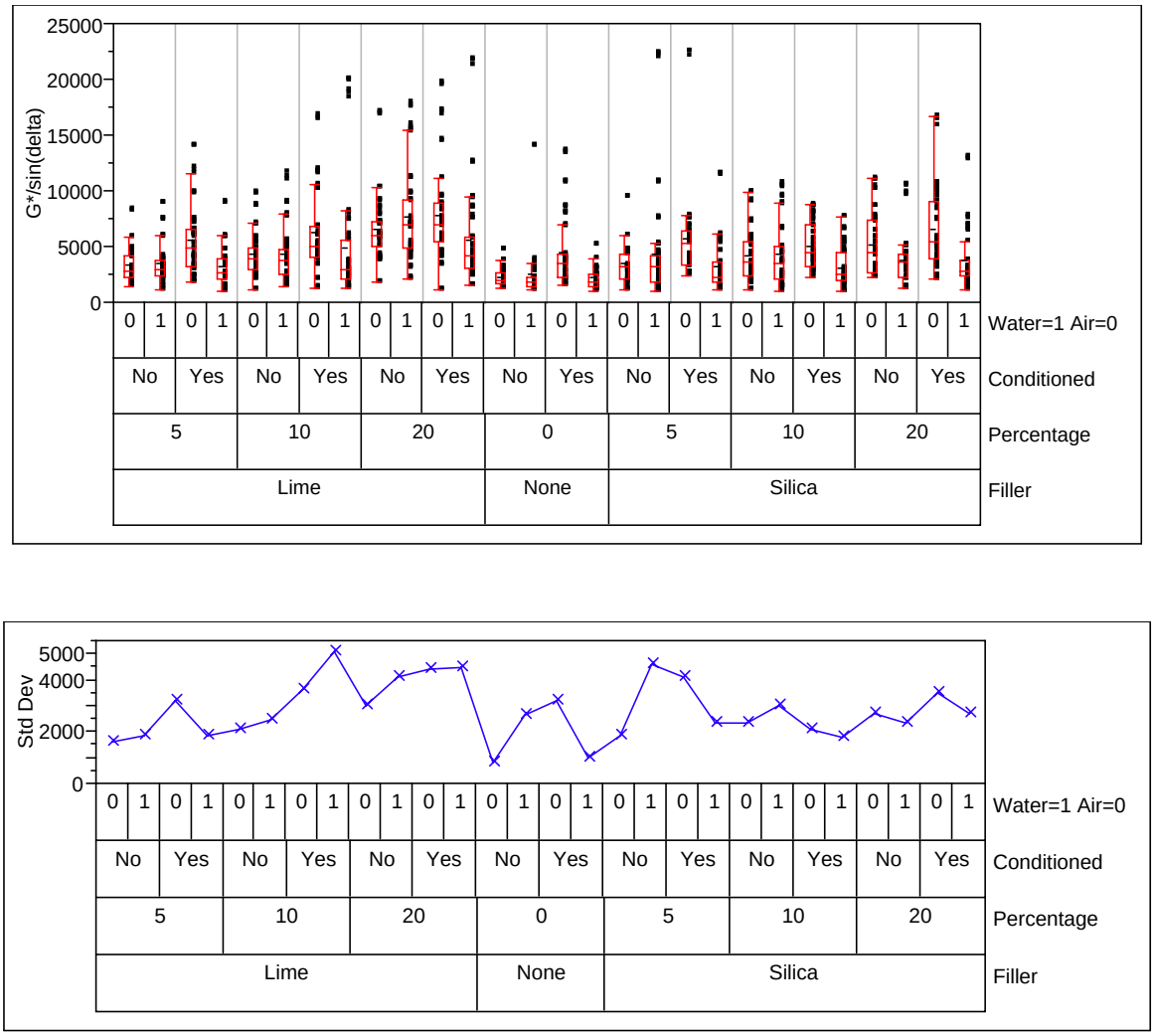

Figure 8.69 Variability Plot of G*/sin(δ)

Figure 8.70 illustrates the difference in mean G*/sin(δ) values for original binders grouped by testing environment and condition status. The mean G*/sin(δ) for unconditioned specimens tested in air is almost the same as the conditioned specimens tested in water. The unconditioned specimens tested in water were only slightly greater than the unconditioned specimens tested in air on average. The greatest difference can be seen with the conditioned specimens tested in air (Kvasnak 2006).

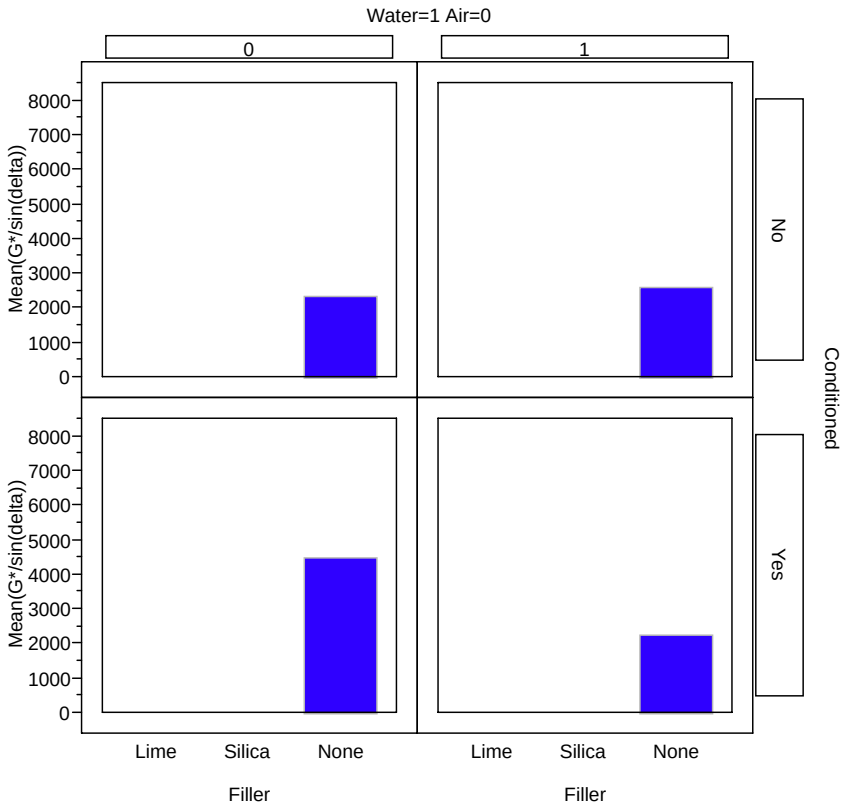

Figure 8.70 Chart of Mean G*/sin(δ) for Neat Binders

Figure 8.71 relates the G*/sin(δ) means for binders with 5% filler grouped by testing environment and condition status. Once again the unconditioned specimens tested in air and conditioned specimens tested in water yielded equivalent G*/sin(δ) means. Interestingly, the binders with silica yielded almost the same mean G*/sin(δ) as the binders with hydrated lime. As with the original binders, the conditioned specimens tested in air yielded the greatest average G*/sin(δ) values. Another possibility is that the saturation process leached out the lighter components of the asphalt binder. Specimens tested after conditioning were exposed to temperatures close to the PG high temperature for longer periods of time due to two test cycles in comparison to the unconditioned test specimens which only endure one test cycle. The difference between the air chamber conditioned specimens and the water bath conditioned

specimens could be attributed to the water bath specimens not having an opportunity for the water logged specimens to dry out, thus the moisture was allowed to soften the binder making it more prone to rutting. The most significant difference between mean G*/sin(δ) values for hydrated lime and silica occurs with the unconditioned specimens tested in water (Kvasnak 2006).

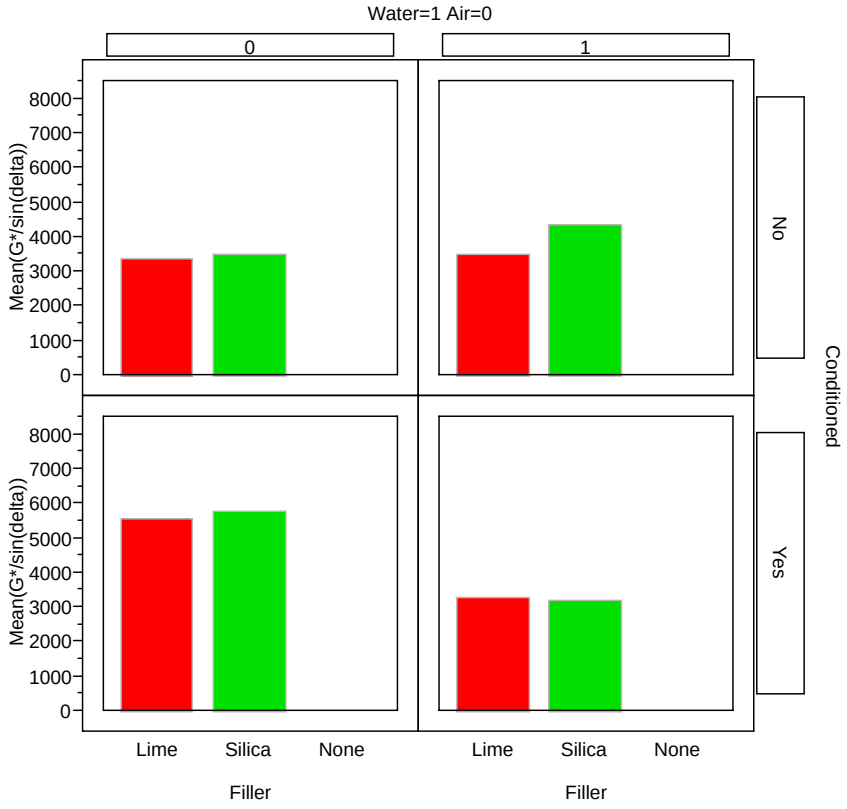

Figure 8.71 Chart of Mean G*/sin(δ) of Binders with 5% Filler

Figure 8.72 graphically summarizes the mean G*/sin(δ) values for binders with 10% filler grouped by testing environment and condition status. With 10% filler, on average, hydrated lime and silica unconditioned specimens tested in water or air are equivalent indicating that at 10% neither filler has a significant effect on the binders prior to moisture saturation

(Kvasnak 2006). Substantial differences between hydrated lime and silica at 10% are seen for the conditioned specimens tested in either water or air (Kvasnak 2006).

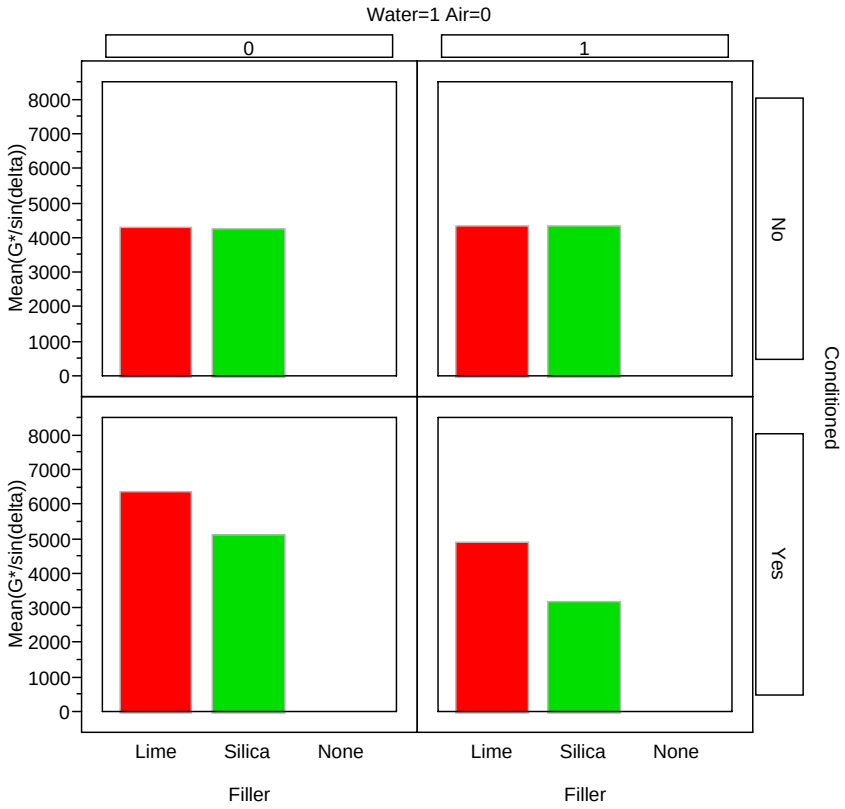

Figure 8.72 Chart of Mean G*/sin(δ) of Binders with 10% Filler

Figure 8.73 illustrates the mean G*/sin(δ) values for binders with 20% filler grouped by condition status and testing environment. It can be seen that for all four testing environment and conditioning combinations, on average, the hydrated lime specimens perform better than the binders with silica. The greatest difference occurs with the unconditioned specimens test in water (Kvasnak 2006).

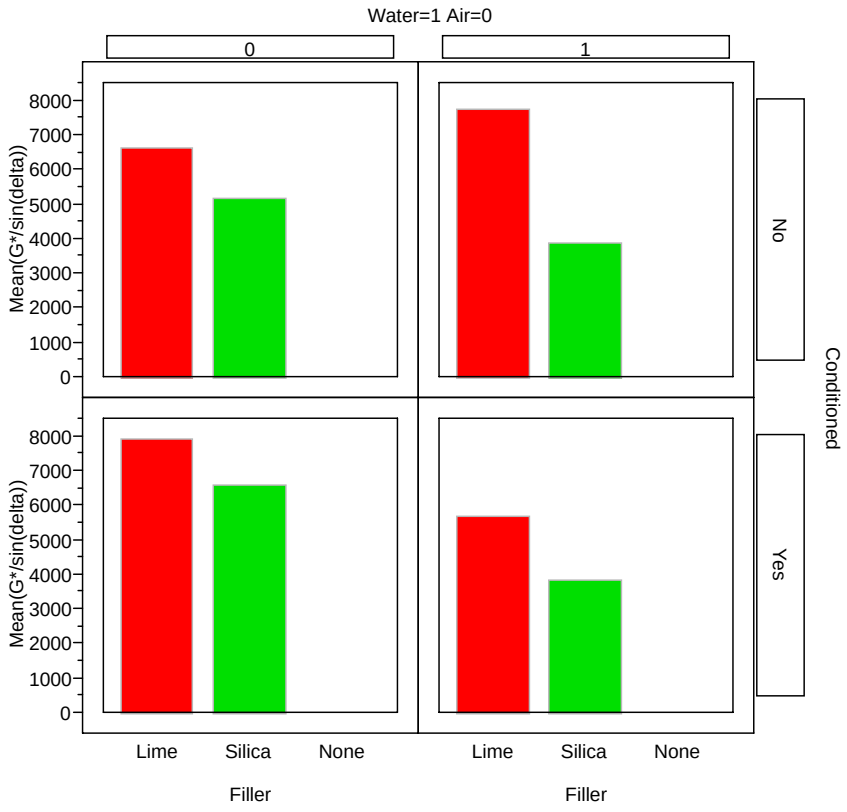

Figure 8.73 Chart of Mean G*/sin(δ) of Binders with 20% Filler

In general, Figures 4.4 through 4.6 relate that as the amount of filler increases the difference in G*/sin(δ) values between the two fillers becomes more pronounced. In comparing the figure of the original binders, to the figures for binders with silica or hydrated lime, it can also be seen that the addition of binder tends to slightly increase the G*/sin(δ) value in most cases, which reiterates that most of the ratios were greater than 1 for both fillers (Kvasnak 2006).

An ANOVA was conducted to determine which factors may be significant. Several variable combinations were examined, altering the variable entered into the analysis first. The analysis indicated that filler type, filler percentage, testing condition, and specimen conditioning are all significant factors contributing to changes in G*/sin(δ) (Kvasnak 2006).

8.11.2 Conclusions about Filler Effects

A new test method for determining moisture susceptibility was developed and this dissertation outlines the results of fillers on binders tested using the new method. The new method appears to be sensitive to the addition of fillers in the binders and is able to distinguish between moisture susceptible fillers and non-moisture susceptible fillers. Interestingly, binders with hydrated lime did not always perform the best. This would indicate that hydrated lime cannot be used for all binders to deter moisture damage. Hydrated lime may not be chemically compatible with all binders for resisting moisture damage (Kvasnak 2006).

None of the binders examined in this dissertation failed the Superpave minimum criteria of $G^*/\sin(\delta)$ being at least 1.0 kPa, however several of the binders did exhibit degradation during testing. During the saturation process many of the binders maintained the original shape prior to saturation, however there were a few binders that tended to spread and even experienced the loss of small sections of binder. The binders which did tend to creep during saturation also emitted a visible oil sheen. Specimens displaying creep and oil sheens tended to yield $G^*/\sin(\delta)$ close to the Superpave minimum of 1.0 kPa indicating that perhaps the criteria should be re-evaluated if used for moisture susceptibility testing (Kvasnak 2006).

8.12 Moisture Damage Factors Affecting TSR and E* Values

This section considers several factors that initiate moisture damage in laboratory tested specimens. The factors being considered are gradation, NMAS, traffic level (mix type), polymer modification, aggregate type, permeability, asphalt content, FAA, RAP, and with dynamic modulus testing frequency. Table 8.44 shows the factors and levels considered for statistical analysis. The general linear models (GLM) procedure was used to determine which factors were considered statistically significant and a multiple comparison procedure using a 5% level of

significance was used to determine if there were statistical differences within the levels for each factor. The GLM procedure gives an F-statistic for each factor based on Type I sum of squares error (SSE) and Type III SSE. For this analysis the Type I SSE will be used to select the appropriate factors that are statistically significant. For this analysis only the Type I SSE will be considered because performing the GLM and analyzing the type I SSE is analogous to performing an eight-way ANVOA on the data set. The GLM is better to use because the user has better control over how the data is input into the model.

Some factors have levels that are determined prior to analysis. Other factors such as permeability, asphalt content, and RAP required classification. Classification was based on clustering observed in graphical representation of data. This method of classification has been employed for permeability in a previous MDOT study concerning the use of a Corelok (Williams et al. 2005). Figure 8.74 shows a graph of permeability versus TSR. From this figure one can see that there is a clear division at approximately 0.002 cm/s. Figure 8.75 shows a graph of RAP versus TSR. From this figure, there are approximately, four division, 0%, 1-10%, 10-15%, and greater than 15%. Figure 8.76 shows a graph of asphalt content versus TSR. From this figure one can see that approximately one-half of the data is less than 5.5% and the other half is greater than 5.5%.

Table 8.44 Factors with Levels Considered for Statistical Analysis

Factors	Levels
Gradation	Coarse Fine
NMAS (mm)	19.0 12.5 9.5
Traffic ESAL's (millions)	E3 E10 E30
Polymer	Yes No
Aggregate Type	Gravel Limestone Gabbro
Permeability (cm/s)	<0.002 ≥0.002
Asphalt Content (%)	4.6-5.5 ≥5.5
FAA (%)	<45 ≥45
RAP (%)	0 1-10 10-15 ≥15
Frequency (Hz)	0.02 0.1 1.0 5.0 10.0 25.0

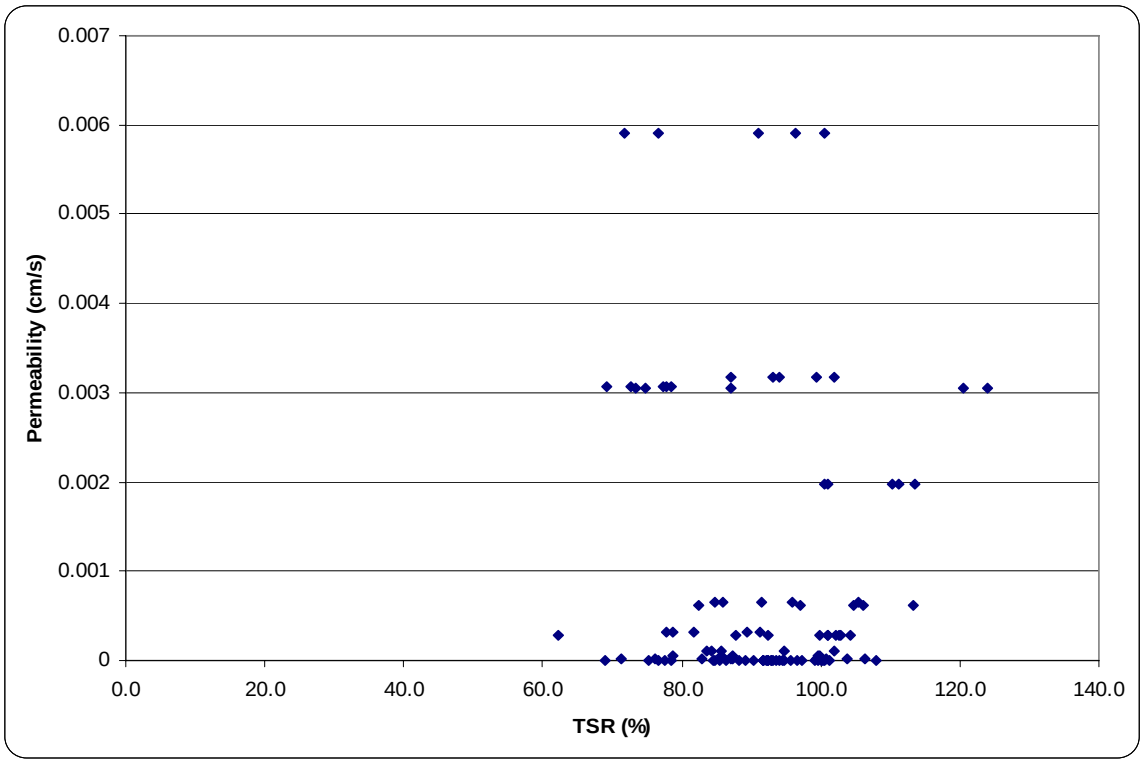

Figure 8.74 TSR versus Permeability

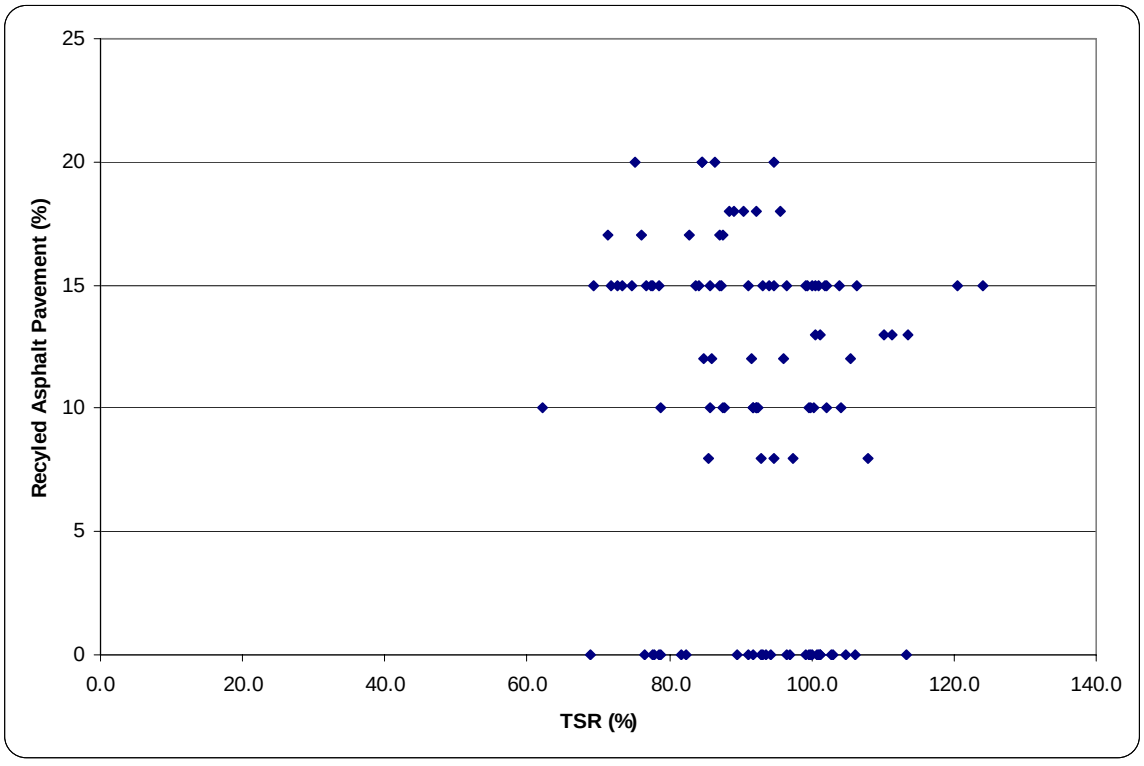

Figure 8.75 TSR versus RAP

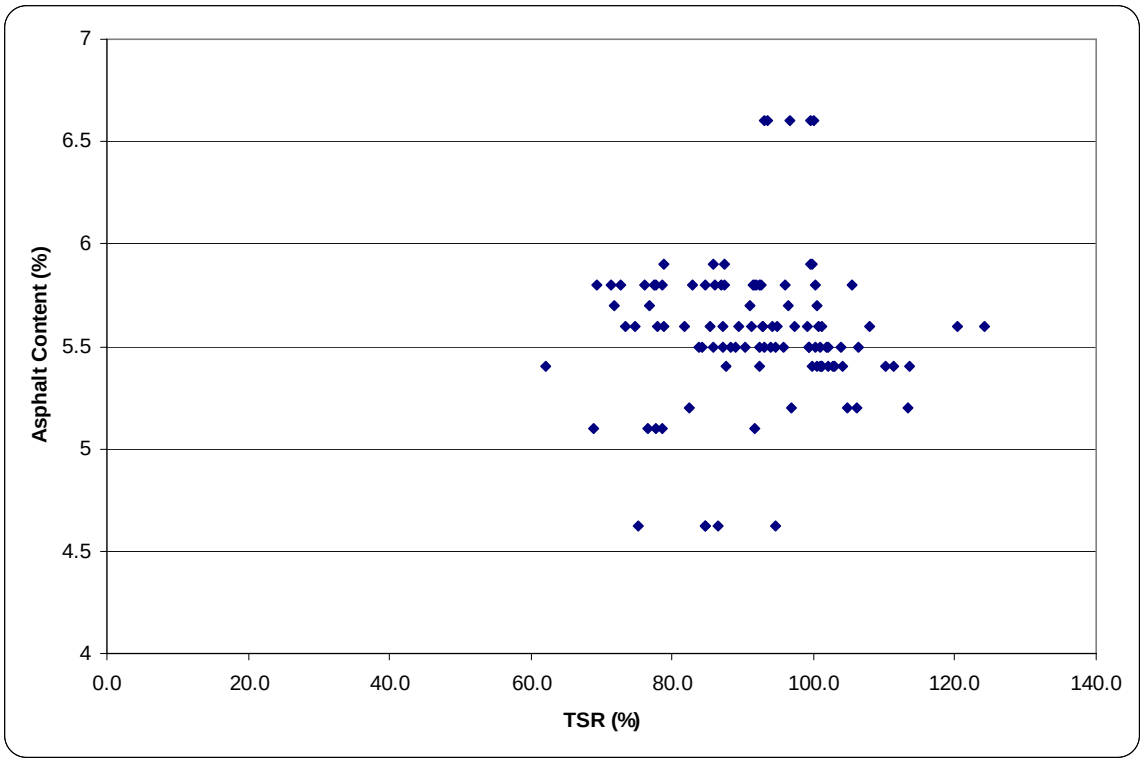

Figure 8.76 TSR versus Asphalt Content

The statistical results (Table 8.45) show that polymer, aggregate type, permeability, and RAP are statistically significant variables when TSR is the dependent variable based on Type I SSE using a 5% level of significance.

Table 8.45 GLM p-values Showing Statistically Significant Variables for TSR

Variable	DF	F-Statistic	p-value
Gradation	1	2.15	0.1478
NMAS	2	0.19	0.8269
Traffic	2	2.91	0.0618
Polymer	**1**	**5.96**	**0.0174**
Aggregate Type	**2**	**3.11**	**0.0513**
Permeability	**1**	**10.85**	**0.0016**
Asphalt Content	1	2.46	0.1213
FAA	1	1.70	0.1975
RAP	**3**	**4.47**	**0.0064**

Table 8.46 shows the results of the LSD mean multiple comparison procedure using a 5% level of significance considering the levels within each factor for the TSR data. Means with the

same letter are not statistically different. The LSD results show that for gradation, NMAS, aggregate type, permeability, and FAA there is no statistical difference among the levels within each factor. However, there are statistical differences among the mean levels of TSR for polymer modification and asphalt content. The traffic variable has statistical differences between E3 (3,000,000 ESALs) and E30 (30,000,000 ESAL) mix types. In terms of RAP content, there are no statistical differences among the mean levels of TSR for 0, 1-10% and 10-15% RAP. However, there are statistical differences in mean TSR among those first three levels with the fourth level (≥15%).

Table 8.46 LSD Results for AASHTO T283

Levels	Factors								
	Gradation	NMAS (mm)	Traffic	Polymer	Aggregate Type	Permeability (cm/s)	Asphalt Content (%)	FAA (%)	RAP (%)
Coarse	A								
Fine	A								
19.0		A							
12.5		A							
9.5		A							
E3			A						
E10			B A						
E30			B						
Yes				A					
No				B					
Gravel					A				
Limestone					A				
Gabbro					A				
<0.002						A			
≥0.002						A			
4.6-5.5							A		
≥5.5							B		
<45								A	
≥45								A	
0									A
1-10									A
10-15									A
≥15									B

The same procedure was used to analyze E* ratio as the dependent variable considering gradation, NMAS, traffic, polymer modification, aggregate type, permeability, asphalt content, FAA, RAP, and frequency. The statistical analysis shows that traffic, aggregate type,

permeability, RAP, and frequency are statistical significant variables based on Type I SSE using a 95% level of significance. The resulting p-values and F-statistic are shown in Table 8.47.

Table 8.47 GLM p-values Showing Statistically Significant Variables for E* Ratio

Variable	DF	F-Statistic	p-value
Gradation	1	0.57	0.4518
NMAS	2	2.46	0.0874
Traffic	**2**	**13.45**	**<0.0001**
Polymer	1	3.49	0.0627
Aggregate Type	**2**	**11.06**	**<0.0001**
Permeability	**1**	**17.04**	**<0.0001**
Asphalt Content	1	0.07	0.7915
FAA	1	0.32	0.5726
RAP	**3**	**5.13**	**0.0018**
Frequency	**5**	**3.06**	**0.0105**

Table 8.48 shows the results of the LSD multiple comparison procedure using a 5% level of significance the levels within each factor for the E* ratio data. Means with the same letter are not statistically different. The LSD results show that gradation and asphalt content show no statistical difference among the levels within each factor. The NMAS variable has statistical differences between 19.0mm and 9.5mm mix types. There are statistical differences among the mean levels of E* ratio for traffic, polymer modification, permeability, and FAA. There appears to be no statistical difference in mean E* values for limestone and gabbro aggregates but there are statistical differences in E* ratio values for between the gravel aggregate and the limestone and gabbro aggregates. In terms of RAP content, there appears to be no statistical difference in E* ratios for 0% and 1-10% RAP and between 10-15% and ≥15% RAP. However, there are statistical differences between 0% and 1-10% RAP and 10-15 and ≥15% RAP. In terms of frequency, E* ratio is statistically the same at 0.02, 0.1, 1.0, and 5.0 Hz while E* ratio is statistically the same at 0.1, 1.0, 5.0, 10.0, and 25.0 Hz.

Table 8.48 LSD Results for E* Ratio

Levels	Factors									
	Gradation	NMAS (mm)	Traffic	Polymer	Aggregate Type	Permeability (cm/s)	Asphalt Content (%)	FAA (%)	RAP (%)	Frequency (Hz)
Coarse	A									
Fine	A									
19.0		A								
12.5		B A								
9.5		B								
E3			A							
E10			B							
E30			C							
Yes				A						
No				B						
Gravel					A					
Limestone					B					
Gabbro					B					
<0.002						A				
≥0.002						B				
4.6-5.5							A			
≥5.5							A			
<45								A		
≥45								B		
0									A	
1-10									A	
10-15									B	
≥15									B	
0.02										A
0.1										A
1.0										A
5.0										A
10.0										A
25.0										B

CHAPTER 9 SUMMARY, CONCLUSIONS, AND RECOMMENDATIONS

9.1 Summary

A number of factors exist that are detrimental to HMA. Moisture damage is a significant factor that impacts HMA; not only the binder but also the mixture component. Moisture damage is important because it can diminish the performance and service life of HMA pavements resulting in increased maintenance and rehabilitation costs of highways. The current method of determining the moisture susceptible of HMA mixtures is AASHTO T283. AASHTO T283 is based upon the Marshall mix design method but current state of the practice for HMA mixture design is the Superpave mix design method. There has not been a transition in test procedure from Marshall mix design to Superpave mix design.

The procedures in AASHTO T283 and NCHRP 9-13 consider the loss of strength due to freeze/thaw cycling and the effects of moisture existing in specimens compared to unconditioned specimens. However, mixtures do not experience such a controlled phenomenon. Pavements undergo cycling of environmental conditions, but when moisture is present, there is repeated hydraulic loading with development of pore pressure in mixtures. Thus, AASHTO T283 and the NCHRP 9-13 study do not consider the effect of pore pressure, but rather consider a single load effect on environmentally conditioned specimens.

This report shows the development of moisture susceptibility procedures which utilize repeated loading testing devices to evaluate mixes and a DSR to evaluate binders and mastics. The two devices used were an APA and an uniaxial compressive tester.

The work outlined in this final report has formed a basis from which MDOT can update their current criteria for TSR and to also update their current method of determining the moisture susceptibility of HMA mixtures.

9.2 Conclusions

Prior to testing of the Michigan asphalt mixtures, extensive research was conducted on determining an equivalent number of freeze/thaw cycles that would achieve moisture damage effects equivalent to ones obtained for 100mm Marshall specimens tested using the original AASHTO T283 specification using the newer Superpave method. The affects of size and compaction method on results obtained following AASHTO T283 procedure were analyzed. Finally, a new minimum TSR can be determined by the analysis instead of using the original TSR of 80% which was based on the original AASHTO T283 specification. Additional preliminary studies were conducted to consider the effects of test temperature and conditioning on dynamic modulus and APA test specimens prior to testing all of the Michigan mixes collected. A binder and mastic preliminary study were also conducted to determine test temperature, condition, interface material, and testing environment. The conclusion of the preliminary testing and final testing are summarized below.

9.2.1 AASHTO T283 – Phase I

The Phase I parametric study considered factors affecting the wet strength of a specimen and new TSR criteria for AASHTO T283 when Superpave compaction method is employed in lieu of the Marshall compaction method. AASHTO T283 was developed based on 100mm Marshall compacted specimens. With the transition from 100mm Marshall compacted specimens to 150mm Superpave compacted specimens it was felt that the requirements outlined in AASHTO T283 should be re-evaluated. It was discovered that one freeze/thaw cycle for conditioning still is satisfactory when using specimens created using the Superpave method. However, to maintain the same probability level as attained with a TSR value for 80% for 100mm Marshall compacted specimens, a TSR value of 87 and 85% should be used,

respectively, with 150mm and 100mm Superpave compacted specimens. An 80% TSR for 150mm Superpave specimens corresponds to a TSR of 70% for 100mm Marshall specimens.

According to the results obtained in this report, three freeze/thaw cycles are adequate when using the AASHTO T283 method in conjunction with 150mm Superpave specimens. Three freeze/thaw cycles for 150mm Superpave gyratory compacted specimens corresponds to one freeze/thaw cycle for 100mm Marshall specimens. The threshold value should be altered accordingly, as stated above, based on the specimen size.

9.2.2 Moisture Testing – Phase II

Phase II testing of Michigan HMA mixtures outlines moisture susceptibility procedures and preliminary criteria that utilizes repeated loading test devices on specimens in saturated conditions and compares them to unconditioned specimens in a dry test environment. The test criteria for APA tested specimens is the ratio of conditioned rut depth to unconditioned rut depth with values greater than 1 suggesting the mix is moisture damage prone accounting for a maximum allowable rut depth. The criterion developed to determine whether or not a mix is moisture susceptible indicated that 2 of the 21 mixes were moisture susceptible. There is not a strong relationship between DSR and APA test results, nor is there a strong relationship between TSR results and APA test results. It is recommended that if a loaded wheel tester is to be used for moisture susceptibility testing that more than three specimens be tested. The variability of the rut depth data was rather high and it is believed that additional specimens tested would yield data less affected by outliers. Also, a maximum allowable rut depth based on Michigan mixes should be established. The dynamic modulus test procedure test criteria suggested is a retained modulus of 60% of conditioned specimens to unconditioned specimens.

Pavements undergo cycling of environmental conditions, but when moisture is present, there is repeated hydraulic loading with development of pore pressure in mixtures. Thus, AASHTO T283 does not consider the effect of pore pressure, but rather considers a single load effect on environmentally conditioned specimens. Dynamic modulus and APA testing of saturated mixtures better simulates the repeated hydraulic loading pavements undergo. Validation of the proposed criteria will need to be conducted through longer term field monitoring prior to implementing either criterion as a mix design specification for moisture susceptibility testing of HMA.

A number of factors exist that cause or accelerate moisture damage. A statistical analysis performed to determine which factors are significant. It appears that the factors affecting AASHTO T283 are polymer modification, aggregate type, permeability, and RAP. The factors affecting dynamic modulus are traffic, polymer modification, aggregate type, permeability, RAP, and frequency. It has been known that aggregate type, polymer modification, and permeability affect moisture damage. RAP is a highly variable material and it makes sense as to why it may impact moisture damage in HMA pavements. The factors affecting APA test results are test temperature, certain sieve sizes, polymer modification, binder content, fines to binder ratio, NMAS, and traffic level.

A new test method for determining moisture susceptibility of asphalt binders and mastic was developed and this report outlines the results of fillers on binders tested using the new method. The new method appears to be sensitive to the addition of fillers in the binders and is able to distinguish between moisture susceptible fillers and non-moisture susceptible fillers.

None of the binders examined in this report failed the Superpave minimum criteria of $G^*/\sin(\delta)$ being at least 1.0kPa, at the high temperature performance grade, however several of

the binders did exhibit degradation during testing. During the saturation process many of the binders maintained the original shape prior to saturation, however there were a few binders that tended to spread and even lose small sections of the binder. The binders which did tend to creep during saturation also emitted a visible oil sheen in the water bath. Specimens displaying creep and oil sheens tended to yield G*/sin(δ) close to the Superpave minimum of 1.0kPa indicating that another criterion should be used for moisture susceptibility testing. The criterion suggested in this report is to evaluate the viscous and elastic components. If both the viscous and elastic components decrease with moisture saturation, then the binder is deemed moisture susceptible.

Several mixes and binders were deemed moisture damage prone by the three mix tests and binder tests. Table 9.1 summarizes the mixes that might be moisture damage prone. A dot in a box indicates that the material (either mix or binder) failed the criterion for moisture resistance.

Table 9.1 Summary of Moisture Damage Prone Materials

Site	Water Absorbed	Dynamic Shear Rheometer	Asphalt Pavement Analyzer	Asphalt Pavement Analyzer Based on Ratio and Maximum Allowable Rut Depth	AASHTO T283 Current	AASHTO T283 Modified	E* Ratio Current	E* Ratio Modified
Ann Arbor								
Battle Creek	•	•	•					
Brighton	•					•		
Clarkston								
Detroit	•		•					
Dundee 19.0mm NMAS	•		•					
Dundee 12.5mm NMAS			•					
Grand Rapids I-196				•		•		
Grand Rapids M-45			•	•	•	•	•	•
Hartland	•	•	•					
Howell	•		•					
Levering	•		•				•	•
Michigan Ave 19.0mm NMAS			•				•	•
Michigan Ave 12.5mm NMAS							•	•
Michigan International Speedway	•					•		
Owosso			•					
Pinckney	•				•	•	•	•
Saginaw			•			•		•
St. Johns			•					
Toledo			•					
Van Dyke			•					

9.3 Recommendations

Extensive testing has been conducted as part of this research project. This testing has brought to light many issues that are involved in the determining the moisture susceptibility of HMA mixtures. These issues should be addressed prior to their implementation by owner/agencies and industry. Additional research is needed as discussed in the following points:

- The aggregate chemistry and asphalt binder chemistry should be looked at to consider if it is an aggregate issue or a binder issue or both. This testing could be accomplished by using the Wilhelmy Plate and Universal Sorption Device. Extra HMA and binder was sampled during the 2004 and 2005 construction season from each of projects tested therefore the binder can be tested in the Wilhelmy Plate and the aggregate can be extracted from the HMA and then placed in the Universal Sorption Device.
- Additional dynamic modulus testing at the intermediate test temperature and mid-range temperatures.
- Conducting dynamic creep testing using a 0.1sec load time and a longer rest period instead of 0.1sec.
- Field monitoring of sampled mixtures should be done to correlate with the extensive laboratory studied here.
- An examination should be undertaken to apply the Hirsh predictive model. The Hirsh model is a newer predictive equation developed by Christensen and Bonaquist (2003) and has been shown to address the issues of over prediction seen with the Witczak model.
- Use the AASHTO Mechanistic-Empirical Pavement Design Guide (M-E PDG) to analyze these pavements using Level 1 mix design on the control and moisture

conditioned specimens to look at how distress change when the E* changes due to moisture damage.

- Additional testing should be conducted with the APA.
- Results from the APA testing should be compared with field data to calibrate the criterion.
- Binders should be tested with a DSR using a modified spindle and base plate, as described in this report, and the results compared with field results prior to implementing as a specification.. The binder that should be tested is original binder and binder with a filler. A binder with filler should be tested to allow for breaks in an asphalt binder specimen membrane surface, which enables water to permeate a specimen faster than a specimen without surface breaks. Surface breaks occur in pavements; therefore inducing breaks by adding a filler simulates, to an extent, reality.
- In conjunction with DSR testing results, specimens should be evaluated to determine water absorbing tendencies.

APPENDIX A JOB MIX FORMULAS

Project: M-50 Dundee

Project Information		Asphalt Information	
Project No.:	50651A	Asphalt Source:	Marathon Det.
Location:	M-50 Dundee	Asphalt Grade (PG):	58-28
Contractor:	Cadillac LLC Asphalt	Asphalt Content:	5.4
Traffic Level:	E1	Asphalt Additives:	None
Aggregate Type:	Limestone	Asphalt Additives (%):	N/A
Mix Size:	3	**SuperPave Consensus Properties**	
Gradation:	Coarse	Angularity (%):	45.1
Specifc Gravities		Dust Corr.:	
G_{mm}	2.511	1 Face Crush (%):	96.6
G_{mb}	2.436	2 Face Crush (%):	93.8
G_b	1.025	**Volumetrics**	
G_{se}	2.737	VMA:	14.9
G_{sb}	2.708	VFA:	79.9
Temperature		AV:	3
Mixing (^oF):	311-322	F/P_{be}:	1.1
Compacting (^oF):	275	P_{be}:	5.36

Sieve Size	Mix/Gradation (%P)	Material/Producer	Percent
1 (25)	100	HL1	13
3/4 (19)	99.4	3/4 x 1/2	13
1/2 (12.5)	87.8	1/2 x 3/8	21
3/8 (9.5)	68.1	3/8 x 4	16
#4 (4.75)	37.1	LimeSAND	27
#8 (2.36)	25.3	RAP	10
#16 (1.18)	16.9		
#30 (0.60)	12.8		
#50 (0.30)	9.9		
#100 (0.15)	7.5		
#200 (0.075)	5.9		

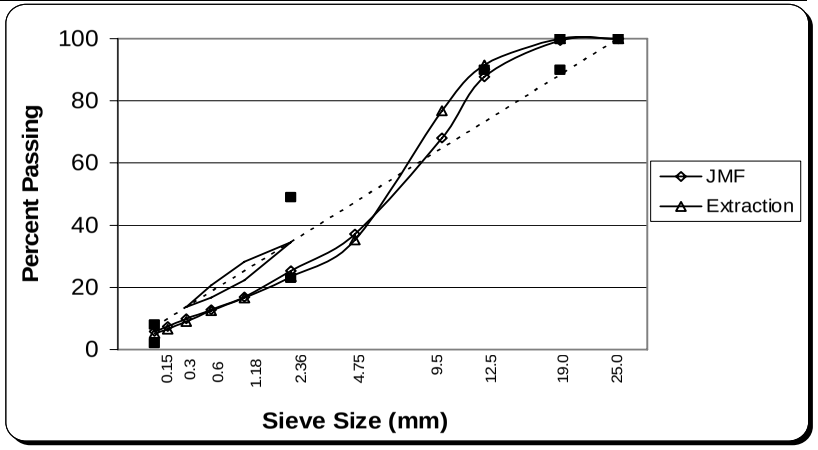

Project: M-36 Pinckney

Project Information		Asphalt Information	
Project No.:	50717A	Asphalt Source:	Marathon Det.
Location:	M-36	Asphalt Grade (PG):	64-22
Contractor:	Ajax Materials Corp.	Asphalt Content:	5.8
Traffic Level:	E3	Asphalt Additives:	None
Aggregate Type:		Asphalt Additives (%):	N/A
Mix Size:	3	**SuperPave Consensus Properties**	
Gradation:	Coarse	Angularity (%):	45.4
Specifc Gravities		Dust Corr.:	0.4
G_{mm}	2.488	1 Face Crush (%):	99.3
G_{mb}	2.413	2 Face Crush (%):	98.8
G_b	1.031	**Volumetrics**	
G_{se}	2.725	VMA:	13.7
G_{sb}	2.634	VFA:	78
Temperature		AV:	3
Mixing (^oF):	312-323	F/P_{be}:	1.16
Compacting (^oF):	294	P_{be}:	4.57

Sieve Size	Mix/Gradation (%P)	Material/Producer	Percent
1 (25)	100	4's	35
3/4 (19)	100	1/2"	25
1/2 (12.5)	85.3	Man. Sand	15
3/8 (9.5)	71	Man. Sand	10
#4 (4.75)	43.8	RAP	15
#8 (2.36)	25.9		
#16 (1.18)	17.5		
#30 (0.60)	13.3		
#50 (0.30)	9.6		
#100 (0.15)	6.8		
#200 (0.075)	5.3		

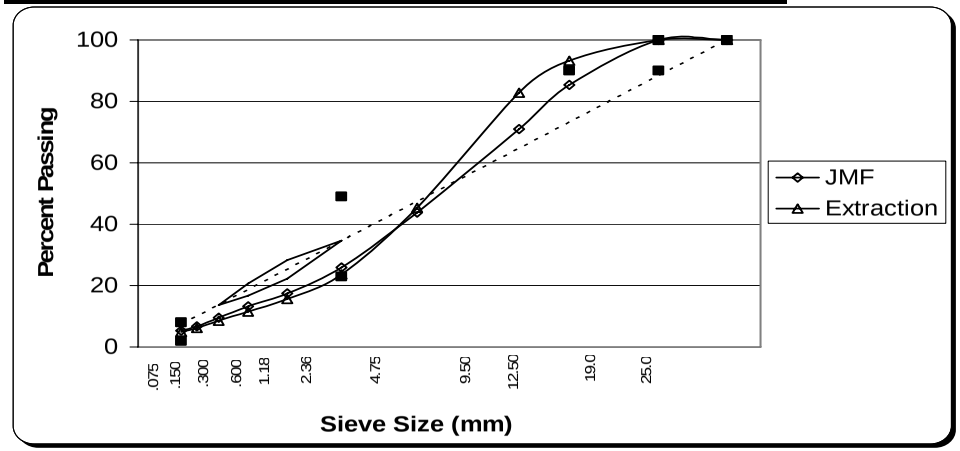

Project: M-45 Grand Rapids

Project Information		Asphalt Information	
Project No.:	06767A	Asphalt Source:	T & M Oil
Location:	M-45 Grand Rapids	Asphalt Grade (PG):	58-28
Contractor:	Thompson McCully	Asphalt Content:	5.1
Traffic Level:	E3	Asphalt Additives:	Anti-Strip Agent
Aggregate Type:		Asphalt Additives (%):	0.3
Mix Size:	3	**SuperPave Consensus Properties**	
Gradation:	Fine	Angularity (%):	42.2
Specifc Gravities		Dust Corr.:	0
G_{mm}	2.509	1 Face Crush (%):	92.4
G_{mb}	2.405	2 Face Crush (%):	N/A
G_b		**Volumetrics**	
G_{se}	2.72	VMA:	13.7
G_{sb}	2.644	VFA:	69.7
Temperature		AV:	4
Mixing:		F/P_{be}:	1.01
Compacting:	135	P_{be}:	4.06

Sieve Size	Mix/Gradation (%P)	Material/Producer	Percent
1 (25)	100	6AA	17
3/4 (19)	98.3	Birdeye Sand	25
1/2 (12.5)	89.6	#4-0	48
3/8 (9.5)	85.7	WW Sand	8.5
#4 (4.75)	74	Baghouse	1.5
#8 (2.36)	48.5		
#16 (1.18)	35.7		
#30 (0.60)	27.6		
#50 (0.30)	16		
#100 (0.15)	6.1		
#200 (0.075)	4.1		

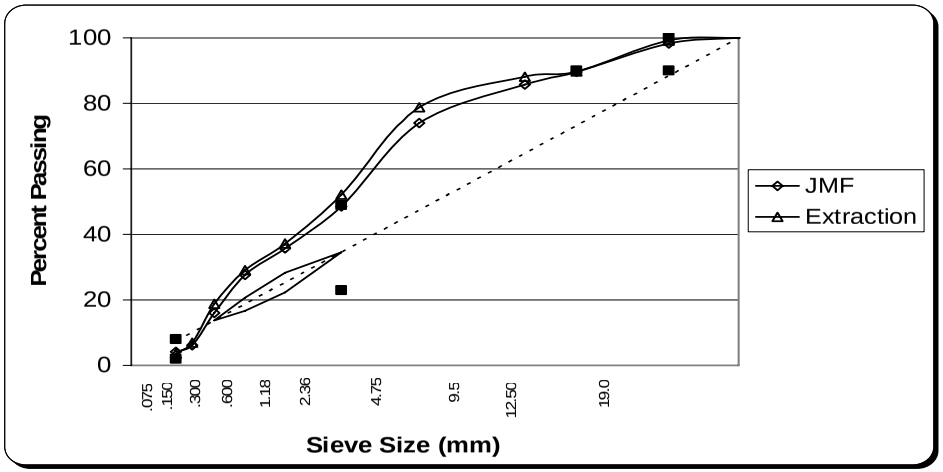

Project: M-84 Saginaw

Project Information		Asphalt Information	
Project No.:	31804A	Asphalt Source:	Marathon Detroit
Location:	M-84 Saginaw	Asphalt Grade (PG):	58-28
Contractor:	Saginaw Asphalt	Asphalt Content:	4.62
Traffic Level:	E3	Asphalt Additives:	None
Aggregate Type:	Slag	Asphalt Additives (%):	N/A
Mix Size:	3	**SuperPave Consensus Properties**	
Gradation:	Fine	Angularity (%):	44
Specifc Gravities		Dust Corr.:	0.5
G_{mm}	2.55	1 Face Crush (%):	98
G_{mb}	2.448	2 Face Crush (%):	N/A
G_b	1.022	**Volumetrics**	
G_{se}	2.749	VMA:	14.19
G_{sb}	2.721	VFA:	71.81
Temperature		AV:	4
Mixing:	303	F/P_{be}:	1.27
Compacting:	280	P_{be}:	4.25

Sieve Size	Mix/Gradation (%P)	Material/Producer	Percent
1 (25)	100	5/8 CLR	29
3/4 (19)	100	3/16 Slag	15
1/2 (12.5)	84.6	JK	36
3/8 (9.5)	73.9	RAP	20
#4 (4.75)	67.4		
#8 (2.36)	48.5		
#16 (1.18)	32.1		
#30 (0.60)	22.3		
#50 (0.30)	13.7		
#100 (0.15)	8.2		
#200 (0.075)	5.4		

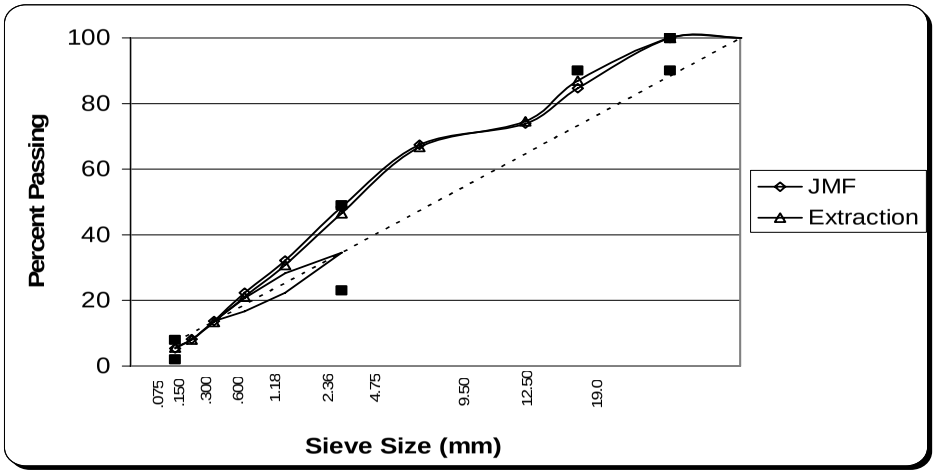

Project: M-21 St. Johns

Project Information		Asphalt Information	
Project No.:	46023A	Asphalt Source:	Michigan Paving & Materials
Location:	M-21 St. Johns	Asphalt Grade (PG):	58-22
Contractor:	Michigan Paving & Materials	Asphalt Content:	5.4
Traffic Level:	E3	Asphalt Additives:	None
Aggregate Type:	Gravel	Asphalt Additives (%):	N/A
Mix Size:	3	**SuperPave Consensus Properties**	
Gradation:	Coarse	Angularity (%):	46.8
Specifc Gravities		Dust Corr.:	0.4
G_{mm}	2.488	1 Face Crush (%):	94.3
G_{mb}	2.414	2 Face Crush (%):	N/A
G_b	1.028	**Volumetrics**	
G_{se}	2.708	VMA:	13.92
G_{sb}	2.653	VFA:	78.63
Temperature		AV:	2.99
Mixing:	292-299	F/P_{be}:	0.9
Compacting:	276	P_{be}:	4.78

Sieve Size	Mix/Gradation (%P)	Material/Producer	Percent
1 (25)	100	2304	15
3/4 (19)	99.9	2384	17
1/2 (12.5)	89.3	2217	17
3/8 (9.5)	76.3	2354	25
#4 (4.75)	45.4	2343	13
#8 (2.36)	27.9	RAP	13
#16 (1.18)	20.1		
#30 (0.60)	15.3		
#50 (0.30)	10.2		
#100 (0.15)	6.1		
#200 (0.075)	4.3		

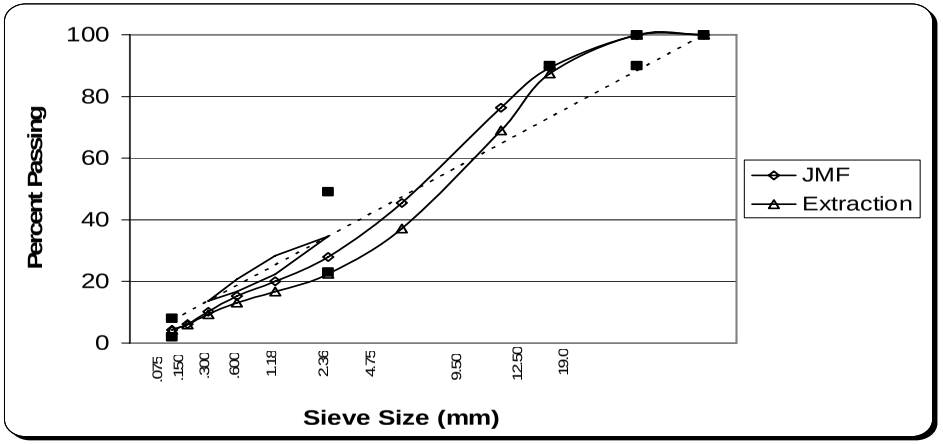

Project: BL I-96 Howell

Project Information		Asphalt Information	
Project No.:	50650A	Asphalt Source:	Michigan Paving & Materials
Location:	BL I-96Howell	Asphalt Grade (PG):	70-28
Contractor:	Rieth-Riley	Asphalt Content:	5.5
Traffic Level:	E3	Asphalt Additives:	None
Aggregate Type:	Limestone	Asphalt Additives (%):	N/A
Mix Size:	4	**SuperPave Consensus Properties**	
Gradation:	Fine	Angularity (%):	42.2
Specifc Gravities		Dust Corr.:	0.4
G_{mm}	2.48	1 Face Crush (%):	82.5
G_{mb}	2.381	2 Face Crush (%):	N/A
G_b	1.028	**Volumetrics**	
G_{se}	2.702	VMA:	14.8
G_{sb}	2.641	VFA:	73
Temperature		AV:	4
Mixing (^oF):	313-319	F/P_{be}:	1.09
Compacting (^oF):	295	P_{be}:	4.68

Sieve Size	Mix/Gradation (%P)	Material/Producer	Percent
1 (25)	100	25B	19
3/4 (19)	100	Chelsea Man. Sand	15
1/2 (12.5)	94.6	Fine Crush	16
3/8 (9.5)	86.3	2NS	35
#4 (4.75)	71.1	RAP	15
#8 (2.36)	54.7		
#16 (1.18)	43.5		
#30 (0.60)	32.7		
#50 (0.30)	18.3		
#100 (0.15)	7.6		
#200 (0.075)	5.1		

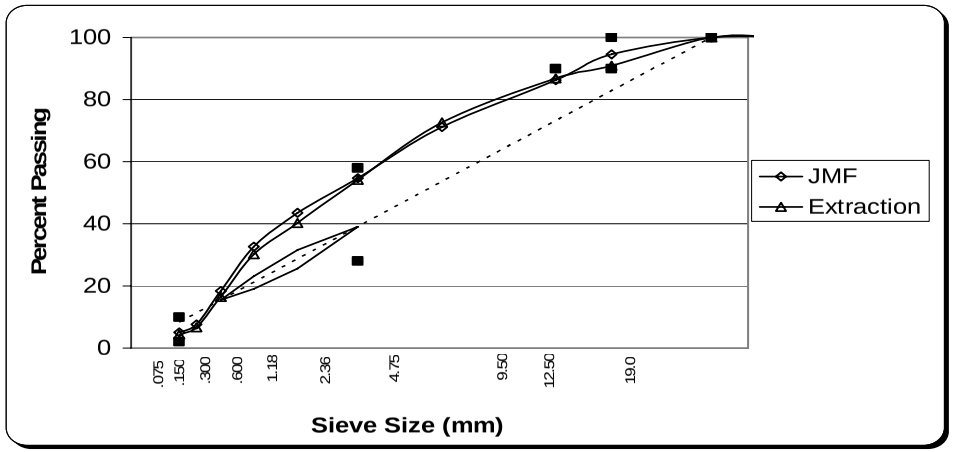

Project: M-21 Owosso

Project Information		Asphalt Information	
Project No.:	48612A	Asphalt Source:	Michigan Paving & Materials
Location:	M-21 Owosso	Asphalt Grade (PG):	64-28
Contractor:	Michigan Paving & Materials	Asphalt Content:	5.9
Traffic Level:	E3	Asphalt Additives:	None
Aggregate Type:	Limestone	Asphalt Additives (%):	N/A
Mix Size:	5	**SuperPave Consensus Properties**	
Gradation:	Fine	Angularity (%):	43.8
Specifc Gravities		Dust Corr.:	0.4
G_{mm}	2.47	1 Face Crush (%):	81.8
G_{mb}	2.371	2 Face Crush (%):	N/A
G_b	1.028	**Volumetrics**	
G_{se}	2.708	VMA:	15.4
G_{sb}	2.637	VFA:	74
Temperature		AV:	4
Mixing (^oF):	302-315	F/P_{be}:	1.09
Compacting (^oF):	266	P_{be}:	4.95

Sieve Size	Mix/Gradation (%P)	Material/Producer	Percent
1 (25)	100	3/8 x 4	10
3/4 (19)	100	Blend Sand	35
1/2 (12.5)	99.6	Fine MFG Sand	15
3/8 (9.5)	98.8	MFG Sand	30
#4 (4.75)	79.5	RAP	10
#8 (2.36)	55.5		
#16 (1.18)	39.1		
#30 (0.60)	27		
#50 (0.30)	14.8		
#100 (0.15)	7.9		
#200 (0.075)	5.4		

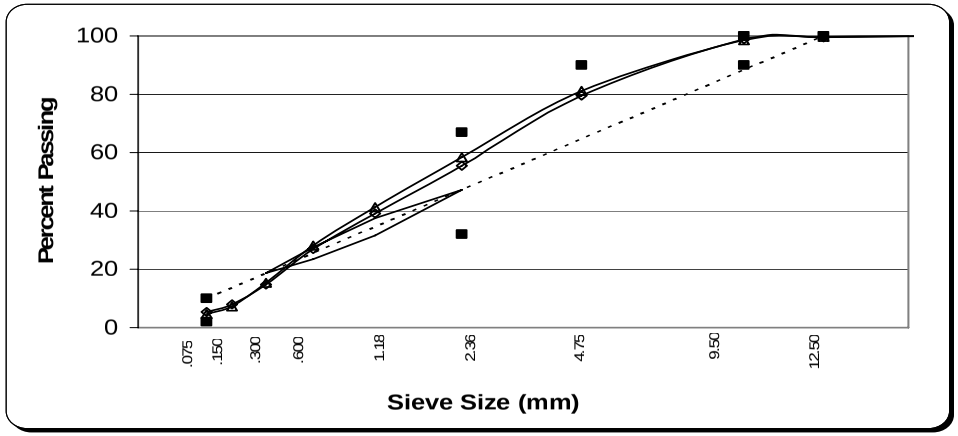

Project: M-66 Battle Creek

Project Information		Asphalt Information	
Project No.:	50759A	Asphalt Source:	Michigan Paving & Materials
Location:	Battle Creek	Asphalt Grade (PG):	64-28
Contractor:	Rieth-Riley	Asphalt Content:	5.5
Traffic Level:	E3	Asphalt Additives:	None
Aggregate Type:		Asphalt Additives (%):	N/A
Mix Size:	4	**SuperPave Consensus Properties**	
Gradation:	Fine	Angularity (%):	42.2
Specifc Gravities		Dust Corr.:	0.4
G_{mm}	2.48	1 Face Crush (%):	82.5
G_{mb}	2.38	2 Face Crush (%):	N/A
G_b	1.027	**Volumetrics**	
G_{se}	2.702	VMA:	14.8
G_{sb}	2.641	VFA:	72.8
Temperature		AV:	4
Mixing (^oF):	302-315	F/P_{be}:	1.09
Compacting (^oF):	266	P_{be}:	4.68

Sieve Size	Mix/Gradation (%P)	Material/Producer	Percent
1 (25)	100	25B	19
3/4 (19)	100	Chelsea Man. Sand	15
1/2 (12.5)	94.6	Fine Crush	16
3/8 (9.5)	86.3	2NS	35
#4 (4.75)	71.1	RAP	15
#8 (2.36)	54.7		
#16 (1.18)	43.5		
#30 (0.60)	32.7		
#50 (0.30)	18.3		
#100 (0.15)	7.6		
#200 (0.075)	5.1		

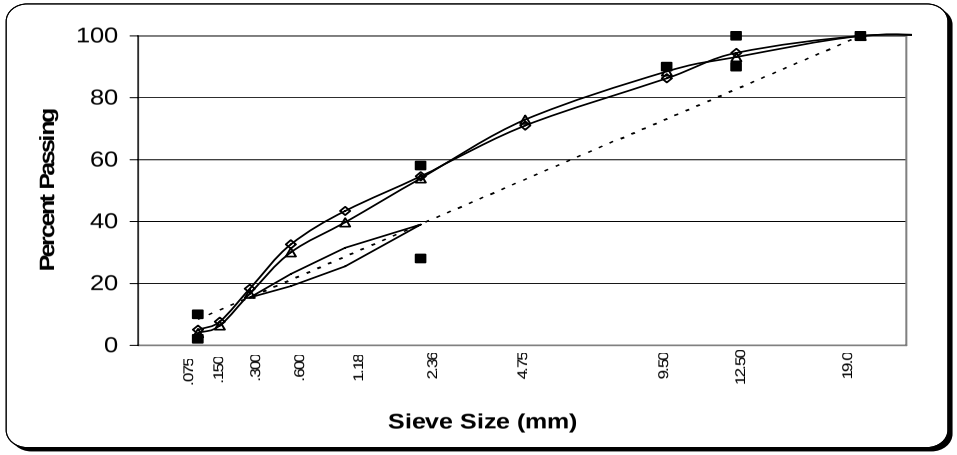

Project: M-50 Dundee

Project Information		Asphalt Information	
Project No.:	50651A	Asphalt Source:	MTM Oil
Location:	M-50	Asphalt Grade (PG):	64-28
Contractor:	Cadillac LLC Asphalt	Asphalt Content:	5.6
Traffic Level:	E3	Asphalt Additives:	None
Aggregate Type:		Asphalt Additives (%):	N/A
Mix Size:	4	**SuperPave Consensus Properties**	
Gradation:	Coarse	Angularity (%):	46
Specifc Gravities		Dust Corr.:	
G_{mm}	2.52	1 Face Crush (%):	98
G_{mb}	2.419	2 Face Crush (%):	96
G_b	1.027	**Volumetrics**	
G_{se}	2.759	VMA:	16
G_{sb}	2.717	VFA:	74.9
Temperature		AV:	4
Mixing (^oF):	311-322	F/P_{be}:	1
Compacting (^oF):	275	P_{be}:	5.10

Sieve Size	Mix/Gradation (%P)	Material/Producer	Percent
1 (25)	100	1/4 Chip	10
3/4 (19)	100	1/2 x 3/8	24
1/2 (12.5)	99.1	3/8 x 4	18
3/8 (9.5)	86.9	Trap. Sand	18
#4 (4.75)	58.3	Lime Sand	30
#8 (2.36)	37.2	RAP	0
#16 (1.18)	21.1		
#30 (0.60)	14		
#50 (0.30)	9.5		
#100 (0.15)	7.3		
#200 (0.075)	5.1		

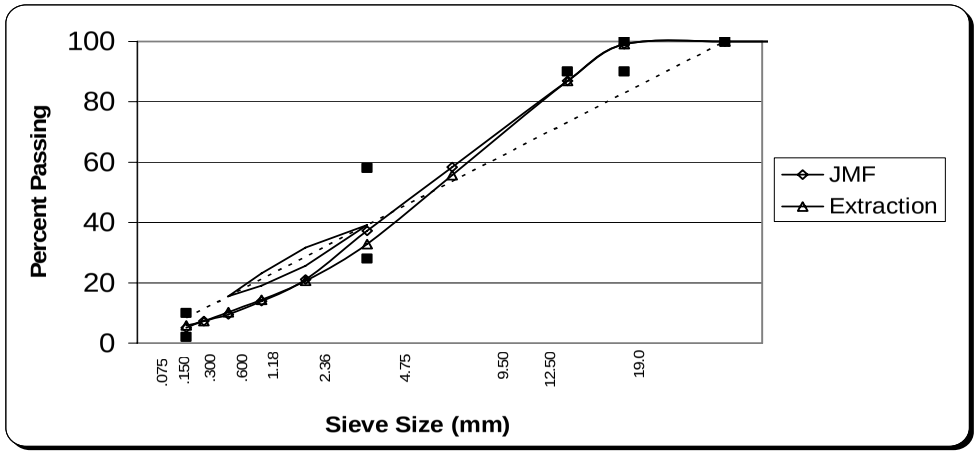

Project: US-12 MIS

Project Information		Asphalt Information	
Project No.:	50714A	Asphalt Source:	Marathon Det.
Location:	US-12 MIS	Asphalt Grade (PG):	64-28
Contractor:	Ajax Materials Corp.	Asphalt Content:	5.8
Traffic Level:	E3	Asphalt Additives:	None
Aggregate Type:		Asphalt Additives (%):	N/A
Mix Size:	4	**SuperPave Consensus Properties**	
Gradation:	Coarse	Angularity (%):	42.4
Specifc Gravities		Dust Corr.:	
G_{mm}	2.49	1 Face Crush (%):	98.7
G_{mb}	2.39	2 Face Crush (%):	98.5
G_b	1.026	**Volumetrics**	
G_{se}	2.729	VMA:	14.8
G_{sb}	2.641	VFA:	72.9
Temperature		AV:	4
Mixing (^oF):	309-321	F/P_{be}:	1.1
Compacting (^oF):	286-296	P_{be}:	4.55

Sieve Size	Mix/Gradation (%P)	Material/Producer	Percent
1 (25)	100	Man. Sand	12
3/4 (19)	100	3/8 x #4	28
1/2 (12.5)	91	Man. Sand	26
3/8 (9.5)	83.1	3/4 x 1/2	17
#4 (4.75)	52.5	RAP	17
#8 (2.36)	30.8		
#16 (1.18)	20.2		
#30 (0.60)	14.6		
#50 (0.30)	9.9		
#100 (0.15)	6.7		
#200 (0.075)	5		

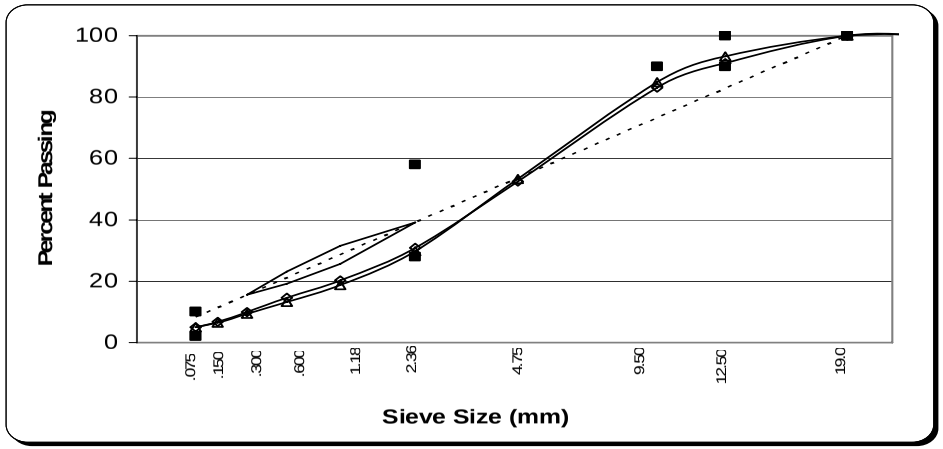

Project: M-59 Brighton

Project Information		Asphalt Information	
Project No.:	34519A	Asphalt Source:	Marathon Det.
Location:	US-23/M-59 Interchange	Asphalt Grade (PG):	58-22
Contractor:	Ajax	Asphalt Content:	5.7
Traffic Level:	E10	Asphalt Additives:	None
Aggregate Type:	Limestone	Asphalt Additives (%):	N/A
Mix Size:	3	**SuperPave Consensus Properties**	
Gradation:	Coarse	Angularity (%):	45.5
Specifc Gravities		Dust Corr.:	0.4
G_{mm}	2.485	1 Face Crush (%):	98.1
G_{mb}	2.41	2 Face Crush (%):	97.7
G_b	1.027	**Volumetrics**	
G_{se}	2.718	VMA:	14.3
G_{sb}	2.652	VFA:	78.9
Temperature		AV:	3
Mixing (^oF):	302-314	F/P_{be}:	0.96
Compacting (^oF):	284	P_{be}:	4.79

Sieve Size	Mix/Gradation (%P)	Material/Producer	Percent
1 (25)	100	1/2 x 3/8	20
3/4 (19)	99.9	3/4 x 1/2	20
1/2 (12.5)	88.2	Man. Sand	15
3/8 (9.5)	72.6	Man. Sand	30
#4 (4.75)	49.1	RAP	15
#8 (2.36)	31.8		
#16 (1.18)	20.7		
#30 (0.60)	14.5		
#50 (0.30)	9.9		
#100 (0.15)	6.3		
#200 (0.075)	4.6		

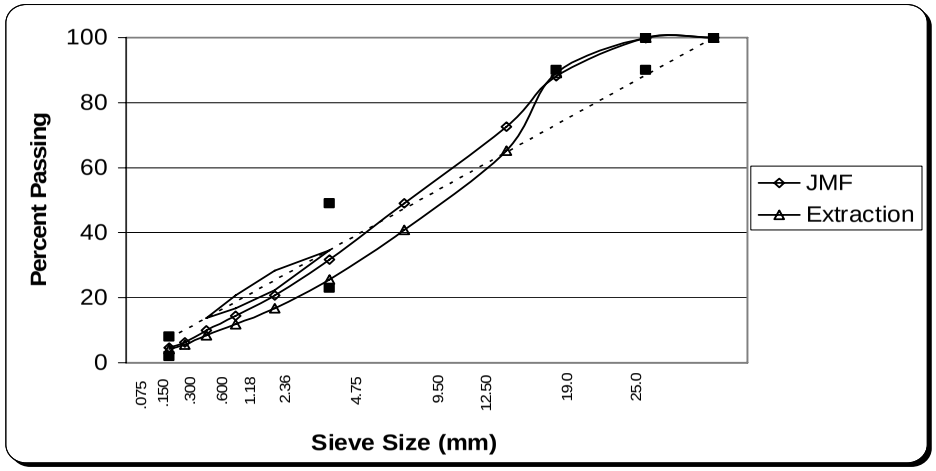

Project: Michigan Avenue, Dearborn

Project Information		Asphalt Information	
Project No.:	47064A	Asphalt Source:	Marathon Det.
Location:	Michigan Ave.	Asphalt Grade (PG):	58-28
Contractor:	Ajax Materials Corp.	Asphalt Content:	5.6
Traffic Level:	E10	Asphalt Additives:	None
Aggregate Type:		Asphalt Additives (%):	N/A
Mix Size:	3	**SuperPave Consensus Properties**	
Gradation:	Coarse	Angularity (%):	45.4
Specifc Gravities		Dust Corr.:	
G_{mm}	2.496	1 Face Crush (%):	99.3
G_{mb}	2.419	2 Face Crush (%):	98.8
G_b	1.025	**Volumetrics**	
G_{se}	2.725	VMA:	13.3
G_{sb}	2.634	VFA:	76.7
Temperature		AV:	3.1
Mixing (^oF):	297-309	F/P_{be}:	1.2
Compacting (^oF):	274-284	P_{be}:	4.42

Sieve Size	Mix/Gradation (%P)	Material/Producer	Percent
1 (25)	100	#4's	33
3/4 (19)	100	1/2"	25
1/2 (12.5)	85.3	Man. Sand	15
3/8 (9.5)	71	Man. Sand Sora	12
#4 (4.75)	43.8	RAP	15
#8 (2.36)	25.9		
#16 (1.18)	17.5		
#30 (0.60)	13.3		
#50 (0.30)	9.6		
#100 (0.15)	6.8		
#200 (0.075)	5.3		

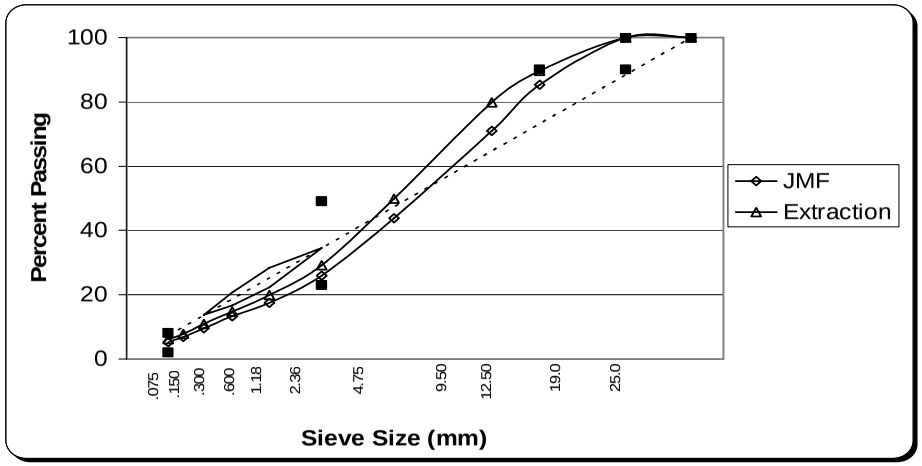

Project: Vandyke, Detroit

Project Information		Asphalt Information	
Project No.:	46273A	Asphalt Source:	Marathon Det.
Location:	M53/28 Mi to 31 Mi Rd.	Asphalt Grade (PG):	64-22
Contractor:	National Asphalt Products	Asphalt Content:	5.2
Traffic Level:	E30	Asphalt Additives:	None
Aggregate Type:		Asphalt Additives (%):	N/A
Mix Size:	3	**SuperPave Consensus Properties**	
Gradation:	Fine	Angularity (%):	45.8
Specifc Gravities		Dust Corr.:	
G_{mm}	2.577	1 Face Crush (%):	98.4
G_{mb}	2.495	2 Face Crush (%):	98.4
G_b	1.031	**Volumetrics**	
G_{se}	2.81	VMA:	14.6
G_{sb}	2.769	VFA:	78.2
Temperature		AV:	3.2
Mixing (^oF):	310-322	F/P_{be}:	0.86
Compacting (^oF):	288-298	P_{be}:	5.00

Sieve Size	Mix/Gradation (%P)	Material/Producer	Percent
1 (25)	100	2NS	15
3/4 (19)	98.9	HL3	8
1/2 (12.5)	90	Otr.	43
3/8 (9.5)	83.9	Mfg. Sand	15
#4 (4.75)	66.6	6A	19
#8 (2.36)	43.7	RAP	
#16 (1.18)	30.5		
#30 (0.60)	21.2		
#50 (0.30)	11		
#100 (0.15)	6.2		
#200 (0.075)	4.3		

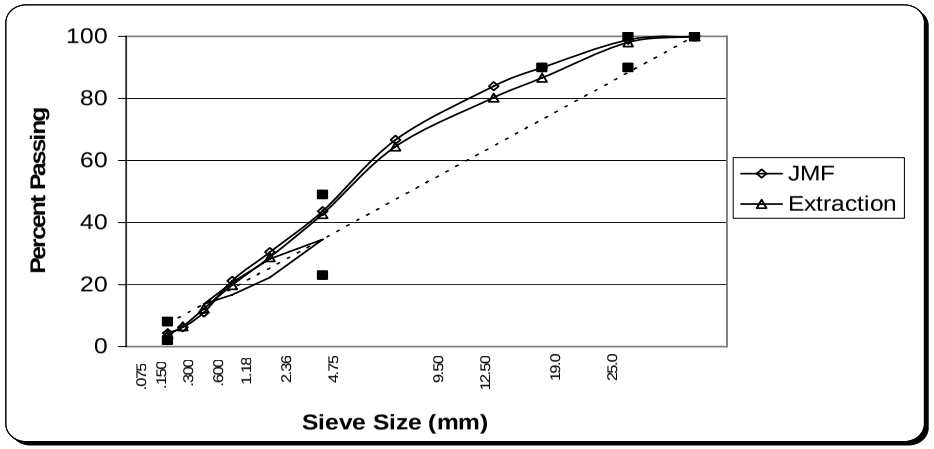

Project: US-23 Heartland

Project Information		Asphalt Information	
Project No.:	34519A	Asphalt Source:	Marathon Detroit
Location:	US-23/M-59 Interchange	Asphalt Grade (PG):	64-22
Contractor:	Ajax	Asphalt Content:	5.5
Traffic Level:	E30	Asphalt Additives:	None
Aggregate Type:	Limestone	Asphalt Additives (%):	N/A
Mix Size:	3	**SuperPave Consensus Properties**	
Gradation:	Coarse	Angularity (%):	45.5
Specifc Gravities		Dust Corr.:	0.4
G_{mm}	2.494	1 Face Crush (%):	98.1
G_{mb}	2.419	2 Face Crush (%):	97.7
G_b	1.031	**Volumetrics**	
G_{se}	2.718	VMA:	13.8
G_{sb}	2.652	VFA:	78.2
Temperature		AV:	3
Mixing (^oF):	312-323	F/P_{be}:	1
Compacting (^oF):	294	P_{be}:	4.60

Sieve Size	Mix/Gradation (%P)	Material/Producer	Percent
1 (25)	100	1/2 x 3/8	20
3/4 (19)	99.9	3/4 x 1/2	20
1/2 (12.5)	88.2	Man. Sand	15
3/8 (9.5)	72.6	Man. Sand	30
#4 (4.75)	49.1	RAP	15
#8 (2.36)	31.8		
#16 (1.18)	20.7		
#30 (0.60)	14.5		
#50 (0.30)	9.9		
#100 (0.15)	6.3		
#200 (0.075)	4.6		

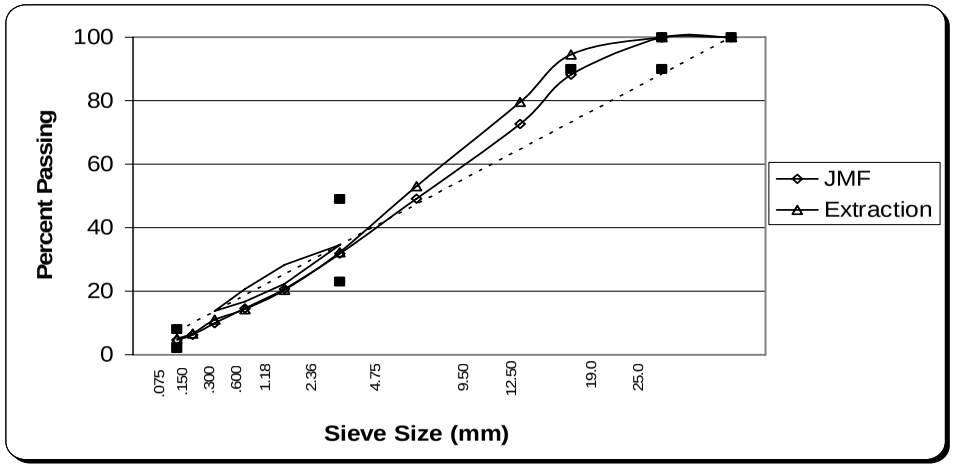

Project: I-75 Levering Road

Project Information		Asphalt Information	
Project No.:	53288A	Asphalt Source:	BP
Location:	I-75 Levering Rd.	Asphalt Grade (PG):	58-28
Contractor:	H & D Inc.	Asphalt Content:	5.5
Traffic Level:	E10	Asphalt Additives:	None
Aggregate Type:		Asphalt Additives (%):	N/A
Mix Size:	3	**SuperPave Consensus Properties**	
Gradation:	Fine	Angularity (%):	43.1
Specifc Gravities		Dust Corr.:	0.5
G_{mm}	2.43	1 Face Crush (%):	95.9
G_{mb}	2.357	2 Face Crush (%):	N/A
G_b	1.031	**Volumetrics**	
G_{se}	2.639	VMA:	14.1
G_{sb}	2.592	VFA:	79
Temperature		AV:	3
Mixing:	290	F/P_{be}:	1.11
Compacting:	266	P_{be}:	4.86

Sieve Size	Mix/Gradation (%P)	Material/Producer	Percent
1 (25)	100	3/4" Stone	12
3/4 (19)	100	9/16" Stone	28
1/2 (12.5)	89.4	Wash Fines	17
3/8 (9.5)	80.5	Cr. Sand	25
#4 (4.75)	59.3	RAP	18
#8 (2.36)	48.2		
#16 (1.18)	38.3		
#30 (0.60)	28.7		
#50 (0.30)	12.9		
#100 (0.15)	6.8		
#200 (0.075)	5.4		

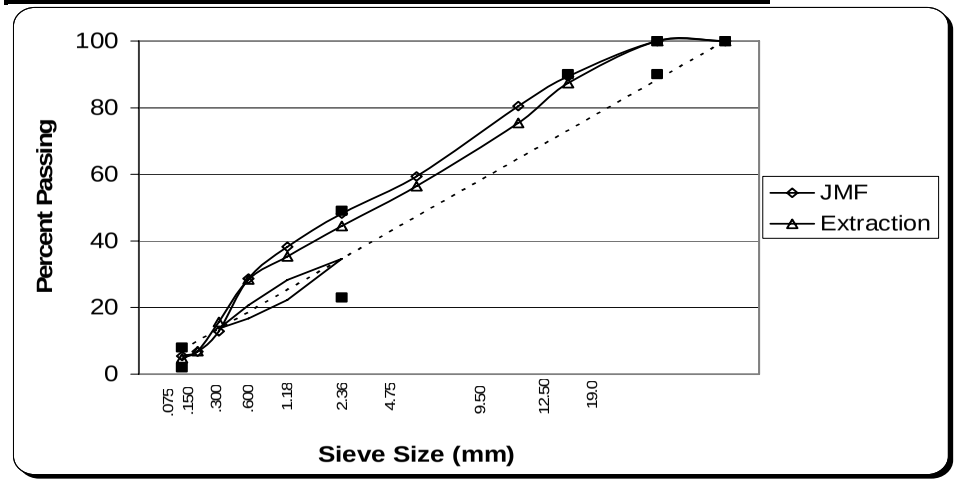

Project: I-196 Grand Rapids

Project Information		Asphalt Information	
Project No.:	74784A	Asphalt Source:	Michigan Paving & Materials
Location:	I-196 Grand Rapids	Asphalt Grade (PG):	64-22
Contractor:	Michigan Paving & Materials	Asphalt Content:	5.6
Traffic Level:	E10	Asphalt Additives:	None
Aggregate Type:	Limestone	Asphalt Additives (%):	N/A
Mix Size:	5	**SuperPave Consensus Properties**	
Gradation:	Coarse	Angularity (%):	45.6
Specifc Gravities		Dust Corr.:	
G_{mm}	2.499	1 Face Crush (%):	91
G_{mb}	2.399	2 Face Crush (%):	86.3
G_b	1.036	**Volumetrics**	
G_{se}	2.73	VMA:	15.3
G_{sb}	2.637	VFA:	73.8
Temperature		AV:	4
Mixing (^oF):	311-322	F/P_{be}:	1.2
Compacting (^oF):	286-298	P_{be}:	4.58

Sieve Size	Mix/Gradation (%P)	Material/Producer	Percent
1 (25)	100	3/8 x 4	12
3/4 (19)	100	Man. Sand	45
1/2 (12.5)	100	31A	10
3/8 (9.5)	99.9	Fine Crush	20
#4 (4.75)	74.3	FA-20	13
#8 (2.36)	43		
#16 (1.18)	27.8		
#30 (0.60)	19.5		
#50 (0.30)	11.7		
#100 (0.15)	7.8		
#200 (0.075)	5.5		

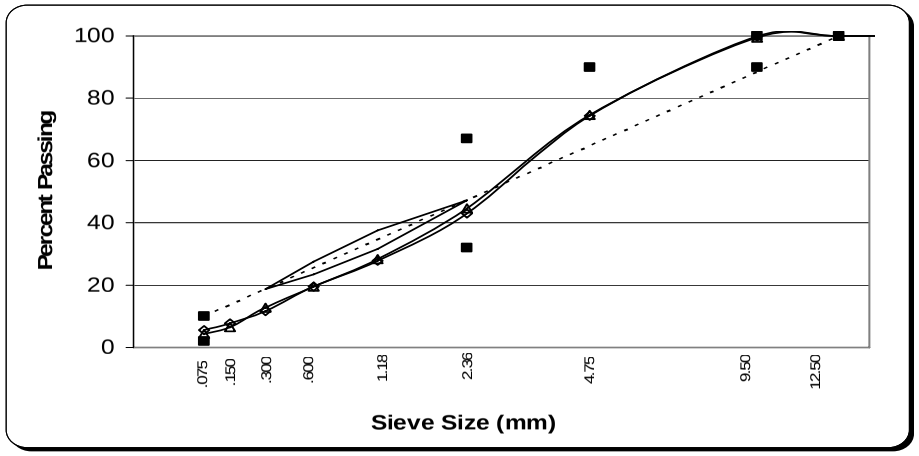

Project: I-75 Clarkston

Project Information		Asphalt Information	
Project No.:	51472A	Asphalt Source:	Marathon Det.
Location:	I-75 Clarkston	Asphalt Grade (PG):	70-22
Contractor:	Ace Asphalt & Paving	Asphalt Content:	5.8
Traffic Level:	E30	Asphalt Additives:	None
Aggregate Type:	Slag	Asphalt Additives (%):	N/A
Mix Size:	4	**SuperPave Consensus Properties**	
Gradation:	Coarse	Angularity (%):	45.3
Specifc Gravities		Dust Corr.:	
G_{mm}	2.467	1 Face Crush (%):	98.5
G_{mb}	2.369	2 Face Crush (%):	95.1
G_b	1.035	**Volumetrics**	
G_{se}	2.699	VMA:	14.7
G_{sb}	2.616	VFA:	72.8
Temperature		AV:	4
Mixing (^oF):	309-329	F/P_{be}:	0.9
Compacting (^oF):	289-309	P_{be}:	4.56

Sieve Size	Mix/Gradation (%P)	Material/Producer	Percent
1 (25)	100	3/8 x #4	16
3/4 (19)	100	MS-6	33
1/2 (12.5)	91.1	#3's	14
3/8 (9.5)	85.9	3CS	9
#4 (4.75)	54.1	3/8 x #4 BF	15
#8 (2.36)	35	RAP	12
#16 (1.18)	25.5		
#30 (0.60)	18.7		
#50 (0.30)	12.7		
#100 (0.15)	6		
#200 (0.075)	4.1		

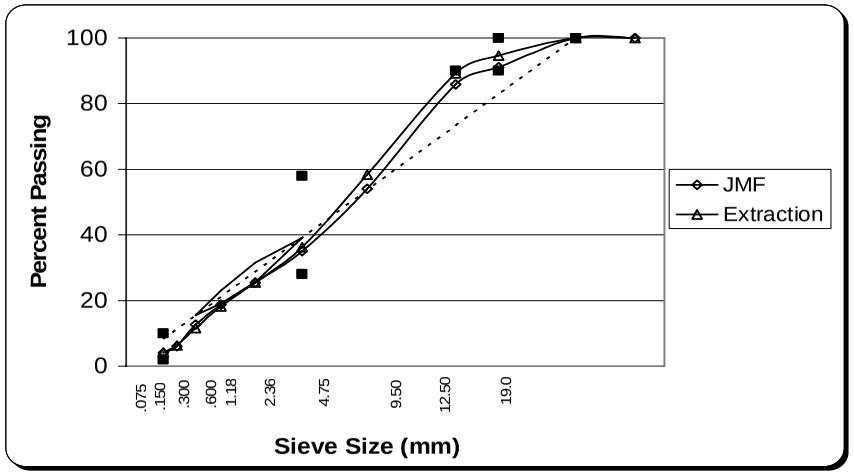

Project: M-53 Detroit, 8 Mile Road

Project Information		Asphalt Information	
Project No.:	52804A/52805A	Asphalt Source:	Marathon Det.
Location:	M-53/M-3 to M-102	Asphalt Grade (PG):	70-22
Contractor:	National Asphalt Products	Asphalt Content:	5.6
Traffic Level:	E10	Asphalt Additives:	None
Aggregate Type:		Asphalt Additives (%):	N/A
Mix Size:	4	**SuperPave Consensus Properties**	
Gradation:	Coarse	Angularity (%):	45.9
Specifc Gravities		Dust Corr.:	
G_{mm}	2.553	1 Face Crush (%):	95.6
G_{mb}	2.451	2 Face Crush (%):	92.8
G_b	1.035	**Volumetrics**	
G_{se}	2.796	VMA:	15.5
G_{sb}	2.738	VFA:	74.2
Temperature		AV:	4
Mixing (^oF):	309-329	F/P_{be}:	0.99
Compacting (^oF):	289-309	P_{be}:	4.55

Sieve Size	Mix/Gradation (%P)	Material/Producer	Percent
1 (25)	100	1/2"	10
3/4 (19)	100	4 x 3/8"	13
1/2 (12.5)	98.6	Otr Sand	34
3/8 (9.5)	86.7	Mfg. Sand	11
#4 (4.75)	51.1	HL3	24
#8 (2.36)	29.3	RAP	8
#16 (1.18)	19.7		
#30 (0.60)	14		
#50 (0.30)	9.5		
#100 (0.15)	6.1		
#200 (0.075)	4.5		

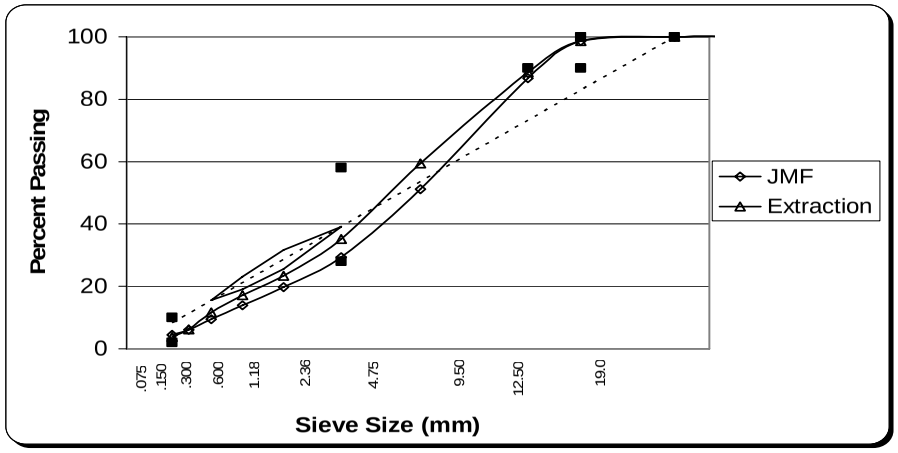

Project: Michigan Avenue, Dearborn

Project Information		Asphalt Information	
Project No.:	47064A	Asphalt Source:	Marathon Det.
Location:	Michigan Ave.	Asphalt Grade (PG):	70-22
Contractor:	Ajax Materials Corp.	Asphalt Content:	5.8
Traffic Level:	E10	Asphalt Additives:	None
Aggregate Type:		Asphalt Additives (%):	N/A
Mix Size:	4	**SuperPave Consensus Properties**	
Gradation:	Coarse	Angularity (%):	45.5
Specifc Gravities		Dust Corr.:	
G_{mm}	2.464	1 Face Crush (%):	98.8
G_{mb}	2.366	2 Face Crush (%):	97.9
G_b	1.035	**Volumetrics**	
G_{se}	2.693	VMA:	15.7
G_{sb}	2.644	VFA:	74.5
Temperature		AV:	4
Mixing (^oF):	309-329	F/P_{be}:	0.9
Compacting (^oF):	289-309	P_{be}:	5.11

Sieve Size	Mix/Gradation (%P)	Material/Producer	Percent
1 (25)	100	Man. Sand	10
3/4 (19)	100	1/2 x 3/8	25
1/2 (12.5)	98.8	Man. Sand	37
3/8 (9.5)	90	#9's	18
#4 (4.75)	57.1	RAP	10
#8 (2.36)	30.6		
#16 (1.18)	20		
#30 (0.60)	14.6		
#50 (0.30)	10		
#100 (0.15)	6.4		
#200 (0.075)	4.6		

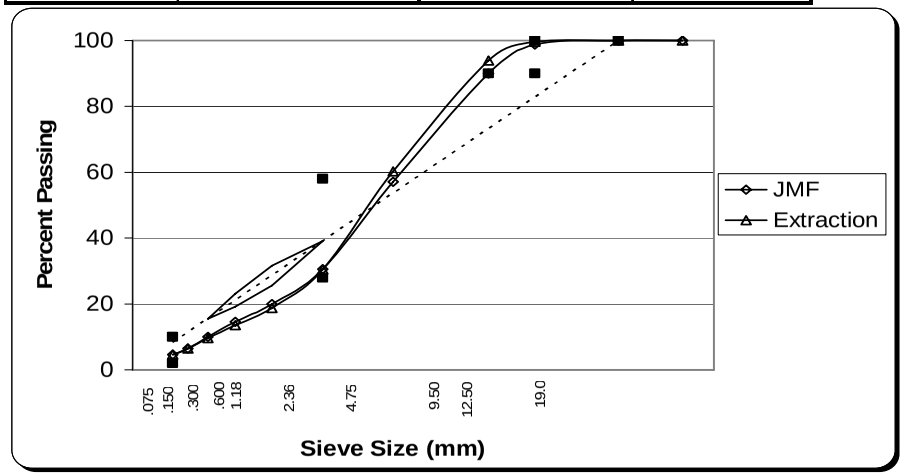

Project: I-75 Toledo

Project Information		Asphalt Information	
Project No.:	74577A	Asphalt Source:	6505 MPM Oil
Location:	I-75	Asphalt Grade (PG):	70-22
Contractor:	Cadillac Asphalt L.L.C.	Asphalt Content:	5.4
Traffic Level:	E30	Asphalt Additives:	None
Aggregate Type:		Asphalt Additives (%):	N/A
Mix Size:	5	**SuperPave Consensus Properties**	
Gradation:	Coarse	Angularity (%):	46
Specifc Gravities		Dust Corr.:	
G_{mm}	2.51	1 Face Crush (%):	98
G_{mb}	2.409	2 Face Crush (%):	96.1
G_b	1.029	**Volumetrics**	
G_{se}	2.737	VMA:	15.9
G_{sb}	2.711	VFA:	74.8
Temperature		AV:	4
Mixing (^oF):	311-322	F/P_{be}:	1.07
Compacting (^oF):	290	P_{be}:	5.05

Sieve Size	Mix/Gradation (%P)	Material/Producer	Percent
1 (25)	100	3/8 x #4	10
3/4 (19)	100	Man. Sand	28
1/2 (12.5)	100	Fine Crush	10
3/8 (9.5)	95.4	Man. Sand	32
#4 (4.75)	64.5	1/4" Chip	10
#8 (2.36)	36.4	1/2" Clear	10
#16 (1.18)	22.4		
#30 (0.60)	16.5		
#50 (0.30)	11.6		
#100 (0.15)	7.4		
#200 (0.075)	5.4		

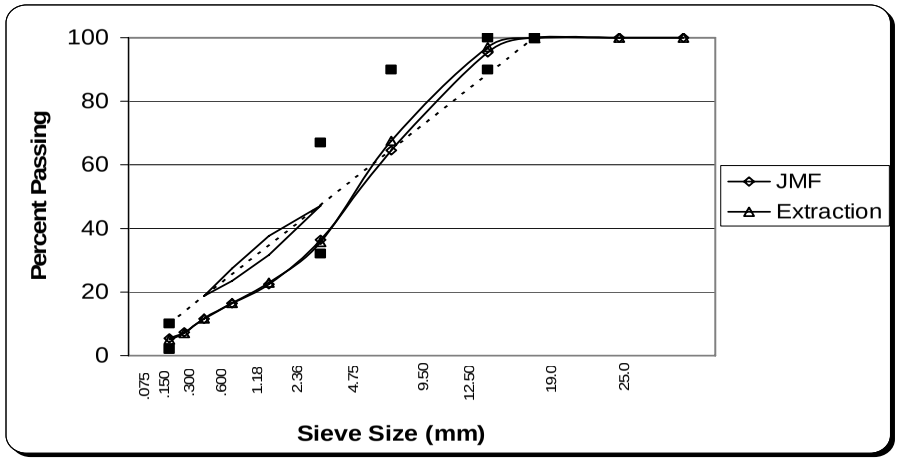

Project: I-94 Ann Arbor

Project Information		Asphalt Information	
Project No.:	47546A	Asphalt Source:	T & M Oil
Location:	I-94 Ann Arbor	Asphalt Grade (PG):	70-22
Contractor:	Thompson McCully	Asphalt Content:	6.6
Traffic Level:	E30	Asphalt Additives:	Cellulose Fibers
Aggregate Type:		Asphalt Additives (%):	0.3
Mix Size:	4	**SuperPave Consensus Properties**	
Gradation:	SMA	Angularity (%):	46.4
Specifc Gravities		Dust Corr.:	0.4
G_{mm}	2.514	1 Face Crush (%):	99.7
G_{mb}	2.413	2 Face Crush (%):	99.5
G_b		**Volumetrics**	
G_{se}	2.798	VMA:	17.8
G_{sb}	2.742	VFA:	77.4
Temperature		AV:	4
Mixing:		F/P_{be}:	1.41
Compacting:	163	P_{be}:	5.89

Sieve Size	Mix/Gradation (%P)	Material/Producer	Percent
1 (25)	100	3/8 x 0	21.5
3/4 (19)	100	3/8 x 4	14.7
1/2 (12.5)	96.7	3/8	14.7
3/8 (9.5)	79	Trap Chip	14.7
#4 (4.75)	35.8	HL1	28.3
#8 (2.36)	17.8	Mineral Filler	4
#16 (1.18)	13.7	Break-down	2.1
#30 (0.60)	11.8		
#50 (0.30)	10.7		
#100 (0.15)	9.5		
#200 (0.075)	8.3		

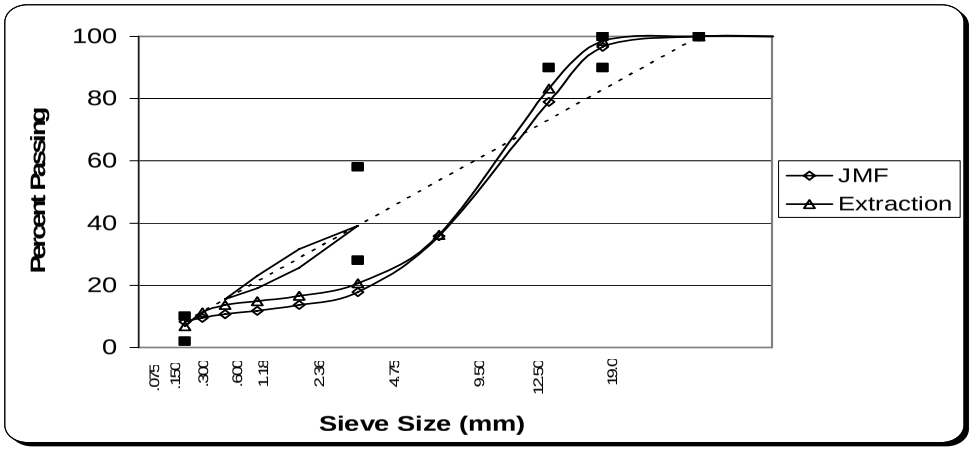

APPENDIX B SPECIMEN VOLUMETRICS

Phase I – Compaction Curves for Marshall Specimens

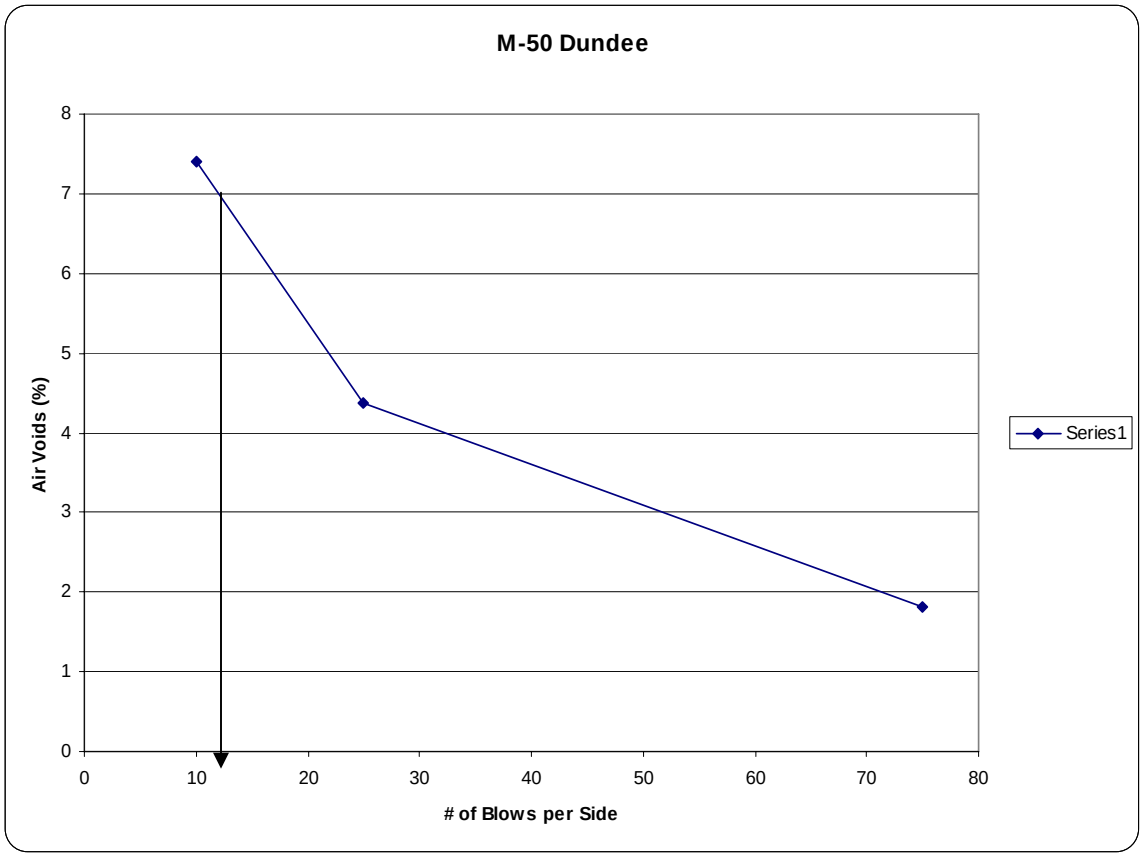
M-50 Dundee
Air Voids (%)
8
7
6
5
4
3
2
1
0
0
10
20
30
40
50
60
70
80
# of Blows per Side
Series1

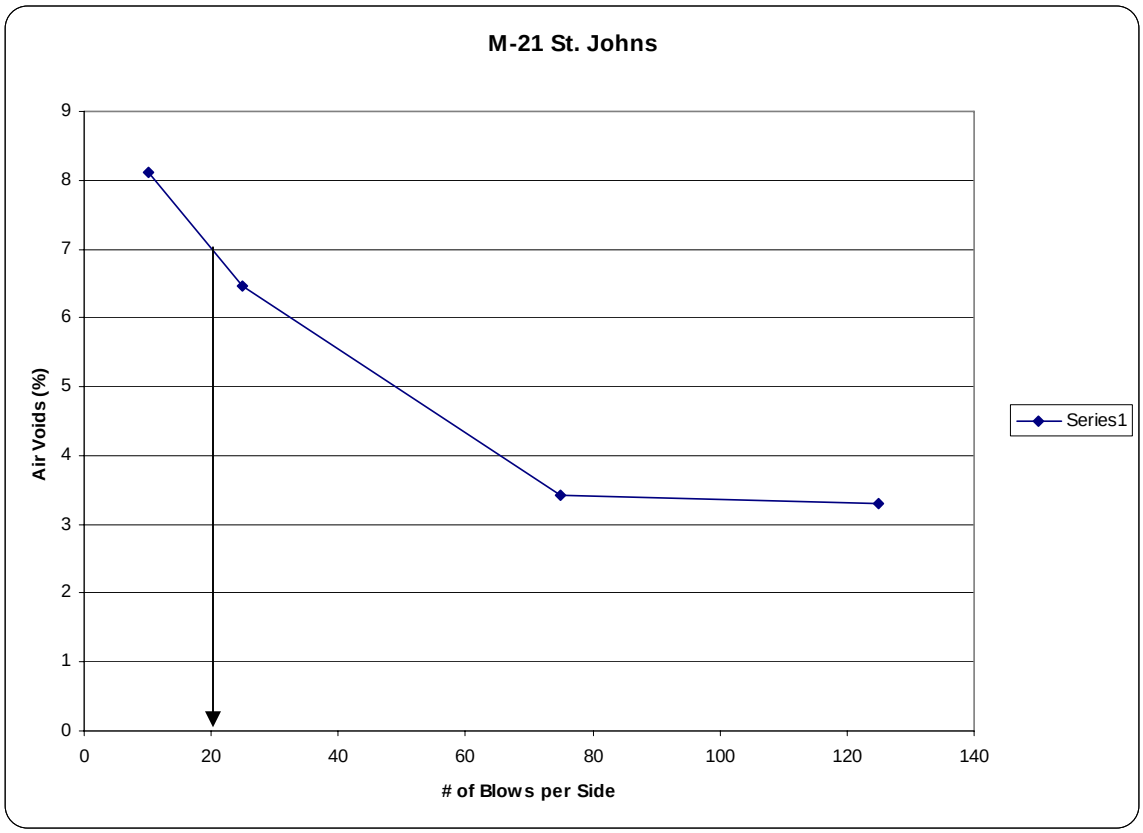
M-21 St. Johns
Air Voids (%)
9
8
7
6
5
4
3
2
1
0
0
20
40
60
80
100
120
140
# of Blows per Side
Series1

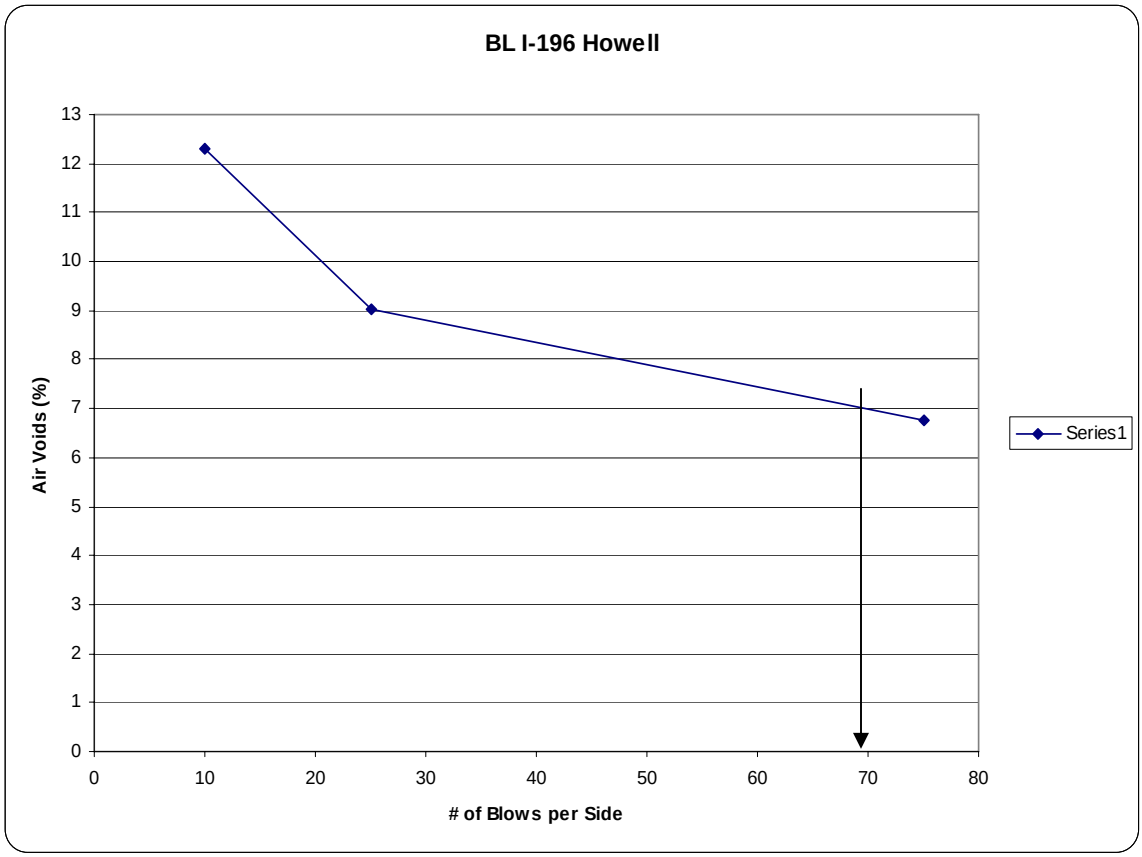
BL I-196 Howell
Air Voids (%)
13
12
11
10
9
8
7
6
5
4
3
2
1
0
0
10
20
30
40
50
60
70
80
# of Blows per Side
Series1

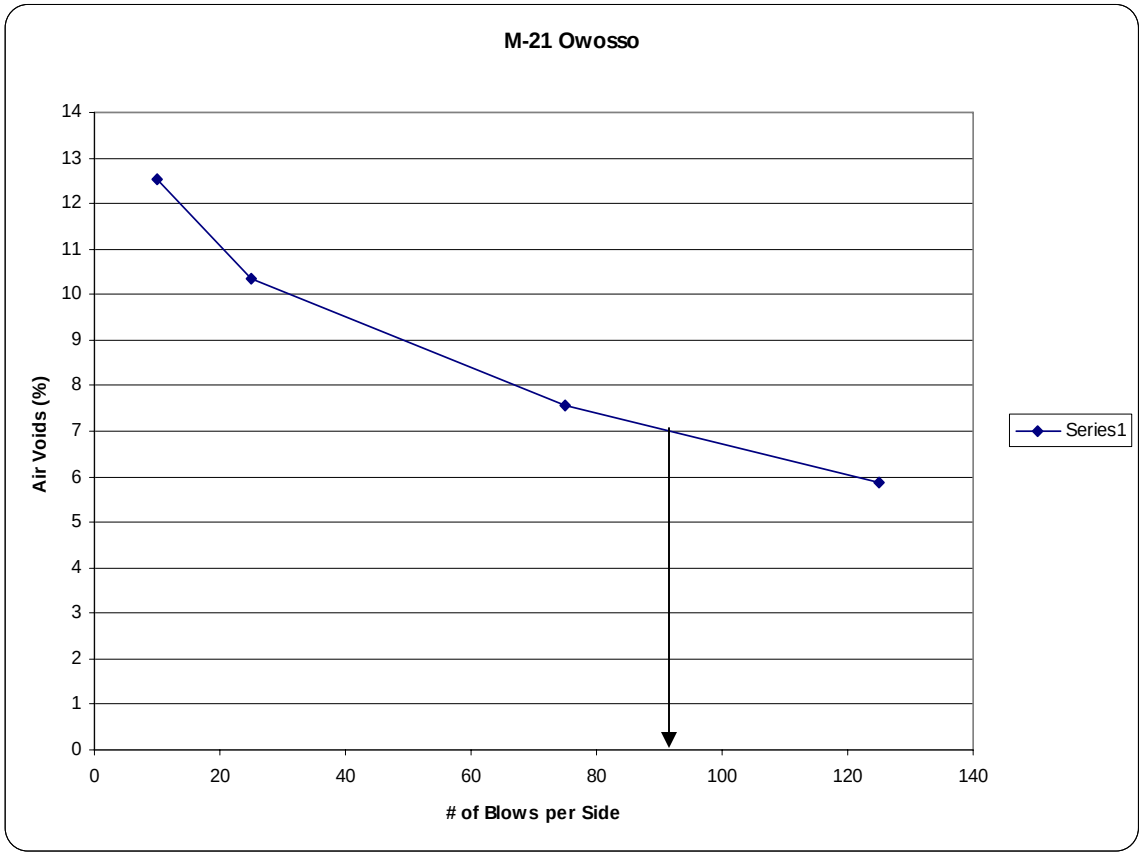
M-21 Owosso
Air Voids (%)
14
13
12
11
10
9
8
7
6
5
4
3
2
1
0
0
20
40
60
80
100
120
140
# of Blows per Side
Series1

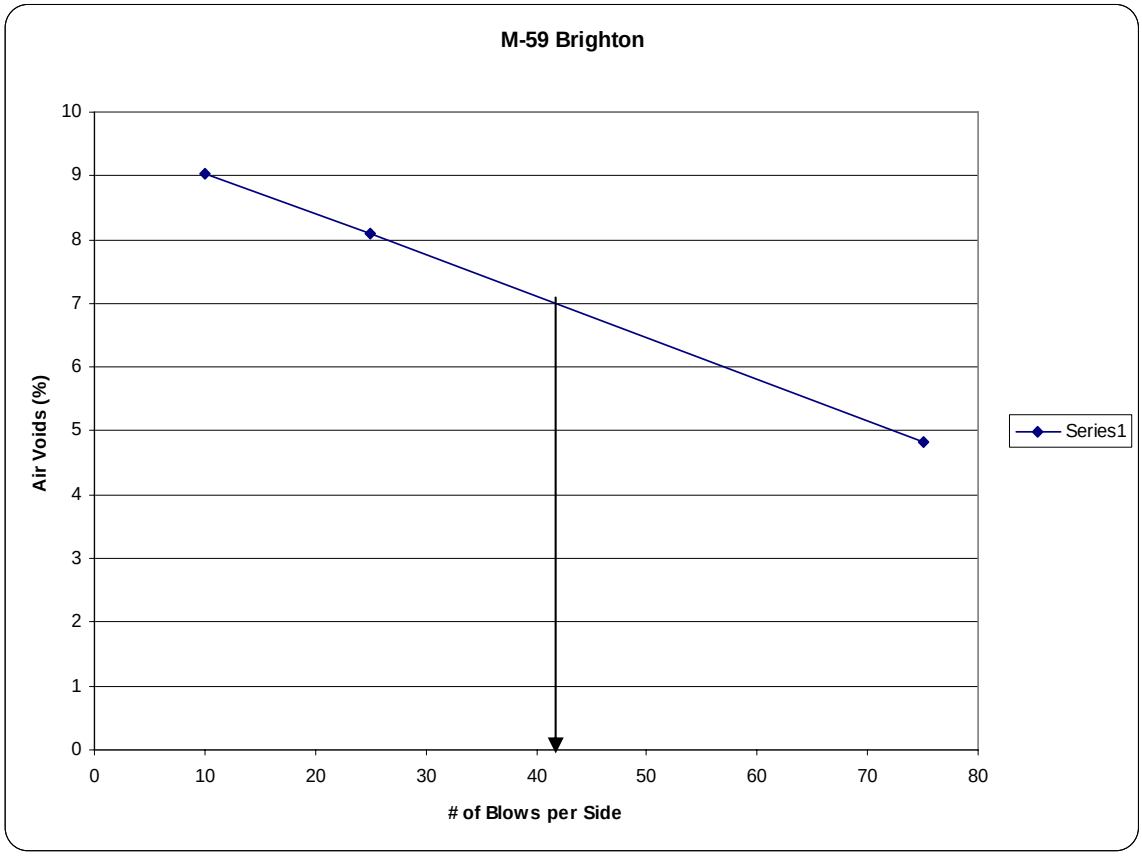
M-59 Brighton
Air Voids (%)
10
9
8
7
6
5
4
3
2
1
0
0
10
20
30
40
50
60
70
80
# of Blows per Side
Series1

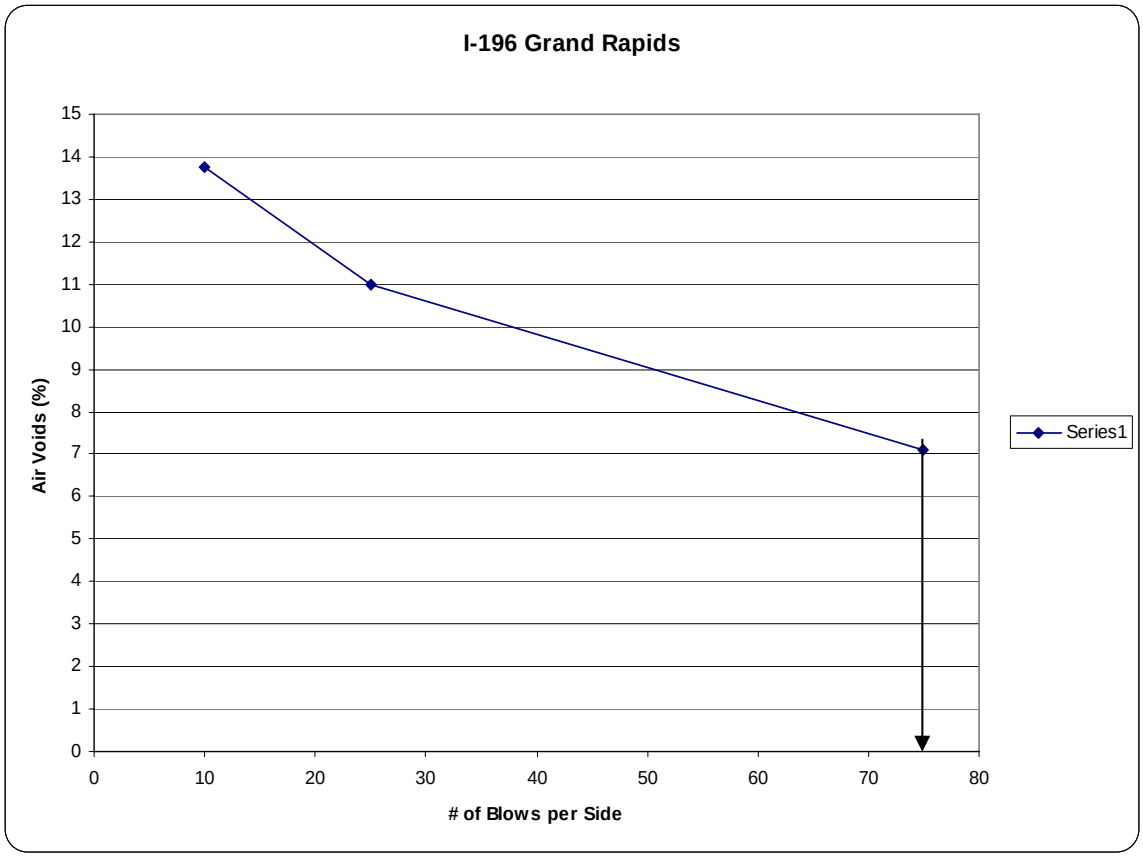
I-196 Grand Rapids
Air Voids (%)
15
14
13
12
11
10
9
8
7
6
5
4
3
2
1
0
0
10
20
30
40
50
60
70
80
# of Blows per Side
Series1

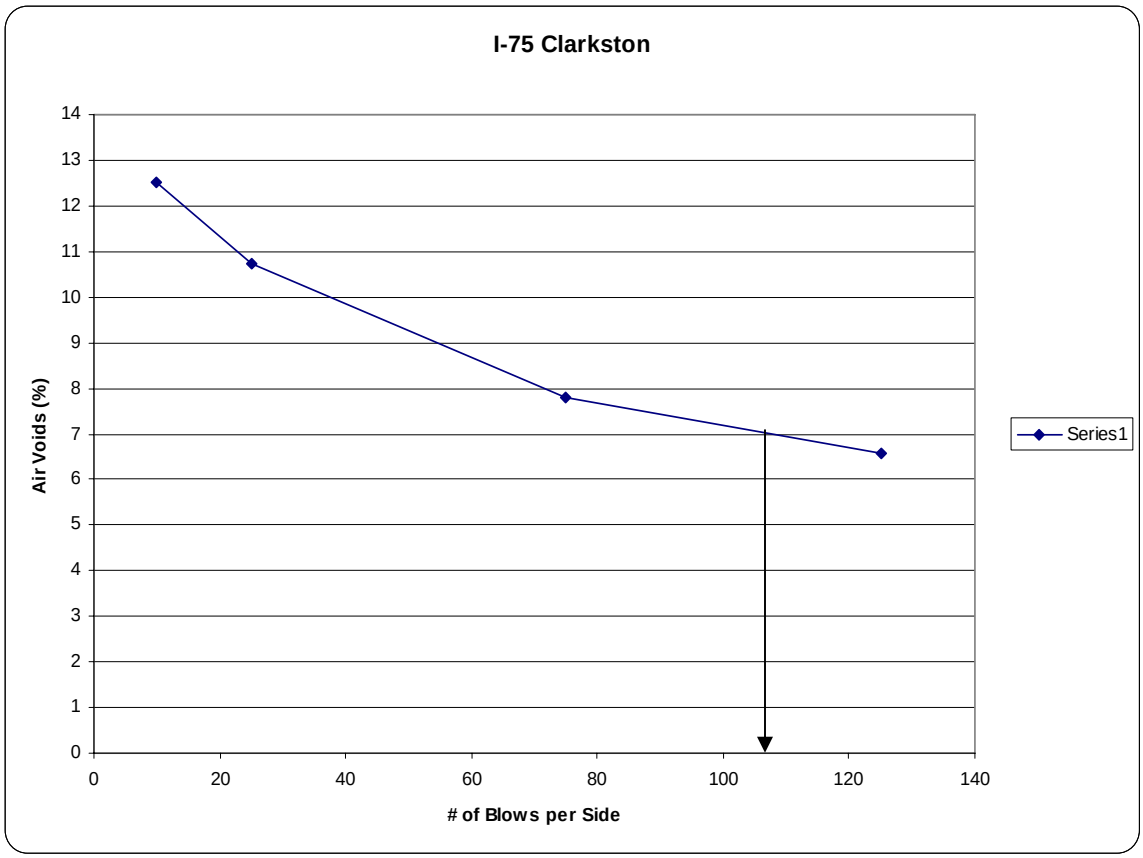
I-75 Clarkston
Air Voids (%)
14
13
12
11
10
9
8
7
6
5
4
3
2
1
0
0
20
40
60
80
100
120
140
# of Blows per Side
Series1

Phase I – 100mm Marshall Specimens

Project Number: 50651A
Location: M-50 Dundee
Contractor: Cadillac LLC
Mix: Asphalt
Gradation: 3E1
G_{mm} Coarse
2.52

	Sample	1	2	3	4	5	6	7	8	9	10	11	12	13	14	15	16	17	18	19	20
A	Dry Mass	1195.8	1192.3	1193.7	1190.2	1194.9	1186.8	1199.7	1196.2	1198.3	1198.8	1194.3	1201.1	1192.4	1191.3	1194.8	1196.2	1196.6	1190	1186	1185.8
B	Height 1	66.90	66.74	65.13	64.32	67.06	64.73	68.04	66.53	67.28	66.20	64.40	67.34	68.47	69.00	68.71	68.57	68.01	68.63	67.73	66.65
C	Height 2	66.49	65.79	66.30	65.42	67.03	65.33	68.27	65.86	67.18	66.12	64.37	67.31	69.22	3.00	69.25	68.34	68.22	68.59	67.45	67.83
D	Height 3	66.59	65.88	66.09	65.65	67.40	64.41	68.53	65.42	67.21	66.31	64.94	67.92	68.47	68.80	68.68	68.72	68.57	68.07	67.49	68.04
E	Height 4	66.28	65.91	65.16	64.50	67.45	64.50	67.94	66.02	67.85	66.67	64.11	68.66	68.12	68.30	68.24	69.27	68.53	69.38	67.72	66.83
F	Average Height	66.57	66.08	65.67	64.97	67.24	64.74	68.20	65.96	67.38	66.33	64.46	67.81	68.57	67.97	68.72	68.73	68.33	68.67	67.60	67.34
G	Diameter 1	101.970	101.090	101.310	101.630	101.480	101.690	100.970	101.500	100.840	101.860	101.120	101.180	100.520	102.240	101.420	101.580	101.640	101.270	101.900	102.360
H	Diameter 2	101.270	101.050	101.350	101.410	101.930	101.900	101.240	101.770	101.540	101.940	101.220	101.140	101.390	101.770	100.960	101.190	101.520	101.500	101.720	102.100
I	Average Diameter	101.620	101.070	101.330	101.520	101.695	101.795	101.105	101.635	101.190	101.900	101.170	101.160	100.955	102.005	101.190	101.385	101.580	101.385	101.810	102.230
J	G_{mb} [A/(F-e/1^2/4)]	2.215	2.249	2.254	2.263	2.188	2.252	2.191	2.235	2.211	2.216	2.305	2.204	2.172	2.145	2.162	2.156	2.161	2.147	2.155	2.145
K	Air Voids [(G$_{mm}$-J)/G$_{mm}$]	12.1	10.8	10.6	10.2	13.2	10.6	13.0	11.3	12.2	12.1	8.5	12.5	13.8	14.9	14.2	14.4	14.3	14.8	14.5	14.9

SATURATED SURFACE DRY METHOD

	Sample	1	2	3	4	5	6	7	8	9	3	11	12	13	14	15	16	17	18	19	20
A	Dry Mass	1195.8	1192.3	1193.7	1190.3	1194.9	1186.7	1199.7	1196.2	1198.3	1198.8	1194.3	1201.1	1192.3	1191.3	1194.3	1196.1	1196.4	1190	1185.7	1185.8
B	Submerged Mass	696.4	691.6	693.3	691.6	695.7	687.7	697.2	696.7	697.6	693.3	691.1	698.7	697.7	698.5	699.4	699.6	698.7	696.8	693.1	687.4
C	SSD Mass	1202.7	1196.7	1197.5	1194	1207.1	1192.1	1211.4	1202.8	1209.6	1205.8	1198.5	1210.6	1210.7	1212.4	1213	12136	1212.1	1207.5	1200.4	1198.5
D	G_{mb} [A/(C-B)]	2.362	2.361	2.368	2.369	2.337	2.353	2.333	2.364	2.340	2.339	2.354	2.346	2.324	2.318	2.325	2.327	2.330	2.330	2.337	2.320
E	Air Voids [(G$_{mm}$-D)/G$_{mm}$]	6.3	6.3	6.1	6.0	7.3	6.6	7.4	6.2	7.1	7.2	6.6	6.9	7.8	8.0	7.7	7.7	7.5	7.5	7.3	7.9

Project Number:	46023A
Location:	M-21 St. Johns
Contractor:	Michigan Paving & Materials
Mix:	3E3
Gradation:	Coarse
G_{mm}	2.489

VOLUMETRIC ANALYSIS

	Sample	1	2	3	4	5	6	7	8	9	1	11	12	13	14	15	16	17	18	19	20
A	Dry Mass (g)	1196.9	1194.3	1182.8	1196.2	1194.6	1191.9	1204.7	1195.2	1190	1199.3	1196.2	1194.8	1212.4	1196.6	1196.4	1195.1	1206.8	1197.3	1200.4	1199.8
B	Height 1 (mm)	68.00	67.16	68.73	69.04	69.04	69.17	69.34	68.74	69.19	68.96	68.07	68.45	69.90	68.01	67.29	68.05	69.63	68.85	68.49	68.82
C	Height 2 (mm)	68.28	66.96	68.49	69.02	69.08	69.14	68.68	68.33	69.18	69.34	68.01	68.55	69.36	67.72	67.95	68.12	70.14	69.37	69.09	69.03
D	Height 3 (mm)	67.98	67.14	68.49	68.98	68.57	69.22	69.25	68.31	69.23	69.12	68.28	68.39	69.63	67.89	67.29	68.08	69.77	69.32	68.72	69.72
E	Height 4 (mm)	67.78	67.58	68.70	69.28	68.74	69.20	69.93	68.55	69.85	68.80	68.45	68.16	69.90	68.72	67.13	67.98	69.33	68.79	68.43	69.80
F	Average Height (mm)	68.01	67.21	68.60	69.08	68.86	69.18	69.30	68.48	69.36	69.06	68.20	68.39	69.70	68.09	67.42	68.06	69.72	69.08	68.68	69.34
G	Diameter 1 (mm)	102.41	101.94	102.05	102.26	102.25	101.76	101.95	102.13	102.55	102.03	102.28	102.43	102.20	102.24	101.77	102.01	102.24	102.14	102.85	102.79
H	Diameter 2 (mm)	102.83	101.81	101.84	102.77	102.79	101.79	101.99	102.14	102.60	102.10	101.93	102.51	102.55	102.02	101.90	102.01	102.13	102.36	102.45	101.90
I	Average Diameter (mm)	102.62	101.88	101.95	102.52	102.52	101.78	101.97	102.14	102.58	102.07	102.11	102.47	102.38	102.13	101.84	102.01	102.19	102.25	102.65	102.35
J	G_{mb} [A/(F*π*I^2/4)]	2.128	2.180	2.112	2.098	2.102	2.118	2.129	2.130	2.076	2.123	2.142	2.119	2.113	2.145	2.179	2.149	2.111	2.111	2.112	2.103
K	Air Voids [(G_{mm}-J)/G_{mm}]	14.5	12.4	15.1	15.7	15.6	14.9	14.5	14.4	16.6	14.7	13.9	14.9	15.1	13.8	12.5	13.7	15.2	15.2	15.2	15.5

SATURATED SURFACE DRY METHOD

	Sample	1	2	3	4	5	6	7	8	9	1	11	12	13	14	15	16	17	18	19	20
A	Dry Mass (g)	1196.9	1194.3	1182.8	1196.2	1194.6	1191.9	1204.7	1195.2	1190	1199.3	1196.2	1194.8	1212.4	1196.6	1196.4	1195.1	1206.8	1197.3	1200.4	1199.8
B	Submerged Mass (g)	686.4	685	690	691.6	689	692.6	697.3	688.7	687.4	691.7	692	689.1	702.4	689.4	685	687.5	699.1	693.5	692	695.8
C	SSD Mass (g)	1208.8	1203	1202.6	1210.9	1209.7	1209.9	1219.6	1209	1206.5	1214.8	1211.2	1210.1	1228.5	1210.3	1203.3	1207.1	1222.4	1216.1	1215.8	1217.7
D	G_{mb} [A/(C-B)]	2.29	2.31	2.31	2.30	2.29	2.30	2.31	2.30	2.29	2.29	2.30	2.29	2.30	2.30	2.31	2.30	2.31	2.29	2.29	2.30
E	Air Voids [(G_{mm}-D)/G_{mm}]	7.9	7.4	7.3	7.5	7.8	7.4	7.3	7.7	7.9	7.9	7.4	7.9	7.4	7.7	7.3	7.6	7.3	8.0	7.9	7.6

Project Number: 50650A

Location: BL I-96 Howell

Contractor: Rieth-Riley

Mix: Fine

Gradation: 4E3

G_{mm} 2.501

	Sample	1	2	3	4	5	6	7	8	9	10	11	12	13	14	15	16	17	18	19	20
A	Dry Mass	1223.4	1265.2	1190.4	1190.3	1194.6	1195.1	1193	1198.6	1188.5	1198.6	1192.6	1196.5	1190.7	1201.5	1198	1193.8	1187.1	1203.8	1193.3	1200.9
B	Height 1	66.24	68.82	65.39	64.95	65.96	65.69	65.20	64.79	64.86	65.28	65.21	65.44	64.93	65.22	66.21	64.80	64.92	65.13	64.90	64.84
C	Height 2	67.42	68.59	65.30	64.20	65.36	66.12	65.63	65.65	64.47	64.94	64.65	65.24	64.48	65.50	65.72	64.47	65.18	65.59	65.81	64.63
D	Height 3	66.63	67.90	64.93	64.45	64.80	64.49	64.48	66.61	64.58	65.45	64.76	64.26	64.53	65.90	64.75	65.75	65.72	66.36	65.41	64.68
E	Height 4	65.56	68.17	64.00	65.37	64.41	65.65	64.38	64.96	65.33	66.79	65.27	64.91	65.14	65.62	65.38	65.40	64.92	65.57	65.19	64.68
F	Average Height	66.46	68.37	64.91	64.74	65.13	65.49	64.92	65.50	64.81	65.62	64.97	64.96	64.77	65.56	65.52	65.11	65.19	65.66	65.33	64.71
G	Diameter 1	101.55	101.2	100.83	101.76	101.3	101.44	101.53	101.65	101.36	101.35	101.37	101.65	101.28	101.39	101.47	101.55	101.47	101.67	101.2	101.88
H	Diameter 2	101.76	101.5	101.25	101.65	101.94	101.61	102.32	101.79	101.19	101.54	101.37	101.47	101.3	101.37	101.55	101.43	101.73	101.46	101.39	101.91
I	Average Diameter	101.655	101.350	101.040	101.705	101.620	101.525	101.925	101.720	101.275	101.445	101.370	101.560	101.290	101.380	101.510	101.490	101.600	101.565	101.295	101.895
J	G_{mb} [A/(F*π*I^2/4)]	2.268	2.294	2.287	2.263	2.261	2.254	2.252	2.252	2.276	2.260	2.274	2.274	2.281	2.270	2.259	2.267	2.246	2.263	2.267	2.276
K	Air Voids [(G_{mm}-J)/G_{mm}]	9.3	8.3	8.5	9.5	9.6	9.9	10.0	10.0	9.0	9.6	9.1	9.1	8.8	9.2	9.7	9.4	10.2	9.5	9.4	9.0

SATURATED SURFACE DRY METHOD

	Sample	1	2	3	4	5	6	7	8	9	10	11	12	13	14	15	16	17	18	19	20
A	Dry Mass	1223.4	1265.2	1190.4	1190.3	1194.6	1195.1	1193	1198.6	1188.5	1198.6	1192.6	1196.5	1190.7	1201.5	1198	1193.8	1187.1	1203.8	1193.3	1200.9
B	Submerged Mass	696.1	722.1	680.7	677.1	680.9	676.8	678.9	680	677.7	681.3	678.5	682.1	677.1	685.2	683.7	679.1	673.8	684.8	677.6	682.6
C	SSD Mass	1224.8	1267.6	1193	1192.5	1196.5	1196.3	1196.6	1200.9	1192.3	1202.2	1196.1	1199.6	1194.1	1203.9	1201	1197.4	1189.6	1206.7	1196	1204.5
D	G_{mb} [A/(C-B)]	2.314	2.319	2.324	2.309	2.317	2.300	2.304	2.301	2.310	2.301	2.304	2.312	2.303	2.316	2.316	2.303	2.301	2.307	2.302	2.301
E	Air Voids [(G_{mm}-D)/G_{mm}]	7.5	7.3	7.1	7.7	7.4	8.0	7.9	8.0	7.7	8.0	7.9	7.6	7.9	7.4	7.4	7.9	8.0	7.8	8.0	8.0

Project Number:	48612A
Location:	M-21 Owosso
Contractor:	Michigan Paving & Materials
Mix:	5E3
Gradation:	Fine
G_{mm}	2.470

VOLUMETRIC ANALYSIS

	Sample	1	2	3	4	5	6	7	8	9	10	11	12	13	14	15	16	17	18	19	20
A	Dry Mass (g)	1192.2	1209.6	1196.8	1212.8	1199.9	1212.1	1194.2	1197.1	1194.2	1199.9	1189.3	1192.6	1194	1179.3	1186	1191	1198.1	1191.1	1195.7	1194.2
B	Height 1 (mm)	64.49	65.46	64.93	66.19	66.31	66.06	65.74	65.82	64.64	67.33	66.48	65.11	66.58	63.85	63.98	64.24	65.60	65.88	65.86	65.33
C	Height 2 (mm)	65.34	65.44	65.46	67.19	65.02	65.68	65.83	65.62	64.70	65.13	64.88	65.92	65.41	64.43	64.14	65.45	64.70	65.49	65.65	65.96
D	Height 3 (mm)	64.43	66.01	65.52	66.81	65.31	66.02	64.97	65.05	65.87	65.35	65.10	66.30	64.47	64.81	65.47	65.68	66.30	65.34	64.48	65.44
E	Height 4 (mm)	64.41	66.04	65.60	65.83	66.57	66.36	65.13	65.32	65.86	66.12	65.97	64.66	65.13	64.68	65.44	64.85	66.83	65.58	64.65	64.42
F	Average Height (mm)	64.67	65.74	65.38	66.51	65.80	66.03	65.42	65.45	65.27	65.98	65.61	65.50	65.40	64.44	64.76	65.06	65.86	65.57	65.16	65.29
G	Diameter 1 (mm)	101.37	101.31	101.23	101.30	101.27	101.29	101.37	101.35	101.29	101.37	101.27	101.32	101.36	101.43	101.38	101.33	101.16	101.37	101.34	101.45
H	Diameter 2 (mm)	101.27	101.47	101.31	101.37	101.36	101.31	101.32	101.40	101.33	101.42	101.28	101.30	101.63	101.35	101.39	101.20	101.35	101.32	101.21	101.33
I	Average Diameter (mm)	101.32	101.39	101.27	101.34	101.32	101.30	101.35	101.38	101.31	101.40	101.28	101.31	101.50	101.39	101.39	101.27	101.26	101.35	101.28	101.39
J	G_{mb} [A/(Pi*r^2/4)]	2.287	2.279	2.273	2.261	2.262	2.278	2.263	2.266	2.270	2.252	2.250	2.259	2.257	2.267	2.269	2.273	2.259	2.252	2.278	2.266
K	Air Voids [(G_{mm}-J)/G_{mm}]	7.4	7.7	8.0	8.5	8.4	7.8	8.4	8.3	8.1	8.8	8.9	8.6	8.6	8.2	8.2	8.0	8.5	8.8	7.8	8.3

SATURATED SURFACE DRY METHOD

	Sample	1	2	3	4	5	6	7	8	9	10	11	12	13	14	15	16	17	18	19	20
A	Dry Mass (g)	1192.2	1209.6	1196.8	1212.8	1193.9	1212.1	1194.2	1197.1	1194.2	1199.9	1189.3	1192.6	1194	1179.3	1186	1191	1198.1	1191.1	1195.7	1194.2
B	Submerged Mass (g)	679.3	685.5	677.1	685.3	673.4	687.1	673.2	676.5	676	676.7	671.8	673.3	674.9	667	671	673.5	677	671.7	676	675.5
C	SSD Mass (g)	1194.4	1211.9	1198.8	1215.5	1196.4	1214.6	1197.2	1200.3	1196.9	1202.1	1192.7	1195.6	1196.8	1181.8	1187.8	1193.5	1200.5	1192.6	1197.8	1197
D	G_{mb} [A/(C-B)]	2.31	2.30	2.29	2.29	2.28	2.30	2.28	2.29	2.29	2.28	2.28	2.28	2.29	2.29	2.29	2.29	2.29	2.29	2.29	2.29
E	Air Voids [(G_{mm}-D)/G_{mm}]	6.3	7.0	7.1	7.4	7.6	7.0	7.7	7.5	7.2	7.5	7.6	7.6	7.4	7.3	7.1	7.3	7.3	7.4	7.2	7.3

Project Number: 34519A

Location: M-59 Brighton

Contractor: Ajax Paving

Mix: 3E10

Gradation: Coarse

G_{mm} 2.503

	Sample	1	2	3	4	5	6	7	8	9	10	11	12	13	14	15	16	17	18	19	20
A	Dry Mass	1211.5	1194.8	1195.8	1198	1208.9	1197.1	1200.7	1203.8	1201.6	1198	1209.2	1188.6	1189.5	1192.9	1194	1195	1207	1196.4	1196.6	1186.7
B	Height 1	70.26	68.03	67.36	68.03	70.00	68.08	65.29	67.81	69.90	68.68	70.00	68.26	65.89	67.12	69.60	68.45	70.66	68.78	66.43	65.13
C	Height 2	70.43	68.79	67.50	68.34	69.86	68.52	65.03	67.73	69.80	69.29	70.26	68.07	65.82	67.48	69.48	67.90	71.69	68.56	65.56	65.36
D	Height 3	70.51	67.92	67.67	68.04	69.89	67.81	66.29	67.46	69.69	69.09	69.97	68.20	64.88	67.38	69.08	67.98	71.19	68.95	65.10	65.33
E	Height 4	69.96	67.62	68.07	67.77	69.87	67.51	65.97	68.20	70.03	68.54	69.51	68.84	64.98	67.13	69.07	68.35	70.84	68.98	65.23	65.84
F	Average Height	70.29	68.09	67.65	68.05	69.91	67.98	65.65	67.80	69.86	68.90	69.94	68.34	65.39	67.28	69.31	68.17	71.10	68.82	65.58	65.42
G	Diameter 1	101.23	101.41	101.38	101.49	100.86	101.56	101.61	101.51	101.18	101.26	101.22	101.28	102.28	101.29	101.24	100.89	101.48	101.41	101.31	101.42
H	Diameter 2	101.61	101.36	101.56	101.51	101.44	101.49	101.33	101.43	101.74	101.33	101.51	101.44	102.01	101.48	101.47	101.44	101.79	101.41	101.71	101.87
I	Average Diameter	101.420	101.385	101.470	101.500	101.150	101.525	101.470	101.470	101.460	101.295	101.365	101.360	102.145	101.385	101.355	101.165	101.635	101.410	101.510	101.645
J	G_{mb} [A/(F*π*I^2/4)]	2.134	2.174	2.186	2.176	2.152	2.175	2.262	2.196	2.128	2.158	2.143	2.155	2.220	2.196	2.135	2.181	2.093	2.152	2.255	2.236
K	Air Voids [(G_{mm}-J)/G_{mm}]	14.8	13.2	12.7	13.1	14.0	13.1	9.6	12.3	15.0	13.8	14.4	13.9	11.3	12.3	14.7	12.9	16.4	14.0	9.9	10.7

SATURATED SURFACE DRY METHOD

	Sample	1	2	3	4	5	6	7	8	9	10	11	12	13	14	15	16	17	18	19	20
A	Dry Mass	1211.5	1194.8	1195.8	1198	1208.9	1197.1	1200.7	1203.8	1201.6	1198	1209.2	1188.6	1189.5	1192.9	1194	1195	1207	1196.4	1196.6	1186.7
B	Submerged Mass	708.6	691.2	691.6	695.8	706.3	694.6	693.1	696.4	701.4	701.4	705.2	692.4	687.3	689	694.7	696.7	706.6	698	690.7	687.4
C	SSD Mass	1234.8	1207.4	1210.4	1212.2	1231.5	1211.2	1204.6	1217.4	1219.8	1221.2	1230.2	1207.9	1194.7	1206.5	1210.6	1209.6	1230.4	1216.3	1199.9	1193.4
D	G_{mb} [A/(C-B)]	2.30	2.31	2.30	2.32	2.30	2.32	2.35	2.31	2.32	2.30	2.30	2.31	2.34	2.31	2.31	2.33	2.30	2.31	2.35	2.35
E	Air Voids [(G_{mm}-D)/G_{mm}]	8.0	7.5	7.9	7.3	8.0	7.4	6.2	7.7	7.4	7.9	8.0	7.9	6.3	7.9	7.5	6.9	7.9	7.8	6.1	6.3

Project Number:	74784A
Location:	I-196 Grand Rapids Michigan
Contractor:	Paving & Materials
Mix:	5E10
Gradation:	Coarse
G_{mm}	2.499

	Sample	1	2	3	4	5	6	7	8	9	10	11	12	13	14	15	16	17	18	19	20
A	Dry Mass	1197.6	1213.2	1207.2	1199.9	1191.5	1220.7	1193.9	1200.9	1213.1	1201.5	1191.8	1221.4	1208	1203	1205.4	1193.8	1194.7	1199.2	1192.2	1197.5
B	Height 1	64.94	65.51	65.36	65.71	65.19	66.72	63.96	64.01	65.15	63.70	64.26	66.31	65.24	64.19	66.18	64.21	64.90	65.85	63.72	64.34
C	Height 2	64.60	64.39	64.21	65.38	64.94	65.66	63.82	64.97	65.21	64.20	64.92	66.62	64.88	65.44	64.75	64.76	64.09	64.89	65.13	65.52
D	Height 3	64.75	64.61	64.26	65.32	64.78	64.98	64.42	65.91	65.96	65.65	64.61	65.46	64.68	65.96	64.24	64.32	64.70	64.50	64.11	66.11
E	Height 4	64.87	65.27	65.35	65.80	65.11	65.46	65.46	65.06	66.36	64.87	64.60	65.00	64.83	64.29	64.68	64.02	65.44	64.57	63.75	64.60
F	Average Height	64.79	64.95	64.80	65.55	65.01	65.71	64.42	64.99	65.67	64.61	64.60	65.85	64.91	64.97	64.96	64.33	64.78	64.95	64.18	65.14
G	Diameter 1	102.300	101.720	101.180	101.420	101.410	101.220	101.540	101.270	101.870	101.070	101.060	101.360	101.280	101.370	101.260	101.440	101.500	101.110	101.240	101.610
H	Diameter 2	102.270	101.790	101.230	101.180	101.670	101.170	101.440	101.190	101.720	101.680	101.330	101.780	101.330	101.590	101.200	101.300	101.560	101.900	101.270	101.530
I	Average Diameter	102.285	101.755	101.205	101.300	101.540	101.195	101.490	101.230	101.795	101.375	101.195	101.570	101.305	101.480	101.230	101.370	101.530	101.505	101.255	101.570
J	G_{mb} [A/(F*π*I^2/4)]	2.250	2.297	2.316	2.271	2.264	2.310	2.291	2.296	2.270	2.304	2.294	2.289	2.309	2.289	2.305	2.299	2.278	2.282	2.307	2.269
K	Air Voids [(G_{mm}-J)/G_{mm}]	10.0	8.1	7.3	9.1	9.4	7.6	8.3	8.1	9.2	7.8	8.2	8.4	7.6	8.4	7.7	8.0	8.9	8.7	7.7	9.2

SATURATED SURFACE DRY METHOD

	Sample	1	2	3	4	5	6	7	8	9	10	11	12	13	14	15	16	17	18	19	20
A	Dry Mass	1197.6	1213.1	1207.3	1199.9	1191.5	1220.5	1193.9	1200.8	1213.2	1201.5	1191.8	1221.4	1208	1203	1205.4	1193.8	1194.8	1199.2	1192.2	1197.5
B	Submerged Mass	686.3	696.3	694.5	687.8	680.2	700.9	683.6	688	695.5	691.4	684.3	699.9	694.6	689.9	693.6	686.2	684.3	687.3	685	683.3
C	SSD Mass	1200.9	1215.6	1209.3	1205.2	1195.7	1222.4	1196.5	1204.1	1216.5	1203.2	1194.5	1223.8	1210.7	1205.8	1207.4	1196	1197.5	1201.9	1194.5	1201.1
D	G_{mb} [A/(C-B)]	2.327	2.336	2.345	2.319	2.311	2.340	2.328	2.327	2.329	2.348	2.336	2.331	2.341	2.332	2.346	2.342	2.328	2.330	2.340	2.313
E	Air Voids [(G_{mm}-D)/G_{mm}]	6.9	6.5	6.2	7.2	7.5	6.3	6.9	6.9	6.8	6.1	6.5	6.7	6.3	6.7	6.1	6.3	6.8	6.7	6.4	7.5

Project Number:	51472A
Location:	I-75 Clarkston
Contractor:	Ace Asphalt
Mix:	4E30
Gradation:	Coarse
G_{mm}	2.487

	Sample	1	2	3	4	5	6	7	8	9	10	11	12	13	14	15	16	17	18	19	20
A	Dry Mass	1233.9	1191.8	1191.2	1197	1191.9	1201	1233	1204	1196.2	1193.6	1192.3	1203.5	1194.3	1197.1	1200.9	1196.1	1223.6	1197.4	1205	1199.2
B	Height 1	67.67	66.58	65.09	66.20	65.47	66.64	69.01	66.47	64.66	65.57	65.52	67.20	65.21	64.55	64.21	65.83	67.42	65.65	65.49	66.84
C	Height 2	67.22	66.30	65.93	65.18	65.16	65.81	69.10	67.15	65.37	63.81	64.78	67.10	65.98	64.62	64.40	64.76	66.98	65.16	66.50	65.10
D	Height 3	67.86	66.37	65.85	65.58	65.21	66.96	68.23	66.35	65.28	64.11	66.09	65.73	66.58	65.47	65.62	65.52	67.28	66.97	66.53	65.15
E	Height 4	67.44	66.54	64.90	66.12	65.36	65.75	68.58	65.73	65.59	65.27	66.09	65.58	66.13	65.75	65.41	66.62	68.49	66.87	65.83	66.33
F	Average Height	67.55	66.45	65.44	65.77	65.30	66.29	68.73	66.43	65.23	64.69	65.62	66.40	65.98	65.10	64.91	65.68	67.54	66.16	66.09	65.86
G	Diameter 1	101.19	101.67	101.32	101.21	101.37	101.34	101.44	101.22	101.33	101.22	101.68	101.75	101.01	101.25	101.13	101.2	101.15	101.48	101.31	101.38
H	Diameter 2	101.88	101.68	101.44	101.23	101.39	101.34	101.59	101.35	101.4	101.2	101.71	101.78	102.06	101.3	101.42	101.31	101.26	101.14	101.4	101.29
I	Average Diameter	101.535	101.675	101.380	101.220	101.380	101.340	101.515	101.285	101.365	101.210	101.695	101.765	101.535	101.275	101.275	101.255	101.205	101.310	101.355	101.335
J	G_{mb} [A/(F*π*I^2/4)]	2.256	2.209	2.255	2.262	2.261	2.246	2.216	2.250	2.273	2.293	2.237	2.228	2.236	2.283	2.297	2.261	2.252	2.245	2.260	2.258
K	Air Voids [(G_{mm}-J)/G_{mm}]	9.3	11.2	9.3	9.1	9.1	9.7	10.9	9.5	8.6	7.8	10.1	10.4	10.1	8.2	7.7	9.1	9.4	9.7	9.1	9.2

SATURATED SURFACE DRY METHOD

	Sample	1	2	3	4	5	6	7	8	9	10	11	12	13	14	15	16	17	18	19	20
A	Dry Mass	1233.9	1191.8	1191.2	1197	1191.9	1201	1233	1204	1196.2	1193.6	1192.3	1203.5	1194.3	1197.1	1200.9	1196.1	1223.6	1197.4	1205	1199.2
B	Submerged Mass	705.9	678.2	681.1	684.6	681.3	685.3	706.6	690.9	685.1	683.2	678.5	686.3	680.8	685	686.8	684.6	695.4	679.8	687.3	683.8
C	SSD Mass	1240.8	1199.2	1193.8	1202.8	1195.7	1209.5	1243.6	1215	1201	1196.1	1197.4	1209.8	1200.2	1201.5	1204.1	1201.7	1229.3	1202	1210	1202.2
D	G_{mb} [A/(C-B)]	2.307	2.288	2.323	2.310	2.317	2.291	2.296	2.297	2.319	2.327	2.298	2.299	2.299	2.318	2.321	2.313	2.292	2.293	2.305	2.313
E	Air Voids [(G_{mm}-D)/G_{mm}]	7.2	8.0	6.6	7.1	6.8	7.9	7.7	7.6	6.8	6.4	7.6	7.6	7.5	6.8	6.7	7.0	7.8	7.8	7.3	7.0

Phase I – 100mm Superpave Specimens

Project Number: 50651A
Location: M-50 Dundee
Contractor: Cadillac LLC
Mix: Asphalt 3E1
Gradation: Coarse
G_{mm} 2.52

	Sample	1	2	3	4	5	6	7	8	9	10	11	12	13	14	15	16	17	18	19	20
A	Dry Mass	1084.9	1085.7	1085.1	1084.9	1086.8	1085.7	1089.5	1091.7	1087	1088.1	1082.4	1084.9	1083.6	1089	1084.1	1089.5	1086.4	1086.3	1089.5	1083.5
B	Height 1	63.47	62.93	62.77	63.47	62.84	63.01	62.95	62.95	62.95	62.97	63.16	63.10	62.94	62.88	63.13	63.06	63.01	63.08	63.04	62.90
C	Height 2	62.90	62.95	63.00	62.90	63.05	62.97	63.04	63.06	62.81	62.91	63.08	63.19	63.03	62.95	63.13	63.12	63.31	63.06	63.14	63.10
D	Height 3	63.01	63.04	63.07	63.01	62.98	63.02	62.94	63.27	62.87	62.93	63.04	63.06	63.08	62.95	63.17	63.21	63.22	63.17	63.31	63.10
E	Height 4	63.53	63.03	63.31	63.53	62.81	63.16	63.13	63.12	62.95	63.47	62.93	63.12	63.19	62.92	62.97	63.14	63.19	63.19	63.30	63.02
F	Average Height	63.23	62.99	63.04	63.23	62.92	63.04	63.02	63.10	62.90	63.07	63.05	63.12	63.06	62.93	63.10	63.13	63.18	63.13	63.20	63.03
G	Diameter 1	99.540	99.590	98.950	99.540	99.180	99.560	99.190	99.800	99.260	99.770	99.570	99.770	99.280	99.400	99.420	99.510	99.950	99.570	99.680	99.630
H	Diameter 2	99.660	98.970	99.600	99.860	99.740	99.610	99.810	100.070	99.220	99.600	99.600	99.740	99.250	99.640	99.700	99.900	99.580	99.830	99.750	99.370
I	Average Diameter	99.700	99.280	99.275	99.700	99.460	99.585	99.500	99.935	99.240	99.685	99.585	99.755	99.265	99.520	99.560	99.705	99.765	99.700	99.715	99.500
J	G_{mb} [A/(F*+I^2/4)]	2.198	2.227	2.224	2.198	2.223	2.211	2.224	2.206	2.234	2.211	2.204	2.199	2.220	2.225	2.207	2.210	2.200	2.204	2.208	2.211
K	Air Voids [(G_{mm}-J)/G_{mm}]	12.8	11.6	11.8	12.8	11.8	12.3	11.8	12.5	11.3	12.3	12.5	12.7	11.9	11.7	12.4	12.3	12.7	12.5	12.4	12.3

SATURATED SURFACE DRY METHOD

	Sample	1	2	3	4	5	6	7	8	9	10	11	12	13	14	15	16	17	18	19	20
A	Dry Mass	1084.9	1085.7	1085.1	1084.9	1086.8	1085.7	1089.5	1091.7	1087	1088.1	1082.4	1084.9	1083.6	1089	1084.1	1089.5	1086.4	1086.3	1089.5	1083.5
B	Submerged Mass	633.3	633.4	632.9	633.3	634.8	632.2	636.4	637.6	634.9	635.2	629.7	632.6	632.1	637.6	633.2	634.8	635.9	635.2	634.3	631.6
C	SSD Mass	1092	1091.9	1091.4	1092	1094.9	1093.5	1096.1	1099.7	1094.3	1094.8	1089.1	1093.3	1092.2	1098.1	1091.8	1099.2	1094.9	1094.9	1098.4	1090
D	G_{mb} [A/(C-B)]	2.365	2.368	2.367	2.365	2.362	2.354	2.370	2.362	2.366	2.367	2.356	2.355	2.355	2.365	2.364	2.346	2.367	2.363	2.348	2.364
E	Air Voids [(G_{mm}-D)/G_{mm}]	6.1	6.0	6.1	6.1	6.3	6.6	6.0	6.3	6.1	6.1	6.5	6.6	6.5	6.2	6.2	6.9	6.1	6.2	6.8	6.2

Project Number:	46023A
Location:	M-21 St. Johns
Contractor:	Michigan Paving & Materials
Mix:	3E3
Gradation:	Coarse
G_{mm}	2.489

VOLUMETRIC ANALYSIS

	Sample	1	2	3	4	5	6	7	8	9	10	11	12	13	14	15	16	17	18	19	20
A	Dry Mass (g)	1081.9	1084.9	1084.7	1092.6	1075.4	1077.8	1081.6	1088.8	1083.1	1087.6	1094.7	1089.7	1084.5	1085.3	1085.3	1079.2	1080.5	1079	1090	1071.1
B	Height 1 (mm)	62.98	63.07	63.12	63.02	62.99	63.31	63.14	62.65	62.86	63.11	63.08	63.08	63.02	63.10	63.06	63.03	62.96	63.05	63.07	63.02
C	Height 2 (mm)	62.90	63.12	63.15	62.98	62.99	63.20	62.99	63.03	62.97	63.19	63.03	63.04	63.08	63.15	62.96	62.99	63.03	62.85	62.94	63.03
D	Height 3 (mm)	63.13	63.05	63.14	62.94	62.90	63.39	63.04	63.08	63.08	63.11	63.09	63.06	63.02	63.11	63.26	62.98	62.88	62.88	63.12	62.96
E	Height 4 (mm)	63.07	62.85	63.16	62.79	62.82	63.25	63.24	63.03	63.18	63.16	63.13	62.99	63.12	63.05	63.07	63.04	63.01	62.85	63.00	63.10
F	Average Height (mm)	63.02	63.02	63.14	62.93	62.93	63.29	63.10	62.95	63.02	63.14	63.08	63.04	63.06	63.10	63.09	63.01	62.97	62.91	63.03	63.03
G	Diameter 1 (mm)	100.05	100.20	100.57	100.19	100.17	100.72	100.77	100.15	100.24	100.34	100.18	100.22	100.14	100.22	100.11	100.17	100.14	100.21	100.06	100.08
H	Diameter 2 (mm)	100.26	100.11	100.62	100.10	100.14	100.09	100.41	100.28	100.15	100.15	100.11	100.08	100.07	100.15	100.30	100.26	100.15	100.38	100.04	100.07
I	Average Diameter (mm)	100.16	100.16	100.60	100.15	100.16	100.41	100.59	100.22	100.20	100.25	100.15	100.15	100.11	100.19	100.21	100.22	100.15	100.30	100.05	100.08
J	G_{mb} [A/(F*π*I^2/4)]	2.179	2.185	2.161	2.204	2.169	2.151	2.157	2.193	2.180	2.182	2.203	2.194	2.185	2.182	2.181	2.171	2.178	2.171	2.200	2.161
K	Air Voids [(G_{mm}-J)/G_{mm}]	12.5	12.2	13.2	11.4	12.8	13.6	13.3	11.9	12.4	12.3	11.5	11.8	12.2	12.3	12.4	12.8	12.5	12.8	11.6	13.2

SATURATED SURFACE DRY METHOD

	Sample	1	2	3	4	5	6	7	8	9	10	11	12	13	14	15	16	17	18	19	20
A	Dry Mass (g)	1081.9	1084.9	1084.7	1092.6	1075.4	1077.8	1081.6	1088.8	1083.1	1087.6	1094.7	1089.7	1084.5	1085.3	1085.3	1079.2	1080.5	1079	1090	1071.1
B	Submerged Mass (g)	623.2	625.1	627.7	631.6	619.9	621.3	621.4	629.6	624.2	623.3	631.1	627.8	627.6	628.4	628.7	622.9	621.9	618.9	630.7	614.4
C	SSD Mass (g)	1089.7	1091.6	1092.1	1098.4	1083.3	1085.3	1089.4	1095.5	1089.7	1094.1	1100.2	1094.7	1091.5	1092.2	1093.1	1085.4	1087.3	1084.5	1097.8	1077.6
D	G_{mb} [A/(C-B)]	2.32	2.33	2.34	2.34	2.32	2.32	2.31	2.34	2.33	2.31	2.33	2.33	2.34	2.34	2.34	2.33	2.32	2.32	2.33	2.31
E	Air Voids [(G_{mm}-D)/G_{mm}]	6.8	6.6	6.2	6.0	6.8	6.7	7.1	6.1	6.5	7.2	6.2	6.2	6.1	6.0	6.1	6.3	6.7	6.9	6.2	7.1

Project Number:	50650A
Location:	BL I-96 Howell
Contractor:	Rieth-Riley
Mix:	Fine
Gradation:	4E3
G_{mm}	2.501

	Sample	1	2	3	4	5	6	7	8	9	10	11	12	13	14	15	16	17	18	19	20
A	Dry Mass	1143.6	1142	1145.8	1141	1141.2	1144.6	1137.2	1142.9	1145	1141.2	1142.2	1145.1	1147.7	1147	1132.5	1144	1140.1	1139.2	1136	1139.6
B	Height 1	63.04	62.96	63.20	63.27	63.21	63.32	63.40	63.07	62.79	63.09	62.84	63.55	63.40	63.42	63.25	63.22	63.35	63.27	63.32	63.26
C	Height 2	63.07	63.29	63.02	63.09	63.27	63.02	63.35	63.37	63.07	63.42	63.14	62.87	63.45	63.25	63.35	63.25	63.42	63.30	63.27	63.23
D	Height 3	62.81	63.31	62.99	62.99	63.33	63.04	63.20	62.92	63.78	62.71	63.25	62.89	63.37	63.30	63.35	63.32	63.32	63.27	63.12	63.29
E	Height 4	62.81	63.33	63.12	63.07	63.21	62.99	63.20	62.99	63.12	62.74	62.89	63.22	63.75	63.40	63.42	63.25	63.27	63.35	63.32	63.28
F	Average Height	62.93	63.22	63.08	63.11	63.26	63.09	63.29	63.09	63.19	62.99	63.03	63.13	63.49	63.34	63.34	63.26	63.34	63.30	63.26	63.27
G	Diameter 1	99.7204	99.08	99.7712	99.6696	99.75	99.9236	99.949	99.8982	99.8728	99.7458	99.9744	99.8474	99.8474	99.8728	99.822	99.8474	99.8474	99.8474	99.9744	99.17
H	Diameter 2	99.695	99.89	99.8474	99.822	99.74	99.949	99.8982	99.9236	99.9236	99.9236	99.9236	99.9236	99.8728	99.8474	99.822	99.8728	99.8982	99.8982	99.8474	98.32
I	Average Diameter	99.708	99.485	99.809	99.746	99.745	99.936	99.924	99.911	99.898	99.835	99.949	99.886	99.860	99.860	99.822	99.860	99.873	99.873	99.911	98.745
J	G_{mb} [A/(F*π*I^2/4)]	2.327	2.324	2.321	2.314	2.309	2.313	2.291	2.311	2.312	2.314	2.310	2.315	2.308	2.312	2.285	2.309	2.298	2.297	2.291	2.352
K	Air Voids [(G_{mm}-J)/G_{mm}]	6.9	7.1	7.2	7.5	7.7	7.5	8.4	7.6	7.6	7.5	7.7	7.4	7.7	7.6	8.7	7.7	8.1	8.1	8.4	6.0

SATURATED SURFACE DRY METHOD

	Sample	1	2	3	4	5	6	7	8	9	10	11	12	13	14	15	16	17	18	19	20
A	Dry Mass	1143.6	1142	1145.8	1141	1141.2	1144.6	1137.2	1142.9	1145	1141.2	1142.2	1145.1	1147.7	1147	1132.5	1144	1140.1	1139.2	1136	1139.6
B	Submerged Mass	657.4	655.5	659	655.4	655.4	659.3	655.2	656.7	659.5	657.5	656.9	659.8	658.2	660.7	648.5	659.4	655.2	652.9	649.8	653.9
C	SSD Mass	1145.7	1144	1147.3	1142.6	1143.2	1146	1139.5	1144.1	1147	1143.9	1143.8	1146.8	1148.9	1148.7	1135.4	1146.2	1141.8	1140.9	1138.4	1142.2
D	G_{mb} [A/(C-B)]	2.342	2.338	2.347	2.342	2.339	2.352	2.348	2.345	2.349	2.346	2.346	2.351	2.339	2.350	2.326	2.350	2.343	2.334	2.325	2.334
E	Air Voids [(G_{mm}-D)/G_{mm}]	6.4	6.5	6.2	6.4	6.5	6.0	6.1	6.2	6.1	6.2	6.2	6.0	6.5	6.0	7.0	6.0	6.3	6.7	7.0	6.7

Project Number:	48612A
Location:	M-21 Owosso
Contractor:	Michigan Paving & Materials
Mix:	5E3
Gradation:	Fine
G_{mm}	2.470

VOLUMETRIC ANALYSIS

	Sample	1	2	3	4	5	6	7	8	9	10	11	12	13	14	15	16	17	18	19	20
A	Dry Mass (g)	1120.2	1124.5	1120.1	1126.9	1126.5	1124.4	1126.9	1128.4	1124.1	1127.8	1127	1121.5	1128.4	1128.8	1128.4	1123.6	1127	1129.6	1128.6	1129.5
B	Height 1 (mm)	63.25	63.35	63.25	63.39	63.50	63.25	63.25	62.99	63.50	63.25	63.25	63.25	62.99	63.41	62.99	63.39	62.99	62.99	62.99	63.25
C	Height 2 (mm)	63.25	63.67	63.23	63.30	63.75	63.50	63.25	63.25	63.25	63.25	62.99	63.25	63.25	63.45	63.50	63.28	62.99	63.25	63.25	62.99
D	Height 3 (mm)	63.25	63.23	63.28	63.24	63.50	62.99	62.99	63.25	63.25	63.50	63.25	63.50	63.50	63.45	63.25	63.32	63.25	63.50	63.25	63.25
E	Height 4 (mm)	62.99	63.28	63.32	63.27	63.25	63.25	62.99	63.25	63.50	63.50	63.25	63.25	62.99	63.40	63.25	63.28	63.25	63.25	62.99	63.25
F	Average Height (mm)	63.18	63.38	63.27	63.30	63.50	63.25	63.12	63.18	63.37	63.37	63.18	63.31	63.18	63.43	63.25	63.32	63.12	63.25	63.12	63.18
G	Diameter 1 (mm)	99.70	98.91	99.96	99.17	99.80	99.94	99.86	99.85	99.90	99.86	99.87	99.90	99.86	99.61	99.85	99.30	99.85	99.82	99.90	99.78
H	Diameter 2 (mm)	99.93	99.43	99.95	99.41	99.89	99.82	99.79	99.83	99.85	99.85	99.89	99.91	99.86	99.89	99.82	99.44	99.84	99.91	99.85	99.87
I	Average Diameter (mm)	99.82	99.17	99.96	99.29	99.85	99.88	99.83	99.84	99.88	99.86	99.88	99.91	99.86	99.75	99.84	99.37	99.85	99.87	99.88	99.83
J	G_{mb} [A/(F*π*I^2/4)]	2.266	2.297	2.256	2.299	2.266	2.269	2.281	2.281	2.264	2.272	2.277	2.260	2.280	2.277	2.279	2.288	2.280	2.280	2.282	2.284
K	Air Voids [(G_{mm}-J)/G_{mm}]	8.3	7.0	8.7	6.9	8.3	8.1	7.6	7.6	8.3	8.0	7.8	8.5	7.7	7.8	7.7	7.4	7.7	7.7	7.6	7.5

SATURATED SURFACE DRY METHOD

	Sample	1	2	3	4	5	6	7	8	9	10	11	12	13	14	15	16	17	18	19	20
A	Dry Mass (g)	1120.2	1124.5	1120.1	1126.9	1126.5	1124.4	1126.9	1128.4	1124.1	1127.8	1127	1121.5	1128.4	1128.8	1128.4	1123.6	1127	1129.6	1128.6	1129.5
B	Submerged Mass (g)	636	640	636.5	642.8	640.9	640.1	641.3	643.4	638.5	642.3	642.7	636.3	643.2	645.3	644.1	640	641.5	643.6	643.2	644.3
C	SSD Mass (g)	1121.4	1126.8	1122.5	1129.1	1128.9	1126.4	1128.3	1129.5	1124.9	1129	1128.9	1123.1	1130.5	1131.6	1130.3	1126.6	1128.3	1130.8	1129.9	1130.7
D	G_{mb} [A/(C-B)]	2.31	2.31	2.30	2.32	2.31	2.31	2.31	2.32	2.31	2.32	2.32	2.30	2.32	2.32	2.32	2.31	2.32	2.32	2.32	2.32
E	Air Voids [(G_{mm}-D)/G_{mm}]	6.6	6.5	6.7	6.2	6.5	6.4	6.3	6.0	6.4	6.2	6.2	6.7	6.3	6.0	6.0	6.5	6.3	6.1	6.1	6.0

Project Number:	34519A
Location:	M-59 Brighton
Contractor:	Ajax Paving
Mix:	3E10
Gradation:	Coarse
G_{mm}	2.503

	Sample	1	2	3	4	5	6	7	8	9	10	11	12	13	14	15	16	17	18	19	20
A	Dry Mass	1082.7	1096.6	1098.8	1101.8	1091.8	1103.9	1083.2	1094.6	1084.5	1091.5	1088.7	1085.6	1084.1	1096.3	1098.5	1083	1085.1	1076.8	1099.1	1096.7
B	Height 1	63.47	63.54	63.64	63.13	63.51	63.29	63.22	63.31	63.10	63.15	63.08	63.25	63.23	63.35	64.05	63.10	63.05	63.01	63.44	63.30
C	Height 2	63.39	63.24	63.44	63.18	63.37	63.33	63.21	63.32	63.05	63.10	63.13	62.89	63.05	63.30	63.26	63.04	63.15	63.14	63.19	63.40
D	Height 3	63.37	63.17	63.25	63.22	63.30	63.30	63.17	63.32	63.10	63.33	63.09	63.20	63.27	63.31	63.34	63.24	63.24	63.17	63.36	63.71
E	Height 4	63.29	63.28	63.41	63.22	63.18	63.30	63.15	63.21	63.22	63.06	63.06	63.13	63.22	63.29	63.34	63.24	63.12	63.15	63.15	63.46
F	Average Height	63.38	63.31	63.44	63.19	63.34	63.31	63.19	63.29	63.12	63.16	63.09	63.12	63.19	63.31	63.50	63.16	63.14	63.12	63.29	63.47
G	Diameter 1	99.6	99.93	99.66	100.06	100.21	100.04	99.53	100.06	99.56	99.02	99.56	99.66	99.35	99.7	100.06	99.44	99.49	99.72	99.9	100.18
H	Diameter 2	99.87	99.2	99.94	100.06	100.11	100.01	99.25	99.98	99.71	99.53	99.51	99.64	99.72	99.9	99.96	99.61	99.4	99.7	99.93	100.09
I	Average Diameter	99.735	99.565	99.800	100.060	100.160	100.025	99.390	100.020	99.635	99.275	99.535	99.650	99.535	99.800	100.010	99.525	99.445	99.710	99.915	100.135
J	G_{mb} [A/(F*π*I^2/4)]	2.187	2.225	2.214	2.217	2.188	2.219	2.210	2.201	2.204	2.233	2.218	2.205	2.205	2.214	2.202	2.204	2.213	2.185	2.215	2.194
K	Air Voids [(G_{mm}-J)/G_{mm}]	12.6	11.1	11.5	11.4	12.6	11.3	11.7	12.1	12.0	10.8	11.4	11.9	11.9	11.6	12.0	11.9	11.6	12.7	11.5	12.3

SATURATED SURFACE DRY METHOD

	Sample	1	2	3	4	5	6	7	8	9	10	11	12	13	14	15	16	17	18	19	20
A	Dry Mass	1082.7	1096.6	1098.8	1101.8	1091.8	1103.9	1083.2	1094.6	1084.5	1091.5	1088.7	1085.6	1084.1	1096.3	1098.5	1083	1085.1	1076.8	1099.1	1096.7
B	Submerged Mass	629.7	636.4	637.2	642.1	633.7	637.1	626.8	633.7	630.4	634.8	634.5	629.6	626.4	637.2	637.9	631.5	630.6	620.2	636	639.2
C	SSD Mass	1090.6	1103.3	1105	1110.3	1098.4	1109.5	1091.9	1100.3	1091.9	1099.5	1097.6	1093.5	1090.6	1103.7	1104.7	1093.1	1092.7	1086.6	1104.5	1105.8
D	G_{mb} [A/(C-B)]	2.35	2.35	2.35	2.35	2.35	2.34	2.33	2.35	2.35	2.35	2.35	2.34	2.34	2.35	2.35	2.35	2.35	2.31	2.35	2.35
E	Air Voids [(G_{mm}-D)/G_{mm}]	6.1	6.2	6.2	6.0	6.1	6.6	7.0	6.3	6.1	6.2	6.1	6.5	6.7	6.1	6.0	6.3	6.2	7.8	6.3	6.1

Project Number:	74784A
Location:	I-196 Grand Rapids Michigan
Contractor:	Paving & Materials
Mix:	5E10
Gradation:	Coarse
G_{mm}	2.499

	Sample	1	2	3	4	5	6	7	8	9	10	11	12	13	14	15	16	17	18	19	20
A	Dry Mass	1125.5	1126.6	1130.1	1130	1127	1131.3	1132.8	1123.1	1130.9	1135.2	1129.3	1129.4	1130.7	1131.1	1126.7	1135.1	1133.2	1128.2	1129.3	1133.4
B	Height 1	63.37	63.36	63.14	63.44	63.28	63.07	63.42	63.71	63.12	63.35	63.35	63.71	63.30	63.48	63.34	63.35	63.09	63.56	63.80	63.31
C	Height 2	63.30	63.47	63.30	63.42	63.43	63.45	63.09	63.39	63.30	63.50	63.45	63.51	63.20	63.38	63.25	63.09	63.14	63.46	63.54	63.35
D	Height 3	63.17	63.30	63.53	63.43	63.38	63.50	63.20	63.53	63.32	63.32	63.22	63.61	63.22	63.47	63.41	63.17	63.35	63.42	63.63	63.31
E	Height 4	63.27	63.34	63.47	63.42	63.40	63.45	63.37	63.61	63.09	63.17	63.27	63.50	63.35	63.53	63.43	63.30	63.30	63.43	63.60	63.31
F	Average Height	63.28	63.37	63.36	63.43	63.37	63.37	63.27	63.56	63.21	63.34	63.32	63.58	63.27	63.47	63.36	63.23	63.22	63.47	63.64	63.32
G	Diameter 1	99.797	99.940	99.924	99.950	99.700	99.924	99.949	99.450	99.898	99.873	99.593	99.690	99.974	99.500	99.520	99.924	99.898	99.460	99.430	99.410
H	Diameter 2	99.873	99.950	99.949	99.720	99.570	99.847	99.974	99.780	99.898	99.644	99.720	99.700	99.949	99.790	99.550	99.898	99.949	99.330	99.580	99.760
I	Average Diameter	99.835	99.945	99.937	99.835	99.635	99.886	99.962	99.615	99.898	99.759	99.657	99.695	99.962	99.645	99.535	99.911	99.924	99.395	99.505	99.585
J	G_{mb} [A/(F*π*I^2/4)]	2.272	2.266	2.274	2.276	2.281	2.278	2.281	2.267	2.283	2.293	2.286	2.275	2.277	2.285	2.285	2.290	2.286	2.291	2.282	2.298
K	Air Voids [(G_{mm}-J)/G_{mm}]	9.1	9.3	9.0	8.9	8.7	8.8	8.7	9.3	8.7	8.2	8.5	8.9	8.9	8.5	8.5	8.4	8.5	8.3	8.7	8.0

SATURATED SURFACE DRY METHOD

	Sample	1	2	3	4	5	6	7	8	9	10	11	12	13	14	15	16	17	18	19	20
A	Dry Mass	1125.5	1126.6	1130.1	1130	1127	1131.3	1132.8	1123.1	1130.9	1135.2	1129.3	1129.4	1130.7	1131.1	1126.7	1135.1	1133.2	1128.2	1129.3	1133.4
B	Submerged Mass	651	649.9	648.4	652.4	648.4	651.1	653.3	646.1	653.2	655.6	650.3	651.7	651.8	653.4	649.9	654.6	654.4	652.2	651.3	654.5
C	SSD Mass	1130.6	1130.3	1131.8	1133.5	1131.4	1135	1136.8	1128.2	1136.2	1138.7	1132.3	1134.5	1134.2	1135.2	1132.2	1138.1	1137.3	1133.7	1134.1	1138.4
D	G_{mb} [A/(C-B)]	2.347	2.345	2.338	2.349	2.333	2.338	2.343	2.330	2.341	2.350	2.343	2.339	2.344	2.348	2.336	2.348	2.347	2.343	2.339	2.342
E	Air Voids [(G_{mm}-D)/G_{mm}]	6.1	6.2	6.4	6.0	6.6	6.4	6.2	6.8	6.3	6.0	6.2	6.4	6.2	6.1	6.5	6.1	6.1	6.2	6.4	6.3

Project Number:	51472A
Location:	I-75 Clarkston
Contractor:	Ace Asphalt
Mix:	4E30
Gradation:	Coarse
G_{mm}	2.487

	Sample	1	2	3	4	5	6	7	8	9	10	11	12	13	14	15	16	17	18	19	20
A	Dry Mass	1112.5	1112.6	1112.3	1110.5	1107.1	1113.3	1110.8	1111	1113.9	1111.4	1115.6	1099.5	1117.8	1117.4	1119.2	1118.6	1114	1113.4	1114.4	1115.1
B	Height 1	63.19	63.59	63.53	63.42	63.17	63.55	63.35	63.13	63.22	63.30	63.29	63.28	63.57	63.30	63.31	63.26	63.52	63.45	63.23	62.48
C	Height 2	63.38	63.34	63.38	63.30	63.18	63.34	63.19	63.16	63.30	63.32	63.26	63.24	63.50	63.31	63.29	63.28	63.34	63.29	63.19	63.37
D	Height 3	63.42	63.34	63.37	63.28	63.28	63.30	63.22	63.19	63.29	63.40	63.30	63.31	63.76	63.27	63.22	63.27	63.20	63.21	63.09	63.25
E	Height 4	63.50	63.38	63.39	63.27	63.20	63.24	63.28	63.18	63.31	63.38	63.22	63.21	63.39	63.27	63.41	63.42	63.22	63.19	63.20	63.25
F	Average Height	63.37	63.41	63.42	63.32	63.21	63.36	63.26	63.17	63.28	63.35	63.27	63.26	63.56	63.29	63.31	63.31	63.32	63.29	63.18	63.09
G	Diameter 1	99.9	99.91	99.77	99.97	99.83	99.89	99.61	99.83	99.85	99.92	99.9	99.56	99.93	99.86	99.87	99.84	99.82	99.85	99.88	99.88
H	Diameter 2	99.83	99.95	99.87	99.87	99.64	99.81	99.95	99.86	99.67	99.82	99.86	99.7	99.78	99.66	99.77	99.86	99.83	99.72	99.86	99.84
I	Average Diameter	99.865	99.930	99.820	99.920	99.735	99.850	99.780	99.845	99.760	99.870	99.880	99.630	99.855	99.760	99.820	99.850	99.825	99.785	99.870	99.860
J	G_{mb} [A/(F*π*I^2/4)]	2.241	2.237	2.241	2.237	2.242	2.244	2.246	2.246	2.252	2.240	2.251	2.229	2.246	2.259	2.259	2.256	2.248	2.250	2.252	2.257
K	Air Voids [(G_{mm}-J)/G_{mm}]	9.9	10.0	9.9	10.1	9.9	9.8	9.7	9.7	9.4	9.9	9.5	10.4	9.7	9.2	9.2	9.3	9.6	9.5	9.5	9.3

SATURATED SURFACE DRY METHOD

	Sample	1	2	3	4	5	6	7	8	9	10	11	12	13	14	15	16	17	18	19	20
A	Dry Mass	1112.5	1112.6	1112.3	1110.5	1107.1	1113.3	1110.8	1111	1113.9	1111.4	1115.6	1099.5	1117.8	1117.4	1119.2	1118.6	1114	1113.4	1114.4	1115.1
B	Submerged Mass	638.7	640.8	638.2	637.2	634.1	639.8	639.1	638.1	639.6	636.7	640.5	631.3	643.4	643.5	646.1	644.2	640.7	640.6	641.2	640.1
C	SSD Mass	1116.6	1118.7	1118.5	1115.7	1115.7	1119.2	1115.6	1118	1119.4	1116.3	1120.1	1106	1123.4	1121.5	1124.6	1123.4	1121	1119.9	1120.6	1119.8
D	G_{mb} [A/(C-B)]	2.328	2.328	2.316	2.321	2.299	2.322	2.331	2.315	2.322	2.317	2.326	2.316	2.329	2.338	2.339	2.334	2.319	2.323	2.325	2.325
E	Air Voids [(G_{mm}-D)/G_{mm}]	6.4	6.4	6.9	6.7	7.6	6.6	6.3	6.9	6.7	6.8	6.5	6.9	6.4	6.0	6.0	6.1	6.7	6.6	6.5	6.5

Phase I – 150mm Superpave Specimens

Project Number: 50651A
Location: M-50 Dundee
Contractor: Cadillac LLC
Mix: Asphalt
Gradation: 3E1
G_{mm} Coarse
2.52

	Sample	1	2	3	4	5	6	7	8	9	10	11	12	13	14	15	16	17	18	19	20
A	Dry Mass	3723	3715.7	3724.2	3720.8	3727.4	3723.9	3723	3731.4	3722.8	3723.4	3720.6	3726.6	3719.5	3720.9	3719.8	3722.4	3719.2	3719.6	3721.9	3716.9
B	Height 1	94.56	94.59	94.33	94.70	94.29	94.44	94.61	94.29	94.42	94.69	94.46	94.80	94.20	94.12	94.50	94.29	94.24	94.70	94.31	94.23
C	Height 2	94.41	94.61	94.59	94.72	94.64	94.54	94.44	94.51	94.39	94.31	94.50	94.41	94.33	94.40	94.32	94.24	94.09	94.56	94.38	94.24
D	Height 3	94.48	94.50	94.90	94.35	94.48	94.34	94.56	94.44	94.67	94.55	94.39	94.47	94.44	94.47	94.23	94.70	94.37	94.31	94.32	94.17
E	Height 4	94.48	94.33	94.56	94.40	94.32	94.39	94.47	94.49	94.34	94.84	94.52	94.52	94.63	94.62	94.35	94.38	94.84	94.39	94.27	94.32
F	Average Height	94.48	94.51	94.60	94.54	94.44	94.43	94.52	94.43	94.46	94.60	94.47	94.55	94.40	94.40	94.35	94.40	94.39	94.49	94.32	94.24
G	Diameter 1	150.630	150.540	150.200	150.590	150.360	150.420	149.800	150.200	150.090	150.840	150.260	150.250	150.870	150.250	150.300	150.660	150.480	150.510	150.320	150.710
H	Diameter 2	150.590	150.680	150.510	150.410	150.480	150.360	150.150	149.810	150.380	150.220	150.360	150.590	150.600	150.610	150.470	150.690	150.320	150.440	150.610	150.460
I	Average Diameter	150.610	150.610	150.355	150.500	150.420	150.390	149.975	150.005	150.225	150.535	150.310	150.420	150.735	150.430	150.385	150.775	150.400	150.475	150.465	150.585
J	G_{mb} [A/(F*π^2/4)]	2.212	2.207	2.217	2.212	2.221	2.220	2.230	2.236	2.224	2.212	2.220	2.218	2.208	2.218	2.220	2.208	2.218	2.214	2.219	2.215
K	Air Voids [(G_{mm}-J)/G_{mm}]	12.2	12.4	12.0	12.2	11.9	11.9	11.5	11.3	11.8	12.2	11.9	12.0	12.4	12.0	11.9	12.4	12.0	12.2	11.9	12.1

SATURATED SURFACE DRY METHOD

	Sample	1	2	3	4	5	6	7	8	9	10	11	12	13	14	15	16	17	18	19	20
A	Dry Mass	3723	3715.7	3724.2	3720.8	3727.4	3723.9	3723	3731.4	3722.8	3723.4	3720.6	3726.6	3719.5	3720.9	3719.8	3722.4	3719.2	3719.6	3721.9	3716.9
B	Submerged Mass	2163.9	2156.6	2167.9	2164	2166.7	2174.2	2168	2176.7	2172.8	2164.1	2163.8	2170.8	2148.4	2158.4	2163	2167.7	2159.3	2164.1	2162.4	2156.5
C	SSD Mass	3748.7	3734.8	3747.8	3746.6	3753.7	3747.6	3742.5	3758.3	3748.5	3744	3742.1	3752.4	3738.7	3738.6	3739.7	3745.5	3742.9	3739.8	3742.3	3741.2
D	G_{mb} [A/(C-B)]	2.349	2.354	2.357	2.351	2.349	2.367	2.365	2.359	2.363	2.357	2.357	2.356	2.339	2.355	2.359	2.359	2.349	2.361	2.356	2.345
E	Air Voids [(G_{mm}-D)/G_{mm}]	6.8	6.6	6.5	6.7	6.8	6.1	6.2	6.4	6.2	6.5	6.5	6.5	7.2	6.6	6.4	6.4	6.8	6.3	6.5	6.9

Project Number:	46023A
Location:	M-21 St. Johns
Contractor:	Michigan Paving & Materials
Mix:	3E3
Gradation:	Coarse
G_{mm}	2.489

VOLUMETRIC ANALYSIS

	Sample	1	2	3	4	5	6	7	8	9	10	11	12	13	14	15	16	17	18	19	20
A	Dry Mass (g)	3657.7	3655.9	3665.4	3656.6	3658.8	3666.3	3657.8	3664.2	3659.2	3662.2	3662.4	3658.7	3660.9	3655.9	3665.3	3659.3	3660.7	3660.2	3662.3	3655.2
B	Height 1 (mm)	94.24	94.20	94.29	94.63	94.34	94.22	94.10	94.44	94.14	94.28	94.24	94.14	94.08	94.24	94.43	94.18	94.32	94.23	94.56	94.48
C	Height 2 (mm)	94.08	94.31	94.20	94.39	94.05	94.14	94.25	94.08	94.25	94.26	94.05	94.29	94.14	94.06	94.19	94.48	94.28	94.21	94.40	94.44
D	Height 3 (mm)	94.36	94.45	94.39	94.54	94.27	94.09	94.25	94.25	94.04	94.24	94.40	94.29	94.24	94.35	94.23	94.37	94.14	94.29	94.49	94.38
E	Height 4 (mm)	94.38	94.20	94.49	94.52	94.19	94.28	94.13	94.13	94.21	94.17	94.20	94.23	94.26	94.43	94.34	94.06	94.49	94.34	94.61	94.37
F	Average Height (mm)	94.27	94.29	94.34	94.52	94.21	94.18	94.18	94.23	94.16	94.24	94.22	94.24	94.18	94.27	94.30	94.27	94.31	94.27	94.52	94.42
G	Diameter 1 (mm)	150.28	150.27	150.36	150.51	150.60	150.44	150.78	150.40	150.55	150.46	150.53	150.33	150.26	150.34	150.31	150.65	150.70	150.74	150.57	151.03
H	Diameter 2 (mm)	150.46	150.10	150.49	150.62	150.35	150.54	150.43	150.46	150.49	150.43	150.57	150.32	150.30	150.40	150.55	150.70	150.75	150.43	150.30	150.53
I	Average Diameter (mm)	150.37	150.19	150.43	150.57	150.48	150.49	150.61	150.43	150.52	150.45	150.55	150.33	150.28	150.37	150.43	150.68	150.73	150.59	150.44	150.78
J	G_{mb} [A/(F*π*I^2/4)]	2.185	2.189	2.186	2.173	2.184	2.189	2.180	2.188	2.184	2.186	2.184	2.188	2.191	2.184	2.187	2.177	2.175	2.180	2.180	2.168
K	Air Voids [(G_{mm}-J)/G_{mm}]	12.2	12.1	12.2	12.7	12.3	12.1	12.4	12.1	12.3	12.2	12.3	12.1	12.0	12.3	12.1	12.5	12.6	12.4	12.4	12.9

SATURATED SURFACE DRY METHOD

	Sample	1	2	3	4	5	6	7	8	9	10	11	12	13	14	15	16	17	18	19	20
A	Dry Mass (g)	3657.7	3655.9	3665.4	3656.6	3658.8	3666.3	3657.8	3664.2	3659.2	3662.2	3662.4	3658.7	3660.9	3655.9	3665.3	3659.3	3660.7	3660.2	3662.3	3655.2
B	Submerged Mass (g)	2118.4	2119.3	2131.9	2117.1	2119.5	2115.9	2109.5	2118.9	2118.9	2120.2	2114.4	2117.7	2113.1	2107.4	2114.6	2114.9	2108.9	2105.3	2107.6	2107.7
C	SSD Mass (g)	3696.3	3688.4	3708.1	3691	3692.8	3697.4	3692.4	3693.4	3696.3	3698.5	3691.3	3689.7	3694.8	3692.6	3703.7	3694.8	3698.1	3695.1	3693.8	3694.5
D	G_{mb} [A/(C-B)]	2.32	2.33	2.33	2.32	2.33	2.32	2.31	2.33	2.32	2.32	2.32	2.33	2.31	2.31	2.31	2.32	2.30	2.30	2.31	2.30
E	Air Voids [(G_{mm}-D)/G_{mm}]	6.9	6.4	6.6	6.7	6.6	6.9	7.2	6.5	6.8	6.8	6.7	6.5	7.0	7.3	7.3	6.9	7.5	7.5	7.2	7.5

Project Number:	50650A
Location:	BL I-96 Howell
Contractor:	Rieth-Riley
Mix:	Fine
Gradation:	4E3
G_{mm}	2.501

	Sample	1	2	3	4	5	6	7	8	9	10	11	12	13	14	15	16	17	18	19	20
A	Dry Mass	3857.9	3855	3852.7	3856.4	3848.2	3860.8	3858	3859.5	3857.9	3858	3857.6	3860.6	3863.2	3862.9	3859.7	3860.8	3860.7	3862.5	3859.4	3854.4
B	Height 1	94.56	94.61	94.52	94.55	94.53	94.45	94.59	94.47	94.50	94.44	94.50	94.52	94.48	94.55	94.55	94.36	94.53	94.48	94.43	94.40
C	Height 2	94.34	94.47	94.41	94.35	94.72	94.45	94.51	94.40	94.52	94.48	94.42	94.47	94.33	94.46	94.29	94.44	94.65	94.41	94.43	94.42
D	Height 3	94.45	94.41	94.42	94.53	94.55	94.43	94.45	94.45	94.53	94.46	94.46	94.48	94.47	94.48	94.51	94.46	94.48	94.34	94.44	94.36
E	Height 4	94.53	94.47	94.49	94.64	94.55	94.37	94.42	94.50	94.58	94.49	94.52	94.36	94.48	94.49	94.59	94.44	94.40	94.48	94.40	94.27
F	Average Height	94.47	94.49	94.46	94.52	94.59	94.43	94.49	94.46	94.53	94.47	94.48	94.46	94.44	94.50	94.49	94.43	94.52	94.43	94.43	94.36
G	Diameter 1	150.04	150.13	150.08	150.36	150.08	150.03	150.12	149.99	150.12	149.92	149.97	150.02	150.05	150.01	150.02	150.38	150.06	149.84	149.98	150.03
H	Diameter 2	150.11	150.07	150.2	150.13	149.96	150.03	149.87	149.98	150.19	149.92	150.05	150.04	149.99	149.97	150.02	150.15	150	150.04	149.93	150.02
I	Average Diameter	150.075	150.100	150.140	150.245	150.020	150.030	149.995	149.985	150.155	149.920	150.010	150.030	150.020	149.990	150.020	150.265	150.030	149.940	149.955	150.025
J	G_{mb} [A/(F*π*I^2/4)]	2.309	2.306	2.304	2.301	2.302	2.313	2.311	2.313	2.305	2.314	2.310	2.312	2.314	2.314	2.311	2.306	2.311	2.317	2.314	2.311
K	Air Voids [(G_{mm}-J)/G_{mm}]	7.7	7.8	7.9	8.0	8.0	7.5	7.6	7.5	7.9	7.5	7.6	7.6	7.5	7.5	7.6	7.8	7.6	7.4	7.5	7.6

SATURATED SURFACE DRY METHOD

	Sample	1	2	3	4	5	6	7	8	9	10	11	12	13	14	15	16	17	18	19	20
A	Dry Mass	3857.9	3855	3852.7	3856.4	3848.2	3860.8	3858	3859.5	3857.9	3858	3857.6	3860.6	3863.2	3862.9	3859.7	3860.8	3860.7	3862.5	3859.4	3854.4
B	Submerged Mass	2216.3	2210.5	2208.9	2209.1	2204.9	2219	2216.4	2216.9	2210.6	2214.6	2216	2220.3	2221.2	2218.7	2217.6	2213.8	2220.1	2223	2221	2211.7
C	SSD Mass	3862	3862.2	3859.2	3861.7	3852.5	3865.9	3862.1	3863.2	3863.4	3862.5	3861.8	3865.2	3867.1	3866.8	3864.1	3865.5	3866	3867.7	3865.5	3858
D	G_{mb} [A/(C-B)]	2.344	2.334	2.335	2.334	2.336	2.344	2.344	2.344	2.334	2.341	2.344	2.347	2.347	2.344	2.344	2.337	2.346	2.348	2.347	2.341
E	Air Voids [(G_{mm}-D)/G_{mm}]	6.3	6.7	6.7	6.7	6.6	6.3	6.3	6.3	6.7	6.4	6.3	6.2	6.2	6.3	6.3	6.5	6.2	6.1	6.2	6.4

Project Number:	48612A
Location:	M-21 Owosso
Contractor:	Michigan Paving & Materials
Mix:	5E3
Gradation:	Fine
G_{mm}	2.470

VOLUMETRIC ANALYSIS

	Sample	1	2	3	4	5	6	7	8	9	10	11	12	13	14	15	16	17	18	19	20
A	Dry Mass (g)	3814.9	3816.1	3816.9	3815	3815.3	3813	3813.1	3816.4	3812.5	3815	3815.1	3812.7	3819.3	3818.7	3815.5	3815.9	3801.2	3814.5	3818.6	3792
B	Height 1 (mm)	94.59	94.50	94.54	94.42	94.54	94.61	94.59	94.68	94.49	94.49	94.57	94.32	94.54	94.58	94.52	94.39	94.42	94.52	94.40	94.49
C	Height 2 (mm)	94.52	94.53	94.53	94.53	94.63	94.54	94.45	94.57	94.46	94.53	94.44	94.29	94.53	94.50	94.38	94.51	94.69	94.57	94.56	94.55
D	Height 3 (mm)	94.56	94.60	94.53	94.59	94.58	94.47	94.50	94.55	94.47	94.56	94.53	94.30	94.47	94.55	94.46	94.49	94.49	94.60	94.44	94.36
E	Height 4 (mm)	94.60	94.56	94.60	94.52	94.50	94.46	94.59	94.47	94.58	94.56	94.50	94.28	94.45	94.53	94.50	94.38	94.43	94.36	94.37	94.40
F	Average Height (mm)	94.57	94.55	94.55	94.52	94.56	94.52	94.53	94.57	94.50	94.54	94.51	94.30	94.50	94.54	94.47	94.44	94.51	94.51	94.44	94.45
G	Diameter 1 (mm)	150.01	149.95	150.01	149.99	149.84	150.02	150.01	149.88	150.01	150.05	150.00	149.99	150.01	149.94	150.03	150.01	149.94	150.02	150.02	149.76
H	Diameter 2 (mm)	149.99	149.95	150.10	150.02	149.95	150.01	150.02	150.03	150.01	149.95	149.90	150.05	149.96	149.85	150.05	149.96	149.56	150.06	150.01	149.95
I	Average Diameter (mm)	150.00	149.95	150.06	150.01	149.90	150.02	150.02	149.96	150.01	150.00	149.95	150.02	149.99	149.90	150.04	149.99	149.75	150.04	150.02	149.86
J	G_{mb} [A/(F*π*I^2/4)]	2.283	2.286	2.283	2.284	2.286	2.282	2.282	2.285	2.283	2.284	2.286	2.287	2.288	2.289	2.284	2.287	2.284	2.283	2.288	2.276
K	Air Voids [(G_{mm}-J)/G_{mm}]	7.6	7.5	7.6	7.5	7.4	7.6	7.6	7.5	7.6	7.5	7.5	7.4	7.4	7.3	7.5	7.4	7.5	7.6	7.4	7.8

SATURATED SURFACE DRY METHOD

	Sample	1	2	3	4	5	6	7	8	9	10	11	12	13	14	15	16	17	18	19	20
A	Dry Mass (g)	3814.9	3816.1	3816.9	3815	3815.3	3813	3813.1	3816.4	3812.5	3815	3815.1	3812.7	3819.3	3818.7	3815.5	3815.9	3801.2	3814.5	3818.6	3792
B	Submerged Mass (g)	2172.2	2174.3	2174	2174.1	2175.7	2173.4	2173.6	2178.2	2174.8	2176.8	2175.2	2177.1	2180.1	2181.4	2179.2	2178.1	2159.7	2177.1	2180.4	2152.2
C	SSD Mass (g)	3819.8	3820.8	3822.1	3821.6	3820.9	3819.5	3819	3822.5	3819.5	3822	3822.3	3819	3824.2	3825.6	3822.5	3822.2	3806.8	3820.9	3825.2	3798.7
D	G_{mb} [A/(C-B)]	2.32	2.32	2.32	2.32	2.32	2.32	2.32	2.32	2.32	2.32	2.32	2.32	2.32	2.32	2.32	2.32	2.31	2.32	2.32	2.30
E	Air Voids [(G_{mm}-D)/G_{mm}]	6.3	6.2	6.2	6.2	6.1	6.2	6.2	6.0	6.2	6.1	6.2	6.0	6.0	6.0	6.0	6.0	6.6	6.1	6.0	6.8

Project Number: 34519A

Location: M-59 Brighton

Contractor: Ajax Paving

Mix: 3E10

Gradation: Coarse

G_{mm} 2.503

	Sample	1	2	3	4	5	6	7	8	9	10	11	12	13	14	15	16	17	18	19	20
A	Dry Mass	3747.4	3742.1	3743.3	3750.5	3751.3	3752.3	3719.8	3718.5	3754.6	3753.3	3753.1	3757.3	3750.8	3749.5	3748.4	3748.3	3750.7	3751.2	3749.7	3753.5
B	Height 1	94.68	94.45	94.35	94.66	94.47	94.53	94.61	94.47	94.56	94.85	94.47	94.45	94.42	94.69	94.40	94.47	94.37	94.54	94.62	94.43
C	Height 2	94.54	94.68	94.38	94.63	94.83	94.66	94.64	94.51	94.61	94.76	94.45	94.54	94.48	94.74	94.42	94.55	94.44	94.49	94.64	94.51
D	Height 3	94.79	94.48	94.27	94.39	94.79	94.29	94.80	94.39	94.62	94.32	94.70	94.27	94.52	94.48	94.65	94.44	94.57	94.54	94.77	94.50
E	Height 4	94.64	94.50	94.45	94.64	94.59	94.51	94.37	94.47	94.38	94.55	94.52	94.51	94.45	94.29	94.46	94.30	94.46	94.47	94.78	94.48
F	Average Height	94.66	94.53	94.36	94.58	94.67	94.50	94.61	94.46	94.54	94.62	94.54	94.44	94.47	94.55	94.48	94.44	94.46	94.51	94.70	94.48
G	Diameter 1	150.44	150.4	150.76	150.48	150.3	150.35	150.22	149.63	150.23	151.09	150.1	150.24	150.32	150.32	150.16	150.13	150.14	150.29	151.6	150.28
H	Diameter 2	150.39	150.95	151.1	150.51	150.49	150.42	150.14	150.39	150.18	150.87	150.25	150.22	150.37	150.15	150.12	150.07	150.09	150.32	150.97	150.11
I	Average Diameter	150.415	150.675	150.930	150.495	150.395	150.385	150.180	150.010	150.205	150.980	150.175	150.230	150.345	150.235	150.140	150.100	150.115	150.305	151.285	150.195
J	G_{mb} [A/(F*π*I^2/4)]	2.228	2.220	2.217	2.229	2.231	2.236	2.220	2.227	2.241	2.216	2.241	2.244	2.237	2.237	2.241	2.243	2.244	2.237	2.203	2.242
K	Air Voids [(G_{mm}-J)/G_{mm}]	11.0	11.3	11.4	10.9	10.9	10.7	11.3	11.0	10.5	11.5	10.5	10.3	10.6	10.6	10.5	10.4	10.4	10.6	12.0	10.4

SATURATED SURFACE DRY METHOD

	Sample	1	2	3	4	5	6	7	8	9	10	11	12	13	14	15	16	17	18	19	20
A	Dry Mass	3747.4	3742.1	3743.3	3750.5	3751.3	3752.3	3719.8	3718.5	3754.6	3753.3	3753.1	3757.3	3750.8	3749.5	3748.4	3748.3	3750.7	3751.2	3749.7	3753.5
B	Submerged Mass	2162.5	2157.8	2151.4	2163.7	2161.3	2167.6	2138.1	2136.2	2173.7	2159.6	2175.1	2169.8	2175.3	2164.5	2174.2	2170.3	2171.7	2162.4	2148	2164.3
C	SSD Mass	3765.4	3756.1	3755.7	3765.9	3766.7	3767.3	3736.8	3742.3	3771.9	3775	3770.8	3772.7	3769	3767.1	3767.1	3767.4	3766.4	3765.7	3769.5	3768.5
D	G_{mb} [A/(C-B)]	2.34	2.34	2.33	2.34	2.34	2.35	2.33	2.32	2.35	2.32	2.35	2.34	2.35	2.34	2.35	2.35	2.35	2.34	2.31	2.34
E	Air Voids [(G_{mm}-D)/G_{mm}]	6.6	6.5	6.8	6.5	6.6	6.3	7.0	7.5	6.1	7.2	6.0	6.3	6.0	6.5	6.0	6.2	6.0	6.5	7.6	6.5

Project Number:	74784A
Location:	I-196 Grand Rapids Michigan
Contractor:	Paving & Materials
Mix:	5E10
Gradation:	Coarse
G_{mm}	2.499

	Sample	1	2	3	4	5	6	7	8	9	10	11	12	13	14	15	16	17	18	19	20
A	Dry Mass	3825	3822.9	3824.3	3825.3	3823.8	3821.6	3822.4	3826.4	3824.2	3823.6	3822.2	3822.9	3821.5	3827.6	3822.2	3826.2	3824.6	3829.2	3823.9	3826.1
B	Height 1	94.63	94.58	94.43	94.42	94.63	94.56	94.42	94.55	94.49	94.62	94.62	94.46	94.68	94.73	94.61	94.50	94.49	94.63	94.62	94.60
C	Height 2	94.55	94.51	94.41	94.56	94.60	94.46	94.47	94.63	94.42	94.44	94.60	94.56	94.53	94.52	94.53	94.79	94.58	94.53	94.45	94.60
D	Height 3	94.64	94.58	94.54	94.49	94.61	94.51	94.53	94.44	94.54	94.57	94.57	94.46	94.61	94.61	94.60	94.69	94.59	94.50	94.51	94.52
E	Height 4	94.62	94.59	94.47	94.51	94.58	94.61	94.45	94.58	94.55	94.54	94.73	94.38	94.40	94.61	94.61	94.72	94.68	94.51	94.58	94.64
F	Average Height	94.61	94.57	94.46	94.50	94.61	94.54	94.47	94.55	94.50	94.54	94.63	94.47	94.56	94.62	94.59	94.68	94.59	94.54	94.54	94.59
G	Diameter 1	150.090	150.000	149.990	150.040	150.000	150.090	150.010	150.010	150.040	149.970	150.090	150.030	150.040	150.140	150.020	150.150	150.040	149.980	150.080	149.890
H	Diameter 2	150.110	150.010	150.150	150.030	150.060	150.010	149.930	150.020	150.010	150.010	150.090	150.000	149.990	150.020	149.970	149.980	150.020	150.040	149.980	149.930
I	Average Diameter	150.100	150.005	150.070	150.035	150.030	150.050	149.970	150.015	150.025	149.990	150.090	150.015	150.015	150.080	149.995	150.065	150.030	150.010	150.030	149.910
J	G_{mb} [A/(F*π*I^2/4)]	2.285	2.288	2.289	2.290	2.286	2.286	2.291	2.290	2.289	2.289	2.283	2.290	2.287	2.287	2.287	2.285	2.287	2.292	2.288	2.292
K	Air Voids [(G_{mm}-J)/G_{mm}]	8.6	8.5	8.4	8.4	8.5	8.5	8.3	8.4	8.4	8.4	8.6	8.4	8.5	8.5	8.5	8.6	8.5	8.3	8.4	8.3

SATURATED SURFACE DRY METHOD

	Sample	1	2	3	4	5	6	7	8	9	10	11	12	13	14	15	16	17	18	19	20
A	Dry Mass	3825	3822.9	3824.3	3825.3	3823.8	3821.6	3822.4	3826.4	3824.2	3823.6	3822.2	3822.9	3821.5	3827.6	3822.2	3826.2	3824.6	3829.2	3823.9	3826.1
B	Submerged Mass	2207.4	2203.1	2202	2208.6	2202	2201.8	2201.3	2199.9	2202.1	2202.1	2198.7	2207.2	2202.4	2203.4	2200	2205.9	2207.5	2212.5	2200.9	2208.9
C	SSD Mass	3840.8	3837.8	3836	3836.7	3836.7	3834.6	3834.3	3836.5	3835	3835.8	3833.3	3837.3	3833	3837.3	3835	3838.3	3838.6	3844.2	3834.7	3839.3
D	G_{mb} [A/(C-B)]	2.342	2.339	2.340	2.350	2.339	2.341	2.341	2.338	2.342	2.340	2.338	2.345	2.344	2.343	2.338	2.344	2.345	2.347	2.340	2.347
E	Air Voids [(G_{mm}-D)/G_{mm}]	6.3	6.4	6.3	6.0	6.4	6.3	6.3	6.4	6.3	6.3	6.4	6.2	6.2	6.3	6.5	6.2	6.2	6.1	6.3	6.1

Project Number:	51472A
Location:	I-75 Clarkston
Contractor:	Ace Asphalt
Mix:	4E30
Gradation:	Coarse
G_{mm}	2.487

	Sample	1	2	3	4	5	6	7	8	9	10	11	12	13	14	15	16	17	18	19	20
A	Dry Mass	3766.4	3770.4	3768.5	3767.6	3770.1	3773.3	3768.5	3769.8	3772.8	3770.2	3769	3772.6	3774.8	3770.6	3771	3769.9	3769.2	3766.9	3776	3768.5
B	Height 1	94.67	94.63	94.67	94.53	94.51	94.60	94.55	94.48	94.42	94.51	94.49	94.54	94.54	94.65	94.54	94.46	94.57	94.60	94.51	94.60
C	Height 2	94.65	94.60	94.71	94.46	94.60	94.68	94.60	94.56	94.60	94.51	94.45	94.64	94.48	94.59	94.63	94.44	94.54	94.63	94.54	94.54
D	Height 3	94.53	94.59	94.57	94.76	94.66	94.55	94.48	94.50	94.51	94.50	94.49	94.67	94.59	94.50	94.63	94.47	94.53	94.62	94.58	94.60
E	Height 4	94.55	94.61	94.61	94.58	94.51	94.59	94.55	94.71	94.56	94.38	94.52	94.54	94.48	94.61	94.61	94.57	94.48	94.53	94.44	94.62
F	Average Height	94.60	94.61	94.64	94.58	94.57	94.61	94.55	94.56	94.52	94.48	94.49	94.60	94.52	94.59	94.60	94.49	94.53	94.60	94.52	94.59
G	Diameter 1	150.06	149.91	149.94	150	149.96	150.01	149.99	149.98	150.02	150.07	149.92	150.05	150.07	149.94	150.02	150	149.96	150.08	150.06	149.96
H	Diameter 2	150.04	149.97	150.03	150.05	149.93	150.08	150.05	149.9	149.99	149.96	149.88	150.07	149.94	149.9	150	150.03	149.96	150.06	150.05	149.97
I	Average Diameter	150.050	149.940	149.985	150.025	149.945	150.045	150.020	149.940	150.005	150.015	149.900	150.060	150.005	149.920	150.010	150.015	149.960	150.070	150.055	149.965
J	G_{mb} [A/(F*π*I^2/4)]	2.252	2.257	2.254	2.253	2.258	2.256	2.255	2.258	2.259	2.258	2.260	2.255	2.260	2.258	2.255	2.257	2.258	2.251	2.259	2.256
K	Air Voids [(G_{mm}-J)/G_{mm}]	9.5	9.2	9.4	9.4	9.2	9.3	9.3	9.2	9.2	9.2	9.1	9.3	9.1	9.2	9.3	9.2	9.2	9.5	9.2	9.3

SATURATED SURFACE DRY METHOD

	Sample	1	2	3	4	5	6	7	8	9	10	11	12	13	14	15	16	17	18	19	20
A	Dry Mass	3766.4	3770.4	3768.5	3767.6	3770.1	3773.3	3768.5	3769.8	3772.8	3770.2	3769	3772.6	3774.8	3770.6	3771	3769.9	3769.2	3766.9	3776	3768.5
B	Submerged Mass	2159.3	2159.1	2163.5	2154.3	2159	2166.8	2155.9	2157.7	2161.4	2160.3	2159.3	2159.2	2164.4	2165.3	2161.2	2160	2163.3	2157.5	2163.5	2167.1
C	SSD Mass	3782.1	3782.5	3784.8	3784.6	3784.8	3788.8	3781.3	3783.2	3786.5	3785.2	3782.2	3785.6	3788	3784.6	3787.1	3783.3	3783.3	3783.1	3789.3	3785.5
D	G_{mb} [A/(C-B)]	2.321	2.323	2.324	2.311	2.319	2.326	2.319	2.319	2.322	2.320	2.322	2.320	2.325	2.329	2.319	2.322	2.327	2.317	2.323	2.329
E	Air Voids [(G_{mm}-D)/G_{mm}]	6.7	6.6	6.5	7.1	6.8	6.5	6.8	6.7	6.7	6.7	6.6	6.7	6.5	6.4	6.7	6.6	6.4	6.8	6.6	6.4

Phase II – 150mm Superpave Specimens for AASHTO T283

Project Number:
Location: M-50 Dundee
Contractor:
Mix: 3E1
Gradation:
G_{mm} 2.52

	Sample	1	2	3	4	5	6	7	8	9	10
A	Dry Mass	3701.4	3702.8	3701.1	3701.1	3697.5	3697.2	3699.4	3690.6	3699	3702.8
B	Height 1	93.53	93.87	93.72	93.89	93.99	93.97	94.08	93.92	94.16	94.27
C	Height 2	93.83	93.84	93.72	93.96	93.89	94.04	93.89	93.92	93.9	94.09
D	Height 3	93.96	93.88	94.25	93.86	93.94	93.95	94.15	93.9	94.14	94.22
E	Height 4	93.73	93.88	94.05	93.94	94.09	93.83	93.95	93.81	94.16	94.26
F	Average Height	93.7625	93.8675	93.935	93.9125	93.9775	93.9475	94.0175	93.8875	94.09	94.21
G	Diameter 1	150.49	150.31	150.35	150.49	150.6	150.4	150.31	150.27	150.32	150.89
H	Diameter 2	151.36	150.7	150.29	150.39	150.38	150.28	150.35	150.28	150.14	150.53
I	Average Diameter	150.925	150.505	150.32	150.44	150.49	150.34	150.33	150.275	150.23	150.71
J	G_{mb} [A/(F*π*I^2/4)]	2.207	2.217	2.220	2.217	2.212	2.217	2.217	2.216	2.218	2.203
K	Air Voids [(G_{mm}-J)/G_{mm}]	12.4	12.0	11.9	12.0	12.2	12.0	12.0	12.1	12.0	12.6
	Sample	1	2	3	4	5	6	7	8	9	10
A	Dry Mass	3701.4	3702.8	3701.1	3701.1	3697.5	3697.2	3699.4	3690.6	3699	3702.8
B	Submerged Mass	2147.1	2149.8	2151.8	2145.7	2144	2150.5	2160.3	2150.5	2153.2	2153.7
C	SSD Mass	3729.4	3729.8	3727.8	3730.8	3724.8	3725.6	3736.9	3719.1	3726.6	3737.5
D	G_{mb} [A/(C-B)]	2.339	2.344	2.348	2.335	2.339	2.347	2.346	2.353	2.351	2.338
E	Air Voids [(G_{mm}-D)/G_{mm}]	7.2	7.0	6.8	7.3	7.2	6.9	6.9	6.6	6.7	7.2

Project Number:
Location: M-36 Pinckney
Contractor:
Mix:
Gradation:
G_{mm} 2.511

	Sample	1	2	3	4	5	6	7	8	9	10
A	Dry Mass	3694.1	3700.3	3695.2	3691.1	3730.3	3691.4	3692.7	3726.1	3730.4	3696.1
B	Height 1	94.55	94.34	94.65	94.35	94.44	94.39	94.6	94.47	94.56	94.45
C	Height 2	94.47	94.56	94.63	94.23	94.69	94.53	94.22	94.5	94.66	94.51
D	Height 3	94.53	94.38	94.42	94.52	94.6	94.54	94.38	94.57	94.62	94.57
E	Height 4	94.51	94.38	94.52	94.49	94.43	94.44	94.46	94.63	94.52	94.66
F	Average Height	94.515	94.415	94.555	94.3975	94.54	94.475	94.415	94.5425	94.59	94.5475
G	Diameter 1	150.21	150.45	150.21	150.17	150.18	150.1	150.25	150.07	150.066	150.35
H	Diameter 2	150.15	150.44	150.06	150.19	150.27	150.2	150.26	150.09	150.09	150.38
I	Average Diameter	150.18	150.445	150.135	150.18	150.225	150.15	150.255	150.08	150.078	150.365
J	G_{mb} [A/(F*π*I^2/4)]	2.206	2.205	2.207	2.207	2.226	2.207	2.206	2.228	2.229	2.201
K	Air Voids [(G_{mm}-J)/G_{mm}]	12.1	12.2	12.1	12.1	11.3	12.1	12.2	11.3	11.2	12.3
	Sample	1	2	3	4	5	6	7	8	9	10
A	Dry Mass	3694.1	3700.3	3695.2	3691.1	3730.3	3691.4	3692.7	3726.1	3730.4	3696.1
B	Submerged Mass	2127.4	2135.8	2127.3	2122.2	2154.3	2122	2124.2	2150.2	2164	2118.1
C	SSD Mass	3719.3	3730.6	3721.5	3715.5	3758	3715.9	3717.8	3754.1	3765	3718.5
D	G_{mb} [A/(C-B)]	2.321	2.320	2.318	2.317	2.326	2.316	2.317	2.323	2.330	2.309
E	Air Voids [(G_{mm}-D)/G_{mm}]	7.6	7.6	7.7	7.7	7.4	7.8	7.7	7.5	7.2	8.0

Project Number:
Location: M-21 St. Johns
Contractor:
Mix:
Gradation:
G_{mm} 2.489

	Sample	1	2	3	4	5	6	7	8	9	10
A	Dry Mass	3662.2	3662.1	3671.9	3666.7	3660.6	3665.4	3665.9	3665.5	3656.8	3665
B	Height 1	94.4	94.46	94.4	93.9	94.44	93.47	94.49	94.16	94.28	94.86
C	Height 2	94.73	94.23	94.51	94.35	94.38	94.43	94.37	94.56	94.5	94.48
D	Height 3	94.6	94.18	94.29	94.58	94.56	94.31	94.23	94.14	94.55	94.53
E	Height 4	94.5	94.54	94.49	94.63	94.2	94.39	94.38	94.29	94.54	94.62
F	Average Height	94.5575	94.3525	94.4225	94.365	94.395	94.15	94.3675	94.2875	94.4675	94.6225
G	Diameter 1	150.59	150.21	150.15	149.65	149.85	149.76	150.19	150.32	150.66	150.85
H	Diameter 2	150.03	150.12	150.4	150.62	150.6	149.91	150.12	150.03	150.53	149.83
I	Average Diameter	150.31	150.165	150.275	150.135	150.225	149.835	150.155	150.175	150.595	150.34
J	G_{mb} [A/(F*π*I^2/4)]	2.183	2.192	2.193	2.195	2.188	2.208	2.194	2.195	2.173	2.182
K	Air Voids [(G_{mm}-J)/G_{mm}]	12.3	12.0	11.9	11.8	12.1	11.3	11.9	11.8	12.7	12.3
	Sample	1	2	3	4	5	6	7	8	9	10
A	Dry Mass	3662.3	3662.7	3672.3	3667.3	3660.8	3665.6	3666.5	3654.7	3656.8	3655
B	Submerged Mass	2121.5	2113.9	2130.3	2118.8	2111.5	2119.2	2117.8	2108.4	2110.1	2091.6
C	SSD Mass	3700.3	3696.7	3704.5	3695.5	3696.5	3697.7	3694.9	3687.2	3689.5	3681.1
D	G_{mb} [A/(C-B)]	2.320	2.314	2.333	2.326	2.310	2.322	2.325	2.315	2.315	2.299
E	Air Voids [(G_{mm}-D)/G_{mm}]	6.8	7.0	6.3	6.6	7.2	6.7	6.6	7.0	7.0	7.6

Project Number:
Location: M-45 Grand Rapids
Contractor:
Mix:
Gradation:
G_{mm} 2.513

	Sample	1	2	3	4	5	6	7	8	9	10
A	Dry Mass	3831.9	3839.3	3837.2	3837.4	3845.3	3843.4	3850	3844.1	3843.8	3841.8
B	Height 1	94.64	94.88	94.38	94.43	94.43	94.42	94.25	94.32	94.22	94.18
C	Height 2	95.37	94.75	94.58	94.28	94.39	94.28	94.17	94.22	94.26	94.47
D	Height 3	94.35	95.15	94.69	94.4	94.4	94.5	94.05	94.3	94.31	94.5
E	Height 4	94.97	95.91	94.36	94.31	94.57	94.38	94.13	94.58	94.14	94.2
F	Average Height	94.8325	95.1725	94.5025	94.355	94.4475	94.395	94.15	94.355	94.2325	94.3375
G	Diameter 1	150.07	150.41	150.04	149.94	149.85	149.95	149.99	149.91	149.97	150.1
H	Diameter 2	150.1	150.82	149.884	149.99	149.93	150.15	150	150	149.97	150.11
I	Average Diameter	150.085	150.615	149.962	149.965	149.89	150.05	149.995	149.955	149.97	150.105
J	G_{mb} [A/(F*π*I^2/4)]	2.284	2.264	2.299	2.303	2.307	2.303	2.314	2.307	2.309	2.301
K	Air Voids [(G_{mm}-J)/G_{mm}]	9.1	9.9	8.5	8.4	8.2	8.4	7.9	8.2	8.1	8.4
	Sample	1	2	3	4	5	6	7	8	9	10
A	Dry Mass	3831.9	3839.3	3837.2	3837.4	3845.3	3843.4	3850	3844.1	3843.8	3841.8
B	Submerged Mass	2205.1	2203	2205.1	2221.2	2219.3	2214.9	2212.9	2214.9	2208.1	2216.4
C	SSD Mass	3848	3860	3849.2	3852.9	3858.9	3854.4	3856.3	3853.8	3850.9	3852.9
D	G_{mb} [A/(C-B)]	2.332	2.317	2.334	2.352	2.345	2.344	2.343	2.346	2.340	2.348
E	Air Voids [(G_{mm}-D)/G_{mm}]	7.2	7.8	7.1	6.4	6.7	6.7	6.8	6.7	6.9	6.6

Project Number:
Location: M-84 Saginaw
Contractor:
Mix:
Gradation:
G_{mm} 2.543

	Sample	1	2	3	4	5	6	7	8	9	10
A	Dry Mass	3826.2	3879.4	3883.9	3879.8	3887.4	3883.7	3887.8	3885	3882.5	3883.4
B	Height 1	94.67	94.23	94.45	94.04	94.28	94.06	94.12	94.34	94.12	94.39
C	Height 2	94.35	94.36	94.4	94.06	94.35	94.16	94.26	94.3	94.39	94.41
D	Height 3	94.43	94.56	94.66	94.37	94.17	94.24	94.7	94.24	94.34	94.28
E	Height 4	94.03	94.2	94.32	94.49	94.8	94.31	93.76	94.41	94.76	94.45
F	Average Height	94.37	94.3375	94.4575	94.24	94.4	94.1925	94.21	94.3225	94.4025	94.3825
G	Diameter 1	150.08	150.22	149.79	149.86	149.87	149.73	149.54	149.57	149.83	149.81
H	Diameter 2	150.54	150.04	149.73	149.91	149.84	149.76	149.94	149.77	149.88	149.77
I	Average Diameter	150.31	150.13	149.76	149.885	149.855	149.745	149.74	149.67	149.855	149.79
J	G_{mb} [A/(F*π*I^2/4)]	2.285	2.323	2.334	2.333	2.335	2.341	2.343	2.341	2.332	2.335
K	Air Voids [(G_{mm}-J)/G_{mm}]	10.1	8.6	8.2	8.2	8.2	7.9	7.9	7.9	8.3	8.2
	Sample	1	2	3	4	5	6	7	8	9	10
A	Dry Mass	3876.6	3880	3884.3	3880.2	3887.3	3884	3887.7	3884.9	3882.3	3883.2
B	Submerged Mass	2264	2265.5	2264.1	2260.7	2269.6	2267.6	2271.1	2267.1	2263.1	2267.9
C	SSD Mass	3895.6	3901.5	3898.9	3894.9	3904.5	3903.6	3903.2	3901.8	3901.6	3902.2
D	G_{mb} [A/(C-B)]	2.376	2.372	2.376	2.374	2.378	2.374	2.382	2.377	2.369	2.376
E	Air Voids [(G_{mm}-D)/G_{mm}]	6.6	6.7	6.6	6.6	6.5	6.6	6.3	6.5	6.8	6.6

Project Number:
Location: BL I-96 Howell
Contractor:
Mix:
Gradation:
G_{mm} 2.501

	Sample	1	2	3	4	5	6	7	8	9	10
A	Dry Mass	3845.3	3841.3	3841.2	3850.3	3820.8	3844.8	3849.2	3847.7	3847.7	3847.1
B	Height 1	94.78	94.67	94.59	94.77	94.7	94.75	94.71	94.5	94.51	94.52
C	Height 2	94.88	94.83	94.79	94.92	94.76	94.55	94.63	94.54	94.55	94.5
D	Height 3	94.91	94.87	94.8	94.83	97.62	94.54	94.58	94.62	94.63	94.65
E	Height 4	94.86	94.8	94.69	94.86	94.9	94.68	94.74	94.68	94.6	94.52
F	Average Height	94.8575	94.7925	94.7175	94.845	95.495	94.63	94.665	94.585	94.5725	94.5475
G	Diameter 1	150.25	150.15	149.78	150.04	150.06	150.02	150.07	149.3	150.05	150.07
H	Diameter 2	150.28	150.25	150.14	150.01	150.04	150.06	150.09	150	150.01	150.09
I	Average Diameter	150.265	150.2	149.96	150.025	150.05	150.04	150.08	149.65	150.03	150.08
J	G_{mb} [A/(F*π*I^2/4)]	2.286	2.287	2.296	2.296	2.263	2.298	2.299	2.313	2.301	2.300
K	Air Voids [(G_{mm}-J)/G_{mm}]	8.6	8.6	8.2	8.2	9.5	8.1	8.1	7.5	8.0	8.0
	Sample	1	2	3	4	5	6	7	8	9	10
A	Dry Mass	3845.3	3841.3	3841.2	3850.3	3820.8	3844.8	3849.2	3847.7	3847.7	3847.1
B	Submerged Mass	2204.9	2201	2200.7	2207.8	2209.3	2206	2209.2	2207.5	2212.1	2205.2
C	SSD Mass	3855	3852	3850.4	3858.1	3857.8	3853.6	3858.9	3856.9	3858.2	3855.6
D	G_{mb} [A/(C-B)]	2.330	2.327	2.328	2.333	2.318	2.334	2.333	2.333	2.337	2.331
E	Air Voids [(G_{mm}-D)/G_{mm}]	6.8	7.0	6.9	6.7	7.3	6.7	6.7	6.7	6.5	6.8

Project Number:
Location: M-21 Owosso
Contractor:
Mix:
Gradation:
G_{mm} 2.47

	Sample	1	2	3	4	5	6	7	8	9	10
A	Dry Mass	3798.3	3796	3841	3796.1	3796.4	3799.4	3800.6	3796.6	3815.9	3797.9
B	Height 1	94.43	94.39	94.49	94.41	94.3	94.41	94.5	94.36	94.28	94.37
C	Height 2	94.4	94.33	94.29	94.52	94.35	94.46	94.36	94.48	94.35	94.43
D	Height 3	94.32	94.4	94.36	94.38	94.32	94.4	94.37	94.41	94.38	94.51
E	Height 4	94.35	94.34	94.35	94.35	94.37	94.35	94.36	94.32	94.33	94.29
F	Average Height	94.375	94.365	94.3725	94.415	94.335	94.405	94.3975	94.3925	94.335	94.4
G	Diameter 1	149.96	149.71	149.93	149.92	149.85	149.96	149.88	149.91	149.9	149.95
H	Diameter 2	149.83	149.78	149.92	149.98	149.86	149.98	149.95	149.93	149.88	149.91
I	Average Diameter	149.895	149.745	149.925	149.95	149.855	149.97	149.915	149.92	149.89	149.93
J	G_{mb} [A/(F*π*I^2/4)]	2.281	2.284	2.305	2.277	2.282	2.278	2.281	2.278	2.292	2.279
K	Air Voids [(G_{mm}-J)/G_{mm}]	7.7	7.5	6.7	7.8	7.6	7.8	7.7	7.8	7.2	7.7
	Sample	1	2	3	4	5	6	7	8	9	10
A	Dry Mass	3798.3	3796	3841	3796.1	3796.4	3799.4	3800.6	3796.6	3815.9	3797.9
B	Submerged Mass	2166.7	2163.1	2203.3	2159.9	2162.7	2164.8	2160.6	2156.5	2178.2	2156.9
C	SSD Mass	3809.5	3806.1	3848.9	3804.8	3805.7	3809.3	3807.7	3804.2	3823.5	3804.7
D	G_{mb} [A/(C-B)]	2.312	2.310	2.334	2.308	2.311	2.310	2.307	2.304	2.319	2.305
E	Air Voids [(G_{mm}-D)/G_{mm}]	6.4	6.5	5.5	6.6	6.5	6.5	6.6	6.7	6.1	6.7

Project Number:
Location: M-66 Battle Creek
Contractor:
Mix:
Gradation:
G_{mm} 2.47

	Sample	1	2	3	4	5	6	7	8	9	10
A	Dry Mass	3822.1	3829.2	3806.2	3804.9	3813.3	3809.2	3825.4	3822.3	3807.9	3822.9
B	Height 1	94.47	94.51	94.36	94.49	94.51	94.53	94.5	94.37	94.42	94.24
C	Height 2	94.5	94.37	94.41	94.58	94.49	94.52	94.49	94.44	94.32	94.32
D	Height 3	94.44	94.4	94.45	94.45	94.49	94.37	94.46	95.04	94.43	94.28
E	Height 4	94.48	94.47	94.36	94.47	94.55	94.56	94.76	94.92	94.51	94.47
F	Average Height	94.4725	94.4375	94.395	94.4975	94.51	94.495	94.5525	94.6925	94.42	94.3275
G	Diameter 1	149.95	149.94	149.99	149.99	150.02	149.94	150.23	150.07	149.97	149.76
H	Diameter 2	149.94	149.98	149.92	149.98	150.01	150.06	149.88	149.84	149.99	149.99
I	Average Diameter	149.945	149.96	149.955	149.985	150.015	150	150.055	149.955	149.98	149.875
J	G_{mb} [A/(F*π*I^2/4)]	2.291	2.296	2.283	2.279	2.283	2.281	2.288	2.286	2.283	2.297
K	Air Voids [(G_{mm}-J)/G_{mm}]	7.2	7.1	7.6	7.7	7.6	7.6	7.4	7.5	7.6	7.0
	Sample	1	2	3	4	5	6	7	8	9	10
A	Dry Mass	3822.1	3829.2	3806.2	3804.9	3813.3	3809.2	3825.4	3822.3	3807.9	3822.9
B	Submerged Mass	2181.8	2187.5	2166.7	2162.3	2173.6	2168.8	2184.8	2179.8	2167.5	2180.6
C	SSD Mass	3829.5	3836.9	3812.7	3811.3	3820.3	3817	3832.3	3828.7	3815.2	3829.8
D	G_{mb} [A/(C-B)]	2.320	2.322	2.312	2.307	2.316	2.311	2.322	2.318	2.311	2.318
E	Air Voids [(G_{mm}-D)/G_{mm}]	6.1	6.0	6.4	6.6	6.2	6.4	6.0	6.2	6.4	6.2

Project Number:
Location: M-50 Dundee
Contractor:
Mix: 4 E 3
Gradation:
G_{mm} 2.538

	Sample	1	2	3	4	5	6	7	8	9	10
A	Dry Mass	3823.3	3824.6	3825.3	3825.7	3829.5	3827	3829.8	3826.7	3829.5	3831.4
B	Height 1	94.65	94.3	94.5	94.42	94.28	94.37	94.38	94.24	94.4	94.19
C	Height 2	94.24	94.46	94.45	94.41	94.44	94.47	94.19	94.18	94.45	94.3
D	Height 3	94.34	94.35	94.58	94.58	94.49	94.41	94.28	94.1	94.51	94.8
E	Height 4	94.36	94.71	94.54	94.33	94.56	94.5	94.28	94.4	94.39	94.37
F	Average Height	94.3975	94.455	94.5175	94.435	94.4425	94.4375	94.2825	94.23	94.4375	94.415
G	Diameter 1	150.01	149.97	149.93	150.12	150	150	150.05	150.01	150.02	150.15
H	Diameter 2	150.06	149.96	149.96	149.99	149.91	150.11	150.01	150.04	150.05	150.01
I	Average Diameter	150.035	149.965	149.945	150.055	149.955	150.055	150.03	150.025	150.035	150.08
J	G_{mb} [A/(F*π*I^2/4)]	2.291	2.292	2.292	2.291	2.296	2.292	2.298	2.297	2.294	2.294
K	Air Voids [(G_{mm}-J)/G_{mm}]	9.7	9.7	9.7	9.7	9.5	9.7	9.5	9.5	9.6	9.6
	Sample	1	2	3	4	5	6	7	8	9	10
A	Dry Mass	3823.3	3824.6	3825.3	3825.7	3829.5	3827	3829.8	3826.7	3829.5	3831.4
B	Submerged Mass	2221.1	2220.8	2220.3	2226	2231.4	2231	2229.4	2229	2231.9	2232.9
C	SSD Mass	3838.2	3839.8	3840.4	3841.4	3849.3	3851.1	3846.4	3842.1	3847.6	3849.5
D	G_{mb} [A/(C-B)]	2.364	2.362	2.361	2.368	2.367	2.362	2.368	2.372	2.370	2.370
E	Air Voids [(G_{mm}-D)/G_{mm}]	6.8	6.9	7.0	6.7	6.7	6.9	6.7	6.5	6.6	6.6

Project Number:
Location: US-12 MIS
Contractor:
Mix:
Gradation:
G_{mm} 2.491

	Sample	1	2	3	4	5	6	7	8	9	10
A	Dry Mass	3741.2	3713.7	3740.4	3714.4	3711.4	3741.3	3715.3	3717.5	3719.9	3722.1
B	Height 1	94.6	94.41	94.63	94.39	94.32	94.48	94.33	94.33	94.33	94.33
C	Height 2	94.4	94.34	94.59	94.74	94.54	94.39	94.3	94.24	94.29	94.39
D	Height 3	94.47	94.53	94.55	94.36	94.5	94.37	94.36	94.29	94.42	94.52
E	Height 4	94.5	94.33	94.62	94.55	94.52	94.4	94.29	94.29	94.36	94.39
F	Average Height	94.4925	94.4025	94.5975	94.51	94.47	94.41	94.32	94.2875	94.35	94.4075
G	Diameter 1	150.11	150.15	150.09	150.31	150.22	150.31	150.21	150.1	150.16	150.16
H	Diameter 2	150.06	150.29	150.1	150.29	150.39	150.14	150.3	150.14	150.06	150.17
I	Average Diameter	150.085	150.22	150.095	150.3	150.305	150.225	150.255	150.12	150.11	150.165
J	G_{mb} [A/(F*π*I^2/4)]	2.238	2.220	2.235	2.215	2.214	2.236	2.221	2.228	2.228	2.226
K	Air Voids [(G_{mm}-J)/G_{mm}]	10.2	10.9	10.3	11.1	11.1	10.2	10.8	10.6	10.6	10.6
	Sample	1	2	3	4	5	6	7	8	9	10
A	Dry Mass	3741.2	3713.7	3740.4	3714.4	3711.4	3741.3	3715.3	3717.5	3719.9	3722.1
B	Submerged Mass	2143.9	2112.9	2144	2125.1	2130	2128.6	2139.3	2137.9	2143.6	2136.6
C	SSD Mass	3760.1	3732.1	3760.3	3739.8	3731.1	3739.9	3747.5	3745.3	3748.9	3747.1
D	G_{mb} [A/(C-B)]	2.315	2.294	2.314	2.300	2.318	2.322	2.310	2.313	2.317	2.311
E	Air Voids [(G_{mm}-D)/G_{mm}]	7.1	7.9	7.1	7.7	6.9	6.8	7.3	7.2	7.0	7.2

Project Number:
Location: M-59 Brighton
Contractor:
Mix:
Gradation:
G_{mm} 2.503

	Sample	1	2	3	4	5	6	7	8	9	10
A	Dry Mass	3716.6	3722.2	3727.5	3717.7	3725	3725.1	3725.5	3718.8	3721	3719.6
B	Height 1	94.13	94.29	94.79	94.42	94.3	94.28	94.39	94.38	94.48	94.84
C	Height 2	94.19	94.47	94.41	94.12	94.37	94.18	94.3	94.2	94.43	94.45
D	Height 3	94.55	93.87	94.29	94.42	94.21	94.7	94.5	94.42	94.1	94.43
E	Height 4	94.32	94.54	94.98	94.49	94.48	94.25	94.56	94.35	94.63	94.54
F	Average Height	94.2975	94.2925	94.6175	94.3625	94.34	94.3525	94.4375	94.3375	94.41	94.565
G	Diameter 1	149.89	149.87	150.73	150.2	149.85	150.16	149.89	150.28	150.22	149.88
H	Diameter 2	150.25	149.91	150.85	150.11	150.04	149.98	149.99	150.12	150.19	150.08
I	Average Diameter	150.07	149.89	150.79	150.155	149.945	150.07	149.94	150.2	150.205	149.98
J	G_{mb} [A/(F*π*I^2/4)]	2.228	2.237	2.206	2.225	2.236	2.232	2.234	2.225	2.224	2.226
K	Air Voids [(G_{mm}-J)/G_{mm}]	11.0	10.6	11.9	11.1	10.7	10.8	10.7	11.1	11.1	11.0
	Sample	1	2	3	4	5	6	7	8	9	10
A	Dry Mass	3716.6	3722.2	3727.5	3717.7	3725	3725.1	3725.5	3718.8	3721	3719.6
B	Submerged Mass	2136.5	2145.7	2142.5	2139.6	2149.5	2143.9	2161.3	2160.7	2143.5	2150.6
C	SSD Mass	3737	3740.3	3748.4	3738	3747.2	3744.4	3749.8	3740.5	3743	3740.7
D	G_{mb} [A/(C-B)]	2.322	2.334	2.321	2.326	2.331	2.327	2.345	2.354	2.326	2.339
E	Air Voids [(G_{mm}-D)/G_{mm}]	7.2	6.7	7.3	7.1	6.9	7.0	6.3	6.0	7.1	6.5

Project Number:
Location: Michigan Ave. Dearborn
Contractor:
Mix: 3 E 10
Gradation:
G_{mm} 2.493

	Sample	1	2	3	4	5	6	7	8	9	10
A	Dry Mass	3749.2	3768.2	3755.1	3743.4	3748.4	3735.4	3745.3	3754.4	3743.5	3762
B	Height 1	94.74	94.42	94.29	95.04	94.86	94.89	95.04	94.42	94.4	94.55
C	Height 2	94.71	94.29	94.42	95.01	94.61	96.52	95.12	94.52	94.9	94.5
D	Height 3	94.97	94.29	94.31	95.05	94.49	95.2	94.8	94.4	94.82	94.39
E	Height 4	94.6	94.39	95.37	95.12	94.8	94.89	95.26	94.44	94.35	94.6
F	Average Height	94.755	94.3475	94.5975	95.055	94.69	95.375	95.055	94.445	94.6175	94.51
G	Diameter 1	149.5	150.05	151.37	150.5	149.73	149.86	150.32	150.65	149.8	150.5
H	Diameter 2	149.72	149.98	150.68	149.81	149.5	149.95	149.92	150.38	149.64	150.57
I	Average Diameter	149.61	150.015	151.025	150.155	149.615	149.905	150.12	150.515	149.72	150.535
J	G_{mb} [A/(F*π*I^2/4)]	2.251	2.260	2.216	2.224	2.252	2.219	2.226	2.234	2.247	2.237
K	Air Voids [(G_{mm}-J)/G_{mm}]	9.7	9.4	11.1	10.8	9.7	11.0	10.7	10.4	9.9	10.3
	Sample	1	2	3	4	5	6	7	8	9	10
A	Dry Mass	3749.2	3768.2	3755.1	3743.4	3748.4	3735.4	3745.3	3754.4	3743.5	3762
B	Submerged Mass	2156	2171.1	2138.8	2160	2154.3	2118.8	2131.3	2146.4	2139.6	2151.8
C	SSD Mass	3760.7	3780.8	3764.5	3759	3756	3743.1	3750.8	3760.9	3750.9	3769.5
D	G_{mb} [A/(C-B)]	2.336	2.341	2.310	2.341	2.340	2.300	2.313	2.325	2.323	2.326
E	Air Voids [(G_{mm}-D)/G_{mm}]	6.3	6.1	7.3	6.1	6.1	7.8	7.2	6.7	6.8	6.7

Project Number:
Location: Vandyke, Detroit
Contractor:
Mix:
Gradation:
G_{mm} 2.604

	Sample	1	2	3	4	5	6	7	8	9	10
A	Dry Mass	3977.7	3982.6	3985.4	3967	3982.1	3983.6	3977.8	3962	3980.7	3958.8
B	Height 1	94.39	94.46	94.4	94.73	94.35	94.34	94.47	94.61	94.14	94.66
C	Height 2	94.48	94.37	94.43	94.69	94.42	94.4	94.38	94.55	94.37	94.61
D	Height 3	94.36	94.5	94.44	94.62	94.53	94.31	94.33	94.69	94.41	94.5
E	Height 4	94.51	94.38	94.43	94.83	94.2	94.33	94.29	94.64	94.37	94.62
F	Average Height	94.435	94.4275	94.425	94.7175	94.375	94.345	94.3675	94.6225	94.3225	94.5975
G	Diameter 1	150.1	149.99	150.02	149.96	150.04	150	150.02	149.92	150.16	150.05
H	Diameter 2	149.96	150.1	149.94	149.95	150	150.13	149.99	150.02	150.06	149.93
I	Average Diameter	150.03	150.045	149.98	149.955	150.02	150.065	150.005	149.97	150.11	149.99
J	G_{mb} [A/(F*π*I^2/4)]	2.383	2.385	2.389	2.371	2.387	2.387	2.385	2.370	2.385	2.368
K	Air Voids [(G_{mm}-J)/G_{mm}]	8.5	8.4	8.3	8.9	8.3	8.3	8.4	9.0	8.4	9.0
	Sample	1	2	3	4	5	6	7	8	9	10
A	Dry Mass	3977.7	3982.6	3985.4	3967	3982.1	3983.6	3977.8	3962	3980.7	3958.8
B	Submerged Mass	2362.2	2360.9	2363.2	2341.5	2360.7	2367.6	2364.8	2339.8	2364.7	2337.2
C	SSD Mass	3990.9	3993	3992.1	3981.4	3992.2	3995.6	3989.6	3976.9	3996.5	3973.8
D	G_{mb} [A/(C-B)]	2.442	2.440	2.447	2.419	2.441	2.447	2.448	2.420	2.439	2.419
E	Air Voids [(G_{mm}-D)/G_{mm}]	6.2	6.3	6.0	7.1	6.3	6.0	6.0	7.1	6.3	7.1

Project Number:
Location: US-23 Heartland
Contractor:
Mix:
Gradation:
G_{mm} 2.492

	Sample	1	2	3	4	5	6	7	8	9	10
A	Dry Mass	3683.5	3676.6	3680	3675	3684.4	3684	3680.1	3681.2	3681.5	3680.5
B	Height 1	94.3	94.3	94.44	94.31	94.5	94.5	94.76	94.69	94.77	94.5
C	Height 2	94.34	94.39	94.18	94.55	94.3	94.66	94.55	94.75	95.21	93.91
D	Height 3	94.16	94.21	94.86	94.6	94.98	94.15	94.44	94.91	94.55	94.54
E	Height 4	94.4	94.31	94.3	94.84	94.42	94.74	94.57	94.66	95.13	94.52
F	Average Height	94.3	94.3025	94.445	94.575	94.55	94.5125	94.58	94.7525	94.915	94.3675
G	Diameter 1	150.04	149.87	150.04	149.67	149.91	150.2	150.11	150.32	149.77	150.01
H	Diameter 2	150.24	149.99	150.17	150.21	150.54	150.22	150.23	150.04	150.66	150.14
I	Average Diameter	150.14	149.93	150.105	149.94	150.225	150.21	150.17	150.18	150.215	150.075
J	G_{mb} [A/(F*π*I^2/4)]	2.206	2.208	2.202	2.201	2.199	2.200	2.197	2.193	2.189	2.205
K	Air Voids [(G_{mm}-J)/G_{mm}]	11.5	11.4	11.6	11.7	11.8	11.7	11.8	12.0	12.2	11.5
	Sample	1	2	3	4	5	6	7	8	9	10
A	Dry Mass	3683.5	3676.6	3680	3675	3684.4	3684	3680.2	3681.1	3681.5	3680.5
B	Submerged Mass	2108.7	2108.1	2101.8	2123.7	2126.6	2128.8	2122.2	2114.2	2105.9	2108.5
C	SSD Mass	3713.6	3704.8	3706.2	3708.6	3715.1	3711.4	3710.8	3706.6	3706.2	3703.4
D	G_{mb} [A/(C-B)]	2.295	2.303	2.294	2.319	2.319	2.328	2.317	2.312	2.301	2.308
E	Air Voids [(G_{mm}-D)/G_{mm}]	7.9	7.6	8.0	7.0	6.9	6.6	7.0	7.2	7.7	7.4

Project Number:
Location: I-75 Levering Rd
Contractor:
Mix:
Gradation:
G_{mm} 2.443

	Sample	1	2	3	4	5	6	7	8	9	10
A	Dry Mass	3737.1	3737.7	3736.4	3734.9	3736.2	3742.7	3737.9	3736.3	3743.9	3738.3
B	Height 1	94.88	94.29	94.6	94.31	94.3	94.46	94.41	94.34	94.29	94.56
C	Height 2	94.77	94.28	94.75	94.37	94.3	94.61	94.68	94.54	94.33	94.38
D	Height 3	94.45	94.84	94.82	94.25	94.5	94.41	94.33	94.76	94.3	94.53
E	Height 4	94.57	94.13	94.34	94.26	94.57	94.32	94.46	94.4	94.42	94.36
F	Average Height	94.6675	94.385	94.6275	94.2975	94.4175	94.45	94.47	94.51	94.335	94.4575
G	Diameter 1	149.96	149.76	150.07	149.88	149.94	150	150.01	149.96	149.67	149.96
H	Diameter 2	149.91	149.9	150.03	149.88	150.02	149.98	150.03	149.94	150	150
I	Average Diameter	149.935	149.83	150.05	149.88	149.98	149.99	150.02	149.95	149.835	149.98
J	G_{mb} [A/(F*π*I^2/4)]	2.236	2.246	2.233	2.245	2.240	2.243	2.238	2.239	2.251	2.240
K	Air Voids [(G_{mm}-J)/G_{mm}]	8.5	8.1	8.6	8.1	8.3	8.2	8.4	8.4	7.9	8.3
	Sample	1	2	3	4	5	6	7	8	9	10
A	Dry Mass	3736.9	3737.4	3736.5	3734.9	3736.2	3742.6	3737.5	3736.1	3743.7	3738.6
B	Submerged Mass	2111.3	2115.6	2110.8	2113.6	2121.8	2124.6	2118	2115.2	2123.3	2118.9
C	SSD Mass	3747.3	3748.9	3747.5	3748.7	3750.7	3753.9	3752.8	3748.5	3757.3	3750.8
D	G_{mb} [A/(C-B)]	2.284	2.288	2.283	2.284	2.294	2.297	2.286	2.287	2.291	2.291
E	Air Voids [(G_{mm}-D)/G_{mm}]	6.5	6.3	6.6	6.5	6.1	6.0	6.4	6.4	6.2	6.2

Project Number:
Location: I-196 Grand Rapids
Contractor:
Mix:
Gradation:
G_{mm} 2.499

	Sample	1	2	3	4	5	6	7	8	9	10
A	Dry Mass	3806.2	3810.7	3806.6	3808.3	3808.8	3806.3	3805.4	3812.1	3806.1	3804.2
B	Height 1	94.48	94.5	94.27	94.73	94.53	94.58	94.64	94.49	94.51	94.56
C	Height 2	94.57	94.53	94.36	94.44	94.48	94.41	94.48	94.56	94.46	94.65
D	Height 3	94.5	94.51	94.51	94.49	94.58	94.57	94.73	94.59	94.75	94.46
E	Height 4	94.41	94.53	94.5	94.88	94.55	94.53	94.7	94.4	94.54	94.46
F	Average Height	94.49	94.5175	94.41	94.635	94.535	94.5225	94.6375	94.51	94.565	94.5325
G	Diameter 1	150.05	149.98	150.02	150.12	150.03	149.9	150.15	150.02	150.05	150.07
H	Diameter 2	150.08	150.2	150.03	150.15	150.11	150.07	150.06	150.14	150.08	150.1
I	Average Diameter	150.065	150.09	150.025	150.135	150.07	149.985	150.105	150.08	150.065	150.085
J	G_{mb} [A/(F*π*I^2/4)]	2.277	2.279	2.281	2.273	2.278	2.279	2.272	2.280	2.276	2.275
K	Air Voids [(G_{mm}-J)/G_{mm}]	8.9	8.8	8.7	9.0	8.9	8.8	9.1	8.8	8.9	9.0
	Sample	1	2	3	4	5	6	7	8	9	10
A	Dry Mass	3806.2	3810.7	3806.6	3808.3	3808.8	3806.3	3805.4	3812.1	3806.1	3804.2
B	Submerged Mass	2184.4	2193.5	2190.2	2185.2	2185.7	2187.7	2183.5	2193.6	2186	2188.6
C	SSD Mass	3819.6	3829.5	3823.3	3826.1	3822.6	3821.2	3819.4	3827.4	3822.2	3822.5
D	G_{mb} [A/(C-B)]	2.328	2.329	2.331	2.321	2.327	2.330	2.326	2.333	2.326	2.328
E	Air Voids [(G_{mm}-D)/G_{mm}]	6.9	6.8	6.7	7.1	6.9	6.8	6.9	6.6	6.9	6.8

Project Number:
Location: I-75 Clarkston
Contractor:
Mix:
Gradation:
G_{mm} 2.487

	Sample	1	2	3	4	5	6	7	8	9	10
A	Dry Mass	3764.5	3763.5	3770.9	3766.9	3766.3	3763.7	3767.2	3770.3	3763.3	3767.8
B	Height 1	94.39	94.44	94.46	94.42	94.42	94.36	94.37	94.36	94.33	94.4
C	Height 2	94.56	94.46	94.64	94.36	94.34	94.28	94.52	94.48	94.23	94.34
D	Height 3	94.39	94.42	94.39	94.3	94.3	94.49	94.59	94.4	94.47	94.42
E	Height 4	94.26	94.49	94.45	94.31	94.52	94.4	94.44	94.34	94.45	94.39
F	Average Height	94.400	94.453	94.485	94.348	94.395	94.383	94.480	94.395	94.370	94.388
G	Diameter 1	150.18	150.07	149.96	150.09	149.96	150.06	150.14	149.94	150.14	150.01
H	Diameter 2	150.08	150.11	150.04	150	150.07	150.03	150.31	149.92	150.08	150.02
I	Average Diameter	150.130	150.090	150.000	150.045	150.015	150.045	150.225	149.930	150.110	150.015
J	G_{mb} [A/(F*π*I^2/4)]	2.253	2.252	2.258	2.258	2.257	2.255	2.250	2.262	2.253	2.258
K	Air Voids [(G_{mm}-J)/G_{mm}]	9.4	9.4	9.2	9.2	9.2	9.3	9.5	9.0	9.4	9.2
	Sample	1	2	3	4	5	6	7	8	9	10
A	Dry Mass	3764.5	3763.5	3770.9	3766.9	3766.3	3763.7	3767.2	3770.3	3763.3	3767.8
B	Submerged Mass	2155.2	2158.2	2162.9	2154.6	2157.2	2156.6	2152.4	2158.6	2154.1	2155.9
C	SSD Mass	3778.3	3781.5	3784.5	3782.5	3781.4	3778.3	3782.5	3783.8	3778.9	3780
D	G_{mb} [A/(C-B)]	2.319	2.318	2.325	2.314	2.319	2.321	2.311	2.320	2.316	2.320
E	Air Voids [(G_{mm}-D)/G_{mm}]	6.7	6.8	6.5	7.0	6.8	6.7	7.1	6.7	6.9	6.7

Project Number:
Location: M-53 Detroit
Contractor:
Mix:
Gradation:
G_{mm} 2.563

	Sample	1	2	3	4	5	6	7	8	9	10
A	Dry Mass	3884	3886.4	3891.6	3884.7	3878.5	3883.8	3878.4	3879.4	3879.4	3877.3
B	Height 1	94.39	94.25	94.3	94.31	94.48	94.31	94.28	94.55	94.29	94.43
C	Height 2	94.31	94.3	94.59	94.46	94.23	94.35	94.4	94.36	94.45	94.34
D	Height 3	94.35	94.18	94.41	94.51	94.28	94.36	94.4	94.45	94.53	94.37
E	Height 4	94.4	94.54	94.34	94.72	94.5	94.37	94.41	94.41	94.4	94.57
F	Average Height	94.3625	94.3175	94.41	94.5	94.3725	94.3475	94.3725	94.4425	94.4175	94.4275
G	Diameter 1	150.02	150.11	149.98	149.95	150.09	150.07	149.98	150.07	150.01	150.17
H	Diameter 2	150.19	150.03	150.1	150	150.16	150.09	149.95	150.17	150.26	150.06
I	Average Diameter	150.105	150.07	150.04	149.975	150.125	150.08	149.965	150.12	150.135	150.115
J	G_{mb} [A/(F*π*I^2/4)]	2.326	2.330	2.331	2.327	2.322	2.327	2.327	2.321	2.321	2.320
K	Air Voids [(G_{mm}-J)/G_{mm}]	9.2	9.1	9.0	9.2	9.4	9.2	9.2	9.5	9.4	9.5
	Sample	1	2	3	4	5	6	7	8	9	10
A	Dry Mass	3884	3886.4	3891.6	3884.7	3878.5	3883.8	3878.4	3879.4	3879.4	3877.3
B	Submerged Mass	2293.8	2290.2	2294.1	2289.5	2279.5	2288.9	2284.4	2276.4	2278.6	2272.6
C	SSD Mass	3905.9	3907.9	3911.7	3903.1	3897.3	3904	3898	3898.5	3896.7	3894.5
D	G_{mb} [A/(C-B)]	2.409	2.402	2.406	2.407	2.397	2.405	2.404	2.392	2.398	2.391
E	Air Voids [(G_{mm}-D)/G_{mm}]	6.0	6.3	6.1	6.1	6.5	6.2	6.2	6.7	6.5	6.7

Project Number:
Location: Michigan Ave Dearborn
Contractor:
Mix: 4 E 10
Gradation:
G_{mm} 2.485

	Sample	1	2	3	4	5	6	7	8	9	10
A	Dry Mass	3740.3	3735.1	3738.8	3747.1	3742.2	3746.6	3742.2	3747.3	3748.3	3748.2
B	Height 1	94.45	94.41	94.55	94.28	94.38	94.18	94.44	94.28	94.54	94.27
C	Height 2	94.46	94.53	94.6	94.25	94.46	94.39	94.33	94.3	94.43	94.37
D	Height 3	94.9	94.38	94.46	94.41	94.34	94.43	94.32	94.54	94.32	94.41
E	Height 4	94.5	94.5	94.34	94.27	94.45	94.27	94.45	94.34	94.25	94.42
F	Average Height	94.5775	94.455	94.4875	94.3025	94.4075	94.3175	94.385	94.365	94.385	94.3675
G	Diameter 1	150.09	150.27	150.46	150.13	150.18	150.17	150.06	150.01	150.17	150.15
H	Diameter 2	150.2	150.22	150.24	150.16	150.09	150.09	149.97	150.05	150.08	150.06
I	Average Diameter	150.145	150.245	150.35	150.145	150.135	150.13	150.015	150.03	150.125	150.105
J	G_{mb} [A/(F*π*I^2/4)]	2.234	2.230	2.229	2.244	2.239	2.244	2.243	2.246	2.244	2.245
K	Air Voids [(G_{mm}-J)/G_{mm}]	10.1	10.2	10.3	9.7	9.9	9.7	9.7	9.6	9.7	9.7
	Sample	1	2	3	4	5	6	7	8	9	10
A	Dry Mass	3740.3	3735.1	3738.8	3747.1	3742.2	3746.6	3742.2	3747.3	3748.3	3748.2
B	Submerged Mass	2139.7	2136.7	2139.5	2146	2139.5	2146.8	2144.8	2141	2146	2141.6
C	SSD Mass	3753.5	3749.7	3752.4	3760.5	3754.7	3763.1	3762.1	3758.2	3766.5	3762
D	G_{mb} [A/(C-B)]	2.318	2.316	2.318	2.321	2.317	2.318	2.314	2.317	2.313	2.313
E	Air Voids [(G_{mm}-D)/G_{mm}]	6.7	6.8	6.7	6.6	6.8	6.7	6.9	6.8	6.9	6.9

Project Number:
Location: I-75 Toledo
Contractor:
Mix:
Gradation:
G_{mm} 2.507

	Sample	1	2	3	4	5	6	7	8	9	10
A	Dry Mass	3808.9	3801.3	3802.1	3812.6	3803.6	3805.5	3803.6	3808.4	3805.9	3806.9
B	Height 1	94.45	94.46	94.52	94.27	94.5	94.37	94.38	94.43	94.46	94.39
C	Height 2	94.37	94.39	94.41	94.42	94.54	94.43	94.49	94.55	94.47	94.62
D	Height 3	94.35	94.43	94.35	94.41	94.49	94.4	94.62	94.42	94.41	94.5
E	Height 4	94.47	94.45	94.37	94.46	94.46	94.54	94.46	94.37	94.42	94.3
F	Average Height	94.41	94.4325	94.4125	94.39	94.4975	94.435	94.4875	94.4425	94.44	94.4525
G	Diameter 1	149.92	150.14	150.14	149.94	150.07	149.98	150.06	150.04	149.95	150.09
H	Diameter 2	149.98	150.09	150.13	149.97	150.07	149.99	150.07	150.04	150.02	150.23
I	Average Diameter	149.95	150.115	150.135	149.955	150.07	149.985	150.065	150.04	149.985	150.16
J	G_{mb} [A/(F*π*I^2/4)]	2.285	2.274	2.275	2.287	2.276	2.281	2.276	2.281	2.281	2.276
K	Air Voids [(G_{mm}-J)/G_{mm}]	8.9	9.3	9.3	8.8	9.2	9.0	9.2	9.0	9.0	9.2
	Sample	1	2	3	4	5	6	7	8	9	10
A	Dry Mass	3808.9	3801.3	3802.1	3812.6	3803.6	3805.5	3803.6	3808.4	3805.9	3806.9
B	Submerged Mass	2203.3	2196.7	2197.7	2207.1	2206.8	2205	2202.5	2203.1	2204.1	2200.5
C	SSD Mass	3826.4	3822.4	3823.2	3831.1	3828.5	3829.6	3823.7	3828.1	3827.3	3826.5
D	G_{mb} [A/(C-B)]	2.347	2.338	2.339	2.348	2.345	2.342	2.346	2.344	2.345	2.341
E	Air Voids [(G_{mm}-D)/G_{mm}]	6.4	6.7	6.7	6.4	6.4	6.6	6.4	6.5	6.5	6.6

Project Number:
Location: I-94 Ann Arbor
Contractor:
Mix: SMA
Gradation:
G_{mm} 2.515

	Sample	1	2	3	4	5	6	7	8	9	10
A	Dry Mass	3757.4	3758.7	3750	3753.8	3759.2	3756.3	3754.7	3757	3756.8	3757.7
B	Height 1	94.24	94.11	94.37	94.33	94.46	94.34	94.38	94.23	94.26	94.27
C	Height 2	94.3	94.3	94.36	94.59	94.23	94.41	94.23	94.3	94.45	94.25
D	Height 3	94.03	94.3	94.17	95.16	94.07	94.17	94.21	94.36	94.4	94.34
E	Height 4	93.84	94.25	94.37	94.39	94.26	94.06	94.36	94.37	94.25	94.53
F	Average Height	94.1025	94.24	94.3175	94.6175	94.255	94.245	94.295	94.315	94.34	94.3475
G	Diameter 1	150.01	150.12	150	149.98	149.93	149.96	150.15	149.93	149.94	150.04
H	Diameter 2	150.25	150.16	150.06	150.2	149.9	149.95	150.06	149.98	149.92	150.07
I	Average Diameter	150.13	150.14	150.03	150.09	149.915	149.955	150.105	149.955	149.93	150.055
J	G_{mb} [A/(F*π*I^2/4)]	2.256	2.253	2.249	2.242	2.259	2.257	2.250	2.256	2.256	2.252
K	Air Voids [(G_{mm}-J)/G_{mm}]	10.3	10.4	10.6	10.8	10.2	10.3	10.5	10.3	10.3	10.5
	Sample	1	2	3	4	5	6	7	8	9	10
A	Dry Mass	3757.4	3758.7	3750	3753.8	3759.2	3756.3	3754.7	3757	3756.8	3757.7
B	Submerged Mass	2197.4	2198.4	2191.2	2189.1	2192.4	2190.1	2189.2	2189.5	2198.8	2186.8
C	SSD Mass	3786.3	3787.8	3783.2	3784.4	3788	3782.5	3783.4	3782.8	3789.2	3781.6
D	G_{mb} [A/(C-B)]	2.365	2.365	2.356	2.353	2.356	2.359	2.355	2.358	2.362	2.356
E	Air Voids [(G_{mm}-D)/G_{mm}]	6.0	6.0	6.3	6.4	6.3	6.2	6.4	6.2	6.1	6.3

Phase II – 150mm Superpave Specimens for Dynamic Modulus (Parametric Study)

G_{mb}'S

Project I-196 Grand Rapids
Gmm 2.499

H_2O Temp: _____ Saturated Surface Dry Method

Sample	1	2	3	4	5	6	7	8	9	10	11	12	13	14	15	16	17	18
A) Dry Mass	6809.1	6816.0	6815.2	6814.0	6820.3	6813.4	6816.7	6815.1	6809.2	6812.4	6813.1	6816.5	6822.2	6813.5	6816.1	6809.9	6815.1	6820.1
B) Submerged Mass	3899.4	3903.5	3903.8	3914.3	3906.0	3910.5	3906.7	3910.4	3907.4	3916.8	3914	3910.4	3910.5	3909.6	3908.1	3911.9	3907.5	3907
C) SSD Mass	6853.2	6853.7	6856.7	6865.9	6860.6	6863.7	6870.2	6860.1	6860.9	6863.6	6864.4	6861.8	6861.4	6859	6863.4	6858.2	6861.6	6859.6
D) G_{mb} [A/(C-B)]	2.305	2.310	2.308	2.309	2.308	2.307	2.300	2.310	2.305	2.312	2.309	2.310	2.312	2.310	2.306	2.311	2.307	2.310
E) Air Voids [(G_{mm}-D)/G_{mm}]	7.8%	7.5%	7.6%	7.6%	7.6%	7.7%	8.0%	7.5%	7.7%	7.5%	7.6%	7.6%	7.5%	7.6%	7.7%	7.5%	7.7%	7.6%

G_{mb}'s

Project I-75 Clarkston
Gmm 2.487

H_2O Temp: _____

Saturated Surface Dry Method

Sample	1	2	3	4	5	6	7	8	9	10	11	12	13	14	15	16	17	18
A) Dry Mass	6741.4	6742.7	6753.5	6741.6	6751.4	6743.0	6748.8	6749.6	6748.3	6750.9	6745.1	6747.3	6749.9	6752.1	6742.3	6746.8	6749.1	6748.4
B) Submerged Mass	3842.8	3842.0	3861.5	3849.1	3860.2	3853.8	3853.4	3852.7	3857	3855.5	3850.6	3856.5	3855.5	3860.8	3851.5	3850.3	3860.1	3847.9
C) SSD Mass	6783.4	6781.2	6799.2	6786.8	6792.1	6785.2	6789.3	6791.4	6791	6792.8	6785.5	6787.9	6790.5	6796.8	6785.3	6787.6	6793.9	6784.9
D) G_{mb} [A/(C-B)]	2.293	2.294	2.299	2.295	2.303	2.300	2.299	2.297	2.300	2.298	2.298	2.302	2.300	2.300	2.298	2.297	2.300	2.298
E) Air Voids $[(G_{mm}-D)/G_{mm}]$	7.8%	7.8%	7.6%	7.7%	7.4%	7.5%	7.6%	7.6%	7.5%	7.6%	7.6%	7.4%	7.5%	7.5%	7.6%	7.6%	7.5%	7.6%

Phase II – 100mm Superpave Specimens for Dynamic Modulus (Parametric Study) Cut and Cored from 150mm Diameter Superpave Specimens

Project Number:
Location: I-196 Grand Rapids
Contractor:
Mix:
Gradation:
G_{mm} 2.499

	Sample	1	2	3	4	5	6	7	8	9	10	11	12	13	14	15	16	17	18
A	Dry Mass	2842.8	2847.9	2848.9	2850	2854.5	2853.9	2846.9	2857.3	2849.6	2858.7	2861.4	2855.6	2859.4	2858.5	2855.8	2862.7	2855.3	2855.1
B	Height 1	151.3	151.35	151.23	151.52	151.39	151.32	151.37	151.45	151.23	151.33	151.49	151.38	151.52	151.45	151.55	151.92	151.43	151.54
C	Height 2	151.43	151.31	151.18	151.34	151.36	151.44	151.47	151.47	151.44	151.33	151.34	151.44	151.41	151.42	151.45	151.69	151.34	151.55
D	Height 3	151.41	151.36	151.46	151.27	151.41	151.34	151.43	151.66	151.25	151.27	151.37	151.45	151.4	151.5	151.55	151.55	151.43	151.47
E	Height 4	151.21	151.48	151.37	151.51	151.41	151.61	151.42	151.43	151.43	151.44	151.44	151.33	151.63	151.42	151.59	151.53	151.53	151.53
F	Average Height	151.3375	151.375	151.31	151.41	151.3925	151.4275	151.4225	151.5025	151.3375	151.3425	151.41	151.4	151.49	151.4475	151.535	151.6725	151.4325	151.5225
G	Top Diameter 1	100.98	100.98	101.01	101.02	101.08	101.04	101	101.08	101.12	101.15	101.09	101.14	101.05	101.07	101.07	101.07	101	101.13
H	Top Diameter 2	101.09	101.07	101.1	101.09	101.06	101.05	101.07	101.08	101.1	101.05	101.1	101.05	101.08	101.01	101.04	100.96	101.03	100.93
	Middle Diameter 1	100.98	100.98	101.06	101.02	101.02	101	101	100.99	101.05	101.13	101.06	101.05	101.03	101.12	101.05	101.06	101.05	101.04
	Middle Diameter 2	100.97	101.02	101.03	101.03	101.07	101.13	101.13	101.03	101.07	100.97	101.06	101.02	101.09	101.09	101.03	101.02	101.03	100.96
	Bottom Diameter 1	101.01	101.06	101.16	101.08	101.08	101.06	101.08	101.1	101.1	101.15	101.15	101.21	101.12	101.09	101.02	101.08	101.07	101.06
	Bottom Diameter 2	101.01	101.03	101.02	101.01	101.02	101	101.03	101.05	101.1	101.04	101.04	101.09	101.06	101.06	101.09	101.05	101.01	101.05
I	Average Diameter	101.0067	101.0233	101.0633	101.0417	101.055	101.0467	101.0517	101.055	101.09	101.0817	101.0833	101.0933	101.0717	101.0733	101.05	101.04	101.0317	101.0283
J	G_{mb} [A/(Pi*r^2*4)]	2.344	2.347	2.347	2.347	2.351	2.350	2.344	2.351	2.346	2.354	2.355	2.350	2.353	2.352	2.350	2.354	2.352	2.351
K	Air Voids [(G_{mm}-J)/G_{mm}]	6.2	6.1	6.1	6.1	5.9	6.0	6.2	5.9	6.1	5.8	5.8	6.0	5.9	5.9	6.0	5.8	5.9	5.9

	Sample	1	2	3	4	5	6	7	8	9	10	11	12	13	14	15	16	17	18
A	Dry Mass	2842.8	2847.9	2848.9	2850	2854.5	2853.9	2846.9	2857.3	2849.6	2858.7	2861.4	2855.6	2859.4	2858.5	2855.8	2862.7	2855.3	2855.1
B	Submerged Mass	1635.5	1639.6	1639.4	1643.5	1644.1	1645	1638.1	1647.3	1640.8	1650.3	1651.2	1645.4	1648.6	1648.2	1645.4	1652.3	1645.6	1645.2
C	SSD Mass	2855.5	2860	2859.6	2863.8	2866	2866	2859.6	2868.2	2860.6	2869.8	2871.8	2865.9	2869.3	2868.9	2866.6	2874	2866.7	2866.8
D	G_{mb} [A/(C-B)]	2.330	2.334	2.335	2.335	2.336	2.337	2.331	2.340	2.336	2.344	2.344	2.340	2.342	2.342	2.339	2.343	2.338	2.337
E	Air Voids [(G_{mm}-D)/G_{mm}]	6.8	6.6	6.6	6.5	6.5	6.5	6.7	6.3	6.5	6.2	6.2	6.4	6.3	6.3	6.4	6.2	6.4	6.5

Project Number:
Location: I-75 Clarkston
Contractor:
Mix:
Gradation:
G_{mm} 2.487

	Sample	1	2	3	4	5	6	7	8	9	10	11	12	13	14	15	16	17	18
A	Dry Mass	2828.9	2827.4	2840.5	2827.7	2832.3	2839.3	2841.5	2829.7	2859.8	2842.8	2840.1	2847.9	2840.2	2847.3	2835.9	2841.1	2843.7	2847.2
B	Height 1	151.45	151.41	151.4	151.39	151.33	151.27	151.31	151.51	151.69	151.45	151.72	151.13	151.3	151.22	151.4	151.48	151.2	151.35
C	Height 2	151.22	151.57	151.45	151.38	151.34	151.33	151.51	151.32	151.67	151.36	151.64	151.14	151.21	151.38	151.37	151.56	151.68	151.28
D	Height 3	151.2	151.42	151.39	151.43	151.2	151.64	151.4	151.4	152.02	151.16	151.25	151.33	151.34	151.4	151.26	151.36	151.26	151.43
E	Height 4	151.4	151.5	151.38	151.26	151.38	151.47	151.26	151.44	151.87	151.15	151.33	151.6	151.41	151.5	151.37	151.43	151.67	151.56
F	Average Height	151.3175	151.475	151.405	151.365	151.3125	151.4275	151.37	151.4175	151.8125	151.28	151.485	151.3	151.315	151.375	151.35	151.4575	151.4525	151.405
G	Top Diameter 1	101.28	100.99	101.01	101.07	101.03	100.99	101.08	100.96	101.11	101.1	101.01	101.09	101.03	101.05	101.1	101.08	100.94	101.02
H	Top Diameter 2	101.04	101.01	101.11	100.97	101.08	101.02	101.02	101.09	100.98	100.96	100.55	101.04	100.96	101.02	100.96	100.93	100.66	101.15
	Middle Diameter 1	101.03	100.99	100.98	101.01	100.99	100.95	101.12	101.05	101.03	101	100.86	100.97	101.01	101.02	101.07	100.99	100.69	101.01
	Middle Diameter 2	101	100.99	101.07	100.99	100.99	101.03	100.99	101.13	100.93	101.01	100.98	101.04	100.96	101.11	100.99	100.93	101.13	101.05
	Bottom Diameter 1	100.97	101.05	101.03	100.95	101	101.04	100.98	100.99	101.04	100.98	101	100.94	100.95	101.16	100.95	101.13	100.99	101.23
	Bottom Diameter 2	101.1	100.97	101.06	101.06	101.01	100.93	101.04	101.01	101.03	100.97	101.01	101.07	101.11	100.98	101.12	100.94	101.04	101.03
I	Average Diameter	101.07	101.00	101.04	101.01	101.02	100.99	101.04	101.04	101.02	101.00	100.90	101.03	101.00	101.06	101.03	101.00	100.91	101.08
J	G_{mb} [A/(F*π*t^2/4)]	2.330	2.330	2.340	2.331	2.336	2.341	2.341	2.331	2.350	2.345	2.345	2.348	2.343	2.345	2.337	2.341	2.348	2.343
K	Air Voids [(G_{mm}-J)/G_{mm}]	6.3	6.3	5.9	6.3	6.1	5.9	5.9	6.3	5.5	5.7	5.7	5.6	5.8	5.7	6.0	5.9	5.6	5.8

	Sample	1	2	3	4	5	6	7	8	9	10	11	12	13	14	15	16	17	18
A	Dry Mass	2828.9	2827.4	2840.5	2827.7	2832.3	2839.3	2841.5	2829.7	2859.8	2842.8	2840.1	2847.9	2840.2	2847.3	2835.9	2841.1	2843.7	2847.2
B	Submerged Mass	1623.1	1619.5	1632.8	1620.5	1626	1629.3	1633.3	1621.2	1646.1	1630.3	1634.8	1638.9	1631	1637.9	1627.6	1632.1	1638.3	1637.1
C	SSD Mass	2842.5	2838.5	2852.4	2838.8	2843.9	2849.6	2852.4	2840.3	2870.1	2850.4	2852	2858	2849.5	2857.1	2846.9	2852.2	2854.4	2857.4
D	G_{mb} [A/(C-B)]	2.320	2.319	2.329	2.321	2.326	2.327	2.331	2.321	2.336	2.330	2.333	2.336	2.331	2.335	2.326	2.329	2.338	2.333
E	Air Voids [(G_{mm}-D)/G_{mm}]	6.7	6.7	6.4	6.7	6.5	6.4	6.3	6.7	6.1	6.3	6.2	6.1	6.3	6.1	6.5	6.4	6.0	6.2

Phase II – 150mm Superpave Specimens for Dynamic Modulus Testing

Project Number:
Location: M-50 Dundee
Contractor:
Mix: 3 E 1
Gradation:
G_{mm} 2.52

	Sample	1	2	3	4	5	6	7	8	9	10
A	Dry Mass	6695.8	6614.4	6693.8	6622	6621.5	6677.9	6619.6	6682.8	6622.6	6623.73
B	Height 1	168.31	168.92	168.04	168.35	168.21	168.53	168.4	168.24	168.51	168.74
C	Height 2	168.4	168.59	167.93	168.36	168.52	168.72	168.65	168.09	168.45	168.74
D	Height 3	168.15	168.68	167.81	168.5	168.42	168.43	168.63	168.54	168.34	168.57
E	Height 4	168.39	169.07	168.04	168.47	168.53	168.72	168.82	168.46	168.08	168.47
F	Average Height	168.3125	168.815	167.955	168.42	168.42	168.6	168.625	168.3325	168.345	168.63
G	Diameter 1	150.61	150.61	150.18	150.91	150.49	150.36	150.77	150.13	150.76	150.46
H	Diameter 2	150.58	150.58	150.42	150.41	150.63	150.38	150.63	150.03	151.11	150.27
I	Average Diameter	150.595	150.595	150.3	150.66	150.56	150.37	150.7	150.08	150.935	150.365
J	G_{mb} [A/(F*π*I^2/4)]	2.233	2.200	2.246	2.206	2.208	2.230	2.201	2.244	2.199	2.212
K	Air Voids [(G_{mm}-J)/G_{mm}]	11.4	12.7	10.9	12.5	12.4	11.5	12.7	10.9	12.8	12.2
	Sample	1	2	3	4	5	6	7	8	9	10
A	Dry Mass	6695.8	6614.4	6693.8	6622	6621.5	6677.9	6619.6	6682.8	6622.6	6623.73
B	Submerged Mass	3852.7	3840.2	3848.4	3839	3865.1	3856.8	3843.8	3890	3847.1	3871.1
C	SSD Mass	6738.2	6679.2	6728.1	6695.3	6695.5	6732.5	6699.6	6750.3	6700.8	6701.8
D	G_{mb} [A/(C-B)]	2.320	2.330	2.324	2.318	2.339	2.322	2.318	2.336	2.321	2.340
E	Air Voids [(G_{mm}-D)/G_{mm}]	7.9	7.5	7.8	8.0	7.2	7.8	8.0	7.3	7.9	7.1

Project Number:
Location: M-36 Pinckney
Contractor:
Mix:
Gradation:
G_{mm} 2.511

	Sample	1	2	3	4	5	6	7	8	9	10
A	Dry Mass	6611.6	6616	6705.6	6617	6713.5	6715.2	6714.6	6707.6	6611.5	6711.9
B	Height 1	169.03	169.2	169.26	169.23	169.31	169.3	169.38	169.23	169.29	169.27
C	Height 2	169.02	169.2	169.38	169.07	169.28	169.32	169.34	169.62	169.05	169.26
D	Height 3	169.3	169.08	169.27	169.32	169.46	169.34	169.21	169.34	169.19	169.32
E	Height 4	169.08	169.04	169.25	169.26	169.56	169.26	169.17	169.25	169.33	169.25
F	Average Height	169.1075	169.13	169.29	169.22	169.4025	169.305	169.275	169.36	169.215	169.275
G	Diameter 1	150.21	150.12	150.11	150.08	150.16	150.14	150.02	150.02	150.13	150.07
H	Diameter 2	150.06	150.14	150.03	150.25	150.24	150.26	150.02	150.08	150.14	149.97
I	Average Diameter	150.135	150.13	150.07	150.165	150.2	150.2	150.02	150.05	150.135	150.02
J	G_{mb} [A/(F*π*I^2/4)]	2.208	2.210	2.239	2.208	2.237	2.239	2.244	2.240	2.207	2.243
K	Air Voids [(G_{mm}-J)/G_{mm}]	12.0	12.0	10.8	12.1	10.9	10.9	10.6	10.8	12.1	10.7
	Sample	1	2	3	4	5	6	7	8	9	10
A	Dry Mass	6611.6	6616	6705.6	6617	6713.5	6715.2	6714.6	6707.6	6611.5	6711.9
B	Submerged Mass	3835.5	3830.9	3873.3	3835.5	3876.9	3885	3883.8	3865.6	3843.1	3870.1
C	SSD Mass	6681.9	6682.2	6763.4	6681.2	6769.9	6765.8	6775.3	6764.5	6687.4	6755
D	G_{mb} [A/(C-B)]	2.323	2.320	2.320	2.325	2.321	2.331	2.322	2.314	2.324	2.327
E	Air Voids [(G_{mm}-D)/G_{mm}]	7.5	7.6	7.6	7.4	7.6	7.2	7.5	7.9	7.4	7.3

Project Number:
Location: M-45 Grand Rapids
Contractor:
Mix:
Gradation:
G_{mm} 2.513

	Sample	1	2	3	4	5	6	7	8	9	10
A	Dry Mass	6877.6	6876.8	6879.6	6874.6	6877.6	6875.6	6880.3	6878.9	6886.1	6878.9
B	Height 1	168.91	168.49	168.81	168.65	168.72	168.97	168.64	168.82	168.57	168.73
C	Height 2	168.63	168.73	169.05	169.04	168.77	168.78	168.91	168.73	168.94	168.72
D	Height 3	168.66	168.64	168.9	168.84	169.11	168.66	168.86	168.65	168.9	168.84
E	Height 4	168.84	168.6	168.68	168.7	168.94	168.7	168.61	168.81	168.75	169.26
F	Average Height	168.76	168.615	168.86	168.8075	168.885	168.7775	168.755	168.7525	168.79	168.8875
G	Diameter 1	149.99	149.9	149.93	149.93	150.01	150.01	149.93	149.97	149.98	150.11
H	Diameter 2	150.02	149.97	150	149.94	149.93	149.98	149.99	149.91	150.05	149.97
I	Average Diameter	150.005	149.935	149.965	149.935	149.97	149.995	149.96	149.94	150.015	150.04
J	G_{mb} [A/(F*π*I^2/4)]	2.306	2.310	2.307	2.307	2.305	2.305	2.308	2.309	2.308	2.304
K	Air Voids [(G_{mm}-J)/G_{mm}]	8.2	8.1	8.2	8.2	8.3	8.3	8.1	8.1	8.2	8.3
	Sample	1	2	3	4	5	6	7	8	9	10
A	Dry Mass	6877.6	6876.8	6879.6	6874.6	6877.6	6875.6	6880.3	6878.9	6886.1	6878.9
B	Submerged Mass	3976.8	3973.5	3973.1	3963.4	3969.4	3972.4	3973.3	3967.3	3954.6	3969.9
C	SSD Mass	6922	6922.8	6925.8	6915.4	6916.9	6919.1	6924.6	6918.4	6916	6923.7
D	G_{mb} [A/(C-B)]	2.335	2.332	2.330	2.329	2.333	2.333	2.331	2.331	2.325	2.329
E	Air Voids [(G_{mm}-D)/G_{mm}]	7.1	7.2	7.3	7.3	7.1	7.1	7.2	7.2	7.5	7.3

Project Number:
Location: M-21 St. Johns
Contractor:
Mix:
Gradation:
G_{mm} 2.489

	Sample	1	2	3	4	5	6	7	8	9	10
A	Dry Mass	6550.4	6553.7	6555.1	6551	6553.3	6556.7	6549.6	6559	6547.5	6557.7
B	Height 1	168.71	168.56	168.44	168.62	169.93	168.94	168.42	168.46	168.91	168.88
C	Height 2	169.27	168.44	168.36	168.48	169.93	168.82	168.47	168.34	169.14	168.54
D	Height 3	168.8	169.35	168.75	168.33	168.77	168.74	168.54	168.44	169.02	169.12
E	Height 4	168.88	168.86	168.44	168.96	168.91	168.68	168.6	168.69	168.88	169.66
F	Average Height	168.915	168.8025	168.4975	168.5975	169.385	168.795	168.5075	168.4825	168.9875	169.05
G	Diameter 1	150.03	150.25	150.37	150.86	150.24	150.06	150.37	150.52	150.3	150.26
H	Diameter 2	150.07	150.32	150.08	150.58	150.25	150.2	150.18	150.23	150.2	150.2
I	Average Diameter	150.05	150.285	150.225	150.72	150.245	150.13	150.275	150.375	150.25	150.23
J	G_{mb} [A/(F*π*I^2/4)]	2.193	2.189	2.195	2.178	2.182	2.194	2.191	2.192	2.185	2.188
K	Air Voids [(G_{mm}-J)/G_{mm}]	11.9	12.1	11.8	12.5	12.3	11.8	12.0	11.9	12.2	12.1
	Sample	1	2	3	4	5	6	7	8	9	10
A	Dry Mass	6551.2	6553.5	6556.1	6551.7	6554	6557.2	6550	6559.7	6547.7	6558.1
B	Submerged Mass	3788.9	3784.8	3781.1	3773.2	3792.3	3797.2	3787.2	3781	3789.8	3799
C	SSD Mass	6645.4	6647.7	6641.2	6631.2	6640.5	6643.3	6628.2	6643.6	6632.2	6644.7
D	G_{mb} [A/(C-B)]	2.293	2.289	2.292	2.292	2.301	2.304	2.306	2.292	2.304	2.305
E	Air Voids [(G_{mm}-D)/G_{mm}]	7.9	8.0	7.9	7.9	7.5	7.4	7.4	7.9	7.4	7.4

Project Number:
Location: M-84 Saginaw
Contractor:
Mix:
Gradation:
G_{mm} 2.543

	Sample	1	2	3	4	5	6	7	8	9	10
A	Dry Mass	6946.1	6945.2	6947.1	6948.9	6948	6951.5	6944.6	6944.4	6948.1	6952.9
B	Height 1	169.16	168.87	169.98	169.94	169.34	168.71	168.86	168.86	168.88	169.09
C	Height 2	168.87	168.93	168.84	168.92	169.12	168.71	169.36	168.96	168.69	169.04
D	Height 3	169.05	168.68	169.12	169.91	168.82	169.14	169.09	169.9	169.04	168.63
E	Height 4	168.7	168.64	169.17	169.02	169.15	168.9	169.08	169.21	169.13	169.11
F	Average Height	168.945	168.78	169.2775	169.4475	169.1075	168.865	169.0975	169.2325	168.935	168.9675
G	Diameter 1	149.93	149.5	149.68	150.08	149.31	149.83	149.96	149.45	149.86	149.8
H	Diameter 2	149.85	150.32	149.81	150.27	149.76	149.83	149.75	149.82	149.76	149.66
I	Average Diameter	149.89	149.91	149.745	150.175	149.535	149.83	149.855	149.635	149.81	149.73
J	G_{mb} [A/(F*π*I^2/4)]	2.330	2.331	2.330	2.315	2.339	2.335	2.329	2.333	2.333	2.337
K	Air Voids [(G_{mm}-J)/G_{mm}]	8.4	8.3	8.4	9.0	8.0	8.2	8.4	8.2	8.2	8.1
	Sample	1	2	3	4	5	6	7	8	9	10
A	Dry Mass	6947.1	6945.8	6947.7	6949.7	6948.6	6952.4	6945.2	6945	6948.7	6953.5
B	Submerged Mass	4047.2	4046.6	4047.9	4045.9	4050.8	4055	4039.5	4053.4	4033.6	4063.8
C	SSD Mass	6992.1	6991.1	6992.3	6991.9	6992.7	6991.9	6987.3	6993.9	6979.1	6997.7
D	G_{mb} [A/(C-B)]	2.359	2.359	2.360	2.359	2.362	2.367	2.356	2.362	2.359	2.370
E	Air Voids [(G_{mm}-D)/G_{mm}]	7.2	7.2	7.2	7.2	7.1	6.9	7.4	7.1	7.2	6.8

Project Number:
Location: BL I-96 Howell
Contractor:
Mix:
Gradation:
G_{mm} 2.501

	Sample	1	2	3	4	5	6	7	8	9	10
A	Dry Mass	6892.8	6890.7	6887	6883.7	6885.9	6886.7	6889.1	6893.8	6892.8	6883.4
B	Height 1	169.75	169.46	169.53	169.49	169.48	169.71	169.85	169.4	169.52	169.42
C	Height 2	169.42	169.73	169.42	169.69	169.33	169.39	170.2	169.56	169.59	169.84
D	Height 3	169.65	169.81	169.45	169.37	169.35	169.56	169.77	169.59	169.58	169.57
E	Height 4	169.36	170.04	169.76	169.59	169.42	169.67	169.68	169.41	169.49	169.59
F	Average Height	169.545	169.76	169.54	169.535	169.395	169.5825	169.875	169.49	169.545	169.605
G	Diameter 1	149.99	149.84	150.04	149.98	150.08	150.14	149.87	150	149.45	150.05
H	Diameter 2	150.02	150.16	149.94	150.04	150.13	150.04	149.85	150.07	149.94	150.01
I	Average Diameter	150.005	150	149.99	150.01	150.105	150.09	149.86	150.035	149.695	150.03
J	G_{mb} [A/(F*π*I^2/4)]	2.300	2.297	2.299	2.297	2.297	2.295	2.299	2.301	2.310	2.296
K	Air Voids [(G_{mm}-J)/G_{mm}]	8.0	8.2	8.1	8.1	8.2	8.2	8.1	8.0	7.6	8.2
	Sample	1	2	3	4	5	6	7	8	9	10
A	Dry Mass	6893.2	6891	6888.1	6884.1	6885.9	6886.7	6889.1	6893.8	6892.8	6883.4
B	Submerged Mass	3944.4	3934.9	3936.8	3938.8	3949.6	3952.1	3954.6	3953.3	3958.2	3945.1
C	SSD Mass	6906.7	6903.3	6900.4	6901.1	6916.6	6917.3	6916.2	6919	6920.9	6903.6
D	G_{mb} [A/(C-B)]	2.327	2.321	2.324	2.324	2.321	2.323	2.326	2.325	2.327	2.327
E	Air Voids [(G_{mm}-D)/G_{mm}]	7.0	7.2	7.1	7.1	7.2	7.1	7.0	7.1	7.0	7.0

Project Number:
Location: M-21 Owosso
Contractor:
Mix:
Gradation:
G_{mm} 2.47

	Sample	1	2	3	4	5	6	7	8	9	10
A	Dry Mass	6799.3	6792.1	6796.4	6794.6	6797	6797.4	6797.4	6797.8	6797.1	6797.2
B	Height 1	169.14	169.3	169.17	169.29	169.52	169.56	169.36	169.53	169.27	169.39
C	Height 2	169.29	169.47	169.17	169.22	169.32	169.33	169.41	169.28	169.38	169.43
D	Height 3	169.42	169.3	169.26	169.4	169.13	169.18	169.27	169.2	169.39	169.26
E	Height 4	169.33	169.43	169.32	169.48	169.36	169.41	169.19	169.45	169.25	169.21
F	Average Height	169.295	169.375	169.23	169.3475	169.3325	169.37	169.3075	169.365	169.3225	169.3225
G	Diameter 1	149.93	149.9	150.04	149.89	149.97	150	149.94	149.96	150	150.03
H	Diameter 2	149.86	150.14	149.91	149.89	149.86	149.98	149.94	149.88	150.02	149.91
I	Average Diameter	149.895	150.02	149.975	149.89	149.915	149.99	149.94	149.92	150.01	149.97
J	G_{mb} [A/(F*π*I^2/4)]	2.276	2.269	2.273	2.274	2.274	2.271	2.274	2.274	2.271	2.273
K	Air Voids [(G_{mm}-J)/G_{mm}]	7.9	8.2	8.0	7.9	7.9	8.0	7.9	7.9	8.0	8.0
	Sample	1	2	3	4	5	6	7	8	9	10
A	Dry Mass	6799.3	6792.1	6796.4	6794.6	6797	6797.4	6797.4	6797.8	6797.1	6797.2
B	Submerged Mass	3861.6	3862.9	3859.7	3850.2	3853.9	3857	3861.4	3853.8	3848.6	3858.3
C	SSD Mass	6819.6	6824.6	6823.1	6820.3	6817.7	6821.4	6824	6816.5	6815.9	6822.1
D	G_{mb} [A/(C-B)]	2.299	2.293	2.293	2.288	2.293	2.293	2.294	2.294	2.291	2.293
E	Air Voids [(G_{mm}-D)/G_{mm}]	6.9	7.2	7.1	7.4	7.2	7.2	7.1	7.1	7.3	7.1

Project Number:
Location: M-66 Battle Creek
Contractor:
Mix:
Gradation:
G_{mm} 2.47

	Sample	1	2	3	4	5	6	7	8	9	10
A	Dry Mass	6840.3	6836.2	6841	6842.3	6841.4	6844	6845.1	6845.8	6844.9	6847
B	Height 1	169.37	169.47	169.42	169.06	169.27	169.31	169.04	169.11	169.14	169.1
C	Height 2	169.68	169.44	169.46	169.19	169.17	169.26	169.08	169.17	169.01	169.18
D	Height 3	169.4	169.29	169.48	169.08	169.22	169.34	169.43	169.29	169.3	169.29
E	Height 4	169.34	169.57	169.18	169.05	169.17	169.32	169.14	169.27	169.21	169.21
F	Average Height	169.4475	169.4425	169.385	169.095	169.2075	169.3075	169.1725	169.21	169.165	169.195
G	Diameter 1	149.99	150.01	149.98	149.94	149.89	149.96	150.05	150.06	150.03	150.02
H	Diameter 2	150.01	150.02	150.05	149.89	150.11	149.94	150.04	149.71	150.08	149.92
I	Average Diameter	150	150.015	150.015	149.915	150	149.95	150.045	149.885	150.055	149.97
J	G_{mb} [A/(F*π*I^2/4)]	2.284	2.283	2.285	2.292	2.288	2.289	2.288	2.293	2.288	2.291
K	Air Voids [(G_{mm}-J)/G_{mm}]	7.5	7.6	7.5	7.2	7.4	7.3	7.4	7.2	7.4	7.2
	Sample	1	2	3	4	5	6	7	8	9	10
A	Dry Mass	6841.2	6838.9	6841.7	6843.3	6842.2	6844.7	6845.8	6846.8	6845.7	6851.8
B	Submerged Mass	3896.7	3899.9	3901.2	3894.4	3899.5	3897.5	3906.7	3911.8	3901.9	3904.8
C	SSD Mass	6861.8	6864.5	6857.7	6855.6	6859.3	6859.5	6867.9	6866.4	6861.3	6866.6
D	G_{mb} [A/(C-B)]	2.307	2.307	2.314	2.311	2.312	2.311	2.312	2.317	2.313	2.313
E	Air Voids [(G_{mm}-D)/G_{mm}]	6.6	6.6	6.3	6.4	6.4	6.4	6.4	6.2	6.3	6.3

Project Number:
Location: M-50 Dundee
Contractor:
Mix: 4 E 3
Gradation:
G_{mm} 2.538

	Sample	1	2	3	4	5	6	7	8	9	10
A	Dry Mass	6848	6842	6842.6	6845.6	6851.8	6840.2	6845.2	6849.1	6846.6	6842.4
B	Height 1	169.04	168.88	168.79	168.85	168.89	169.03	168.98	168.73	168.83	168.84
C	Height 2	168.84	168.87	169.09	168.88	168.83	168.76	169.01	168.89	169.02	168.8
D	Height 3	168.8	168.73	169.07	168.9	168.78	168.79	168.98	168.93	169.11	168.85
E	Height 4	168.86	168.93	168.89	168.82	168.83	168.98	168.85	168.83	168.93	168.85
F	Average Height	168.885	168.8525	168.96	168.8625	168.8325	168.89	168.955	168.845	168.9725	168.835
G	Diameter 1	149.98	150.02	150.05	149.95	150.02	149.98	150	149.8	150.02	149.96
H	Diameter 2	150	150.01	149.92	150.04	149.98	150	149.98	149.93	150.11	149.94
I	Average Diameter	149.99	150.015	149.985	149.995	150	149.99	149.99	149.865	150.065	149.95
J	G_{mb} [A/(F*π*I^2/4)]	2.295	2.293	2.292	2.294	2.297	2.292	2.293	2.300	2.291	2.295
K	Air Voids [(G_{mm}-J)/G_{mm}]	9.6	9.7	9.7	9.6	9.5	9.7	9.7	9.4	9.7	9.6
	Sample	1	2	3	4	5	6	7	8	9	10
A	Dry Mass	6848	6842	6842.6	6845.6	6851.8	6840.2	6845.2	6849.1	6846.6	6842.4
B	Submerged Mass	3996.7	3995.1	3994.3	3993.8	3997.3	3995.4	3994.9	4001.4	3997.4	3995.2
C	SSD Mass	6905	6904.6	6903.8	6903.7	6904	6903.6	6901.3	6910.8	6904.5	6903.5
D	G_{mb} [A/(C-B)]	2.355	2.352	2.352	2.353	2.357	2.352	2.355	2.354	2.355	2.353
E	Air Voids [(G_{mm}-D)/G_{mm}]	7.2	7.3	7.3	7.3	7.1	7.3	7.2	7.2	7.2	7.3

Project Number:
Location: US-12 MIS
Contractor:
Mix:
Gradation:
G_{mm} 2.491

	Sample	1	2	3	4	5	6	7	8	9	10
A	Dry Mass	6755.5	6753.5	6754.9	6751.3	6752	6751.7	6653.8	6756.2	6752.7	6647.8
B	Height 1	169.15	169.28	169.31	169.57	169.3	169.42	169.38	169.17	169.22	169.27
C	Height 2	169.21	169.22	169.26	169.3	169.37	169.33	169.22	169.15	169.26	169.28
D	Height 3	169.2	169.16	169.24	169.62	169.24	169.24	169.07	169.4	169.39	169.31
E	Height 4	169.26	169.33	169.33	169.65	169.26	169.23	169.11	169.14	169.36	169.22
F	Average Height	169.205	169.2475	169.285	169.535	169.2925	169.305	169.195	169.215	169.3075	169.27
G	Diameter 1	150.01	150.1	150.19	150.42	150.05	150	150.04	150.12	150.4	150.05
H	Diameter 2	150.06	150.05	150.11	150.24	150.25	149.98	149.93	150.09	150.04	150.03
I	Average Diameter	150.035	150.075	150.15	150.33	150.15	149.99	149.985	150.105	150.22	150.04
J	G_{mb} [A/(F*π*I^2/4)]	2.258	2.256	2.254	2.244	2.252	2.257	2.226	2.256	2.250	2.221
K	Air Voids [(G_{mm}-J)/G_{mm}]	9.3	9.4	9.5	9.9	9.6	9.4	10.6	9.4	9.7	10.8
	Sample	1	2	3	4	5	6	7	8	9	10
A	Dry Mass	6755.5	6753.5	6754.9	6751.3	6752	6751.7	6653.8	6756.2	6752.7	6647.8
B	Submerged Mass	3877.8	3866.3	3863.6	3851.4	3870.7	3869.4	3838.3	3875	3870.8	3830
C	SSD Mass	6799.3	6794.2	6791.1	6785.1	6801.6	6796	6729.9	6800.4	6789.7	6725
D	G_{mb} [A/(C-B)]	2.312	2.307	2.307	2.301	2.304	2.307	2.301	2.309	2.313	2.296
E	Air Voids [(G_{mm}-D)/G_{mm}]	7.2	7.4	7.4	7.6	7.5	7.4	7.6	7.3	7.1	7.8

Project Number:
Location: M-59 Brighton
Contractor:
Mix:
Gradation:
G_{mm} 2.503

	Sample	1	2	3	4	5	6	7	8	9	10
A	Dry Mass	6671	6659.1	6667.5	6667.4	6657.1	6669.3	6664.7	6661.6	6661.9	6668.9
B	Height 1	168.59	168.56	168.85	168.71	168.72	168.88	168.71	168.82	168.75	169.08
C	Height 2	168.79	168.32	168.98	168.76	169.06	168.76	168.88	168.91	168.65	168.74
D	Height 3	168.88	168.86	168.58	169.04	169.09	168.55	168.94	168.99	168.63	168.65
E	Height 4	168.81	168.73	168.78	169.03	168.84	168.77	168.95	168.49	168.74	168.97
F	Average Height	168.7675	168.6175	168.7975	168.885	168.9275	168.74	168.87	168.8025	168.6925	168.86
G	Diameter 1	150.44	150.89	149.92	150.02	150.04	149.66	150.18	150.22	149.95	149.94
H	Diameter 2	150.48	149.88	149.99	150.22	149.86	150.02	150.04	150.03	149.95	149.91
I	Average Diameter	150.46	150.385	149.955	150.12	149.95	149.84	150.11	150.125	149.95	149.925
J	G_{mb} [A/(F*π*I^2/4)]	2.223	2.223	2.237	2.230	2.232	2.241	2.230	2.229	2.236	2.237
K	Air Voids [(G_{mm}-J)/G_{mm}]	11.2	11.2	10.6	10.9	10.8	10.5	10.9	10.9	10.7	10.6
	Sample	1	2	3	4	5	6	7	8	9	10
A	Dry Mass	6670.9	6659	6657.5	6664.8	6654.8	6669.3	6663.5	6661.3	6661.9	6668.8
B	Submerged Mass	3848.6	3845.8	3848.6	3855.1	3853.2	3847.4	3853	3845	3834.8	3881.6
C	SSD Mass	6717.5	6717.3	6715.4	6716	6716.2	6724.6	6721.3	6716.5	6713.8	6742.4
D	G_{mb} [A/(C-B)]	2.325	2.319	2.322	2.330	2.324	2.318	2.323	2.320	2.314	2.331
E	Air Voids [(G_{mm}-D)/G_{mm}]	7.1	7.4	7.2	6.9	7.1	7.4	7.2	7.3	7.6	6.9

Project Number:
Location: Michigan Ave. Dearborn
Contractor:
Mix: 3 E 10
Gradation:
G_{mm} 2.493

	Sample	1	2	3	4	5	6	7	8	9	10
A	Dry Mass	6719.5	6731	6724.4	6723.4	6729.9	6715.1	6728.8	6725.9	6709.9	6716.2
B	Height 1	169.17	169.35	169.19	169.21	169.07	169.49	169	169.3	168.75	169.02
C	Height 2	169.1	169.02	169	168.86	169.21	169.05	169.15	169.07	168.73	169.06
D	Height 3	169.24	169.41	168.89	169.31	169.02	169.31	169.05	169.35	169.05	169.04
E	Height 4	168.93	169.02	168.9	169.05	169.19	169.52	169.08	169.21	168.81	168.86
F	Average Height	169.11	169.2	168.995	169.1075	169.1225	169.3425	169.07	169.2325	168.835	168.995
G	Diameter 1	149.95	149.86	149.95	149.91	150.04	149.92	149.98	149.95	149.87	150.31
H	Diameter 2	149.96	149.98	150.14	149.86	149.99	149.88	149.94	149.7	149.95	149.8
I	Average Diameter	149.955	149.92	150.045	149.885	150.015	149.9	149.96	149.825	149.91	150.055
J	G_{mb} [A/(F*π*I^2/4)]	2.250	2.254	2.250	2.253	2.251	2.247	2.253	2.254	2.252	2.247
K	Air Voids [(G_{mm}-J)/G_{mm}]	9.8	9.6	9.7	9.6	9.7	9.9	9.6	9.6	9.7	9.9
	Sample	1	2	3	4	5	6	7	8	9	10
A	Dry Mass	6719.5	6731	6724.4	6723.4	6729.9	6715.1	6728.8	6725.9	6709.9	6716.2
B	Submerged Mass	3879.5	3886.2	3877.6	3873.4	3875.8	3866.4	3881	3876.2	3853.2	3848.4
C	SSD Mass	6765.1	6771.8	6772.1	6763.6	6771.3	6760.4	6768.2	6768	6744.9	6750.1
D	G_{mb} [A/(C-B)]	2.329	2.333	2.323	2.326	2.324	2.320	2.331	2.326	2.320	2.315
E	Air Voids [(G_{mm}-D)/G_{mm}]	6.6	6.4	6.8	6.7	6.8	6.9	6.5	6.7	6.9	7.2

Project Number:
Location: Vandyke Detroit
Contractor:
Mix:
Gradation:
G_{mm} 2.604

	Sample	1	2	3	4	5	6	7	8	9	10
A	Dry Mass	7127.5	7127.8	7129.1	7127.3	7125.1	7123.6	7153.8	7125.8	7124.8	7130.6
B	Height 1	169.09	169.08	169.02	169.18	169	169.14	169.3	169.05	169.25	169.12
C	Height 2	169.1	168.97	169.11	169.05	169.15	169.24	169.19	169.15	169.09	169.2
D	Height 3	169.29	169.03	169.28	169.04	169.17	169.08	169.01	169.33	169.08	169.47
E	Height 4	169.27	169.21	169.34	169.19	169.07	169.03	169.19	169.21	169.16	169.18
F	Average Height	169.1875	169.0725	169.1875	169.115	169.0975	169.1225	169.1725	169.185	169.145	169.2425
G	Diameter 1	150	150.05	150.06	150.1	150.01	150.01	150.25	150.13	150.03	150.01
H	Diameter 2	150.06	150.06	149.98	150.1	150.04	149.98	150.05	150.05	150.01	150.07
I	Average Diameter	150.03	150.055	150.02	150.1	150.025	149.995	150.15	150.09	150.02	150.04
J	G_{mb} [A/(F*π*I^2/4)]	2.383	2.384	2.384	2.382	2.384	2.384	2.388	2.381	2.383	2.383
K	Air Voids [(G_{mm}-J)/G_{mm}]	8.5	8.5	8.5	8.5	8.5	8.5	8.3	8.6	8.5	8.5
	Sample	1	2	3	4	5	6	7	8	9	10
A	Dry Mass	7127.5	7127.8	7129.1	7127.3	7125.1	7123.6	7153.8	7125.8	7124.8	7130.6
B	Submerged Mass	4236.5	4229.2	4236.3	4235.1	4236.5	4234.7	4233.6	4222.9	4227.5	4225.1
C	SSD Mass	7171.1	7163.8	7165.9	7176.2	7168.3	7166.7	7173.1	7166.2	7164.7	7163.4
D	G_{mb} [A/(C-B)]	2.429	2.429	2.433	2.423	2.430	2.430	2.434	2.421	2.426	2.427
E	Air Voids [(G_{mm}-D)/G_{mm}]	6.7	6.7	6.5	6.9	6.7	6.7	6.5	7.0	6.8	6.8

Project Number:
Location: US-23 Heartland
Contractor:
Mix:
Gradation:
G_{mm} 2.492

	Sample	1	2	3	4	5	6	7	8	9	10
A	Dry Mass	6592.6	6704.4	6702.2	6586.2	6705	6699	6703.9	6705.4	6708.5	6586.9
B	Height 1	169.04	169.12	169.23	169.12	169.07	169.05	168.91	169.01	168.88	169.07
C	Height 2	169.33	169.15	169.13	168.76	168.95	168.95	169.32	169.17	168.96	169.14
D	Height 3	169.19	169.13	168.94	168.86	168.83	169.07	169.07	169.28	169.07	169.25
E	Height 4	169.25	169.2	169.25	169.53	169.14	169.08	168.76	169.1	169.07	169.28
F	Average Height	169.2025	169.15	169.1375	169.0675	168.9975	169.0375	169.015	169.14	168.995	169.185
G	Diameter 1	150.04	150.06	149.92	150.04	150.06	150.23	150.01	150.03	150.1	150.16
H	Diameter 2	150.19	150.13	150	149.4	150.03	150.16	149.94	150.32	150.09	150.14
I	Average Diameter	150.115	150.095	149.96	149.72	150.045	150.195	149.975	150.175	150.095	150.15
J	G_{mb} [A/(F*π*I^2/4)]	2.201	2.240	2.244	2.213	2.244	2.237	2.245	2.238	2.244	2.199
K	Air Voids [(G_{mm}-J)/G_{mm}]	11.7	10.1	10.0	11.2	10.0	10.2	9.9	10.2	10.0	11.8
	Sample	1	2	3	4	5	6	7	8	9	10
A	Dry Mass	6721.1	6704.4	6702.2	6586.2	6705	6699	6703.9	6705.4	6708.5	6586.9
B	Submerged Mass	3885.8	3882.5	3883	3795.8	3870.6	3849.1	3884.3	3863.7	3865.5	3856.5
C	SSD Mass	6769.2	6768.4	6769.3	6662.5	6773.9	6759.9	6767.7	6772.9	6764.5	6701
D	G_{mb} [A/(C-B)]	2.331	2.323	2.322	2.297	2.309	2.301	2.325	2.305	2.314	2.316
E	Air Voids [(G_{mm}-D)/G_{mm}]	6.5	6.8	6.8	7.8	7.3	7.6	6.7	7.5	7.1	7.1

Project Number:
Location: I-75 Levering Rd.
Contractor:
Mix:
Gradation:
G_{mm} 2.443

	Sample	1	2	3	4	5	6	7	8	9	10
A	Dry Mass	6682.4	6687.5	6683.7	6684.6	6685.7	6681.6	6684.5	6680.5	6686.2	6686.1
B	Height 1	168.94	168.69	168.72	168.98	169.15	168.65	168.62	168.57	169.11	169.06
C	Height 2	168.63	168.81	168.92	169.06	168.81	168.51	168.89	168.94	168.57	168.43
D	Height 3	168.96	169.4	169.02	169.01	169.03	168.89	168.85	168.96	168.87	168.73
E	Height 4	168.88	168.97	169.82	168.81	169	169.05	169.15	168.58	169.22	168.95
F	Average Height	168.8525	168.9675	169.12	168.965	168.9975	168.775	168.8775	168.7625	168.9425	168.7925
G	Diameter 1	149.7	149.65	149.66	149.97	149.6	149.76	149.85	149.65	149.88	149.63
H	Diameter 2	149.92	149.83	149.77	149.92	149.63	150.2	149.76	149.83	149.66	149.93
I	Average Diameter	149.81	149.74	149.715	149.945	149.615	149.98	149.805	149.74	149.77	149.78
J	G_{mb} [A/(F*π*I^2/4)]	2.245	2.247	2.245	2.240	2.250	2.241	2.246	2.248	2.246	2.248
K	Air Voids [(G_{mm}-J)/G_{mm}]	8.1	8.0	8.1	8.3	7.9	8.3	8.1	8.0	8.0	8.0
	Sample	1	2	3	4	5	6	7	8	9	10
A	Dry Mass	6684.7	6689.8	6686.1	6685.8	6687.3	6682.9	6686.7	6682.7	6687.7	6687.8
B	Submerged Mass	3793.3	3793.4	3787.6	3768.2	3766.9	3783.7	3785	3776	3769.8	3784
C	SSD Mass	6719.7	6733	6722.8	6712.8	6716.6	6716.6	6716.5	6717.3	6714.9	6717.3
D	G_{mb} [A/(C-B)]	2.284	2.276	2.278	2.271	2.267	2.279	2.281	2.272	2.271	2.280
E	Air Voids [(G_{mm}-D)/G_{mm}]	6.5	6.8	6.8	7.1	7.2	6.7	6.6	7.0	7.0	6.7

Project Number:
Location: I-196 Grand Rapids
Contractor:
Mix:
Gradation:
G_{mm} 2.499

	Sample	1	2	3	4	5	6	7	8	9	10
A	Dry Mass	6814.9	6813.8	6793.8	6818.3	6812.5	6818.7	6814.1	6817.3	6812	6815
B	Height 1	169	170.4	169.66	169.67	169.41	169.27	169.26	169.44	169.64	169.33
C	Height 2	169.45	170.59	169.52	169.35	169.35	169.49	169.3	169.62	169.62	169.5
D	Height 3	169.93	170.35	169.85	169.27	169.5	169.44	169.29	169.68	170.09	169.46
E	Height 4	169.25	169.93	170.22	169.6	169.48	169.32	169.33	169.52	169.7	169.35
F	Average Height	169.4075	170.3175	169.8125	169.4725	169.435	169.38	169.295	169.565	169.7625	169.41
G	Diameter 1	150.06	150.22	150.2	150.04	150.23	150.07	150	150.05	150.05	149.96
H	Diameter 2	150.02	150.07	150.12	150.01	149.99	149.96	149.99	150.06	150.18	149.95
I	Average Diameter	150.04	150.145	150.16	150.025	150.11	150.015	149.995	150.055	150.115	149.955
J	G_{mb} [A/(F*π*I^2/4)]	2.275	2.260	2.259	2.276	2.272	2.278	2.278	2.273	2.267	2.278
K	Air Voids [(G_{mm}-J)/G_{mm}]	9.0	9.6	9.6	8.9	9.1	8.9	8.9	9.0	9.3	8.9
	Sample	1	2	3	4	5	6	7	8	9	10
A	Dry Mass	6814.9	6813.8	6793.8	6818.3	6812.5	6818.7	6814.1	6817.3	6812	6815
B	Submerged Mass	3922.6	3914.3	3914.3	3926.4	3918.9	3935.3	3922.2	3921.6	3916	3926.4
C	SSD Mass	6870.5	6819.6	6863.9	6871.7	6868.8	6878.5	6865.1	6871.7	6878.5	6867.9
D	G_{mb} [A/(C-B)]	2.312	2.345	2.303	2.315	2.309	2.317	2.315	2.311	2.299	2.317
E	Air Voids [(G_{mm}-D)/G_{mm}]	7.5	6.2	7.8	7.4	7.6	7.3	7.3	7.5	8.0	7.3

Project Number:
Location: I-75 Clarkston
Contractor:
Mix:
Gradation:
G_{mm} 2.487

	Sample	1	2	3	4	5	6	7	8	9	10
A	Dry Mass	6747.8	6749.7	6736	6742.5	6750.5	6747.1	6742.7	6816.5	6746.2	6745.4
B	Height 1	169.42	169.03	169.11	169.17	169.19	169.13	169.09	169.26	169.16	169.18
C	Height 2	169.24	169.16	169.26	169.1	169.28	169.25	169.21	169.12	169.26	169.19
D	Height 3	168.99	169.12	169	169.22	169.28	169.05	169.02	169.02	169.25	169.33
E	Height 4	169.08	169.14	169.07	169.06	169.19	169.07	169.14	169.18	169.16	169.26
F	Average Height	169.1825	169.1125	169.11	169.1375	169.235	169.125	169.115	169.145	169.2075	169.24
G	Diameter 1	149.95	150.09	149.99	150.01	150.06	149.95	150.06	149.9	149.95	149.95
H	Diameter 2	149.97	150.01	150.06	149.99	149.99	149.98	150.18	149.95	150.02	149.91
I	Average Diameter	149.96	150.05	150.025	150	150.025	149.965	150.12	149.925	149.985	149.93
J	G_{mb} [A/(F*π*I^2/4)]	2.258	2.257	2.253	2.256	2.256	2.259	2.253	2.283	2.257	2.258
K	Air Voids [(G_{mm}-J)/G_{mm}]	9.2	9.2	9.4	9.3	9.3	9.2	9.4	8.2	9.3	9.2
	Sample	1	2	3	4	5	6	7	8	9	10
A	Dry Mass	6747.8	6749.7	6736	6742.5	6750.5	6747.1	6742.7	6816.5	6746.2	6745.4
B	Submerged Mass	3870.9	3871.2	3862.9	3860	3871.1	3869	3860.2	3924.3	3864.2	3861.6
C	SSD Mass	6788.2	6793.4	6785.3	6791.9	6793.8	6792.5	6787.6	6855.2	6793.8	6786.6
D	G_{mb} [A/(C-B)]	2.313	2.310	2.305	2.300	2.310	2.308	2.303	2.326	2.303	2.306
E	Air Voids [(G_{mm}-D)/G_{mm}]	7.0	7.1	7.3	7.5	7.1	7.2	7.4	6.5	7.4	7.3

Project Number:
Location: M-53 Detroit
Contractor:
Mix:
Gradation:
G_{mm} 2.563

	Sample	1	2	3	4	5	6	7	8	9	10
A	Dry Mass	6949.6	6947.4	6947.3	6943	6947.4	6937.7	6952.6	6949.7	6947.8	6951.3
B	Height 1	168.9	168.91	168.99	169.09	168.89	168.91	168.92	168.88	168.99	168.97
C	Height 2	169.08	169.08	169.19	168.79	169.27	169.16	168.92	169.14	169.2	168.92
D	Height 3	169.06	168.93	168.87	168.71	168.96	168.91	169.06	169.13	169.04	169.06
E	Height 4	168.9	168.97	168.71	168.88	168.76	168.79	168.83	169.06	168.84	168.78
F	Average Height	168.985	168.9725	168.94	168.8675	168.97	168.9425	168.9325	169.0525	169.0175	168.9325
G	Diameter 1	149.97	149.93	149.91	149.94	149.97	149.9	149.98	149.97	149.93	149.92
H	Diameter 2	149.98	150.05	150.04	149.9	149.94	149.94	150	150.08	149.95	149.91
I	Average Diameter	149.975	149.99	149.975	149.92	149.955	149.92	149.99	150.025	149.94	149.915
J	G_{mb} [A/(F*π*I^2/4)]	2.328	2.327	2.328	2.329	2.328	2.326	2.329	2.326	2.328	2.331
K	Air Voids [(G_{mm}-J)/G_{mm}]	9.2	9.2	9.2	9.1	9.2	9.2	9.1	9.3	9.2	9.0
	Sample	1	2	3	4	5	6	7	8	9	10
A	Dry Mass	6949.6	6947.4	6947.3	6943	6947.4	6937.7	6952.6	6949.7	6947.8	6951.3
B	Submerged Mass	4083.9	4079.8	4081.1	4084.2	4085.6	4073.6	4097.9	4096.7	4076.7	4093.5
C	SSD Mass	7000.7	6995.4	6996.5	6995.2	7001.5	6989.8	7006.8	7005.2	7000.9	7003
D	G_{mb} [A/(C-B)]	2.383	2.383	2.383	2.385	2.383	2.379	2.390	2.389	2.376	2.389
E	Air Voids [(G_{mm}-D)/G_{mm}]	7.0	7.0	7.0	6.9	7.0	7.2	6.7	6.8	7.3	6.8

Project Number:
Location: Michigan Ave. Dearborn
Contractor:
Mix: 4 E 10
Gradation:
G_{mm} 2.485

	Sample	1	2	3	4	5	6	7	8	9	10
A	Dry Mass	6703.2	6704.4	6700	6705.5	6701.2	6700.8	6701.3	6704.4	6702.1	6701.8
B	Height 1	169.04	169.26	169.16	169.07	169.35	169.15	169.46	169.53	169	169.27
C	Height 2	169.58	169.18	169.08	169.92	169.59	169.33	169.33	169.63	169.19	169.24
D	Height 3	169.21	169.35	169.2	169.47	169.37	169.6	169.41	169.12	169.59	169.38
E	Height 4	169.37	169.34	169.67	169.58	169.45	169.49	169.5	169.47	169.61	169.35
F	Average Height	169.3	169.2825	169.2775	169.51	169.44	169.3925	169.425	169.4375	169.3475	169.31
G	Diameter 1	149.94	150.05	150.03	149.49	149.93	149.98	149.97	150.04	150.04	150.04
H	Diameter 2	149.97	150.19	150.07	149.96	149.94	149.95	149.97	149.96	150.09	150.03
I	Average Diameter	149.955	150.12	150.05	149.725	149.935	149.965	149.97	150	150.065	150.035
J	G_{mb} [A/(F*π*I^2/4)]	2.242	2.238	2.238	2.247	2.240	2.240	2.239	2.239	2.238	2.239
K	Air Voids [(G_{mm}-J)/G_{mm}]	9.8	10.0	9.9	9.6	9.9	9.9	9.9	9.9	10.0	9.9
	Sample	1	2	3	4	5	6	7	8	9	10
A	Dry Mass	6703.4	6704.1	6699.6	6705.9	6700.8	6701	6700.9	6704.7	6701.7	6702.3
B	Submerged Mass	3836	3839.8	3826.3	3841.4	3827.4	3826.5	3830.8	3831.8	3828.8	3840.7
C	SSD Mass	6753.4	6751.7	6736.5	6751	6738.9	6746	6745.1	6746	6743.3	6747.5
D	G_{mb} [A/(C-B)]	2.298	2.302	2.302	2.305	2.301	2.295	2.299	2.301	2.299	2.306
E	Air Voids [(G_{mm}-D)/G_{mm}]	7.5	7.4	7.4	7.3	7.4	7.6	7.5	7.4	7.5	7.2

Project Number:
Location: I-75 Toledo
Contractor:
Mix:
Gradation:
G_{mm} 2.507

	Sample	1	2	3	4	5	6	7	8	9	10
A	Dry Mass	6813.8	6818.3	6811.9	6809.6	6811.5	6809.8	6814.8	6811.8	6811.9	6812.9
B	Height 1	169.3	169.36	169.19	169.4	169.37	169.32	169.38	169.28	169.17	169.28
C	Height 2	169.33	169.49	169.26	169.24	169.26	169.18	169.35	169.38	169.46	169.36
D	Height 3	169.1	169.34	169.32	169.19	169.12	169.25	169.32	169.51	169.45	169.31
E	Height 4	169.19	169.26	169.33	169.35	169.27	169.37	169.27	169.23	169.23	169.24
F	Average Height	169.23	169.3625	169.275	169.295	169.255	169.28	169.33	169.35	169.3275	169.2975
G	Diameter 1	150.01	149.86	150.11	149.99	149.96	150.04	149.94	149.98	150.03	149.94
H	Diameter 2	149.96	150.01	149.98	149.88	149.98	150.08	150.01	150.02	149.97	150.04
I	Average Diameter	149.985	149.935	150.045	149.935	149.97	150.06	149.975	150	150	149.99
J	G_{mb} [A/(F*π*I^2/4)]	2.279	2.280	2.276	2.278	2.278	2.275	2.278	2.276	2.277	2.278
K	Air Voids [(G_{mm}-J)/G_{mm}]	9.1	9.0	9.2	9.1	9.1	9.3	9.1	9.2	9.2	9.2
	Sample	1	2	3	4	5	6	7	8	9	10
A	Dry Mass	6813.8	6818.3	6811.9	6809.6	6811.5	6809.8	6814.8	6811.8	6811.9	6812.9
B	Submerged Mass	3945.2	3958.5	3951.8	3945.5	3951.8	3946.8	3954.7	3947.9	3947.1	3950.2
C	SSD Mass	6877.6	6881.3	6883.1	6874.5	6877.7	6872.9	6877.2	6873.4	6879.2	6875.9
D	G_{mb} [A/(C-B)]	2.324	2.333	2.324	2.325	2.328	2.327	2.332	2.328	2.323	2.329
E	Air Voids [(G_{mm}-D)/G_{mm}]	7.3	6.9	7.3	7.3	7.1	7.2	7.0	7.1	7.3	7.1

Project Number:
Location: I-94 Ann Arbor
Contractor:
Mix: SMA
Gradation:
G_{mm} 2.515

	Sample	1	2	3	4	5	6	7	8	9	10
A	Dry Mass	6730	6729.3	6720.4	6722.6	6730.7	6724	6729.9	6727.7	6721.8	6727.8
B	Height 1	168.95	168.95	168.81	168.9	168.79	168.96	168.97	168.91	169.04	168.89
C	Height 2	168.65	168.92	169.03	168.99	169.16	169.03	168.85	168.84	169.15	169.01
D	Height 3	168.65	168.82	168.7	168.84	168.92	168.89	168.8	168.62	168.91	168.97
E	Height 4	168.89	168.89	168.79	168.8	169.06	168.91	168.75	168.54	168.85	168.8
F	Average Height	168.785	168.895	168.8325	168.8825	168.9825	168.9475	168.8425	168.7275	168.9875	168.9175
G	Diameter 1	149.92	149.97	149.9	149.98	150.15	149.93	150.01	150	149.96	149.93
H	Diameter 2	150.12	150	150	149.95	149.94	150.02	150	149.99	149.98	150.12
I	Average Diameter	150.02	149.985	149.95	149.965	150.045	149.975	150.005	149.995	149.97	150.025
J	G_{mb} [A/(F*π*I^2/4)]	2.256	2.255	2.254	2.254	2.253	2.253	2.255	2.257	2.252	2.253
K	Air Voids [(G_{mm}-J)/G_{mm}]	10.3	10.3	10.4	10.4	10.4	10.4	10.3	10.3	10.5	10.4
	Sample	1	2	3	4	5	6	7	8	9	10
A	Dry Mass	6730	6729.3	6720.4	6722.6	6730.7	6724	6729.9	6727.7	6721.8	6727.8
B	Submerged Mass	3937.5	3935.3	3927.1	3936.8	3939.9	3941.4	3940.2	3942.7	3930.6	3938.4
C	SSD Mass	6801.4	6797.4	6792.2	6801.8	6796.5	6801.5	6803.3	6809.1	6791.6	6795.1
D	G_{mb} [A/(C-B)]	2.350	2.351	2.346	2.346	2.356	2.351	2.351	2.347	2.349	2.355
E	Air Voids [(G_{mm}-D)/G_{mm}]	6.6	6.5	6.7	6.7	6.3	6.5	6.5	6.7	6.6	6.4

Phase II – 100mm Superpave Specimens for Dynamic Modulus Testing
Cut and Cored from 150mm Diameter Superpave Specimens

Project Number:
Location: M-50 Dundee
Contractor:
Mix: 3 E 1
Gradation:
G_{mm} 2.52

	Sample	1	2	3	4	5	6	7	8	9	10
A	Dry Mass	2869.3	2816.3	2868.7	2825.2	2834.7	2859.7	2809.2	2893	2803.4	2832.8
B	Height 1	151.03	151.11	151.17	151.5	151.13	150.89	151.01	150.85	150.97	150.95
C	Height 2	151.52	151.13	151.45	151.48	151.31	151.11	150.88	150.92	150.98	151.02
D	Height 3	151.14	151.3	151.23	151.54	151.24	150.88	151.19	151.24	150.89	151.03
E	Height 4	150.96	151.37	151.12	151.34	151.02	151.07	151.07	151.06	150.81	150.82
F	Average Height	151.1625	151.2275	151.2425	151.465	151.175	150.9875	151.0375	151.0175	150.9125	150.955
G	Top Diameter 1	101.5	101.37	101.22	101.12	101.41	101.2	101.31	101.45	101.27	101.24
H	Top Diameter 2	101.26	101.32	101.44	101.42	101.43	101.31	101.43	101.4	101.27	101.28
	Middle Diameter 1	101.22	101.27	101.29	101.3	100.99	101.11	101.32	101.2	101.3	101.13
	Middle Diameter 2	101.3	101.29	101.22	101.35	101.27	101.25	101.26	101.27	101.25	101.35
	Bottom Diameter 1	101.49	101.28	101.44	101.27	101.36	101.06	101.45	101.32	101.23	101.11
	Bottom Diameter 2	101.43	101.28	101.26	101.41	101.25	101.35	101.26	101.29	101.38	101.49
I	Average Diameter	101.3667	101.3017	101.3	101.3117	101.285	101.2133	101.3383	101.3217	101.2833	101.2667
J	G_{mb} [A/(F*π*I^2/4)]	2.352	2.311	2.353	2.314	2.327	2.354	2.306	2.376	2.306	2.330
K	Air Voids [(G_{mm}-J)/G_{mm}]	6.7	8.3	6.6	8.2	7.6	6.6	8.5	5.7	8.5	7.5

	Sample	1	2	3	4	5	6	7	8	9	10
A	Dry Mass	2869.3	2816.3	2868.7	2825.2	2834.7	2859.7	2809.2	2893	2803.4	2832.8
B	Submerged Mass	1664.3	1634.6	1663.4	1637.6	1654	1658	1625.2	1692	1623.9	1649.4
C	SSD Mass	2884.1	2846.3	2883.7	2850.7	2862.4	2875.8	2834	2910.7	2828.1	2861.9
D	G_{mb} [A/(C-B)]	2.352	2.324	2.351	2.329	2.346	2.348	2.324	2.374	2.328	2.336
E	Air Voids [(G_{mm}-D)/G_{mm}]	6.7	7.8	6.7	7.6	6.9	6.8	7.8	5.8	7.6	7.3

Project Number:
Location: M-36 Pinckney
Contractor:
Mix:
Gradation:
G_{mm} 2.511

	Sample	1	2	3	4	5	6	7	8	9	10
A	Dry Mass	2821.1	2835.1	2852.2	2840.7	2852.2	2874.5	2869.3	2850.3	2845.3	2887.7
B	Height 1	151.55	151.34	151.85	151.62	151.35	151.17	152.41	151.51	151.44	152.82
C	Height 2	151.39	151.45	151.52	151.48	151.41	151.42	152.25	151.34	151.5	152.05
D	Height 3	151.37	151.58	151.47	151.47	151.31	151.29	152.57	151.3	151.58	152.13
E	Height 4	151.55	151.56	151.38	151.52	151.38	151.32	152.61	151.34	151.46	152.15
F	Average Height	151.47	151.48	151.56	151.52	151.36	151.30	152.46	151.37	151.50	152.29
G	Top Diameter 1	102.05	101.94	102.05	102.12	101.82	102.07	102	102.01	101.86	102.13
H	Top Diameter 2	101.93	102.03	102.1	102.03	102.03	102.01	102.08	101.88	101.91	102.03
	Middle Diameter 1	101.63	101.67	101.79	101.66	101.62	101.74	101.58	101.53	101.76	101.57
	Middle Diameter 2	101.63	101.66	101.71	101.71	101.6	101.74	101.67	101.48	101.72	101.56
	Bottom Diameter 1	101.61	101.83	101.76	101.64	101.6	101.64	101.59	101.51	101.63	101.54
	Bottom Diameter 2	101.82	101.64	101.74	101.53	101.88	101.79	101.6	101.66	101.64	101.62
I	Average Diameter	101.78	101.80	101.86	101.78	101.76	101.83	101.75	101.68	101.75	101.74
J	G_{mb} [A/(F*π*I^2/4)]	2.289	2.300	2.310	2.304	2.317	2.333	2.314	2.319	2.310	2.332
K	Air Voids [(G_{mm}-J)/G_{mm}]	8.8	8.4	8.0	8.2	7.7	7.1	7.8	7.6	8.0	7.1

	Sample	1	2	3	4	5	6	7	8	9	10
A	Dry Mass	2821.1	2835.1	2852.2	2840.7	2852.2	2874.5	2869.3	2850.3	2845.3	2887.7
B	Submerged Mass	1627	1636	1649.8	1642.7	1651	1672	1656.6	1645.4	1648	1671.9
C	SSD Mass	2842.6	2855.2	2870	2862	2870.3	2891	2883.7	2864	2866.1	2899.7
D	G_{mb} [A/(C-B)]	2.321	2.325	2.337	2.330	2.339	2.358	2.338	2.339	2.336	2.352
E	Air Voids [(G_{mm}-D)/G_{mm}]	7.6	7.4	6.9	7.2	6.8	6.1	6.9	6.9	7.0	6.3

Project Number:
Location: M-45 Grand Rapids
Contractor:
Mix:
Gradation:
G_{mm} 2.513

	Sample	1	2	3	4	5	6	7	8	9	10
A	Dry Mass	2901.3	2901.3	2895.4	2897.7	2898.2	2905.9	2902.8	2910.1	2902.4	2898.3
B	Height 1	151.23	151.46	151.4	151.61	151.68	151.97	151.8	151.54	151.64	151.7
C	Height 2	151.32	151.4	151.32	151.42	151.43	151.54	151.79	151.58	151.61	151.84
D	Height 3	151.5	151.53	151.52	151.57	151.35	151.67	151.67	151.51	151.64	151.86
E	Height 4	151.36	151.4	151.51	151.41	151.22	151.55	151.68	151.4	151.69	151.77
F	Average Height	151.35	151.45	151.44	151.50	151.42	151.68	151.74	151.51	151.65	151.79
G	Top Diameter 1	101.95	101.95	101.97	102.03	101.96	101.93	101.95	101.92	101.93	101.89
H	Top Diameter 2	101.97	101.82	101.87	101.91	101.89	102.18	102.02	101.86	101.98	102.02
	Middle Diameter 1	101.67	101.48	101.69	101.5	101.51	101.63	101.73	101.74	101.55	101.52
	Middle Diameter 2	101.53	101.57	101.43	101.71	101.6	101.61	101.55	101.65	101.51	101.5
	Bottom Diameter 1	101.42	101.65	101.46	101.91	101.66	101.56	101.54	101.5	101.53	101.62
	Bottom Diameter 2	101.75	101.31	101.87	101.61	101.51	101.83	101.81	101.83	101.92	101.44
I	Average Diameter	101.72	101.63	101.72	101.78	101.69	101.79	101.77	101.75	101.74	101.67
J	G_{mb} [A/(F*π*I^2/4)]	2.359	2.362	2.353	2.351	2.357	2.354	2.352	2.362	2.354	2.352
K	Air Voids [(G_{mm}-J)/G_{mm}]	6.1	6.0	6.4	6.5	6.2	6.3	6.4	6.0	6.3	6.4
	Sample	1	2	3	4	5	6	7	8	9	10
A	Dry Mass	2901.3	2901.3	2895.4	2897.7	2898.2	2905.9	2902.8	2910.1	2902.4	2898.3
B	Submerged Mass	1687.1	1686.6	1681.9	1682.3	1681.2	1688.7	1687.5	1692.3	1684.5	1680.7
C	SSD Mass	2913.4	2913	2908.6	2909.7	2908.4	2917.3	2915.9	2920.6	2913.5	2909.4
D	G_{mb} [A/(C-B)]	2.366	2.366	2.360	2.361	2.362	2.365	2.363	2.369	2.362	2.359
E	Air Voids [(G_{mm}-D)/G_{mm}]	5.9	5.9	6.1	6.1	6.0	5.9	6.0	5.7	6.0	6.1

Project Number:
Location: M-21 St. Johns
Contractor:
Mix:
Gradation:
G_{mm} 2.489

	Sample	1	2	3	4	5	6	7	8	9	10
A	Dry Mass	2821.8	2818.6	2831.5	2831.5	2827.1	2840.4	2833.2	2785.4	2812.7	2814.7
B	Height 1	151.96	152.57	153.07	152.98	153.53	153.28	153.03	151.76	152.07	152.58
C	Height 2	152.16	152.67	153.05	153.55	153.73	152.9	152.9	151.52	152.14	152.89
D	Height 3	152.46	152.09	153.33	153.6	153.06	153.03	152.47	151.54	152.45	153.02
E	Height 4	152.25	152.14	153.46	153.03	152.87	153.49	152.55	151.66	152.6	152.83
F	Average Height	152.21	152.37	153.23	153.29	153.30	153.18	152.74	151.62	152.32	152.83
G	Top Diameter 1	101.68	101.53	101.65	101.41	101.56	101.37	101.74	101.4	101.51	101.42
H	Top Diameter 2	101.48	101.42	101.35	101.48	101.31	101.49	101.42	101.37	101.4	101.67
	Middle Diameter 1	101.56	101.51	101.53	101.46	101.54	101.56	101.48	101.52	101.56	101.62
	Middle Diameter 2	101.74	101.67	101.57	101.42	101.47	101.59	101.49	101.63	101.62	101.55
	Bottom Diameter 1	101.69	101.59	101.65	101.69	101.46	101.56	101.65	101.62	101.65	101.53
	Bottom Diameter 2	101.57	101.71	101.57	101.54	101.57	101.5	101.42	101.44	101.63	101.65
I	Average Diameter	101.62	101.57	101.55	101.50	101.49	101.51	101.53	101.50	101.56	101.57
J	G_{mb} [A/(F*π*I^2/4)]	2.286	2.283	2.281	2.283	2.280	2.291	2.291	2.271	2.279	2.273
K	Air Voids [(G_{mm}-J)/G_{mm}]	8.2	8.3	8.3	8.3	8.4	7.9	8.0	8.8	8.4	8.7
	Sample	1	2	3	4	5	6	7	8	9	10
A	Dry Mass	2821.8	2818.6	2831.5	2831.5	2827.1	2840.4	2833.2	2785.4	2812.7	2814.7
B	Submerged Mass	1616.1	1612.5	1618.9	1619.8	1621.2	1630.2	1627	1590.2	1611.2	1612.2
C	SSD Mass	2843.3	2840.1	2850.8	2851.5	2851.6	2861.2	2854.9	2810.7	2835.9	2841.6
D	G_{mb} [A/(C-B)]	2.299	2.296	2.298	2.299	2.298	2.307	2.307	2.282	2.297	2.289
E	Air Voids [(G_{mm}-D)/G_{mm}]	7.6	7.8	7.7	7.6	7.7	7.3	7.3	8.3	7.7	8.0

Project Number:
Location: M-84 Saginaw
Contractor:
Mix:
Gradation:
G_{mm} 2.543

	Sample	1	2	3	4	5	6	7	8	9	10
A	Dry Mass	2950.9	2944.7	2931.1	2916.1	2937.5	2953.6	2951.6	2952.9	2940.7	2965.8
B	Height 1	152.6	152.41	151.83	151.65	151.65	152.04	152.93	152.89	152.08	152.52
C	Height 2	152.42	152.83	152.06	151.64	152.13	152.11	152.97	153.07	152	152.44
D	Height 3	152.5	152.83	151.77	151.74	152.01	152.29	152.54	153.1	152.28	152.82
E	Height 4	152.75	152.46	151.78	151.57	151.78	152.53	152.64	153.22	152.23	152.15
F	Average Height	152.57	152.63	151.86	151.65	151.89	152.24	152.77	153.07	152.15	152.48
G	Top Diameter 1	101.43	101.53	101.52	101.59	101.42	101.49	101.48	101.49	101.46	101.54
H	Top Diameter 2	101.55	101.53	101.39	101.46	101.71	101.54	101.43	101.43	101.54	101.58
	Middle Diameter 1	101.53	101.66	101.45	101.47	101.58	101.47	101.43	101.52	101.58	101.56
	Middle Diameter 2	101.56	101.52	101.53	101.65	101.45	101.48	101.44	101.49	101.56	101.65
	Bottom Diameter 1	101.53	101.44	101.5	101.59	101.6	101.59	101.58	101.65	101.58	101.66
	Bottom Diameter 2	101.59	101.51	101.56	101.56	101.52	101.4	101.34	101.55	101.53	101.53
I	Average Diameter	101.53	101.53	101.49	101.55	101.55	101.50	101.45	101.52	101.54	101.59
J	G_{mb} [A/(F*π*I^2/4)]	2.389	2.383	2.386	2.374	2.388	2.398	2.390	2.383	2.387	2.400
K	Air Voids [(G_{mm}-J)/G_{mm}]	6.1	6.3	6.2	6.6	6.1	5.7	6.0	6.3	6.1	5.6
	Sample	1	2	3	4	5	6	7	8	9	10
A	Dry Mass	2950.9	2944.7	2931.1	2916.1	2937.5	2953.6	2951.6	2952.9	2940.7	2965.8
B	Submerged Mass	1725	1719.2	1712.4	1697.8	1717.1	1730.4	1723.6	1723.5	1718.7	1738.4
C	SSD Mass	2960.9	2952.7	2940.4	2925.2	2946.3	2962.7	2960	2961.8	2949.5	2974.3
D	G_{mb} [A/(C-B)]	2.388	2.387	2.387	2.376	2.390	2.397	2.387	2.385	2.389	2.400
E	Air Voids [(G_{mm}-D)/G_{mm}]	6.1	6.1	6.1	6.6	6.0	5.7	6.1	6.2	6.0	5.6

Project Number:
Location: BL I-96 Howell
Contractor:
Mix:
Gradation:
G_{mm} 2.501

	Sample	1	2	3	4	5	6	7	8	9	10
A	Dry Mass	2897.3	2880.6	2907.8	2901.8	2899.8	2846.9	2882.1	2890.9	2894.7	2888.5
B	Height 1	152.08	151.66	152.72	152.68	152.38	152.3	151.73	152.3	152.64	151.89
C	Height 2	152.39	151.92	152.8	152.89	152.92	152.54	151.59	152.24	152.7	152.11
D	Height 3	152.09	151.9	153.08	152.86	153.09	152.24	151.71	152.39	152.17	151.86
E	Height 4	152.02	151.67	153.29	152.67	152.48	152.07	151.63	152.49	152.26	151.68
F	Average Height	152.15	151.79	152.97	152.78	152.72	152.29	151.67	152.36	152.44	151.89
G	Top Diameter 1	101.37	101.47	101.49	101.5	101.51	99.88	101.43	101.51	101.49	101.42
H	Top Diameter 2	101.57	101.66	101.59	101.58	101.39	99.79	101.39	101.55	101.35	101.55
	Middle Diameter 1	101.59	101.61	101.49	101.53	101.43	100.24	101.67	101.51	101.43	101.57
	Middle Diameter 2	101.52	101.46	101.54	101.48	101.54	101.31	101.61	101.58	101.53	101.58
	Bottom Diameter 1	101.52	101.6	101.58	101.48	101.54	101.69	101.51	101.59	101.62	101.63
	Bottom Diameter 2	101.55	101.55	101.55	101.56	101.52	101.57	101.68	101.54	101.52	101.58
I	Average Diameter	101.52	101.56	101.54	101.52	101.49	100.75	101.55	101.55	101.49	101.56
J	G_{mb} [A/(F*π*I^2/4)]	2.353	2.343	2.347	2.346	2.347	2.345	2.346	2.343	2.347	2.348
K	Air Voids [(G_{mm}-J)/G_{mm}]	5.9	6.3	6.1	6.2	6.1	6.2	6.2	6.3	6.1	6.1
	Sample	1	2	3	4	5	6	7	8	9	10
A	Dry Mass	2897.3	2880.6	2907.8	2901.8	2899.8	2846.9	2882.1	2890.9	2894.7	2888.5
B	Submerged Mass	1674.1	1658.4	1679	1674	1671.3	1661.2	1664.4	1669.2	1666.4	1641.5
C	SSD Mass	2905.2	2888.5	2917.3	2910.3	2907.9	2889	2897.9	2902.5	2895.6	2855.1
D	G_{mb} [A/(C-B)]	2.353	2.342	2.348	2.347	2.345	2.319	2.337	2.344	2.355	2.380
E	Air Voids [(G_{mm}-D)/G_{mm}]	5.9	6.4	6.1	6.2	6.2	7.3	6.6	6.3	5.8	4.8

Project Number:
Location: M-21 Owosso
Contractor:
Mix:
Gradation:
G_{mm} 2.47

	Sample	1	2	3	4	5	6	7	8	9	10
A	Dry Mass	2855.8	2848.3	2849.8	2842	2845.1	2847.8	2848.6	2856.8	2840.5	2860
B	Height 1	151.77	151.81	151.67	151.53	151.66	151.61	151.78	151.85	151.65	152.4
C	Height 2	151.86	151.52	151.67	151.53	151.6	151.7	151.94	152.19	151.62	152.67
D	Height 3	151.62	151.48	151.62	151.76	151.66	151.49	151.59	152.09	151.67	152.71
E	Height 4	151.65	151.55	151.91	151.49	151.52	151.59	151.62	151.79	151.56	152.32
F	Average Height	151.73	151.59	151.72	151.58	151.61	151.60	151.73	151.98	151.63	152.53
G	Top Diameter 1	101.56	101.56	101.55	101.55	101.42	101.51	101.52	101.53	101.56	101.47
H	Top Diameter 2	101.58	101.49	101.58	101.48	101.49	101.44	101.5	101.5	101.54	101.53
	Middle Diameter 1	101.61	101.58	101.57	101.56	101.54	101.58	101.52	101.57	101.59	101.58
	Middle Diameter 2	101.58	101.59	101.57	101.55	101.54	101.54	101.57	101.63	101.6	101.56
	Bottom Diameter 1	101.55	101.54	101.55	101.58	101.56	101.61	101.56	101.59	101.55	101.53
	Bottom Diameter 2	101.56	101.52	101.61	101.54	101.55	101.48	101.56	101.58	101.58	101.55
I	Average Diameter	101.57	101.55	101.57	101.54	101.52	101.53	101.54	101.57	101.57	101.54
J	G_{mb} [A/(F*π*I^2/4)]	2.323	2.320	2.318	2.315	2.318	2.320	2.318	2.320	2.312	2.316
K	Air Voids [(G_{mm}-J)/G_{mm}]	6.0	6.1	6.1	6.3	6.1	6.1	6.1	6.1	6.4	6.2
	Sample	1	2	3	4	5	6	7	8	9	10
A	Dry Mass	2855.8	2848.3	2849.8	2842	2845.1	2847.8	2848.6	2856.8	2840.5	2860
B	Submerged Mass	1635.4	1629.2	1630.8	1621.5	1624	1629.1	1628.4	1632.9	1620.1	1635.3
C	SSD Mass	2863.8	2857.2	2857.7	2848.5	2851.6	2856	2856.4	2864.1	2848.4	2868.8
D	G_{mb} [A/(C-B)]	2.325	2.319	2.323	2.316	2.318	2.321	2.320	2.320	2.313	2.319
E	Air Voids [(G_{mm}-D)/G_{mm}]	5.9	6.1	6.0	6.2	6.2	6.0	6.1	6.1	6.4	6.1

Project Number:
Location: M-66 Battle Creek
Contractor:
Mix:
Gradation:
G_{mm} 2.47

	Sample	1	2	3	4	5	6	7	8	9	10
A	Dry Mass	2858.6	2862.1	2863.9	2863.4	2876.6	2866.3	2876.8	2873.2	2869.5	2867.1
B	Height 1	152.09	151.75	151.81	151.82	151.88	151.77	151.67	151.65	151.67	151.71
C	Height 2	151.66	151.55	151.67	151.71	151.95	151.83	151.73	151.7	151.58	151.71
D	Height 3	151.67	151.68	151.75	151.9	151.91	151.89	152.09	151.77	151.56	151.52
E	Height 4	152.08	151.71	151.84	151.76	151.99	151.88	151.83	151.54	151.64	151.65
F	Average Height	151.88	151.67	151.77	151.80	151.93	151.84	151.83	151.67	151.61	151.65
G	Top Diameter 1	101.43	101.48	101.42	101.57	101.34	101.57	101.65	101.46	101.63	101.5
H	Top Diameter 2	101.55	101.44	101.53	101.47	101.52	101.58	101.45	101.53	101.59	101.47
	Middle Diameter 1	101.59	101.47	101.63	101.6	101.63	101.59	101.48	101.59	101.57	101.54
	Middle Diameter 2	101.56	101.63	101.54	101.58	101.51	101.64	101.62	101.61	101.64	101.53
	Bottom Diameter 1	101.59	101.6	101.61	101.59	101.54	101.71	101.63	101.59	101.71	101.62
	Bottom Diameter 2	101.56	101.51	101.65	101.64	101.65	101.53	101.53	101.6	101.57	101.58
I	Average Diameter	101.55	101.52	101.56	101.58	101.53	101.60	101.56	101.56	101.62	101.54
J	G_{mb} [A/(F*π*I^2/4)]	2.324	2.331	2.329	2.328	2.338	2.328	2.339	2.338	2.334	2.335
K	Air Voids [(G_{mm}-J)/G_{mm}]	5.9	5.6	5.7	5.8	5.3	5.7	5.3	5.3	5.5	5.5
	Sample	1	2	3	4	5	6	7	8	9	10
A	Dry Mass	2858.6	2862.1	2863.9	2863.4	2876.6	2866.3	2876.8	2873.2	2869.5	2867.1
B	Submerged Mass	1638.8	1642.8	1644.2	1641.6	1654.8	1645	1653.4	1653	1648.8	1647.4
C	SSD Mass	2867.2	2870.4	2872	2870.2	2884.4	2873.4	2883.3	2880.4	2876.3	2875.4
D	G_{mb} [A/(C-B)]	2.327	2.331	2.333	2.331	2.339	2.333	2.339	2.341	2.338	2.335
E	Air Voids [(G_{mm}-D)/G_{mm}]	5.8	5.6	5.6	5.6	5.3	5.5	5.3	5.2	5.4	5.5

Project Number:
Location: M-50 Dundee
Contractor:
Mix: 4 E 3
Gradation:
G_{mm} 2.538

	Sample	1	2	3	4	5	6	7	8	9	10
A	Dry Mass	2919.3	2913	2907.1	2916.7	2919.9	2911	2922	2921.2	2932.3	2915.5
B	Height 1	151.37	151.13	151.17	151.27	151.51	151.29	151.3	151.53	151.9	151.41
C	Height 2	151.38	151.2	151.18	151.24	151.58	151.22	151.22	151.84	151.93	151.35
D	Height 3	151.27	151.19	151.17	151.2	151.57	151.22	151.15	151.65	152.19	151.16
E	Height 4	151.39	151.2	151.28	151.3	151.47	151.18	151.15	151.65	152.02	151.19
F	Average Height	151.3525	151.18	151.2	151.2525	151.5325	151.2275	151.205	151.6675	152.01	151.2775
G	Top Diameter 1	101.83	101.76	101.84	101.95	101.92	102	101.89	101.9	101.87	101.89
H	Top Diameter 2	101.96	101.82	101.98	101.81	101.89	101.96	101.87	101.97	101.95	101.86
	Middle Diameter 1	101.53	101.46	101.58	101.64	101.67	101.63	101.64	101.55	101.42	101.71
	Middle Diameter 2	101.65	101.71	101.55	101.62	101.65	101.59	101.51	101.47	101.63	101.56
	Bottom Diameter 1	101.69	101.87	101.52	101.65	101.41	101.7	101.56	101.53	101.7	101.6
	Bottom Diameter 2	101.48	101.68	101.63	101.69	101.5	101.74	101.56	101.73	101.65	101.48
I	Average Diameter	101.69	101.72	101.68	101.73	101.67	101.77	101.67	101.69	101.70	101.68
J	G_{mb} [A/(F*π*I^2/4)]	2.375	2.371	2.368	2.373	2.373	2.366	2.380	2.371	2.375	2.373
K	Air Voids [(G_{mm}-J)/G_{mm}]	6.4	6.6	6.7	6.5	6.5	6.8	6.2	6.6	6.4	6.5
	Sample	1	2	3	4	5	6	7	8	9	10
A	Dry Mass	2919.3	2913	2907.1	2916.7	2919.9	2911	2922	2921.2	2932.3	2915.5
B	Submerged Mass	1706.9	1702	1694.8	1702.9	1706.2	1701.5	1710.2	1706.6	1712.7	1705.8
C	SSD Mass	2929	2924.2	2916.9	2925.9	2930.8	2922.8	2933.1	2932.1	2942.3	2928.6
D	G_{mb} [A/(C-B)]	2.389	2.383	2.379	2.385	2.384	2.384	2.389	2.384	2.385	2.384
E	Air Voids [(G_{mm}-D)/G_{mm}]	5.9	6.1	6.3	6.0	6.1	6.1	5.9	6.1	6.0	6.1

Project Number:
Location: US-21 MIS
Contractor:
Mix:
Gradation:
G_{mm} 2.491

	Sample	1	2	3	4	5	6	7	8	9	10
A	Dry Mass	2864.2	2859.6	2854.2	2831.8	2830.3	2840	2859.1	2850.1	2854.6	2814.9
B	Height 1	151.54	151.24	151.17	151.23	151.14	151.14	153.33	151.32	151.14	151.13
C	Height 2	151.47	151.35	151.04	151.12	150.97	151.24	153.38	151.24	151.05	151.28
D	Height 3	151.48	151.6	151.22	151.19	151.24	151.55	153.61	151.22	151.14	151.6
E	Height 4	151.66	151.27	151.07	151.09	151.25	151.03	153.66	151.31	151.17	151.26
F	Average Height	151.54	151.37	151.13	151.16	151.15	151.24	153.50	151.27	151.13	151.32
G	Top Diameter 1	102.05	102.08	101.96	101.89	101.73	101.94	101.82	101.74	101.84	101.86
H	Top Diameter 2	101.87	102.01	101.9	102.06	101.94	101.8	101.75	101.65	101.8	101.73
	Middle Diameter 1	101.66	101.65	101.69	101.52	101.58	101.33	101.49	101.52	101.52	101.51
	Middle Diameter 2	101.62	101.74	101.67	101.65	101.53	101.68	101.7	101.55	101.58	101.47
	Bottom Diameter 1	101.85	101.77	101.82	101.66	101.29	101.42	101.61	101.52	101.55	101.51
	Bottom Diameter 2	101.73	101.67	101.81	101.57	101.39	101.39	101.41	101.45	101.41	101.5
I	Average Diameter	101.80	101.82	101.81	101.73	101.58	101.59	101.63	101.57	101.62	101.60
J	G_{mb} [A/(F*π*I^2/4)]	2.322	2.320	2.320	2.305	2.311	2.316	2.296	2.325	2.329	2.295
K	Air Voids [(G_{mm}-J)/G_{mm}]	6.8	6.9	6.9	7.5	7.2	7.0	7.8	6.7	6.5	7.9
	Sample	1	2	3	4	5	6	7	8	9	10
A	Dry Mass	2864.2	2859.6	2854.2	2831.8	2830.3	2840	2859.1	2850.1	2854.6	2814.9
B	Submerged Mass	1645.1	1641.6	1637.6	1619	1621.4	1631.3	1642	1639.9	1643.5	1613.3
C	SSD Mass	2871.8	2866.8	2862.4	2840.2	2839.3	2849.7	2875.5	2859.7	2863.3	2831.4
D	G_{mb} [A/(C-B)]	2.335	2.334	2.330	2.319	2.324	2.331	2.318	2.337	2.340	2.311
E	Air Voids [(G_{mm}-D)/G_{mm}]	6.3	6.3	6.4	6.9	6.7	6.4	6.9	6.2	6.1	7.2

Project Number:
Location: M-59 Brighton
Contractor:
Mix:
Gradation:
G_{mm} 2.503

	Sample	1	2	3	4	5	6	7	8	9	10
A	Dry Mass	2881.1	2870.2	2861.9	2869.9	2858.7	2873.6	2870.4	2875.2	2863.7	2876.1
B	Height 1	151.62	151.5	151.55	151.7	152.02	151.84	151.76	151.66	151.73	151.82
C	Height 2	151.59	151.7	151.55	151.68	151.63	151.84	151.91	151.84	151.68	151.8
D	Height 3	151.77	151.59	151.74	151.77	151.69	151.77	151.98	151.8	151.72	151.98
E	Height 4	151.86	151.72	151.65	151.58	151.78	151.54	151.93	151.81	151.95	152.53
F	Average Height	151.71	151.6275	151.6225	151.6825	151.78	151.7475	151.895	151.7775	151.77	152.0325
G	Top Diameter 1	101.33	101.3	101.32	101.34	101.39	101.39	101.34	101.27	101.28	101.32
H	Top Diameter 2	101.3	101.35	101.33	101.34	101.38	101.46	101.33	101.54	101.6	101.25
	Middle Diameter 1	101.33	101.4	101.35	101.37	101.37	101.38	101.31	101.56	101.43	101.36
	Middle Diameter 2	101.35	101.38	101.28	101.37	101.41	101.49	101.32	101.3	101.49	101.35
	Bottom Diameter 1	101.29	101.33	101.43	101.38	101.3	101.24	101.36	101.39	101.41	101.49
	Bottom Diameter 2	101.35	101.42	101.47	101.39	101.47	101.37	101.27	101.3	101.47	101.35
I	Average Diameter	101.325	101.3633	101.3633	101.365	101.3867	101.3883	101.3217	101.3933	101.4467	101.3533
J	G_{mb} [A/(F*π*I^2/4)]	2.355	2.346	2.339	2.345	2.333	2.346	2.344	2.346	2.334	2.345
K	Air Voids [(G_{mm}-J)/G_{mm}]	5.9	6.3	6.6	6.3	6.8	6.3	6.4	6.3	6.7	6.3
	Sample	1	2	3	4	5	6	7	8	9	10
A	Dry Mass	2881.1	2870.2	2861.9	2869.9	2858.7	2873.6	2870.4	2875.2	2863.7	2876.1
B	Submerged Mass	1678.2	1665.6	1659.8	1666.9	1660.5	1665.5	1660.6	1666	1654.4	1672.5
C	SSD Mass	2900.7	2890.5	2882.5	2890.6	2881.4	2889.8	2885.7	2891.7	2879.7	2897.4
D	G_{mb} [A/(C-B)]	2.357	2.343	2.341	2.345	2.341	2.347	2.343	2.346	2.337	2.348
E	Air Voids [(G_{mm}-D)/G_{mm}]	5.8	6.4	6.5	6.3	6.5	6.2	6.4	6.3	6.6	6.2

Project Number:
Location: Michigan Ave. Dearborn
Contractor:
Mix: 3 E 10
Gradation:
G_{mm} 2.493

	Sample	1	2	3	4	5	6	7	8	9	10
A	Dry Mass	2860.4	2888.4	2871.8	2881.7	2875.2	2871.7	2887.9	2880.7	2875.1	2873.1
B	Height 1	151.41	151.65	151.66	151.83	151.94	151.77	151.81	151.94	151.89	151.97
C	Height 2	151.27	151.59	151.84	151.7	152	151.66	151.72	151.52	151.65	151.92
D	Height 3	151.06	151.83	151.72	151.72	151.8	151.65	151.93	151.9	151.69	151.9
E	Height 4	151.17	151.81	151.86	151.8	151.78	151.66	151.87	151.79	151.68	151.93
F	Average Height	151.23	151.72	151.77	151.76	151.88	151.69	151.83	151.79	151.73	151.93
G	Top Diameter 1	101.66	101.64	101.42	101.48	101.52	101.52	101.46	101.53	101.56	101.49
H	Top Diameter 2	101.7	101.6	101.5	101.43	101.53	101.52	101.65	101.54	101.72	101.57
	Middle Diameter 1	101.6	101.54	101.43	101.54	101.59	101.63	101.57	101.6	101.68	101.53
	Middle Diameter 2	101.6	101.49	101.54	101.67	101.55	101.43	101.57	101.62	101.53	101.53
	Bottom Diameter 1	101.58	101.47	101.45	101.59	101.58	101.7	101.6	101.41	101.46	101.68
	Bottom Diameter 2	101.48	101.61	101.64	101.49	101.67	101.45	101.65	101.64	101.71	101.35
I	Average Diameter	101.60	101.56	101.50	101.53	101.57	101.55	101.58	101.56	101.61	101.53
J	G_{mb} [A/(F*π*I^2/4)]	2.333	2.350	2.339	2.345	2.336	2.338	2.347	2.343	2.337	2.336
K	Air Voids [(G_{mm}-J)/G_{mm}]	6.4	5.7	6.2	5.9	6.3	6.2	5.9	6.0	6.3	6.3
	Sample	1	2	3	4	5	6	7	8	9	10
A	Dry Mass	2860.4	2888.4	2871.8	2881.7	2875.2	2871.7	2887.9	2880.7	2875.1	2873.1
B	Submerged Mass	1652	1673.8	1658.2	1666.1	1661.5	1658.4	1674.9	1667.7	1663.5	1657.8
C	SSD Mass	2872.2	2899	2882.6	2891.3	2886.7	2883.7	2898.6	2892	2888.5	2884.6
D	G_{mb} [A/(C-B)]	2.344	2.357	2.345	2.352	2.347	2.344	2.360	2.353	2.347	2.342
E	Air Voids [(G_{mm}-D)/G_{mm}]	6.0	5.4	5.9	5.7	5.9	6.0	5.3	5.6	5.9	6.1

Project Number:
Location: Vandyke Detroit
Contractor:
Mix:
Gradation:
G_{mm} 2.604

	Sample	1	2	3	4	5	6	7	8	9	10
A	Dry Mass	3011.6	3007.4	3016.3	3002.3	3011.5	3014.6	3002.4	3011.8	3008.4	3009.1
B	Height 1	151.18	151.29	151.28	151.33	151.11	151.22	151.28	151.3	151.24	151.72
C	Height 2	151.23	151.33	151.16	151.18	151.2	151.34	151.21	151.35	151.24	151.39
D	Height 3	151.24	151.13	151.18	151.36	151.08	151.28	151.4	151.37	151.1	151.7
E	Height 4	151.19	151.2	151.32	151.06	151.18	151.14	151.35	151.25	151.34	151.66
F	Average Height	151.21	151.24	151.24	151.23	151.14	151.25	151.31	151.32	151.23	151.62
G	Top Diameter 1	101.82	101.96	101.93	101.9	101.85	101.84	101.9	101.8	101.91	101.84
H	Top Diameter 2	101.86	101.94	101.89	101.97	101.84	101.89	101.99	101.89	101.87	102.07
	Middle Diameter 1	101.65	101.53	101.67	101.55	101.55	101.6	101.69	101.57	101.71	101.56
	Middle Diameter 2	101.49	101.48	101.57	101.6	101.66	101.69	101.53	101.73	101.52	101.69
	Bottom Diameter 1	101.53	101.73	101.69	101.8	101.75	101.87	101.47	101.84	101.63	101.64
	Bottom Diameter 2	101.68	101.48	101.6	101.57	101.62	101.73	101.79	101.54	101.5	101.64
I	Average Diameter	101.67	101.69	101.73	101.73	101.71	101.77	101.73	101.73	101.69	101.74
J	G_{mb} [A/(F*π*I^2/4)]	2.453	2.449	2.454	2.442	2.452	2.450	2.441	2.449	2.449	2.441
K	Air Voids [(G_{mm}-J)/G_{mm}]	5.8	6.0	5.8	6.2	5.8	5.9	6.2	6.0	5.9	6.2
	Sample	1	2	3	4	5	6	7	8	9	10
A	Dry Mass	3011.6	3007.4	3016.3	3002.3	3011.5	3014.6	3002.4	3011.8	3008.4	3009.1
B	Submerged Mass	1797.3	1793.3	1802.3	1788.1	1797	1800.1	1785.9	1797	1792.1	1792.1
C	SSD Mass	3021.3	3016.6	3025.6	3011.6	3019.8	3024.1	3010.1	3020.9	3016.1	3018.4
D	G_{mb} [A/(C-B)]	2.460	2.458	2.466	2.454	2.463	2.463	2.453	2.461	2.458	2.454
E	Air Voids [(G_{mm}-D)/G_{mm}]	5.5	5.6	5.3	5.8	5.4	5.4	5.8	5.5	5.6	5.8

Project Number:
Location: US-23 Heartland
Contractor:
Mix:
Gradation:
G_{mm} 2.492

	Sample	1	2	3	4	5	6	7	8	9	10
A	Dry Mass	2904.8	2897.3	2902.7	2854.3	2883.3	2860.5	2900.6	2861.4	2878.5	2863.8
B	Height 1	153.66	152.63	152.94	153.9	152.61	153.08	153.63	152.14	152.16	153.43
C	Height 2	153.55	152.6	152.75	153.81	152.53	152.31	153.33	152.34	152.49	153.09
D	Height 3	153.21	153.09	152.13	153.25	153.23	152.7	152.85	152.27	151.98	153.18
E	Height 4	153.43	153.07	152.39	153.32	153.18	152.6	152.69	152.62	152.09	153.62
F	Average Height	153.46	152.85	152.55	153.57	152.89	152.67	153.13	152.34	152.18	153.33
G	Top Diameter 1	101.43	101.44	101.56	101.48	101.53	101.55	101.59	101.48	101.56	101.4
H	Top Diameter 2	101.47	101.48	101.44	101.63	101.56	101.59	101.52	101.59	101.51	101.6
	Middle Diameter 1	101.55	101.59	101.65	101.56	101.57	101.54	101.56	101.53	101.52	101.55
	Middle Diameter 2	101.64	101.5	101.61	101.52	101.58	101.62	101.61	101.64	101.58	101.51
	Bottom Diameter 1	101.54	101.48	101.53	101.53	101.6	101.6	101.54	101.64	101.73	101.29
	Bottom Diameter 2	101.46	101.52	101.6	101.51	101.53	101.58	101.53	101.51	101.65	101.52
I	Average Diameter	101.52	101.50	101.57	101.54	101.56	101.58	101.56	101.57	101.59	101.48
J	G_{mb} [A/(F*π*I^2/4)]	2.339	2.343	2.349	2.295	2.328	2.312	2.338	2.318	2.333	2.309
K	Air Voids [(G_{mm}-J)/G_{mm}]	6.2	6.0	5.8	7.9	6.6	7.2	6.2	7.0	6.4	7.3
	Sample	1	2	3	4	5	6	7	8	9	10
A	Dry Mass	2904.8	2897.3	2902.7	2854.3	2883.3	2860.5	2900.6	2861.4	2878.5	2863.8
B	Submerged Mass	1682	1679.3	1684.9	1638.2	1667.8	1645.5	1684.4	1649.1	1663.2	1659.1
C	SSD Mass	2919	2911.1	2919.2	2875	2901	2877.5	2916.8	2880.3	2891	2889.9
D	G_{mb} [A/(C-B)]	2.348	2.352	2.352	2.308	2.338	2.322	2.354	2.324	2.344	2.327
E	Air Voids [(G_{mm}-D)/G_{mm}]	5.8	5.6	5.6	7.4	6.2	6.8	5.6	6.7	5.9	6.6

Project Number:
Location: I-75 Levering Rd.
Contractor:
Mix:
Gradation:
G_{mm} 2.443

	Sample	1	2	3	4	5	6	7	8	9	10
A	Dry Mass	2848.2	2850.6	2849.6	2834.8	2828.2	2845.8	2858.7	2836.5	2832.8	2845.2
B	Height 1	151.81	152.46	151.82	152.27	151.92	152.37	152.95	152.28	152.1	151.76
C	Height 2	151.93	152.04	151.71	152.2	151.98	152.39	152.55	152.28	151.89	151.93
D	Height 3	152.05	151.99	151.89	152.06	152.18	151.89	152.36	151.98	151.96	152.26
E	Height 4	152.17	152.33	151.96	152.21	152.27	151.88	152.56	152	152.31	152.46
F	Average Height	151.99	152.21	151.85	152.19	152.09	152.13	152.61	152.14	152.07	152.10
G	Top Diameter 1	101.63	101.56	101.55	101.68	101.66	101.66	101.54	101.6	101.49	101.44
H	Top Diameter 2	101.45	101.52	101.45	101.58	101.3	101.42	101.44	101.42	101.57	101.43
	Middle Diameter 1	101.49	101.69	101.54	101.49	101.45	101.48	101.44	101.5	101.57	101.59
	Middle Diameter 2	101.63	101.6	101.53	101.64	101.64	101.58	101.69	101.59	101.52	101.58
	Bottom Diameter 1	101.59	101.58	101.65	101.74	101.7	101.69	101.58	101.72	101.37	101.63
	Bottom Diameter 2	101.54	101.66	101.44	101.54	101.65	101.49	101.38	101.51	101.59	101.65
I	Average Diameter	101.56	101.60	101.53	101.61	101.57	101.55	101.51	101.56	101.52	101.55
J	G_{mb} [A/(F*π*I^2/4)]	2.313	2.310	2.318	2.297	2.295	2.309	2.315	2.302	2.301	2.309
K	Air Voids [(G_{mm}-J)/G_{mm}]	5.3	5.4	5.1	6.0	6.0	5.5	5.3	5.8	5.8	5.5
	Sample	1	2	3	4	5	6	7	8	9	10
A	Dry Mass	2848.2	2850.6	2849.6	2834.8	2828.2	2845.8	2858.7	2836.5	2832.8	2845.2
B	Submerged Mass	1623.9	1626.3	1626.6	1610	1605.6	1621.4	1630	1611.8	1608.9	1619.9
C	SSD Mass	2856.2	2859.6	2858.2	2843.9	2837	2854.8	2866	2845.5	2841.9	2853.3
D	G_{mb} [A/(C-B)]	2.311	2.311	2.314	2.297	2.297	2.307	2.313	2.299	2.297	2.307
E	Air Voids [(G_{mm}-D)/G_{mm}]	5.4	5.4	5.3	6.0	6.0	5.6	5.3	5.9	6.0	5.6

Project Number:
Location: I-196 Grand Rapids
Contractor:
Mix:
Gradation:
G_{mm} 2.499

	Sample	1	2	3	4	5	6	7	8	9	10
A	Dry Mass	2865.7	2837.7	2851.1	2869.8	2859.3	2868.4	2871.8	2862.4	2851.3	2872.1
B	Height 1	151.02	151.28	151.07	151.31	151.33	151.33	151.17	151.25	151.19	151.29
C	Height 2	151	151.38	151.21	151.09	151.36	151.57	151.42	151.09	151.28	151.33
D	Height 3	150.87	151.28	151.28	151.05	151.3	151.25	151.07	151.14	151.39	151.2
E	Height 4	150.92	151.33	151.2	151.15	151.45	151.22	151.22	151.17	151.29	151.29
F	Average Height	150.9525	151.3175	151.19	151.15	151.36	151.3425	151.22	151.1625	151.2875	151.2775
G	Top Diameter 1	101.37	101.32	101.47	101.35	101.3	101.38	101.34	101.36	101.37	101.366
H	Top Diameter 2	101.4	101.28	101.33	101.27	101.16	101.3	101.36	101.43	101.34	101.4
	Middle Diameter 1	101.4	101.26	101.41	101.28	101.24	101.35	101.28	101.3	101.33	101.44
	Middle Diameter 2	101.38	101.22	101.41	101.33	101.23	101.23	101.17	101.54	101.31	101.46
	Bottom Diameter 1	101.47	101.24	101.19	101.39	101.27	101.59	101.31	101.32	101.28	101.33
	Bottom Diameter 2	101.36	101.25	101.39	101.28	101.28	101.33	101.3	101.36	101.4	101.42
I	Average Diameter	101.3967	101.2617	101.3667	101.3167	101.2467	101.3633	101.2933	101.385	101.3383	101.4027
J	G_{mb} [A/(F*π*I^2/4)]	2.351	2.329	2.337	2.355	2.346	2.349	2.357	2.346	2.337	2.351
K	Air Voids [(G_{mm}-J)/G_{mm}]	5.9	6.8	6.5	5.8	6.1	6.0	5.7	6.1	6.5	5.9
	Sample	1	2	3	4	5	6	7	8	9	10
A	Dry Mass	2865.7	2837.7	2851.1	2869.8	2859.3	2868.4	2871.8	2862.4	2851.3	2872.1
B	Submerged Mass	1648.8	1628.4	1641.8	1656.6	1645.3	1657.4	1659.5	1650	1641.2	1657.6
C	SSD Mass	2873.8	2853	2864.1	2881.6	2871	2881.3	2883.9	2874.7	2865.8	2883.6
D	G_{mb} [A/(C-B)]	2.339	2.317	2.333	2.343	2.333	2.344	2.345	2.337	2.328	2.343
E	Air Voids [(G_{mm}-D)/G_{mm}]	6.4	7.3	6.7	6.3	6.7	6.2	6.1	6.5	6.8	6.3

Project Number:
Location: I-75 Clarkston
Contractor:
Mix:
Gradation:
G_{mm} 2.487

	Sample	1	2	3	4	5	6	7	8	9	10
A	Dry Mass	2863.3	2857.5	2838.5	2849.3	2855.9	2854.1	2850.6	2889.7	2855.5	2850.6
B	Height 1	151.14	151.05	150.79	150.84	151.03	151	150.89	151.25	150.97	151.09
C	Height 2	151.15	151.43	151.14	150.86	150.99	150.97	150.97	151.09	151.11	151.2
D	Height 3	151.34	151.36	151.09	150.99	151.02	151.01	151.03	151.14	151.16	151.24
E	Height 4	151.37	151.04	151.19	151.07	151.2	151.06	150.95	151.17	150.98	151.07
F	Average Height	151.25	151.22	151.0525	150.94	151.06	151.01	150.96	151.1625	151.055	151.15
G	Top Diameter 1	101.83	101.84	101.8	101.77	101.84	101.79	101.84	101.83	101.83	101.94
H	Top Diameter 2	101.85	101.76	101.78	101.97	101.85	101.73	101.86	101.77	101.9	101.91
	Middle Diameter 1	101.62	101.5	101.62	101.61	101.5	101.54	101.58	101.58	101.58	101.55
	Middle Diameter 2	101.62	101.52	101.57	101.51	101.52	101.7	101.5	101.6	101.56	101.6
	Bottom Diameter 1	101.61	101.73	101.75	101.37	101.53	101.83	101.53	101.52	101.46	101.73
	Bottom Diameter 2	101.48	101.66	101.81	101.53	101.81	101.59	101.61	101.73	101.62	101.49
I	Average Diameter	101.67	101.67	101.72	101.63	101.68	101.70	101.65	101.67	101.66	101.70
J	G_{mb} [A/(F*π*I^2/4)]	2.332	2.328	2.312	2.327	2.328	2.327	2.327	2.355	2.329	2.321
K	Air Voids [(G_{mm}-J)/G_{mm}]	6.2	6.4	7.0	6.4	6.4	6.4	6.4	5.3	6.4	6.7
	Sample	1	2	3	4	5	6	7	8	9	10
A	Dry Mass	2863.3	2857.5	2838.5	2849.3	2855.9	2854.1	2850.6	2889.7	2855.5	2850.6
B	Submerged Mass	1651.2	1645.1	1629.8	1640.6	1646.7	1643.7	1638.7	1675.2	1644.9	1640.8
C	SSD Mass	2872.7	2867.1	2849.7	2860.5	2866.7	2865.2	2859.5	2897.8	2866.6	2862.6
D	G_{mb} [A/(C-B)]	2.344	2.338	2.327	2.336	2.341	2.337	2.335	2.364	2.337	2.333
E	Air Voids [(G_{mm}-D)/G_{mm}]	5.7	6.0	6.4	6.1	5.9	6.0	6.1	5.0	6.0	6.2

Project Number:
Location: M-53 Detroit
Contractor:
Mix:
Gradation:
G_{mm} 2.563

	Sample	1	2	3	4	5	6	7	8	9	10
A	Dry Mass	2953.2	2957.8	2957.9	2961.8	2955.4	2954.5	2982.1	2964.7	2944.4	2963.8
B	Height 1	151.1	151.22	151.23	150.95	151.31	151.3	151.56	151.44	150.91	150.95
C	Height 2	151.16	151.11	151.17	151.22	151.09	151.26	151.71	151.05	151.07	151.07
D	Height 3	150.95	151.28	151.09	151.21	151.3	151.26	151.76	151.05	150.85	151
E	Height 4	151.23	151.12	151.3	151.12	151.26	151.24	151.6	151.27	151.08	150.88
F	Average Height	151.11	151.1825	151.1975	151.125	151.24	151.265	151.6575	151.2025	150.9775	150.975
G	Top Diameter 1	101.31	101.33	101.28	101.51	101.54	101.34	101.54	101.34	101.33	101.3
H	Top Diameter 2	101.42	101.47	101.39	101.51	101.34	101.33	101.34	101.32	101.38	101.32
	Middle Diameter 1	101.35	101.47	101.3	101.29	101.27	101.23	101.3	101.39	101.25	101.29
	Middle Diameter 2	101.43	101.36	101.34	101.32	101.33	101.3	101.32	101.17	101.27	101.27
	Bottom Diameter 1	101.38	101.52	101.27	101.45	101.33	101.43	101.31	101.36	101.32	101.39
	Bottom Diameter 2	101.49	101.36	101.31	101.36	101.39	101.5	101.3	101.34	101.31	101.19
I	Average Diameter	101.3967	101.4183	101.315	101.4067	101.3667	101.355	101.3517	101.32	101.31	101.2933
J	G_{mb} [A/(F*π*I^2/4)]	2.420	2.422	2.427	2.427	2.421	2.421	2.437	2.432	2.419	2.436
K	Air Voids [(G_{mm}-J)/G_{mm}]	5.6	5.5	5.3	5.3	5.5	5.5	4.9	5.1	5.6	5.0
	Sample	1	2	3	4	5	6	7	8	9	10
A	Dry Mass	2953.2	2957.8	2957.9	2961.8	2955.4	2954.5	2982.1	2964.7	2944.4	2963.8
B	Submerged Mass	1741.8	1746.8	1744.2	1749.3	1743.6	1737.2	1763.7	1752.3	1734.5	1752.5
C	SSD Mass	2964.7	2969.1	2968.1	2972.7	2966.3	2962.2	2992	2974.1	2956.1	2974.4
D	G_{mb} [A/(C-B)]	2.415	2.420	2.417	2.421	2.417	2.412	2.428	2.427	2.410	2.426
E	Air Voids [(G_{mm}-D)/G_{mm}]	5.8	5.6	5.7	5.5	5.7	5.9	5.3	5.3	6.0	5.4

Project Number:
Location: Michigan Ave. Dearborn
Contractor:
Mix: 4 E 10
Gradation:
G_{mm} 2.485

	Sample	1	2	3	4	5	6	7	8	9	10
A	Dry Mass	2841	2842	2844.6	2846.5	2842	2844.8	2835.3	2852.8	2844.3	2853.9
B	Height 1	151.76	151.72	151.71	151.64	151.66	151.75	151.77	151.66	151.77	151.79
C	Height 2	151.58	151.72	151.75	151.71	151.74	151.55	151.81	151.59	151.74	151.76
D	Height 3	151.54	151.81	151.76	151.76	151.6	151.79	151.69	151.77	151.75	151.81
E	Height 4	151.51	151.82	151.58	151.81	151.93	151.57	151.8	151.65	151.82	151.78
F	Average Height	151.60	151.77	151.70	151.73	151.73	151.67	151.77	151.67	151.77	151.79
G	Top Diameter 1	101.47	101.42	101.45	101.55	101.45	101.49	101.53	101.51	101.58	101.46
H	Top Diameter 2	101.48	101.48	101.42	101.55	101.42	101.46	101.52	101.57	101.47	101.55
	Middle Diameter 1	101.54	101.55	101.51	101.54	101.52	101.53	101.47	101.57	101.53	101.58
	Middle Diameter 2	101.52	101.46	101.51	101.58	101.51	101.54	101.52	101.59	101.56	101.63
	Bottom Diameter 1	101.55	101.57	101.52	101.62	101.59	101.58	101.59	101.7	101.7	101.58
	Bottom Diameter 2	101.5	101.58	101.56	101.48	101.57	101.64	101.56	101.58	101.58	101.63
I	Average Diameter	101.51	101.51	101.50	101.55	101.51	101.54	101.53	101.59	101.57	101.57
J	G_{mb} [A/(F*π*I^2/4)]	2.316	2.314	2.318	2.316	2.314	2.316	2.307	2.321	2.313	2.320
K	Air Voids [(G_{mm}-J)/G_{mm}]	6.8	6.9	6.7	6.8	6.9	6.8	7.1	6.6	6.9	6.6
	Sample	1	2	3	4	5	6	7	8	9	10
A	Dry Mass	2841	2842	2844.6	2846.5	2842	2844.8	2835.3	2852.8	2844.3	2853.9
B	Submerged Mass	1629.4	1629.9	1627.9	1634.3	1629.4	1629.9	1623.2	1637.9	1629.4	1640.2
C	SSD Mass	2851.6	2853.1	2852.7	2857.8	2853.2	2854.6	2847	2862.4	2855.4	2864.3
D	G_{mb} [A/(C-B)]	2.324	2.323	2.323	2.327	2.322	2.323	2.317	2.330	2.320	2.331
E	Air Voids [(G_{mm}-D)/G_{mm}]	6.5	6.5	6.5	6.4	6.5	6.5	6.8	6.2	6.6	6.2

Project Number:
Location: I-75 Toledo
Contractor:
Mix:
Gradation:
G_{mm} 2.507

	Sample	1	2	3	4	5	6	7	8	9	10
A	Dry Mass	2874.2	2882.7	2881.4	2878	2877.4	2878.7	2880.4	2879.9	2871.2	2868.2
B	Height 1	151.4	151.9	151.93	151.55	151.61	151.93	151.63	151.57	151.61	151.55
C	Height 2	151.71	151.87	152.02	151.5	151.78	151.63	151.64	151.61	151.66	151.58
D	Height 3	151.29	151.52	151.93	151.59	151.76	151.59	151.85	151.68	151.62	151.53
E	Height 4	151.54	151.77	151.88	151.64	151.94	151.7	151.74	151.6	151.58	151.7
F	Average Height	151.49	151.77	151.94	151.57	151.77	151.71	151.72	151.62	151.62	151.59
G	Top Diameter 1	101.5	101.52	101.46	101.36	101.46	101.55	101.37	101.4	101.38	101.5
H	Top Diameter 2	101.53	101.53	101.71	101.63	101.58	101.45	101.61	101.36	101.41	101.51
	Middle Diameter 1	101.59	101.54	101.64	101.48	101.5	101.6	101.58	101.38	101.56	101.47
	Middle Diameter 2	101.48	101.57	101.51	101.54	101.55	101.43	101.52	101.46	101.48	101.47
	Bottom Diameter 1	101.54	101.59	101.64	101.53	101.64	101.52	101.57	101.47	101.58	101.52
	Bottom Diameter 2	101.53	101.58	101.62	101.58	101.56	101.51	101.56	101.48	101.52	101.56
I	Average Diameter	101.53	101.56	101.60	101.52	101.55	101.51	101.54	101.43	101.49	101.51
J	G_{mb} [A/(F*π*I^2/4)]	2.344	2.345	2.339	2.346	2.341	2.345	2.345	2.351	2.341	2.338
K	Air Voids [(G_{mm}-J)/G_{mm}]	6.5	6.5	6.7	6.4	6.6	6.5	6.5	6.2	6.6	6.7
	Sample	1	2	3	4	5	6	7	8	9	10
A	Dry Mass	2874.2	2882.7	2881.4	2878	2877.4	2878.7	2880.4	2879.9	2871.2	2868.2
B	Submerged Mass	1661	1670.1	1667.8	1664	1664.4	1664.7	1670	1671.8	1662.7	1659.8
C	SSD Mass	2885.8	2895.3	2893.9	2888.9	2890.3	2890.4	2895.5	2893.1	2886.3	2882.4
D	G_{mb} [A/(C-B)]	2.347	2.353	2.350	2.350	2.347	2.349	2.350	2.358	2.347	2.346
E	Air Voids [(G_{mm}-D)/G_{mm}]	6.4	6.1	6.3	6.3	6.4	6.3	6.2	5.9	6.4	6.4

Project Number:
Location: I-94 Ann Arbor
Contractor:
Mix: SMA
Gradation:
G_{mm} 2.515

	Sample	1	2	3	4	5	6	7	8	9	10
A	Dry Mass	2906.1	2913.9	2902.1	2885	2907.7	2907.7	2889.2	2890.7	2895	2881.1
B	Height 1	152.01	152.24	152.36	151.03	152.19	152.97	151.82	151.82	151.85	151.75
C	Height 2	152.32	152.26	152.38	151.14	152.2	152.65	151.93	151.5	151.98	151.95
D	Height 3	152.18	152.32	152.93	151.16	152.02	152.79	151.77	151.56	151.84	151.62
E	Height 4	151.84	152.39	152.69	151.06	151.94	152.72	151.95	151.77	151.95	151.68
F	Average Height	152.0875	152.3025	152.59	151.0975	152.0875	152.7825	151.8675	151.6625	151.905	151.75
G	Top Diameter 1	101.38	101.44	101.59	101.32	101.31	101.31	101.3	101.33	101.35	101.49
H	Top Diameter 2	101.48	101.56	101.59	101.34	101.34	101.3	101.25	101.33	101.31	101.3
	Middle Diameter 1	101.64	101.46	101.63	101.33	101.27	101.36	101.28	101.32	101.48	101.28
	Middle Diameter 2	101.48	101.59	101.59	101.28	101.3	101.3	101.33	101.31	101.32	101.36
	Bottom Diameter 1	101.62	101.6	101.83	101.35	101.33	101.3	101.34	101.32	101.32	101.29
	Bottom Diameter 2	101.6	101.62	101.61	101.28	101.27	101.33	101.37	101.47	101.45	101.43
I	Average Diameter	101.5333	101.545	101.64	101.3167	101.3033	101.3167	101.3117	101.3467	101.3717	101.3583
J	G_{mb} [A/(F*π*I^2/4)]	2.360	2.362	2.344	2.368	2.372	2.361	2.360	2.363	2.361	2.353
K	Air Voids [(G_{mm}-J)/G_{mm}]	6.2	6.1	6.8	5.8	5.7	6.1	6.2	6.1	6.1	6.4
	Sample	1	2	3	4	5	6	7	8	9	10
A	Dry Mass	2906.1	2913.9	2902.1	2885	2907.7	2907.7	2889.2	2890.7	2895	2881.1
B	Submerged Mass	1696.1	1703.1	1684.5	1692.4	1703.9	1709.9	1691.7	1689.6	1696.3	1678.1
C	SSD Mass	2924.4	2932.9	2911.4	2908.7	2931.2	2934.7	2915.4	2911.8	2917.1	2900.1
D	G_{mb} [A/(C-B)]	2.366	2.369	2.365	2.372	2.369	2.374	2.361	2.365	2.371	2.358
E	Air Voids [(G_{mm}-D)/G_{mm}]	5.9	5.8	5.9	5.7	5.8	5.6	6.1	6.0	5.7	6.3

APPENDIX C SAS OUTPUTS

Distribution Fitting Outputs for Phase I and Phase II
Phase I Moisture Study
150mm Superpave – 1 Freeze/thaw Cycle

The UNIVARIATE Procedure
Variable: tsrS1

Moments

N	35	Sum Weights	35
Mean	93.2857143	Sum Observations	3265
Std Deviation	11.8534468	Variance	140.504202
Skewness	-0.5350362	Kurtosis	0.019754
Uncorrected SS	309355	Corrected SS	4777.14286
Coeff Variation	12.7066046	Std Error Mean	2.0035982

Basic Statistical Measures

Location		Variability	
Mean	93.2857	Std Deviation	11.85345
Median	96.0000	Variance	140.50420
Mode	100.0000	Range	52.00000
		Interquartile Range	15.00000

Tests for Location: Mu0=0

Test	-Statistic-		-----p Value------
Student's t	t	46.55909	Pr > |t| <.0001
Sign	M	17.5	Pr >= |M| <.0001
Signed Rank	S	315	Pr >= |S| <.0001

Fitted Distributions for tsrS1

Parameters for Normal Distribution

Parameter	Symbol	Estimate
Mean	Mu	93.28571
Std Dev	Sigma	11.85345

Goodness-of-Fit Tests for Normal Distribution

Test	---Statistic----		-----p Value-----
Kolmogorov-Smirnov	D	0.14302463	Pr > D 0.070
Cramer-von Mises	W-Sq	0.07795230	Pr > W-Sq 0.220
Anderson-Darling	A-Sq	0.43589260	Pr > A-Sq >0.250

Parameters for Lognormal Distribution

Parameter	Symbol	Estimate
Threshold	Theta	0
Scale	Zeta	4.527278
Shape	Sigma	0.133903
Mean		93.3395
Std Dev		12.55466

Goodness-of-Fit Tests for Lognormal Distribution

Test	---Statistic----		-----p Value-----	
Kolmogorov-Smirnov	D	0.15094143	Pr > D	0.045
Cramer-von Mises	W-Sq	0.10546672	Pr > W-Sq	0.093
Anderson-Darling	A-Sq	0.63226708	Pr > A-Sq	0.093

Parameters for Weibull Distribution

Parameter	Symbol	Estimate
Threshold	Theta	0
Scale	Sigma	98.27725
Shape	C	9.635224
Mean		93.34722
Std Dev		11.63131

Goodness-of-Fit Tests for Weibull Distribution

Test	---Statistic----		-----p Value-----	
Cramer-von Mises	W-Sq	0.05761474	Pr > W-Sq	>0.250
Anderson-Darling	A-Sq	0.29976607	Pr > A-Sq	>0.250

150mm Superpave – 2 Freeze/thaw Cycle

The UNIVARIATE Procedure
Variable: tsrS2

Moments

N	35	Sum Weights	35
Mean	87.9428571	Sum Observations	3078
Std Deviation	13.0315067	Variance	169.820168
Skewness	0.09469332	Kurtosis	-0.8544696
Uncorrected SS	276462	Corrected SS	5773.88571
Coeff Variation	14.8181526	Std Error Mean	2.20272667

Basic Statistical Measures

Location		Variability	
Mean	87.94286	Std Deviation	13.03151
Median	89.00000	Variance	169.82017
Mode	73.00000	Range	51.00000
		Interquartile Range	22.00000

Tests for Location: Mu0=0

Test	-Statistic-	-----p Value------
Student's t	t 39.92454	Pr > |t| <.0001
Sign	M 17.5	Pr >= |M| <.0001
Signed Rank	S 315	Pr >= |S| <.0001

Fitted Distributions for tsrS2

Parameters for Normal Distribution

Parameter	Symbol	Estimate
Mean	Mu	87.94286
Std Dev	Sigma	13.03151

Goodness-of-Fit Tests for Normal Distribution

Test	---Statistic----	-----p Value-----
Kolmogorov-Smirnov	D 0.12012127	Pr > D >0.150
Cramer-von Mises	W-Sq 0.06963466	Pr > W-Sq >0.250
Anderson-Darling	A-Sq 0.45030797	Pr > A-Sq >0.250

Parameters for Lognormal Distribution

Parameter	Symbol	Estimate
Threshold	Theta	0
Scale	Zeta	4.465882
Shape	Sigma	0.149769
Mean		87.97896
Std Dev		13.25076

Goodness-of-Fit Tests for Lognormal Distribution

Test	---Statistic----		-----p Value-----
Kolmogorov-Smirnov	D	0.10983981	Pr > D >0.150
Cramer-von Mises	W-Sq	0.09047980	Pr > W-Sq 0.147
Anderson-Darling	A-Sq	0.53068504	Pr > A-Sq 0.170

Parameters for Weibull Distribution

Parameter	Symbol	Estimate
Threshold	Theta	0
Scale	Sigma	93.5345
Shape	C	7.540292
Mean		87.82856
Std Dev		13.77098

Goodness-of-Fit Tests for Weibull Distribution

Test	---Statistic----		-----p Value-----
Cramer-von Mises	W-Sq	0.05364863	Pr > W-Sq >0.250
Anderson-Darling	A-Sq	0.41954107	Pr > A-Sq >0.250

150mm Superpave – 3 Freeze/thaw Cycle

The UNIVARIATE Procedure
Variable: tsrS3

Moments

N	35	Sum Weights	35
Mean	83.4857143	Sum Observations	2922
Std Deviation	15.5324545	Variance	241.257143
Skewness	0.32710397	Kurtosis	-0.2173961
Uncorrected SS	252148	Corrected SS	8202.74286
Coeff Variation	18.604925	Std Error Mean	2.625464

Basic Statistical Measures

Location		Variability	
Mean	83.48571	Std Deviation	15.53245
Median	84.00000	Variance	241.25714
Mode	91.00000	Range	63.00000
		Interquartile Range	21.00000

Tests for Location: Mu0=0

Test	-Statistic-		-----p Value------
Student's t	t	31.79846	Pr > |t| <.0001
Sign	M	17.5	Pr >= |M| <.0001
Signed Rank	S	315	Pr >= |S| <.0001

Fitted Distributions for tsrS3

Parameters for Normal Distribution

Parameter	Symbol	Estimate
Mean	Mu	83.48571
Std Dev	Sigma	15.53245

Goodness-of-Fit Tests for Normal Distribution

Test	---Statistic----		-----p Value-----
Kolmogorov-Smirnov	D	0.08639713	Pr > D >0.150
Cramer-von Mises	W-Sq	0.03624281	Pr > W-Sq >0.250
Anderson-Darling	A-Sq	0.28216379	Pr > A-Sq >0.250

Parameters for Lognormal Distribution

Parameter	Symbol	Estimate
Threshold	Theta	0
Scale	Zeta	4.407805
Shape	Sigma	0.187024
Mean		83.53737
Std Dev		15.76111

Goodness-of-Fit Tests for Lognormal Distribution

Test	---Statistic----		-----p Value-----
Kolmogorov-Smirnov	D	0.10919085	Pr > D >0.150
Cramer-von Mises	W-Sq	0.04567675	Pr > W-Sq >0.500
Anderson-Darling	A-Sq	0.27629087	Pr > A-Sq >0.500

Parameters for Weibull Distribution

Parameter	Symbol	Estimate
Threshold	Theta	0
Scale	Sigma	89.93046
Shape	C	5.782065
Mean		83.2585
Std Dev		16.69232

Goodness-of-Fit Tests for Weibull Distribution

Test	---Statistic----		-----p Value-----
Cramer-von Mises	W-Sq	0.04837711	Pr > W-Sq >0.250
Anderson-Darling	A-Sq	0.43219627	Pr > A-Sq >0.250

100mm Marshall – 1 Freeze/thaw Cycle

The UNIVARIATE Procedure
Variable: tsrM1
Moments

N	35	Sum Weights	35
Mean	97.7714286	Sum Observations	3422
Std Deviation	21.0895649	Variance	444.769748
Skewness	-0.2211672	Kurtosis	-0.9689605
Uncorrected SS	349696	Corrected SS	15122.1714
Coeff Variation	21.5702739	Std Error Mean	3.5647871

Basic Statistical Measures

Location		Variability	
Mean	97.7714	Std Deviation	21.08956
Median	99.0000	Variance	444.76975
Mode	116.0000	Range	73.00000
		Interquartile Range	39.00000

Tests for Location: Mu0=0

Test	-Statistic-		-----p Value------
Student's t	t	27.427	Pr > |t| <.0001
Sign	M	17.5	Pr >= |M| <.0001
Signed Rank	S	315	Pr >= |S| <.0001

Parameters for Normal Distribution

Parameter	Symbol	Estimate
Mean	Mu	97.77143
Std Dev	Sigma	21.08956

Goodness-of-Fit Tests for Normal Distribution

Test	---Statistic----		-----p Value-----
Kolmogorov-Smirnov	D	0.09900318	Pr > D >0.150
Cramer-von Mises	W-Sq	0.06880207	Pr > W-Sq >0.250
Anderson-Darling	A-Sq	0.43242541	Pr > A-Sq >0.250

Parameters for Lognormal Distribution

Parameter	Symbol	Estimate
Threshold	Theta	0
Scale	Zeta	4.558176
Shape	Sigma	0.229319
Mean		97.9512
Std Dev		22.76068

Goodness-of-Fit Tests for Lognormal Distribution

Test	---Statistic----		-----p Value-----	
Kolmogorov-Smirnov	D	0.13930827	Pr > D	0.084
Cramer-von Mises	W-Sq	0.12833590	Pr > W-Sq	0.045
Anderson-Darling	A-Sq	0.72762170	Pr > A-Sq	0.053

Parameters for Weibull Distribution

Parameter	Symbol	Estimate
Threshold	Theta	0
Scale	Sigma	106.1106
Shape	C	5.522241
Mean		97.98391
Std Dev		20.49222

Goodness-of-Fit Tests for Weibull Distribution

Test	---Statistic----		-----p Value-----	
Cramer-von Mises	W-Sq	0.04951851	Pr > W-Sq	>0.250
Anderson-Darling	A-Sq	0.35492956	Pr > A-Sq	>0.250

100mm Marshall – 2 Freeze/thaw Cycle

The UNIVARIATE Procedure
Variable: tsrM2
Moments

N	35	Sum Weights	35
Mean	94.7428571	Sum Observations	3316
Std Deviation	20.0826862	Variance	403.314286
Skewness	0.00533005	Kurtosis	-0.4631701
Uncorrected SS	327880	Corrected SS	13712.6857
Coeff Variation	21.1970452	Std Error Mean	3.39459354

Basic Statistical Measures

Location		Variability	
Mean	94.7429	Std Deviation	20.08269
Median	94.0000	Variance	403.31429
Mode	105.0000	Range	83.00000
		Interquartile Range	28.00000

Tests for Location: Mu0=0

Test	-Statistic-	-----p Value------
Student's t	t 27.90993	Pr > |t| <.0001
Sign	M 17.5	Pr >= |M| <.0001
Signed Rank	S 315	Pr >= |S| <.0001

Parameters for Normal Distribution

Parameter	Symbol	Estimate
Mean	Mu	94.74286
Std Dev	Sigma	20.08269

Goodness-of-Fit Tests for Normal Distribution

Test	---Statistic----	-----p Value-----
Kolmogorov-Smirnov	D 0.07773968	Pr > D >0.150
Cramer-von Mises	W-Sq 0.03579673	Pr > W-Sq >0.250
Anderson-Darling	A-Sq 0.22153527	Pr > A-Sq >0.250

Parameters for Lognormal Distribution

Parameter	Symbol	Estimate
Threshold	Theta	0
Scale	Zeta	4.528125
Shape	Sigma	0.221542
Mean		94.88501
Std Dev		21.28165

Goodness-of-Fit Tests for Lognormal Distribution

Test	---Statistic----		-----p Value-----
Kolmogorov-Smirnov	D	0.11497959	Pr > D >0.150
Cramer-von Mises	W-Sq	0.07922535	Pr > W-Sq 0.213
Anderson-Darling	A-Sq	0.43786178	Pr > A-Sq 0.293

Parameters for Weibull Distribution

Parameter	Symbol	Estimate
Threshold	Theta	0
Scale	Sigma	102.751
Shape	C	5.343813
Mean		94.70432
Std Dev		20.41195

Goodness-of-Fit Tests for Weibull Distribution

Test	---Statistic----		-----p Value-----
Cramer-von Mises	W-Sq	0.03110473	Pr > W-Sq >0.250
Anderson-Darling	A-Sq	0.21469917	Pr > A-Sq >0.250

100mm Marshall – 3 Freeze/thaw Cycle

The UNIVARIATE Procedure
Variable: tsrM3
Moments

N	35	Sum Weights	35
Mean	83.4571429	Sum Observations	2921
Std Deviation	19.1454846	Variance	366.54958
Skewness	-0.1889456	Kurtosis	-0.8930737
Uncorrected SS	256241	Corrected SS	12462.6857
Coeff Variation	22.9404985	Std Error Mean	3.23617755

Basic Statistical Measures

Location		Variability	
Mean	83.45714	Std Deviation	19.14548
Median	86.00000	Variance	366.54958
Mode	68.00000	Range	71.00000
		Interquartile Range	31.00000

Tests for Location: Mu0=0

Test	-Statistic-		-----p Value------
Student's t	t	25.7888	Pr > |t| <.0001
Sign	M	17.5	Pr >= |M| <.0001
Signed Rank	S	315	Pr >= |S| <.0001

Parameters for Normal Distribution

Parameter	Symbol	Estimate
Mean	Mu	83.45714
Std Dev	Sigma	19.14548

Goodness-of-Fit Tests for Normal Distribution

Test	---Statistic----		-----p Value-----
Kolmogorov-Smirnov	D	0.09087113	Pr > D >0.150
Cramer-von Mises	W-Sq	0.06741259	Pr > W-Sq >0.250
Anderson-Darling	A-Sq	0.40882763	Pr > A-Sq >0.250

Parameters for Lognormal Distribution

Parameter	Symbol	Estimate
Threshold	Theta	0
Scale	Zeta	4.396524
Shape	Sigma	0.244979
Mean		83.6408
Std Dev		20.80157

Goodness-of-Fit Tests for Lognormal Distribution

Test	---Statistic----		-----p Value-----	
Kolmogorov-Smirnov	D	0.13629187	Pr > D	0.096
Cramer-von Mises	W-Sq	0.13019416	Pr > W-Sq	0.043
Anderson-Darling	A-Sq	0.72986888	Pr > A-Sq	0.052

Parameters for Weibull Distribution

Parameter	Symbol	Estimate
Threshold	Theta	0
Scale	Sigma	90.92177
Shape	C	5.146386
Mean		83.62063
Std Dev		18.65498

Goodness-of-Fit Tests for Weibull Distribution

Test	---Statistic----		-----p Value-----	
Cramer-von Mises	W-Sq	0.04754713	Pr > W-Sq	>0.250
Anderson-Darling	A-Sq	0.32296421	Pr > A-Sq	>0.250

100mm Superpave – 1 Freeze/thaw Cycle

The UNIVARIATE Procedure
Variable: tsrS1
Moments

N	35	Sum Weights	35
Mean	88.8	Sum Observations	3108
Std Deviation	16.4742223	Variance	271.4
Skewness	0.27572465	Kurtosis	0.48623737
Uncorrected SS	285218	Corrected SS	9227.6
Coeff Variation	18.5520521	Std Error Mean	2.78465181

Basic Statistical Measures

Location		Variability	
Mean	88.80000	Std Deviation	16.47422
Median	89.00000	Variance	271.40000
Mode	78.00000	Range	76.00000
		Interquartile Range	22.00000

Tests for Location: Mu0=0

Test	-Statistic-		-----p Value------
Student's t	t	31.88909	Pr > |t| <.0001
Sign	M	17.5	Pr >= |M| <.0001
Signed Rank	S	315	Pr >= |S| <.0001

Parameters for Normal Distribution

Parameter	Symbol	Estimate
Mean	Mu	88.8
Std Dev	Sigma	16.47422

Goodness-of-Fit Tests for Normal Distribution

Test	---Statistic----		-----p Value-----
Kolmogorov-Smirnov	D	0.11366899	Pr > D >0.150
Cramer-von Mises	W-Sq	0.04746100	Pr > W-Sq >0.250
Anderson-Darling	A-Sq	0.30226604	Pr > A-Sq >0.250

Parameters for Lognormal Distribution

Parameter	Symbol	Estimate
Threshold	Theta	0
Scale	Zeta	4.469278
Shape	Sigma	0.189772
Mean		88.87983
Std Dev		17.01994

Goodness-of-Fit Tests for Lognormal Distribution

Test	---Statistic----		-----p Value-----
Kolmogorov-Smirnov	D	0.10134991	Pr > D >0.150
Cramer-von Mises	W-Sq	0.04657419	Pr > W-Sq >0.500
Anderson-Darling	A-Sq	0.30444000	Pr > A-Sq >0.500

Parameters for Weibull Distribution

Parameter	Symbol	Estimate
Threshold	Theta	0
Scale	Sigma	95.59641
Shape	C	5.746508
Mean		88.47348
Std Dev		17.83878

Goodness-of-Fit Tests for Weibull Distribution

Test	---Statistic----		-----p Value-----
Cramer-von Mises	W-Sq	0.08698467	Pr > W-Sq 0.162
Anderson-Darling	A-Sq	0.55683460	Pr > A-Sq 0.156

100mm Superpave – 2 Freeze/thaw Cycle

The UNIVARIATE Procedure
Variable: tsrS2
Moments

N	35	Sum Weights	35
Mean	79.8857143	Sum Observations	2796
Std Deviation	15.2966191	Variance	233.986555
Skewness	0.12837539	Kurtosis	-0.0897758
Uncorrected SS	231316	Corrected SS	7955.54286
Coeff Variation	19.1481283	Std Error Mean	2.58560054

Basic Statistical Measures

Location		Variability	
Mean	79.88571	Std Deviation	15.29662
Median	80.00000	Variance	233.98655
Mode	83.00000	Range	65.00000
		Interquartile Range	18.00000

Tests for Location: Mu0=0

Test	-Statistic-		-----p Value------
Student's t	t	30.89639	Pr > |t| <.0001
Sign	M	17.5	Pr >= |M| <.0001
Signed Rank	S	315	Pr >= |S| <.0001

Parameters for Normal Distribution

Parameter	Symbol	Estimate
Mean	Mu	79.88571
Std Dev	Sigma	15.29662

Goodness-of-Fit Tests for Normal Distribution

Test	---Statistic----		-----p Value-----
Kolmogorov-Smirnov	D	0.10808692	Pr > D >0.150
Cramer-von Mises	W-Sq	0.05481793	Pr > W-Sq >0.250
Anderson-Darling	A-Sq	0.33928688	Pr > A-Sq >0.250

Parameters for Lognormal Distribution

Parameter	Symbol	Estimate
Threshold	Theta	0
Scale	Zeta	4.362207
Shape	Sigma	0.196774
Mean		79.96324
Std Dev		15.88827

Goodness-of-Fit Tests for Lognormal Distribution

Test	---Statistic----		-----p Value-----
Kolmogorov-Smirnov	D	0.14599732	Pr > D 0.058
Cramer-von Mises	W-Sq	0.09973698	Pr > W-Sq 0.111
Anderson-Darling	A-Sq	0.55293931	Pr > A-Sq 0.147

Parameters for Weibull Distribution

Parameter	Symbol	Estimate
Threshold	Theta	0
Scale	Sigma	86.13012
Shape	C	5.732775
Mean		79.70183
Std Dev		16.10556

Goodness-of-Fit Tests for Weibull Distribution

Test	---Statistic----		-----p Value-----
Cramer-von Mises	W-Sq	0.05705911	Pr > W-Sq >0.250
Anderson-Darling	A-Sq	0.37172290	Pr > A-Sq >0.250

100mm Superpave – 3 Freeze/thaw Cycle

The UNIVARIATE Procedure
Variable: tsrS3
Moments

N	35	Sum Weights	35
Mean	74.4857143	Sum Observations	2607
Std Deviation	18.2311489	Variance	332.37479
Skewness	0.55300249	Kurtosis	0.70812845
Uncorrected SS	205485	Corrected SS	11300.7429
Coeff Variation	24.4760342	Std Error Mean	3.08162661

Basic Statistical Measures

Location		Variability	
Mean	74.48571	Std Deviation	18.23115
Median	71.00000	Variance	332.37479
Mode	70.00000	Range	84.00000
		Interquartile Range	23.00000

Tests for Location: Mu0=0

Test	-Statistic-	-----p Value------
Student's t	t 24.17091	Pr > |t| <.0001
Sign	M 17.5	Pr >= |M| <.0001
Signed Rank	S 315	Pr >= |S| <.0001

Parameters for Normal Distribution

Parameter	Symbol	Estimate
Mean	Mu	74.48571
Std Dev	Sigma	18.23115

Goodness-of-Fit Tests for Normal Distribution

Test	---Statistic----	-----p Value-----
Kolmogorov-Smirnov	D 0.09009951	Pr > D >0.150
Cramer-von Mises	W-Sq 0.03320896	Pr > W-Sq >0.250
Anderson-Darling	A-Sq 0.22272842	Pr > A-Sq >0.250

Parameters for Lognormal Distribution

Parameter	Symbol	Estimate
Threshold	Theta	0
Scale	Zeta	4.281421
Shape	Sigma	0.247093
Mean		74.58571
Std Dev		18.71454

Goodness-of-Fit Tests for Lognormal Distribution

Test	---Statistic----		-----p Value-----
Kolmogorov-Smirnov	D	0.07556771	Pr > D >0.150
Cramer-von Mises	W-Sq	0.02364675	Pr > W-Sq >0.500
Anderson-Darling	A-Sq	0.17885336	Pr > A-Sq >0.500

Parameters for Weibull Distribution

Parameter	Symbol	Estimate
Threshold	Theta	0
Scale	Sigma	81.54436
Shape	C	4.310017
Mean		74.22941
Std Dev		19.46317

Goodness-of-Fit Tests for Weibull Distribution

Test	---Statistic----		-----p Value-----
Cramer-von Mises	W-Sq	0.05684418	Pr > W-Sq >0.250
Anderson-Darling	A-Sq	0.39553700	Pr > A-Sq >0.250

Phase II Moisture Study - TSR

The UNIVARIATE Procedure
Variable: tsr
Moments

N	105	Sum Weights	105
Mean	91.952381	Sum Observations	9655
Std Deviation	11.57813	Variance	134.053095
Skewness	-0.0367541	Kurtosis	-0.0117542
Uncorrected SS	901741.76	Corrected SS	13941.5219
Coeff Variation	12.5914413	Std Error Mean	1.1299098

Basic Statistical Measures

Location		Variability	
Mean	91.95238	Std Deviation	11.57813
Median	92.50000	Variance	134.05310
Mode	92.30000	Range	62.00000
		Interquartile Range	15.60000

Tests for Location: Mu0=0

Test	-Statistic-		-----p Value------
Student's t	t	81.38028	Pr > |t| <.0001
Sign	M	52.5	Pr >= |M| <.0001
Signed Rank	S	2782.5	Pr >= |S| <.0001

Parameters for Normal Distribution

Parameter	Symbol	Estimate
Mean	Mu	91.95238
Std Dev	Sigma	11.57813

Goodness-of-Fit Tests for Normal Distribution

Test	---Statistic----		-----p Value-----
Kolmogorov-Smirnov	D	0.07719145	Pr > D 0.125
Cramer-von Mises	W-Sq	0.07815315	Pr > W-Sq 0.223
Anderson-Darling	A-Sq	0.49132013	Pr > A-Sq 0.223

Parameters for Lognormal Distribution

Parameter	Symbol	Estimate
Threshold	Theta	0
Scale	Zeta	4.51321
Shape	Sigma	0.128664
Mean		91.97225
Std Dev		11.88264

Goodness-of-Fit Tests for Lognormal Distribution

Test	---Statistic----		-----p Value-----	
Kolmogorov-Smirnov	D	0.08659458	Pr > D	0.051
Cramer-von Mises	W-Sq	0.15037342	Pr > W-Sq	0.024
Anderson-Darling	A-Sq	0.86510204	Pr > A-Sq	0.025

Parameters for Weibull Distribution

Parameter	Symbol	Estimate
Threshold	Theta	0
Scale	Sigma	97.01041
Shape	C	8.590305
Mean		91.66893
Std Dev		12.72391

Goodness-of-Fit Tests for Weibull Distribution

Test	---Statistic----		-----p Value-----	
Cramer-von Mises	W-Sq	0.07307117	Pr > W-Sq	0.242
Anderson-Darling	A-Sq	0.64161236	Pr > A-Sq	0.093

Phase II Moisture Study – E* Ratio

The UNIVARIATE Procedure
Variable: estar 0.02 Hz

Moments

N	62	Sum Weights	62
Mean	86.9080645	Sum Observations	5388.3
Std Deviation	25.527679	Variance	651.662393
Skewness	0.46366812	Kurtosis	-0.3990607
Uncorrected SS	508038.13	Corrected SS	39751.406
Coeff Variation	29.3731993	Std Error Mean	3.24201847

Basic Statistical Measures

Location		Variability	
Mean	86.90806	Std Deviation	25.52768
Median	83.80000	Variance	651.66239
Mode	76.30000	Range	111.90000
		Interquartile Range	35.80000

Tests for Location: Mu0=0

Test	-Statistic-		-----p Value------
Student's t	t	26.80678	Pr > |t| <.0001
Sign	M	31	Pr >= |M| <.0001
Signed Rank	S	976.5	Pr >= |S| <.0001

Parameters for Normal Distribution

Parameter	Symbol	Estimate
Mean	Mu	86.90806
Std Dev	Sigma	25.52768

Goodness-of-Fit Tests for Normal Distribution

Test	---Statistic----		-----p Value-----
Kolmogorov-Smirnov	D	0.09684781	Pr > D >0.150
Cramer-von Mises	W-Sq	0.08336662	Pr > W-Sq 0.191
Anderson-Darling	A-Sq	0.51915095	Pr > A-Sq 0.189

Parameters for Lognormal Distribution

Parameter	Symbol	Estimate
Threshold	Theta	0
Scale	Zeta	4.422043
Shape	Sigma	0.297241
Mean		87.02706
Std Dev		26.45008

Goodness-of-Fit Tests for Lognormal Distribution

Test	---Statistic----		-----p Value-----
Kolmogorov-Smirnov	D	0.06143057	Pr > D >0.150
Cramer-von Mises	W-Sq	0.04192032	Pr > W-Sq >0.500
Anderson-Darling	A-Sq	0.27122326	Pr > A-Sq >0.500

Parameters for Weibull Distribution

Parameter	Symbol	Estimate
Threshold	Theta	0
Scale	Sigma	96.32195
Shape	C	3.691709
Mean		86.91536
Std Dev		26.21509

Goodness-of-Fit Tests for Weibull Distribution

Test	---Statistic----		-----p Value-----
Cramer-von Mises	W-Sq	0.07911830	Pr > W-Sq 0.208
Anderson-Darling	A-Sq	0.52055657	Pr > A-Sq 0.195

The UNIVARIATE Procedure
Variable: estar 0.1 Hz

Moments

N	62	Sum Weights	62
Mean	80.3080645	Sum Observations	4979.1
Std Deviation	20.7464182	Variance	430.413868
Skewness	0.15279987	Kurtosis	-0.881308
Uncorrected SS	426117.13	Corrected SS	26255.246
Coeff Variation	25.8335428	Std Error Mean	2.63479775

Basic Statistical Measures

Location		Variability	
Mean	80.30806	Std Deviation	20.74642
Median	79.55000	Variance	430.41387
Mode	60.20000	Range	80.30000
		Interquartile Range	30.60000

Tests for Location: Mu0=0

Test	-Statistic-	-----p Value------
Student's t	t 30.47978	Pr > |t| <.0001
Sign	M 31	Pr >= |M| <.0001
Signed Rank	S 976.5	Pr >= |S| <.0001

Parameters for Normal Distribution

Parameter	Symbol	Estimate
Mean	Mu	80.30806
Std Dev	Sigma	20.74642

Goodness-of-Fit Tests for Normal Distribution

Test	---Statistic----	-----p Value-----
Kolmogorov-Smirnov	D 0.07683534	Pr > D >0.150
Cramer-von Mises	W-Sq 0.06178074	Pr > W-Sq >0.250
Anderson-Darling	A-Sq 0.48208726	Pr > A-Sq 0.230

Parameters for Lognormal Distribution

Parameter	Symbol	Estimate
Threshold	Theta	0
Scale	Zeta	4.351487
Shape	Sigma	0.268491
Mean		80.44152
Std Dev		21.99301

Goodness-of-Fit Tests for Lognormal Distribution

Test	---Statistic----		-----p Value-----	
Kolmogorov-Smirnov	D	0.08809599	Pr > D	>0.150
Cramer-von Mises	W-Sq	0.06645013	Pr > W-Sq	0.326
Anderson-Darling	A-Sq	0.46893534	Pr > A-Sq	0.245

Parameters for Weibull Distribution

Parameter	Symbol	Estimate
Threshold	Theta	0
Scale	Sigma	88.27489
Shape	C	4.342228
Mean		80.39079
Std Dev		20.93678

Goodness-of-Fit Tests for Weibull Distribution

Test	---Statistic----		-----p Value-----	
Cramer-von Mises	W-Sq	0.07277117	Pr > W-Sq	0.242
Anderson-Darling	A-Sq	0.53598981	Pr > A-Sq	0.180

The UNIVARIATE Procedure
Variable: estar 1.0 Hz

Moments

N	62	Sum Weights	62
Mean	78.2645161	Sum Observations	4852.4
Std Deviation	22.8424906	Variance	521.779376
Skewness	0.15583434	Kurtosis	-0.6377257
Uncorrected SS	411599.28	Corrected SS	31828.5419
Coeff Variation	29.1862669	Std Error Mean	2.9009992

Basic Statistical Measures

Location		Variability	
Mean	78.26452	Std Deviation	22.84249
Median	76.85000	Variance	521.77938
Mode	44.40000	Range	93.70000
		Interquartile Range	31.80000

NOTE: The mode displayed is the smallest of 5 modes with a count of 2.

Tests for Location: Mu0=0

Test	-Statistic-	-----p Value------
Student's t	t 26.97847	Pr > |t| <.0001
Sign	M 31	Pr >= |M| <.0001
Signed Rank	S 976.5	Pr >= |S| <.0001

Parameters for Normal Distribution

Parameter	Symbol	Estimate
Mean	Mu	78.26452
Std Dev	Sigma	22.84249

Goodness-of-Fit Tests for Normal Distribution

Test	---Statistic----	-----p Value-----
Kolmogorov-Smirnov	D 0.11159274	Pr > D 0.054
Cramer-von Mises	W-Sq 0.08062584	Pr > W-Sq 0.207
Anderson-Darling	A-Sq 0.50855646	Pr > A-Sq 0.201

Parameters for Lognormal Distribution

Parameter	Symbol	Estimate
Threshold	Theta	0
Scale	Zeta	4.31521
Shape	Sigma	0.308956
Mean		78.48729
Std Dev		24.83946

Goodness-of-Fit Tests for Lognormal Distribution

Test	---Statistic----		-----p Value-----
Kolmogorov-Smirnov	D	0.14446214	Pr > D <0.010
Cramer-von Mises	W-Sq	0.12531582	Pr > W-Sq 0.050
Anderson-Darling	A-Sq	0.87500643	Pr > A-Sq 0.024

Parameters for Weibull Distribution

Parameter	Symbol	Estimate
Threshold	Theta	0
Scale	Sigma	86.65676
Shape	C	3.827929
Mean		78.35128
Std Dev		22.87194

Goodness-of-Fit Tests for Weibull Distribution

Test	---Statistic----		-----p Value-----
Cramer-von Mises	W-Sq	0.07165103	Pr > W-Sq 0.248
Anderson-Darling	A-Sq	0.46314926	Pr > A-Sq 0.249

The UNIVARIATE Procedure
Variable: estar 5.0 Hz

Moments

N	62	Sum Weights	62
Mean	82.1564516	Sum Observations	5093.7
Std Deviation	24.536561	Variance	602.042827
Skewness	0.05808302	Kurtosis	-0.8134506
Uncorrected SS	455204.93	Corrected SS	36724.6124
Coeff Variation	29.8656533	Std Error Mean	3.11614637

Basic Statistical Measures

Location		Variability	
Mean	82.15645	Std Deviation	24.53656
Median	83.00000	Variance	602.04283
Mode	60.20000	Range	98.50000
		Interquartile Range	37.80000

NOTE: The mode displayed is the smallest of 3 modes with a count of 2.

Tests for Location: Mu0=0

Test	-Statistic-	-----p Value------
Student's t	t 26.36476	Pr > |t| <.0001
Sign	M 31	Pr >= |M| <.0001
Signed Rank	S 976.5	Pr >= |S| <.0001

Parameters for Normal Distribution

Parameter	Symbol	Estimate
Mean	Mu	82.15645
Std Dev	Sigma	24.53656

Goodness-of-Fit Tests for Normal Distribution

Test	---Statistic----	-----p Value-----
Kolmogorov-Smirnov	D 0.06415837	Pr > D >0.150
Cramer-von Mises	W-Sq 0.04640869	Pr > W-Sq >0.250
Anderson-Darling	A-Sq 0.28258419	Pr > A-Sq >0.250

Parameters for Lognormal Distribution

Parameter	Symbol	Estimate
Threshold	Theta	0
Scale	Zeta	4.360459
Shape	Sigma	0.322349
Mean		82.46825
Std Dev		27.28929

Goodness-of-Fit Tests for Lognormal Distribution

Test	---Statistic----		-----p Value-----
Kolmogorov-Smirnov	D	0.10132484	Pr > D 0.113
Cramer-von Mises	W-Sq	0.09662889	Pr > W-Sq 0.125
Anderson-Darling	A-Sq	0.59715939	Pr > A-Sq 0.119

Parameters for Weibull Distribution

Parameter	Symbol	Estimate
Threshold	Theta	0
Scale	Sigma	91.0848
Shape	C	3.786947
Mean		82.30549
Std Dev		24.26081

Goodness-of-Fit Tests for Weibull Distribution

Test	---Statistic----		-----p Value-----
Cramer-von Mises	W-Sq	0.04026210	Pr > W-Sq >0.250
Anderson-Darling	A-Sq	0.24437811	Pr > A-Sq >0.250

The UNIVARIATE Procedure
Variable: estar 10.0 Hz

Moments

N	62	Sum Weights	62
Mean	83.8387097	Sum Observations	5198
Std Deviation	25.0797244	Variance	628.992575
Skewness	0.04089549	Kurtosis	-0.7006048
Uncorrected SS	474162.16	Corrected SS	38368.5471
Coeff Variation	29.9142538	Std Error Mean	3.18512818

Basic Statistical Measures

Location		Variability	
Mean	83.83871	Std Deviation	25.07972
Median	83.15000	Variance	628.99258
Mode	.	Range	103.30000
		Interquartile Range	38.80000

Tests for Location: Mu0=0

Test	-Statistic-	-----p Value------
Student's t	t 26.32193	Pr > |t| <.0001
Sign	M 31	Pr >= |M| <.0001
Signed Rank	S 976.5	Pr >= |S| <.0001

Parameters for Normal Distribution

Parameter	Symbol	Estimate
Mean	Mu	83.83871
Std Dev	Sigma	25.07972

Goodness-of-Fit Tests for Normal Distribution

Test	---Statistic----	-----p Value-----
Kolmogorov-Smirnov	D 0.07933165	Pr > D >0.150
Cramer-von Mises	W-Sq 0.04215164	Pr > W-Sq >0.250
Anderson-Darling	A-Sq 0.31214487	Pr > A-Sq >0.250

Parameters for Lognormal Distribution

Parameter	Symbol	Estimate
Threshold	Theta	0
Scale	Zeta	4.380063
Shape	Sigma	0.325821
Mean		84.19564
Std Dev		28.17716

Goodness-of-Fit Tests for Lognormal Distribution

Test	---Statistic----		-----p Value-----	
Kolmogorov-Smirnov	D	0.11101509	Pr > D	0.057
Cramer-von Mises	W-Sq	0.14502390	Pr > W-Sq	0.027
Anderson-Darling	A-Sq	0.79593914	Pr > A-Sq	0.039

Parameters for Weibull Distribution

Parameter	Symbol	Estimate
Threshold	Theta	0
Scale	Sigma	92.93645
Shape	C	3.777766
Mean		83.96732
Std Dev		24.80494

Goodness-of-Fit Tests for Weibull Distribution

Test	---Statistic----		-----p Value-----	
Cramer-von Mises	W-Sq	0.03745174	Pr > W-Sq	>0.250
Anderson-Darling	A-Sq	0.28262365	Pr > A-Sq	>0.250

The UNIVARIATE Procedure
Variable: estar 25.0 Hz

Moments

N	62	Sum Weights	62
Mean	92.3306452	Sum Observations	5724.5
Std Deviation	37.0172294	Variance	1370.27527
Skewness	1.79088158	Kurtosis	4.55105856
Uncorrected SS	612133.57	Corrected SS	83586.7918
Coeff Variation	40.0920294	Std Error Mean	4.70119284

Basic Statistical Measures

Location		Variability	
Mean	92.33065	Std Deviation	37.01723
Median	87.25000	Variance	1370
Mode	83.70000	Range	199.50000
		Interquartile Range	39.80000

NOTE: The mode displayed is the smallest of 3 modes with a count of 2.

Tests for Location: Mu0=0

Test	-Statistic-	-----p Value------
Student's t	t 19.63983	Pr > |t| <.0001
Sign	M 31	Pr >= |M| <.0001
Signed Rank	S 976.5	Pr >= |S| <.0001

Parameters for Normal Distribution

Parameter	Symbol	Estimate
Mean	Mu	92.33065
Std Dev	Sigma	37.01723

Goodness-of-Fit Tests for Normal Distribution

Test	---Statistic----	-----p Value-----
Kolmogorov-Smirnov	D 0.13900007	Pr > D <0.010
Cramer-von Mises	W-Sq 0.29676684	Pr > W-Sq <0.005
Anderson-Darling	A-Sq 2.06508708	Pr > A-Sq <0.005

Parameters for Lognormal Distribution

Parameter	Symbol	Estimate
Threshold	Theta	0
Scale	Zeta	4.458921
Shape	Sigma	0.359555
Mean		92.16323
Std Dev		34.23815

Goodness-of-Fit Tests for Lognormal Distribution

Test	---Statistic----		-----p Value-----
Kolmogorov-Smirnov	D	0.07586343	Pr > D >0.150
Cramer-von Mises	W-Sq	0.04381118	Pr > W-Sq >0.500
Anderson-Darling	A-Sq	0.35843326	Pr > A-Sq 0.457

Parameters for Weibull Distribution

Parameter	Symbol	Estimate
Threshold	Theta	0
Scale	Sigma	103.8658
Shape	C	2.561806
Mean		92.21539
Std Dev		38.60632

Goodness-of-Fit Tests for Weibull Distribution

Test	---Statistic----		-----p Value-----
Cramer-von Mises	W-Sq	0.28834246	Pr > W-Sq <0.010
Anderson-Darling	A-Sq	2.01222721	Pr > A-Sq <0.010

GENERAL LINEAR MODEL - REGRESSION
AASHOT T283

The SAS System 09:38 Friday, July 28, 2006 127

The GLM Procedure

Class Level Information

Class	Levels	Values
grad	2	0 1
nmas	3	0 1 2
traf	3	0 1 2
poly	2	0 1
agg	3	0 1 2
k	2	0 1
ac	2	0 1
faa	2	0 1
rap	4	0 1 2 3

Number of Observations Read	105
Number of Observations Used	80

The GLM Procedure

Dependent Variable: tsr

Source	DF	Sum of Squares	Mean Square	F Value	Pr > F
Model	14	5174.25688	369.58978	3.50	0.0003
Error	65	6870.63700	105.70211		
Corrected Total	79	12044.89388			

R-Square	Coeff Var	Root MSE	tsr Mean
0.429581	11.07182	10.28115	92.85875

Source	DF	Type I SS	Mean Square	F Value	Pr > F
grad	1	226.787042	226.787042	2.15	0.1478
nmas	2	40.287944	20.143972	0.19	0.8269
traf	2	614.550361	307.275181	2.91	0.0618
poly	1	629.918099	629.918099	5.96	0.0174
agg	2	657.623067	328.811533	3.11	0.0513
k	1	1146.676766	1146.676766	10.85	0.0016
ac	1	260.459703	260.459703	2.46	0.1213
faa	1	179.168042	179.168042	1.70	0.1975
rap	3	1418.785851	472.928617	4.47	0.0064

Source	DF	Type III SS	Mean Square	F Value	Pr > F
grad	1	1165.367405	1165.367405	11.03	0.0015
nmas	2	1463.532377	731.766189	6.92	0.0019
traf	2	1187.556818	593.778409	5.62	0.0056
poly	1	1869.826118	1869.826118	17.69	<.0001
agg	2	1816.637940	908.318970	8.59	0.0005
k	1	684.352000	684.352000	6.47	0.0133
ac	1	291.852800	291.852800	2.76	0.1014
faa	1	953.285950	953.285950	9.02	0.0038
rap	3	1418.785851	472.928617	4.47	0.0064

Dynamic Modulus

The SAS System 11:01 Friday, July 28, 2006 24

The GLM Procedure

Class Level Information

Class	Levels	Values
grad	2	0 1
nmas	3	0 1 2
traf	3	0 1 2
poly	2	0 1
agg	3	0 1 2
k	2	0 1
ac	2	0 1
faa	2	0 1
rap	4	0 1 2 3
freq	6	0 1 2 3 4 5

Number of Observations Read	372
Number of Observations Used	288

The GLM Procedure

Dependent Variable: estar

Source	DF	Sum of Squares	Mean Square	F Value	Pr > F
Model	19	54938.7583	2891.5136	5.59	<.0001
Error	268	138719.8074	517.6112		
Corrected Total	287	193658.5658			

R-Square	Coeff Var	Root MSE	estar Mean
0.283689	25.33635	22.75107	89.79618

Source	DF	Type I SS	Mean Square	F Value	Pr > F
grad	1	293.88334	293.88334	0.57	0.4518
nmas	2	2546.66251	1273.33125	2.46	0.0874
traf	2	13922.15758	6961.07879	13.45	<.0001
poly	1	1808.01875	1808.01875	3.49	0.0627
agg	2	11448.72186	5724.36093	11.06	<.0001
k	1	8819.90288	8819.90288	17.04	<.0001
ac	1	36.25349	36.25349	0.07	0.7915
faa	1	165.21534	165.21534	0.32	0.5726
rap	3	7971.68895	2657.22965	5.13	0.0018
freq	5	7926.25366	1585.25073	3.06	0.0105

Source	DF	Type III SS	Mean Square	F Value	Pr > F
grad	1	2288.290932	2288.290932	4.42	0.0364
nmas	2	3637.787637	1818.893818	3.51	0.0312
traf	2	1179.722080	589.861040	1.14	0.3215
poly	1	1943.952196	1943.952196	3.76	0.0537
agg	2	2485.267833	1242.633916	2.40	0.0926
k	1	11.793185	11.793185	0.02	0.8801
ac	1	3220.128290	3220.128290	6.22	0.0132
faa	1	3411.955796	3411.955796	6.59	0.0108
rap	3	7412.616266	2470.872089	4.77	0.0029
freq	5	7926.253657	1585.250731	3.06	0.0105

REFERENCES

AASHTO TP48 (1997) Standard Test Procedure for Viscosity Determination of Asphalt Binders Using Rotational Viscometer. *Standard Specifications for Transportation Materials and Methods and Sampling and Testing Part II: Tests*. Washington D.C.

AASHTO T165-55. (1997) Effect of Water on Cohesion of Compacted Bituminous Mixtures. *Standard Specifications for Transportation Materials and Methods and Sampling and Testing Part II: Tests*. Washington D.C.

AASHTO T166-93. (1997) Bulk Specific Gravity of Compacted Bituminous Mixtures Using Saturated Surface-Dry Specimens. *Standard Specifications for Transportation Materials and Methods and Sampling and Testing Part II: Tests*. Washington D.C.

AASHTO T182-84. (1997) Coating and Stripping of Bitumen-Aggregate Mixtures. *Standard Specifications for Transportation Materials and Methods and Sampling and Testing Part II: Tests*. Washington D.C.

AASHTO T209-94. (1997) Theoretical Maximum Specific Gravity and Density of Bituminous Paving Mixtures. *Standard Specifications for Transportation Materials and Methods and Sampling and Testing Part II: Tests*. Washington D.C.

AASHTO T269-94. (1997) % Air Voids in Compacted Dense and Open Bituminous Paving Mixtures. *Standard Specifications for Transportation Materials and Methods and Sampling and Testing Part II: Tests*. Washington D.C.

AASHTO T283-89. (1993) Resistance of Compacted Bituminous Mixture to Moisture Induced Damage. *Standard Specifications for Transportation Materials and Methods and Sampling and Testing Part II: Tests*. Washington D.C.

ASTM D5. (2004) Standard Test Method for Penetration of Bituminous Materials. *Annual Book of ASTM Standards* 4.03. West Conshohocken, PA: ASTM International.

ASTM D140. (2004) Standard Practice for Sampling Bituminous Materials. *Annual Book of ASTM Standards* 4.03. West Conshohocken, PA: ASTM International.

ASTM D1075. (2004) Standard Test Method for Effect of Water on Compressive Strength of Compacted Bituminous Mixtures. *Annual Book of ASTM Standards* 4.03. West Conshohocken, PA: ASTM International.

ASTM D2041. (2004) Standard Test Method for Theoretical Maximum Specific Gravity and Density of Bituminous Paving Mixtures. *Annual Book of ASTM Standards* 4.03. West Conshohocken, PA: ASTM International.

ASTM D2172. (2004) Standard Test Method for Quantitative Extraction of Bitumen from Bituminous Paving Mixtures. *Annual Book of ASTM Standards* 4.03. West Conshohocken, PA: ASTM International.

ASTM D2726. (2004) Standard Test Method for Bulk Specific Gravity and Density of Non-Absorptive Compacted Bituminous Mixtures. *Annual Book of ASTM Standards* 4.03. West Conshohocken, PA: ASTM International.

ASTM D4867. (2004) Standard Test Method for Effect of Moisture on Asphalt Concrete Paving Mixtures. *Annual Book of ASTM Standards* 4.03. West Conshohocken, PA: ASTM International.

ASTM C702. (2004) Standard Practice for Reducing Samples of Aggregate to Testing Size. *Annual Book of ASTM Standards* 4.02. West Conshohocken, PA: ASTM International.

Alam, Muhammad Murshed; Tandon, Vivek; Nazarian, Soheil; and Tahmoressi; Maghsoud. "Identification of Moisture-Susceptible Asphalt Concrete Mixes Using Modified Environmental Conditioning System." *Transportation Research Record 1630*, TRB, National Highway Research Council, Washington, D.C., 1998, pp. 106–116.

Al-Swailmi, Saleh and Terrel, Ronald. "Evaluation of Water Damage of Asphalt Concrete Mixtures Using the Environmental Conditioning System (ECS)." *Journal of the Association of Asphalt Paving Technologists*, Vol. 61, 1992a, pp. 405–435.

Al-Swailmi, Saleh and Terrel, Ronald. "Evaluation of the Environmental Conditioning System (ECS) with AASHTO T-283." *Journal of the Association of Asphalt Paving Technologists*, Vol. 61, 1992b, pp. 150–171.

Al-Swailmi, Saleh; Scholz, Todd V.; and Terrel, Ronald L. "Development and Evaluation of Test System to Induce and Monitor Moisture Damage to Asphalt Concrete Mixtures." *Transportation Research Record 1353*, TRB, National Highway Research Council, Washington, D.C., 1992c, pp. 39–45.

APA User's Manual 5.11.01. Pavement Technology, Inc, 2002.

Aschenbrener, T.; McGennis, R.B; and Terrel, R.L. "Comparison of Several Moisture Susceptibility Tests to Pavements of Known Field Performance." *Journal of the Association of Asphalt Paving Technologists*, Vol. 64, 1995, pp. 163–208.

Asphalt Institute. *Cause and Prevention of Stripping in Asphalt Pavements*. Educational Series No. 10, College Park, Md. 1981.
Asphalt Institute. *Superpave Mix Design*. Superpave Series No. 2. 2001.

Barak, John, Michigan Department of Transportation Bituminous Engineer, Email correspondence, Fall 2005.

Barcena, R., Epps Martin, A., and D. Hazlett. "Performance-Graded Binder Specification for Surface Treatments." *Transportation Research Record 1810*, National Highway Research Council, Washington D.C., 2002.

Bausano, J.P., Kvasnak, A.N., and R.C. Williams, "Transitioning Moisture Susceptibility Testing to Accommodate Superpave Gyratory Compaction" Canadian Technical Asphalt Association 2006 Conference, Charlottetown, Prince Edward Island, 2006.

Bhasin, Amit; Masad, Eyad; Little, Dallas; and Lytton, Robert. "Limits of Adhesive Bond Energy for Improved Resistance to Hot Mix Asphalt to Moisture Damage." *Transportation Research Board CD-ROM*. 85th Annual Meeting, January 22-26, 2006.

Birgisson, Bjorn; Roque, Reynaldo; and Page, Gale C. "Evaluation of Water Damage Using Hot Mix Asphalt Fracture Mechanics." *Association of Asphalt Paving Technologists* CD-ROM. 2003.

Birgisson, B, G. Sholar, R. Roque, "Evaluation of Predicted Dynamic Modulus for Florida Mixtures," Transportation Research Board CD-ROM. 84th Annual Meeting, January 9-13, 2005.

Bonaquist, Ramon and Christensen, Donald. *NCHRP Report 513: Simple Performance Tester for Superpave Mix Design: First Article Development and Evaluation.* Transportation Research Board, National Highway Research Council, Washington D.C. 2003.

Brown, E.R.; Kandhal, P.S.; Zhang, J. "Performance Testing for Hot Mix Asphalt," National Center for Asphalt Technology (NCAT) Report 2001-05, 2001.

California Test 302. "Method of Test for Film Stripping." State of California Department of Transportation. 1999.

California Test 307. "Method of Test for Moisture Vapor Susceptibility of Bituminous Mixtures." State of California Department of Transportation. 2000.

Cheng, DingXin; Little, Dallas N.; Lytton, Robert L.; Holste, James C . "Surface Energy Measurements of Asphalt and Its Application to Predicting Fatigue and Healing in Asphalt Mixtures." *Transportation Research Record 1810*, TRB, National Highway Research Council, Washington, D.C., 2002, pp. 44–53.

Cheng, DingXin; Little, Dallas N.; Lytton, Robert L.; Holste, James C . "Moisture Damage Evaluation of Asphalt Mixtures by Considering Both Moisture Diffusion and Repeated-Load Conditions." *Transportation Research Record 1832*, TRB, National Highway Research Council, Washington, D.C., 2003, pp. 42–49.

Choubane, Bouzid; Page, Gale; and Musselman, James. "Effects of Water Saturation Level on Resistance of Compacted Hot-Mix Asphalt Samples to Moisture-Induced Damage."

Transportation Research Record 1723, TRB, National Highway Research Council, Washington, D.C., 2000, pp. 97–106.

Cooley, L.A., P.S. Kandhal, M.S. Buchanan, F. Fee, and A. Epps, "Loaded Wheel Testers in the United States: State of the Practice," Transportation Research E-Circular, Number E-C016, Transportation Research Board, Washington, D.C., July 2000.

Coplantz, John and Newcomb, David. "Water Sensitivity Test Methods for Asphalt Concrete Mixtures: A Laboratory Comparison." *Transportation Research Record 1171*, TRB, National Highway Research Council, Washington, D.C., 1988, pp. 44–50.

Cross, S.A., Voth, D.M., and G.A. Fager, "Effects of Sample Preconditioning on Asphalt Pavement Analyzer Wet Rut Depths," Mid-Continent Transportation Symposium 2000 Proceedings, 2000.

Curtis, C.W.; Lytton, Robert L.; and Brannan, C.J. "Influence of Aggregate Chemistry on the Adsorption and Desorption of Asphalt." *Transportation Research Record 1362*, TRB, National Highway Research Council, Washington, D.C., 1992, pp. 1–9.

Curtis, C.W.; Ensley, K; and Epps, J. "Fundamental Properties of Asphalt-Aggregate Interactions Including Adhesion and Absorption." SHRP-A-341. Strategic Highway Research Program, National Highway Research Council, Washington, D.C., 1993.

DATAPAVE, http://www.datapave.com, LTPP DataPave Online 2004.

Dongre, Raj. Personal Communication on June 26, 2006.

Epps Martin, A. and D.W. Park, "Use of the Asphalt Pavement Analyzer and Repeated Simple Shear Test at Constant Height to Augment Superpave Volumetric Mix Design," Journal of Transportation Engineering, Volume 129, Issue 5, 2003.

Epps, J.; Sebaaly, Peter; Penaranda, Jorge; Maher, Michele; McCann, Martin; and Hand Adam. *NCHRP 444: Compatibility of a Test for Moisture-Induced Damage with Superpave Volumetric Mix Design*. Transportation Research Board, National Highway Research Council, Washington, D.C. 2000.

Ford, M.C.; Manke, P.G.; and O'Bannon, C.E. "Quantitative Evaluation of Stripping by the Surface Reaction Test." *Transportation Research Record 515*, TRB, National Highway Research Council, Washington, D.C., 1974, pp. 40–54.

Fromm, H.J. The Mechanisms of Asphalt Stripping from Aggregate Surfaces. *Journal of the Association of Asphalt Paving Technologists*, Vol. 43, 1974, pp 191–223.

Goode, F.F. "Use of Immersion Compression Test in Evaluating and Designing Bituminous Paving Mixtures." In American Society of Testing and Materials (ASTM) Special Technical Publication (STP) 252, 1959, pp. 113–126.

Graf, Peter. "Factors Affecting Moisture Susceptibility of Asphalt Concrete Mixes." *Journal of the Association of Asphalt Paving Technologists*, Vol. 55, 1986, pp. 175 –204.

Hicks, Gary. *NCHRP 175: Moisture Damage in Asphalt Concrete*. Transportation Research Board, National Highway Research Council, Washington, D.C. 1991.

IPC Global. UTM 38 Dynamic Modulus Software Package, Version 1.01, 2000a.

IPC Global. UTM 19 Dynamic Creep Software Package, Version 1.0, 2000b.

Isacsson, W. and Jorgensen, T. Laboratory Methods for Determination of the Water Susceptibility of Bituminous Pavements. VIT Report, Swedish Road and Traffic Research Institute, No. 324A, 1987.

Jackson, N.M. and C.D. Baldwin, "Evaluation of the Asphalt Pavement Analyzer to Predict the Relative Rutting Susceptibility of HMA in Tennessee," International Conference on Accelerated Pavement Testing October 18-20, 1999 Dissertation Number CS6-3, 1999.

Jimenez, R.A. "Testing for Debonding of Asphalt from Aggregates." *Transportation Research Record 515,* TRB, National Highway Research Council, Washington, D.C., 1974, pp. 1–17.

Johnston, A.G., Yeung, K., and D. Tannahill, "Use of Asphalt Pavement Analyzer Testing for Evaluating Premium Surfacing Asphalt Mixtures for Urban Roadways," 2005 Annual Conference of the Transportation Association of Canada, 2005.

Kandhal, P. "Field and Laboratory Investigation of Stripping in Asphalt Pavements: State of the Art Report." *Transportation Research Record 1454,* TRB, National Highway Research Council, Washington, D.C., 1994, pp. 36–47.

Kanitpong, K. and H.U. Bahia, "Role of Adhesion and Thin Film Tackiness of Asphalt Binders in Moisture Damage of HMA." *Journal of the Association of Asphalt Paving Technologists,* Vol. 72, 2003, pp 502–528.

Kanitpong, Kunnawee and Bahia, Hussain. "Evaluation of HMA Moisture Damage in Wisconsin as it Related to Pavement Performance." Transportation Research Board CD-ROM. 85th Annual Meeting, January 22-26, 2006a.

Kanitpong, Kunnawee and Bahia, Hussain. "Relating Adhesion and Cohesion of Asphalts to Effect of Moisture ON Asphalt Mixtures' Laboratory Performance." Transportation Research Board CD-ROM. 85th Annual Meeting, January 22-26, 2006b.

Kennedy, Thomas W; Roberts, Freddy, L.; and Lee, Kang W. "Evaluation of the Moisture Effects on Asphalt Concrete Mixtures." *Transportation Research Record 911,* TRB, National Highway Research Council, Washington, D.C., 1983, pp. 134–143.

Kennedy, Thomas W; Roberts, Freddy, L.; and Lee, Kang W. "Evaluating Moisture Susceptibility of Asphalt Mixtures Using the Texas Boiling Test." *Transportation Research Record 968,* TRB, National Highway Research Council, Washington, D.C., 1984a , pp. 45–54,

Kennedy, T.W. and W.V. Ping, "Comparison Study of Moisture Damage Test Methods for Evaluating Antistripping Treatments in Asphalt Mixtures." *Transportation Research Record 1323,* TRB, National Highway Research Council, Washington D.C., 1984b. pp 94–111.

Kvasnak, A.N., "Development and Evaluation of Test Procedures to Identify Moisture Damage Prone Hot Mix Asphalt Pavements," Ph.D Dissertation, Iowa State University, 2006.

Little, Dallas N. and Jones IV, David R. "Chemical and Mechanical Processes of Moisture Damage in Hot-Mix Asphalt Pavements." Moisture Sensitivity of Asphalt Pavements A National Seminar. February 4-6, 2003.

Lottman, R.P. *NCHRP 192: Predicting Moisture-Inducted Damage to Asphaltic Concrete*. Transportation Research Board, National Highway Research Council, Washington, D.C. 1978.

Lottman, R.P. *NCHRP 246: Predicting Moisture-Inducted Damage to Asphaltic Concrete – Field Evaluation*. Transportation Research Board, National Highway Research Council, Washington, D.C. 1982.

Lottman, Robert P.; Chen, R.P.; Kumar, K.S.; and Wolf, L.W. "A Laboratory Test System for Prediction of Asphalt Concrete Moisture Damage." *Transportation Research Record 515,* TRB, National Highway Research Council, Washington, D.C., 1974, pp. 18–26.

Lottman, Robert P. "Laboratory Test Method for Predicting Moisture-Induced Damage to Asphalt Concrete." *Transportation Research Record 843,* TRB, National Highway Research Council, Washington, D.C., 1982, pp. 88–95.

Mack, C. *Bituminous Materials,* Vol. 1 (A Holberg, ed.), Interscience Publishers, New York. 1964

Majidzadeh, K. and Brovold, F.N. "Special Report 98: State of the Art: Effect of Water on Bitumen-Aggregate Mixtures." *Highway Research Board (HRB),* National Research Council, Washington, D.C. 1968.

Mallick, R.B, Gould, J.S., Bhattacharjee, S., Regimand, A., James, L.H., and E.R. Brown, "Development of a Rational Procedure for Evaluation of Moisture Susceptibility of Asphalt Paving Mixes," 82nd Annual Meeting of the Transportation Research Board, Washington, D.C., 2003.

Masad, Eyad; Zollinger, Corey; Bulut, Rifat; Little, Dallas; and Lytton, Robert. "Characterization of HMA Moisture Damage Using Surface Energy and Fracture Properties." *Association of Asphalt Paving Technologists* CD-ROM. 2006.

NCHRP 9-34. Improved Conditioning Procedure for Predicting the Moisture Susceptibility of HMA Pavements, National Cooperative Highway Research Program, March 2002.

Petersen, J.C., H. Plancher, E.K. Ensley, R.L. Venable, and G. Miyake, "Chemistry of Asphalt-Aggregate Interaction: Relationship with Pavement Moisture-Damage Prediction Test." *Transportation Research Record 843*, TRB, National Highway Research Council, Washington D.C., 1982. pp 95–104.

Plancher, H.; Miyake, G.; Venable, R.L.; and Peterson, J.C. "A Simple Laboratory Test to Indicate Moisture Susceptibility of Asphalt-Aggregate Mixtures to Moisture Damage During Repeated Freeze-Thaw Cycling." *Canadian Technical Asphalt Association Proceedings*, Vol. 25, 1980, pp. 247–262.

Roberts, Freddy L.; Kandhal, Prithvi S.; Brown, E. Ray; Lee, Dah-Yinn; and Kennedy, Thomas W. *Hot Mix Asphalt Materials, Mixture Design, and Construction*. 2nd Ed. 1996.

Robinette, Christopher. "Testing Wisconsin Asphalt Mixtures for the 2002 AASHTO Mechanistic Design Guide." Master Thesis, Michigan Technological University, 2005.

Romero, F.L. and Stuart, K.D. "Evaluating Accelerated Rut Testers." *Public Roads*, Vol. 62, No. 1, July-August, pp 50–54. 1998.

Rottermond, Matthew P., "Development of a Prototype Moisture Sensitivity Test for Asphalt Binder." M.S. Thesis Michigan Technological University, 2004.

SAS Institute, Inc. SAS for Windows XP Version 9.1.3, 2006.

Scherocman, James; Mesch, Keith; and Proctor, J. Joseph. "The Effect of Multiple Freeze-Thaw Cycle Conditioning on the Moisture Damage of Asphalt Concrete Mixtures." *Journal of the Association of Asphalt Paving Technologists*, Vol. 55, 1986, pp. 213–228.

Scholz, T.V. and S.F. Brown, "Rheological Characteristics of Bitumen in Contact with Mineral Aggregate (With Discussion)," Journal of the Association of Asphalt Paving Technologists, Volume 65, Bookcrafters Inc., Chelsea, MI, 1996.

Scholz, T.V.; Terrel, R.L.; Al-Joaib, A; and Bea, J. "Water Sensitivity: Binder Validation." SHRP-A-402. Strategic Highway Research Program, National Research Council, Washington, D.C., 1994.

Scott, J.A.N. "Adhesion and Disbonding Mechanisms of Asphalt Used in Highway Construction and Maintenance." *Journal of the Association of Asphalt Paving Technologists*, Vol. 47, 1978. pp19–44.

Shatnawi, S; Nagarajaiah, M.; and Harvey, J. "Moisture Sensitivity Evaluation of Binder-Aggregate Mixtures." *Transportation Research Record 1492,* TRB, National Highway Research Council, Washington, D.C., 1995, pp. 71–84.

Solaimanian, Mansour; Harvey, John; Tahmoressi, Maghsoud; and Tandon, Vivek. "Test Methods to Predict Moisture Sensitivity of Hot-Mix Asphalt Pavements." *Moisture Sensitivity of Asphalt Pavements A National Seminar*. February 4-6, 2003.

Solaimanian, Mansour; Fedor, David; Bonaquist, Ramon; Soltani, Ali; and Tandon, Vivek. "Simple Performance Test for Moisture Damage Prediction in Asphalt Concrete." *Association of Asphalt Paving Technologists CD-ROM*. 2006.

Stroup-Gardiner, Mary and Epps, J. "Laboratory Tests for Assessing Moisture Damage of Asphalt Concrete Mixtures." *Transportation Research Record 1353,* TRB, National Highway Research Council, Washington, D.C., 1992, pp. 15–23.

Tandon, Vivek; Alam, Muhammad Murshed; Nazarian, Soheil; and Vemuri, Nalini. "Significance of Conditioning Parameters Affecting Distinction of Moisture Susceptible Asphalt Concrete Mixtures in the Laboratory." *Journal of the Association of Asphalt Paving Technologists*, Vol. 67, 1998, pp. 334–353.

Tarrer, A.R. and Wagh, V. *The Effect of the Physical and Chemical Characteristics of the Aggregate on Bonding*. Strategic Highway Research Program, National Highway Research Council, Washington, DC., 1991.

Terrel, R.L. and Shute, W.J. Summary Report on Water Sensitivity. SHRP-A/IR-89-003. Strategic Highway Research Program, National Research Council, Washington D.C., 1989.

Terrel, R.L. and Al-Swailmi, S. "Final Report on Water Sensitivity of Asphalt-Aggregate Mixtures Test Development." SHRP-A-403. Strategic Highway Research Program, National Research Council, Washington, D.C., 1994.

Terrel, Ronald and Al-Swailmi, Saleh. "Role of Pessimum Voids Concept in Understanding Moisture Damage to Asphalt Concrete Mixtures." *Transportation Research Record 1386*, TRB, National Highway Research Council, Washington, D.C., 1993, pp. 31–37.

Thelen, Edmund. "Surface Energy and Adhesion Properties in Asphalt-Aggregate Systems." *Highway Research Board*, Volume 192, 1958, pp. 63–74.

Tunnicliff, D.G. and Root, R. 1982. *NCHRP Report 274*: *Use of Antistripping Additives in Asphaltic Concrete Mixtures. Laboratory phase*. TRB, National Highway Research Council, Washington, DC.

Tunnicliff, D.G. and R.E. Root. *NCHRP 373: Use of Antistripping Additives in Asphalt Concrete Mixtures – Field Evaluation*. Transportation Research Board, National Highway Research Council, Washington, D.C., 1995.

West, R., Zhang, J. and A. Cooley Jr., "Evaluation of Asphalt Pavement Analyzer for Moisture Sensitivty Testing," NCAT Report 04-04, Auburn, AL., 2003

Williams, R. Christopher. Iowa State University Associate Professor, Personal Conversion, Fall 2006.

Williams, R.C. and B.D. Prowell, "Comparison of Laboratory Wheel-Tracking Test Results with WesTrack Performance," Transportation Research Record 1681, Transportation Research Board, National Research Council, Washington, D.C., 1999.

Witczak, M.W.; Kaloush, K.; Pellinen, T.; El-Basyouny, M.; and Von Quintus, H. *NCHRP 465: Simple Performance Test for Superpave Mix Design.* Transportation Research Board, National Highway Research Council, Washington D.C., 2002.

Witczak, M.W. *NCHRP Report 547: Simple Performance Tests: Summary of Recommended Methods and Database.* Transportation Research Board, National Highway Research Council, Washington D.C., 2005.

Youtcheff, J.S. and Aurilio, V. "Moisture Sensitivity of Asphalt Binders: Evaluation and Modeling of the Pneumatic Adhesion Test Results." *Canadian Technical Asphalt Association Proceedings*, 1997.

Youtcheff, J.S.; Williams, R.C.; and Branthaver, J. "Evaluation of Relationships Between Moisture Sensitivity of Paving Asphalts, Modified Asphalt Binders, and Asphalt Components, and Their Chemistries." *American Chemical Society – Fuel Division, Symposium*, Vol. 34, 1998.